The Turbulent Single Phase Forced Convection Heat Transfer and Pressure Drop Characteristics of Circular Ducts Containing Swirl Flow Inducers or Pall Rings

by D. Burfoot

A Doctoral Thesis

Submitted in partial fulfilment of the requirements for the award of Doctor of Philosophy of Loughborough University of Technology

September 1982

Abstract

The heat transfer and pressure drop characteristics of tubes containing either Pall rings, or helical (180^{o}) strips of metal, were studied experimentally. Tests were performed with water in the Reynolds number range of 11000 to 104000, approximately.

Rotameters were used to measure the volumetric flowrate of the water. The effect of fluid temperature on this measurement was determined.

The insertion of a continuous length of Pall rings into a tube increases the Nusselt number and pressure drop by factors of 1.5 and 15. (These factors are relative to the empty tube over the same flow range). Smaller increases were obtained while using rings that were equidistantly spaced along the tube.

The effects of the twist direction, the orientation of consecutive helices, and the spacing of the helices, were examined. Equidistantly spaced pairs of helices with identical twist direction, and aligned leading edges, was found to be a better device than the continuous full length twisted strip. For the conditions of this work, the optimum spacing was equal to the length of each of the pairs of helices. Further work, with other geometries, is required to examine this optimum spacing. The Nusselt number and pressure drop increases, relative to the empty tube, were found to be 2.0 and 11, respectively, when using the optimum spacing.

Tubes containing continuous lengths of alternately twisted helices, with aligned leading edges, produced Nusselt number and pressure drop increases, again compared to the empty tube, of 2.6 and 26. A configuration formed with the above helices, but with the leading edges positioned perpendicularly, is known as a Kenics static mixer. When such a device was located in a tube, the Nusselt number and pressure drop increases were 2.8 and 73, approximately.

The equidistant spacing of pairs of alternately twisted helices was found to be more beneficial than the use of an empty tube section and a continuous length of helices.

I am responsible for the work submitted in this thesis. The original work is my own except as specified at the appropriate location in the text or in the Preface. This thesis and the original work contained herein has not been submitted previously for a higher degree.

D. Burfoot

September, 1982

Table of Contents

Preface

I extend a sincere thanks to the Science and Engineering Research Council for providing the financial support which enabled this work to be undertaken.

During the first 9 months of this project the experimental flow circuit was constructed, the equipment was calibrated, and the relevant literature was surveyed. A large amount of literature concerning various in-line mixers was collected during this, and later, periods. Much of this information is not directly applicable to the present work and therefore it has not been included in the review. However, to assist further workers who may benefit from such information, I have prepared a bibliography of the literature and this may be obtained from the address noted at the end of this preface. The purpose of the literature survey in this thesis is not simply to direct the reader to pertinent references, it also provides substantial justification of the reasons for undertaking the work, the assumptions used in some parts, and the agreement with previous work. A brief review of previously proposed devices, for heat transfer enhancement, is also provided. For these reasons the survey is necessarily long.

While awaiting the manufacture of the swirl inducing inserts, a study of the characteristics of Pall rings in tubes was carried out. These experiments, which extended over 6 months, allowed the equipment to be tested under conditions which produced enhanced heat transfer. The results show interesting trends and they have been included in this thesis. I thank Mr. K. Robinson (Norton Chemical Process Products (Europe) Ltd.) for supplying the Pall rings.

The following 12 months of work involved a study of the characteristics of swirl inducing inserts. I thank Mr. R.G. Stanbury (Kenics Europe) for supplying a considerable amount of information concerning the characteristics of one such device - the Kenics static mixer. Acknowledgement is also due to Mr. T.C. Carnavos (Noranda Metal Industries Inc.) for similar assistance regarding internally finned tubing.

Throughout the project a number of articles have been submitted for publication. The form of presentation of some of the work in this thesis has been affected, to a certain extent, by the constructive comments of the referees of these articles. The following articles have

been produced :

Burfoot, D., Rice, P.; "The effect of temperature on the measurement of water volumetric flowrate using a rotameter", J. Phys. E: Sci. Instrum., 14, 921 (1981).

Burfoot, D., Rice, P.; "Comparison of the heat transfer and pressure drop characteristics of packed beds and those of Pall rings in a tube", Chem. Eng. Sci., 37, No.3, 497-498 (1982).

Burfoot, D., Rice, P.; "Turbulent forced convection heat transfer enhancement using Pall rings in a circular duct", To be published in Ind. Eng. Chem. Proc. Des. Dev..

Burfoot, D., Rice, P.; "The heat transfer and pressure drop characteristics of short lengths of swirl flow inducers interspaced along a circular duct", To be published in Trans. IChemE.

A further manuscript, which considers the effects of using swirl flow inducing inserts, has been adapted according to the comments of the referees and this article is currently being reviewed.

I thank my supervisor, Dr. P. Rice, for his assistance in submitting the above articles and also for his support throughout the project.

I extend my gratitude to all members of the staff at Loughborough University who helped during my study. Particular recognition is given to Mr. H. Peters for his assistance as laboratory technician and to the staff of the library services. I am also grateful to Mr. G. Boyden for producing the photographs and to Mrs. S. Hoone for typing the manuscript.

Although they were not involved with the research, I wish to thank my parents, and my friend, Miss C.A. Garratt, for their support throughout the period of this work.

The bibliography of references concerned with in-line mixers, and the raw experimental data obtained during the experiments, may be obtained from :

Dr. P. Rice,
Department of Chemical Engineering,
University of Technology,
Loughborough,
Leicestershire.
LE11 3TU.

Systems of units

The units used in this thesis are usually those of the Sytème International d'Unités (S.I.). Traditional quantities are written between brackets which directly follow the S.I. values. While developing some computer programs it was found to be considerably easier to use the traditional systems of units. For this reason some conversion factors are listed below. Dimensionless ratios have been used whenever possible and particularly when considering the results of experimental work.

1 Btu	=	1.055 kJ
1 Btu ft^{-1} hr^{-1} $^oF^{-1}$	=	1.731 W m^{-1} K^{-1}
	=	4.134×10^{-3} cal cm^{-1} s^{-1} $^oC^{-1}$
1 Btu ft^{-2} hr^{-1} $^oF^{-1}$	=	5.678 W m^{-2} K^{-1}
	=	1.355×10^{-4} cal cm^{-2} s^{-1} $^oC^{-1}$
1 Btu lb^{-1} $^oF^{-1}$	=	4.187 kJ kg^{-1} K^{-1}
	=	1 cal g^{-1} $^oC^{-1}$
1 cP	=	0.0010 kg m^{-1} s^{-1}
	=	6.72×10^{-4} lb ft^{-1} s^{-1}
1 ft	=	0.3048 m
1 gall	=	4.546×10^{-3} m^3
1 hp	=	745.7 W
1 in = 1"	=	25.40 mm
1 lb	=	0.4536 kg
1 psi	=	6.895 kN m^{-2}

1 Literature survey and scope of the present work

1.1 Introduction

Section 1.2 of this chapter presents some of the correlations used by previous workers for the representation of the heat transfer and pressure drop characteristics of empty tubes. Almost all of the correlations presented in this chapter apply in the conventional turbulent flow regime: it was in this range that the results of the present work were obtained. The advantages of certain of the forms of correlation are discussed. The following section of this chapter briefly describes the type of objects which previous workers have placed inside tubes with the aim of increasing the heat transfer rate through the tube wall. Several review articles have been published on this subject and the reader is referred to these for further details. The twisted tape arrangement is described and previous results obtained by using this type of insert are considered in detail since this device, and modifications of it, were used in the present work.

Various static inline mixers have been suggested for the enhancement of heat transfer and some of the more common versions of these devices are described. For instances where such data exists, the pressure drop and heat transfer characteristics of each of these types of tube insert are correlated using a common basis. The characteristics of one particular device, the Kenics static mixer, are studied in detail. This form of tube insert, and some modifications of it, were tested.

The increase in the rate of heat transfer that results from the insertion of objects into a tube is accompanied by an increase in the pressure drop along the tube. The latter leads to an increased pumping power and the associated cost increase. Various methods have been proposed for the estimation of the economic viability, or effectiveness, of the use of tube inserts for increasing the heat transfer rate; the applications of these methods are also discussed.

Section 1.5 clearly outlines the scope of the work discussed in this thesis. It is seen that these objectives are closely related to previous studies which used swirl inducing inserts.

1.2 The characteristics of empty circular ducts

1.2.1 Isothermal friction factor in long straight ducts.

Using hydrodynamically smooth tubes, Blasius (7) found that :

$$\phi = (100\ Re)^{-0.25}/8 \qquad (1.1)$$

$$= 0.0395\ Re^{-0.25}$$

where ϕ = friction factor

$$= \frac{\Delta p\ d}{4\ l\ \rho\ u^2} \qquad (1.2)$$

and Re = Reynolds number

$$= \frac{du\rho}{\mu} \qquad (1.3)$$

Nunner (90) and Round (105) suggest that equation (1.1) applies in the turbulent flow regime upto Reynolds numbers of approximately 10^5. Kays and Perkins (103, p. 7-4) limit the flow range to $5000 < Re < 30000$. Davies (31, p. 31) uses a constant of 0.04 in equation (1.1) and uses a flow range of $3000 < Re < 10^5$ and Coulson and Richardson (29, p. 49) use a constant of 0.0396 over the range $2500 < Re < 10^5$. The variation in the suggested ranges of application, and of the constant, appears to be due to the personal judgement of the authors in view of which constant, range, and degree of accuracy, suits the experimental data available at that time.

The work of Colburn (27) suggests that the following equation may be used :

$$\phi = 0.023\ Re^{-0.2} \qquad (1.4)$$

This correlation is an approximation of equation (1.5), see (27). The suggested range of application is :

$5000 < Re < 2 \times 10^5$ - McAdams (81, p. 155)

$30000 < Re < 10^6$ - Kays and Perkins (103, p. 7-4)

For long smooth pipes Drew, Koo, and McAdams (36) experimentally found that

$$\phi = 0.0007 + 0.0625\ Re^{-0.32} \qquad (1.5)$$

for $3000 < Re < 10^6$

Hermann (90, p. 3) correlates data using the same equation form as that above. He suggests that :

$$\phi = 0.000675 + 0.0495\ Re^{-0.3} \qquad (1.6)$$

in the range $10^5 < Re < 2 \times 10^6$

Von Karman and Prandtl correlated the results of Nikuradse, see (85) and (106, p. 204), in the form :

$$(2\phi)^{-0.5} = 4.0 \log_{10}(Re\ (2\phi)^{0.5}) - 0.40 \qquad (1.7)$$

As shown in reference (37) this equation may be represented to within 1% by

$$2\phi = \left[4 \log_{10}\left[\frac{Re}{4.53 \log_{10}(Re) - 3.82} \right]\right]^{-2} \qquad (1.8)$$

for $10^4 < Re < 2.5 \times 10^8$

and by

$$2\phi = \left[3.6 \log_{10}\left[\frac{Re}{7} \right]\right]^{-2} \qquad (1.9)$$

for $10^4 < Re < 10^7$

Rouse (106, pp. 191 to 204) shows that equation (1.7) is an empirical modification of the result which is obtained using the velocity profile data obtained by Nikuradse. The latter profile shows that :

$$(2\phi)^{-0.5} = 4.06 \log_{10}(Re\ (2\phi)^{0.5}) - 0.6 \qquad (1.10)$$

Colebrook, see (85, p. 676), developed a correlation which applies for Reynolds numbers greater than approximately 3000 :

$$(2\phi)^{-0.5} = -4 \log_{10}\left[\frac{e}{3.7d} + \frac{1.255}{Re(2\phi)^{0.5}} \right] \qquad (1.11)$$

This equation embodies the result of Von Karman that for the fully rough pipe zone :

$$(2\phi)^{-0.5} = -4 \log_{10}\left[\frac{e}{3.7d} \right] \qquad (1.12)$$

The adequacy of equation (1.11) is shown by the more recent results of Robertson et. al. (102).

The often used Moody chart (85) is based on the Colebrook function over the range commonly known as the transition, or partially rough wall, zone. In that zone the tubes do not behave as fully rough pipes. Moody considered that the boundary between the fully rough and transition zones occurred when the difference between the friction factors found by using equations (1.11) and (1.12) was less than $\frac{1}{2}\%$. It is important not to confuse the transition zone with the region denoted by Moody as the critical zone. The latter, which begins at Reynolds numbers of approximately 2000, represents the change from a laminar to a turbulent flow regime.

The Colebrook function is a useful representation of the Moody chart. However, this function is an implicit equation, and it is for these reasons that in recent years some work has been directed towards obtaining explicit equations. The interested reader is referred to Pham (98) and Chen (23). A notable discussion on the merits of developing explicit forms of the Colebrook function, which are often performed using the methods of successive substitution, is given by Schorle, Churchill, Shacham, and Chen (109). The reader is also referred to the work of Round (105) who modifies an equation proposed in the Russian literature and shows that the following equation is a good representation of the data available at that time :

$$(2\emptyset)^{-0.5} = 3.6\left[\log_{10}\left[\frac{Re}{0.135\ (Re)\ \frac{e}{d} + 6.5}\right]\right] \qquad (1.13)$$

It will be seen later that the results of the present work have been compared to the predictions of some of the above equations.

The above review clearly demonstrates the wide range of equation forms used to represent friction factor data for empty tubes. On first sight, it may be considered that correlations of the form of equation (1.11), for instance, could be used for the presentation of results obtained using tubes containing inserts. In such cases the constants could be modified and the relative roughness, e/d, replaced by a function which is characteristic of the insert geometry. However, many of the above equations have been developed using a very large number of experimental observations: this is a necessary requirement of any equation involving a large number of constants. The present work involved pressure loss and heat transfer measurements and it was considered that, over the available time period, insufficient pressure

loss data would be collected to allow accurate determination of a large number of constants. For this reason, and because of the computational simplicity, the results of the present tests, using empty and packed tubes, were correlated using the same form as equations (1.1) and (1.4).

1.2.2 The effect of tube length on the friction factor.

The entry length, x_{ent}, is the distance from the pipe inlet within which the turbulent velocity profile develops and thereafter remains constant. Davies (31, p. 47) uses a theoretical analysis which provides the following estimate of the smallest possible entry length in a smooth tube :

$$\frac{x_{ent}}{d} = C_1 Re^{0.25} \qquad (1.14)$$

where $C_1 = 1.41$ (1.15)

Over the flow range of the present work, equation (1.14) predicts that $x_{ent}/d = 14.4$ (Re = 11000) and $x_{ent}/d = 25.3$ (Re = 104000).

According to reference (90), the results of Nikuradse show that :

$$\frac{x_{ent}}{d} = 50 \qquad (1.16)$$

Latzko (103, p. 7-6) predicts that the pipe length required for the friction factor to attain a constant value is given by :

$$\frac{x}{d} = 0.623 Re^{0.25} \qquad (1.17)$$

which shows that $x/d = 6.3$ (Re = 11000) and 11.2 (Re = 104000).

Using water over the Reynolds number range of 16000 to 70000, Olsen and Sparrow (91) found that after the first 25 pipe diameters the pressure gradient is within 5% of the fully developed value.

Later it will be seen that the experimental equipment, of the present work, was constructed such that the distance between the upstream pressure tapping and the nearest object which projects through the tube wall upstream of that tapping was 53.3 tube diameters.

1.2.3 The effect of fluid property variation across the flow field.

The results of sections 1.2.1 and 1.2.2 apply for fluids flowing along tubes with no heat being transferred through the tube wall.

For situations where the fluid is a liquid and heat is being transferred, the velocity profile across the tube is deformed mainly due to the viscosity variation. To allow for this effect the following equation may be used :

$$\frac{\phi_h}{\phi_{iso}} = \left[\frac{\mu_s}{\mu}\right]^m \qquad (1.18)$$

where ϕ_h, ϕ_{iso} = friction factors determined under heat transfer and isothermal conditions at the same bulk Reynolds number

and μ_s, μ = liquid viscosities evaluated at the surface temperature of the tube wall and at the bulk fluid temperature.

Kays and Perkins (103, p. 7-158) show that predicted values of m, for heating conditions, decrease with increasing Prandtl number. Typical results show that m = 0.063 (Pr = 3) and m = 0.028 (Pr = 10). However, they also note that some experimental evidence shows that m = 0.25 for water with a Prandtl number of 8. On the basis of these findings it is expected that for Pr = 4.94, the value used in the present work, the value of m will exceed 0.25. This conclusion is supported by Lopina and Bergles (79) who suggest that m = 0.35 for water. However, McAdams (81, p. 157) suggests that m = 0.14 which shows that the data reported in the literature is somewhat inconclusive. This is probably because equation (1.18) is a simplification and later in this thesis (section 5.4.4) it is shown that m probably depends on the Reynolds and Prandtl numbers.

1.2.4 The heat transfer characteristics of long smooth circular ducts.

The so-called Dittus-Boelter equation is presented by McAdams (81, p. 219) in the form :

$$Nu = \frac{hd}{k} = 0.023 \left[\frac{d\,u\,\rho}{\mu}\right]^{0.8} \left[\frac{c_p\,\mu}{k}\right]^{0.4} = 0.023\, Re^{0.8}\, Pr^{0.4} \qquad (1.19)$$

The restrictions on the use of this equation are :

(i) $0.7 < Pr < 120$

(ii) $10^4 < Re < 1.2 \times 10^5$

(iii) $l/d > 60$

(iv) moderate $(t_s - t_b)$

It is interesting to note that conversion of the equation determined by Dittus and Boelter (34, p. 450) into dimensionless form, and noting that the Reynolds number exponent had been misprinted as 0.08 as opposed to 0.8, it is found that :

$$Nu = 0.024\ Re^{0.8}\ Pr^{0.4} \text{ for a fluid being heated} \qquad (1.20)$$

and $$Nu = 0.026\ Re^{0.8}\ Pr^{0.3} \text{ for cooling} \qquad (1.21)$$

It is considered here that McAdams found that equation (1.19) was a better representation of all of the data available at that time than were equations (1.20) and (1.21). Equation (1.19) correlates the data within an average deviation of $\pm$ 20% (81, p. 202).

Incorporating the physical properties of water in equation (1.19), McAdams (81, p. 228) shows that :

$$h = 5700\ (1 + 0.015\ t_{av})\ \frac{u^{0.8}}{d^{0.2}} \quad W\ m^{-2}\ K^{-1} \qquad (1.22)$$

where t_{av} = mean bulk temperature of the fluid, ^oC

u = fluid velocity, $m\ s^{-1}$

and d = tube diameter, mm

Nunner (90, p. 6) states that the result of Kraussold, for $Re > 5000$, may be represented in the form

$$Nu = 0.024\ Re^{0.8}\ Pr^{\frac{1}{3}} \qquad (1.23)$$

The commonly used Sieder - Tate equation may be written as :

$$Nu = (\text{Constant})\ Re^{0.8} Pr^{\frac{1}{3}} \left[\frac{\mu}{\mu_s}\right]^{0.14} \qquad (1.24)$$

The original work of Sieder and Tate (114), which shows the results of tests using oils, paraffin, benzene, and water, indicates that the constant in equation (1.24) is 0.027. However, McAdams (81, p. 219) states that results obtained using air show that the constant may be 0.023 or 0.021. Perry and Chilton (97, p. 10-14) use a constant of 0.023 and propose the following limitations for the use of equation (1.24):

(i) $Re > 10^4$

(ii) $0.7 < Pr < 700$

(iii) $l/d > 60$

In discussing the above equations, the results in the original source of the equation and in a number of commonly used textbooks have been cited. The original material was often based on a limited number of experimental measurements and the complete limitations of the equations were often unknown at that time. However, the comments made in some of the textbooks are often based on the experience of using the equations and in noting their limitations. Nonetheless, this should not be accepted as a rigid guideline. For example, Kern (62, p. 104) suggests that equation (1.24), with a constant of 0.027, should not be used when water is the process fluid : the results of Evans (43, Figure 13), obtained using water, are in good agreement with equation (1.24) with a constant of 0.027.

Equation (1.24) involves a similar term to that incorporated in the friction factor equations for the allowance of the physical property variation with temperature. This viscosity ratio allows the equation to be applied to situations where the fluid properties are significantly temperature dependent and it can be used for either heating or cooling conditions.

Using a total of 651 individual data points which had been selected from a number of sources, reference (38) produced an equation which represents the data with a root mean square absolute percentage deviation (R.A.D.) of 10.2%. The proposed correlation may be rewritten in the form :

$$Nu = 0.0225\ Re^{0.795}\ Pr^{G} \qquad (1.25)$$

where $G = 0.495 - 0.0225\ \ln[Pr]$

Using the same data, reference (38) also shows that the R.A.D. was 13% when using equation (1.19). Adjustment of the constants and exponents in equation (1.19) by a least squares procedure, showed that (38) :

$$Nu = 0.0204\ Re^{0.805}\ Pr^{0.415} \qquad (1.26)$$

for which R.A.D. = 11.5%

The data used by reference (38) lay within the following ranges :

(i) $l/d > 40$

(ii) $T_s/T_b < 1.15$, gases

(iii) $t_s - t_b$ is small, liquids

All of the above empirical correlations indicate that the Reynolds number exponent is 0.8. This is an important finding which is of considerable importance in the calculation procedure adopted in the present work.

1.2.5 The effect of the conditions at the entrance to the heated length of the tube on the heat transfer factor, $Nu/Pr^{0.4}$.

Knudsen and Katz (68, p. 400 et. seq.) review the available data concerning entrance effects on the heat transfer coefficients. One of the most common methods of representing this data, see for example (68, p. 403), (97, p. 10-15), (59, p. 196), uses

$$\frac{h}{h_\infty} = 1 + X\left[\frac{d}{l}\right] \qquad (1.27)$$

Where h is the mean heat transfer coefficient over the heated length, l, and h_∞ is the assymptotic value of the heat transfer coefficient. The parameter X, evaluated from integrations of curves showing h_x / h versus x/d, are tabulated by Boelter et. al. (10), and are reproduced in the references cited above. Using air with a straight calming section ($l/d = 11.2$) preceding the heated tube length which had the same bore, Boelter et. al. found that $X = 1.4$, for $27200 < Re < 53000$. In the present work the length of the heated tube was 53.3 tube diameters. Using this length with $X = 1.4$ in equation (1.27), the constant in the Dittus-Boelter equation (1.19) may be adjusted; the resulting constant is 0.024. Reporting on the results of other workers, reference (39) states that data obtained using water exhibits a lack of quantitative agreement, although similar trends to those found by Boelter et. al. are noted as l/d is increased.

1.3 The type and characteristics of tube inserts used by previous workers

Various methods have been suggested for the enhancement of heat transfer. Some methods, for instance tube vibration, require a power source which is not a component of the flow circuit. These types of augmentation techniques are not the concern of the present work, they are discussed by Bergles (2). However, it was considered that the reader should be given a description of the heat transfer enhancement that is made possible by the use of techniques which require no external power source. Consideration is limited to single phase heat transfer generally in the range $10^4 < Re < 10^5$. The actual flow range is stated if the latter restriction is not imposed. The discussion is divided into sections concerning roughened tube walls, extended surfaces, displaced promoters, inserts which extend across the tube diameter but do not induce swirl flow, swirl flow inducers, twisted tapes, static mixers, and the Kenics static mixer. Although the twisted tape and Kenics mixer are swirl inducers they are considered in separate sections because of their particular importance in the present work. Also the use of any stationary object, located inside a tube, may be considered to be a static mixer, however the section of that name describes devices which have actually been used for the purpose of mixing.

Bergles (2) provides a survey of the heat transfer enhancement that is obtained using some of the techniques listed above. His work is an extension of reference (5). Ouellette and Bejan (92) also provide a useful survey. Bergles (2) compares the various techniques using the constant pumping power basis. This method, which is described more fully in section 1.4, is a measure of the heat transfer improvement relative to the same length of empty tube requiring the same pumping power. The results obtained with this method are expressed in the form $(h/h_o)_p$ where h and h_o are the heat transfer coefficients in the tubes with and without the enhancement technique.

1.3.1 Internally roughened tube surface.

The results of Nunner's tests (90) using naturally roughened pipes show that $(h/h_o)_p$ lies in the range 1.1 to 0.9 (2). The results used by Bergles (2) show that tubes with machined roughnesses are not beneficial and $(h/h_o)_p < 1$. However, the more recent data surveyed by Norris (6, p. 16 et. seq.) do not support that conclusion. His survey, which embodies a far greater number of experimental studies, shows that the heat transfer coefficient may be increased by a factor of 2 for pumping power increases of a factor of 3 when using widely spaced ribs ($s/e = 10$). The results in Bergles (2) apply to closely spaced ribs ($s/e < 2.24$).

Dipprey and Sabersky (33) produced tubes with a sand grain roughness. Their tests were performed in the range $1.2 < Pr < 5.94$. Bergles (2) used their results to show that $(h/h_o)_p$ increases with increasing Prandtl number. The most beneficial tubes had the largest roughness of the tests and showed that $(h/h_o)_p$ may be as large as 1.95. Extrapolating the results of Dipprey and Sabersky to a Prandtl number of 0.7, Norris (6) found that tubes possessing a sand grain roughness have little advantage over tubes with a machined roughness.

Piston rings may be inserted into a tube to provide the same roughness form on the tube wall as may be produced by machine roughening. Bergles (2) refers to this form of insert as "small ring-type". Adapting the results of Nunner (90), who used various shapes and axial spacings of piston rings, reference (2) shows that $(h/h_o)_p$ may attain maximum values of 1.6 ($s/e = 10$) with a mean value of approximately 1.3 for all of the tests. Koch (69) used thin metal discs with apertures of various diameters. The diameter of the discs was approximately the same as that of the tube bore. The results determined by Koch show that $(h/h_o)_p$ may be as high as 1.4 but the mean value for all of the tests over the entire flow range is 1.0 (2).

The results used by reference (2) to indicate the effect of using wire coils inside tubes shows considerable data scatter. The present author considers that this is a result of comparing results obtained using a large range of geometrical parameters. Bergles (2) uses results which were determined using coils which were loosely wound and coils which were tightly wound, the latter results show that $(h/h_o)_p$ decreases extremely rapidly with increasing Reynolds number.

This trend is not apparent for other types of insert and it implies that the friction factor and heat transfer factor, $Nu/Pr^{0.4}$, do not follow similar trends as the empty tube with respect to Reynolds number changes. Probably the best data used by Bergles (2) in discussing the effect of wire coil inserts is that of the Trane Co. (130). Their results show that $(h/h_o)_p$ is approximately 1.35 (heating) and 1.3 (cooling) when the process fluid is water. These values are only slightly lower than those found using the results of Nunner's work (90) with piston rings. In the latter case, a good contact between the rings and the tube wall was obtained, but using wire coils only a small fraction of the circumference of the wire is in contact with the tube. For these reasons the piston rings may increase the effective heat transfer surface area while wire coils will not produce such a large increase.

1.3.2 Extended Surfaces.

Hilding and Coogan (56) used a number of tubes which possessed various numbers of fins and fin heights. Their results show that the most beneficial tubes contained a large number of fins with large fin heights. Using fins which extended across the entire tube diameter, or by placing a smooth tube within a finned tube, it was found that $(h/h_o)_p$ may be as large as 2 (2).

The tests of Hilding and Coogan (56) were performed by heating air in the tubes, the later work of Bergles et. al. (4) was performed by heating water. The results of reference (4) show that $1.2 < (h/h_o)_p < 2.7$, where the greater improvements were obtained using short spiral fins. Watkinson et. al. (135) also used the heating mode of operation with water. They define low fin heights as those for which the ratio of the fin height to the tube diameter is less than 0.05. Using straight fins it was found that the mean value of $(h/h_o)_p$, over the flow range, was within the range 1.0 to 1.4 for each of the tubes; the higher values being produced in tubes containing a low number of fins. The tests using spiral fins showed that the mean values of $(h/h_o)_p$ were in the range of 1.1 to 1.6 (low fins) and 1.0 to 1.4 (high fins). It was also found that $(h/h_o)_p$ decreased with increasing Reynolds number, increasing angle of rotation of the fins, and increasing number fins for a given angle of rotation.

Watkinson et. al. (134) performed heating tests using air in

finned tubes. They experienced considerable difficulty in obtaining useful results due to the effects of flow transition from the laminar to the turbulent regime, and due to heat conduction at the ends of the tubes. The main conclusions were that $(h/h_o)_p$, for spiral fins, may be increased by reducing the helix angle of the fins or by increasing the peripheral spacing between the fins. For straight fins, the latter parameter had only a slight effect on $(h/h_o)_p$. Russell and Carnavos (107) performed tests using a tube with the same fin configuration but a slightly larger diameter than one of the tubes used by Watkinson et. al. (134). The Nusselt numbers and friction factors determined by Russell and Carnavos were greater than those found by reference (134). Russell and Carnavos could not explain this finding although it may be due to the different mode of operation; reference (107) operated in the cooling mode. The results of reference (107) are also interesting because each of their tubes contained 10 straight fins and only the tube diameter and fin tip thickness was varied. As a reasonable approximation it can be stated that the results for all of the tubes show that $(h/h_o)_p$ is approximately 1.3. Two anomalies exist in their results; one of the tubes, which used a slightly smaller fin tip thickness than the others, produced very large values of $(h/h_o)_p$ and also the friction factors determined under cooling conditions were lower than those found under isothermal conditions. The latter effect, which was found using all of the tubes, including the empty smooth tubes, is unexpected.

A quintuplex finned tube consists of five internally finned tubes fitted tightly in a concentric form. Other configurations may be produced, for example, a triplex finned tube is formed using three finned tubes. Soliman and Feingold (119) performed tests using a smooth tube, a single spiral finned tube, and a quintuplex spiral finned tube. They concluded that, because of the large pumping power requirements, quintuplex tubes should generally only be used for instances where the main priority is heat exchanger size reduction. The tests involved the cooling of lubricating oil in the laminar and transition (laminar to turbulent) flow regimes. However, Carnavos (18) performed air cooling tests in the turbulent flow regime with a variety of compounded finned tubes. Carnavos calculated the ratios $(h/h_o)_p$ and found that the values produced by a quintuplex spiral finned tube are approximately 5. It is also shown that using a triplex tube, formed using two spiral finned tubes and a central

smooth tube, the ratio $(h/h_o)_p$ is 3.9. Further tests using three forms of duplex tubes produced values of $(h/h_o)_p$ in the range 1.7 to 2.4. The merits of this type of tubing are considered further in section 1.4.

Carnavos (17), (19) studied the effects of using single finned tubes with water and water/ethylene glycol mixtures under heating conditions and using air under cooling conditions. The heating tests show that $1.24 < (h/h_o)_p < 1.72$, with the higher values being obtained with the tubes possessing the highest helix angles of the spiral fins and with the highest internal surface areas. The cooling tests produced similar conclusions over the range $1.15 < (h/h_o)_p < 1.6$. The results of these two studies have been used in a parametric analysis of finned tubes, see Webb and Scott (136).

Kreith and Margolis (74) and Gambill et. al. (49) mention that helical tubes may be formed by flattening tubes to produce an oval cross section and then, after packing the tube with sand, it is possible to twist the tube about its axis. The heat transfer and pressure drop characteristics of this type of tube have recently been studied by Ievlev et. al. (57). Some tubes, which are now commercially available, have a similarity to those produced by the above method. It is now possible to produce a number of tubes with different numbers of flutes (corrugations) and with various pitches of the flutes (131), (132). The data of one of the manufacturers of such tubes (131) suggests that, in the turbulent flow regime, the increased rate of heat transfer produced by using the tubes is a result of the increased heat transfer surface area and not the result of any changes in the film heat transfer coefficients. Although the data in reference (131) is unclear it appears that (hA_T) may be increased above the empty tube value by a factor of up to 2.5 in the turbulent flow regime; comparative pressure loss results are not given. Further discussion of these forms of tubing is not given because the present author considers that they are probably only useful for processes where the heat transfer resistances on the inside and outside tube surfaces are large. Tube inserts are used where the dominant resistance to heat transfer would exist in the tube side fluid if empty tubes were to be used.

1.3.3 Displaced promoters.

One of the factors producing the heat transfer enhancement which results from the use of fins is the increased surface area available for heat transfer. The surface area of tube inserts, which are in contact with the tube wall, does not always increase the effective surface area available for heat transfer. The effective area depends on the thermal contact of the tube wall and the insert. If the contact is very poor then the insert may actually reduce the heat transfer surface area compared to the empty tube. Displaced promoters are objects which do not have any contact with the tube wall, their ability to increase the rate of heat transfer is a result of flow disturbances.

It was previously noted that Koch (69) used rings, with a central orifice, such that the circumference of the rings were in contact with the tube wall (maximum clearance 0.3 mm). Koch also performed tests using two tubes which contained undersized rings. Bergles (2) shows that over the range $10^4 < Re < 10^5$, the mean values of $(h/h_o)_p$ for the two arrangements were 0.95 and 1.2. The orifice diameter and ring spacing were different in each of the tests and it is therefore difficult to suggest any trends concerning the most beneficial geometry. It is noted that $(h/h_o)_p$ decreases with increasing Reynolds number.

Discs may be axially located on a rod which may then be centrally positioned inside a tube. Koch (69) and Evans (43) performed heat transfer and pressure drop tests using this type of insert. Koch (69) uses the term "baffle plates" in reference to these inserts. Bergles (2) uses the results of references (69) and (43) to show that $(h/h_o)_p$ is generally less than 1 for Reynolds numbers greater than approximately 40000. Both sets of results show similar magnitudes for $(h/h_o)_p$ and also that this ratio decreases with increasing Reynolds number. However, it should be stated that the friction factors and Nusselt numbers determined by Koch are greater than those determined by Evans who suggests reasons for the differences.

Evans (43) also replaced the discs by streamline shapes. Bergles (2) used the results of that study to show that they produce mean values of $(h/h_o)_p$, for $10^4 < Re < 10^5$, in the range 0.95 to 0.75.

1.3.4 Inserts which extend across the tube diameter but do not induce a swirling flow.

Some of the fins described in section 1.3.2 could have been considered in this section. In general however, the inserts considered here do not necessarily produce significant increases in the effective area available for heat transfer.

Nauman (88) suggests that the fluid mixing process associated with the use of static inserts inside a tube may be considered as the result of two components - flow division and flow inversion. It is shown that the fluid near to the tube wall at the entrance of a flow divider is also near to the tube wall at the exit of the insert. Flow inverters produce a flow transformation which results in fluid near to the tube wall being transferred to the centre of the tube. On this simple basis, it is clear that flow inverters are expected to produce larger Nusselt numbers than flow dividers. Nauman suggests one geometrical arrangement that produces flow inversion. Over part of its length the proposed device extends across the tube; it is for this reason that it is mentioned here. The interested reader is referred to reference (88) for further details. However, it is important to realise that reference (88) uses an analysis that is based on the existence of laminar flow regimes. In turbulent flows, where fluid is continually removed from the boundary layers by turbulent eddies, the analysis of Nauman using hypothetical inversion and division processes will be difficult, if not impossible, to use with certainty.

The Corpak turbulence promoter (129) consists of continuous lengths of loosely wound wire spirals which produce a high free voidage. When located inside tubes the device may be used to increase the rate of heat transfer and/or degree of fluid mixing compared to an empty pipe of the same diameter. Unfortunately, comparable heat transfer and pressure drop data in reference (129) apply to the conventional empty tube laminar flow range and therefore are not of particular interest in the present work.

Megerlin et. al. (82) studied the effects of mesh inserts and brush inserts. The mesh inserts were produced from pads of stainless steel fibres which were copper plated. The brush inserts were formed using commercially available spiral brushes manufactured from stainless steel. Although the brushes induced a significant spiral component in

the flow, this type of insert is considered here, rather than in section 1.3.5, because of the similarity with mesh inserts. The free voidage of Corpak turbulators, see above, is unknown, however it appears that it is greater than those of the inserts used by Megerlin et. al.. The mesh, brush, and Corpak, inserts increase the rate of heat transfer by increasing the effective surface area and by disrupting the boundary layer fluid; the brush inserts also create a swirling flow, as noted above.

The results of reference (82) show that the heat transfer coefficient may be very sensitive to any local variations in the mesh porosity. For two of the three tubes with mesh inserts, it was found that $(h/h_o)_p$ is approximately 1.25, for $10^4 < Re < 3 \times 10^4$. The film heat transfer coefficients were approximately 9 times those that would exist in an empty tube at the same Reynolds numbers. For the other tube containing a mesh insert, it was found that $(h/h_o)_p$ was approximately 0.65; this lower value was considered to be a result of measuring the exit fluid temperature near to a region of high mesh porosity. The results obtained with brush inserts show that $(h/h_o)_p$, again for $10^4 < Re < 3 \times 10^4$, is approximately 0.7, and the increase in the heat transfer coefficient, compared to an empty tube at the same Reynolds number, is a factor of 5 (82).

Sparrow et. al. (121) studied the thermal and hydraulic characteristics of tubes containing an asymmetrical slat blockage, see Figure 1.1. The thickness of the blockage relative to the tube length was small ($l'/t' = 392$). They also report on similar tests that used asymmetrical segmental blockages. In both studies the local heat transfer coefficients and static pressures were determined downstream of the blockage. Water (Pr = 4) was used for the heat transfer tests and air was used in the pressure drop determinations. It was found that very large Nusselt numbers were obtained at small values of x/d, where x is the distance from the downstream face of the blockage. The Nusselt numbers in this region, when expressed as a ratio to the fully developed value, were approximately 4.8 (flow area blockage of $\frac{3}{4}$), 3.3 ($\frac{1}{2}$ blockage) and 2.3 ($\frac{1}{4}$ blockage). These ratios are mean values over the Reynolds number range of 11000 to 60000. The values given were determined using slat blockages and unless otherwise stated the remainder of the following discussion will be restricted to this geometrical form. At the lower Reynolds numbers, the Nusselt number ratios were greatest and for the $\frac{3}{4}$ blockage it was found that maximum

values of the ratios occurred approximately $2\frac{1}{2}$ pipe diameters downstream of the blockage; thereafter the ratios decreased to unity. Using segmental blockages maxima in the curves of Nu/Nu_0 versus x/d were found using blockages of $\frac{1}{4}$, $\frac{1}{2}$ and $\frac{3}{4}$. Sparrow et. al. suggest that the maxima are caused by the reattachment of the separated flow and by the impact, on the tube wall, of the fluid that is displaced by the blockage. They conclude that both of these effects occur further downstream of a segmental blockage compared to a slat blockage. For the slat blockages, the thermal development (to within five per cent) is completed approximately 10, 15, and 18 diameters downstream of the blockage for respective area ratios of $\frac{1}{4}$, $\frac{1}{2}$ and $\frac{3}{4}$.

Sparrow et. al. define the angle θ as shown in Figure 1.1. They produce graphs which show the local circumferential Nusselt number, expressed as a ratio to the fully developed value, versus the non-dimensional axial location, x/d, for various values of θ. They deduce that the flow reattachments and impacts, discussed above, occur at $x/d<1$ for all values of θ, when using a $\frac{1}{4}$ slat blockage. For the case of a $\frac{1}{2}$ blockage, there is a peak in the Nusselt number ratio for $\theta = 90^{\circ}$ at high Reynolds numbers. However, for the same Reynolds numbers and $\theta = 0^{\circ}$, the maximum appears to occur at $x/d<1$ and this is because the maximum is a result of the impact effect. At lower Reynolds numbers, it was found that there was no maximum for $\theta = 90^{\circ}$, but a maximum existed for $\theta = 0^{\circ}$. It was considered that this is a result of the shorter reattachment region and smaller impact effect than was observed at higher Reynolds numbers. The results for a $\frac{3}{4}$ blockage agree with the above deductions. It was also found that the circumferential variations of the Nusselt number did not exist for $x/d > 5$. For segmental blockages the circumferential variations persisted at considerably greater distances downstream.

The form in which Sparrow et. al. present their pressure analyses does not allow the local friction factors downstream of the blockages to be determined. However, Koch (69) used an instrument which allowed the measurement of the local wall shear stress in the regions downstream of objects located within a tube. From the results thereby obtained, Koch suggests that the local wall shear stress, τ_w, is a dominant factor affecting the local heat transfer coefficient. This is not surprising since the major part of the resistance to heat transfer lies in the boundary layer, near to the tube wall, and it is the wall shear stress that determines the thickness of the boundary

layer. On the basis of this proposition, beneficial tube inserts must increase the wall shear stress. However, a large number of the forms of tube inserts, for example displaced promoters, indirectly cause the boundary layer disruption by producing substantial mixing of the core fluid. The kinetic energy losses associated with this mixing lead to the need for large pumping powers and it is now clear that only a fraction of that power is used to increase the wall shear stress and hence the heat transfer coefficient. Koch (69) deduces that as the degree of mixing in the core fluid increases so the relative proportion of the total resistance to heat transfer that lies in the boundary layer is also increased and this effect is similar to that produced by increasing the Prandtl number of the fluid.

The suggestion that the heat transfer coefficient is dependent on the wall shear stress indicates that some form of analogy exists between heat and momentum transfer. Such analogies have been developed for the empty tube; these are discussed by Knudsen and Katz (68, Chapter 15). However, as noted by Koch (69), the same equations cannot be applied to tubes which contain discontinuous inserts because the intermittent boundary layer disruption, caused by the inserts, violates the assumptions on which the equations are based.

1.3.5 Swirl flow inducers (excluding the twisted tape).

Blum and Oliver (9) measured the local heat transfer coefficients, for carbon dioxide and air, downstream of an inlet vortex generator. The device used was basically a tangential slot through the tube wall. Near to the generator the heat transfer coefficients for air were larger than those obtained using carbon dioxide. However, the decrease of the coefficients with respect to the axial distance from the generator was more rapid for the air. This was due to the higher viscosity of air compared to carbon dioxide. No generalisations were made concerning the tube length for which the vortex effect completely decayed.

Koch (69) produced propeller-shaped promoters using brass plates (1 mm thick). The vanes of the propellers were formed by making 6 radial slits through the plates and twisting the resulting vanes through approximately 45° relative to the axis of the plate. The propellers were located at various equidistant positions on a brass rod which was inserted into a tube. Bergles (2) uses the results of (69) to show that $(h/h_o)_p$ is approximately 1.1 over the range

$10^4 < Re < 10^5$, and decreases with increasing Reynolds number. However, on the basis of these results, it is difficult to suggest the best possible spacing of the inserts.

1.3.6 Twisted tape inserts.

A sketch of a twisted tape is shown as Figure 1.2. This form of tube insert is usually produced by twisting thin strips of metal. Margolis (80), (73) and Koch (69) discuss some of the pertinent tests performed prior to 1958. Since then a large number of experimental studies and literature surveys have been concerned with twisted tapes. In the following survey, continuous twisted tapes, i.e. those which extend along the total heated tube length, are considered prior to a discussion of the use of short twisted tapes and the flow in the region downstream of the tapes. The work is presented in a chronological sequence and emphasis is placed on those studies which have received the largest number of favourable citations in the published literature.

(a) Continuous twisted tapes extending along the entire heated tube length.

The work described in reference (49) is outlined by Gambill et. al. (50). The test sections used in that work were electrically heated although heat generation in the twisted tapes was negligible. In a later study, Gambill (46) performed boiling and burnout tests using electrically heated twisted tapes. The present author has not located any reference to the use of this type of system in single phase tests. Gambill et. al. (50) found that their results, determined under heating and isothermal conditions, could be correlated with an average absolute percentage deviation (A.A.D.) of 12.3% by

$$\phi = \frac{0.000111}{(yd^2)^{0.6}}\left[\frac{\mu_s}{\mu}\right]^{0.18} \qquad (1.28)$$

where ϕ = friction factor defined by equation (1.2) with the fluid velocity based on the inside diameter, d, of the tube

and y = twist ratio of the tape, which is defined as the number of tube diameters per 180^o degrees of insert rotation.

Gambill et. al. specifically state that equation (1.28) should not be extrapolated beyond the values of y and d used in their tests. These geometrical constraints are given in Table 1.1. The results were also correlated with an A.A.D. of 20.1% by using an empty tube correlation, and equation (1.2), with the length, velocity and diameter replaced by the characteristic values l_{si}, u_{ri}, and D_e. The definitions of these quantities are given in Appendix A.1. Also it should be noted that in this method the Reynolds number to be used in equation (1.11) is also based on D_e and u_{ri}.

Gambill et. al. (49, 50) correlate their heat transfer results, with an A.A.D. of 10.1%, by

$$\frac{Nu}{Nu_o} = \frac{2.18}{y^{0.09}} \qquad (1.29)$$

or by

$$\frac{Nu}{Nu_o} = \frac{2.43\ (\beta_f\ \Delta t_f)^{0.042}}{y^{0.084}} \qquad (1.30)$$

where Nu = Nusselt number obtained using the twisted tape. This value is based on the tube inside diameter and the total circumference of the tube

Nu_o = Nusselt number obtained in an empty pipe at the same nominal Reynolds number as that used to produce Nu

β_f = volumetric coefficient of thermal expansion evaluated at the film temperature

Δt_f = temperature drop across the film of fluid at the tube wall = $(t_s - t_b)$

Nu and Nu_o were determined under heating conditions and, unless otherwise stated, all of the heat transfer correlations presented in this thesis apply to that mode of operation. The Nusselt number, Nu_o, was determined using

$$Nu_o = 0.023\ Re^{0.8}\ Pr^{\frac{1}{3}}\ (1 + (d/l)^{0.7}) \qquad (1.31)$$

Gambill and Bundy (47) present a survey of the swirl flow tests that were performed prior to 1962. They suggest that the pressure loss determinations of references (49) and (50), as given above, may be low due to a small system leakage and incorrect locations of the pressure tappings. Unfortunately, the distance between the downstream edge of

the tapes and the pressure tappings is not specified. Gambill and Bundy (47) correlate all of the available friction factor data in the form :

$$\phi_e - \phi_{oe} = \frac{0.02625}{y^{1.31}} \left[\frac{Re_e}{2000} \right]^{-n} \quad (1.32)$$

where $n = 0.81 \exp(-1700\ (e/D_e))$ (1.33)

$\phi_{oe} = 0.023\ Re_e^{-0.2}$

ϕ_e = friction factor defined by equation (1.2) with the diameter and velocity evaluated using equations (A.1.2) and (A.1.3)

and Re_e = Reynolds number based on the equivalent diameter and velocity as given by equations (A.1.2) and (A.1.3).

Gambill and Bundy suggest that the ratio of the Nusselt number for swirl flow compared to that in an empty tube is smaller for air than for water because of the compressibility of air. This effect leads to denser air lying at the tube wall though it is more beneficial, due to centrifugal forces, for the denser fluid to exist in the central core of the fluid. It is also this effect that produces the greater Nusselt number ratios determined under heating conditions as opposed to the cooling mode of operation. Gambill and Bundy considered that insufficient details were available to enable the correlation of all of the heat transfer results into a single equation. However, they refer to equation (1.30) and a correlation which was later published in reference (48) and is discussed later.

Gambill and Bundy (48) state that isothermal friction factors, determined by tests using ethylene glycol, were represented to within 16.5% by equations (1.32) and (1.33). They suggest that equation (1.18), when used with equations (1.32) and (1.33), accounts for the mode of operation when using :

$$m = 0.043 \text{ for cooling, } y = 4.8 \quad (1.34)$$

$$m = 0.140 - \frac{0.3465}{y^2} \text{ for heating, } 2.26 < y < \infty \quad (1.35)$$

Gambill and Bundy (48) correlate the results of reference (49) and their own results to show that, under heating conditions :

$$Nu = 0.00675\ Re^{0.89}\ Pr^{0.6} \left[\frac{(\rho\ \beta\ \Delta t)_f\ u^2}{y^2\ d} \right]^{0.0344} \qquad (1.36)$$

where Nu and Re are based on the inside diameter of the tube, the circumference of the tube wall, and the fluid velocity is also based on the tube i.d.. The following units are to be employed in equation (1.36): ρ, lb ft^{-3}, u, ft s^{-1}; d, ft. The maximum tube diameter used in the tests, for which equation (1.36) is representative, was 6.3 mm. Since this equation is dimensional it may be that its range of application is limited; no further citations of this equation have been located. Gambill and Bundy (48) note that the Prandtl number exponent of 0.6, compared to the value of 0.4 for empty tubes, implies that the improvement in the Nusselt number caused by tape insertion is greatest for fluids with a large Prandtl number. However, Koch (69, p. 103) suggests that the improvement is expected to fall as the Prandtl number is increased. As noted previously, Koch considered that for large Prandtl numbers the proportion of the fluid's resistance to heat transfer that lies in the core fluid is relatively small and hence any changes in the fluid core have only a small effect on the Nusselt number. This conflict of views is again discussed after reviewing some of the later studies of twisted tapes.

The parameter and flow ranges of the tests performed by Seymour (110) are outlined in Table 1.1. The pressure losses measured in that work are considerably less than those reported in a further article, Seymour (111). In the latter, Seymour suggests that the reason for the discrepency is possibly the use of an insufficient tape length in the earlier work. However, the results presented in reference (111) do not support that suggestion. In reference (110) the heat transfer results of that work are correlated to within 5% by

$$Nu = \frac{Re^{0.75}\ (\Delta t_f\ \beta)^{0.125}}{11.89\quad y^{0.25}} \qquad (1.37)$$

where Re is evaluated as for equation (1.36). Although not stated, β is presumably evaluated at the film temperature. The heat transfer correlation for the empty tube results is not given.

Smithberg and Landis (118) analytically found that

$$\phi_e = \frac{0.058\ (2\phi_e)^{0.5}}{y^2} + \frac{0.01245}{Re_e\ y}\left[\frac{A_f}{A_c}\right]\left[1125\ \ln(Re_e\ (2\phi_e)^{0.5}) - 3170\right] + 0.023\ Re_e^{-0.2} \qquad (1.38)$$

where the subscript "e" indicates the use of the equivalent diameter and velocity basis. It should again be recalled that ϕ_e is given by equation (1.2) with D_e and the actual fluid velocity which allows for the tape thickness. A_f and A_c are the cross sectional free flow areas of an empty tube and a tube of the same diameter with a tape. Smithberg and Landis also present a simpler equation which agrees to within 11% with equation (1.38). Experimental tests were performed over the ranges indicated in Table 1.1. The results and those of Koch generally agreed with equation (1.38) to within ± 10%.

An analytical study by Smithberg and Landis (118) showed that

$$Nu = \frac{h\ d}{k} = \left[\frac{(1 + (2\eta/\pi))\ Re_e\ Pr}{1 + \frac{175}{Re_e\ \phi_e\ y}\ \frac{D_e}{d}\ Pr^{0.731}}\right]\left[(A) + (B)\right] \qquad (1.39)$$

where

$$(A) = \frac{18.0}{Re_e\ \phi_e^{0.5}\ y}$$

and

$$(B) = \frac{0.023}{Re_e^{0.2}\ Pr^{\frac{1}{3}}}\left[\frac{d}{D_e}\right]\left[1 + \frac{0.00274}{y^2\ \phi_e}\right]^{0.5}$$

In the above equation it is important to realise that Nu is defined using the inside diameter of the tube but ϕ_e and Re_e are defined using the equivalent diameter basis as in the friction factor analysis. The experimental empty tube data were correlated by equation (1.24) with a constant of 0.023 and either an exponent of 0.36 on the viscosity ratio (water tests), or with the viscosity ratio replaced by the term $(T_s / T_b)^{0.575}$ (air tests). These corrections

were also applied to the analytical predictions. Only one of the experimental results obtained using air by references (118) and (69) differed from the predictions of equation (1.39) by more than 10%. However, at low Reynolds numbers the predicted values of Nu are lower than the experimental results of Koch (69), at high flowrates the predictions are high. The experimental water data and the predicted results agreed to within ± 20%. It should be noted that in using equation (1.39) the fin effectiveness of the tape, η, needs to be estimated. It is seen from equation (1.39) that the Nusselt number for a 100% fin efficiency is 64% greater than the value for zero fin efficiency. This may be one of the factors causing the slight discrepancy, seen later, between the results of various workers.

Poppendiek and Gambill (99) discuss some possible uses of swirl inducing inserts and the relative importance of the phenomena affecting the thermal and hydraulic characteristics. Most of the ideas in reference (99) have appeared in previous references. However, one effect which is not generally apparent from other papers is the effect of heat addition on the hydraulic characteristics of tubes containing swirl inducers. Gambill and Bundy suggest that under the conditions of high heat fluxes, for fluids with large values of β and low μ/ρ, the "free" convection produced during swirl flow increases the friction factor.

The analysis of Migay (83) shows that for fully developed swirl flow with a twisted tape :

$$\phi_e = \frac{0.0124}{Re_e\, y}\left(1125 \ln\left(Re_e\,(2\phi_e)^{0.5}\right) - 3170\right) + 0.023\, Re_e^{-0.2}\, C^{2.8} \qquad (1.40)$$

where $$C = \frac{\pi}{\left[\frac{\pi}{2} + 1\right]}\left[\frac{(A^{-1} + 1)^{0.5}}{2} + \frac{1}{4y}\left[(A + 1)^{0.5} + A \ln(B)\right]\right]$$

$$A = \frac{4\, y^2}{\pi^2}$$

and $$B = \left(A^{-0.5} + (A^{-1} + 1)^{0.5}\right)$$

In the above equation, the suffix "e" refers to the use of the equivalent diameter and fluid velocity with the tape inserted. To allow for the formation of the vortex flow, Migay uses the equation proposed by Smithberg and Landis (118), such that

$$\phi_{eTOT} = \phi_e + \phi'_e \qquad (1.41)$$

where $$\phi'_e = \frac{D_e \pi^2}{64 y^2 l} \qquad (1.42)$$

and l = length of the twisted tape

For Migay's tests in the range indicated in Table 1.1 the results and the predictions of equation (1.41) generally agreed to within 3%.

Migay (83), again by analytical methods, showed that

$$\frac{h D_e}{k} = \frac{\dfrac{15\,(1 + 1.75/(Pr + 8))\,Pr\,D_e}{\phi_e^{0.5}\; y\; d} + B}{1 + \left[\dfrac{D_e}{15\, y\, d\, Re_e}\right](5050\, Pr^{0.69} + 0.00006\, Pr^{3})} \qquad (1.43)$$

where $$B = \frac{0.023\, Re_e^{0.8}\, Pr\, (A^{-1} + 1)^{0.4}}{1 + 2.14\, Re_e^{-0.1}\, (A^{-1} + 1)^{-0.05}(Pr^{\frac{2}{3}} - 1)}$$

and $$A = \frac{4 y^2}{\pi^2}$$

Migay also includes an additive term to allow for the fin effect which is neglected by equation (1.43). This equation is applicable in the turbulent flow regime with $0.7 < Pr < 1000$ (83).

The range of variables used by Seymour (111) are noted in Table 1.1. Empirical correlation of the results, which were determined under isothermal conditions, showed that

$$\log_{10}(\phi_1 / \phi_o) = (0.905 / y) + 0.29 \qquad (1.44)$$

for $13000 < Re_1 < 10^5$; M.A.D. = 10%

The friction factor and Reynolds number have been designated the subscript "1" since it appears from reference (111) that ϕ_1 and Re_1 are

determined using the inside diameter of the tube but with a fluid velocity which allows for the thickness of the tape. The empty tube results were correlated by equation (1.7). Seymour also used a semi-empirical method which fitted the experimental results, for $10^3 < Re_l < 10^5$, with an M.A.D. of approximately 35%.

The semi-empirical analysis of Thorsen and Landis (128) shows that

$$\phi_e = 0.023 \left[\frac{\Gamma}{B_T}\right] Re_{el}^{-0.2} \left[\frac{T_s}{T_b}\right]^{-0.1} \quad \text{for } Re_{el} > 10^4 \qquad (1.45)$$

where $\Gamma = 1.126 + 0.031 \left[\frac{\gamma^2}{(1+\gamma^2)\, r}\right]$

r = tube radius, ft

$\gamma = (\pi/2\, y)$

$$B_T = \frac{(1+\gamma^2)^{0.5}\, B}{\left[\frac{2}{3\gamma^2}\left[(1+\gamma^2)^{1.5} - 1\right]\right]^2}$$

$$B = \frac{(\pi + 2)\, d - 2\delta}{\left[\frac{4}{3}\gamma r^2 \left[\frac{3\pi\gamma}{d} + \frac{\pi A}{y\, d}\right] + 2\, d\, A + \pi d - 2\delta A\right]}$$

and $A = (1+\gamma^2)^{0.5}$

The temperature ratio is an empirical modification of their analysis and allows for the variation of the physical properties of gases. The same modification applies to their empty tube results. The Reynolds number is defined by

$$Re_{el} = \frac{D_e\, \bar{v}\, \rho}{\mu} \qquad (1.46)$$

where $\bar{v}$ is the average total velocity, which includes the tangential and axial components of the flow, based on the forced vortex model outlined in Appendix A.1. In using this model, the analysis is considerably simplified if the thickness of the tape is neglected; this allows integrations to be performed across the flow field from the centre of the pipe to the tube wall. Hence

$$\bar{v} = \frac{1}{A_c}\int_0^r 2\pi R\, u_r\, (dR) \qquad (1.47)$$

The resultant fluid velocity, u_r, is found using equation (A.1.7) in the same way as that used to determine equation (A.1.9). However, the true mean axial fluid velocity, u_e, is used in these calculations. This shows that

$$\bar{v} = \frac{1}{A_c}\int_0^r 2\pi R\, (1 + \gamma^2(R/r)^2)^{0.5} u_e\, (dR) \qquad (1.48)$$

$$= \frac{2 A_f u_e}{3 A_c \gamma^2}\, ((1+\gamma^2)^{1.5} - 1)$$

where $\gamma = (\pi/2y)$

It follows that

$$Re_{el} = \frac{2 A_f}{3 A_c \gamma^2}\, ((1+\gamma^2)^{1.5} - 1)\, Re_e \qquad (1.49)$$

The anomaly concerning the definition of the flow area also occurs in the work of Gambill et. al. (49), Smithberg and Landis (118), and Seymour (111). All of these workers assume in their analysis that the thickness of the tape may be neglected. This may be a reasonable approximation in view of the approximate nature of the forced vortex model and because they used thin tapes, see Table 1.1. The approximation may be invalid for large area blockage ratios.

Thorsen and Landis (128) also derive the following semi-empirical equations :

$$Nu_e = C_h\, Re_e^{0.8}\, Pr^{0.4} \left[\frac{T_s}{T_b}\right]^{-0.32} (1 + 0.25(Gr)^{0.5}/Re_e) \qquad (1.50)$$

for heating

$$Nu_e = C_c \, Re_e^{0.8} \, Pr^{\frac{1}{3}} \left[\frac{T_s}{T_b}\right]^{-0.1} \left(1 - 0.25(Gr)^{0.5}/Re_e\right) \qquad (1.51)$$

for cooling

where $$C_h = 0.021 \left[1 + \frac{0.07 \ \gamma^2}{(1 + \gamma^2) \ r}\right]$$

and $$C_c = 0.023 \left[1 + \frac{0.07 \ \gamma^2}{(1 + \gamma^2) \ r}\right]$$

In the above equations, Nu_e is defined using D_e. The empty tube results were correlated with equations (1.50) and (1.51) by neglecting the terms in the round brackets and using $\gamma = 0$.

Lopina and Bergles (79) correlated their isothermal friction factors using

$$\frac{\phi_e}{\phi_{oe}} = 2.75 \ y^{-0.406} \qquad (1.52)$$

where $$\phi_{oe} = 0.023 \ Re_e^{-0.2}$$

This equation represented the experimental results of reference (79) to within 20%. Generally, the agreement between the results of six other workers and equation (1.52) was good. One friction factor, obtained from Gambill and Bundy (47), was approximately 60% greater than the predicted result. This was considered to be a result of the greater roughness of the tube in that test.

Lopina and Bergles allow for the effect on the friction factor of heat transfer by using equation (1.52) and equation (1.18) with

$$m = 0.35 \qquad \text{for the empty tube, heating} \qquad (1.53)$$

$$m = 0.35\left[\frac{D_e}{d}\right] \qquad \text{for tubes containing twisted tapes, heating} \qquad (1.54)$$

They performed heating and cooling tests with water and a tape with a twist ratio of 3.15. It was found that the Nusselt numbers determined during the cooling tests were approximately 25% below those determined under heating conditions. The Nusselt numbers obtained using a tape which was insulated from the tube wall were approximately 10% lower than the results obtained using an embedded tape. Using an additive

method, involving the components of the Nusselt number that are the result of the increased fluid velocity, flow length, and the centrifugal convection and fin effects in swirling flow, it is shown that

$$Nu_e = \frac{h\,D_e}{k} = F\left[0.023\,(\propto Re_e)^{0.8}\,Pr^{0.4} + 0.193\left\{\frac{Re_e^2\,D_e\,\beta\,\Delta t_f\,Pr}{y^2\,d}\right\}^{\frac{1}{3}}\right] \qquad (1.55)$$

where $\propto = \frac{(4y^2 + \pi^2)^{0.5}}{2y}$

This equation applies for heating conditions; for cooling applications the second term in the square brackets should be neglected. The factor, F, allows for the fin effect of the tape. Lopina and Bergles used $F = 1.10$ for $Re > 3 \times 10^4$, this value was estimated using the experimental method discussed above, and by analytical methods. They also modified the constant of 0.023 to fit their actual empty tube results which showed that the constant was 0.025. In this way the results determined under heating and cooling conditions agreed with equation (1.55) to within 10%. The results of references (118) and (49) generally agreed with the predictions to within 15%.

Klaczak (64) correlated his results, obtained by the steam heating of water, to show that

$$Nu = 2.519\,Re^{0.44}\,Pr^{0.36}\,y^{0.33} \qquad (1.56)$$

$\pm$ 10% for 95% probability

The following range of variables were used :

d	=	6.8 mm
δ /d	=	0.074
l/d	=	30
y	=	1.63, 2.64, and 3.79
$1700 < Re < 20000$		
$2.5 < Pr < 9$		

The actual experimental data in reference (64) shows that the Reynolds number exponent is greater than 0.44 at Reynolds numbers greater than 10^4. Nonetheless the exponent, 0.44, is lower than the values determined by other workers. Unfortunately Klaczak does not give details of the tube section upstream of the twisted tapes, the empty tube results, nor any pressure loss measurements. The Reynolds numbers are low in the Klaczak study which may indicate that the results were

obtained in a laminar/turbulent transition regime. Blackwelder and Kreith (6, pp. 102-108) show that the Nusselt number, in a twisted tape arrangement, deviates from the turbulent flow trend at Reynolds numbers less than 3000 and that laminar flow exists at $Re < 1200$. The tube length used by Blackwelder and Kreith was 102 pipe diameters, this is considerably greater than the length used in Klaczak's tests.

Date (30) reviews the studies performed using twisted tapes. In that thesis the correlations proposed by previous workers are tabulated. However, many of the correlations are misprinted and it is for this reason that many of them have been restated in the present review. Date suggests that equation (1.40) is the best correlation of the available friction factor data for all twist ratios. Due to the complexity of that equation, Date recorrelates the available data into the form :

$$\phi_e = 0.023\ Re_e^{-0.2} \left[\frac{y}{y-1}\right]^b \qquad (1.57)$$

where $b = 1.15 + (0.15\ (7 \times 10^4 - Re_e) / 6.5 \times 10^4)$

This equation applies for

$$1.5 < y < \infty$$

$$5000 < Re_e < 70000$$

Date does not correlate the heat transfer data, probably because an adequate correlation would require that the fin effect for each set of data is known. It is suggested that equations (1.39), (1.43), and (1.55) are the best representations of the available data.

Reference (30) notes that there is some inconsistency in the literature concerning the Prandtl number effect. It is proposed, in reference (30), that a Prandtl number exponent of 0.4 is adequate, although no experimental data has been obtained for Prandtl numbers considerably greater than unity. This is not surprising since a fluid flowing with high Reynolds and Prandtl numbers exhibits a large pressure loss (and possibly viscous heating). This is undesirable in many practical applications.

Date (30) solves the partial differential equations of momentum and heat transfer for laminar and turbulent flows in twisted tapes. The calculated Nusselt numbers in that reference should be multiplied by a factor of 2 since Date considered only one half of the duct (112, p. 382). Due to the difficulty in modelling the Reynolds stresses

using an effective viscosity, the calculated friction factors and Nusselt numbers, in the turbulent flow regime, did not agree with the experimental results.

Using electrical resistance heating of tubes with nitrogen flow, Klepper (65) determined the following correlations :

$$\frac{Nu}{Nu_o} = 1.105 + \frac{0.59\ Re^{0.05}}{y^{0.6}} \qquad (1.58)$$

where Nu = Nusselt number for fully developed flow in a tube containing a twisted tape

and Nu_o = Nusselt number for fully developed flow in an empty tube

$$= 0.023\ Re^{0.8}\ Pr^{0.4} \left[\frac{T_s}{T_b}\right]^{-0.5} \qquad (1.59)$$

Equations (1.58) and (1.59) correlated Klepper's data to within 8% and 5% respectively. The range of the tests is indicated in Table 1.1. Using a tape twist of 2.38 a peaking of the local Nusselt number occurred near to the leading edge of the tape; this effect was not found using other twist ratios. For all twist ratios, fully developed flow was established within 26 pipe diameters of the leading edge of the tape.

Klepper (65) correlates friction factor data using a fluid viscosity and density evaluated at a temperature θ_1, where $\theta_1 = 0.3\ (T_s - T_b) + T_b$. This method of calculation probably only applies for gases and will not be considered in detail in the present work. For y = 2.38 and 4.42, Klepper's proposed correlation predicts friction factors which are 10% greater than those found by Thorsen and Landis (128).

Nazmeev and Nikolaev (89) suggest that empty tube correlations may be used for the prediction of the heat transfer characteristics of tubes containing twisted tapes provided that the true flow area is used in the calculations. Reference (89) is a translation of the work of Nazmeev and Nikolaev and, although not stated in the reference, an hydraulic diameter must be used in the empty tube equations so that agreement with the experimental results is obtained.

Subtracting the cross sectional area of the tape from the flow area derived by Gambill et. al. (49), see equation (A.1.14), one obtains

equation (A.1.15). This is the flow area used by Nazmeev and Nikolaev. The hydraulic diameter, D_H', to be used in the empty tube correlations, is derived in Appendix A.1. Those correlations, as shown earlier in this thesis, show that the Reynolds number exponent is 0.8, therefore

$$\frac{Nu}{Nu_o} = \left[\frac{A_f}{A_f''}\right]^{0.8} \left[\frac{d}{D_H'}\right]^{0.2} \qquad (1.60)$$

where Nu, Nu_o = Nusselt numbers, based on the tube i.d., for tubes with and without twisted tapes

A_f = cross sectional area of the empty tube of diameter, d

A_f'' = corrected true flow area, see equation (A.1.15)

D_H' = corrected hydraulic diameter, see equation (A.1.23)

From the comparisons presented by Nazmeev and Nikolaev, equation (1.60) appears to represent the results of references (69), (118), (110), and (64) to within approximately 25%.

(b) The effect of tape length and swirl decay downstream of twisted tapes.

Seymour (110) used a tape (y = 2.63) with the leading edge at the beginning of the heated tube section. The length of the tape was varied and the result of these variations were correlated to within 5% by :

$$\log_{10}\left[\frac{Nu}{Nu_T}\right] = \left[\frac{3.1}{Re^{0.31}}\right] \log_{10}\left[\frac{x_1}{l}\right] \qquad (1.61)$$

where Nu = Nusselt number based on the total heated length of the tube

Nu_T = Nusselt number for a continuous full length twisted tape arrangement. (Both Nu and Nu_T are defined using the inside diameter of the tube)

x_1 = tape length

l = heated length of the tube

Kreith and Sonju (75) perform an order of magnitude analysis of the Navier Stokes equations with the aim of investigating the swirl decay downstream of a twisted tape. They solve the resulting equation

by incorporating an approximation of the Reynolds stresses which involves the eddy diffusivity. The magnitude of this factor was determined by experimental tests. The theoretical and experimental analyses showed that within 100 pipe diameters downstream of the tape the swirl intensity decays to approximately 20% of the value at the tape outlet, (see Figures 7 and 8 in reference (75)).

Blackwelder and Kreith (6, pp. 102-108) experimentally investigated the heat transfer and pressure drop characteristics of a decaying swirl flow downstream of a twisted tape. Tests were performed in the range $2 \times 10^4 < Re < 6 \times 10^4$ and $1.77 < y < 11.0$. The decay of the local Nusselt number was almost exponential upto 15 to 30 diameters downstream of the trailing edge of the tape. Nusselt numbers characteristic of turbulent flow in an empty tube were determined approximately 60 to 80 diameters downstream of the tape. The rate of attenuation of the swirl increased with increasing heat flux through the tube wall, decreasing twist ratio of the tape, and decreasing Reynolds numbers. Allowance for the heat flow and twist ratio was obtained by multiplying the local Nusselt number by the ratio :

$$\left[\frac{T_s}{T_b}\right]^{(K_1 x/d)}$$

where T_s = tube wall surface temperature

T_b = local bulk fluid temperature

x = distance downstream of the tape

K_1 = a function of the twist ratio

It appears that within 5 tube diameters of the tape edge the decay may, for practical purposes, be considered independent of the heat flux and twist ratio. Blackwelder and Kreith used air in their tests; it is probable that had a liquid been used then the above ratio would involve fluid viscosities. Furthermore, they used a tape thickness of 0.041 tube diameters and fully developed swirl flow existed at the tape exit in all of the tests. The rate of decay may also be affected by these two factors.

The local friction factors decayed to the values which are typical of empty tubes at approximately 60 diameters downstream of the tape (6, pp. 102-108). The local friction factor decreases very rapidly in the empty tube section downstream of the trailing edge of the twisted tape. For instance, the local friction factor within the tape

section (y = 4.25, Re = 42000) may be approximately a factor of 3 greater than the corresponding empty tube value, while 3 diameters downstream of the tape the friction factor is approximately 1.8 times the empty tube value. The rate of reduction of the local friction factor with respect to the distance from the tape appears to increase with decreasing twist ratio.

The local Nusselt number, Nu_x, downstream of the trailing edge of a twisted tape was determined under heating conditions using nitrogen gas, see Klepper (65). The results were correlated to within 10% by

$$Nu_x = 0.023\ Re^{0.8}\ Pr^{0.4} \left[\frac{T_s}{T_b}\right]^{-0.5} (A)\ (B) \qquad (1.62)$$

where $$(A) = \frac{(0.7 + 0.000042\ Re)}{(1.0 + 0.000039\ Re)}$$

$$(B) = 1.0 + \frac{1.05}{\left[y + 0.0025\ y \left[\frac{x}{d}\right]^2\right]^{0.6}}$$

and x = distance from the trailing edge of the tape to the measurement position

The range of the tests is noted in Table 1.1. As also found by Blackwelder and Kreith, the local friction factor rapidly decreased beyond the tape. The increase of the average friction factor above the empty tube factor, over the range $0 < x/d < 10$ in the region downstream of the tape, was only one third of the increase determined in the tape region.

The correlations proposed by previous workers have been used to determine the values of $(h/h_o)_p$ that may be expected when using the conditions of the present work. The friction factor correlations of previous workers were adapted using equations (1.53) and (1.54) and calculations were performed assuming zero fin effect. The predictions found using the work of Smithberg and Landis (118) showed that $(h/h_o)_p$ would be 1.39 and 1.23 at Reynolds numbers of 15500 and 104000. The proposals of Thorsen and Landis (128) and Lopina and Bergles (79) show that $(h/h_o)_p$ would be respectively 1.36 and 1.19 at a Reynolds number of 15500, and 1.35 and 1.16 at a Reynolds number of 104000. The empty tube correlations that were adopted by the reference authors were used in the above calculations.

1.3.7 Motionless inline mixers ("Static mixer" is a registered trademark of the Kenics Corporation).

A motionless inline mixer may be generally described as any stationary body, or assembly of bodies, which are located within a duct and thereby cause transformations of the fluid velocity and hence result in the mixing of the fluid. Simpson (15, pp. 280-305) outlines the factors for consideration in the design or purchasing of a motionless inline mixer. Reference (96) describes some applications of the mixers, including the Kenics and Dow/Ross devices. References (100) and (54) also consider those mixers and the Sulzer/Koch device. Compared to the flow in empty tubes, the increased shear stress at the duct wall and the fluid mixing produced in motionless mixers lead to larger heat transfer coefficients. Pahl and Muschelknautz (93, 94 and 95) and Chakrabarti (21) consider the mixing, pressure drop, and heat transfer (fluid to tube wall) characteristics of motionless mixer systems. The references cited above generally limit their observations to the laminar flow regime. For comparison with the results of the present work the turbulent flow thermal and hydraulic characteristics of some commercially available mixers are reviewed in the next two sections of this thesis.

A schematic diagram of an Etoflo LV (low viscosity) mixer is shown in Figure 1.3. The pressure drop across a standard six element Etoflo unit is given by (42) :

K = ratio of the friction factors, based on the tube with and without the mixer at the same nominal Reynolds number

$= 50$ (approximately) for $Re > 3000$ (1.63)

The heat transfer characteristics of the Etoflo mixer are not available (11).

The arrangement of the three-bladed elements of the Lightnin In-line blender are shown in Figure 1.3. The pressure loss associated with these turbulent flow devices is given by (77), (84):

$$K = A\, Re^{0.086}\, \mu^{0.064} \qquad (1.64)$$

where

$A = 66.5$ for $25\text{ mm} < d < 254\text{ mm}$, standard modules

or $A = 84.32$ for $300\text{ mm} < d < 1829\text{ mm}$, non standard modules (1.65)

and μ = fluid viscosity, centipoise

The overall heat transfer coefficient for a jacketed Lightnin mixer is 5 to 10 times greater than the value for a double pipe heat exchanger (77). It is probable that these increases were obtained in the laminar flow regime.

The LPD (low pressure drop), LLPD (lower pressure drop) and ISG (interfacial surface generator) mixers are shown in Figure 1.3. These mixers are manufactured by Charles Ross Co. under license from Dow Chemical Co. (22) hence the reason for various sources in the literature using different names for these devices. From the graphs in reference (22) it was estimated that in the turbulent flow regime (Re > 500):

$$\phi = \frac{Y\ N\ d\ A}{l} \tag{1.66}$$

where $Y = 1.11$ for LPD mixers (1.67)

$Y = 0.51$ for LLPD mixers (1.68)

$Y = 16.2$ for ISG mixers (1.69)

N = number of elements forming the mixer; typically $N = 6$ (LPD) or $N = 4$ (ISG)

d = tube diameter

l = length of the mixer

and A = viscosity correction factor. The tabulated data in reference (22) may be represented by $A = \mu^{0.056}$, where μ is the fluid viscosity, cP.

Unfortunately no heat transfer data pertinent to these mixers could be located.

Rearranging the equations given in reference (70) it is found that the pressure drop across Komax motionless mixers, see Figure 1.3, may be calculated using

$$\phi = \frac{0.288\ N\ d^{0.6}\ B_1}{l} \tag{1.70}$$

where ϕ = friction factor defined in equation (1.2)

N = number of elements forming the mixer; typically $N = 6$

d = tube diameter, ft

l = length of the mixer, ft

and B_1 = viscosity correction factor. The graph in reference (70) may be represented by $B_1 = \mu^{0.053}$, where μ is the fluid viscosity, cP.

Equation (1.70) applies for standard Komax modules, for which

$$l = d\,(1 + 1.25N) \qquad (1.71)$$

Nested Komax elements may be used in applications where extremely vigorous mixing is required. For these elements the pressure loss is double that given by equation (1.70) and

$$l = d\,(1 + 0.9N) \qquad (1.72)$$

The data in a later Komax bulletin (71) are correlated by

$$\phi = \frac{(N - 1)\,\mu^{0.08}\,d^{1.28}}{l}$$

where μ = fluid viscosity, cP

d = pipe diameter, ft

and l = pipe length, ft

The above equation will not be considered further in the present work because reference (71) does not include any information concerning the length of the mixers.

The overall heat transfer coefficient, U, of a Komax mixer with a heating or cooling jacket is approximately 3 times the value obtained with an empty pipe double pipe heat exchanger (72). Although no statement is given concerning the flow regime and geometrical details of the tests used to obtain this approximation, it appears that the tests were performed in the laminar flow regime and the increase is conservative. Later work (63) showed approximately 5 fold increases of U in the laminar flow regime. Further data from Komax (113) is presented in graphical form as ln(u) versus U, where u is the fluid velocity and U is the overall heat transfer coefficient for a double pipe heat exchanger containing a Komax mixer. The graph shows that

$$U = 178 \ln\left[\frac{u}{Y_1}\right] \qquad (1.73)$$

where

Y_1 = 0.046 for a fluid cooling (average temperature 60°C) (1.74)

Y_1 = 0.030 for a fluid being heated (average temperature 26.7°C) (1.75)

U = overall heat transfer coefficient, Btu $ft^{-2}\,hr^{-1}\,{}^{o}F^{-1}$

u = fluid velocity, based on the pipe diameter, ft s^{-1}

The tube of the heat exchanger used in the above tests was a 25.4 mm o.d. (22.1 mm i.d.) 316 stainless steel tube and water was used in the tube and shell. Replotting equations (1.73) and (1.75) in the form of the conventional Wilson plot,* $1/U$ versus $1/u^{0.8}$, a gradual curve was produced which shows that either the scale or the annulus fluid film resistances to heat transfer were not constant, or that the film heat transfer coefficients of a fluid flowing through a Komax mixer are not dependent on $u^{0.8}$. However, using the results for u = 2,4,6,8 and 10 ft s^{-1} (Re = 15600 to 78000) a straight line approximation using the Wilson plot method showed that

$$h = \text{inside fluid film heat transfer coefficient in a tube containing a Komax mixer (heating, } 26.7^{o}C)$$

$$\simeq 1300\ u^{0.8}\ \text{Btu ft}^{-2}\ \text{hr}^{-1}\ {}^{o}\text{F}^{-1} \qquad (1.76)$$

Substituting the fluid temperature and tube diameter into equation (1.22) and converting to compatible units, it is found that

$$\frac{h}{h_o} = 4.5 \text{ (approximately)} \qquad (1.77)$$

where h_o is the film heat transfer coefficient for the empty tube. Equation (1.77) is an approximation and certainly should not be used in design calculations.

Sulzer mixers were developed by Sulzer Bros. from a distillation column packing. They are sometimes referred to as Koch mixers because they are also manufactured by Koch Eng. Inc. in U.S.A. (133). A large variety of these mixers are available; the arrangement to be used in a given application is based on the allowable pressure loss, length limitations, the required degree of mixing, the flow regime, and the duct shape. The main types which are currently available are the SMV, SMX and SMXL. The sections of an SMV mixer consist of a number of corrugated plates, consecutive plates are in contact with each other and thereby form intersecting channels. The sections of the mixers may be aligned or perpendicular. Unlike the SMV mixer, the SMX and SMXL types are generally used in the laminar flow regime (125). These mixers consist of intersecting flat plates; the SMXL type is less densely packed

---

* This analysis technique is discussed in section 4.8.2.

than the SMX and it is also used for heat transfer applications.

Due to the large number of geometrical variations and hence the large range of resulting friction factors it would be misleading to propose a typical equation for determination of the friction factors applicable to Sulzer mixers. The reader is therefore directed to the original literature in which turbulent flow results are reported. References (133), (124), and (127) used air in SMV mixers in square ducts (450 mm diameter). Reference (124) observes the effect of the number of plates and length of the mixer.

Limited data concerning type SMX mixers are also reported in (124). References (126) and (123) discuss the use of Sulzer mixers for the inline dispersion of liquids; they present some pressure loss data for the turbulent flow regime. Reference (125) provides good photographs of the three types of Sulzer mixers, noted above, and presents some of the mixing and pressure drop characteristics.

References (53) and (55) investigate the laminar flow heat transfer characteristics of SMXL mixers, but no turbulent flow data could be located.

1.3.8 The Kenics static mixer.

A Kenics static mixer, see Figure 1.2, consists of a number of helices each of which possesses a twist of 180^{o} either in a clockwise or anticlockwise direction. The elements, generally 6 in turbulent flow applications, are positioned inside circular ducts so that consecutive elements have alternate twist direction and perpendicular leading edges.

Table 1.2 shows typical values of the friction factor ratio, K, which have been reported in the literature concerning Kenics static mixers. However, by far the most extensive amount of data is that of Chen (24) and Kenics Corp. (60). The latter references use the following notation :

K = ratio of the friction factors, based on the inside diameter of the tube and the superficial fluid velocity, for the mixer and the empty tube at the same superficial Reynolds number

$$= Z\, K_{oT} \qquad (1.78)$$

Chen (24) shows that Z is a parameter which is dependent on the Reynolds number only. A good approximation to the data of Chen is :

$$Z = 0.62\ Re^{0.104} \qquad (1.79)$$

Values of K_{oT}, for various pipe diameters, are given by (24) and (60). These values were correlated by regression analyses during the present work using terms which involved the tube diameter and either the twist ratio of the inserts, y, or the term $y/(y-1)$; the latter factor was proposed by Date (30) for the correlation of twisted tape data, see equation (1.57). Using the resulting correlations with equations (1.78) and (1.79) it was found that for the data of (24) :

$$\text{either} \quad K = 72.0\ D^{-0.190}\ y^{-2.24}\ Re^{0.104} \qquad (1.80)$$

M.A.D. = 6.2 A.A.D. = 1.1

$$\text{or} \quad K = 5.24\ D^{-0.196}\ (y/(y-1))^{1.61}\ Re^{0.104} \qquad (1.81)$$

M.A.D. = 6.6 A.A.D. = 1.2

Regression analyses of the data in (60) showed that :

$$\text{either} \quad K = 75.8\ D^{-0.207}\ y^{-2.46}\ Re^{0.104} \qquad (1.82)$$

M.A.D. = 5.9 A.A.D. = 0.81

$$\text{or} \quad K = 5.08\ D^{-0.211}\ (y/(y-1))^{1.57}\ Re^{0.104} \qquad (1.83)$$

M.A.D. = 6.5 A.A.D. = 0.83

Four important notes concerning equations (1.80) to (1.83) are:

(i) The inside diameter of the pipe, D, is evaluated in units of inches. This procedure was adopted since the manufacturers generally use these units.

(ii) The data of Chen (24) for d = 20.8 mm (D = 0.82 inches) was not used in the analyses since the value of K_{oT} for that pipe diameter was a misprint (122).

(iii) It is to be expected that K is dependent on the thickness of the elements, δ . Insufficient details were available to allow for this parameter in the regression analyses. Over the range of interest in the present study, $d < 38$ mm, the thickness of commercial Kenics mixers is approximated by $\delta/d = 0.1$, and for larger tube diameters $\delta/d < 0.1$, (20).

(iv) The data in references (24) and (60) were obtained over the respective ranges $1.5 < y < 1.9$ and $1.5 < y < 1.8$.

Grace (51) suggests that the Nusselt number for a gas turbulently flowing in a Kenics static mixer may be calculated using equation (1.19) with the constant, 0.023, replaced by 0.075. It appears from reference (32) that this equation was determined using tests with air in a 12 mm diameter pipe.

Morris and Benyon (86) measured the rate of transfer of naphthalene, to air, from the walls of tubes which contained Kenics mixers. Their results were generally correlated to within 10% (M.A.D. = 20%) by

$$\frac{Sh}{Sh_o} = 1 + 0.06N^{0.288}\, Re^{0.32}\, Sc^{0.4} \qquad (1.84)$$

$$\text{for } 10^4 < Re < 3.5 \times 10^4$$

$$d = 12.7 \text{ mm}$$

$$\delta/d = 0.079$$

where Sh_o is determined using the mass transfer anologue of equation (1.19) with a length correction of $(1 + (d/l)^{0.7})$. The mixers used in these tests were composed of 2,4,6,8, or 10 elements with a twist ratio of 2.5.

Proctor* (101) used the naphthalene transfer method during studies of Kenics mixers with twist ratios of 1.5 and 2.0. The tube diameter and element thickness were identical to those used by Morris and Benyon (86). It was found that the ratio of the mean Sherwood numbers along the test section with and without the mixers, Sh/Sh_o, was in the range 2 to 3 at superficial Reynolds numbers of approximately 400. The ratio increased with Reynolds number upto Re = 2000 to 3000 when Sh/Sh_o was in the range 5 to 6. Thereafter increasing the Reynolds number produced a reduction in Sh/Sh_o such that at a Reynolds number of 30000 (the maximum used in the tests) the ratio was approximately 2. If the trend found by Proctor is extrapolated to Reynolds numbers in the range 10^5 to 2×10^5 it is found that Sh/Sh_o is 1. However, there are some inconsistencies in the work of Proctor (101). In Figure 18 of Proctor's thesis (alternatively, see Figure 9 of reference (87)) the ratio Sh/Sh_o is seen to decrease with increasing Reynolds number when using Kenics mixers with twist ratios of 2.5.

---

* The mass transfer studies of this work are also reported in reference (87).

The results shown are noted as being the "reevaluated" results of Morris and Benyon (86) but no details of the reevaluation are given. A similar discrepancy also occurs in considering the heat transfer results which were obtained using a 12.7 mm diameter steel tube and Kenics mixers with a twist ratio of 1.5. Figure 33 of Proctor's thesis shows that the ratio of the mean Nusselt numbers along the test section with and without the mixers, Nu/Nu_o, increases with increasing Reynolds number. However, in Figure 32, Proctor implies that Nu/Nu_o decreases with Reynolds number. It appears from the actual experimental data on Figures 32 and 33 that Nu/Nu_o is approximately 3 for Reynolds numbers greater than 2000.

Chen (25) suggests that turbulent flow empty tube data may be correlated in the form of equation (1.23) with the constant, 0.024, replaced by 0.026. It is suggested that the constant is 0.078 for turbulent flow through a Kenics mixer. No details are given of the Reynolds and Prandtl numbers used in the determination of this constant. Figure 3-3 of reference (25) is a graphical representation of Nu versus $(Re^{0.8}Pr^{\frac{1}{3}})$ on linear coordinates. It shows $(Re^{0.8}Pr^{\frac{1}{3}})$ over the range 0 to 2000 and indicates that Nu/Nu_o is approximately 3.7. It is considered here that this graph does not represent the characteristics of the Kenics mixer. The graph does not agree with the equations quoted by Chen and to obtain turbulent flow conditions with low values of the product $(Re^{0.8}Pr^{\frac{1}{3}})$ it is necessary to use a fluid with an extremely small Prandtl number.

Lin et. al. (78) investigated the effect of using a section of Kenics static mixers in the upstream section of a heated tube. Various lengths of static mixer were used, including the full length mixer. One test section included 14 pairs of Kenics elements and a single element equidistantly spaced along the tube length. The latter configurations produced larger (approximately 13%) heat transfer coefficients and smaller (approximately 12%) pressure losses than the configuration consisting of 25 elements lumped together at the tube inlet. The tests were performed in the Reynolds number range of 980 to 5500. At these values, the heat transfer coefficients developed using the full length mixer were factors of 10.6 and 7.3 times greater than the coefficients obtained with the empty tube at the same Reynolds numbers. In the writer's opinion, these large increases are to be expected since in the laminar regime in empty tubes the heat transfer coefficients are low. The insertion of Kenics mixers produces a

turbulent flow and consequently increases the heat transfer coefficients compared to the empty tube laminar flow values at the same superficial Reynolds numbers. Furthermore, it has already been shown that Kenics mixers increase the heat transfer coefficients in the turbulent flow regime and hence considerable increases are obtained in the conventional laminar/turbulent transitional flow regime. This result was also found by Morris et. al. (87).

Azer et. al. (1) used the same equipment as in reference (78) to investigate the effect of the equidistant spacing between pairs of Kenics elements, i.e. a counter clockwise and a clockwise helix with perpendicular leading edges. Their results are not presented in a form which can be converted to conventional $Nu/Pr^{0.4}$, or ϕ, versus Reynolds number curves. Their forced convection results were obtained in a region near to the subcooled nucleate boiling regime and they indicate that the heat transfer factor ratios, and the friction factor ratios, are dependent on the temperature difference between the tube wall and bulk fluid.

1.3.9 Range of application of in-line mixers to heat transfer enhancement.

The friction factors, ϕ, are based on the definition of equation (1.2) in this thesis. Hence it follows that

$$\frac{\Delta p}{\Delta p_o} = \frac{K\, l}{l_o} \qquad (1.85)$$

where K = friction factor ratio as defined previously (see Notation)

Δp = pressure drop across the mixer which is of sufficient length, l, to produce the required degree of mixing

and Δp_o = pressure drop across an empty tube which is of length, l_o, where l_o is the tube length required to produce the same degree of mixing as the in-line mixer of the same diameter.

In the present analysis, the length, l, will be considered to be the length of one standard mixing module as recommended by the manufacturers for turbulent flow applications. The empty tube mixing length, l_o, will be assumed to be 2540 mm (l/d = 95.2). This ratio

was used by Tauscher and Streiff (127).

Also,

$$\frac{q / \Delta t_{LM}}{q_o / \Delta t_{LMo}} = \frac{U\ t}{U_o\ t_o} \qquad (1.86)$$

where $q/\Delta t_{LM}$, $q_o/\Delta t_{LMo}$ = heat flow rates per unit of temperature driving force for the tubes with and without mixers

and U, U_o = overall heat transfer coefficients for the heat exchangers with and without mixers.

Table 1.3 shows the assumptions and the results of an analysis using the above equations. It must be stated that the chosen conditions do not represent the best application of the in-line mixers. It is very unlikely that the ISG mixer would be used at the high flowrate (superficial velocity = 1.87 m s^{-1}) used in the present analysis. However, Table 1.3 shows the important fact that the equipment size reduction, that results from the insertion of the mixers, may lead to insufficient heat transfer area being available. This indicates that in-line mixers are suited to applications where simultaneous mixing and relatively low heat flowrates are required. Most of the mixers were initially conceived to reduce the equipment size necessary for the mixing of fluids at low Reynolds numbers. The need for effective mixing, and sometimes heat transfer, at higher flowrates has led to the development of lower pressure loss devices which necessarily require greater homogenization lengths and consequently increase the area available for heat transfer, for instance the LLPD and SMXL mixers.

The pressure losses given in Table 1.3, when considered with a three fold increase in the film heat transfer coefficient, show that $(h/h_o)_p$ is 0.87 for a Kenics mixer (27.7 mm i.d. pipe) operating at a Reynolds number of 50000.

1.4 Evaluation of the heat transfer enhancement techniques

Bergles et. al. (3) present 8 criteria which may be used as measures of the effectiveness of the enhancement techniques. For each of these criteria there is an objective, for example, increasing the heat transfer rate relative to that obtained using an empty tube, and fixed constraints, for example, the tube diameter and length, the number of tubes, and the fluid mass flowrate, may be equal in the augmented and empty tube applications.

A number of methods have been proposed for comparing the heat duty and pumping power requirements of various enhancement techniques. Glaser, see (69, pp. 118-119), uses curves showing the required heat transfer surface area versus an efficiency, ε_1, where

$$\varepsilon_1 = \frac{\text{Heat flowrate per unit of temperature driving force, } q/\Delta t}{\text{Pumping power}} \tag{1.87}$$

Using this definition, all devices which have the same efficiency, when operating at the same $q/\Delta t$, require the same pumping power. The most beneficial device requires the smallest heat transfer area. This method is similar to the R3 criterion, proposed by Bergles et. al. (3) which is now described.

The pumping power requirement of a given device is

$$\begin{aligned} P &= Q\,\Delta p \\ &= \pi \phi\, l\, d\, \rho\, u^3 \end{aligned} \tag{1.88}$$

Substituting equation (1.3) into (1.88) shows that

$$P = \frac{\phi\, \pi\, l\, Re^3\, \mu^3}{d^2\, \rho^2} \tag{1.89}$$

For empty and augmented tubes requiring equal pumping powers and with equal fluid temperatures and tube diameters and lengths, it follows that

$$\phi_o\, Re_o^3 = \phi\, Re^3 \tag{1.90}$$

where the suffix "o" refers to the empty tube. This equation can be solved easily if the empty tube can be characterised by a simple friction factor correlation. (When ϕ_o is not proportional to Re^B equation (1.90) may be quickly solved using a plot of Re_o versus $\phi_o\, Re_o^3$. A series of such curves, each applicable to a certain tube roughness, may be produced). For instance, substituting equation (1.4)

into (1.90) shows that

$$Re_o = (43.5\ \phi\ Re^3)^{0.357}$$

Hence using Re_o and Re in the heat transfer correlations which apply to the empty and augmented tubes, it is possible to determine the ratio $(h/h_o)_p$, for a constant power requirement. This technique was used in the review articles of Bergles (5), (2) and is used in the present work to allow direct comparison with those reviews.

Alternative methods of presenting the heat transfer/power analysis have been proposed. Morris and Proctor (87) present curves of Nu versus ln $(\phi\ Re^3)$ for the empty and augmented tubes. Nunner (90) uses ln (Nu/Nu_o) versus ln (ϕ / ϕ_o) where each factor is evaluated at the same Reynolds number. On this basis ϕ / ϕ_o is the ratio of the power requirements of the augmented and empty tubes operating at the same Reynolds number. This method of data presentation is useful since it gives a clear indication of the pumping power increases required to produce the heat transfer enhancement when the mass flow-rate is fixed. Norris (6, pp. 16-26) used this method for the correlation of the characteristics of roughened tubes. This method will also be used in the present work.

A further extension of the above graphical presentation method, which was also used in an adapted form by Gambill and Bundy (47), again investigates the Nusselt number increases that are possible by increasing the fluid velocity through an empty tube. Nunner (90) shows that if the empty tube characteristics are such that ϕ_o and Nu_o are respectively proportional to $Re^{-0.25}$ and $Re^{0.8}$, then

$$\frac{Nu_{o2}}{Nu_{o1}} = \left[\frac{P_{o2}}{P_{o1}} \right]^{0.291} \qquad (1.91)$$

where Nu_{o1}, Nu_{o2} = Nusselt numbers at Reynolds numbers of Re_{o1} and Re_{o2} in the empty tube

and P_{o1}, P_{o2} = pumping powers required to produce the Reynolds numbers.

This equation can be shown on the ln-ln coordinates of Nu/Nu_o versus P/P_o, or analogously ϕ / ϕ_o, for the augmented tubes.

It must be noted that the heat transfer coefficient, or Nu, has been used in the above equations. If the equations are to represent the actual benefit resulting from the use of augmentation techniques then the calculations should use the overall heat transfer coefficient, U. Such an analysis introduces other possible variables, for example, the fluid film resistance on the outside of the tube.

Ouellette and Bejan (92) use entropy (available energy) minimisation as the criterion for the suitability of using enhancement devices. They define the "augmentation entropy generation number", N, as the ratio of the rate of total entropy generation, with respect to length, for the augmented and empty tubes. The total entropy generation rate is the sum of the rates associated with the pressure losses and the finite temperature difference between the tube side and annulus side fluids. On the basis of this definition an augmentation device is suitable if $N < 1$; lower values of N indicate better techniques. Throughout the analyses in reference (92) it is assumed that the thermal and frictional available energies have the same cost per energy unit. However, it is shown that the method can be adapted to allow for dissimilar available energy costs, although the method still neglects the fixed costs associated with, for example, the equipment manufacture and maintenance. Nonetheless, these factors were not considered in the constant pumping power analyses.

The evaluation methods used by Evans (43), (44), and Spalding and Lieberam (120) determine the enhancement technique which produces the minimum total (fixed and operating) cost. These methods are necessarily more time consuming to apply than are the simplified criteria suggested by Bergles et. al. (3). However, this type of analysis should be applied at sometime during the design of a heat exchanger.

Other criteria may be important in some applications. Reduction of the equipment mass is a factor when using expensive materials of construction or when the equipment is to be part of mobile machines, for example, aircraft. The power requirement per unit volume of fluid, E_1, is important where blood is used. Bluestein and Mockros (8) used blood in the range $1000 < Re < 4500$ passing through circular tubes, orifice plates and venturi tubes.

They found that

$$h_t = K_1 (E_1)^{1.2} \qquad (1.92)$$

where h_t = hemolysis rate of the blood cells,

mgm cm^{-3} (cells) min^{-1}

and E_1 = power per unit volume of fluid,

erg cm^{-3} (blood) min^{-1}

K_1 is a constant for a given type of tube insert; it increases as the nonuniformity of the energy dissipation, across the flow area, increases. Since most tube inserts increase E_1 and many of them create significant form drag losses and thereby increase K_1, it is unlikely that many forms of tube inserts are beneficial in blood oxygenators or blood heat exchangers.

The use of tube inserts to enhance heat transfer is not as widely applied as may have been expected. This may be due to conservatism or a lack of sufficiently accurate data, or a knowledge of the data, for a given application. Very little work has investigated the scale formation and erosion that may occur while using tube inserts. The comparatively large fluid velocity near the tube wall that is produced by swirl flow inducers may reduce the rate of scale formation that would occur in an empty tube, but erosion may occur. The need to clean the tubes is a possible reason for not using multiplex finned tubes. Also, multiplex tubes, although they provide substantial heat transfer enhancement, are costly due to the number of tubes and the compounding technique required for their production.

Enhancement devices are particularly suited to applications involving large heat fluxes, such as nuclear reactors. In these instances, local hot spots and large temperature gradients may be reduced thereby ensuring the mechanical integrity of the equipment. The use of inserts is also clearly favourable if the pumping power is relatively free, for example, the use of river water in cooling applications (92). As a generalisation, low spiral fins appear to be one of the best devices for heat transfer enhancement. (These fins are used on the outside surface of "cans" containing solid uranium rods in nuclear reactors).

1.5 Scope of the present work

The following comments outline the objectives, the limitations, and the reasons for performing the present work.

(i) The K values in Tables 1.2 and 7.2 show that the pressure drop across a Kenics mixer is significantly greater than that across a twisted tape. The present experimental project examines whether this difference is the result of the alternate twist direction or the perpendicularity of the elements in the Kenics configuration. Heat transfer and pressure drop measurements were performed using water passing through tubes containing a continuous length of any of the configurations shown in Figure 1.4. The effect of the thickness of the inserts was not studied.

(ii) Previous workers had shown that substantial improvements in the heat transfer factor, $Nu/Pr^{0.4}$, are obtained in the region downstream of a twisted tape. However, no data was available for a tube containing discontinuous lengths of twisted tapes spaced along the tube. Heat transfer and pressure drop measurements were therefore performed using the configurations shown in Figure 1.5.

(iii) It has been shown that short lengths of in-line mixers will not satisfy large heat transfer requirements. This project investigates the use, in a heat transfer application, of pairs of elements arranged in the Kenics mixer configuration with empty tube lengths between the pairs, see Figure 1.6. To allow a comparison, the spacings between the inserts were identical to those used in (ii).

(iv) The tests were limited to the turbulent flow regime because most heat exchangers are operated in that regime and because the turbulent flow produces the large heat transfer factors which are required in applications involving large heat fluxes.

(v) No theoretical analysis of the thermal and hydraulic characteristics of the above configurations was attempted. The work of Date (30) had shown that insufficient knowledge concerning the Reynolds stresses is currently available to predict the characteristics of tubes containing a swirling turbulent flow produced around a continuous

twisted tape. Many of the present configurations involve discontinuous lengths of inserts and a decaying swirl flow; the flow around these inserts would be considerably more difficult to model.

After the construction of the experimental facility it was necessary to await the manufacture of the Kenics mixer elements. During this period, the operation of the equipment was tested using Pall rings which had been adapted for insertion into tubes with the same diameter as those to be used with the Kenics elements, see Figure 1.7. Pall rings were readily available and it was considered that they may increase the heat transfer coefficients, relative to those obtained using an empty tube, by a similar mechanism to that produced using ring type tube wall roughnesses. The configurations of the Pall rings are shown in Figure 1.8.

2 Experimental Equipment

2.1 Introduction

Figure 2.1 shows the flow arrangements used in this study. The tube fluid, water at an average temperature of 35°C along the test section, was moved by the centrifugal pump P101 from the tank T101 into the calming section. A by-pass was used in order to reduce the noise level and strain on P101 that would have been caused by greatly throttling the fluid across the gate valve V1. The fluid passed through the mixing mesh M1 and along the calming and test section to the cooler, via the adiabatic mixing chamber M3. From the cooler the water returned to T101 via the rotameter R1. The cooler removed the heat gained by the tube fluid while flowing through the heated length of the test section. The water in tank T102 was heated by the steam injector S1, the fluid prime mover being the pump P103. This annulus fluid was transferred from T102, by the pump P102, along the annulus where its average temperature was maintained at 80°C. From the annulus, the water passed through the adiabatic mixing chamber M2, through the rotameter R2, and returned to the tank T102. The calming section, annular section, mixing chambers, and flanges of the mixing mesh, were all lagged using asbestos flex (4 mm thick) and magnesia blocks (25 mm thick). Other lengths of pipe work were lagged, either for reasons of safety or to reduce the steam requirement of the injector S1.

Throughout the period of study a number of modifications to the experimental facility were made; these are discussed in more detail in the remaining sections of this chapter.

2.2 Tubes, pressure tappings, manometers and connections

2.2.1 Connections.

During the initial empty tube tests, and those performed using Pall rings, the calming section and test section were connected together by a 35 mm length of clear flexible P.V.C. tubing and two jubilee clips. The bore of the flexible tubing was equal to the outside diameter of the two tubes. The pressures encountered while using the swirl flow inducers enforced the use of a compression fitting pipe connector internally bored so that the ends of the tubes were in

intimate contact. The olives of the compression fitting were constructed in polytetrafluoro-ethylene (P.T.F.E. or TEFLON); this allowed the test section to be disconnected easily. An identical arrangement was used to connect the calming section and short length of tube through which the thermocouple stem, T1, was placed, see Figure 2.4.

2.2.2 *Tubes.*

The copper tubes, forming the calming and test sections, had inside and outside diameters of 20 mm and 22 mm respectively. The reproducibility of these dimensions was confirmed by the agreement of the pressure drop and heat transfer results obtained using different sections of tubing. The calming section and test sections had total lengths of 1016 mm (40 ins.) and 1270 mm (50 ins.). The distances between the pressure tappings were 965 mm (38 ins.) and 1219 mm (48 ins.) for the distances P1 to P2 and P2 to P3, respectively.

2.2.3 Pressure tappings.

For the initial empty tube tests pressure tappings were made at the points P1, P2, and P3, see Figure 2.1, corresponding to the positions 25.4 mm (1 ins.), 991 mm (39 ins.) and 2210 mm (87 ins.) from the calming section inlet. For the tests using the Pall rings, the tappings at P1 were not used. For the tests using the swirl flow inducers, tappings were made at points P2 and P3 only.

The tappings at each position consisted of four circumferentially equidistant holes of 2 mm diameter. Tubes, 25.4 mm (1 ins.) long, with the inside bore equal to the hole size given above, were soldered to the outside surfaces of the test tubes in order to complete the pressure tapping arrangement. It was always ensured that the inner tube wall was smooth after this soldering process.

For the relatively low pressure Pall ring tests, clear flexible P.V.C. tubing, 4.8 mm (3/16 ins.) inside diameter, was used to connect the pressure tappings to the manometers. With the latter arrangement, valves on the connecting tubing were of the simple thumb-screw type. Short lengths of thick walled rubber tubing were used at the positions of the thumb screw valves in order to ensure that they could be closed effectively.

During the higher pressure tests using the swirl flow inducers, the P.V.C. connecting tube was replaced by nylon tube, 4 mm (5/32 ins.) inside diameter and 6 mm ($\frac{1}{4}$ ins.) outside diameter, and the thumb screw valves were replaced by 6 mm ($\frac{1}{4}$ ins.) ball valves. Compression fittings were used to connect the pressure tappings and nylon tubing, while Serkeit nylon tees (6 mm, $\frac{1}{4}$ ins.) were used as the common manifolds of the pressure tappings and manometers, see Figure 2.2.

2.2.4 Manometers.

All of the manometers were the U-tube type, produced from glass (5 mm inside diameter and 8 mm outside diameter). The Pall ring tests utilised two manometers each 1000 mm (39.4 ins.) long, one contained a carbon tetrachloride/iodine mixture with a specific gravity of 1.6, the other contained mercury. The tests with the swirl flow inducers utilised four manometers, each 2000 mm (78.7 ins.) long, one contained carbon tetrachloride, the other three, which could be connected in series, contained mercury, (see Figure 2.2).

2.3 Heating jacket (See Figures 2.3.A to 2.3.E and Figure 2.4)

The heating jacket and test section formed the annulus through which the hot water was circulated. The outer faces of the brass flanges of the jacket were 102 mm (4 ins.) and 51 mm (2 ins.) from the tappings at P2 and P3, respectively. The cross sectional areas of the inlet and outlet ports of the heating jacket were approximately the same as that of the annular space formed by the jacket and the tube. The tube wall thermocouples, T11 and T12, passed through the P.V.C. flanges of the jacket and were as close as reasonably practical to the heated section. Although the grade of P.V.C. used to produce the end flanges did not noticeably distort at the maximum temperatures encountered, approximately 90°C, it was found that they could be distorted slightly while being attached to the brass flanges of the jacket. The use of the Q.V.F. flanges, shown in Figures 2.3.B and 2.3.E, eliminated the latter effect.

Again it should be noted that the brass compression fittings of the P.V.C. flanges were used with P.T.F.E. olives to facilitate

removal of the test section. Early tests using copper olives within the compression fittings showed that heating of the test section resulted in such olives deeply indenting the test section and therefore led to difficulty in removal of the tube, and would have precluded removal of any inserts within the tube.

2.4 Adiabatic mixing chambers and mixing mesh (See Figure 2.5)

Due to the formation of temperature profiles within the annulus and test tubes it is imperative that some device is used to mix the fluid of which the bulk temperature is to be measured. The present work used adiabatic mixing chambers in the exit fluids streams and a mixing mesh on an inlet stream. Tests with and without a mixing mesh on the inlet to the annulus showed that a mesh was unnecessary; the bend and multiple fittings, immediately preceding the thermocouple T3, mixed the fluid stream sufficiently. The mixing mesh M1 destroyed any velocity profile in the upstream length of tube and allowed a bulk temperature to be measured by the thermocouple, T1. Such a device was produced by placing a mesh of 1 mm (0.04 ins.) diameter holes between two gaskets and sealing with water resistant adhesive. This arrangement was positioned between brass flanges and connected to the pipework using compression fittings.

2.5 Steam injector and associated circulating system

Constructional details of the steam injector are shown as Figure 2.6. Steam at a pressure of 830 to 1030 kN m^{-2} (gauge) (120 to 150 psig) was reduced down to 440 kN m^{-2} (gauge) (64 psig) prior to injection. Although the steam pressure remained relatively constant, early tests showed that using the injector in the piping circuit downstream of the rotameter, R2, produced slight fluctuations in the annulus fluid flowrate; this effect was eliminated by using a separate water heating circuit as shown in Figure 2.1.

2.6 Pumps and holding tanks

During the Pall rings tests an already available pump of rating 4 kW (5.5 hp) was used as the prime mover, P101, of the tube side fluid. The higher pressures required for the testing of the swirl flow inducers led to the installation of a 15 kW (20 hp) pump. Fluid was circulated through the annulus flow loop by the 210 W ($\frac{1}{4}$ hp) pump, P102. An identical pump was sufficient for use in the steam injector flow loop upto a heating rate of approximately 16 kW (55000 Btu hr^{-1}); for further tests the previously used 4 kW pump was installed as P103.

The capacities of the tanks T101, which was baffled, and T102, were 0.205 m^3 (45 galls) and 0.114 m^3 (25 galls), respectively.

2.7 Fluid flowrate determination

The tube fluid flowrate was determined using the rotameter, R1. This rotameter was a Metric 47 X F manufactured by GEC - Elliot Process Instruments Ltd.. The rotameter, R2, used to determine the annulus fluid flowrate, was a Metric 35 manufactured by Rotameter MFG. Co. Ltd.. Both rotameters utilised stainless steel floats and were calibrated against orifice plates. The orifice plates were made to the specifications of BS 1042: 1963 (13). A brass plate with an orifice diameter of 10.02 mm (0.394 ins.) and a 302 stainless steel plate with an orifice diameter of 19.05 mm (0.750 ins.) were used; both of the latter measurements were made at 20°C. The pressure differential was determined using corner tappings with a piezometer ring; this arrangement is shown by Figure 22b of BS 1042: 1963 (13), further dimensional details are shown by Figure 3 of BS 1042: 1943 (13). The calming and outlet sections of the whole orifice arrangement were formed from 302 stainless steel pipe with an inside diameter of 52.50 mm (2.067 ins.) at 20°C, their lengths were 1016 mm (40 ins.) and 559 mm (22 ins.), respectively. The orifice sections and connecting pipework to the rotameter were lagged.

While calibrating the rotameter, R1, the cooler shown on Figure 2.1 was replaced by the orifice sections, the fluid being indirectly heated by passing heated water through the annular section. The orifice sections were connected between the mixing chamber, M2,

and the rotameter, R2, while the latter was calibrated. At this stage of the experimental work the steam injector, S1, was positioned downstream of the rotameter, R2, thus fluid heating was by direct steam injection. The fluid temperature was measured using a chromel-alumel thermocouple positioned within the orifice calming section at a distance of 419 mm (16.5 ins.) upstream of the leading face of the orifice plate.

2.8 Temperature measurement

2.8.1 Thermocouples/ice junctions.

Nickel-chromium/nickel-aluminium (chromel-alumel) thermocouples were used throughout. The hot junctions were grounded to the 18/8/1 stainless steel sheaths which were 150 mm (5.9 ins.) long with an outside diameter of 1.5 mm (0.06 ins.). The cold junctions were formed from 30 BSG chromel-alumel cable. The insulation was stripped from one end of each length of cable and the two bare wires were fused together by heating them. Contact between the cold junctions was eliminated by covering the 15 mm (0.6 ins.) length of cable near to the junction with flexible tubing. The cold junctions were placed in a thermally insulated Dewar flask which contained an ice/water mixture.

The hot junctions were held in the fluid streams using brass male stud couplings and P.T.F.E. olives. The measurements of tube wall temperature posed a further problem. Most commercially available devices that are used for tube wall temperature determination utilise a spring mechanism, a similar arrangement, see Figure 2.7, was used in the present work. This procedure allowed the axial heat conduction losses, from the heated section, to be estimated; they were found to be negligible.

2.8.2 Data transfer unit (D.T.U.).

The data transfer unit, manufactured by Schlumberger - Solartron, selects a thermocouple signal and transfers it to the digital voltmeter (D.V.M.). The signal returns to the D.T.U. and is transferred to the output interface. For the present work the output was produced on paper rolls using an Addmaster Model 420 machine.

2.8.3 Digital voltmeter (D.V.M.).

The digital voltmeter, which measures the electromotive force (e.m.f.) between the hot and cold thermocouple junctions, was a Schlumberger - Solartron Type No. A203.

2.9 Cooling requirements

The cooler, C101, consisted of a 22 mm outside diameter copper tube and a 2440 mm (96 ins.) length of Q.V.F. glass tube. Cooling water was passed through the annulus of this double pipe heat exchanger. The tube side fluid was further cooled by continuously passing small amounts of cold water into the tank T101 and thereby displacing the warm water out through the overflow pipe of the tank. Since only small amounts of additional water were used and because the residence time in T101 was sufficient for any air to be released to the atmosphere, no air was seen to be passed along the test section.

2.10 Tube inserts

2.10.1 Stainless steel Pall rings.

One inch Pall rings were adapted for insertion into a tube of 20 mm (0.79 ins.) diameter by cutting away one fifth of the circumference of the rings, see Figure 1.7. The rings, which were manufactured by Norton Chemical Process Products (Europe) Ltd. from 304 stainless steel, were easily reformed and when placed in the tube they remained at their required locations without the need for any additional fixing method. The maximum fluid pressure used during the tests was approximately 410 kN m^{-2} (gauge) (60 psig). Intimate contact of the rings on all of the tube circumference was not obtained.

2.10.2 Stainless steel swirl inducers.

The swirl flow inducers, which were manufactured by the Kenics Corporation using 316 stainless steel, were 3.2 mm (0.125 ins.) thick and 40.5 mm (1.595 ins.) long. Figure 1.4 shows the form of the anti-clockwise and clockwise helices each of which had a rotational angle of 180°. Three elements of each rotational direction were obtained from the Kenics Corporation; for cost reasons further elements were

produced by the method of the following subsection.

2.10.3 Production of swirl inducers by moulding.

Twisted tapes have generally been produced by twisting thin strips of metal subjected to the yield stress of the metal. The present work used thicker inserts than those previously adopted. The aim was to study configurations for which the flow area blockages were similar to those in the commercial Kenics mixers and thereby examine whether the correlations proposed by previous workers, for twisted tapes, could be extrapolated to greater flow blockages using the hydraulic flow concept. Moulding of the stainless steel inserts was chosen as the method of producing further inserts.

Two moulds, one of a left hand and the other of a right hand element, were formed by high pressure moulding of rubber inside a piece of test tube containing the appropriate insert. This procedure required approximately 48 hours at room temperature.

The material to be used in the moulds was ideally to possess the following properties :-

(a) Moulded at atmospheric pressure
(b) Moulded simply and quickly into a helix form
(c) Inexpensive since a large number of elements were to be produced
(d) Low melting point so as not to distort the moulds
(e) Smooth and reproducible surface finish after moulding
(f) Required strength
(g) High thermal conductivity.

Solder alloy (Grade J of BS 219) possesses all of the required properties and was used as the moulded material. Data concerning this material is presented in Table 2.1.

Experimentation showed that dampening the mould with water, prior to the moulding operation, produced the required smooth surface finish shown by Figure 1.4. Using this relatively simple moulding procedure it was not found possible to reproduce the thickness of the stainless steel elements. The solder elements were 2.8 mm (0.11 ins.) thick as opposed to the thickness of 3.2 mm (0.125 ins.) of the steel elements. This difference came as a result of producing moulds under compression while during the actual moulding of the solder elements

the moulds were not in their compressed form.

2.10.4 Insertion and Removal of Inserts.

The Pall rings were positioned within the test section by pushing them into the tube and locating them using a length of tough P.V.C. tube. As noted previously, they did not dislodge from their required locations during the tests, presumably due to their elasticity. The Pall rings were removed using an aluminium rod with a steel hook tapped into one end.

The swirl flow inducers, which fitted tightly within the tube, were located using an aluminium rod with a Terry clip attached to one end, this enabled the inserts to be positioned with aligned or perpendicular trailing edges. To ensure that the elements did not dislodge from their required locations a slight indentation of the tube wall was made at the axial position of each element. This procedure was performed using a tube cutter from which the cutting wheel had been replaced by a small thicker wheel. For configurations 5T, 6T, and 5K, the inserts were soldered together to form the required number of separate pairs of inserts and only one tube identation, per insert pair, was required. For the continuous insert configurations, for example 7T, the elements were soldered together to form one continuous length and therefore only one tube indentation, at the downstream end of the inserts, was required.

The swirl flow inducers were removed from the tube by placing a rubber bung inside the tube and then gently tapping the inserts out of the tube using a metal rod.

3 Experimental Techniques

3.1 Introduction

This section describes the operating procedures used for the calibrations of the equipment. Also described is the general operation of the experimental facility.

3.2 Calibration techniques

3.2.1 Rotameter calibrations.

As stated previously, the orifice sections and connecting pipework to the rotameter were lagged; with this precaution early sample tests showed that the temperature drop between a thermocouple in the orifice calming section and one immediately downstream of the rotameter used, never exceeded $0.1^{o}C$. For this reason calculations were based on the temperature in the calming section. Pressure drops were measured using two 1000 mm (39.4 ins.) manometers, one contained a carbon tetrachloride/iodine mixture, the other contained mercury.

For the scale range 2 to 12, the rotameter R1 was calibrated against the smaller diameter orifice plate. The water in tank T102 was heated up to almost $97^{o}C$ using the steam injector, S1. This water was passed through the heating jacket while the tube side fluid was passed through the test section, orifice and rotameter, R1. When the tube side fluid temperature was approximately $92^{o}C$ the pump P102 was switched off, any air in the lines connecting the orifice section and manometer was bled off, and the rotameter scale reading was adjusted to 2 units. The fluid passing through the orifice section was allowed to cool to approximately $90^{o}C$ and the temperature of the fluid and ambient air and the pressure drop across the orifice plate were recorded. The rotameter scale reading was adjusted to 4 units and the temperatures and pressure drop again recorded; this procedure was repeated for 2 unit rotameter scale increments upto 12 units. The whole process, including the air bleeding operations, was repeated at approximately $5^{o}C$ temperature increments down to ambient temperature. At high temperatures the fluid was allowed to cool by natural convection to the ambient air. However, as the fluid temperature decreased the cooling rate was unnecessarily long and in these cases a small

amount of cold water was added to T102 and the pump P102 was used to circulate the water across the test section. When the tube fluid temperature was approximately 1°C above the required temperature the pump P102 was again switched off and the previous procedure was adopted. The larger diameter orifice plate was used for calibrations with rotameter (R1) scale readings, greater than 12 units, upto 24 units.

Before calibrating the rotameter, R2, the test section was filled with cold water, and the annulus side fluid heated upto approximately 92°C. The fluid was allowed to cool by convection and the method adopted for calibration of R1 was repeated over the scale range of 2 to 10 units for the rotameter R2. The cooling rate could be accelerated by circulating the cold tube side fluid. In performing these calibrations the orifice sections were positioned immediately upstream of R2; the smaller diameter orifice was used throughout. At this time the steam injector was positioned in the flow loop of pump P102 and due to the power limitations of this pump the maximum obtainable rotameter scale reading was 10 units.

One hundred and thirty flowrates were measured using the rotameter, R1, and seventy eight flowrates were measured using R2.

3.2.2 Thermocouple calibrations.

The hot junctions and the probe of a Kane-May-Comark digital thermometer were bound together using rubber bands and then placed inside a 20 mm inside diameter copper tube. This assembly was placed inside a thermostatically controlled water bath. The digital thermometer, previously calibrated by the manufacturers, used temperature graduations of 0.1°C. The water temperature inside the copper tube was indicated by the digital thermometer and the thermocouples at a total of 80 temperatures over the range 0°C to 99.9°C. The e.m.f. outputs of the thermocouples, after conversion to temperature equivalents using BS 4937: 1973: Part 4 (14), always agreed to within ± 0.12°C with the value shown by the thermometer. Frequency distribution charts, frequency versus relative order of the temperature recorded by each thermocouple, were compiled.

Thermocouples T1, T2, T3, and T4 were used for the primary temperature measurements because they showed the most normally distributed frequency charts.

3.2.3 *Determination of the heat losses to the ambient air.*

The calming section and mixing cup, M3, were disconnected from the test section which was then packed with asbestos rope. Hot water was passed through the heating annulus, the inlet temperature of this water was varied over the range 77°C to 95°C (171°F to 203°F) and the scale reading of the rotameter, R2, was varied over the range 6 to 10 units. The annulus section and connecting pipework had previously been lagged. The thirty-two runs performed showed that the heat content of the fluid leaving the annulus, when expressed as a ratio with the heat content of the inlet fluid, lay within the range 1.01 to 0.99. Using the same procedure but with the calming section and mixing chamber, M3, connected to the test section, the same ratio range as above was found. In the latter instance the calming section was also packed with asbestos rope; the use of this material, which has a low thermal conductivity, ensures that heat is only lost to the ambient air. Furthermore, to ensure that heat is not used to raise the temperature of the lagging or packing, the heat input was applied for approximately one hour prior to the initiation of the tests.

3.3 Procedures for the operation of the experimental facility

3.3.1 Isothermal pressure drop measurements.

Prior to experimentation, sodium hypochlorite solution was added to the water in each of the holding tanks. The dilute bleaching solution so formed was passed around the tube side and annulus side flow loops and eventually drained from the system which was then "washed" with water. In this way the formation of scale deposits was almost totally eliminated. These operations were performed almost every day including before the heat transfer tests.

During the isothermal tests the average temperature of the fluid in the test section was maintained to within 0.5°C of the ambient temperature by using the valves V5 and V6. During these tests there was no water in the annular section. The need to cool the fluid was a result of the frictional heating in the pump P101 and the associated pipework. Throughout the tests it was always ensured that no air bubbles existed within the manometers and the tubing connecting the test section to the manometers. Prior to any testing it was also

ensured that the manometer fluid in each leg of the manometers was indicating the same level when there was no flow along the test section. Approximately five minute intervals elapsed between the adjustment of the fluid flowrate and the measurement of the manometer fluid differential and the ambient and fluid temperatures. Three results were obtained at each of nine fluid flowrates.

While testing certain configurations the above procedures were also adopted using an average fluid temperature of 35°C.

3.3.2 Data acquisition under heating conditions.

The tube side fluid flowrate was adjusted using the valves V1 and V2, the annulus side flow, which was maintained at a constant value throughout a set of tests, was adjusted using valve V3. The tube side fluid temperature was controlled using valves V5 and V6 such that the average of the temperatures at T1 and T2 was within 0.13°C of 35°C. Valve V4 was used to control the annulus side fluid temperature. The average of the temperatures at T3 and T4 was maintained at 80°C, again to within 0.13°C. No data was recorded until at least 1½ hours after initiating the heating of the annulus side fluid. At each tube side fluid flowrate three sets of the required data were recorded at 20 minute intervals. Tests were generally performed at nine tube side flowrates. Regular checks of the float levels in the rotameters and the fluid temperatures were made to ensure that steady conditions had been maintained.

The correct functioning of the thermocouples was checked by calculating the heat balance using :

$$\frac{\text{Heat output}}{\text{Heat input}} = (\text{Multiplying factor}) \frac{(T2 - T1)}{(T3 - T4)} \qquad (3.1)$$

The values of the appropriate multiplying factor are given in Table 3.1. Values of the above ratio were in the range of 0.94 to 1.06. On the occasions that these limitations were not satisfied it was found that either one of the thermocouple cold junctions had broken or that physical contact between two cold junctions had occurred. The latter difficulty was overcome by placing short lengths of flexible tube over the lengths of thermocouple cable near to the cold junctions.

Obviously no data was recorded if either of the above two defects prevailed. The thermocouples T5 and T6 acted as readily available checks on the thermocouples T2 and T4.

Pressure loss measurements were made during the heating tests. As with the isothermal tests, it was always ensured that no air bubbles existed in the manometer lines.

4 Data analysis techniques

4.1 Introduction

This chapter presents the equations used for the calculation of the properties of the materials and fluids used in this work. The techniques used to convert the raw experimental data into readily usable forms, such as dimensionless groups, are also considered.

4.2 Conversion of the e.m.f. data

The e.m.f.s which were recorded on paper rolls were converted to equivalent temperatures using the data of BS 4937 : Part 4 : 1973 (14). This standard provides e.m.f. data at $1^{o}C$ temperature intervals; linear interpolation between these values was used. Converted e.m.f.s were "rounded-up" to the nearest $0.01^{o}C$. On three occasions throughout the project the accuracy of the digital voltmeter was checked using a voltage source and a voltmeter which had recently been calibrated by the manufacturers. The agreement was always within 0.001 mV, this corresponds to an equivalent temperature change of approximately $0.02^{o}C$.

4.3 Properties of the materials and fluids

4.3.1 Specific gravities of the manometer fluids.

A small volume thermocouple is susceptable to ambiant temperature deviations which occur over a short time interval, for example, those caused by a brief draught. For this reason a mercury in glass thermometer was used to measure the temperature of the ambient air.

The specific gravity of the carbon tetrachloride/iodine mixture, used during some of the earlier tests, was experimentally found to be 1.6. The density of pure carbon tetrachloride was determined from the large amount of data which was obtained during studies involving mixtures of carbon tetrachloride and other liquids. This data is presented in Landolt and Börnstein (76) and the extracted results for 100% carbon tetrachloride are presented as Figure 4.1 of this thesis. The specific gravity was calculated using the values of the density of water that are presented by Perry and Chilton (97, p. 3-71).

The specific gravity of mercury at various temperatures was

determined from Perry and Chilton (97, pp. 3-71 and 3-72). The data is presented as Figure 4.2.

4.3.2 Properties of water.

Many of the computer programs, see section 4.6, which perform the analyses of the experimental data require the knowledge of the properties of water at various temperatures. The latter requirement enforces the use of equations for the calculation of the properties. This was not necessary when determining the specific gravity of the manometer fluids.

The equations used for the calculation of the properties have been obtained from Dorsey (35) and the interested reader is referred to this source for further details, for example, concerning the effect of dissolved air.

(i) Specific Heat Capacity, c_p

Specific Heat Capacity of Water = 1.00 Btu $lb^{-1}\ ^{o}F^{-1}$ (4.1)

The effect of temperature over the range of the experiments produces deviations from the above value of less than 0.5%, see Dorsey (35, pp. 257 et. seq.).

(ii) Thermal Conductivity, k

$$k = 0.339\ (1 + 0.00281\ (t-20))\ \text{Btu ft}^{-1}\text{hr}^{-1}\ ^{o}F^{-1}$$

$$= 0.00587\ (1 + 0.00281\ (t-20))\ \text{W cm}^{-1}\ ^{o}C^{-1} \quad (4.2)$$

where t = fluid temperature, ^{o}C

See Dorsey (35, pp. 273 et. seq.)

(iii) Viscosity, μ

$$\mu = \frac{100}{2.1482\ [(t-8.435) + (8078.4 + (t-8.435)^2)^{0.5}] - 120} \text{ cP} \quad (4.3)$$

where t = fluid temperature, ^{o}C

See Dorsey (35, pp. 182 et. seq.).

(iv) Density, ρ

$$\rho = 1 - \frac{(t-3.9863)^2\ (t + 288.9414)}{508929.2\ (t + 68.12963)}\ \text{g cm}^{-3} \quad (4.4)$$

where t = fluid temperature, ^{o}C

See Dorsey (35, pp. 250 et. seq.).

4.3.3 Properties of copper.

From Kern (62, p. 799) :

k_w = 218 Btu $ft^{-1}hr^{-1}\,{}^oF^{-1}$ at 212^oF

and k_w = 207 Btu $ft^{-1}hr^{-1}\,{}^oF^{-1}$ at 932^oF

Hence, by linear interpolation :

$$k_w = 221.2 - (11/720)\,t \quad \text{Btu } ft^{-1}hr^{-1}\,{}^oF^{-1} \qquad (4.5)$$

where t = temperature of the copper, ^oF

Converting to SI units, then

$$k_w = 382 - 0.0476\,t \quad W\,m^{-1}\,{}^oC^{-1}$$

where t = temperature of the copper, ^oC

4.4 Pressure differentials

BS 1042 (13), which was used for the rotameter calibrations, relies on the measurement of the pressure drop across an orifice plate. Similarly a friction factor is a representation of the pressure loss along a pipe. For each of these two situations one of the measured quantities is the manometer fluid head differential. This quantity may be converted to an equivalent pressure loss. Coulson and Richardson (29, p. 101) consider the conversion of the fluid differential that is indicated by a simple U-tube manometer. That analysis is presented here in order to show the logical extension to the case of manometers which are connected in series.

(a) Simple U-tube Manometer

As shown in Figure No. 4.3 the manometer fluid is of density ϱ_m, the less dense fluid above is of density ϱ. For equilibrium, the pressure in each limb at level a-a must be the same, thus

$$P_2 + z\varrho g = P_1 + (z - H)\varrho g + H\varrho_m g$$

$$\Rightarrow \Delta p = P_2 - P_1 = H(\varrho_m - \varrho)g$$

$$= H(S - 1)\varrho g \qquad (4.6)$$

(b) U-tube Manometers Connected in Series

Referring to Figure No. 4.3 and applying a pressure balance analysis to the nth manometer of the series, it is found that

$$\Delta P_n = P_{n+1} - P_n = H_n(S - 1)\varrho g \qquad (4.7)$$

Therefore, the total pressure drop is given by

$$\Delta p = P_N - P_1 = \sum_{1}^{(N-1)} \Delta P_n$$

$$= (S - 1)\rho g \sum_{1}^{(N-1)} H_n \qquad (4.8)$$

Since the fluids of density ρ and ρ_m are incompressible it can be stated that if the initial fluid levels are identical in all of the manometers then

$$\Delta p = (S - 1)\rho g (N - 1) H \qquad (4.9)$$

where H is the fluid level differential in each manometer.

4.5 Calibration of the rotameters

As shown in Chapter 6, the accuracies of the heat transfer coefficients and friction factors depend on the accuracy of the mass flowrate measurements. During the initial construction of the experimental facility, each of the rotameters, R1 and R2, was calibrated in situ using water at room temperature. The method used was simply the measurement of the time required to collect a known volume of water at a given rotameter scale reading. At this early stage in the experimental program it was hoped that tests would be performed for average tube side temperatures of 35, 50 and 65^{o}C. It was intuitively considered that the volumetric flowrate indicated by the rotameter scale reading is dependent on the fluid temperature. (As the experimental work progressed it became evident that insufficient time would be available to study the Prandtl number effect on the heat transfer coefficients.)

At the high flowrates required, the determination of the effect of temperature on the measurement of water volumetric flowrate using the rotameters could not be performed using the simple tank and stop watch method since the heating requirement was not available. The rotameter manufacturers were consulted and reference (45) was obtained. However, the manufacturers instructions are not explicit concerning the effect of temperature on the measured flowrates. For a given rotameter tube and float, an 'impedance', 'fiducial' flow, and '% of the fiducial flow', are calculated with the aid of the manufacturer's charts using the density and viscosity of water. The actual volumetric flowrate is the product of the % of the fiducial flow, which is a function of the impedance and scale reading, and the fiducial flow.

The charts are difficult to use for small changes of impedance, and it was considered that the fluid and rotameter temperatures, and not only the fluid properties, would affect the flowrate measurements. Furthermore the conversion of the manufacturer's charts into an equation for use in computer programs may be difficult and somewhat inaccurate due to the use of charts rather than tabulated data.

A typical form of equation that may be used, in certain circumstances, for the calculation of the volumetric flowrate passing through a rotameter, is given by Coulson and Richardson (29, p. 121) as

$$Q = c_D A_2 \left[\frac{2 g V_F (\rho_F - \rho)}{\rho A_F (1 - (A_2 / A_1)^2)} \right]^{0.5} \qquad (4.10)$$

The obvious problems with this form of equation are that the dimensions and thermal properties of the components of the rotameter need to be known accurately. However, the type of glass and steel, forming the rotameter, are often unknown and the drag coefficient, c_D, is dependent on the shape of the float.

A further publication of the rotameter manufacturers (104), which is similar in method to reference (45) but differs in the numerical values of impedance etc., shows that

$$I = \text{'Impedance'} = \log_{10} \left[K_{F1} \mu \left[\frac{10^8}{g V_F (\rho_F - \rho) \rho} \right]^{0.5} \right] \qquad (4.11)$$

$$Q_T = \text{'Fiducial flow'} = K_{F2} \left[\frac{g V_F (\rho_F - \rho)}{\rho} \right]^{0.5} \qquad (4.12)$$

The % of the fiducial flow, f, is obtained from a chart, and the actual flowrate is then given by

$$Q = f Q_T \qquad (4.13)$$

The above shows that any equation used to represent the effect of temperature on the flowrate measurement will be complex. A number of workers have found that, for a given fluid temperature, the volumetric flowrate passing through the rotameter may be represented as a linear function of scale reading, over short scale ranges, or as a quadratic function of scale reading over large scale ranges.

From this it was considered that

$$f = f'(I) + f''(I)\, R_s + f'''(I)\, R_s^2 \qquad (4.14)$$

If each of the functions f', f'', and f''', are considered to be a quadratic then

$$f = a_0 + b_0 I + c_0 I^2 + a_1 R_s + b_1 I R_s + c_1 I^2 R_s + a_2 R_s^2 + b_2 I R_s^2 + c_2 I^2 R_s^2 \qquad (4.15)$$

As previously shown in Chapter 3, the rotameters were calibrated against orifice plates using BS 1042 (13). However, since the above 'impedance' is a function of temperature it was concluded that one possible form for representing the calibration results was :

$$Q = A_0 + B_0 t + C_0 R_s + A_1 t R_s + B_1 R_s^2 + C_1 t R_s^2 + A_2 t^2 + B_2 t^2 R_s + C_2 t^2 R_s^2 \qquad (4.16)$$

As noted above, the effect on the scale reading of the volumetric flowrate may be considered a linear function over small ranges, similarly it was thought that the effect of temperature may also be linear over short temperature intervals. Based on these postulates the following three equations were also considered for use :

$$Q = A_0 + B_0 t + C_0 R_s + A_1 t R_s + B_1 R_s^2 + C_1 t R_s^2 \qquad (4.17)$$

$$Q = A_0 + B_0 t + C_0 R_s + A_1 t R_s + A_2 t^2 + B_2 t^2 R_s \qquad (4.18)$$

$$Q = A_0 + B_0 t + C_0 R_s + A_1 t R_s \qquad (4.19)$$

Furthermore, the following equations which neglect the effect of temperature were also considered :

$$Q = A_0 + C_0 R_s + B_1 R_s^2 \qquad (4.20)$$

$$Q = A_0 + C_0 R_s \qquad (4.21)$$

The deviations of the experimental calibration data from these equations is considered later in this section.

Computer programs were developed to analyse the raw experimental data using the procedures of BS 1042 (13) and to perform regression analyses using equations (4.16) to (4.21). The graphical data in BS 1042 was converted to the equations which are presented in

Appendix A.2. The error analyses obtained using the raw data and the calibration computer program are presented as Table 4.1 and Figure 4.4. The computer program and the raw data have not been presented in order to limit the size of this thesis. The calibrations clearly demonstrate the accuracy of the postulates considered above. For the rotameter R1, which was calibrated over a large scale range, it is necessary to use a quadratic function of scale reading although Figure 4.4 shows that a linear function of temperature is adequate. For rotameter R2, which was calibrated over a relatively short scale range, the difference in using a quadratic or linear function of scale reading is less pronounced; the temperature effect is well correlated using a linear function. Since the volumetric flowrates were to be calculated using computer programs the best fitting equations were used, that is, the equations with quadratic functions of flowrate and temperature. The equations are

for rotameter R1 :

$$Q = 3.402 \times 10^{-3} + 2.6 \times 10^{-6} t + 1.2744 \times 10^{-3} R_s + 3.285 \times 10^{-6} t R_s + 1.3 \times 10^{-5} R_s^2 - 1.1307 \times 10^{-7} t R_s^2 + 6.01 \times 10^{-8} t^2 - 3.622 \times 10^{-8} t^2 R_s + 1.466 \times 10^{-9} t^2 R_s^2$$

for rotameter R2 :

$$Q = 2.912 \times 10^{-3} + 1.09 \times 10^{-5} t + 7.601 \times 10^{-4} R_s - 6.3 \times 10^{-7} t R_s + 9.75 \times 10^{-6} R_s^2 - 2.23 \times 10^{-8} t R_s^2 - 7.14 \times 10^{-8} t^2 + 1.1915 \times 10^{-8} t^2 R_s - 2.14 \times 10^{-10} t^2 R_s^2$$

where

Q = volumetric flowrate, $ft^3 s^{-1}$

t = fluid temperature, ^oC

and R_s = rotameter scale reading

4.6 The computer programs used for the analysis of the experimental data

The analysis of the pressure drop data was performed using the program labelled EX-6010, see Appendix A.3. The symbols and their definitions which have been used in the computer programs are presented as Appendix A.7. The regression analysis of the pressure loss results, ϕ and Re, was performed by the program labelled FRICTION-6010; this is presented as Appendix A.4. The heat transfer data was analysed using the programs EX-6010 and HEAT2-6010, the latter is presented as

Appendix A.5. In the regression analyses, the values of "t_1" from Student's t-distribution, see Perry and Chilton (97, p. 1-40), are required. These values are presented in Appendix A.6.

The three computer programs include a number of "remark" (REM) statements which define the function of the referenced line numbers. The programs were compiled under the BASIC/VM language. This compiler allows the use of larger programs than may be compiled using many other forms of BASIC. BASIC/VM uses 14 figure arithmetic.

Sample computer print-outs are presented in Chapter 5. Some of the equations and data inputs used by the computer programs are considered in the remaining sections of this chapter.

4.7 Pressure drop analyses

The processed data was presented on the conventional co-ordinates of $\ln(\phi)$ versus $\ln(Re)$, where ϕ and Re are defined by equations (1.2) and (1.3). The dimensionless group, ϕ, is referred to as the "friction factor" although it must be emphasised that it does not represent the head loss due to purely frictional losses. For much of this work, ϕ represents such effects as those caused by frictional and form drag, and centrifugal forces. The hydraulic flow concept was not used in the analyses of the experimental data partly because the wetted perimeter and flow area cannot be clearly defined for tubes containing inserts which are interspaced along the tube length.

The processed pressure loss data was correlated by least squares regression in the form :

$$\ln(\phi) = A + B \ln(Re) \qquad (4.22)$$

Curvature of the data about this equation was noted by the determination of the correlation coefficient.

Using an empty tube with the fluid temperature maintained at ambient temperature, the friction factor was based on the total length between the pressure tappings, P2 and P3, that is, l = 1219 mm (48 ins.). The fluid velocity and density were determined at the average bulk fluid temperature between the pressure tappings. The friction factors for an empty tube operated under heating conditions were also based on a length of 1219 mm (48 ins.) but the average bulk fluid temperature over the heated tube length was used in the evaluations.

The friction factors for the tubes containing inserts were based on the axial distance between the upstream and downstream limits of the

section containing the inserts. The pressure drop between the pressure tappings, P2, and the leading edge of the first element of the configuration and the pressure drop between the trailing edge of the last element and the pressure tappings, P3, were calculated using equation (1.1) with a constant of 0.0396. The pressure loss used in the evaluation of the friction factor was determined by subtracting the above calculated values from the measured overall pressure drop. The fluid velocities and densities were determined in the same way as that used with the empty tube results. The implications of these pressure drop corrections are considered in Chapter 6.

4.8 Heat transfer analyses

4.8.1 Heat losses by conduction.

The heat "losses" by conduction along the tube wall were accounted for using :

$$q_{COND} = -k_w A_w \frac{\Delta t_T}{\Delta x} \qquad (4.23)$$

where q_{COND} = heat lost from the annulus section by conduction along the tube

k_w = thermal conductivity of the tube

A_w = cross sectional area of the tube wall

Δt_T = difference between the temperatures of the tube wall at two locations which are separated by a tube length of Δx.

These corrections were used in calculating the fluid properties for use in the pressure drop analyses and therefore they were calculated using the computer program EX-6010. Although the total heat "loss" by conduction never exceeded 0.4% of the total heat transferred between the process fluids, the corrections were applied by the computer program. In this way the program remained of general application, for instance, should it be required to be used with fluids with temperature sensitive properties or with different tubes.

4.8.2 The Wilson plot technique.

The raw data of the heat transfer tests were analysed using an adaptation of the Wilson method (137). The method, the adaptation, and the reasons for using this correlating procedure are given in this section.

The overall heat transfer coefficient for a concentric tube arrangement is given by

$$\frac{1}{U} = \frac{1}{h_a} + \frac{x_w\, d_o}{k_w\, d_m} + R_i + R_o + \frac{d_o}{d\, h} \qquad (4.24)$$

where $h = h\,(t_{av},\, u)$ (4.25)

Wilson only considered the situation where the tube fluid was water and he proposed for fixed annulus fluid, scale, and tube wall, resistances that

$$\frac{1}{U} = C + \frac{\varepsilon}{V^{0.82}} \qquad (4.26)$$

where V = tube side fluid velocity corrected for viscosity and density effects to a reference temperature, see Wilson (137) for further details

C = sum of the annulus fluid film, scale, and tube wall, resistances to heat transfer

ε = constant which depends on the tube dimensions. (ε will also depend on the type of inserts, if any, which are located in the tube).

However, the equations presented in section 1.2.4 all indicate that for fixed fluid properties :

$$h \propto u^{0.8} \qquad (4.27)$$

Presumably because of the substantial evidence which justifies the above proportionality a "Wilson plot" is usually considered to be a graph with ordinates of $1/U$ versus $1/u^{0.8}$.

Russell and Carnavos (107) used a "reverse" procedure to that above: for each tube side fluid flowrate the overall heat transfer coefficient was determined for three annulus fluid velocities, w, that is, the outside film heat transfer coefficient, h_a, was varied. Using the latter method the intercept on the $1/U$ axis, which is shown against an axis of $1/w^{0.8}$, is the sum of the scale, tube wall, and tube side fluid resistances. The tube wall resistance may be calculated, and neglecting any scale resistance the tube side film heat transfer coefficient can be determined. There are two possible disadvantages to this method, namely, any scale resistance is ignored, and the use of an exponent of 0.8 on the annulus fluid velocity may be suspect even with a turbulent flow. The latter disadvantage was noted in a later paper

by Carnavos (19). In this later work the exponent on the tube side velocity was considered to be 0.8. This procedure showed that, for the particular apparatus used in that work, the exponent on the annulus fluid velocity was 0.865.

The description of the calculation procedure in reference (80) shows that Margolis used the Wilson plot technique with the assumption that the tube side fluid velocity exponent is 0.8 for tubes containing coiled wires and twisted tapes. (Carnavos (19) only used the Wilson technique with empty tube results in order to determine the value of C). However, the results of Margolis (80), when presented on logarithmic co-ordinates of Nu versus Re, do not indicate that Nu is proportional to $Re^{0.8}$. Although the work of Kreith and Margolis (73) appears to be based on the work in reference (80) it is shown that Nu increases more rapidly with Re, for tubes containing their inserts, than an exponent of 0.8 would imply.

The apparent anomaly that the Wilson plot technique, with an exponent of 0.8, does not yield a ln(Nu) versus ln(Re) graph with a slope of 0.8, is now discussed.

Returning to the original concept of Wilson (137) with the adjusted exponent, it has been noted that for cases where all of the variables are fixed, except the tube side fluid velocity, then

$$\frac{1}{U} = C + \frac{E}{u^{0.8}} \qquad (4.28)$$

From experimental values of U and u it is possible to determine the value of C by using a graph with ordinates of $1/U$ and $1/u^{0.8}$. The tube side film heat transfer coefficient is then calculated using

$$h = \frac{d_o}{d\,[(1/U) - C]} \qquad (4.29)$$

Heat transfer correlations are often presented in the dimensionless form

$$Nu = Nu\,(Re, Pr) \qquad (4.30)$$

A commonly accepted form of presentation of the data is

$$\ln\left[\frac{Nu}{Pr^{0.4}}\right] = \ln(F) + E \ln(Re) \qquad (4.31)$$

Substituting equation (4.29) into equation (4.31) shows that

$$\ln\left[\frac{Nu}{Pr^{0.4}}\right] = \ln\left[\frac{d_o}{[(1/U) - C]\, k\, Pr^{0.4}}\right]$$

$$= \ln(F) + E \ln(Re) \qquad (4.32)$$

The value of C may be determined by performing a "least squares" fit of the experimental data with equation (4.28). However, using this value of C with equation (4.32) and performing a least squares analysis with this equation will not necessarily show that E = 0.8. Initially it was considered that this ambiguity might be due to any slight fluctuations in the tube side fluid temperature. To test this hypothesis, the following procedure was used :

$$Nu = F\, Re^{E}\, Pr^{G} \qquad (4.33)$$

Rearranging this equation and substituting into equation (4.24), with all resistances except the tube side film resistance assumed to be constant, shows that

$$\frac{1}{U} = C + \left[\frac{d_o}{F\, Pr^{G}\, k}\right]\left[\frac{1}{Re^{E}}\right] \qquad (4.34)$$

The similarity between equations (4.28) and (4.34) is obvious. Correlating the experimental data in the form of equation (4.34), with G = 0.4 and E = 0.8, allows the value of the heat transfer resistance, C, to be determined. Using this value of C in equation (4.32), and performing a regression analysis, again will not necessarily show that the regression parameter, E in equation (4.32), is 0.8. The ambiguity is due to the fact that the data is fitted to two different equation forms and the distribution of the deviations of the experimental data from the least squares equations is different for each equation. The results obtained using these forms of the equation, i.e. (4.32) and (4.34), will only be identical if the data is exactly fitted by the equations.

To eliminate the above ambiguity the experimental data of the present work was processed using regression analysis with equation (4.32). This analysis used a linear regression fit of the logarithms in equation (4.32) and iteration was used to determine the heat transfer resistance, C. The iteration procedure was terminated when the change in the value of C was within a specified limit, or when the value of E was 0.8, again within a specified limit. These calculations were performed by the computer program HEAT2-6010.

As described in Chapter 3, a set of experimental results consists of twenty-seven runs. The procedure used to obtain the processed results and to determine the heat transfer resistance, C, is outlined by the following points :

(i) Obtain experimental data using an empty tube. Use this data with a regression analysis of equation (4.32) with the assumption that E = 0.8. This determines the heat transfer characteristics of the empty tube. This procedure requires the use of the programs EX-6010 and HEAT2-6010.

(ii) Obtain experimental data using the tube with inserts. A number of configurations may be tested.

(iii) Perform experimental tests using the empty tube and process the resultant data by the method used in (i).

(iv) Process all of the fifty-four experimental runs from (i) and (iii) using a regression analysis of equation (4.32) with the assumption that E = 0.8. In this way the average value of the heat transfer resistance (scale, tube wall, annulus fluid film), C, that occurred over the time period between (i) and (iii), is calculated.

(v) Perform regression analyses of equation (4.32) with the results obtained using each configuration in (ii). In this procedure, use the value of C that was obtained in (iv) and do not use the Wilson assumption that E = 0.8.

(vi) Points (ii) to (v) may be repeated. It is unnecessary to repeat (i) since the empty tube results obtained in (iii) may now to used as the first set of empty tube results.

On some occasions it was not possible to easily remove the swirl flow inducing inserts from the tube after the tests in part (ii). This was due to the inserts being too firmly held at their required locations by the slight indentations of the tube wall, see section 2.10.4. Under these circumstances the tube was not used in any further tests. The value of C used in analysing the results obtained with those inserts was considered to be that obtained from a single set of empty tube results (from part (i)) that were obtained immediately prior to the insert tests.

For the periods when the inserts were held by the tube indentations, the value of C that was used in processing the insert data was that obtained using the empty tube with the same number of tube indentations as were required by the insert tests. It will be shown in Chapter 5 that the slight tube indentations had a negligible effect on the heat transfer and pressure drop results.

It is obvious that in using the above procedures a considerable number of sets of empty tube data were obtained. The purpose of these tests was to determine the sum of the scale, tube wall, and annulus fluid film, resistances to heat transfer, C. However, the acquisition of such data also provided a frequent check on the reproducibility of the pressure and temperature measuring equipment.

5 Experimental Results

5.1 Introduction

The raw data obtained experimentally, and the computer outputs of the calculated data, are not presented in this thesis: the data may be obtained from the address noted in the Preface. Sample computer outputs, which demonstrate the various methods of using the computer programs, are given in this chapter. The reference numbers used to identify the insert configurations are those given in Figures 1.5, 1.6, and 1.8.

The calculated data is presented graphically in the conventional forms of $\ln(\emptyset)$, or $\ln(Nu/Pr^{0.4})$, versus $\ln(Re)$. To obtain a clear presentation it has been necessary, due to the close proximity of the data, to present the experimental results in a number of graphs rather than on a single graph. For each type of insert and mode of operation the results are discussed at the point in the text at which they are first introduced. However, certain observed trends were noted which involve the use of results obtained under various modes of operation (e.g. heating and isothermal) and with various configurations (e.g. aligned and perpendicular leading edges of swirl flow inducers). These trends, and the pertinent graphical presentations, are presented in sections 5.2.4 and 5.4.4. The present chapter does not compare the results of this work with those obtained by previous workers using continuous full length twisted tapes and Kenics mixers; those comparisons are the purpose of Chapter 7.

While awaiting the construction of the steam injector and heating jacket, tests were performed using an empty tube under isothermal conditions. These tests showed that fouling of the tube, over a three month period, produced friction factor increases of approximately 1.5% and 3.5% at Reynolds numbers of 15000 and 35000, respectively. The trend of convergence at low Reynolds numbers is characteristic of tube wall roughness effects and this was supported by photographs obtained using an electron microscope. Flushing the tubes with very dilute sodium hypochlorite solution prior to testing, and daily operation of the equipment, produced results which showed no roughness effects.

Empty tube pressure drop measurements between the pressure tappings at P1 and P3, and between P2 and P3, see Figure 2.1, showed that the friction factors calculated for the total tube length were

approximately 1.5% greater than those obtained along the test section alone. The latter may be due to a hydrodynamic entrance length effect or positioning of the tappings at P1 in a region of flow disturbance caused by the mixing mesh, M1. Further tests used only the tappings at P2 and P3.

5.2 Data obtained using Pall rings

5.2.1 Friction factor data obtained under isothermal conditions.

Figure 5.1 shows that the experimentally determined empty tube results are in acceptable agreement with the commonly used Blasius equation. Deviations from the Blasius equation are most noticeable at low Reynolds numbers where the measured manometer fluid differentials are small, typically 5 cm. The use of an inclined manometer would overcome this disadvantage but, due to the small deviations from the Blasius equation, the use of such a manometer was considered unnecessary. During the period of testing the configurations using swirl flow inserts, the manometers were cleaned more frequently and this produced a reduction in the maximum deviations of the experimental empty tube results from those calculated using the Blasius equation.

In most cases the symbols used for the representation of the experimental data denote the results of a number of pressure drop determinations: this can be seen from Table 5.1 which shows the number (No.) of results obtained. Pressure drops were determined using individual and multiple pressure tappings at the points P2 and P3; this provides a reasonably severe test of the reproducibility of the results.

The maximum manometer fluid differential that could be determined was approximately 90 cm. Unfortunately, the head of mercury equivalent to a head of carbon tetrachloride/iodine mixture of slightly greater than 90 cm was found to be insufficiently large for accurate determinations. For this reason there is an absence of experimental data in certain ranges of the friction factor curves. This shortcoming of the apparatus was overcome during the tests using swirl flow inducers by utilizing longer manometers.

5.2.2 Friction factor data obtained under heating conditions.

The comments of section 5.2.1 also apply to the results shown

by Figure 5.2 and Table 5.2. (The calculated friction factors, ϕ_{CALC}, are considered in section 5.2.4).

For the results obtained under heating conditions, the experimental empty tube data shows lower friction factors than those predicted by the Blasius equation; this is due to the reduced fluid viscosity at the tube wall. Comparing Figures 5.1 and 5.2 it is seen that for configurations 0, 1P, and 2P, the isothermal friction factors are greater than the heating values at the same Reynolds number. For configurations 3P and 4P the two sets of results are almost identical, while for configurations 5P and 6P the isothermal friction factors are slightly lower than the corresponding heating values. For the two latter configurations a relatively large proportion of the tube wall is covered by the rings and therefore the reduced fluid viscosity at the tube wall will have a small effect. Furthermore, the Pall rings may be considered to behave as a tube wall roughness with the insets of the rings producing form drag. These two factors may be the dominant effects leading to the resulting friction factors. On this hypothesis the friction factors, obtained under isothermal and heating conditions with large numbers of rings in the tube, are expected to be comparable in magnitude. For configurations 5P and 6P, the results obtained under the two conditions deviate by about 5% (maximum) and generally by less than about 1%. These deviations are within the uncertainty of the experimental data.

5.2.3 Heat transfer factor data.

Figures 5.3 to 5.8 and Table 5.3 show that the scatter of experimental data about the regression lines is quite small. However, it will be shown that, in most cases, the experimental scatter for the results obtained while using the swirl flow inducers is less than that noted while using Pall rings; this reduction in data scatter was produced by placing short rubber sleaves over the thermocouple ice junctions (see section 2.8.1).

Two sets of results obtained using the empty tube, denotations A and B in Table 5.3, were analysed together to calculate a value of the heat transfer resistance, C. This value was used in the analysis of the data obtained using configurations 6P and 4P; the latter configurations were tested during the time period between the tests of denotations A and B. Similarly the remaining four configurations were

tested in the time period between the tests of denotations B and C. Since most of the data was based on the analysis of the latter two sets of empty tube data, the characteristics of the empty tube were considered to be those calculated using the program HEAT2-6010 with the latter empty tube data. Using the average value of the heat transfer factor multiplier, F, for the results of denotations A, B, and C, the value of F would have been only 1.6% lower, i.e. 0.0235. The empty tube results are in good agreement with the results of Dittus and Boelter, see equation (1.19), using the entry length correction outlined in section 1.2.5. The empty tube data has not been represented graphically since it is discussed in section 5.3.

Figure 5.9 shows the regression equations which represent the heat transfer characteristics of the tubes. Discussion of these characteristics is given in the next section.

5.2.4 Discussion of the results obtained using Pall rings.

Figures 5.10 and 5.11 show that the Reynolds number exponents and multipliers of the heat transfer factor and friction factor equations vary between the empty tube values and the values obtained using configuration 6P as the covered fraction of the tube wall area increases. The fraction of the tube wall area, that was uncovered, was calculated by assuming that the circumference of each Pall ring contacted the inner surface of the tube. The surface area of the rings does not include the surface area of their insets.

Leva, see Perry and Chilton (97, p. 4-38), measured the heat transfer through the walls of containers filled with a fixed bed and found that

$$E = 0.90 \quad \text{for } (D_p / d) < 0.35 \qquad (5.1)$$

and

$$E = 0.75 \quad \text{for } 0.35 < (D_p / d) < 0.65 \qquad (5.2)$$

By analogy, it may be tentatively considered that configuration 6P of the present work behaves as a packed bed with $(D_p / d) > 0.65$. The latter restriction implies that a large volume of the bed is unoccupied by the packing and a relatively small proportion of the container wall surface area is covered by the packing; these criteria apply to configuration 6P.

Chilton and Colburn (26) found at high rates of flow through packed beds, that

$$B = -0.15 \quad \text{for } (D_p / d) < 0.25 \qquad (5.3)$$

In the present work, it may be expected that increasing the number of Pall rings in the tube will have a similar effect to that produced by reducing the value of (D_p / d) in a packed bed. Hence it is expected that the value of B would tend towards the value found by Chilton and Colburn (26); Figure 5.11 clearly shows this trend.

It is difficult to calculate an equivalent diameter of the Pall rings which may be used in the available correlations which apply to packed beds. It was because of this difficulty that the tube wall surface coverage was chosen as an ordinate of Figures 5.10 and 5.11. However, this choice involves an anomaly which may be inherent in using inserts interspaced along a tube. Unless the effect of each insert is limited to the axial position in which it is located, the measured heat transfer and pressure drops will be affected by the spacing of the inserts. On this basis the effect of the insert spacing on the parameters of the regression equations should be studied. Replotting the data in this form shows trends similar to those of Figures 5.10 and 5.11.

Figure 5.9 shows the regression equations of the heat transfer data. It is seen that the heat transfer factor line of configuration 4P lies above that representing the data obtained with configuration 5P. This is not the expected trend although the parameters E and F apertaining to these configurations do not deviate from the trends shown in Figure 5.10. However, if it is assumed that the heat transfer coefficients in the inlet region are greater than the average value that was measured, it may be considered that the four rings at the inlet of configuration 5P are unable to significantly increase the heat transfer factor above the undeveloped empty tube value. Configuration 4P uses only two Pall rings in this assumed thermal "entry" region and therefore a higher proportion of the rings of this configuration are used in the region where the empty tube heat transfer coefficients are relatively low. The former discussion indicates that the heat transfer factors for these two configurations will be relatively close and the difference between the pertinent regression equations, which is 6% (approximate maximum), is within the uncertainty of the data.

If it is considered that the effect of each insert is limited to the pipe length in which it is situated then each configuration consists of a packed length and an empty tube length, hence

$$\phi_{CALC} = \frac{\phi_p \, l_p}{(l_p + l_o)} + \frac{\phi_o \, l_o}{(l_p + l_o)} \qquad (5.4)$$

where ϕ_o, ϕ_p = friction factors calculated using the regression equations which represent the characteristics of the empty tube and configuration 6P, respectively

l_p, l_o = actual total length of tube that contains (l_p), or does not contain (l_o), inserts between the upstream and downstream ends of the packed section of the tube.

The results of these calculations are shown by figure 5.2. The difference between the experimental and calculated results are indications of the deviations from a linear relationship between the friction factors and the number of Pall rings. These differences may be explained by referring to the empty tube and configuration 6P as producers of "undisturbed" and "disturbed" fluids. The calculated friction factors are smaller than the experimental values presumably because the empty tube lengths, between the inserts, contain a stream which is partly "disturbed" thereby increasing the pressure drop. Furthermore it may be considered that, for small ring spacings, the fluid will rapidly become "disturbed" upon entering the packed length, thus only small increases in the heat transfer coefficient are to be expected as the spacing is decreased. However, as the number of rings is increased the friction factor will increase due to the form drag on each ring, although the stream will not necessarily become much more "disturbed".

For large ring spacings, the heat transfer factor will rise more rapidly than for the above case since each insert that is added will enhance the "disturbance" of the fluid. The latter effect, and the relatively large increases in the pressure drop that is due to the form drag caused by each of the added inserts, will lead to rapid increases in the friction factor. The above considerations are in agreement with the data shown in Figure 5.12.

Equation (5.4) may be written in the more general form :

$$\phi_{CALC} = G_1 \, Re^{-n} \, H(l_R) + J_1 \, Re^{-p} \, Q(l_R) \qquad (5.5)$$

where $H(l_R)$ and $Q(l_R)$ are weighting functions which are dependent on the fraction of the tube length, l_R, that is occupied by the inserts; n, p G_1 and J_1, are constants. For a given configuration the weighting functions are constant, hence

$$\phi_{CALC} = G_2 \, Re^{-n} + J_2 \, Re^{-p} \qquad (5.6)$$

where G_2 , J_2 , n, and p , are constant. Coulson and Richardson (28, Chapter 1) show that the above equation forms have often been used for the correlation of data obtained using fixed packed beds. In the latter case, the weighting functions are dependent on the properties of the bed used. Such studies generally show that n = 1 and either p = 0, the Ergun (40) type of equation, or p = 0.1, the form used by Carman (16) and Sawistowski (108). The first term in each of the above equations represents the flow resistance due to viscous drag; the second term indicates the effect of kinetic energy losses in turbulent eddies. The correlation form for the packed bed data is generally based on the analogy with flow in empty pipes (28, p.6). Hence, it is not surprising that experimental friction factor data, for a smooth empty tube, is also correlated in the form of equation (5.6), see for example equations (1.5) and (1.6).

The above discussion infers that for a tube containing discontinuous sharp edged inserts the slope of the friction factor curve depends on the proportion of the tube which contains inserts. Tubes with a relatively large fraction of their length occupied by such inserts will exhibit shallow friction factor curves : the present work fully supports this conclusion.

Heat transfer factors for turbulent low viscosity fluids are not generally correlated in the forms of equation (5.5) and (5.6). This may be due to the difficulty in determining accurate and reproducible correlations. However, it is interesting to note that the Colburn analogy (27) was initially proposed using equation (1.5). This produces a two term heat transfer factor versus Reynolds number correlation. Furthermore, the entrance length effect on empty tube heat transfer, see equation (1.27), is also correlated in a similar form to equations (5.5) and (5.6).

5.3 Data obtained using an empty tube (Configuration 0)

5.3.1 Friction factor data obtained under isothermal conditions.

Table 5.4 shows the reproducibility of the experimental friction factor data. The maximum deviations of the 243 data items, denotations A to I in Table 5.4, from the values calculated using the Blasius equation, were +7.0% and -7.7%; the average values of these

maximum deviations were +4.4% and -6.7%, respectively. While the data shows acceptable agreement with the work of Blasius*, the friction factor curves are slightly steeper than that found by Blasius and other workers. As will be seen later, the friction factor slopes, obtained under heating conditions with an average fluid temperature of 35°C, were in good agreement with the values of Blasius and others. This tends to indicate that possible errors in the rotameter calibration may have been the cause of the difference between the experimental and previously reported results. Tests performed using an average fluid temperature of 35°C, but without heat input through the test section wall, produced a friction factor curve with a slope close to that obtained using water at ambient temperature, compare denotations A-I and J-K of Table 5.4. These results exhibit maximum deviations, from the Blasius predictions, of +4.6% and -3.7%, with average values of these maximum deviations of +3.7% and -3.7%. The mean ratio of the experimentally determined values to the Blasius predictions was 0.996; a value of 0.983 was obtained using the results of the ambient temperature tests.

The experimental data was obviously reproducible and the calculations of Chapter 6 show that the deviations from the Blasius predictions are within the uncertainty of the data. The manometers were regularly cleaned and no system leakages occurred hence no further reasons for the deviations considered above can be suggested.

Table A.8.1 (Appendix A.8) presents the raw experimental data which corresponds to denotation H of Table 5.4. The processed results from this sample data are presented as Table A.9.1 (Appendix A.9). The pertinent friction factor curve is shown as Figure 5.13.

5.3.2 Friction factor data obtained under heating conditions.

Pressure drop and heat transfer measurements were performed almost simultaneously. Tables 5.5 and 5.6 are compatible, except that no pressure drop measurements were performed during the tests of denotation A of Table 5.6. The present data, and that obtained under isothermal conditions, show that a straight line, on logarithmic co-

---

* In this work the Blasius equation is considered to be equation (1.1) with a constant of 0.0396.

ordinates, provides a good fit of all the data for each mode of operation. Denotation B-P of Table 5.5 shows that the maximum deviation of the experimental data from the regression equation is 5.11%, thereby indicating the reproducibility of the results. The average values of the mean, maximum, and minimum, ratios of the experimental data compared to the Blasius predictions are 0.907, 0.927, and 0.878, with certain results, or groups of results, deviating from these values by approximately 0.02.

As noted previously, the friction factors determined under heating conditions are reduced below the isothermal values, at the same Reynolds number, due to the reduced fluid viscosity at the tube wall. Using the empty tube friction factor regression equations that were determined using an average fluid temperature of 35°C, under isothermal and heating conditions, it is found that

$$\frac{\phi_{o(h)}}{\phi_{o(iso)}} = 0.908$$

This value was calculated using the regression equations (denotation J-K of Table 5.4 and denotation B-P of Table 5.5) at Reynolds numbers of 15500 and 104000. Using equations (1.18) and (1.53) it is estimated that the inside tube wall temperature was 50°C during the heating tests. The measured tube wall temperatures, T11 and T12, indicate that the outside wall temperature was 52.5°C. In further work the inside tube wall temperature will be considered to be 51°C, that is, the average of the two temperatures determined by the above two methods.

The results which are represented by denotation K of Table 5.5 are presented in Table A.8.2 (Appendix A.8) and Table A.9.2 (Appendix A.9). This sample data is shown as Figure 5.14.

5.3.3 Heat transfer factor data.

Table 5.6 presents the regression equations and analyses obtained from the 16 sets of empty tube heat transfer tests. The data scatter for all of the tests is quite low hence, to avoid repetition, only the data used in the reliability analyses of Chapter 6 are given in this thesis. The raw data, computer outputs, and conventional heat transfer factor graphs, for denotations I, K, and N, are given in Tables A.8.3 to A.8.5, Tables A.9.3 to A.9.5, and in Figures 5.15 to 5.17.

The Wilson assumption, $E = 0.8$, was used in analysing the 16 sets of empty tube results, hence it was judiciously considered that the equation used to represent all of the 432 individual results should use $E = 0.8$. For this reason, the value of F was calculated for each individual result obtained using configuration O. Denotation A-P in Table 5.6 shows the mean value of the regression parameter, F, that was obtained. The latter procedure is not a regression analysis and although a confidence interval and correlation coefficient could be determined for the representation of the distribution of the results about the equation of denotation A-P, such values were not obtained. It is interesting to note that, for the 16 sets of results, the average correlation coefficient and 95% confidence interval are 0.996 and 0.019, respectively.

The empty tube results were reproducible, however, they must be compared to the results reported by previous workers. As noted in section 1.2.5, the combination of equations (1.19) and (1.27) shows that F is expected to be 0.024 for the geometry of the present work. This compares favourably with the experimental result, $F = 0.0253$, when it is recalled that equation (1.19) has an accuracy of 20%. Alternatively rearranging the result of denotation A-P of Table 5.6 into the form of equation (1.24) it is found that the (Constant) is 0.0270. This value is in exact agreement with the result of Sieder and Tate (114) and the value found by Evans (43) using water. In performing the above rearrangement it was recalled that $Pr = 4.94$, and μ and μ_s are evaluated at $35^{o}C$ and $51^{o}C$, respectively.

For the copper tubes, used in the tests of denotations A to J in Table 5.6, the average value of the heat transfer resistance, C, was found to be 2.02×10^{-4} $m^2\ ^{o}C\ W^{-1}$ (1.14×10^{-3} $ft^2\ hr\ ^{o}F\ Btu^{-1}$). The average and maximum percentage deviations of the value of C from the mean value of two consecutive sets of tests were 1.62% and 3.15%. The maximum percentage deviation of any of the values of C from the mean value for all of the tests, A to J, was only 4.6%; this shows that the heat transfer resistance remained almost constant. During the period of these tests, the heat transfer resistance increased very slightly and this was probably due to a slow rate of scale formation. During further tests, K to P of Table 5.6, a greater concentration of sodium hypochlorite solution was used in "flushing" the tubes prior to testing and this eliminated the slight scaling of the tube, as described later.

In section 3.2.1 it was noted that initially the maximum obtainable scale reading on the rotameter, R2, was 10 units. Due to slight steam pressure fluctuations a scale reading of 7.5 units was used. However, as stated previously, the removal of the steam injector from the annulus side flow loop showed that the pressure fluctuations no longer affected the flow conditions and therefore a scale reading of 10 units could have been used. To test the reproducibility of the results, under different conditions, tests were performed using a scale reading on the rotameter, R2, of 10 units. (For the conditions of the tests, rotameter scale readings of 7.5 and 10 units correspond to hydraulic Reynolds numbers, in the annulus, of 17100 and 21100). From Tables 5.5 and 5.6 it is seen that the results obtained using either annulus side fluid flowrates are the same for the empty tube configuration.

For the tests of denotations K to M, in Table 5.6, the average resistance to heat transfer was 1.63×10^{-4} $m^2\ ^oC\ W^{-1}$ (9.3×10^{-4} $ft^2\ hr\ ^oF\ Btu^{-1}$) with a maximum percentage deviation, from this value, of 3.92%. However, for any two consecutive sets of tests the mean and maximum deviations from the average of the two determined values of C were 1.73% and 2.47%. For the tests of denotations N to P, the average heat transfer resistance was 1.89×10^{-4} $m^2\ ^oC\ W^{-1}$ (1.07×10^{-3} $ft^2\ hr\ ^oF\ Btu^{-1}$) with a maximum deviation of 1.73%. The mean and maximum deviations of a single value of C from the average value for two consecutive tests were 0.73% and 1.37%.

As shown in section 4.3.2, the heat transfer resistance, C, is the sum of four resistances, such that

$$C = \frac{1}{h_a} + \frac{x_w\, d_o}{k_w\, d_m} + R_i + R_o \qquad (5.7)$$

For the conditions of the present tests it is estimated that the heat transfer resistance due to the tube wall is 2.8×10^{-6} $m^2\ ^oC\ W^{-1}$ (1.6×10^{-5} $ft^2\ hr\ ^oF\ Btu^{-1}$). Wiegand, see (67), correlated all of the heat transfer data available at that time, for the cooling of liquids in smooth annuli, in the form

$$\frac{h_a\, d_E}{k} = 0.023\, Re_E^{0.8}\, Pr^{0.3} \left[\frac{d_1}{d_o}\right]^{0.45} \qquad (5.8)$$

where d_o = outside diameter of the inner tube

d_1 = inside diameter of the outer tube

and d_E = equivalent diameter of the annulus = $d_1 - d_o$

Using this equation with the calculated tube wall resistance, and neglecting the scale resistances, the estimated total heat transfer resistances are 1.84×10^{-4} $m^2\,^oC\,W^{-1}$ (1.05×10^{-3} $ft^2\,hr\,^oF\,Btu^{-1}$) and 1.56×10^{-4} $m^2\,^oC\,W^{-1}$ (8.9×10^{-4} $ft^2\,hr\,^oF\,Btu^{-1}$) for the two conditions studied experimentally. These results closely agree with the experimental determinations. For scale readings on the rotameter, R2, of 7.5 and 10 units, the calculated heat transfer resistances are 2.6% and 4.3% less than the values found for denotations N to P and K to M of Table 5.6. This indicates the magnitude of the scale resistances.

5.4 Data obtained using swirl flow inducers

5.4.1 Friction factor data obtained under isothermal conditions.

Table 5.7 and Figures 5.18 to 5.20 show the results obtained under isothermal conditions using configurations of inserts possessing an anticlockwise twist. The graphical representations, where each point symbolizes three experimental determinations, show that the data are adequately depicted by straight lines on logarithmic co-ordinates. Figure 5.21, which presents the results of the regression analyses of Table 5.7, clearly shows that the presentation of all the results on a single figure was impractical.

Sample raw data and computer outputs are shown, for denotation A of Table 5.7, as Tables A.8.6 and A.9.6. The results are presented in Figure 5.18.

The pressure drop between the tappings P2 and P3 was measured. For configuration 9T the pressure drop between the pressure tappings and packed length of the tube was calculated and subtracted from the measured pressure loss, as described in section 4.7. This corrected pressure drop was used in conjunction with the packed length of the tube in order to determine the friction factors which are denoted by "9T" in Figures 5.20 and 5.21. Furthermore the pressure drop across the length of tube which is equal to the length of the annulus section was also used to evaluate friction factors. The values so determined are denoted by "9T′". The latter friction factors are of the same magnitude as those obtained using configuration 3T. This infers that a relatively large proportion of the pressure drop across configuration 3T is due to any, or combinations, of the following factors :-

(a) contractions and expansions of the flow area

(b) undeveloped swirl flow in the channels formed by the inserts

(c) swirling flow in the empty tube sections.

The friction factors of configuration 9T' are also similar in magnitude to the results of configuration 4T, and for this comparison the following factor also needs to be considered :-

(d) the pressure drop at the junction of the perpendicular trailing/leading insert edges.

The relative proportions of these factors, which contribute to the overall pressure drop, cannot be determined from the results of the present work. As an example, consider configurations 3T and 4T, where the only difference between the insert arrangements is the perpendicularity of the edges. The difference between the pressure drops across each of these configurations is not only the result of factor (d), instead, it represents the combined effects of factors (a), (b), (c), and (d). On first sight, it may appear that a comparison of the results for configurations 7T and 8T would provide a measure of the effect of the leading/trailing edge arrangement. Although this is true for these configurations, the resulting value of the pressure drop, due to a single leading/trailing edge intercept, is not necessarily representative of the drop due to such an intercept when it is positioned within any other configuration. The latter statement is true because of the different flow patterns at the insert intercepts in each configuration.

The friction factors obtained using configuration 9T are greater than those of configuration 7T. Two possible reasons for this are the effect of an establishment length for fully developed swirl flow and the relative proportion of the total pressure drop that is due to inlet and exit effects, including swirl decay at the tape exit. For a continuous twisted tape, Seymour (111) found that fully developed swirl flow is established approximately 10 to 20 pipe diameters from the tape inlet. In the development section, the local friction factors oscillate about the fully developed value and it appears that the integrated value of the local friction factors is significantly above the terminal result only in the first $3\frac{1}{2}$ pipe diameters. Subtracting the pressure drop across the inserts of configuration 9T from that of tube 7T should yield a friction factor equation which is independent of flow development and entrance and exit effects,

hence

$$\phi_{CORR} = 2.15\ Re^{-0.338} - 1.13\ Re^{-0.329} \qquad (5.9)$$

Using this equation the pressure drop across a twisted tape, of the same length as configuration 7T, can be calculated. The pressure loss, $\Delta p'$, due to the flow development and entrance and exit effects can therefore be estimated :

$$\frac{\Delta p'}{\Delta p} = \frac{\phi - \phi_{CORR}}{\phi} \qquad (5.10)$$

where ϕ is the friction factor calculated using denotation H-I of Table 5.7. At Reynolds numbers of 11000 and 78000, the pressure loss ratios calculated using equation (5.10) are 0.071 and 0.092. Using the estimation method proposed in Appendix A.10, the corresponding ratios are found to be 0.027 and 0.049. In using the estimation method, the tube section containing the twisted tape was considered to behave as an empty tube possessing the same flow area and the flow upstream of the tape was considered to be fully developed. Comparing the values of $\Delta p'/\Delta p$, obtained using the above two methods, it is estimated that the friction factors determined using configuration 7T are approximately $4\frac{1}{2}\%$ larger than would be measured for a fully developed swirl flow.

For certain configurations, pressure drop measurements were recorded while using a fluid temperature of $35^{o}C$ but without heat being passed through the tube wall. The results, obtained over the Reynolds number range of 15500 to 104000, are shown in Table 5.7 and Figures 5.22 to 5.24. Isothermal friction factors were calculated using the regression equations determined for the results with fluid temperatures of $35^{o}C$ and ambient, for Reynolds numbers of 15500 and 78000, that is, those common to the tests at both temperatures. At these Reynolds numbers, the maximum deviations of the friction factors obtained at $35^{o}C$, compared to the ambient results, are 1.9% and 7.6%, with a maximum deviation of the average friction factor, for the two Re values, being 4.0%. All of these maximum deviations were found using the result obtained with tube 6T. Referring to Figures 5.18 to 5.23, it is seen that all of the data exhibits a slight curvature and this is most noticeable for configuration 6T. It is considered that this is a result of using low Reynolds numbers during these tests. The friction factors, which were calculated using the regression equations which apply to the two operating temperatures, differ partly due to the slight curvature. The measured fluid temperature change along the test

section never exceeded 0.2°C while using a fluid at 35°C. This amount is small, hence these results are thought to have been obtained under isothermal conditions. For a given Reynolds number the actual data points are in closer agreement than the regression results tend to imply. It is for this reason that the tabulated equations, Table 5.7, should not be applied outside the Reynolds number range of the present work.

Table 5.8 and Figures 5.25 to 5.28 show the results obtained under isothermal conditions with a fluid at room temperature and configurations of alternate rotation inserts. Figure 5.29 presents the corresponding data obtained using a fluid at 35°C. Sample raw data and computer outputs are shown for denotation I of Table 5.8 as Tables A.8.7 and A.9.7.

It was previously shown that the pressure drop across the empty tube and packed section of configuration 9T was considerably below that across configuration 5T. Both of these configurations use the same number of inserts and empty tube lengths. Using the results obtained with configurations 8K and 9K the friction factors based on the length of the annulus section were calculated and denoted as configurations 8K′ and 9K′. The resulting values of ϕ are considerably greater than the results obtained using 7 pairs of inserts interspaced along the same length of tube. It may have been expected that the flow area changes and swirl flow in the empty tube sections of configuration 5K would have resulted in larger pressure drops than those encountered with tubes 8K′ and 9K′. This was not the case, and the observed phenomenon may be a result of the change of swirl direction caused by consecutive elements. This would produce a relatively small clockwise swirl component in the flow entering consecutive pairs of elements in configuration 5K. However, at each junction of the inserts in configurations 6K, 8K, and 9K, the flow entering each junction has a relatively large swirl component which then has to be transformed into a large swirl component in the opposite direction, thereby leading to a large pressure drop.

The friction factors denoted by 9K′ are slightly greater than those of 8K′. Although the difference is within the uncertainty of the data, it may also be postulated that it is due to the development of a turbulent flow velocity profile in the empty tube section of configuration 9K′.

The results of denotations H and I in Table 5.8 show the re-

producibility of the friction factor results. Comparison of these results with those of denotation M, in the same table, shows that the friction factors are slightly dependent on the number of inserts forming the Kenics mixer. Using Kenics mixers formed from 4, 6, 8, and 10, elements with a twist ratio of 2.5, Morris and Benyon (86) found that the number of elements had little effect on the friction factors in the Reynolds number range of 6000 to 30000. Morris and Proctor (87) obtained the same conclusion using inserts with twist ratios of 1.5 or 2.0.

It may be considered that the elements at the upstream end of a Kenics mixer will produce a well mixed flow. Thereafter only relatively small increases in the degree of mixing will be achieved by each element. On this hypothesis it would be expected that the friction factors are dependent on the number of elements and this would be particularly noticeable in comparing the results obtained by Morris and Benyon (86) with 4 and 10 elements. These authors do not present their results for individual tests hence a direct comparison with the present work is not possible. The friction factor correlation, which they determined, fitted their data "typically to within $\pm$ 8%."

The isothermal results obtained using configurations of anti-clockwise rotating elements with water at 35^{o}C and room temperature have been compared. Using the same procedure and Reynolds numbers with the results of tests on alternate rotation arrangements, the maximum deviations of the friction factors obtained at each temperature are 4.2% and 6.6% at Reynolds numbers of 15500 and 78000. The maximum deviation of the mean of the friction factors determined at the two Reynolds numbers was 5.2%. This maximum deviation was found using the results of configuration 7K; these results show a definite curvature which is further discussed in section 5.4.4.

5.4.2 Friction factor data obtained under heating conditions.

Table 5.9 and Figures 5.30 to 5.33 present the results of the pressure drop analyses performed using arrangements of inserts of anti-clockwise twist. Table 5.10 and Figures 5.34 to 5.37 present the corresponding results for arrangements of inserts of alternate twist direction. Tables A.8.8 and A.9.8 provide the sample raw data and computer outputs appertaining to denotation A of Table 5.9. Tables A.8.9 and A.9.9 provide the pertinent data for denotation H of Table 5.10.

The regression equations of Tables 5.7 and 5.9 were used to evaluate friction factors at Reynolds numbers of 15500 and 78000. For the empty tube results the average deviation of the isothermal and heating friction factors was found to be approximately 10.6%. For the remaining configurations the maximum deviation is 6.6% (configuration 1T using an average fluid temperature of 35^{o}C) with a mean absolute deviation of 2.6%. Using the same procedure with the results of Tables 5.8 and 5.10, the maximum value of the average of the deviations (at Re = 15500 and 78000) of the isothermal and heating friction factors is 3.1%. There is one exception to this limiting value; for configuration 1TS the deviation is 8.4%. For these configurations which used inserts of alternate rotation, the mean absolute deviation of the results obtained using the three methods of operation is 2.4%.

The above discussion shows that the inserts reduce the effect of the fluid viscosity ratio, (μ_s/μ), compared to the effect in an empty tube. The pressure loss across a tube containing inserts is the result of the losses at the tube wall, the surfaces of the inserts, and in the core of the flow stream. A significant proportion of the total pressure loss therefore occurs away from the tube wall where the viscosity reduction occurs. For the tubes containing inserts, the effect of the viscosity reduction was greatest for the tubes with the least number of inserts. However, it was not possible to obtain a correlation between the number of inserts and (μ_s/μ) even when only one type of configuration, for example anticlockwise inserts with aligned edges, was considered.

Most of the discussion presented in section 5.4.1 also applies to the friction factors obtained under heating conditions. That discussion will not be repeated since no further trends were noted from the heating results. In section 5.4.4 the effect of the insert thickness, the orientation of consecutive elements, and the regression parameter A and B, are discussed. The heat transfer results are considered prior to that discussion since they also show trends which clarify those effects.

5.4.3 Heat transfer factor data.

The heat transfer factors, determined from the tests using the type T configurations of Figure 1.5, are shown in Table 5.11 and Figures 5.38 to 5.42. The close proximity of the heat transfer characteristics

of the tubes is clearly shown by Figure 5.43. For the type K configurations of Figure 1.6 the results are shown in Table 5.12 and Figures 5.44 to 5.46. As noted previously, a number of configurations produced heat transfer factors of comparable magnitude thereby enforcing the presentation of data on a number of separate graphs. Figure 5.47 shows the regression equations in graphical form.

The raw data for denotation H of Table 5.11, and denotations G and H of Table 5.12, are shown in Tables A.8.10, A.8.11, and A.8.12. The computer outputs of the heat transfer data determined by analyses of the raw data are shown by Tables A.9.10, A.9.11, and A.9.12.

For each configuration, three heat transfer measurements were performed at each Reynolds number, hence it should be noted that many of the points shown on the heat transfer factor graphs represent three actual results. The figures and tables show that the experimental scatter is adequately within the typical scatter range encountered during heat transfer tests. For each of the tests, the experimental data is well correlated by a straight line on the conventional logarithmic co-ordinates.

In order to maintain a constant heat transfer resistance, C, it was necessary to vary the heat flowrate through the tube wall as the tube side Reynolds number was varied. Tests performed using scale readings of 7.5 and 10* units on the rotameter, R2, required that the heat flowrates, for configuration O, varied from approximately 6.1 kW to 12.4 kW and from 6.5 kW to 14.4 kW, respectively. These values should be multiplied by 14.9 to obtain the heat flux (kW m^{-2}) based on the inside area of the tube wall. For configuration 7T, the corresponding heat flow ranges were 8.9 kW to 14.3 kW and 9.7 kW to 16.4 kW. During the tests using configuration 6K, with the annulus side fluid flowrates stated above, the respective ranges were 10.5 kW to 14.9 kW and 11.6 kW to 17.1 kW. The results shown by denotation G-H of Table 5.11 clearly demonstrate the excellent reproducibility of the tests performed using configuration 7T, even when different conditions were used. The pressure drop measurements performed at the time of the heat transfer tests also show excellent reproducibility, see denotation G-H in Table 5.9.

---

* Scale readings on the rotameter R2 of 7.5 and 10 units indicate respective flowrates of 2.7×10^{-4} m^3 s^{-1} (9.5×10^{-3} ft^3 s^{-1}) and 3.3×10^{-4} m^3 s^{-1} (11.7×10^{-3} ft^3 s^{-1}).

The friction factor correlation used to represent the characteristics of configuration 6K is shown as denotation G-H of Table 5.10. The results obtained over both heat flux ranges are in good agreement. For this configuration, the experimental heat transfer results are shown in Figures 5.44 and 5.45. Comparison of these results, for Reynolds numbers not exceeding 86000, shows that the data is in good agreement. At the highest Reynolds number, Re = 104000, there is a relatively large scatter of the data although only one single experimental result lies considerably away from the observed trend. Denotation G-H of Table 5.12 shows that the average deviation of the data from the overall regression equation is comparable with that obtained using other configurations. The relatively high maximum deviation is caused by the experimental result noted above. This result, compared to the regression line, lies within the experimental uncertainty of the data, as calculated in Chapter 6.

For configurations 9T, 8K and 9K, the heat transfer results shown in the previous figures were all based on the measured inlet and outlet temperatures. The heat transfer factors are therefore the result of the heat transfer in the empty and packed tube sections. It has already been noted that a pressure drop across a type T or type K configuration may be dependent on the number of inserts forming the configuration. Appendix A.11 presents an analysis for the estimation of the heat transfer coefficients in the tube lengths which contain inserts in configurations 9T and 8K. Denotations A to D of Table 5.13 present the results of this analysis. The results obtained assuming a constant heat transfer resistance, C, (case 1) are almost identical to those obtained using the temperature correction of case 2 of Appendix A.11. This is due to the small changes in the bulk annulus fluid temperature. The results of Table 5.13 were determined using equation (A.11.11). This equation was used, as opposed to equation (A.11.10), because the heat flow, Z1 in the computer program, was determined using the temperature difference, (Y-T(I,13)), of the tube side fluid. It was therefore considered that the equation used to determine Y1 should also use this temperature difference. If the heat flow in the empty section had been based on the heat input from the annulus fluid then equation (A.11.8) should have been used to determine Y1. The value of Z1 was based on the tube side fluid since previous calculations, used to determine the results of Figures 5.38 to 5.47, also used this as a measure of the heat transferred.

The procedure of Appendix A.11 is essentially based on the following equation :-

$$U A_T \Delta t_{LM} = U_p A_p \Delta t_{LMp} + U_o A_o \Delta t_{LMo} \qquad (5.11)$$

where $$A_T = d_o l \pi \qquad (5.12)$$

Equations of the same form as (5.12) apply for the empty tube and packed sections. Hence, by rearrangement

$$U = \frac{U_p l_p \Delta t_{LMp}}{l \Delta t_{LM}} + \frac{U_o l_o \Delta t_{LMo}}{l \Delta t_{LM}} \qquad (5.13)$$

Alternatively, we may write

$$h = \frac{h_p l_p \Delta t'_{LMp}}{l \Delta t'_{LM}} + \frac{h_o l_o \Delta t'_{LMo}}{l \Delta t'_{LM}} \qquad (5.14)$$

where $\Delta t'_{LM}$, $\Delta t'_{LMp}$, and $\Delta t'_{LMo}$, are the log mean temperature driving forces between the tube side fluid and the tube wall over the total tube length, and the packed and empty tube sections, respectively. Comparing equations (5.14) and (5.4), it can be seen that substitution of ϕ for Nu in equation (5.4) would produce an equation which is valid only if $\Delta t'_{LM} = \Delta t'_{LMp} = \Delta t'_{LMo}$. It is for this reason that an equation of the form of (5.4) was not used to obtain calculated heat transfer coefficients for the Pall ring data.

Table 5.13, denotation B, shows that for the Kenics mixer arrangement the average Nusselt number for a mixer formed from 14 inserts is 14% greater than that obtained using a 26 insert mixer. For Reynolds numbers greater than 6000, Proctor (101, Figure 31) found that the local Nusselt number increases with the axial distance from the mixer inlet until about the fourth or fifth insert; thereafter the value steadily falls to an assymptotic value maintained after about the twelth insert. The rise and fall of the local Nusselt number appears to become less pronounced as the Reynolds number increases. The discussion which now follows is speculative and is based on the experimental determinations of the local Nusselt numbers in the entry regions of a circular pipe with various inlet configurations. This data is obtained from Boelter et. al. (10). These workers found that for an abrupt sharp edged entrance, and for a 180° bend, situated upstream of the heated section, the local Nu values rise and fall in a manner similar to that found by Proctor with a Kenics mixer. Boelter et. al. suggest that these

characteristics are due to the flow contraction and reexpansion produced by the abrupt entrance. For the tests with a 180° bend it may be the stall region which produces the observed trend. Relating these findings to the Kenics arrangement, it may be postulated that the first few elements contain an accelerating flow which is initiated by the flow area reduction. This leads to an increased wall shear stress and by the heat/momentum analogy, as outlined in section 1.3.4, this corresponds to large heat transfer coefficients. As the fluid flows further along the mixer the flow acceleration effects will be gradually attenuated and the flow will become more mixed. Hence the average Nusselt number over the length of each successive element will gradually fall to an assymptotic value. It should be noted that these ideas are compatible with the suggested mechanisms causing the pressure drop across the mixer. However, it must be stated that the mass transfer tests of Proctor (101), see his Figure 16 for example, show that the local Sherwood number increases in the first two or three elements and then attains a constant value. This suggests that the mass transfer rate may be considerably dependent on the degree of mixing within the flow.

Table 5.13 shows that the heat transfer coefficient for a twisted tape composed of 14 inserts is 13% greater than the coefficient that is produced by a tape of 26 inserts. This is due to the contraction of the flow and the production of the swirl flow velocity and temperature profiles. For the shorter tape a significantly larger proportion of the tape length will contain a developing flow. Using twisted tapes with a thickness ratio, δ/d, of 0.051, Smithberg and Landis (118) found that the heat transfer coefficient in the total length of their tapes was approximately 4% greater than the heat transfer coefficient in the downstream half of the tape length. In that work the heated length was 29.09 tube diameters. It should be realised that the upstream half of their tapes contained the decay region of the inlet effects and the flow entering the downstream half of the tape possessed significantly developed swirl flow velocity and temperature profiles. Using the result found by Seymour (110), see equation (1.61) in Chapter 1, it is found that the heat transfer coefficient, for a tube with $(x_1/l) = 0.53$, is 0.905 (Re = 15000) and 0.946 (Re = 100000) times the coefficient obtained using a tape which extended along the full heated tube length. Seymour used a heated tube length of 28.5 tube diameters. For configuration 9T of the present work, the heat transfer coefficient is 0.792 (Re = 15000) and 0.811 (Re = 100000) times the coefficient obtained using

configuration 7T. The ratios determined using the results of Seymour are greater than those of the present work due to the existence of a swirling flow in the tube section downstream of Seymour's tapes. All of the above work shows that the heat transfer coefficients in the inlet section are greater than those in the downstream section of a tube containing a full length twisted tape.

The method of Appendix A.11 relies on the calculation of the heat transferred in the empty tube section of the examined configurations. For configuration 9K the heat transferred along the empty tube section cannot be determined. However, using the heat transfer correlations for the Kenics mixer, the heat transfer coefficients in the empty tube section may be estimated. These estimated values may then be expressed as a ratio to the empty tube results which are calculated using equation (A.11.21) with $x/d = 24.9$. The correlation used to calculate the heat transfer coefficients in the Kenics mixer was initially considered to be that of denotation G-H in Table 5.12. Using that equation, the results indicated as denotations E and F in Table 5.13 were obtained. The results of denotation F show that the heat transfer factor in the empty tube section, downstream of the inserts, is approximately 17% greater than that which would be found in the inlet section of an empty tube. However, a more truly representative result is estimated if the heat transfer coefficient in the packed section of the tube is calculated using the correlation which applies to the packed section of configuration 8K. For this purpose the results of denotation B in Table 5.13 were used. Denotation H of Table 5.13 shows that the heat transfer factors in the empty section of configuration 9K are approximately 9% greater than those that would exist in an empty tube of the same length with no swirl. Alternatively, the ratio of the heat transfer factors downstream of the mixer and those that would be obtained using the full length empty tube (i.e. denotation A-P of Table 5.6) may be calculated. The average of the ratios evaluated in this way at Reynolds numbers of 15500 and 104000 is 1.24.

The above discussion shows that the heat transfer factors downstream of the Kenics mixer are considerably lower than those produced within the mixer, that is, Nu decays rapidly beyond the mixer outlet. In contrast to this configuration, equation (1.62) may be used to produce curves of Nu/Nu_o versus x/d for $1 < x/d < 24.9$ and Reynolds numbers of 15500 and 104000. From such curves the ratio Nu/Nu_o downstream of a twisted tape may be determined at the specified Reynolds

numbers. The average of the ratios determined at the two Reynolds numbers is found to be approximately 1.45. The Nusselt numbers downstream of the twisted tape are expected to be larger than those downstream of the Kenics mixer because of the greater swirl component of the flow beyond the tape.

5.4.4 Discussion of the results obtained using swirl flow inducers.

Using the regression equations obtained under isothermal and heating conditions, it is found that the friction factors for configuration 1TS (δ/d = 0.16) are approximately 21% greater than those determined using configuration 1T (δ/d = 0.14). Similarly, the friction factors of configuration 1KS (δ/d = 0.16) are approximately 23% greater than those found using configuration 1K (δ/d = 0.14). These increases are presumably caused by the increased blockage of the flow-area and possibly by an increased swirl in the empty tube sections. Again using the isothermal and heating results, the friction factors of configuration 3KS are 4.7% greater than those found with configuration 3K. This increase is significantly less than that found using the configurations formed from three single inserts. The flow entering each of the two downstream inserts of configurations 1K and 1KS may possibly possess a quite small swirl flow component, while the flow received by each downstream insert of the pairs in configurations 3K and 3KS will possess a strong swirl component. Therefore quite large pressure losses, due to the swirl flow reversal, are to be expected at the insert interfaces. These losses are unlikely to be strongly dependent on the flow blockage, for the present range of blockages, and therefore the pressure drops across tubes 3K and 3KS are unlikely to greatly differ. Furthermore, in the empty tube sections the swirl produced by the downstream insert of each pair may be less than that produced by the inserts of configurations 1K and 1KS. This leads to a larger proportion of the total pressure loss being caused by the flow reversal and eddy losses.

For tubes 1TS, 1KS, and 3KS, the heat transfer factors are respectively 7%, 10%, and 5%, greater than those determined using tubes 1T, 1K, and 3K.

Figures 5.48 to 5.50 show the variation of the friction factor regression parameters, A and B in equation (4.22), with the fraction of the tube length which does not contain inserts. It should be recalled that each of the symbols is the result of 27 actual data measurements.

The results obtained using configurations 8K, 9K, and 9T are not included on these graphs. Similarly the results determined using stainless steel inserts are not shown. The data obtained under isothermal conditions, at room temperature and at 35°C, and under heating conditions, exhibit very similar trends. For each configuration it was previously noted that as the Reynolds number is increased the slope of the friction factor curve tends to decrease. The data points referred to as "Isothermal" and "35°C", in Figures 5.48 5.50, clearly show this trend. The "Isothermal" results apply over the approximate range of Reynolds numbers of 11000 to 78000, the "35°C" results were obtained over the range of 15500 to 104000.

The parameters appertaining to the "Heating" tests are smaller than those found at 35°C under isothermal conditions. For the empty tube the fluid viscosity near the hot tube wall is lower than that in the fluid core and it is at the tube wall that a large proportion of the pressure loss occurs. Hence the ratio of the inertial to viscous forces is increased which leads the fluid to behave as if it were flowing with a larger Reynolds number, thereby reducing the friction factor. Since the friction factor curves, at higher Reynolds numbers than those determined by the bulk flow properties, possess a smaller negative slope, it follows that the friction factor curves under heating conditions will exhibit a smaller slope than those obtained under isothermal conditions at the same bulk Reynolds numbers. It will later be shown that the inserts of the present work do not behave as effective fins and therefore there is no fluid viscosity reduction at the surface of the inserts. From this discussion, it is inferred that as the proportion of the total pressure drop that is due to losses at the tube wall is reduced, the difference in the slopes of the friction factor curves, for the heating and isothermal conditions, should become less. For the inserts positioned with perpendicular leading and trailing edges, Figure 5.50 clearly shows this trend. For these configurations a large proportion of the total pressure drop is due to the friction on the insert surfaces, and the kinetic energy losses due to the flow area changes, the leading and trailing edges, and the flow reversals. For inserts with aligned edges, no reduction in the difference between the slopes of the friction factor curves (isothermal and heating) is shown by Figure 5.50. For these arrangements no reduction is seen because there no longer exists the large pressure

losses which were associated with the form drag that is due to the leading and trailing edges of the perpendicular edge configurations.

For the results obtained using configurations formed from inserts with aligned leading edges and identical twist direction, the friction factor curves show a greater curvature than those obtained using perpendicular edges. For the latter configurations the kinetic energy losses are quite large compared to the losses caused by viscous drag, even at low Reynolds numbers. In the configurations formed with aligned inserts the proportion of the total pressure loss that is a result of kinetic energy losses gradually increases as the Reynolds number increases, in much the same way as the empty tube behavior. It is this effect which produces the noted curvature of the graphs of $\ln(\phi)$ versus $\ln(Re)$. For these reasons the heating results shown on Figure 5.48 should be compared with the isothermal results obtained at $35^{o}C$. Such a comparison shows that the difference between the slopes of the friction factor curves reduces as the number of inserts, and hence the relative importance of the form drag, increases. However, for a continuous twisted tape the difference increases above that found using an unoccupied tube length fraction of 0.238. In this case the form drag losses are not dominant and the reduced fluid viscosity at the tube wall has a greater effect.

The present results, and those of many previous workers, support the conclusion that for a continuous twisted tape the friction factor curve is steeper than that found using an empty tube. On this premise it is inferred that the presence of a swirling flow will lead to an increased negative value of the Reynolds number exponent, B. The previous discussion of the friction factor characteristics of Pall rings concluded that increases in the kinetic energy losses results in a reduction of the slope of the friction factor curve. The curves obtained using aligned inserts with anticlockwise twists, under isothermal conditions, show that the magnitude of the slope, B, increases as the unoccupied fraction of the tube length, hereafter denoted by UFTL, is decreased from 0.771 (configuration 3T) to 0.010 (configuration 7T). Strictly the UFTL for configuration 7T is zero, however, for comparison with the heat transfer results the UFTL was calculated using a total tube length equal to the length of the heating jacket. This approximation is very small and does not effect the trends shown in Figures 5.48 to 5.50. The slope of the friction factor plot for a UFTL of 0.886 (configuration 1T) is greater than that determined for the empty

tube. It is difficult to justify this finding; it may be due to a slight error in the determined slope. Denotation A of Table 5.7 shows that the 95% confidence interval on the slope is large enough to allow for the observed effect. A further very tentative proposition is that the swirl produced by the three inserts raises the slope of the friction factor curve above the reference empty tube value. The rapid reduction in the slope, B, in the range of the UFTL of 0.886 to 0.771, may then be due to the slightly increased swirl component of the flow entering the upstream element of each pair of inserts in configuration 3T. This increased swirl may produce an increase in the kinetic energy losses at the leading edge of each pair of inserts, and thereby reduce the slope of the friction factor curve. As noted previously, the downward trend of the regression slope of the heating results of Figure 5.48, in the UFTL range of 0.238 to 0.010, is a result of the fluid viscosity reduction at the tube wall.

Figure 5.50 shows that for pairs of inserts of alternate rotation, with perpendicular edges, the friction factor curves generally become shallower as the number of inserts is increased. This is caused by the kinetic energy losses associated with the insert edges and the flow reversals. The results obtained using a UFTL of 0.467 (configuration 5K) exhibit a steeper slope than may have been expected. The present hypothesis is obviously a simplification in that the friction factor slope is considered to increase, or decrease, according to the proportion of the swirl flow and kinetic energy losses. Using this simplification it is difficult to adequately justify any slight deviations from the overall trend. Furthermore, any noted discrepancies may be due to slight errors in the determined slopes.

For all of the results, except those determined using configurations formed using only inserts with an anticlockwise twist and a UFTL of 0.771, the friction factor curves are steeper for configurations with aligned inserts than for the perpendicular arrangement. From the present simple hypothesis this is to be expected.

Figure 5.51 shows that the Reynolds number exponent, E, in the heat transfer factor regression equations is not clearly dependent on the UFTL. The values of the exponent deviate about the characteristic empty tube exponent, $E = 0.8$. The present results, and those of previous workers, show that the exponent for a continuous twisted tape arrangement is close to that determined using an empty tube. The fluid

passing through the tubes of the present tests possessed a swirl component and therefore it is to be expected that the observed characteristics would be those appertaining to a swirling flow. In the empty sections of the tubes the flow is intermediate between a developed swirl flow and that in an empty tube. Hence, as found experimentally, it is to be expected that the heat transfer coefficients, for the present tubes, are dependent on the Reynolds number in a similar manner to those in an empty tube and a tube containing a twisted tape. The deviations of the experimentally derived exponents from those of the two latter configurations may be due to experimental error. Furthermore, the deviations will be the result of kinetic energy losses caused by the leading and trailing edges and, in some circumstances, due to flow reversal.

Figures 5.52 to 5.54 show the effect of the number of inserts on the friction factor and heat transfer factor ratios. The ratios have been determined by comparing the regression equations which apply to the packed and empty tubes at Reynolds numbers of 15500 and 104000. The figures show the average packed/empty tube ratios of the two values so determined. It is clearly seen that the perpendicular arrangement of the leading and trailing edges of consecutive elements results in larger values of the friction factor and heat transfer factor compared to the use of aligned edges. The friction factor results, determined using 26 inserts, show that the effect of using perpendicular edges is considerably greater for the use of pairs of inserts of alternate rotation than for pairs of identical rotation. This indicates that the greater pressure drop across the Kenics mixer, compared to a twisted tape of the same length, is the result of the combined effect of the flow reversals and the leading and trailing edges and is not simply dominated by one of these effects.

Koch (69) postulated that heat transfer factors are strongly dependent on the wall shear stresses. In the present work, the parts of the leading and trailing edges of the inserts that touch the tube wall will disrupt the fluid boundary layer. Also the leading and trailing edges produce a flow separation from the insert surfaces; this flow may interact with the fluid near the tube wall. These mechanisms were considered by Sparrow et. al. (121), see section 1.3.4. The flow separation may increase the mixedness of the fluid stream but it will also produce a significant increase in the pressure drop (15, p. 301).

It is considered that these mechanisms cause the observed differences in the heat transfer factors obtained using the aligned and perpendicular edge arrangements. In the conventional empty tube turbulent flow regime the fluid may be quite well mixed in an empty pipe. It is expected that the inclusion of aligned inserts into the pipe will produce further mixing. However, a relatively small proportion of the fluid resistance to heat transfer lies in the bulk of the fluid, hence any increases in the mixedness of this fluid, obtained by the use of perpendicular edge inserts, will cause somewhat small increases in the heat transfer factor. This important deduction leads to the conclusion that any inline mixer which is used in the hope of substantially increasing the mixedness of the core fluid by flow splitting, and which therefore requires a large power input, may be an inefficient device for increasing the heat transfer factor in the turbulent flow regime. On this basis, it is suggested that mixing studies should be performed using tubes containing inserts arranged as in configuration 7K. This arrangement provides flow reversal which aids fluid mixing in the semi-circular channels formed by the inserts and the tube wall and increases the wall shear stress. It is later shown that this configuration is a comparatively useful device for heat transfer enhancement.

Figures 5.52 and 5.54 show the results obtained using configurations 8K and 9K. These results, which are based on the actual heated length of the tube, do not distinguish between the data determined using each of these arrangements. The friction factor and heat transfer factor ratios, for these two configurations, deviated by only 0.57% and 2.37% from the mean values shown on the figures. It is clear that configuration 5K is far more beneficial than 8K or 9K even though each arrangement contains the same number of inserts in the same tube length. This tends to indicate that mixing studies using configuration 5K may prove to be beneficial. Unfortunately, it may be that the fluids to be mixed in such a device may coalesce in the empty tube sections: the manufacturers (61) state that the distance between Kenics mixer modules should not exceed 2 to 3 pipe diameters.

Some of the heat transfer data obtained using 3 and 6 inserts appears to show a discrepancy. The difference between the two results determined using 3 inserts is very small and may be due to experimental error. The inserts of configuration 1T will produce a swirling flow which will not greatly decay within the empty tube sections of one insert length immediately downstream of the insert: this is supported by

the work of (6, pp. 102-108) and (75). However, the additional inserts of configuration 3T, compared to 1T, will produce further insert surface drag. It is therefore expected that only a small increase in the heat transfer factor will be observed as the number of inserts, in a type T arrangement, is increased from 3 to 6. A more significant increase in the friction factor will occur. The above discussion strongly suggests that the use of equidistant spacing of individual inserts, of the same twist direction, would be more beneficial than the use of pairs of inserts. In the present work, this would not have allowed such a clear comparison of the effects of the leading edge orientation and the insert twist direction. Nonetheless it is a promising direction for further research.

One of the most interesting trends shown by the present work is the almost asymptotic behavior of the friction factor ratios shown in Figure 5.53. The ratios obtained using 14 inserts (configuration 5T) and 20 inserts (configuration 6T) are 1.7% and 3.8% greater than the value found using 26 inserts (configuration 7T). Although these deviations are within the experimental uncertainty of the data, the possible reasons for the observed trend will be discussed since this helps in the consideration of the heat transfer determinations.

In the previous discussion of the effects of the leading and trailing edges it was suggested that they produce a flow separation from the insert surfaces. In the empty tube regions of configuration 5T the separated flow may cause fluid to interact with the boundary layer at the tube wall. Upon reaching the leading edge of the next pair of inserts the fluid must contract due to the reduction in the flow area. The fluid in the empty tube regions of configuration 6T may be expected to undergo a part of the procedure described, i.e. as the fluid leaves one pair of inserts it begins to interact with the tube wall fluid but it soon reaches the next contraction of the flow area. On this basis,it may be expected that the friction factor ratio obtained using configuration 5T would be greater than that of 6T. This is not found to be the case due to the greater surface area of the inserts in the latter configuration, and hence the greater losses due to shear stress on the inserts. The friction factor ratio determined using tube 7T is less than the ratios found using tubes 5T and 6T due to the lack of flow separations and hence the reduced form drag. However, the foregoing discussion infers that as the number of inserts is increased from 14 to 26 the shear stress at the tube wall decreases and

therefore the heat transfer factor ratios are expected to decrease. This trend is shown by Figure 5.54.

It is interesting to note that the peak in the heat transfer factor ratio occurs when the distance between consecutive pairs of inserts was almost exactly equal to the length of a pair of inserts. To check if this is a coincidence it would be interesting, in further work, to use pairs of inserts with a different twist ratio from that of the present work. Also, the results obtained using individual inserts, equidistantly spaced along a tube, would be of interest. Further possible modifications to the inserts, and the configurations, are suggested in Chapter 7.

6 Accuracy Assessment

6.1 Introduction

The regression analyses, performed using the computer programs FRICTION-6010 and HEAT2-6010, show the data scatter about the regression equations. These ln-ln linear regression correlations between the variables ϕ and Re, and $Nu/Pr^{0.4}$ and Re, are essentially models which have been proposed for the representation of the physical events. The correlation coefficients and 95% confidence intervals compare the experimental data and the model. For tests in the turbulent flow regime, the use of such models has been repeatedly justified; the latter may be considered to provide a multiple-sample test of the model. The results of the present work agree significantly with the ln-ln linear regression model and this indicates a certain confidence in the results.

The preceding discussion does not provide any information concerning the reliability of the experimental data, and therefore of the constants and exponents of the regression equations; this is the purpose of the present chapter.

6.2 Methods considered for the reliability estimations

This subsection discusses the proposals, presented by Kline and McLintock (66), concerning reliability estimates in single sample experiments. The available methods are considered in general terms and are applied specifically to the present work in sections 6.3 and 6.4.

Consider y to be a function of n independent variables*:

$$y = y(x_1, x_2, \ldots\ldots, x_n) \qquad (6.1)$$

A Taylor expansion of equation (6.1), neglecting all terms after the second term, allows the error in y, here denoted by δy, to be found. This approximation of the possible deviation of y from the

---

* In the present chapter y and $x_1, x_2, \ldots, x_n$, are arbitrary variables; they are not used to represent the twist ratio of a tape, or a tube length. The latter definitions have been used in the other chapters of this thesis.

true value applies for small error terms in the variables. Hence

$$\delta y = \left|\frac{\partial y}{\partial x_1}\delta x_1\right| + \left|\frac{\partial y}{\partial x_2}\delta x_2\right| + \ldots + \left|\frac{\partial y}{\partial x_n}\delta x_n\right| \qquad (6.2)$$

If the errors in the variables are considered to be the maximum possible errors then

$$\delta y_{MAX} = \left|\frac{\partial y}{\partial x_1}\delta x_{1MAX}\right| + \left|\frac{\partial y}{\partial x_2}\delta x_{2MAX}\right| + \ldots + \left|\frac{\partial y}{\partial x_n}\delta x_{nMAX}\right| \qquad (6.3)$$

This equation is often used to rapidly estimate the reliability of experimentally determined results. Kline and McLintock (66) call equation (6.3) the "linear" equation. They place "odds" on the values of the error terms, for instance, there may be a 20 to 1 chance that the error in x_1 is less than or equal to δx_1. Using equation (6.3) the odds on the value of δy is far greater than the odds for the terms δx_1, δx_2, ..., and δx_n (66).

The use of standard deviations rather than error terms, for the result, y, and the variables, has also been considered; this approach may also place unacceptably large odds on the value of the standard deviation of y, and therefore on the value of δy (66).

Reference (66) proposes that the best method of reliability estimation is obtained using their "second power" equation :

$$\delta y = \left[\left[\frac{\partial y}{\partial x_1}\delta x_1\right]^2 + \left[\frac{\partial y}{\partial x_2}\delta x_2\right]^2 + \ldots + \left[\frac{\partial y}{\partial x_n}\delta x_n\right]^2\right]^{0.5} \qquad (6.4)$$

Again they suggest that for each variable the error should be expressed such that it is "b to 1" certain that x is within the range In BS 1042: Part 1: 1964 (13, pp. 67-73) the 95% confidence limits on x are used as the value of δx. The merit of equation (6.4) is that "b to 1 odds", or 95% confidence limits, on the values of the variables also leads to the same odds, or confidence, on the value of δy. There are two principal drawbacks to the use of equation (6.4) :

(i) the odds on δy and $\delta x_{1\to n}$ will be the same only if all of the errors exhibit normal distributions.

(ii) the odds on the errors are difficult to specify.

Kline and McLintock (66) show that equation (6.4), compared to equation (6.2), provides a better

measure of δy when the errors are not normally distributed. The difficulty of point (ii) must be overcome in any reliability analysis; for example, the use of maximum error terms is essentially stating the values of δx for very large odds.

The reliability analysis of the present work shows the results obtained using equation (6.2), which is hereafter referred to as the "linear" equation, and the "second power" equation, that is, equation (6.4). Sample experimental data, obtained while operating over a wide range of variables, are analysed.

6.3 Reliability analysis of the friction factors

The friction factors were determined using the overall equation :

$$\phi = \frac{\pi^2 d^5 H \rho_1 g (S - 1)}{64 l \rho Q^2} - \frac{\phi_E (l_{in} + l_{out})}{l} \qquad (6.5)$$

where l = length of tube on which the friction factor, ϕ, is based, for example, the heated or packed tube length. More precise definitions of this symbol are given at its point of application in the text

l_{in} = tube length between the upstream pressure tapping and either the upstream end of the heated section or the upstream end of the packed section of the tube

and l_{out} = tube length between the downstream pressure tapping and either the downstream end of the heated section or the downstream end of the packed section of the tube.

The Reynolds numbers were determined using :

$$Re = \frac{4 Q \rho}{\pi d \mu} \qquad (6.6)$$

The second term of equation (6.5), later denoted by the symbol ϕ_{T2}, represents the correction applied to the experimentally determined pressure drop to allow for the empty tube length between the packed tube length and the pressure tappings.

6.3.1 Isothermal empty tube tests.

For this mode of operation, the second term of equation (6.5) is not considered. Applying a reliability analysis with equation (6.5)

it is found that :

$$\frac{\partial \phi}{\partial d} = \frac{5 \pi^2 d^4 H \rho_1 g (S - 1)}{64 l \rho Q^2} \qquad (6.7)$$

$$\frac{\partial \phi}{\partial H} = \frac{\pi^2 d^5 \rho_1 g (S - 1)}{64 l \rho Q^2} \qquad (6.8)$$

$$\frac{\partial \phi}{\partial l} = \frac{\pi^2 d^5 H \rho_1 g (1 - S)}{64 l^2 \rho Q^2} \qquad (6.9)$$

and

$$\frac{\partial \phi}{\partial Q} = \frac{2 \pi^2 d^5 H \rho_1 g (1 - S)}{64 l \rho Q^3} \qquad (6.10)$$

where l = tube length between the pressure tappings.

The fluid properties ρ, ρ_1, and S, may deviate slightly from the true values due to very small errors in the recorded temperature. These deviations will not be considered since the fluid properties are not significantly temperature dependent.

Substituting equations (6.7) to (6.10) into equation (6.2) and dividing throughout by ϕ, gives

$$\frac{\delta \phi}{\phi} = \frac{5 \delta d}{d} + \frac{\delta H}{H} + \frac{\delta l}{l} + \frac{2 \delta Q}{Q} \qquad (6.11)$$

Alternatively, substituting equations (6.7) to (6.10) into the "second power" equation, (6.4), gives

$$\frac{\delta \phi}{\phi} = \left[\left[\frac{5 \delta d}{d}\right]^2 + \left[\frac{\delta H}{H}\right]^2 + \left[\frac{\delta l}{l}\right]^2 + \left[\frac{2 \delta Q}{Q}\right]^2 \right]^{0.5} \qquad (6.12)$$

Sample calculations using experimental empty tube data are shown in Tables 6.1 and 6.2. The experimental results which are represented by denotation H of Table 5.4, are shown in Tables A.8.1 and A.9.1 and in Figure 5.13. Tables 6.1 and 6.2 present the results of the reliability analysis when it is applied using the estimated "maximum" deviations and the estimated "mean" deviations of the variables.

6.3.2 Isothermal tests using inserts.

If the friction factors for tubes containing inserts had been based on the tube length between the pressure tappings, i.e. including the empty tube end lengths, L_{in} and L_{out}, then the analysis of section 6.3.1 would apply. However, the friction factors were based on the actual packed length of the tube and therefore the reliability estimations are evaluated using a slightly different procedure to that of the previous section.

An energy balance between two sets of pressure tappings at points 2 and 3, between which swirl inducing inserts are placed with the last insert situated close to point 3, shows that for a horizontal tube :

$$\frac{P_2}{\rho g} + \frac{u^2}{2g} = \frac{P_3}{\rho g} + \frac{u^2}{2g} + \frac{u_t^2}{2g} + H_f \qquad (6.13)$$

where u_t = tangential velocity of the fluid
H_f = fluid head loss
P = fluid pressure

The friction factors determined in the present work include the tangential velocity head term of equation (6.13). This term is included in the friction factors since it is an energy "loss" involved in swirl flow. For the insert arrangements of the present work it is estimated, based on the work of Kreith and Sonju (75) and assuming a fully developed swirl flow, that the tangential flow velocity at point 3, is approximately a factor of 0.96 times the value calculated using the forced vortex model. Using this model, Gambill, Bundy, and Wansbrough (49) show that the radial pressure gradient caused by the swirl flow is given by :

$$\Delta P_{C-R} = \frac{\rho}{3755}\left[\frac{u}{y}\right]^2\left[\frac{R}{r}\right]^2 \qquad (6.14)$$

where Δp_{C-R} is calculated in psi, u in ft s^{-1}, and ρ in lb ft^{-3}, and y is the twist ratio of the twisted tape.

By integrating equation (6.14) across the flow field it can be shown that the average pressure gradient between the tube centreline and the tube wall is one half of the value calculated using equation (6.14). The tangential velocity used in determining equation (6.14) was obtained from equation (A.1.7). Using the factor of 0.96 that was estimated from

the work of Kreith and Sonju, see above, it is therefore possible to estimate the average value of Δp_{C-R} at the axial tube position of P3. In this way it is found that

δH_T = differential manometer fluid head equivalent to the average pressure gradient at the axial position of P3, cm

$$= \frac{0.5386}{(S - 1)} \left[\frac{\rho}{\rho_1}\right]\left[\frac{u}{y}\right]^2 \qquad (6.15)$$

where u is expressed in units of ft s^{-1}. The value of δH_T, obtained using equation (6.15), may be considered as an estimate of the difference in pressure readings at the axial position P3, when measured using a p-stat tube traverse across the tube and when using a wall pressure tapping. On this basis δH_T represents a possible error in the measured manometer fluid differentials due to the apparatus used in the tests.

The value of ϕ_E, calculated by the computer program EX-6010, was determined using $\phi_o = 0.0396\ Re^{-0.25}$. However, the experimental isothermal empty tube friction factor data was correlated well using $\phi_o = 0.0651\ Re^{-0.300}$ and it may be considered that this equation should have been used to determine ϕ_E. Furthermore, in the empty tube section between the inserts and the downstream pressure tapping, P3, the data of Blackwelder and Kreith (6, pp. 102-108) for a fully developed upstream swirl flow, show that the friction factor is approximately 2.3 times the empty tube value. Based on the preceding discussion the possible error in the value of ϕ_E, is given by

$$\delta\phi_E = 0.0396\ Re^{-0.25} - \left[\frac{l_{in}}{(l_{in} + l_{out})} + \frac{(2.3)\ l_{out}}{(l_{in} + l_{out})}\right](0.0651\ Re^{-0.300}) \qquad (6.16)$$

where l_{in}, (l_{out}) = tube length between the upstream (downstream) pressure tapping and the upstream (downstream) end of the packed section of the tube

The above estimates of δH_T and $\delta\phi_E$ are considered to be overestimates since they assume that a fully developed swirl flow exists at the exit of the packed section. This will not be true for all of the configurations tested.

The method of Kline and McLintock is now applied to each of the component terms of equation (6.5), hence it is found that :

$$\frac{\delta\phi}{\phi} = \frac{\delta\phi_{T1} + \delta\phi_{T2}}{\phi} \qquad (6.17)$$

The term $\delta\phi_{T1}$ is calculated using the same method as that required to determine $\delta\phi$ in the empty tube analyses. The analysis to obtain $\delta\phi_{T2}$ is :

$$\phi_{T2} = \phi_E \frac{(l_{in} + l_{out})}{l} \qquad (6.18)$$

where l = packed length of the tube

Hence, using equation (6.2) :

$$\frac{\delta\phi_{T2}}{\phi_{T2}} = \frac{\delta\phi_E}{\phi_E} + \frac{\delta(l_{in} + l_{out})}{(l_{in} + l_{out})} + \frac{\delta l}{l} \qquad (6.19)$$

Alternatively, using equation (6.4) :

$$\frac{\delta\phi_{T2}}{\phi_{T2}} = \left[\left[\frac{\delta\phi_E}{\phi_E}\right]^2 + \left[\frac{\delta(l_{in} + l_{out})}{(l_{in} + l_{out})}\right]^2 + \left[\frac{\delta l}{l}\right]^2\right]^{0.5} \qquad (6.20)$$

In section 6.3.1 the reliability estimation used the results for sample empty tube tests; some of these tests exhibited small manometer fluid differentials. The results for a full length Kenics mixer arrangement required the measurements of the largest manometer fluid differentials obtained in the present study. The estimation procedures considered in this section are applied to sample experimental data obtained using the Kenics system, in Tables 6.1 and 6.2. The experimental data corresponds to the results of denotation I of Table 5.8. Tables 6.1 and 6.2 show that the effects of δH_T and $\delta\phi_E$ are negligible for insert configurations where the empty tube pressure drop corrections are small compared to the total pressure drop along the tube. For comparison, the results of tests performed using three equidistantly spaced, anticlockwise twisting, inserts with aligned leading edges are also considered in Tables 6.1 and 6.2. The experimental data for these tests is presented in the graph and tables that are noted in Table 6.1; this data is represented by denotation A of Table 5.7.

6.3.3 Empty tube tests performed under heating conditions.

The analysis of this mode of operation is already stated in

section 6.3.1. However, friction factors quoted in the literature as "non-isothermal friction factors" are generally obtained such that the total length of tube between the pressure tappings is either heated or cooled. For the present work it may be considered that the empty tube lengths between the pressure tappings and the heated section act under an isothermal mode. Neglecting fluid density changes it can be shown that :

$$\phi_h = \phi_{oM} \frac{(l + l_{in} + l_{out})}{l} - \phi_{o(iso)}^{t_i} \frac{l_{in}}{l} - \phi_{o(iso)}^{t_o} \frac{l_{out}}{l} \qquad (6.21)$$

where ϕ_h = friction factor acting along the heated tube length

ϕ_{oM} = experimentally determined value of the friction factor

$\phi_{o(iso)}^{t_i}$ = friction factor calculated using the experimental empty tube isothermal regression equation at a Reynolds number based on the fluid inlet temperature

$\phi_{o(iso)}^{t_o}$ = friction factor evaluated as for $\phi_{o(iso)}^{t_i}$ but using a Reynolds number based on the outlet fluid temperature

l = heated length of the tube

l_{in}, (l_{out}) = tube lengths between the upstream (downstream) pressure tapping and the upstream (downstream) end of the heated section.

Tables 6.3 and 6.4 present the results of a reliability estimation using the analysis of section 6.3.1. The sample empty tube results obtained under heating conditions are those which pertain to denotation K of Table 5.5. For these tests, the values of $((\phi_h - \phi_{oM})/\phi_{oM})$, that were calculated using the above procedure, are 0.027 and 0.002 for run numbers 1 and 27, respectively.

6.3.4 Tests performed using heating conditions and inserts.

Applying the procedures of sections 6.3.2 and 6.3.3 it is found that :

$$\delta\phi_E = 0.0396\, Re_{t_{av}}^{-0.25} - \frac{l_{in}}{(l_{in} + l_{out})}(0.0651 Re_{t_i}^{-0.300}) - \frac{l_{out}}{(l_{in} + l_{out})}(2.3)(0.0651 Re_{t_o}^{-0.300}) \qquad (6.22)$$

where Re_{t_i}, Re_{t_o}, $Re_{t_{av}}$ = Reynolds numbers evaluated at the inlet, outlet, and average fluid temperatures. For the purpose of the present estimations t_i, t_o, and t_{av}, are considered to be the temperatures indicated by the thermocouples T1, T2, and the mean value (T1 + T2)/2, see Figure 2.4.

The value of δH_T is evaluated using the method of section 6.3.2. The reliability estimations for tests using the continuous Kenics system, and for the use of three aligned equidistantly spaced inserts of the same twist direction, are given in Tables 6.3 and 6.4. The experimental results for the continuous Kenics mixer are those represented by denotation H of Table 5.10. The experimental results for the configuration of three inserts are those represented by denotation A of Table 5.9.

6.3.5 Reliability of the Reynolds number.

The Reynolds number is defined by :

$$Re = \frac{du\rho}{\mu} = \frac{4Q\rho}{\pi d\mu} \qquad (6.23)$$

Neglecting any deviations of the fluid properties due to possible errors in temperature measurement, a reliability analysis using the linear equation, (6.2), shows that

$$\frac{\delta Re}{Re} = \frac{\delta d}{d} + \frac{\delta Q}{Q} \qquad (6.24)$$

Alternatively, using the second power equation, (6.4), then

$$\frac{\delta Re}{Re} = \left[\left[\frac{\delta d}{d}\right]^2 + \left[\frac{\delta Q}{Q}\right]^2 \right]^{0.5} \qquad (6.25)$$

Substituting $(\delta d/d) = 0.01$ and $(\delta Q/Q) = 0.03558$ into equations (6.24) and (6.25) it is found that $(\delta Re/Re)$ is approximately equal to 0.046 and 0.037, respectively. Using the more probable estimates, $(\delta d/d) = 0.005$ and $(\delta Q/Q) = 0.01575$, then $(\delta Re/Re)$ is found to be 0.021 and 0.017 using equations (6.24) and (6.25), respectively.

6.3.6 Discussion of the reliability of the friction factor data.

From Table 6.2, the maximum and probable deviations that may exist in the determined friction factors for the isothermal empty tube data are found to be 8.8% and 4.3% using the second power equation. These values are reasonable representations of the actual deviations of the present data and the results obtained using the Blasius equation. The results, for isothermal and heating modes, show that the possible errors have maximum values in the range 8% to 14% and more probable values in the range 4% to 11%, for all of the data obtained. Assuming a Reynolds number exponent of -0.33, the largest value determined experimentally, the errors in the friction factors calculated using the regression equations would only be 1.5% greater than the errors noted above. This calculation was based on the maximum error determined using the linear equation of the Reynolds number analysis, and hence is a maximum possible additional error.

The reliability estimations were separately performed on the terms ϕ_{T1} and ϕ_{T2} and the overall reliability of ϕ was determined from these values. This procedure is an approximation since it requires the addition of the two error terms which both depend on the error δl. However, since the term $\delta\phi_{T2}$ has only a small effect on $\delta\phi$ the approximate method is adequate. Strictly, equation (6.5) should be rearranged in the form

$$\phi = \frac{1}{l}\left[\frac{\pi^2 d^5 H \rho_1 g (S-1)}{64 \rho Q^2} - \phi_E (l_{in} + l_{out})\right] \qquad (6.26)$$

6.4 Reliability analysis of the heat transfer factors

While analysing the heat transfer data obtained using inserts, the heat transfer resistance, C, was considered to be known exactly. Using this assumption the 95% confidence intervals and correlation coefficients, for the regression equations, were found. Had the value of C been unknown, a regression analysis with no assumptions would not have been possible.

The heat transfer factor, $Nu/Pr^{0.4}$, is calculated using

$$\frac{Nu}{Pr^{0.4}} = \frac{d_o}{\left[(1/U) - C\right] k\, Pr^{0.4}} \tag{6.27}$$

A heat balance over the double pipe heat exchanger gives

$$q = Q \rho c_p (t_o - t_i) = Q \rho c_p \Delta t \tag{6.28}$$

$$q = U \pi d_o l \Delta t_{LM} \tag{6.29}$$

where $$\Delta t_{LM} = \frac{(T_o - t_i) - (T_i - t_o)}{\ln\left[\frac{T_o - t_i}{T_i - t_o}\right]} \tag{6.30}$$

Combining equations (6.27) to (6.29) and rearranging we obtain

$$\frac{Nu}{Pr^{0.4}} = \frac{1}{\left[\frac{\pi l \Delta t_{LM}}{Q \rho c_p \Delta t} - \frac{C}{d_o}\right] k\, Pr^{0.4}} \tag{6.31}$$

In order that dependent terms are not combined in the reliability analysis the temperature variables are compounded into the single term ($\Delta t_{LM}/\Delta t$). An approximation of the reliability of this term is derived below.

Using the substitutions

$$G_o = (T_o - t_i) \tag{6.32}$$

and $$H_o = (T_i - t_o) \tag{6.33}$$

we obtain

$$\frac{\partial(\Delta t_{LM}/\Delta t)}{\partial T_o} = \frac{\ln\left[\frac{G_o}{H_o}\right] - \frac{(G_o - H_o)}{G_o}}{\Delta t\left[\ln\left[\frac{G_o}{H_o}\right]\right]^2} \tag{6.34}$$

$$\frac{\partial(\Delta t_{LM}/\Delta t)}{\partial T_i} = \frac{\frac{(G_o - H_o)}{H_o} - \ln\left[\frac{G_o}{H_o}\right]}{\Delta t\left[\ln\left[\frac{G_o}{H_o}\right]\right]^2} \tag{6.35}$$

$$\frac{\partial(\Delta t_{LM}/\Delta t)}{\partial t_i} = \frac{(G_o - H_o)\left[\ln\left[\frac{G_o}{H_o}\right] + \left[\frac{\Delta t}{G_o}\right]\right] - \left[\Delta t \ln\left[\frac{G_o}{H_o}\right]\right]}{\left[\Delta t \ln\left[\frac{G_o}{H_o}\right]\right]^2} \tag{6.36}$$

$$\frac{\partial(\Delta t_{LM}/\Delta t)}{\partial t_o} = \frac{\left[\Delta t \ln\left[\frac{G_o}{H_o}\right]\right] - (G_o - H_o)\left[\ln\left[\frac{G_o}{H_o}\right] + \left[\frac{\Delta t}{H_o}\right]\right]}{\left[\Delta t \ln\left[\frac{G_o}{H_o}\right]\right]^2} \tag{6.37}$$

The equations (6.32) to (6.37) are used in either a "linear" or "second power" reliability analysis equation to obtain $\delta(\Delta t_{LM}/\Delta t)$.

A "linear" reliability analysis of equation (6.31) shows that

$$\frac{\delta(C/d_o)}{(C/d_o)} = \frac{\delta C}{C} + \frac{\delta d_o}{d_o} \tag{6.38}$$

and

$$\frac{\delta Y}{Y} = \frac{\delta l}{l} + \frac{\delta(\Delta t_{LM}/\Delta t)}{(\Delta t_{LM}/\Delta t)} + \frac{\delta Q}{Q} \tag{6.39}$$

where

$$Y = \frac{\pi \; l \; \Delta t_{LM}}{Q \; \rho \; c_p \; \Delta t} \tag{6.40}$$

and

$$\frac{\delta(Nu/Pr^{0.4})}{(Nu/Pr^{0.4})} = \frac{\delta Y + \delta(C/d_o)}{\left[Y - (C/d_o)\right]} \tag{6.41}$$

A number of possible methods for the estimation of δC were considered, these are outlined below :

(i) The regression equation used for the analysis of the raw experimental empty tube data may be written in the form :

$$\frac{1}{\left[Y - (C/d_o)\right]} = F \; Re^E \; k \; Pr^{0.4} \tag{6.42}$$

Rearranging, we obtain

$$(C/d_o) = Y - X \tag{6.43}$$

where $$X = \frac{1}{F\ Re^{E}\ k\ Pr^{0.4}} \tag{6.44}$$

Hence $$\delta X = \frac{E\ \delta Re}{k\ Pr^{0.4}\ F\ Re^{(E+1)}} \tag{6.45}$$

For a given set of empty tube results, F is known, E = 0.8, and δRe is obtained using the method of section 6.3.5. Using a "linear" reliability analysis it is found that

$$\delta(C/d_o) = \delta Y + \delta X \tag{6.46}$$

Alternatively, a "second power" analysis may be used.

The above method has two faults: the terms Y and X both involve the term $(Q\rho)$ and therefore the terms δY and δX should not be combined since they are not independent, also, substituting equation (6.46) into equation (6.41) shows that the term δY is used twice, which again involves the combination of two dependent terms. The former fault may be partly surmounted by rearranging equation (6.42) and making the approximation given below :

$$(C/d_o) = \frac{\pi\ l\ \Delta t_{LM}}{Q\ \rho\ c_p\ \Delta t} - \left[\frac{\pi\ d\ \mu}{4\ Q\ \rho}\right]^{E} \frac{1}{F\ k\ Pr^{0.4}}$$

$$\approx \frac{1}{Q\rho}\left[\frac{\pi\ l\ \Delta t_{LM}}{c_p\ \Delta t} - \left[\frac{\pi\ d\ \mu}{4}\right]^{E} \frac{1}{F\ k\ Pr^{0.4}}\right] \tag{6.47}$$

(ii) Since tests using the empty tube were, in some instances, performed prior to and after the insert tests, the value of δC may be considered to be the difference of the values of C for the two empty tube tests. Alternatively, if the tube was destroyed after the insert tests, or if a relatively long time period existed between the empty tube tests, thereby possibly leading to scale formation, the value of δC may be obtained from the two values of C found by assuming that E = 0.8 and E = (0.8 - CON.) for the empty tube data analysis using the ln-ln linear regression.

(iii) The value of δC may be considered to be the difference in the values of C obtained using the regression analysis with the assumptions that E equals the actual regression Reynolds number exponent, and that E equals the regression exponent minus the 95% confidence interval on the exponent. For empty tube tests this method is the alternative procedure used in method (ii). Provided that the data scatter of the insert tests and of the tests for the empty tube which provide the heat transfer resistance value, C, are approximately equal, then methods (ii) and (iii) will produce approximately the same reliability analysis results.

For the reasons discussed above, methods (i) and (ii) were applied to the analysis of the present work. Tables 6.5 and 6.6 show reliability analyses based on estimates of the possible errors in the measured variables which may be considered as "mean" values. Tables 6.7 and 6.8 show the results obtained using the same analyses with the "maximum" possible deviations of the variables.

6.4.1 Discussion of the reliability of the heat transfer factors.

As stated previously, method (i) of section 6.4 is not considered to be a good method for the estimation of $\delta(C/d_o)$. The use of the method results in extremely large possible errors in the heat transfer factors. If these errors are due to ramdom errors in the measured variables then these should be demonstrated by considerable data scatter on the heat transfer factor charts. Since this is not found to be the case the possible errors may almost be considered to be fixed errors i.e. approximately the same error occurs in each of the variables when it is determined on consecutive occasions. Considering this to be true, the possible error in $\delta(C/d_o)$ should not be considered to be caused by errors in X and Y but only by the scatter of the data about a Wilson plot line (Y versus X): method (ii) is based on this procedure.

From Tables 6.6 and 6.8 the possible errors in the empty tube heating data, obtained using the second power equation with method (ii), are seen to be approximately 7% (mean) and 13% (maximum). Using the approximate linear equation and the maximum possible error in the Reynolds number, the possible errors in the heat transfer factors obtained using the linear regression equation are 3.6% greater than the values stated above.

Since the possible errors in the heat transfer factors are inversely proportional to $((1/U) - C)$ it is clear that the use of a very low heat transfer resistance, C, is to be preferred. This effect is shown by comparing the reliability analysis results of denotations C and D, and G and H (Tables 6.6 and 6.8). These results were obtained using identical insert configurations but for denotations C and D the annulus fluid flowrate was greater than that used in determining the results for denotations G and H. The possible error limits on the data obtained using the full length Kenics arrangement (configuration 6K) are quite large, but they are considered to be acceptable for most design situations. It should be noted that the full length arrangements (configurations 6K and 7T) used insert lengths which did not quite extend along the full heated tube length. To allow for this effect, and also the possible error in the insert length due to the method of constructing the lengths, the heated length of tube has been considered to possess a possible error of 2.24% (maximum).

Configuration 6K yields an approximately three fold increase of the heat transfer factor compared to the empty tube value; configuration 7T, the full length twisted tape, yields an approximately two fold increase. Due to the intermediate results obtained using configuration 7T, this arrangement has also been analysed in order to provide a reasonably complete reliability analysis over the total range of the measured heat transfer factors.

7 Comparisons with previous work

7.1 Introduction

This chapter compares the hydraulic and thermal characteristics of tubes containing either the twisted tape or Kenics configuration with the results obtained by previous workers. Also, all of the present work is presented in the form of $\ln(Nu/Nu_o)$ versus $\ln(\phi / \phi_o)$ and using the constant pumping power criterion adopted in Chapter 1.

7.2 Pall rings

The packed/empty tube ratios of the Nusselt numbers and friction factors were evaluated at Reynolds numbers of 15500 and 86500 (the maximum value obtainable with a fully packed tube) using the regression equations in Tables 5.2 and 5.3. The average values of the ratios determined at these Reynolds numbers are shown in Figure 7.1. Also shown are some of the data presented by Norris (6, pp. 16-26). The results for large roughness spacings were obtained using $s/e = 10$, which is the optimum spacing. These roughnesses were either an integral part of the tube wall or there was a small resistance between the tube and the roughness elements. The Pall rings did not intimately contact all of the circumference of the tube and therefore they provide little, or no, fin effect, instead they may have actually reduced the effective heat transfer surface area. This is one of the reasons for the lower Nusselt numbers produced using Pall rings as opposed to other forms of tube roughness. Furthermore, portions of the Pall rings projected into the bulk flow stream thereby leading to form drag and increasing the ratio ϕ / ϕ_o.

For reasons of clarity, the line corresponding to equation (1.91) has not been included in Figure 7.1. This line would pass through the origin of Figure 7.1 and the point where $\phi / \phi_o = 10$, $Nu/Nu_o = 1.95$. All of the results obtained using Pall rings would lie below the line and therefore the use of Pall rings is not an effective method for heat transfer enhancement, based on the constant power criterion. Table 7.1, which was formed using equation (1.90), clearly demonstrates this conclusion. It can be seen that the Reynolds number, Re_{op}, may be larger than the highest values used in the empty tube tests, however it was assumed that the empty tube characteristics were specified by the results in Tables 5.2 and 5.3.

While reviewing some previously published work it was necessary to estimate the friction factor and/or heat transfer factor for the empty tube. In these instances the viscosity effect at the tube wall and the effect of the tube length were neglected. This procedure was also adopted by Bergles et. al. (2), (5). The empty tube characteristics were considered to be those which are represented by equation (1.4) and by equation (1.19). The results of the present work have also been analysed using these equations and the constant pumping power criterion. The resulting Nusselt number ratios for a constant power, $(Nu/Nu_o)^*_p$ are presented in Table 7.1. The difference between $(Nu/Nu_o)_p$ and $(Nu/Nu_o)^*_p$ never exceeds 8%. The experimental empty tube characteristics should be used in evaluating the results with the constant power criterion; however for comparison with the effectiveness of some devices the values of $(Nu/Nu_o)^*_p$ may provide a better, although not strictly correct, relative comparison.

7.3 The twisted tape (Configuration 7T)

Equation (5.9) represents the isothermal (room temperature) pressure drop characteristics of the twisted tape configuration used in the present work. The results obtained under heating conditions can also be formulated into an equation which is independent of the flow area changes and flow development :

$$\phi_{CORR} = 1.20\ Re^{-0.281} - 0.593\ Re^{-0.268} \qquad (7.1)$$

The friction factor ratios evaluated using equations (5.9) and (7.1) and the equations presented in Chapter 1 are compared in Table 7.2. These results, which have been evaluated at the limits of the Reynolds number range of the present work, provide a reasonable comparison of the work of various authors because most of the available correlations are almost straight line presentations on logarithmic co-ordinates. The results of Seymour (111) are not used in this comparison because they show that a "laminar/turbulent" flow transition occurs at Reynolds numbers greater than 10^4. This result was not found in the present work, or by other workers, it may occur as a result of the smooth entrance conditions and thin tapes used by Seymour. Converting equation (1.44) to the equivalent flow basis and using the conditions of the present work, as outlined in Table 7.2, it is found that $\phi / \phi_o = 8.51$

± 0.03, over the Reynolds number range 11000 to 78000. This result agrees reasonably well with the present work although for the above reasons it is a tentative comparison.

The correlation proposed by Gambill and Bundy (47) severely underpredicts the present results. However, they note that some of the results, used to obtain their correlation, may be in error. The average percentage difference between the present results and the predictions of the remaining authors in Table 7.2 is 39% for isothermal conditions (Re = 11000 and 78000). This difference may be due to the fact that the values of (δ/d) used by previous workers were considerably less than that of the present work. It may be that the equivalent flow concept cannot be used to extrapolate the available correlations to larger values of (δ/d). An alternative reason for the deviations is the effect of the roughness of the tube and inserts. Lopina and Bergles (79), see section 1.3.6 of this thesis, suggest that the tube roughness has a significant effect on the pressure drop with swirling flows. Furthermore, Koch (69, p. 51) suggests that the friction on the tape surface accounts for the majority of the pressure drop. Although the joints between consecutive elements appeared to be reasonably smooth, it is possible that the difference between the results of this study and those predicted using the correlations in section 1.3.6, is the result of an increased pressure loss at the surface of the tape. If the above argument is correct, and it is assumed that the tape does not act as a fin, then the heat transfer results of the present work should be adequately predicted by the correlations of previous workers. Table 7.3 shows the good agreement of the results. The heat transfer correlations of Gambill et. al. (49, 50) were not converted to the equivalent flow basis because of the range of values of d and δ used in their studies and because some of their tests were performed using $(\delta/d) = 0.1$; this is reasonably close to the value used in this work. It may be this effect which results in the slightly lower heat transfer factors obtained using equations (1.29) and (1.30).

The heat transfer correlation proposed by Migay (83), see equation (1.43), was not used in Table 7.3. For the geometry of the present work, the correlation predicts heat transfer factor ratios of 5.37 and 2.86 at Reynolds numbers of 15500 and 104000. These values are considerably greater than those obtained using the correlations that were proposed by other workers. Migay's correlation has not been used by any

previous authors other than Date (30). This may indicate that equation (1.43) does not produce satisfactory predictions.

The friction factor correlations of the reference authors were adjusted to heating conditions in Table 7.2 by using equations (1.53) and (1.54). These correlations were obtained using water. For the conditions of the present work, these equations show that

$$\frac{\phi_h}{\phi_{iso}} = 0.947 \qquad \text{for the twisted tape}$$

and $$\frac{\phi_{o(h)}}{\phi_{o(iso)}} = 0.903 \qquad \text{for the empty tube}$$

where the friction factors are evaluated at the same bulk Reynolds number and the following subscripts have been used :

h = heating conditions

iso = isothermal conditions

o = empty tube

Using the correlations of the results obtained under isothermal and heating conditions, with an average bulk fluid temperature of $35^{o}C$, and with allowance for the effects of the tape ends and flow development, the present work shows that

$$\frac{\phi_{CORR(h)}}{\phi_{CORR(iso)}} = 0.985 \qquad \text{for the twisted tape}$$

and $$\frac{\phi_{o(h)}}{\phi_{o(iso)}} = 0.908 \qquad \text{for the empty tube}$$

The effect of heating is seen to reduce the isothermal friction factors by a smaller amount than is predicted by equation (1.54). This is because, in the present tests, a larger proportion of the total pressure loss occurs at the tape surface rather than at the tube wall where the viscosity reduction is effective. This is a result of the slight roughness of the tapes used in this work.

Figure 7.2 presents all of the results obtained using solder inserts under heat transfer conditions. These results have previously been presented in Figures 5.52 to 5.54. The actual friction factors associated with the powers required to produce the heat transfer coefficients have been used in these graphs i.e. no allowance has been made for the flow development and tape end effects with configuration 7T. At Reynolds numbers of 15500 and 104000 the values of (Nu/Nu_o) and (ϕ / ϕ_o) do not deviate from the mean values shown in Figure 7.2 by

more than 3.2% and 6.5%, respectively, and generally the deviations are considerably smaller. The dashed line on Figure 7.2 shows the effect of increasing the number of type T (LH:LH) inserts with aligned (0^{o}) leading edges. Comparing this line with Figure 7.1 clearly shows that the relationship between the heat transfer and friction factor increases is different for these enhancement devices. The complex form of the line must represent the changing proportional contributions of the swirling flow, form drag and flow disturbances, and surface friction, on the heat transfer and pressure drop characteristics. Obviously, Figure 7.2 is not a good method of representing the results obtained with these inserts.

Table 7.4 shows that type T configurations are not effective for heat transfer enhancement when used with the conditions of this work. However, it is interesting to note that configuration 5T is a better device than the full length tape, configuration 7T. The former configuration requires approximately one half of the insert material needed to produce a full length tape; this may be important in applications where equipment weight reduction is a design criterion.

The results for configurations 1T and 1TS show that the effect of the insert thickness on the ratio $(Nu/Nu_o)_p$ is negligible for tubes containing 3 inserts. Table 7.4 also shows that the use of the full length perpendicular edge arrangement, or locating the inserts near to the tube exit (configuration 9T), are to be avoided if the constant power criterion is to be used as a measure of the effectiveness.

The following modifications of the present insert configurations may produce more beneficial results :

(i) The use of smooth inserts will reduce the pressure drop across configuration 7T, possibly by upto 40%. A lower reduction would occur with configuration 5T, for example.

(ii) The inserts used in this work did not behave as effective fins. Enhancement of the contact between the inserts and the tube wall, for example by redrawing the tube over the inserts or by a tube rolling process at the location of the inserts, would increase the heat transfer coefficients. The fin effect determined by Lopina and Bergles (79), see section 1.3.6, was obtained using a redrawn tube.

(iii) Configurations 1T, 1TS, 2T, ... to 6T, do not benefit from the swirl flow downstream of the inserts which are located at the exit of the heated section. If these inserts had not been included

then the pressure loss across the tube would have been significantly reduced, although there would have been a smaller reduction in the heat transfer coefficients. These comments also apply to the type K configurations.

(iv) The use of thinner inserts would reduce the power requirements of all of the configurations. However, the heat transfer coefficients are dependent on the fluid mixing between the inserts and the interaction of the tube wall fluid with the flow which has separated at the leading edges of the inserts. (This has been discussed in section 5.4.4 and by Sparrow et. al. (121), see section 1.3.4). Furthermore, the greater fluid velocities associated with the larger values of (δ/d) will produce larger heat transfer coefficients in the packed sections of the tube. It is likely that there exists an optimum insert thickness, for each configuration, which produces the largest values of $(Nu/Nu_o)_p$. It was not the purpose of the present work to determine the optimum insert thickness.

7.4 The Kenics static mixer arrangement (Configuration 6K)

No previous workers have proposed generalised correlations which may be used for the comparison of the pressure drop results of various studies. For this reason the friction factors are to be compared with equations (1.80) to (1.83). Allowance for the relative insert thickness, (δ/d), is based on the equivalent flow concept using equations (A.1.2) and (A.1.3). This procedure cannot be theoretically justified and it is only used because of a lack of any further information. Furthermore, it is possible that the effect of the tube diameter, as proposed in equations (1.80) to (1.83), does partially include the effect of the thickness of the inserts, although since no geometrical details are available it is impossible to determine this possible effect. Details of the comparison procedure and the calculated results are presented in Appendix A.12 and Table 7.5.

The isothermal results of the present work are slightly greater than the predicted results. The experimental friction factors were determined using 26 inserts. However, the results in references (24) and (60) may have been obtained using 6 elements since that is the number used to form a standard Kenics mixer module. It has already been shown that the friction factor decreases slightly as the number of

elements is reduced and this is one possible reason for the deviation between the experimental and predicted results. It is also possible that the slight roughnesses, near to the joints of successive elements, may also lead to greater friction factors. This effect is expected to be small due to the high degree of mixing of the fluid stream. However, it must be recalled that equations (1.80) to (1.83) are the results of regression analyses of the manufacturer's data. Their work involved inserts with twist ratios upto 1.8 (60), or 1.9 (24). Extrapolation of the equations to the twist ratio used in the present work ($y = 2.03$) may be a possible source of the deviations which have been noted. Also, it was assumed that $(\delta/d) = 0.1$ for the standard mixer; this is an approximation.

The differences between the predicted and experimental friction factors is greater for the heating results than for those obtained under isothermal conditions. This must be due to an overprediction of the effect of the fluid viscosity near to the tube wall. This indicates that the results given in references (24) and (60), on which the prediction correlations are based, were obtained under isothermal conditions. It is also interesting to note the close agreement of the effect of the Reynolds number on the friction factor ratio; the results of Chen (24) indicate that K is proportional to $Re^{0.104}$ while the present work shows a dependence on $Re^{0.111}$ under isothermal conditions. This again implies that the results in reference (24) were obtained under isothermal conditions.

In Table 7.5, the results of previous workers have been extrapolated to Reynolds numbers of 78000 in order to examine if such extrapolations produce agreement between the previous and predicted work. In the turbulent flow regime the friction factor is proportional to the Reynolds number raised to a given power. The results of Chakrabarti (21) were obtained in the empty tube laminar flow regime and they do show some curvature of the ln-ln friction factor correlation. For this reason the correlation proposed by Chakrabarti has been presented graphically as Figure 7.3. The lowest Reynolds numbers below which Chakrabarti's correlation deviates from the predicted results by more than about 15% is shown in Table 7.5. Although the present work and that of Chakrabarti was performed at considerably different Reynolds numbers the agreement with the predicted friction factors is quite good. The results of Smith (116), (117) also indicate a good agreement over a

wide Reynolds number range, particularly when, as with the previous work considered above, the modified form of equation (1.81) is used for comparison.

Although this work was not directed towards measurements in the laminar flow regime the above conclusions suggest that the modified forms of equations (1.80) to (1.83) may be used at low Reynolds numbers. Figure 7.4 shows some results which have been extracted from the literature concerning the pressure losses associated with the Kenics system. The results obtained from the manufacturer's literature (24), (60) are greater than those determined by Proctor (101) and Lin et. al. (78) who both used a tube diameter of 12.7 mm. No conclusive reason can be offered for the comparatively small friction factors determined by Lin et. al. who used liquid refrigerant-113 in vertical electrically heated tubes. However, it is interesting to note that they sustained a laminar/turbulent flow transition at Reynolds numbers upto 5500. For the above reasons, Figure 7.4 clearly shows that it is not advisable to extrapolate the results of the present work to considerably lower Reynolds numbers.

Morris and Benyon (86) and Proctor (101) used the same equipment in their mass transfer studies. Table 7.5 shows that their experimentally determined friction factors are considerably smaller than the predicted results. Unfortunately, they do not present any empty tube friction factor data which would provide an indication of the accuracy of their measurements and the relative roughness of the surface of the naphthalene layer. The diagram of the apparatus, as shown in reference (101), indicates that the pressure tappings were very close to the Kenics elements and this may have produced some error in the results. Proctor suggests that the difference between the friction factors determined under mass and heat transfer conditions may be partially attributable to a slight deterioration of the contact between the inserts and the naphthalene at the tube wall. In conclusion, Proctor suggests that caution should be exercised in using his friction factor results and that further work is required.

Further possible reasons may be suggested for the difference between the results found by Proctor (101) and those calculated using the modified forms of equations (1.80) to (1.83). These include :

(i) A minimum diameter of 15.7 mm was used in the regression analyses that produced equations (1.80) to (1.83). The tube diameter

was 12.7 mm in the tests of Proctor (101). It is clear therefore that in using the regression equations with the geometrical details of Proctor's work there has been an extrapolation, with respect to the tube diameter, of the regression equations.

(ii) Equations (1.64), (1.66), and (1.70), show that the friction factor characteristics of many in-line mixers depend on the fluid viscosity; lower viscosities lead to lower friction factors. Proctor's studies (101) used air, and since Kenics mixers are generally used with viscous fluids it is likely that the results of reference (24) apply for fluids with viscosities that are greater than that of air. For this reason, it may be expected that the friction factors that were determined by Proctor would be smaller than those found by Chen (24). However, Chen does not indicate that the friction factor is dependent on the fluid viscosity, other than in the manner that is indicated by the Reynolds number effect. The results of Smith (116), (117), for air and water, also indicate that there is no effect of the fluid viscosity, other than that shown by the Reynolds number dependency, on the friction factor characteristics of Kenics mixers.

Previous workers have shown that the insertion of a Kenics mixer, y = 1.5 (approximately), into an empty tube will increase the heat transfer coefficient by approximately a factor of 3. In the present work, the average of the heat transfer factor ratios, evaluated at Reynolds numbers of 15500 and 104000, was found to be 2.79. This result was obtained using inserts with a twist ratio of 2.03 and a slightly greater relative insert thickness than those used by previous workers. Due to the lack of information it is not possible to propose any correlation concerning the effects of y, D, δ, and the fin effect, on the heat transfer characteristics of the Kenics system.

Figure 7.5 compares the present results with those obtained by Lin et. al. (78) in the laminar/turbulent transitional flow regime. Reference (78) does not provide specific geometrical details of their Kenics mixers although it is inferred that they used commercially available mixers. For this reason, their results and those of reference (25) should be similar. The slight disagreement of these two sources is difficult to explain since no experimental data is given in reference (25). It may be that the manufacturers (25) considered that

their proposed correlation adequately represents all of their results for Re > 2000. There may have been some curvature of their data in the Reynolds number range of the laminar/turbulent transitional flow regime. Such curvature may have been neglected in order to produce a straight line (ln-ln) correlation of the results for Re > 2000. If this suggestion is correct, the lines H and D in Figure 7.5 may be considered to represent the characteristics of the Kenics static mixer in the transitional and turbulent flow regimes. On this basis, it appears that extrapolation of the present results, obtained using a full length Kenics configuration, may lead to predictions which are slightly lower than the actual heat transfer factor at low Reynolds numbers. The relative positions of the characteristics of the full length Kenics mixer and configuration 9K are approximately the same in this study and reference (78). Therefore, extrapolation of the present results, obtained with configuration 9K, may also lead to under predictions of the heat transfer factors at low Reynolds numbers.

Figure 7.5 shows the considerable enhancement that may be obtained by using Kenics inserts in the conventional laminar/turbulent flow regime. However in some applications the need for very large heat transfer coefficients necessitates operation in the turbulent regime. It is also interesting to note that Lin et. al. (78) produced conditions which are particularly suitable for heat transfer enhancement. They sustained a flow for which the friction factor decreased rapidly with increasing Reynolds number while the heat transfer factor increased rapidly. It may be that in an industrial application, with flow disturbances upstream of the heat exchanger, these conditions cannot be produced and turbulence will be increased.

Figure 7.2 shows that all of the results obtained using alternately twisted helices, with perpendicular edges, can be represented by a single curve using logarithmic co-ordinates of the heat transfer factor ratio and the friction factor ratio. It may be that this type of correlation is possible because each of the pairs of inserts increases, to approximately the same extent, the magnitude of the effects which result in the heat transfer and pressure drop increases. In contrast, the results obtained using aligned anticlockwise helices could not be correlated in this way because of the changing contribution of each of the effects producing the increases.

Figure 7.2 clearly shows that the use of a continuous length of Kenics mixers extending along part of the heated tube length, that is, configurations 8K and 9K, is not a good method of increasing the heat transfer coefficient. It is also seen that alignment of the leading edges, in a full length configuration of alternately twisted helices, is better than the perpendicular edge arrangement, i.e. the Kenics mixer configuration. Table 7.6 shows that the continuous aligned edge arrangement is considerably better than the other configurations when compared using the constant power basis. This table also indicates that none of the devices were beneficial. However, it would be possible to increase the heat transfer factors by enhancing the contact between the inserts and the tube wall.

The thicker stainless steel inserts produced values of $(Nu/Nu_o)_p$ which were approximately 3 to 4% greater than those obtained using the solder inserts. However, with the available inserts, only two configurations could be tested using both of the insert thicknesses. Due to this low number of tests, it cannot be conclusively stated that the use of thicker inserts is to be preferred for all of the configurations shown in Figure 1.6.

8 Conclusions

This chapter is a summary of the main conclusions and results of this study. For reasons of brevity, and to provide a clear presentation, the conclusions have been annotated.

(i) A survey of the turbulent flow characteristics of various commercial in-line motionless mixers has been presented. The lack of design data in published sources required that the survey was mainly based on the sales literature and personal communication with the manufacturers. The pressure loss data has been presented using a common definition of a friction factor.

(ii) The calibration of the rotameters that were used in this work showed that it was necessary to allow for the effect of temperature on the measurement of the volumetric flowrate of the water. Various calibration correlations were produced. It was found that, for most purposes, a correlation which uses a quadratic function of the rotameter scale reading and a linear function of the fluid temperature will be adequate. This procedure had not been proposed by previous workers.

(iii) An adaptation of the Wilson plot technique has been used. This adaptation eliminates the need to produce two graphs, $1/U$ versus $1/u^{0.8}$ and $\ln(Nu/Pr^{0.4})$ versus $\ln(Re)$, in order to determine the heat transfer characteristics. The adaptation also shows that the use of the above two graphs can lead to the anomaly that the exponent on the fluid velocity is not the same for each of the two graphs. This had been mentioned in the literature but no reasons for it had been proposed.

(iv) Pressure drop and heat transfer tests have been performed using tubes which contained Pall rings. Various empty tube distances, between the Pall rings, were used. The maximum heat transfer factor increase, above the empty tube values that were obtained over the same Reynolds number range, (Nu/Nu_o), was 1.5. This increase was accompanied by a pressure loss increase, (ϕ / ϕ_o), of 15.

(v) None of the configurations of the Pall rings were found to be effective when compared to an empty tube that requires the same pumping

power. This was considered to be due to the form drag, in the central core fluid, that is caused by the insets of the Pall rings. This suggestion was based on the heat/momentum analogy. This analogy has been qualitatively used to explain some of the phenomena observed throughout the present work.

(vi) The characteristics of tubes containing short lengths of twisted tapes interspaced along a tube have been investigated. Over the flow range of the tests, it was found that the optimum empty tube spacing between the pairs of inserts was equal to the length of a pair of the inserts. This may be a coincidence and further tests would be required to examine this finding.

The ratio of the heat transfer coefficient produced by this optimum configuration to that produced in an empty tube requiring the same pumping power, $(Nu/Nu_o)_p$, is 1.0. For the continuous full length twisted tape the ratio was found to be 0.89.

Over the flow range of the tests, the average actual heat transfer factor ratio, (Nu/Nu_o), was 2.0 for the optimum configuration, and 1.8 for the continuous tape. For both of these configurations the above increases were accompanied by friction factor ratios, (ϕ / ϕ_o), of 11, approximately.

(vii) The friction factors which are characteristic of the continuous twisted tape were found to be approximately 40% greater than those calculated using the correlations of previous workers. This was probably due to the slight roughness of the tape at the junctions of consecutive inserts. The relative thickness, (δ/d), of the tape was approximately twice that used by other workers. The equivalent flow concept was used to allow for this difference. The use of this concept may be unjustified and further work is required to clarify this effect.

(viii) Further work using single inserts, as opposed to the pairs used in this study, is recommended. Also, investigations of such configurations for the mixing of turbulently flowing fluids may be beneficial.

(ix) Tests were performed using a continuous Kenics mixer and with pairs of Kenics elements (consecutive alternately twisted helices with

perpendicular leading edges) interspaced along a tube. None of these configurations are beneficial for heat transfer enhancement when using the constant power basis for comparison with the empty tube results of this work. However, heat transfer coefficients were produced which were 2.8 times greater than those obtained while using an empty tube over the same Reynolds number range. This increase was produced with a continuous Kenics mixer for which the friction factor increase, (ϕ / ϕ_o), was 73.

(x) The large difference between the ratios (ϕ / ϕ_o) for the Kenics and twisted tape configurations was due to the combined effects of the flow reversal and perpendicularity of the leading edges of consecutive inserts. For the continuous configurations, formed such that consecutive inserts had either opposite, or identical, twist direction, it was found that alignment of the leading edges of the inserts is to be preferred.

(xi) A continuous length of alternately twisted helices with aligned leading edges was found to be the best arrangement of alternately twisted inserts. For this configuration, the heat transfer coefficient ratio based on the constant power criterion, $(Nu/Nu_o)_p$, was 1.0. The average heat transfer and friction factor increases, relative to an empty tube operating over the same superficial Reynolds number range, were 2.6 and 26, respectively.

(xii) The equidistant spacing of the pairs of inserts is preferred to locating the inserts close to the downstream end of the heated section of the tube. This suggests that the use of pairs of Kenics inserts, spaced along a tube, may be beneficial for the mixing of low viscosity fluids.

(xiii) Correlations have been proposed which acceptably represent the friction factor characteristics, found by various workers, of tubes containing continuous lengths of Kenics mixers operating under isothermal conditions.

(xiv) The friction factor characteristics of tubes that contained various equidistanly spaced pairs of helices have been examined under isothermal conditions and with heat being applied through the

tube wall. Although there is an indication that the effect of the viscosity ratio, (μ_s/μ), is dependent on the number of inserts it was not possible to quantitatively characterize this effect.

(xv) The results have been presented in the form of $\ln(Nu/Nu_o)$ versus $\ln(\phi / \phi_o)$. The results obtained using configurations of alternately twisted inserts, with perpendicular leading edges, were found to lie on a single curve when presented in this form. The results obtained using identically twisted inserts could not be represented by a single curve.

(xvi) The regression parameter, B, where $\phi = A\ Re^B$, was found to vary with the number and arrangement of the inserts in the tube. It has been suggested that the magnitude of B decreases as the kinetic energy losses of the fluid are increased or as the degree of swirl flow is reduced.

(xvii) The configurations that have been studied in this work are unlikely to be used in general heat exchanger applications. However, some of them may be suited to applications where simultaneous heat transfer and fluid mixing is required. Also, they may be suitable where the size reduction of the heat exchanger is a primary consideration. In such instances, it is recommended that the methods of increasing the effectiveness of the inserts, which are suggested in this thesis, should be applied.

(xviii) Estimations of the accuracies of the experimental results were obtained. A number of possible methods of error estimation, involving the Wilson plot technique, are suggested in this thesis. There is a considerable variation in the estimated possible errors that are calculated using these methods. This work shows that, at the present time, there exists a lack of any unified approach for the estimation of the possible errors in many experimental studies.

References

The English translations of foreign material have been cited with the original reference. The page numbers cited in the main body of this thesis apply to the English translations.

(1) Azer, N.Z., Lin, S.T., Fan, L.T.; Ind. Eng. Chem. Proc. Des. Dev., 19, 246-250 (1980).

(2) Bergles, A.E.; Int. J. Heat Mass Trans. Series: Progress in Heat and Mass Transfer, 1, 331-424 (1969).

(3) Bergles, A.E., Blumenkrantz, A.R., Taborek, J.; "Performance evaluation criteria for enhanced heat transfer surfaces", Paper FC6.3, 5th Int. Heat Trans. Conference, II, 239-243, Tokyo (1974).

(4) Bergles, A.E., Brown, G.S., Snider, W.D.; "Heat transfer performance of internally finned tubes", ASME Paper No. 71-HT-31 (August, 1971).

(5) Bergles, A.E., Morton, H.L.; "Survey and evaluation of techniques to augment convective heat transfer", Report No. 5382-34, Dept. of Mech. Eng., Massachusetts Institute of Technology (February, 1965).

(6) Bergles, A.E., Webb, R.L. (Eds.); "Augmentation of convective heat and mass transfer", ASME, New York (1970).

(7) Blasius, H.; Forsch.-Arb. Ing.-Wes., No. 131, 1-40 (1913).

(8) Bluestein, M., Mockros, L.F.; Med. Biol. Eng., 7, 1-16 (1969).

(9) Blum, H.A., Oliver, L.R.; "Heat transfer in a decaying vortex system", ASME Paper No. 66-WA/HT-62 (1966).

(10) Boelter, L.M.K., Young, G., Iverson, H.W.; "An investigation of aircraft heaters - XXVII - Distribution of heat transfer rate in the entrance section of a circular tube", National Advisory Committee on Aeronautics (NACA) technical note TN1451 (1948).

(11) Bolton, P. (Assistant Sales Project Engineer, E.T. Oakes Ltd.); personal communication (December, 1979).

(12) Bor, T.; "The Kenics static mixer and its applications in the chemical process industries", Paper presented at the 4th International Congress of Chemical Equipment Design, Prague, Czechoslovakia (September, 1972).

(13) British Standards Institution; "Flow Measurement", British Standard Code B.S. 1042: 1943. Also "Methods for the measurement of fluid flow in pipes. Part 1. Orifice plates, nozzles and venturi tubes", B.S. 1042: Part 1: 1964 and "Part 3. Guide to the effects of departure from the methods in Part 1", B.S. 1042: Part 3: 1965, London.

(14) British Standards Institute; "International thermocouple reference tables. Part 4. Nickel-chromium/nickel-aluminium thermocouples, Type K", B.S. 4937: Part 4: 1973, London.

(15) Brodkey, R.S. (Ed.); "Turbulence in mixing operations, Theory and application to mixing and reaction", Academic Press, London (1975).

(16) Carman, P.C.; Trans. IChemE, 15, 150-116 (1937).

(17) Carnavos, T.C.; "Cooling air in turbulent flow with internally finned tubes", AIChE4, 17th National Heat Transfer Conference, Salt Lake City (August 1977). This paper is also presented in; Heat Transfer Eng., 1, No.2, 41-46 (1979).

(18) Carnavos, T.C.; "Cooling air in turbulent flow with multi-passage internally finned tubes", ASME Paper No. 78-WA/HT-52 (1978).

(19) Carnavos, T.C.; "Heat transfer performance of internally finned tubes in turbulent flow", Symposium Volume 100122, Advances in Enhanced Heat Transfer, 18th National Heat Transfer Conference, San Diego (August, 1979). This paper is also presented in; Heat Transfer Engineering, 1, No. 4, 32-37 (1980).

(20) Cathie, N.M. (Sales Engineer, Kenics Europe (Belgium)); personal communication (April, 1980).

(21) Chakrabarti, A.; "Mixing of liquids in a static in-line mixer", Ph.D. thesis, University of Bradford (1979).

(22) Charles Ross and Son Company; "Ross motionless mixers", Brochure M-376 (Date unknown). Ross mixers are distributed in England by D.H. Industries.

(23) Chen, N.H.; Ind. Eng. Chem. Fundam., 18, 296-297 (1979).

(24) Chen, S.J.; "Pressure drop in the Kenics Mixer", Kenics Corporation Bulletin KTEK-2 (Revision January, 1978).

(25) Chen, S.J.; "Heat transfer and thermal homogenization of viscous flow in the Kenics mixer", Kenics Corporation Bulletin KTEK-3 (Revision March, 1979).

(26) Chilton, T.H., Colburn, A.P.; Ind. Eng. Chem., 23, 913-919 (1931).

(27) Colburn, A.P.; Trans. AIChE, 29, 174-210 (1933).

(28) Coulson, J.M., Richardson, J.F.; "Chemical Engineering", Vol. 2, 2nd Edition, Pergamon Press, Oxford (1968).

(29) Coulson, J.M., Richardson, J.F.; "Chemical Engineering", Vol. 1, 2nd Edition, Pergamon Press, Oxford (1970).

(30) Date, A.W.; "Prediction of friction and heat transfer characteristics of flow in tubes containing twisted tapes", Ph.D. thesis, University of London (1972).

(31) Davies, J.T.; "Turbulence Phenomena", Academic Press, London (1972).

(32) De Vos, P.; Inform. Chim., 109, 109-123 (June, 1972).

(33) Dipprey, D.F., Sabersky, R.H.; Int. J. Heat Mass Trans., 6, No.3, 329-353 (1963).

(34) Dittus, F.W., Boelter, L.M.K.; "Heat transfer in automobile radiators of the tubular type", University of California Publications in Engineering, 2, No. 13, 443-461 (1930).

(35) Dorsey, N.E.; "Properties of ordinary water substance", Reinhold, New York (1940).

(36) Drew, T.B., Koo, E.C., McAdams, W.H.; Trans. AIChE, 28, 56-72 (1932).

(37) Engineering Sciences Data Unit; "Friction losses for fully developed flow in straight pipes", Item No. 66027, London (1966).

(38) Engineering Sciences Data Unit; "Forced convection heat transfer in tubes, Part I: Correlations for fully developed turbulent flow - their scope and limitations", Item No. 67016, London (1967).

(39) Engineering Sciences Data Unit; "Forced convection heat transfer in circular tubes, Part III : Further data for turbulent flows", Item No. 68007, London (1968).

(40) Ergun, S.; Chem. Eng. Prog., 48, No. 2, 89-94 (1952).

(41) E.T. Oakes Ltd.; "Etoflo process line mixer", Leaflet No. 7022 (February, 1979). Etoflo mixers are now manufactured by Wymbs Engineering Ltd.

(42) E.T. Oakes Ltd.; "Selection guide for Etoflo static mixers" (Date unknown).

(43) Evans, L.B.; "The effects of axial turbulence promoters on heat transfer and pressure drop inside a tube", Ph.D. thesis, University of Michigan (1962).

(44) Evans, L.B., Churchill, S.W.; Chem. Eng. Prog., 58, No. 10, 55-61 (1962).

(45) Fisher Controls Ltd., Process Instrumentation Division; "Rotameter Metric Series C.C.M. Calibration Charts" (Date unknown).

(46) Gambill, W.R.; J. Heat Trans., 87, 342-348 (1965).

(47) Gambill, W.R., Bundy, R.D.; "An evaluation of the present status of swirl flow heat transfer", ASME Paper No. 62-HT-42 (1962).

(48) Gambill, W.R., Bundy, R.D.; AIChE J., 9, 55-59 (1963).

(49) Gambill, W.R., Bundy, R.D., Wansbrough, R.W.; "Heat transfer, burnout, and pressure drop for water in swirl flow through tubes with internal twisted tapes", Oak Ridge National Laboratory Report ORNL-2911 (March, 1960).

(50) Gambill, W.R., Bundy, R.D., Wansbrough, R.W.; Chem. Eng. Prog. Symp. Series, 57, No. 32, 127-137 (1961).

(51) Grace, C.D.; Chem. Proc. Eng., 52, 57-59 (1971).

(52) Gradshteyn, I.S., Rhyzik, I.M.; "Table of Integrals, Series, and Products", Academic Press, London (1965).

(53) Grosz-Röll, F.; Chemie-Anlagen + Verfahren, No. 11, 50-54 (November, 1979).

(54) Hansmann, J.; Gumm: Asbest Kunst, 31, No. 2, 76-80 (1978).

(55) Heierle, A.; Chemie-Technik, 9, No.2, 83-85 (1980).

(56) Hilding, W.E., Coogan, C.H.; "Heat transfer and pressure loss measurements in internally finned tubes" ASME Symposium on Air Cooled Heat Exchangers, 57-85 (1964).

(57) Ievlev, V.M., Dzyukenko, B.W., Dreitser, G.A., Vilemas, Yu. V.; Int. J. Heat Mass Trans., 25, No.3, 317-323 (1982).

(58) Kays, W.M.; Trans. ASME, 72, 1067-1074 (1950).

(59) Kays, W.M.; "Convective Heat and Mass Transfer", McGraw-Hill, New York (1966).

(60) Kenics Corporation; "Static mixer units, Series 10 'Standard Design' Modules", Bulletin KMOD-10 (1977).

(61) Kenics Corporation; "Technical Report No.3, Operation of Kenics mixer units" (1980).

(62) Kern, D.Q.; "Process Heat Transfer", International Student Edition, McGraw-Hill (1976).

(63) King, L.T. (Komax Systems Inc.); personal communication (May, 1981).

(64) Klaczak, A.; J. Heat Trans., 95, 557-559 (1973).

(65) Klepper, O.H.; AIChE Symp. Series, 69, No.131, 87-93 (1973).

(66) Kline, S.J., McLintock, F.A.; Mech. Eng., 75, 3-8 (January, 1953).

(67) Knudsen, J.G., Katz, D.L.; Chem. Eng. Prog., 46, 490-500 (1950).

(68) Knudsen, J.G., Katz, D.L.; "Fluid dynamics and heat transfer", McGraw-Hill, New York (1958).

(69) Koch, R.; VDI-Forschungsheft, 24, Series B, No.469, 1-44 (1958). English translation is AEC-tr-3875.

(70) Komax Systems Inc.; "Komax triple action motionless mixers", Bulletin 103A (Date unknown).

(71) Komax Systems Inc.; "Komax triple action motionless mixers", Bulletin 103B (Date unknown).

(72) Komax Systems Inc.; "Komax motionless mixers", Industry Bulletin No.1016 (February, 1979). Komax mixers are distributed in England by Span Engineering Ltd.

(73) Kreith, F., Margolis, D.; "Heat transfer and friction in swirling turbulent flow", Proc. of the Heat Transfer and Fluid Mechanics Institute, 126-142 (June, 1958).

(74) Kreith, F., Margolis, D.; Appl. Sci, Res., 8, Section A 457-473 (1959).

(75) Kreith, F., Sonju, O.K.; J. Fluid Mech., 22, Part 2, 257-271 (1965).

(76) Landolt, H., Börnstein, R.; "Numerical data and functional relationships in science and technology", IV/1a, New Series, 147-156, Springer-Verlag, Berlin-Heidelberg (1974).

(77) Lightnin Mixers Ltd.; "Lightnin in-line blenders, Series 50, 25-1829 mm", Brochure E520/8 (1977).

(78) Lin, S.T., Fan, L.T., Azer, N.Z.; "Augmentation of single phase convective heat transfer with in-line static mixers", Proceedings of the 1978 Heat Transfer and Fluid Mechanics Institute, 117-130 (June, 1978).

(79) Lopina, R.F., Bergles, A.E.; J. Heat Trans., 91, 434-442 (1969).

(80) Margolis, D.; "The effect of turbulence promoters on the rate of heat transfer and the pressure drop in straight tubes", MS thesis, Lehigh University (1957).

(81) McAdams, W.H.; "Heat transmission", 3rd Edition, McGraw-Hill, New York (1954).

(82) Megerlin, F.E., Murphy, R.W., Bergles, A.E.; J. Heat Trans., 96, 145-151 (1974).

(83) Migay, V.K.; AN SSSR: Izvestiya, Energetika I Transport, No.5, 143-151 (1966). English translation is FTD-HT-23-1258-68.

(84) Mixing Equipment Co. Inc.; "The Lightnin inliner mixer", Bulletin B-564 (1980). United Kingdom contact is Lightnin Mixers Ltd.

(85) Moody, L.F.; Trans. ASME, 66, 671-684 (1944).

(86) Morris, W.D., Benyon, J.; Ind. Eng. Chem. Proc. Des. Dev., 15, No.2, 338-342 (1976).

(87) Morris, W.D., Proctor, R.; Ind. Eng. Chem. Proc. Des. Dev., 16, No.3, 406-412 (1977).

(88) Nauman, E.B., AIChE J., 25, No.2, 246-258 (1979).

(89) Nazmeev, Yu. G., Nikolaev, N.A.; Themal Eng., 27, No.3, 151-152 (1980).

(90) Nunner, W.; V.D.I. Forschungsheft 455, Supplement to Forschung auf dem Gebeite des Ingenieurwesens, 22, Series B, 5-39 (1956). English translation is A.E.R.E. Lib./ Trans. 786.

(91) Olsen, R.M., Sparrow, E.M.; AIChE J., 9, 766-770 (1963).

(92) Ouellette, W.R., Bejan, A.; "Entropy generation criterion applied to various heat transfer augmentation techniques", Report No. CUMER-79-5, Dept. of Mech. Eng., University of Colorado. This report is based on the MS thesis, with the same title, submitted by W.R. Ouellette to the above university.

(93) Pahl, M.H., Muschelknautz, E.; Chem.-Ing.-Tech., 51, No.5, 347-364 (1979).

(94) Pahl, M.H., Muschelknautz, E.; "Comparative investigation of static mixers", FH-Texte, 17, 91-118 (1979).

(95) Pahl, M.H., Muschelknautz, E.; Chem.-Ing.-Tech., 52, No.4, 285-291 (1980).

(96) Pattison, D.; Chem. Eng., 76, No. 11, 94-96 (1969).

(97) Perry, R.H., Chilton, C.H. (Eds.); "Chemical Engineers Handbook", 5th Edition, McGraw-Hill, New York (1973).

(98) Pham, Q.T.; Trans. IChemE, 57, No.4, 281-283 (1979).

(99) Poppendiek, H.F., Gambill, W.R.; "Helical forced flow heat transfer and fluid dynamics in single and two phase systems", Proc. of the 3rd International Confer. on the Peaceful Uses of Atomic Energy, 8, 274-282, United Nations, New York (1965).

(100) Process Industries Review; "Mixing '74", 41-44 (1974).

(101) Proctor, R.; "An investigation into convective heat and mass transfer in the Kenics static mixer", M. Phil. thesis, University of Sussex (1977).

(102) Robertson, J.M., Martin, J.D., Burkhart, T.H.; Ind. Eng. Chem. Fundam., 7, No.2, 253-265 (1968).

(103) Rohsenow, W.M., Hartnett, J.P. (Eds.); "Handbook of heat transfer", McGraw-Hill, New York (1973).

(104) Rotameter Manufacturing Co. Ltd.; "Rotameter Fluid Measurement and Control, Dynamic characteristics of metric series rotameters" (Date unknown).

(105) Round, G.F.; Canadian J. Chem. Eng., 58, 122-123 (1980).

(106) Rouse, H.; "Elementary mechanics of fluids", John Wiley and Sons, New York (1946).

(107) Russell, J.J., Carnavos, T.C.; Chem. Eng. Prog., 73, 84-88 (February, 1977).

(108) Sawistowski, H.; Chem. Eng. Sci., 6, 138-140 (1957).

(109) Schorle, B.J., Churchill, S.W., Shacham, M., Chen, N.H.; Ind. Eng. Chem. Fundam., 19, 228-230 (1980).

(110) Seymour, E.V.; Trans. IChemE, 41, 159-162 (1963).

(111) Seymour, E.V.; The Engineer, 222, 634-642 (1966).

(112) Shah, R.K., London, A.L.; "Laminar flow forced convection in ducts", Academic Press, New York (1978).

(113) Shurvell, B. (Director, Span Engineering Ltd.); Supplied heat transfer data in graphical form (January, 1980). Span Engineering Ltd. is the United Kingdom distributor of Komax mixers.

(114) Sieder, E.N., Tate, G.E.; Ind. Eng. Chem., 28, No.12, 1429-1434 (1936).

(115) Singh, B.S., Dybbs, A.; J. Heat Trans., 491-495 (1976).

(116) Smith, J.M.; "Two phase gas-liquid flow in Kenics static mixers", Paper 74C, Presented at AIChE Meeting, Miami Beach (November, 1978).

(117) Smith, J.M.; The Chemical Engineer, 827-830 (November, 1978).

(118) Smithberg, E., Landis, F.; J. Heat Trans., 86, 38-49 (1964).

(119) Soliman, H.M., Feingold, A.; "Heat transfer, pressure drop, and performance evaluation of a quintuplex internally finned tube", ASME Paper No. 77-HT-46 (1977).

(120) Spalding, D.B., Lieberam, A.; "The selection of the most economical turbulence promoters in the design of heat exchangers", Paper presented at V.D.I. Thermodynamics Colloquium at Trier. See Windscale Trans. 277 (1964).

(121) Sparrow, E.M., Koram, K.K., Charmchi, M.; J. Heat Trans., 102, 64-70 (1980).

(122) Stanbury, R.G. (General Manager, Kenics Europe (Belgium)); personal communication (February, 1980).

(123) Streiff, F.; Sulzer Technical Review, 59, No.3, 108-113 (1977).

(124) Streiff, F.A.; "Adapted motionless mixer design", Paper C2 presented at the 3rd European Conference on Mixing, York, England (April, 1979).

(125) Streiff, F.; Chem.-Ing.-Tech., 52, No.6, 520-522 (1980).

(126) Tauscher, W, Schutz, G.; Sulzer Technical Review, 55, No.2, 157-161 (1973).

(127) Tauscher, W.A., Streiff, F.A.; Chem. Eng. Prog., 75, 61-65 (April, 1979).

(128) Thorsen, R.S., Landis, F.; J. Heat Trans., 90, 87-98 (1968).

(129) Tolltreck Linkrose Ltd.; "Corpak" (Date unknown).

(130) Trane Co.; Catologs DS-365 and DS-385 (1962). Cited in Bergles (2, p.343), but could not be located by the present author.

(131) Turbotec Products Inc.; "Turbotechnology Kit", Brochure TTK-2 (1979 and 1980).

(132) Turbotec Products Inc.; "Turbotec selector guide", Brochure TTK-31 (November, 1980).

(133) Ulbrecht, J.J., Laidler, P.; "Flow distribution in a section of a Sulzer-Koch motionless mixer", Paper presented at 71st AIChE Meeting, Miami Beach (November, 1978).

(134) Watkinson, A.P., Miletti, D.L., Kubanek, G.R.; "Heat transfer and pressure drop of internally finned tubes in turbulent air flow", ASHRAE No. 2347, 330-337, Atlantic City. (January, 1975).

(135) Watkinson, A.P., Miletti, D.L., Tarassoff, P.; AIChE Symp. Series, 69, No. 131, 94-103 (1973).

(136) Webb, R.L., Scott, M.F.; "A parametric analysis of the performance of internally finned tubes for heat exchanger application", Symposium Volume 100122, Advances in Enhanced Heat Transfer, 18th National Heat Transfer Conference, San Diego (August, 1979).

(137) Wilson, E.E.; Trans. ASME, 37, 47-71 (1915).

Nomenclature

In order not to use a large number of multiple subscripts, it has been necessary to use some symbols for the representation of more than one variable. The definitions given below are those which have been most often used. On the few occasions for which these definitions do not apply, the relevant definition appears at the appropriate location in the text.

A = regression parameter in the friction factor correlation, see equation (4.22)

A_c = actual free flow area

A_f = superficial free flow area = $(\pi/4)\ d^2$

A_f' = true flow area, see equation (A.1.14)

A_f'' = corrected true flow area, see equation (A.1.15)

A_o = surface area of the outer wall of the tube section that does not contain inserts = $\pi\ d_o\ l_o$

A_p = surface area of the outer wall of the tube section that does contain inserts = $\pi\ d_o\ l_p$

A_w = cross sectional area of the tube wall

A_F = maximum cross sectional area, in a horizontal plane, of the rotameter float

A_T = total surface area of the outer wall of the tube = $\pi\ d_o\ l$

A_1 = cross sectional area of the rotameter tube on the downstream side of the float

A_2 = cross sectional area of the annulus formed by the tube and float of the rotameter

A.A.D. = average absolute percentage deviation

$$= \frac{1}{(No.)} \sum \left| \frac{\text{Measured - Calculated}}{\text{Measured}} \right| (100)$$

B = Reynolds number exponent in a friction factor correlation, see equation (4.22)

c	=	expansion coefficient
c_c	=	ratio of the flow areas of the vena contracta and the contracted duct
c_p	=	specific heat capacity of the fluid
c_D	=	drag coefficient of the float of the rotameter
C	=	sum of the scale, tube wall, and annulus fluid film, resistances to heat transfer. This quantity is an average value over the total heated length of the tube
C_o	=	see definition of C except that this value applies over the section of the tube that is heated and does not contain inserts
C_p	=	see definition of C except this value applies over the section of the tube that is heated and contains inserts
CON.	=	95% confidence interval on the regression parameter, B or E
d	=	inside diameter of the tube, or container
d_m	=	logarithmic mean diameter of the tube
	=	$(d_o - d) / \ln (d_o/d)$
d_o	=	outside diameter of the tube
d_1	=	inside diameter of the outer tube of an annulus
D	=	inside diameter of the tube, inches
D_e	=	equivalent diameter of a tube containing inserts, see equation (A.1.2)
D_H	=	"true" hydraulic diameter of a tube containing inserts, see equation (A.1.20)
D'_H	=	corrected hydraulic diameter, see equation (A.1.23)
D_o	=	diameter of the orifice
D_p	=	diameter of the particles
D(I,2)	=	tube side fluid density evaluated at the temperature of rotameter R1
D(I,3)	=	annulus side fluid density evaluated at the temperature of rotameter R2
e	=	roughness of the tube wall, or height of a roughness element

E = Reynolds number exponent in the heat transfer factor correlation, see equation (4.32)

E_1 = power per unit volume of fluid, erg cm^{-3} (blood) min^{-1}

f = % of the "fiducial" flow through the rotameter, see section 4.5

F = regression parameter in the heat transfer factor correlation, see equation (4.32)

g = acceleration due to gravity

G = Prandtl number exponent

Gr = Grashof number = $\dfrac{2 \beta \gamma^2 u_e^2 (T_s - T_b) D_e^3 \rho^2}{d \mu^2}$

h, h_a = fluid film heat transfer coefficient on the tube side and the annulus side, respectively

h_o = tube side fluid film heat transfer coefficient in the empty tube or in the empty section of the tube

h_p = tube side fluid film heat transfer coefficient in the section of the tube that contains inserts

h_t = hemolysis rate of the blood cells, mgm cm^{-3} (cells) min^{-1}

h_x = local tube side film heat transfer coefficient at axial location x

h = assymptotic value of h

$(h/h_o)_p$ = ratio of the film heat transfer coefficients for tubes with and without inserts when requiring the same pumping power. The fluid properties, tube length, and tube diameter, are the same in both cases

H_f = fluid head loss

$H_1 \ldots H_N$ = manometer fluid differentials as shown in Figure 4.3

I = "impedance", a parameter used in calculating the volumetric flowrate of the fluid passing through the rotameter, see section 4.5

k, k_w = thermal conductivity of the fluid and tube wall, respectively

K = ratio of the friction factors, based on the inside diameter of the tube and the superficial fluid velocity, for the mixer and the empty tube at the same superficial Reynolds number

K_c = number of velocity heads "lost" due to a flow contraction, see equation (A.10.3)

K_d = momentum correction factor

K_e = number of velocity heads "lost" due to a flow expansion, see equation (A.10.2)

K_{eb} = kinetic energy correction factor

K_{F1}, K_{F2} = constants which depend on the type of rotameter, see equations (4.11) and (4.12)

K_{oT} = parameter which is dependent on the geometry of the Kenics mixer and is used to calculate the pressure drop across such a mixer, see equation (1.78)

K_1 = parameter which depends on the cross section, and changes in the cross section, of the duct, see equation (1.92)

l = length of the tube

l' = length of the tube downstream of a blockage, see Figure 1.1

l_{in} = tube length between the upstream pressure tapping and either the upstream end of the heated section, or the upstream end of the packed section, of the tube

l_o, l_p = actual total length of tube that does not contain (l_o), or does contain (l_p), inserts

l_{out} = tube length between the downstream pressure tapping and either the downstream end of the heated section, or the downstream end of the packed section, of the tube

l_R = fraction of the tube length that is occupied by inserts = $l_p / (l_o + l_p)$

l_{si} = swirl flow path length at the inside surface of the tube wall, see equation (A.1.6)

m = exponent on the viscosity ratio, (μ_s/μ), which is used with the friction factor correlation

m_o = ratio of the cross sectional areas of the orifice and the tube = $(D_o/d)^2$

M.A.D. = maximum absolute percentage deviation, i.e. the maximum value of $\left|\frac{\text{Measured - Calculated}}{\text{Measured}}\right|(100)$

n = Reynolds number exponent as calculated using equation (1.33)

N = number of inserts

No. = number of experimental tests

Nu = Nusselt number = (hd/k)

Nu = Nusselt number evaluated using either the regression equation that applies to the full length configuration (6K or 7T) or equation (A.11.21), see Table 5.13

Nu_e = equivalent flow Nusselt number = $(h\ D_e/k)$

Nu_o = Nusselt number for flow in an empty tube

Nu_{o1}, Nu_{o2} = Nusselt number for flow in an empty tube at a Reynolds number of Re_{o1}, or Re_{o2}

$(Nu/Nu_o)_p$ = ratio of the Nusselts numbers of the flow in the packed and empty tubes which are operating at Reynolds numbers of Re and Re_{op}, respectively. Nu_o is evaluated using the regression equation that was found experimentally

$(Nu/Nu_o)_p^*$ = see definition of $(Nu/Nu_o)_p$ except the packed tube is operated at a Reynolds number of Re_{op}^* and Nu_o is evaluated using equation (1.19)

p = pumping power

P_{o1}, P_{o2} = pumping power required to produce a Reynolds number of Re_{o1}, or Re_{o2}, in an empty tube

$P_1 \ldots P_N$ = fluid pressure, see Figure 4.3

Pr = Prandtl number = $(c_p\ \mu/k)$

q = heat flowrate through the entire tube wall

q_{COND} = heat lost from the annulus section by conduction along the tube

q_{fin} = heat flowrate through the surfaces of the fin

q_o, q_p = heat flowrate through the wall of the tube section that does not (q_o), or does (q_p), contain inserts

Q = volumetric flowrate of the fluid

Q_T = "fiducial", or theoretical, volumetric flowrate of fluid through the rotameter, see section 4.5

$Q(1,2)$ = volumetric flowrate of the tube side fluid at the temperature of rotameter R1

$Q(1,3)$ = volumetric flowrate of the annulus side fluid at the temperature of rotameter R2

r = radius of the tube

R = radial distance measured from the centreline of the tube, when using the forced vortex model

R^2 = (correlation coefficient)^2, when considering the experimental data. (Values of R^2 that are close to 1 indicate that the data is acceptably represented by the linear regression equation)

R_i, R_o = scale resistances to heat transfer on the inside and outside surfaces of the tube wall

R_s = scale reading on the rotameter

R.A.D. = root mean square absolute percentage deviation

$$= \left[\frac{1}{(\text{No.})} \sum \left[\left[\frac{\text{Measured - Calculated}}{\text{Measured}} \right] (100) \right]^2 \right]^{0.5}$$

Re = superficial Reynolds number = $(d\ u\ \rho/\ \mu)$, also referred to as "Reynolds number"

Re_e = equivalent flow Reynolds number = $(D_e\ u_s\ \rho/\ \mu)$

Re_{el} = $(D_e\ \bar{v}\ \rho/\ \mu)$

Re_{oP} = Reynolds number of the flow in an empty tube which requires the same pumping power as the Reynolds number in the tube that contains inserts. The empty tube characteristics are those found experimentally in the present work

Re^*_{oP} = see definition of Re_{oP} except the empty tube characteristics are represented by equation (1.4)

Re_l = $(d\ u_e\ \rho/\ \mu)$

s	=	pitch of roughness elements
S	=	specific gravity of the manometer fluid
Sc	=	Schmidt number
Sh, Sh_o	=	Sherwood number for flow in tubes which contain (Sh), or do not contain (Sh_o), inserts
t	=	fluid temperature, for example, in a rotameter
t'	=	thickness of a blockage, see Figure 1.1
t_{av}, t_i, t_o	=	average, inlet, or outlet, bulk fluid temperature of the tube side fluid
t_b, T_b	=	bulk fluid temperature, (T_b measured in degrees absolute)
t_s, T_s	=	temperature at the inside surface of the tube wall, (T_s measured in degrees absolute)
t_1	=	value obtained from Student's t-distribution, see Appendix A.6
T_{av}, T_i, T_o	=	average, inlet, or outlet, bulk fluid temperature of the annulus side fluid
$T(I,3)$	=	T_i
$T(I,4)$	=	T_o
$T(I,13)$	=	inlet temperature of the tube side fluid corrected for heat conduction losses
$T(I,14)$	=	outlet temperature of the tube side fluid corrected for heat conduction losses
u	=	superficial fluid velocity
u_e	=	fluid velocity based on the actual flow area, see equation (A.1.3)
u_{ri}	=	resultant fluid velocity at the inside surface of the tube wall, see equation (A.1.9)
u_t	=	tangential fluid velocity at radial co-ordinate, R, see equation (A.1.7)
u_{ti}	=	tangential fluid velocity at the inside surface of the tube, see equation (A.1.8)
U	=	average overall heat transfer coefficient acting over the total heated length of the tube

U_o, U_p = overall heat transfer coefficient acting over the empty (U_o), or packed (U_p), section of the heated tube length

UFTL = uncovered fraction of the tube length

$\bar{v}$ = average total velocity, see equation (1.48)

V = tube side fluid velocity corrected, for viscosity and density effects, to a reference temperature

V_F = volume of the rotameter float

w = velocity of the annulus side fluid

x = distance from the tube inlet, or insert. Appropriate definition is specified in the text

x_{ent} = distance from the tube inlet within which the turbulent velocity profile develops

x_w = thickness of the tube wall = $(d_o - d)$

x_l = length of the twisted tape

$x_1 \ldots x_n$ = independent (measured) variable, in Chapter 6

X = parameter which allows for the effect of tube length on the Nusselt number, see equation (1.27)

y = twist ratio, defined as the number of tube diameters per 180^o of insert rotation

y = dependent variable, in Chapter 6

Y = tube side fluid temperature at the interface of the empty and packed sections of the tube

Y1 = annulus side fluid temperature at the axial position of the interface of the empty and packed sections of the tube

z = distance between the manometer fluid level and the top of the manometer, see Figure 4.3

Z = parameter which is dependent on the Reynolds number and is used to calculate the pressure drop across a Kenics mixer, see equations (1.78) and (1.79)

Z1 = q_o

β_f = volumetric coefficient of thermal expansion evaluated at the mean film temperature, $(t_b + t_s)/2$

γ = $\pi/(2y)$

δ = thickness of a swirl inducing insert

δ = "small deviation of", in Chapter 6 only

δH_T = differential manometer fluid head that is equivalent to the average pressure gradient, across the tube, at the axial location of P3

Δp = pressure drop

$\Delta p'$ = pressure loss due to the flow development and the entrance and exit

Δp_o = pressure drop across an empty pipe

Δp_c = pressure loss due to contraction of the flow

Δp_{C-R} = pressure difference between the fluid at the centre-line and distance R from the centreline

Δp_e = pressure loss due to expansion of the flow

Δp_s = pressure loss due to the formation of a fully developed swirl flow, see equation (A.10.1)

Δt = temperature rise of the tube side fluid = $(t_o - t_i)$

Δt_f = temperature drop across the fluid film = $(t_s - t_b)$

Δt_{LM} = logarithmic mean temperature difference between the tube and annulus side fluids. This difference acts over the total length of the heat exchanger

Δt_{LMo} = see definition of Δt_{LM} except this temperature difference acts over the total length of an empty tube or over an empty section of a tube

Δt_{LMp} = see definition of Δt_{LM} except this temperature difference acts over the section of tube which contains inserts

$\Delta t'_{LM}$ = logarithmic mean temperature difference between the tube wall and the tube side fluid. This difference acts over the total length of the heat exchanger

$\Delta t'_{LMo}$ = see definition of $\Delta t'_{LM}$ except this temperature difference acts over the empty section of the tube

$\Delta t'_{LMp}$ = see definition of $\Delta t'_{LM}$ except this temperature difference acts over the packed section of the tube

Δt_T = difference between the temperatures of the tube wall at two locations which are separated by a tube length of Δx

Δx = tube length between two locations

ε = constant which depends on the tube dimensions and on the type of inserts, if any; see equation (4.26)

ε_1 = efficiency of a enhancement device, see equation (1.87)

η = overall fin efficiency = $q_{fin}/(2\ (t_s - t_b)\ d\ l\ h)$

θ = angular co-ordinate, see Figure 1.1

θ_1 = $0.3\ (T_s - T_b) + T_b$

μ = fluid viscosity

μ_s = fluid viscosity evaluated at the temperature at the inside surface of the tube wall

ϱ = fluid density

ϱ_f = fluid density evaluated at the mean film temperature

ϱ_m = *density of the manometer fluid*

ϱ_F = density of the rotameter float material

ϱ_1 = tube side fluid density evaluated at the temperature of the manometer

σ = ratio of the flow areas downstream and upstream of the contraction

$\sum$ = "summation"

τ_w = local shear stress at the tube wall

ϕ = friction factor = $(\Delta p\ d) / (4\ l\ \varrho\ u^2)$

ϕ_e = equivalent flow friction factor = $(\Delta p\ D_e) / (4\ l\ \varrho\ u_e^2)$

ϕ'_e = equivalent flow friction factor for the pressure losses *associated with swirl flow development*, see equations (1.41) and (1.42)

ϕ_{eTOT} = total equivalent flow friction factor, see equations (1.41) and (1.42)

ϕ_h = friction factor under heating conditions

ϕ_{iso} = friction factor under isothermal conditions

ϕ_o = friction factor for the empty tube

ϕ_{oe} = empty tube friction factor evaluated using the equivalent Reynolds number, Re_e

$\phi_{o(h)}$ = empty tube friction factor under heating conditions

$\phi_{o(iso)}$ = empty tube friction factor under isothermal conditions

ϕ_p = friction factor calculated using the regression equation which represents the results obtained with configuration 6P

ϕ_{CALC} = friction factor calculated using equation (5.4)

ϕ_{CORR} = friction factor corrected for the effects of flow development and entrance and exit

ϕ_E = friction factor that is assumed to exist over the lengths l_{in} and l_{out}

$= 0.0396\ Re^{-0.25}$

ϕ_{T1} = first term in equation (6.5)

$$= \frac{\pi^2\ d^5\ H\ \rho_l\ g\ (S - 1)}{64\ l\ \rho\ Q^2}$$

ϕ_{T2} = second term in equation (6.5) $= \phi_E\ (l_{in} + l_{out})\ /\ l$

ϕ_l = $(\Delta p\ d)\ /\ (4\ l\ \rho\ u_s^2)$

The subscript "K" refers to the commercial Kenics mixer for which

$\delta/d = 0.1$ for $d < 38$ mm

TABLES

Table No.1.1 Conditions of the tests performed by various workers using twisted tapes.

Reference	Fluid	Twist ratio	d / mm	δ / d	Re range
Present work	Water	2.03	20	0.14	1.1×10^4–1.04×10^5
Gambill, Bundy, and Wansbrough (49)	Water	2.3–12.0	3.5–6.3	0.06–0.11	5×10^3–4.27×10^5
Gambill and Bundy (47)*	Various	0.28–11.0	3.5–75.9	Various	2.5×10^3–5×10^5
Seymour (110)	Air	1.75–13.2	22	0.037	1.5×10^4–10^5
Smithberg and Landis (118)	Air & Water	1.81–11.0	35.1	0.051	2×10^3–6×10^4
Migay (83)	Air	1.75–10.0	20	0.050	2×10^3–5×10^4
Seymour (111)	Air	1.84–6.55	25.3–75.2	0.063–0.065	10^3–10^5
Thorsen and Landis (128)	Air	1.58–4.0	25.3	Unknown	5×10^3–10^5
Lopina and Bergles (79)	Water	2.48–9.2	4.9	0.070	8×10^3–1.3×10^5
Klepper (65)	Nitrogen gas	2.38–8.05	10.7	0.036	2×10^4–3.8×10^5

* Survey of the available experimental results.

Table No.1.2 Typical values of the friction factor ratio ($K = \phi/\phi_o = G\,Re^{H}$) for the Kenics static mixer configuration

Reference	Conditions	Twist ratio	d / mm	δ / d	Re range	G	H	Average K
Grace [51]	Unknown	@ 1·5	Unknown	Unknown	$5x10^3$–10^7	74·2	0·087	230
Bor [12]	Unknown	Unknown	Unknown	Unknown	Turbulent	——	——	60–80
Morris and Benyon [86]	Mass transfer	2·5	12·7	0·079	$6x10^3$–$3x10^4$	3·47	0·140	13
Proctor [101]	Mass transfer	2·0	12·7	0·079	$1{\cdot}1x10^4$–$3{\cdot}0x10^4$	1·74	0·222	15
Proctor [101]	Mass transfer	1·5	12·7	0·079	$1{\cdot}1x10^4$–$2{\cdot}2x10^4$	2·19	0·240	22
Proctor [101]	Heat transfer	1·5	12·7	0·079	$6x10^3$–$2x10^4$	4·18	0·229	36
Smith+ [117]	Isothermal	1·5	19	0·074	$3x10^2$–10^5	23·6	0·130	85
Chakrabarti[x] [21]	Isothermal	1·43	20·65	Unknown	1·6–$2{\cdot}8x10^3$	——	——	——

Notes

The values of K are based on $\phi_o = 0{\cdot}0396\,Re^{-0{\cdot}25}$. The average K is the mean of the results evaluated at limits of Reynolds number for each of the reference studies.

+Reference [116] is the original source of this correlation; reference [117] presents the correlation more clearly. For this work the average K is based on the results at Re = 2500 and 10^5.

[x]The friction factor correlation in reference [21] is: $\phi = (55/Re) + 0{\cdot}4$. Due to the low Reynolds numbers used in these tests the friction factor ratios have not been determined.

Table No.1.3 Comparison of the heat transfer and pressure loss characteristics of standard lengths of motionless in-line mixers.

Mixer Type	K	$K\frac{l}{l_o}$	$\frac{U}{U_o}$	$\frac{U}{U_o}\frac{l}{l_o}$
Etoflo	50	5	—	——
Lightnin	169	10.1	5	0.299
Ross LPD	293	26.4	—	——
Ross LLPD	116	12.1	—	——
Ross ISG	3950	257	—	——
Komax	203	18.2	3	0.268
Kenics	71.3	7.23	3	0.305

Assumptions and conditions for this table:

(a) The standard length of each of the mixers is considered to produce the same degree of mixing as would be obtained in an empty pipe length of 2540 mm.

(b) d = 27.7 mm (1.05 ins) for all cases except the Lightnin mixers for which the tube outside diameter is 38 mm but the inside diameter is unknown.

(c) μ = 1 cP, specific gravity = 1, Re = 50000.

(d) $\phi_o = 0.0396\ Re^{-0.25}$

(e) K for the Kenics mixer is determined from references (24) and (60).

Table No.2.1 The properties of two solder alloys and 316 stainless steel

The data for the solder alloys was supplied by Fry's Metals Ltd.(London)
The data for stainless steel is extracted from Perry and Chilton (97)

Common name	Plumber's solder	Tinman's solder	316 stainless steel
BS 219	Grade J	Grade K	———
Typical composition	Sn 30% Pb Bal	Sn 60% Pb Bal	Cr 18%,Ni 11%, Mo 2.5%,Max. C 0.1%, Fe Bal
Melting range, ^{o}C	183-255	183-188	1370-1400
Thermal conductivity, cal cm^{-1} $^{o}C^{-1}$ s^{-1}	0.09	0.118	0.04
Thermal expansion, at rosin temperature, m m^{-1} $^{o}C^{-1}$	26.0	24.7	16.0
Specific heat, cal g^{-1} $^{o}C^{-1}$	0.045	0.051	0.12
Charpy V-notch impact strength, J	———	22	———
Tensile strength, MN m^{-2}	———	49	827

The above data represents average values for the temperature range 0-100^{o}C.

Table No. 3.1

Approximate Multiplying Factors
(For the Rapid Determination of Heat Balances)

Multipliers apply for
Average Tubeside Temp.=35C
Average Annulus side Temp.=80C

WHAT IS THE SCALE READING FOR ROTAMETER R2 !7.5

HEAT BALANCE DATA

Flow Rl	Multiplier
2	.656750346116
4	.9507632036908
6	1.253824110097
8	1.565933065335
10	1.887090069405
12	2.217295122306
14	2.556548224039
16	2.904849374604
18	3.262198574
20	3.628595822228
22	4.004041119288
24	4.388534465179

DO YOU WANT TO CHANGE THE SCALE READING !YES
WHAT IS THE SCALE READING FOR ROTAMETER R2 !10

HEAT BALANCE DATA

Flow Rl	Multiplier
2	.5318069555487
4	.7698853724139
6	1.01529049315
8	1.268022317756
10	1.528080846233
12	1.79546607858
14	2.070178014797
16	2.352216654885
18	2.641581998844
20	2.938274046673
22	3.242292798372
24	3.553638253942

Table No.4.1 Analysis of the rotameter calibrations

M.A.D. Maximum absolute percentage deviation
A.A.D. Average absolute percentage deviation
R.A.D. Root mean square absolute percentage deviation

Reference Equation/ Error Type		Rotameter R1	Rotameter R2
	M.A.D.	3.558	2.088
4.16	A.A.D.	1.272	0.441
	R.A.D.	1.575	0.748
	M.A.D.	3.691	2.093
4.17	A.A.D.	1.288	0.448
	R.A.D.	1.575	0.769
	M.A.D.	16.80	2.032
4.18	A.A.D.	2.942	0.688
	R.A.D.	5.089	1.003
	M.A.D.	16.48	2.021
4.19	A.A.D.	2.943	0.684
	R.A.D.	5.101	1.016
	M.A.D.	5.551	3.667
4.20	A.A.D.	1.446	1.432
	R.A.D.	1.850	1.691
	M.A.D.	18.06	3.845
4.21	A.A.D.	3.082	1.472
	R.A.D.	5.181	1.806

Table No.5.1 Friction factor data obtained under isothermal conditions (Pall Rings)

This data is shown as Figure 5.1

Denotation	Config-uration	A	-B	No.	A.A.D.	R.A.D.	M.A.D.	R^2	CON.
A	0	0·0864	0·326	10	1·81	2·18	4·22	0·986	0·031
B	0	0·0868	0·325	21	0·83	1·05	2·36	0·995	0·011
A_B	0	0·0897	0·329	31	1·21	1·60	3·88	0·992	0·011
C	1P	0·157	0·328	45	1·35	1·62	3·68	0·993	0·009
D	2P	0·132	0·278	40	1·58	1·90	4·35	0·988	0·010
E	3P	0·163	0·269	30	1·95	2·31	5·48	0·982	0·014
F	4P	0·184	0·257	35	2·13	2·51	5·58	0·980	0·013
G	5P	0·227	0·245	35	2·18	2·49	5·07	0·978	0·013
H	6P	0·276	0·185	41	0·75	0·93	2·25	0·990	0·006

Table No.5.2 Friction factor data obtained under heating conditions (Pall Rings)

This data is shown as Figure 5.2

Denotation	Config-uration	A	-B	No.	A.A.D.	R.A.D.	M.A.D.	R^2	CON.
A	0	0·0440	0·263	27	1·70	2·00	3·45	0·984	0·014
B	0	0·0543	0·285	24	1·30	1·49	2·48	0·992	0·012
C	0	0·0515	0·278	24	1·13	1·30	2·62	0·992	0·011
A_C	0	0·0491	0·274	75	1·55	1·87	4·44	0·986	0·008
D	1P	0·0890	0·276	24	0·91	1·01	1·63	0·996	0·007
E	2P	0·100	0·252	21	1·20	1·39	2·45	0·992	0·011
F	3P	0·105	0·225	21	1·94	2·08	3·11	0·981	0·015
G	4P	0·139	0·229	21	2·43	2·71	4·34	0·970	0·019
H	5P	0·245	0·248	24	2·55	2·99	5·06	0·965	0·021
I	6P	0·344	0·202	28	1·37	1·59	3·04	0·980	0·012

Table No. 5.3 Heat transfer factor data (Pall Rings)

Denotation	Ht. Trans. Factor Fig. No.	Config-uration	F	E	No.	A.A.D.	R.A.D.	M.A.D.	R^2	CON.
A	___	0	0·0226	0·800	27	6·01	7·21	12·69	0·977	0·050
B	___	0	0·0220	0·800	27	4·30	4·87	7·80	0·990	0·034
C	___	0	0·0260	0·800	27	3·77	4·49	8·85	0·991	0·031
B_C	___	0	0·0239	0·800	54	5·18	6·48	15·10	0·982	0·030
D	5.3	1P	0·0267	0·802	27	2·92	3·49	6·87	0·995	0·024
E	5.4	2P	0·0367	0·779	27	1·88	2·41	6·33	0·997	0·017
F	5.5	3P	0·0320	0·794	27	2·62	3·17	7·25	0·996	0·022
G	5.6	4P	0·0535	0·759	27	3·75	4·58	9·86	0·990	0·032
H	5.7	5P	0·0582	0·746	27	2·31	3·14	10·15	0·995	0·022
I	5.8	6P	0·0692	0·738	22	5·47	6·26	9·87	0·977	0·052

Table No.5.4 Friction factor data obtained under isothermal conditions (Configuration 0)

Denotation	Temp. of operation	A	-B	No.	A.A.D.	R.A.D.	M.A.D.	R^2	CON.
A	Room	0·0685	0·305	27	0·81	1·02	2·72	0·997	0·007
B	Room	0·0695	0·306	27	0·44	0·54	1·46	0·999	0·004
C	Room	0·0695	0·306	27	0·59	0·74	1·68	0·998	0·005
D	Room	0·0677	0·304	27	0·92	1·10	2·48	0·996	0·008
E	Room	0·0759	0·314	27	0·57	0·80	2·69	0·998	0·006
F	Room	0·0558	0·286	27	0·62	0·79	1·73	0·998	0·005
G	Room	0·0579	0·289	27	0·82	0·97	2·15	0·997	0·007
H	Room	0·0584	0·288	27	0·47	0·56	1·28	0·999	0·004
I	Room	0·0663	0·300	27	0·68	0·80	2·14	0·998	0·006
J	35°C	0·0550	0·281	27	0·57	0·69	1·58	0·998	0·005
K	35°C	0·0518	0·278	27	0·45	0·52	0·86	0·999	0·004
A_I	Room	0·0651	0·300	243	1·01	1·27	4·25	0·995	0·003
J_K	35°C	0·0534	0·279	54	0·53	0·67	1·96	0·999	0·003

Table No.5.5 Friction factor data obtained under heating conditions (Configuration 0)

Denotation	Scale on R2	A	-B	No.	A.A.D.	R.A.D.	M.A.D.	R^2	CON.
B	7·5	0·0323	0·240	27	0·41	0·54	1·18	0·999	0·004
C	7·5	0·0440	0·271	27	0·93	1·17	2·86	0·995	0·008
D	7·5	0·0360	0·251	27	0·61	0·79	1·67	0·997	0·005
E	7·5	0·0322	0·240	27	1·07	1·31	3·28	0·992	0·009
F	7·5	0·0361	0·250	27	0·87	1·12	2·83	0·994	0·008
G	7·5	0·0338	0·243	27	0·66	0·80	2·05	0·997	0·006
H	7·5	0·0271	0·224	27	0·90	1·13	2·24	0·993	0·008
I	7·5	0·0300	0·234	27	0·46	0·56	1·11	0·998	0·004
J	7·5	0·0279	0·226	27	0·50	0·63	1·25	0·998	0·004
K	10	0·0243	0·213	27	0·84	1·01	1·82	0·994	0·007
L	10	0·0284	0·227	27	0·58	0·66	1·16	0·998	0·005
M	10	0·0307	0·237	27	0·68	0·84	1·56	0·996	0·006
N	7·5	0·0248	0·214	27	0·88	1·09	2·46	0·993	0·008
O	7·5	0·0275	0·224	27	0·78	0·98	1·64	0·995	0·007
P	7·5	0·0260	0·218	27	0·78	0·97	2·34	0·994	0·007
B_P	7·5&10	0·0304	0·234	405	1·26	1·60	5·11	0·987	0·003

Table No.5.6 Heat transfer factor data (Configuration 0)

Denotation	Scale on R2	F	E	No.	A.A.D.	R.A.D.	M.A.D.	R^2	CON.
A	7·5	0·0249	0·800	27	1·39	1·93	5·66	0·998	0·013
B	7·5	0·0257	0·800	27	2·61	2·98	5·69	0·996	0·021
C	7·5	0·0255	0·800	27	3·46	5·18	16·37	0·989	0·035
D	7·5	0·0250	0·800	27	1·79	2·33	5·49	0·998	0·016
E	7·5	0·0256	0·800	27	1·95	2·51	6·77	0·997	0·017
F	7·5	0·0275	0·800	27	2·40	3·08	6·55	0·996	0·021
G	7·5	0·0256	0·800	27	2·48	3·23	8·70	0·995	0·022
H	7·5	0·0253	0·800	27	2·37	2·96	7·22	0·996	0·021
I	7·5	0·0257	0·800	27	2·85	3·33	6·24	0·995	0·023
J	7·5	0·0244	0·800	27	1·87	2·43	7·04	0·997	0·017
K	10	0·0255	0·800	27	2·06	2·42	4·40	0·997	0·017
L	10	0·0246	0·800	27	1·66	1·91	3·08	0·998	0·013
M	10	0·0251	0·800	27	2·26	2·73	4·77	0·997	0·019
N	7·5	0·0239	0·800	27	2·07	2·43	4·62	0·997	0·017
O	7·5	0·0257	0·800	27	1·67	2·07	5·44	0·998	0·014
P	7·5	0·0246	0·800	27	1·99	2·45	5·95	0·997	0·017
A_P	7·5&10	0·0253	0·800	432	3·21	4·16	15·33	———	———

Table No.5.7 Friction factor data obtained under isothermal conditions

(Inserts of identical twist direction)

Denotation	Friction Factor Fig. No.	Config-uration	Temp. of operation	A	-B	No.	A.A.D.	R.A.D.	M.A.D.	R^2	CON.
		0	Room	0·0651	0·300	243	1·01	1·27	4·25	0·995	0·003
A	5.18	1 T	Room	0·261	0·308	27	1·01	1·14	2·04	0·996	0·008
B	5.18	1 TS	Room	0·330	0·317	27	1·33	1·50	2·91	0·994	0·010
C	5.18	2 TS	Room	0·290	0·303	27	1·54	1·71	3·15	0·991	0·012
D	5.18	3 T	Room	0·261	0·254	27	1·55	1·84	4·50	0·985	0·013
E	5.19	4 T	Room	0·322	0·273	27	1·39	1·59	3·29	0·991	0·011
F	5.19	5 T	Room	0·520	0·274	27	1·75	2·06	3·88	0·984	0·014
G	5.19	6 T	Room	0·981	0·334	27	1·56	1·76	2·80	0·992	0·012
H	5.19	7 T	Room	1·00	0·339	27	1·73	1·99	3·53	0·990	0·014
I	5.20	7 T	Room	0·985	0·337	27	1·87	2·14	3·74	0·989	0·015
J	5.20	8 T	Room	0·786	0·256	27	1·59	1·81	3·19	0·986	0·013
K	5.20	9 T	Room	0·968	0·329	27	1·59	1·72	2·69	0·992	0·012
L	5.20	9 T′	Room	0·525	0·323	27	1·48	1·60	2·51	0·993	0·011
H_I		7 T	Room	0·990	0·338	54	1·82	2·11	4·04	0·989	0·010

Results denoted using a prime (′) were calculated using the "heated" tube length; all of the other results were based on the total length of tube that contained inserts

Cont.....

Table No.5.7 (Continued)

Denotation	Friction Factor Fig. No.	Configuration	Temp. of operation	A	-B	No.	A.A.D.	R.A.D.	M.A.D.	R^2	CON.
		0	35°C	0·0534	0·278	54	0·53	0·68	1·96	0·998	0·003
M	5.22	1 T	35°C	0·206	0·283	27	1·25	1·37	2·12	0·993	0·010
N	5.22	6 T	35°C	0·723	0·300	27	1·91	2·16	3·66	0·985	0·015
O	5.22	7 T	35°C	0·666	0·295	27	2·01	2·36	4·40	0·982	0·016
P	5.23	7 T	35°C	0·796	0·314	27	2·05	2·39	4·16	0·984	0·017
Q	5.23	8 T	35°C	0·672	0·239	27	1·87	2·17	3·87	0·977	0·015
R	5.23	9 T	35°C	0·773	0·304	27	1·78	2·05	3·59	0·987	0·014
S	5.23	9 T′	35°C	0·427	0·300	27	1·65	1·91	3·34	0·989	0·013
O_P		7 T	35°C	0·729	0·305	54	2·16	2·56	4·28	0·980	0·012
H,I,O,P		7 T	Both	0·779	0·313	108	2·69	3·21	6·57	0·972	0·010
K,R		9 T	Both	0·809	0·310	54	2·16	2·59	4·65	0·982	0·012
H,I,O,P,K,R		7 T,9 T	Both	0·787	0·311	162	3·73	4·29	8·95	0·952	0·011

Table No.58 Friction factor data obtained under isothermal conditions

(Inserts of alternate rotation)

Denotation	Friction Factor Fig. No.	Configuration	Temp. of operation	A	-B	No.	A.A.D.	R.A.D.	M.A.D.	R^2	CON.
		0	Room	0·0651	0·300	243	1·01	1·27	4·25	0·995	0·003
A	5.25	1K	Room	0·244	0·281	27	0·39	0·47	0·86	0·999	0·003
B	5.25	1KS	Room	0·194	0·235	27	1·28	1·52	3·25	0·988	0·011
C	5.25	2KS	Room	0·209	0·246	27	1·06	1·31	3·07	0·992	0·009
D	5.25	3K	Room	0·330	0·225	27	1·32	1·47	2·52	0·988	0·010
E	5.25	3KS	Room	0·358	0·229	24	1·50	1·82	3·44	0·979	0·015
F	5.25	4K	Room	0·370	0·245	27	1·43	1·70	4·86	0·986	0·012
G	5.25	5K	Room	0·828	0·245	27	1·60	1·87	3·48	0·984	0·013
H	5.26	6K	Room	1·27	0·187	27	1·30	1·52	2·92	0·981	0·011
I	5.26	6K	Room	1·33	0·190	27	1·08	1·28	2·48	0·987	0·009
J	5.26	7K	Room	1·89	0·321	27	2·39	2·74	4·79	0·980	0·019
K	5.26	8K	Room	1·29	0·193	27	1·36	1·60	3·18	0·981	0·011
L	5.27	8K′	Room	0·702	0·194	27	1·34	1·58	3·14	0·981	0·011
M	5.27	9K	Room	1·36	0·197	27	1·40	1·62	3·02	0·981	0·011
N	5.27	9K′	Room	0·744	0·197	27	1·38	1·60	2·97	0·982	0·011
H_I		6K	Room	1·31	0·189	54	1·31	1·55	3·23	0·981	0·007
K,M		8K,9K	Room	1·31	0·194	54	1·59	1·91	4·26	0·973	0·009

Results denoted using a prime (′) were calculated using the "heated" tube length; all of the other results were based on the total length of tube containing inserts.

Cont.....

Table No.5.8 (Continued)

Denotation	Friction Factor Fig. No.	Configuration	Temp. of operation	A	-B	No.	A.A.D.	R.A.D.	M.A.D.	R^2	CON.
		0	35°C	0·0534	0·278	54	0·53	0·68	1·96	0·998	0·003
O	5.29	1K	35°C	0·208	0·263	27	1·08	1·13	1·78	0·995	0·008
P	5.29	6K	35°C	1·21	0·177	27	1·30	1·53	3·01	0·979	0·011
Q	5.29	7K	35°C	1·35	0·285	27	2·87	3·28	5·61	0·963	0·023
H,I,P		6K	Both	1·15	0·175	81	2·53	2·84	6·31	0·933	0·011
H,I,P,L,N		6K,8K, 9K	Both	1·17	0·179	135	3·45	4·16	8·45	0·871	0·012

Table No.5.9 Friction factor data obtained under heating conditions

(Inserts of identical twist direction)

Denotation	Friction Factor Fig. No.	Configuration	Scale on R2	A	-B	No.	A.A.D.	R.A.D.	M.A.D.	R^2	CON.
		0	7·5&10	0·0304	0·234	405	1·26	1·60	5·11	0·987	0·003
A	5.30	1T	7·5	0·134	0·248	27	1·17	1·39	2·82	0·991	0·010
B	5.30	1TS	7·5	0·175	0·250	27	1·06	1·13	1·67	0·994	0·008
C	5.30	3T	7·5	0·178	0·217	27	0·98	1·12	1·95	0·992	0·008
D	5.30	4T	7·5	0·204	0·227	27	2·06	2·42	5·17	0·968	0·017
E	5.31	5T	7·5	0·334	0·231	27	1·89	2·25	4·47	0·973	0·016
F	5.31	6T	7·5	0·609	0·286	27	1·74	1·97	3·43	0·987	0·014
G	5.31	7T	10	0·542	0·279	27	1·95	2·29	4·14	0·981	0·016
H	5.31	7T	7·5	0·567	0·284	27	1·97	2·33	4·20	0·981	0·016
I	5.32	8T	7·5	0·590	0·228	27	1·53	1·78	3·49	0·983	0·012
J	5.32	9T	7·5	0·508	0·268	27	1·71	2·02	3·69	0·984	0·014
K	5.32	9T′	7·5	0·289	0·266	27	1·58	1·86	3·42	0·986	0·013
G_H		7T	Both	0·554	0·281	54	1·99	2·34	4·22	0·980	0·011
G,H,J		7T,9T	Both	0·539	0·277	81	2·95	3·45	6·44	0·960	0·013

Table No.5.10 Friction factor data obtained under heating conditions

(Inserts of alternate rotation)

Denotation	Friction Factor Fig. No.	Config-uration	Scale on R2	A	-B	No.	A.A.D.	R.A.D.	M.A.D.	R^2	CON.
		0	7·5&10	0·0304	0·234	405	1·26	1·60	5·11	0·987	0·003
A	5.34	1K	7·5	0·159	0·239	27	0·98	1·13	1·92	0·994	0·008
B	5.34	1KS	7·5	0·124	0·199	27	1·16	1·33	2·52	0·987	0·009
C	5.34	3K	7·5	0·256	0·198	27	1·39	1·59	2·83	0·982	0·011
D	5.34	3KS	7·5	0·294	0·208	24	1·78	2·11	3·84	0·965	0·017
E	5.34	4K	7·5	0·250	0·207	27	1·26	1·51	3·27	0·985	0·011
F	5.34	5K	7·5	0·664	0·222	27	1·58	1·81	3·19	0·981	0·013
G	5.35	6K	7·5	1·03	0·164	27	0·83	0·97	1·47	0·990	0·007
H	5.35	6K	10	1·13	0·170	27	1·12	1·33	2·53	0·983	0·009
I	5.35	7K	7·5	1·21	0·276	27	2·66	3·14	5·62	0·964	0·022
J	5.35	8K	7·5	1·05	0·171	27	1·22	1·47	2·88	0·979	0·010
K	5.36	8K'	7·5	0·577	0·172	27	1·20	1·45	2·84	0·980	0·010
L	5.36	9K	7·5	1·20	0·182	24	1·70	1·92	3·44	0·967	0·015
M	5.36	9K'	7·5	0·656	0·183	24	1·68	1·89	3·39	0·969	0·015
G_H		6K	Both	1·08	0·167	54	1·27	1·66	3·99	0·972	0·008
J,L		8K,9K	7·5	1·11	0·176	51	1·49	1·80	4·70	0·970	0·009
G,H,J,L		6K,8K, 9K	Both	1·11	0·173	105	3·15	3·51	6·23	0·893	0·012

Table No.5.11 Heat transfer factor data (Inserts of identical twist direction)

Denotation	Ht.Trans. Factor Fig. No.	Config-uration	Scale on R2	A	-B	No.	A.A.D.	R.A.D.	M.A.D.	R^2	CON.
		0	7·5&10	0·0253	0·800	432	3·21	4·16	15·33	——	——
A	5.38	1T	7·5	0·0301	0·815	27	1·13	1·35	2·43	0·999	0·009
B	5.39	1TS	7·5	0·0286	0·826	27	2·71	3·40	7·34	0·995	0·024
C	5.40	3T	7·5	0·0442	0·783	27	1·90	2·46	5·49	0·997	0·017
D	5.41	4T	7·5	0·0385	0·799	27	2·53	3·21	7·49	0·995	0·022
E	5.38	5T	7·5	0·0567	0·790	27	3·20	3·97	8·55	0·993	0·028
F	5.39	6T	7·5	0·0434	0·813	27	1·53	2·10	4·44	0·998	0·015
G	5.40	7T	10	0·0521	0·787	27	1·80	2·27	5·84	0·998	0·016
H	5.41	7T	7·5	0·0557	0·780	27	1·78	2·15	4·63	0·998	0·015
I	5.42	8T	7·5	0·0552	0·793	27	1·46	2·08	5·54	0·998	0·014
J	5.42	9T	7·5	0·0377	0·796	27	2·34	3·00	6·62	0·996	0·021
G_H		7T	7·5&10	0·0538	0·784	54	1·78	2·22	6·11	0·998	0·011

Table No.5.12 Heat Transfer factor data (Inserts of alternate rotation)

Denotation	Ht. Trans. Factor Fig. No.	Config-uration	Scale on R2	A	B	No.	A.A.D.	R.A.D.	M.A.D.	R^2	CON.
		0	7·5&10	0·0253	0·800	432	3·21	4·16	15·33	____	____
A	5.44	1K	7·5	0·0362	0·794	27	0·86	1·26	3·49	0·999	0·009
B	5.45	1KS	7·5	0·0415	0·790	27	3·13	4·00	9·14	0·993	0·028
C	5.46	3K	7·5	0·0555	0·771	27	4·98	5·85	14·08	0·984	0·041
D	5.46	3KS	7·5	0·0424	0·801	24	3·52	4·68	11·28	0·988	0·039
E	5.44	4K	7·5	0·0480	0·783	27	2·18	2·54	4·87	0·997	0·018
F	5,45	5K	7·5	0·0442	0·818	27	4·68	5·08	7·64	0·989	0·036
G	5.45	6K	7·5	0·0457	0·844	27	3·89	5·01	15·60	0·989	0·036
H	5.44	6K	10	0·0918	0·772	27	2·10	2·70	5·60	0·996	0·019
I	5.46	7K	7·5	0·0872	0·772	27	3·16	3·75	8·08	0·993	0·026
J	5.45	8K	7·5	0·0399	0·808	27	2·96	3·79	8·89	0·994	0·026
K	5.44	9K	7·5	0·0487	0·794	24	4·20	4·72	8·92	0·989	0·036
G_H		6K	7·5&10	0·0648	0·808	54	4·37	5·80	21·27	0·984	0·029

Table No.5.13 Estimated heat transfer factors for the packed sections of configurations 8K and 9T (see denotations A to D)
and Estimated heat transfer factors in the tube section downstream of the inserts of configuration 9K (see denotations E to H)

Denotation	Configuration	Case (1) or (2)	F	E	A.A.D.	R.A.D.	M.A.D.	R^2	CON.	$Nu/Pr^{0.4}$	$\frac{Nu}{Nu'}$
A	8K	(1)	0·0247	0·907	7·48	10·0	26·3	0·967	0·069	517	1·16^{x}
B	8K	(2)	0·0259	0·901	7·33	9·80	25·7	0·968	0·068	509	1·14^{x}
C	9T	(1)	0·0476	0·806	4·98	6·33	14·3	0·982	0·045	320	1·14^{x}
D	9T	(2)	0·0481	0·805	4·86	6·18	13·9	0·983	0·044	318	1·13^{x}
E	9K	(1)	0·0294	0·808	7·65	8·66	17·2	0·965	0·068	202	1·15$^{\bullet}$
F	9K	(2)	0·0279	0·814	7·69	8·70	17·1	0·965	0·068	205	1·17$^{\bullet}$
G	9K	(1)	0·0567	0·744	8·13	9·11	17·8	0·955	0·072	189	1·08$^{\bullet}$
H	9K	(2)	0·0531	0·751	8·17	9·15	17·7	0·955	0·072	192	1·09$^{\bullet}$

For the description of the "case" refer to Appendix A.11.
F,E,A.A.D, etc., are results of the regression analyses of the estimated heat transfer factors and Reynolds numbers.
Nu and Nu' are the mean of the heat transfer factors, evaluated for Re=15500 and 104000, using the regression equations of the estimated heat transfer factors and either
^{x}(i) those determined using the full length configuration (6K or 7T)
or $^{\bullet}$(ii) those determined using the empty tube correlation (Equation (A.11.21).
The results of denotations E and F were found by assuming that the packed length of tube behaves as in configuration 6K. The results of denotations G and H were found assuming that the packed length behaves as for denotation B, above.

Table No. 6.1 Reliability estimation of the experimental friction factors (Isothermal results)

Denotation	Friction Factor Fig. No.	Config-uration	Tables for data	Run No.	$\frac{5\delta d}{d}$	$\frac{\delta H}{H}$	$\frac{\delta H_T}{H_T}$	$\frac{\delta l}{l}$	$\frac{\delta(l_{in}+l_{out})}{(l_{in}+l_{out})}$	$\frac{2\delta Q}{Q}$	$\frac{\delta \phi_E}{\phi_E}$
A	5.13	0	A.8.1, A.9.1	1	0·0500	0·0194	——	0·0025	——	0·0712	——
B	5.13	0	A.8.1, A.9.1	1	0·0250	0·0194	——	0·0025	——	0·0315	——
C	5.13	0	A.8.1, A.9.1	27	0·0500	0·0022	——	0·0025	——	0·0712	——
D	5.13	0	A.8.1, A.9.1	27	0·0250	0·0011	——	0·0025	——	0·0315	——
E	5.18	1T	A.8.6, A.9.6	1	0·0500	0·0057	0·0423	0·0019	0·0328	0·0712	0·4803
F	5.18	1T	A.8.6, A.9.6	1	0·0250	0·0057	0·0423	0·0019	0·0328	0·0315	0·4803
G	5.18	1T	A.8.6, A.9.6	27	0·0500	0·0048	0·0765	0·0019	0·0328	0·0716	0·3465
H	5.18	1T	A.8.6, A.9.6	27	0·0250	0·0048	0·0765	0·0019	0·0328	0·0315	0·3465
I	5.26	6K	A.8.7, A.9.7	1	0·0500	0·0081	0·0028	0·0149	0·0966	0·0716	0·5399
J	5.26	6K	A.8.7, A.9.7	1	0·0250	0·0081	0·0028	0·0149	0·0966	0·0315	0·5399
K	5.26	6K	A.8.7, A.9.7	27	0·0500	0·0015	0·0041	0·0149	0·0966	0·0716	0·4013
L	5.26	6K	A.8.7, A.9.7	27	0·0250	0·0008	0·0041	0·0149	0·0966	0·0315	0·4013

Table No. 6.2 Reliability estimation of the experimental friction factors (Isothermal results)

These results are based on the estimations of Table 6.1

Denotation	ϕ_{T1}	ϕ_{T2}	$\frac{\delta\phi_{T1}}{\phi_{T1}}\Big\vert_L$	$\frac{\delta\phi_{T2}}{\phi_{T2}}\Big\vert_L$	$\frac{\delta\phi_{T1}}{\phi_{T1}}\Big\vert_S$	$\frac{\delta\phi_{T2}}{\phi_{T2}}\Big\vert_S$	$\frac{\delta\phi}{\phi}\Big\vert_L$	$\frac{\delta\phi}{\phi}\Big\vert'_L$	$\frac{\delta\phi}{\phi}\Big\vert_S$	$\frac{\delta\phi}{\phi}\Big\vert'_S$
A	$3\cdot97\times10^{-3}$	—	0·1430	—	0·0891	—	0·1430	0·1430	0·0891	0·0891
B	$3\cdot97\times10^{-3}$	—	0·0784	—	0·0447	—	0·0784	0·0784	0·0447	0·0447
C	$2\cdot25\times10^{-3}$	—	0·1259	—	0·0870	—	0·1259	0·1259	0·0870	0·0870
D	$2\cdot25\times10^{-3}$	—	0·0601	—	0·0403	—	0·0601	0·0601	0·0403	0·0403
E	$1\cdot53\times10^{-2}$	$5\cdot43\times10^{-4}$	0·1710	0·5150	0·0969	0·4815	0·1962	0·1347	0·1181	0·0916
F	$1\cdot53\times10^{-2}$	$5\cdot43\times10^{-4}$	0·1064	0·5150	0·0587	0·4815	0·1291	0·0677	0·0784	0·0434
G	$8\cdot48\times10^{-3}$	$3\cdot37\times10^{-4}$	0·2044	0·3812	0·1160	0·3481	0·2285	0·1345	0·1351	0·0921
H	$8\cdot48\times10^{-3}$	$3\cdot37\times10^{-4}$	0·1397	0·3812	0·0866	0·3481	0·1612	0·0672	0·1046	0·0436
I	$2\cdot33\times10^{-1}$	$5\cdot92\times10^{-4}$	0·1469	0·6513	0·0886	0·5486	0·1490	0·1448	0·0903	0·0891
J	$2\cdot33\times10^{-1}$	$5\cdot92\times10^{-4}$	0·0823	0·6513	0·0437	0·5486	0·0842	0·0799	0·0452	0·0440
K	$1\cdot59\times10^{-1}$	$3\cdot68\times10^{-4}$	0·1417	0·5127	0·0883	0·4130	0·1432	0·1381	0·0895	0·0887
L	$1\cdot59\times10^{-1}$	$3\cdot68\times10^{-4}$	0·0763	0·5127	0·0431	0·4130	0·0776	0·0725	0·0441	0·0432

SUBSCRIPTS : T1 = Term 1 T2 = Term 2 (see equation 6.5) L = Linear equation 6.2
S = Second power equation 6.4

SUPERSCIPT : ′ = Evaluation excluding the terms $\delta H_f/H$ and $\delta\phi_E/\phi_E$

Table No.6.3 Reliability estimation of experimental friction factors (Heating results)

Denotation	Friction Factor Fig. No	Config-uration	Tables for data	Run No.	$\frac{5\delta d}{d}$	$\frac{\delta H}{H}$	$\frac{\delta H_T}{H}$	$\frac{\delta l}{l}$	$\frac{\delta(l_{in}+l_{out})}{(l_{in}+l_{out})}$	$\frac{2\delta Q}{Q}$	$\frac{\delta \phi_E}{\phi_E}$
M	5.14	0	A.8.2, A.9.2	1	0·0500	0·0244	——	0·0025	——	0·0712	——
N	5.14	0	A.8.2, A.9.2	1	0·0250	0·0244	——	0·0025	——	0·0315	——
O	5.14	0	A.8.2, A.9.2	27	0·0500	0·0008	——	0·0025	——	0·0712	——
P	5.14	0	A.8.2, A.9.2	27	0·0250	0·0008	——	0·0025	——	0·0315	——
Q	5.30	1T	A.8.8, A.9.8	1	0·0500	0·0065	0·0495	0·0019	0·0328	0·0712	0·4589
R	5.30	1T	A.8.8, A.9.8	1	0·0250	0·0065	0·0495	0·0019	0·0328	0·0315	0·4589
S	5.30	1T	A.8.8, A.9.8	27	0·0500	0·0050	0·0802	0·0019	0·0328	0·0712	0·3281
T	5.30	1T	A.8.8, A.9.8	27	0·0250	0·0050	0·0802	0·0019	0·0328	0·0315	0·3281
U	5.35	6K	A.8.9, A.9.9	1	0·0500	0·0081	0·0029	0·0149	0·0966	0·0712	0·5086
V	5.35	6K	A.8.9, A.9.9	1	0·0250	0·0081	0·0029	0·0149	0·0966	0·0315	0·5086
W	5.35	6K	A.8.9, A.9.9	27	0·0500	0·0003	0·0041	0·0149	0·0966	0·0712	0·3769
X	5.35	6K	A.8.9, A.9.9	27	0·0250	0·0003	0·0041	0·0149	0·0966	0·0315	0·3769

Table No. 6.4 Reliability estimation of the experimental friction factors (Heating results)

These results are based on the estimates of Table 6.3

Denotation	ϕ_{T1}	ϕ_{T2}	$\frac{\delta\phi_{T1}}{\phi_{T1}}\Big\|_L$	$\frac{\delta\phi_{T2}}{\phi_{T2}}\Big\|_L$	$\frac{\delta\phi_{T1}}{\phi_{T1}}\Big\|_S$	$\frac{\delta\phi_{T2}}{\phi_{T2}}\Big\|_S$	$\frac{\delta\phi}{\phi}\Big\|_L$	$\frac{\delta\phi}{\phi}\Big\|'_L$	$\frac{\delta\phi}{\phi}\Big\|_S$	$\frac{\delta\phi}{\phi}\Big\|'_S$
M	3.07×10^{-3}	—	0.1480	—	0.0904	—	0.1480	0.1480	0.0904	0.0904
N	3.07×10^{-3}	—	0.0834	—	0.0471	—	0.0834	0.0834	0.0471	0.0471
O	2.02×10^{-3}	—	0.1244	—	0.0757	—	0.1244	0.1244	0.0757	0.0757
P	2.02×10^{-3}	—	0.0598	—	0.0403	—	0.0598	0.0598	0.0403	0.0403
Q	1.31×10^{-2}	5.06×10^{-4}	0.1791	0.4936	0.1003	0.4600	0.2063	0.1363	0.1229	0.0921
R	1.31×10^{-2}	5.06×10^{-4}	0.1144	0.4936	0.0641	0.4600	0.1390	0.0690	0.0853	0.0438
S	8.10×10^{-3}	3.15×10^{-4}	0.2082	0.3628	0.1184	0.329	0.2313	0.1346	0.1366	0.0920
T	8.10×10^{-3}	3.15×10^{-4}	0.1435	0.3628	0.0899	0.329	0.1640	0.0673	0.1068	0.0435
U	2.24×10^{-1}	5.45×10^{-4}	0.1470	0.6200	0.0886	0.5179	0.1489	0.1447	0.0901	0.0890
V	2.24×10^{-1}	5.45×10^{-4}	0.0824	0.6200	0.0437	0.5179	0.0841	0.0799	0.0451	0.0440
W	1.60×10^{-1}	3.39×10^{-4}	0.1367	0.4884	0.0882	0.3894	0.1381	0.1368	0.0893	0.0887
X	1.60×10^{-1}	3.39×10^{-4}	0.0757	0.4884	0.0431	0.3894	0.0769	0.0720	0.0440	0.0432

SUBSCRIPTS : T1 = Term 1 T2 = Term 2 (see equation 6.5) L = Linear equation 6.2
S = Second power equation 6.4

SUPERSCRIPT: ′ = Evaluation excluding the terms $\delta H_f/H$ and $\delta\phi_E/\phi_E$

Table No. 6.5 Reliability estimation of the experimental heat transfer factors

Denotation	Ht. Trans. Factor Fig. No.	Config-uration	Tables for data	Run No.	$\frac{\delta(\Delta t'/\Delta t)}{(\Delta t'/\Delta t)}$ L	$\frac{\delta(\Delta t'/\Delta t)}{(\Delta t'/\Delta t)}$ S	$\frac{\delta Y}{Y}$ L	$\frac{\delta Y}{Y}$ S	$\frac{\delta(C/d_o)}{(C/d_o)}$ i.L	$\frac{\delta(C/d_o)}{(C/d_o)}$ i.S	$\frac{\delta(C/d_o)}{(C/d_o)}$ ii.L	$\frac{\delta(C/d_o)}{(C/d_o)}$ ii.S
A	5.16	0	A.8.4, A.9.4	1	0·0075	0·0049	0·0242	0·0165	0·1051	0·0560	0·0220	0·0180
B	5.16	0	A.8.4, A.9.4	27	0·0222	0·0153	0·0389	0·0219	0·0628	0·0319	0·0220	0·0180
C	5.44	6K	A.8.12, A.9.12	1	0·0045	0·0028	0·0212	0·0160	0·1051	0·0560	0·0220	0·0180
D	5.44	6K	A.8.12, A.9.12	27	0·0181	0·0123	0·0348	0·0200	0·0628	0·0319	0·0220	0·0180
E	5.15	0	A.8.3, A.9.3	1	0·0078	0·0051	0·0245	0·0166	0·0918	0·0488	0·0251	0·0211
F	5.15	0	A.8.3, A.9.3	27	0·0255	0·0176	0·0422	0·0236	0·0638	0·0327	0·0251	0·0211
G	5.45	6K	A.8.11, A.9.11	1	0·0049	0·0031	0·0216	0·0161	0·0918	0·0488	0·0251	0·0211
H	5.45	6K	A.8.11, A.9.11	27	0·0206	0·0141	0·0373	0·0218	0·0638	0·0327	0·0251	0·0211
I	5.17	0	A.8.5, A.9.5	1	0·0080	0·0052	0·0247	0·0166	0·1015	0·0536	0·0218	0·0178
J	5.17	0	A.8.5, A.9.5	27	0·0245	0·0168	0·0412	0·0231	0·0638	0·0325	0·0218	0·0178
K	5.41	7T	A.8.10, A.9.10	1	0·0057	0·0036	0·0224	0·0162	0·1015	0·0536	0·0218	0·0178
L	5.41	7T	A.8.10, A.9.10	27	0·0215	0·0147	0·0381	0·0216	0·0638	0·0325	0·0218	0·0178

$\Delta t' = \Delta t_{LM}$ L,S = Utilizes linear or second power equation, respectively

$Y = \frac{\pi l \Delta t'}{Q \rho c_p \Delta t}$ i,ii = Utilizes method (i) or (ii) of section 6.4

The above work is based on the estimates: $\delta d_o/d_o = 0{\cdot}0045$, $\delta Q/Q = 0{\cdot}0157$, $\delta l/l = 0{\cdot}0009$, $\delta d/d = 0{\cdot}005$ and $\delta T_o = \delta T_i = \delta t_o = \delta t_i = 0{\cdot}03°C$

Table No.6.6 Reliability estimation of the experimental heat transfer factors

These results are based on the estimates of Table 6.5

Denotation	$\frac{\delta(Nu/Pr^{0.4})}{(Nu/Pr^{0.4})}$ i.L	$\frac{\delta(Nu/Pr^{0.4})}{(Nu/Pr^{0.4})}$ i.S	$\frac{\delta(Nu/Pr^{0.4})}{(Nu/Pr^{0.4})}$ ii.L	$\frac{\delta(Nu/Pr^{0.4})}{(Nu/Pr^{0.4})}$ ii.S	$\frac{\delta(Nu/Pr^{0.4})}{(Nu/Pr^{0.4})}$ ii.MS
A	0·0885	0·0373	0·0471	0·0263	0·055
B	0·2741	0·1036	0·1791	0·0838	
C	0·2033	0·0897	0·0835	0·0470	0·119
D	0·6677	0·2557	0·4027	0·1900	
E	0·0951	0·0399	0·0547	0·0296	0·067
F	0·3275	0·1240	0·2234	0·1040	
G	0·2242	0·0981	0·1051	0·0585	0·187
H	1·0547	0·4045	0·6658	0·3161	
I	0·0922	0·0384	0·0495	0·0272	0·061
J	0·3115	0·1175	0·2031	0·0944	
K	0·1526	0·0654	0·0611	0·0381	0·094
L	0·5210	0·1974	0·3218	0·1497	

M = Mean value ; for other symbols see Table 6.5

Table No. 6.7 Reliability estimation of the experimental heat transfer factors

Denotation	Ht. Trans. Factor Fig No.	Config-uration	Tables for data	Run No.	$\frac{\delta(\Delta t'/\Delta t)}{(\Delta t'/\Delta t)}$ L	$\frac{\delta(\Delta t'/\Delta t)}{(\Delta t'/\Delta t)}$ S	$\frac{\delta Y}{Y}$ L	$\frac{\delta Y}{Y}$ S	$\frac{\delta(C/d_o)}{(C/d_o)}$ i.L	$\frac{\delta(C/d_o)}{(C/d_o)}$ i.S	$\frac{\delta(C/d_o)}{(C/d_o)}$ ii.L	$\frac{\delta(C/d_o)}{(C/d_o)}$ ii.S
A	5.16	0	A.8.4, A9.4	1	0·0149	0·0097	0·0515	0·0369	0·2260	0·1251	0·0220	0·0180
B	5.16	0	A.8.4, A9.4	27	0·0444	0·0305	0·0809	0·0469	0·1315	0·0683	0·0220	0·0180
C	5.44	6K	A.8.12, A9.12	1	0·0091	0·0056	0·0673	0·0424	0·2260	0·1251	0·0220	0·0180
D	5.44	6K	A.8.12, A9.12	27	0·0361	0·0246	0·0941	0·0487	0·1315	0·0683	0·0220	0·0180
E	5.15	0	A.8.3, A9.3	1	0·0157	0·0102	0·0522	0·0370	0·1970	0·1091	0·0251	0·0211
F	5.15	0	A.8.3, A9.3	27	0·0511	0·0352	0·0876	0·0500	0·1330	0·0694	0·0251	0·0211
G	5.45	6K	A.8.11, A9.11	1	0·0098	0·0062	0·0678	0·0425	0·1970	0·1091	0·0251	0·0211
H	5.45	6K	A.8.11, A9.11	27	0·0372	0·0282	0·0952	0·0506	0·1330	0·0694	0·0251	0·0211
I	5.17	0	A.8.5, A9.5	1	0·0160	0·0105	0·0525	0·0371	0·2181	0·1197	0·0218	0·0178
J	5.17	0	A.8.5, A9.5	27	0·0489	0·0337	0·0855	0·0490	0·1333	0·0691	0·0218	0·0178
K	5.41	6T	A.8.10, A9.10	1	0·0114	0·0072	0·0693	0·0426	0·2181	0·1197	0·0218	0·0178
L	5.41	6T	A.8.10, A9.10	27	0·0429	0·0294	0·1009	0·0513	0·1333	0·0691	0·0218	0·0178

$\Delta t' = \Delta t_{LM}$ L,S = Utilizes linear or second power equation, respectively

$Y = \frac{\pi l \Delta t'}{Q \varrho c_p \Delta t}$ i,ii = Utilizes method (i) or (ii) of section 6.4

The above work is based on the estimates: $\delta d_o/d_o = 0{\cdot}0045$, $\delta d/d = 0{\cdot}01$, $\delta Q/Q = 0{\cdot}0356$, $\delta l/l = 0{\cdot}0009$ (Empty), $\delta l/l = 0{\cdot}0224$, and $\delta T_o = \delta T_i = \delta t_o = \delta t_i = 0{\cdot}06\,^{\circ}C$

Table No. 6.8 Reliability estimation of the experimental heat transfer factors

These results are based on the estimates of Table 6.7

Denotation	$\frac{\delta(Nu/Pr^{0.4})}{(Nu/Pr^{0.4})}$ i.L.	$\frac{\delta(Nu/Pr^{0.4})}{(Nu/Pr^{0.4})}$ i.S	$\frac{\delta(Nu/Pr^{0.4})}{(Nu/Pr^{0.4})}$ ii.L	$\frac{\delta(Nu/Pr^{0.4})}{(Nu/Pr^{0.4})}$ ii.S	$\frac{\delta(Nu/Pr^{0.4})}{(Nu/Pr^{0.4})}$ iiMS
A	0·1897	0·0833	0·0880	0·0560	0·108
B	0·5723	0·2215	0·3189	0·1608	
C	0·4903	0·2080	0·1960	0·1067	0·245
D	1·5575	0·5740	0·8468	0·3830	
E	0·2036	0·0890	0·0991	0·0609	0·127
F	0·6812	0·2628	0·3908	0·1932	
G	0·5411	0·2280	0·2337	0·1242	0·362
H	2·3926	0·8961	1·3064	0·5993	
I	0·1972	0·0856	0·0922	0·0577	0·119
J	0·6488	0·2496	0·3615	0·1811	
K	0·3714	0·1532	0·1650	0·0894	0·198
L	1·2097	0·4399	0·6814	0·3061	

M = Mean value ; for other symbols see Table 6.7

Table No.7.1 The effectiveness of Pall rings for heat transfer enhancement based on the constant power criterion.

Configuration	Re	Re_{oP}	$\left[\frac{Nu}{Nu_o}\right]_P$	$\left[\frac{Nu}{Nu_o}\right]_P^*$
1P	15500	19200	0.964	0.994
1P	104000	129000	0.969	0.962
2P	15500	21800	0.959	0.992
2P	104000	148000	0.911	0.981
3P	15500	24300	0.878	0.910
3P	104000	169000	0.844	0.911
4P	15500	26700	0.971	1.01
4P	104000	185000	0.875	0.944
5P	15500	30700	0.830	0.865
5P	104000	210000	0.742	0.805
6P	15500	40800	0.737	0.772
6P	86500	238000	0.639	0.695

The configurations of the Pall rings are shown in Figure 1.8.

Re = Reynolds number of the flow in the tube containing Pall rings

Re_{oP} = Reynolds number of the flow in an empty tube which requires the same pumping power as Re. The empty tube friction factor is evaluated using denotation A – C of Table 5.2

$\left[\frac{Nu}{Nu_o}\right]_P$ = ratio of the Nusselt numbers of the flow in the packed and empty tubes operating at Re and Re_{oP}, respectively. Nu_o is evaluated using denotation B – C of Table 5.3

$\left[\frac{Nu}{Nu_o}\right]_P^*$ = ratio of the Nusselt numbers obtained using the same pumping power in the packed and empty tubes. (Re^*_{oP}, the Reynolds number required in the empty tube, is not tabulated.) The empty tube characteristics are evaluated using equations (1.4) and (1.19).

Table No.7.2 Comparison of the friction factor ratios, (ϕ / ϕ_o), determined using a continuous twisted tape under isothermal conditions at room temperature and under heating conditions.

Reference	Equation	Friction factor ratio, ϕ / ϕ_o at Reynolds numbers of				% Difference at Reynolds numbers of			
		11000	78000	15500	104000	11000	78000	15500	104000
Present work[1]	(5.9) or (7.1)	9.92	9.00	11.0	9.77	—	—	—	—
Present work[2]	(5.9) or (7.1)	11.1	8.30	11.6	9.61	—	—	—	—
Gambill and Bundy (47)	(1.32), (1.33)	6.67	4.59	6.46	4.62	49	96	71	110
Smithberg and Landis (118)	(1.38)	8.48	5.77	8.10	5.87	17	56	36	66
Migay (83)	(1.40)	8.16	5.95	7.93	6.07	22	51	39	61
Thorsen and Landis (128)	(1.45)	6.85	6.85	7.18	7.18	45	31	54	36
Lopina and Bergles (79)	(1.52)	6.28	6.28	6.58	6.58	58	43	68	48
Date (30)	(1.57)	7.34	6.86	7.66	7.00	35	31	44	40

Notes concerning this table, and the superscripts hereon, are given on the next page.

Notes concerning Table No. 7.2

The friction factor ratios at Re = 11000 and 78000 were evaluated for isothermal conditions. The remaining values apply to heating conditions.

The percentage difference is a comparison of the present work[1] with the stated reference.

Superscript 1 : The friction factor correlation determined in the present work is compared to the actual experimental empty tube correlation i.e. denotation A – I of Table 5.4 for isothermal conditions, or denotation B – P of Table 5.5 for heating conditions.

Superscript 2 : The friction factor correlation of the present work is compared to equation (1.4) for isothermal conditions or to equations (1.4) and (1.53) for heating conditions. These equations were considered to be representative of the empty tube results of the previous workers.

Isothermal friction factors, evaluated using the correlations of the reference authors, were corrected to heating conditions using equations (1.53) and (1.54). The following values were used in the correlations :

$d = 20$ mm

$D_e = 10.62$ mm

$\delta = 2.8$ mm

$y = 2.026$

$t_{av} = 35^{\circ}C$

$t_s = 51^{\circ}C$

Table No. 7.3 Comparison of the heat transfer factor ratios, $(Nu/Pr^{0.4})/(Nu/Pr^{0.4})_o$, determined using a continuous twisted tape

Reference	Equation	Heat transfer factor ratio at Reynolds numbers of		% Difference at Reynolds numbers of	
		15500	104000	15500	104000
Present work	(G - H, Table 5.11)	1.81	1.76	———	———
Gambill et.al. (49)	(1.29)	1.77	1.77	2.3	0.9
Gambill et.al. (49)	(1.30)	1.61	1.61	13	9.4
Smithberg and Landis (118)	(1.39)	2.06	1.67	-12	5.3
Migay (83)	(1.43)				
Thorsen and Landis (128)	(1.50)	2.04	2.04	-11	-14
Lopina and Bergles (79)	(1.55)	1.85	1.80	-2.2	-2.2
Nazmeev and Nikolaev (89)	(1.60)	1.98	1.98	-8.3	-11

The results of the reference authors were evaluated using the above equations with the conditions and geometrical details noted in Table 7.2. All of the equations were referred to the experimental empty tube correlation of the present work i.e. denotation A - P of Table 5.6.

Equation (1.60) was used with the equation suggested by Nazmeev and Nikolaev :

$$Nu_o = 0.021\ Re^{0.8}\ Pr^{0.43}\ (Pr/Pr_s)^{0.25}$$

Table No.7.4 The effectiveness of inserts of identical twist direction for heat transfer enhancement based on the constant power criterion

Configuration	$Re_{oP} \times 10^{-4}$ for Reynolds numbers of		$(Nu/Nu_o)_P$ at Reynolds numbers of		$(Nu/Nu_o)^*_P$ at Reynolds numbers of	
	15500	104000	15500	104000	15500	104000
1T	2.53	16.8	0.928	0.961	1.04	1.10
3T	3.12	21.2	0.845	0.810	0.951	0.928
4T	3.17	21.4	0.854	0.850	0.961	0.974
5T	3.72	25.0	1.01	0.985	1.13	1.13
6T	3.82	24.7	0.941	0.992	1.06	1.14
7T	3.76	24.4	0.893	0.888	1.00	1.02
8T	4.64	31.2	0.853	0.839	0.963	0.966
9T	3.13	20.5	0.819	0.828	0.921	0.948
1TS	2.77	18.4	0.915	0.971	1.03	1.11

The configurations of the inserts are shown in Figure 1.5

The symbols used in this table are the same as those given in Table 7.1, except that the empty tube friction and heat transfer factors are evaluated using denotation B - P of Table 5.5 and denotation A - P of Table 5.6, respectively.

Table No.7.5 Comparison of the friction factors evaluated using the modified forms of equations (1.80) to (1.83) and those experimentally determined

Details of the calculation procedure are given in Appendix A.12
ϕ_P = the friction factor evaluated using the modified equation; subscripts 1, 2, 3, and 4, refer to the use of equations (1.80), (1.81), (1.82), and (1.83), respectively.
ϕ_R = the friction factor determined by the reference author.
$\% = (\phi_P - \phi_R) \times 100 / \phi_R$

The range of the tests performed by each of the reference authors is presented in Table 1.2
* = Results of the present work for heating conditions.(The results at Re = 11000 and 78000 apply to isothermal conditions.)

Reference	Reynolds Number	ϕ_R	ϕ_{P1}	$\%_1$	ϕ_{P2}	$\%_2$	ϕ_{P3}	$\%_3$	ϕ_{P4}	$\%_4$
Present work	11000	0.226	0.194	-14	0.205	-9	0.168	-26	0.194	-14
	78000	0.156	0.132	-15	0.140	-10	0.114	-27	0.132	-15
	15500*	0.215	0.159	-26	0.168	-22	0.138	-36	0.159	-26
	104000*	0.157	0.124	-21	0.131	-16	0.107	-31	0.124	-21
Morris and Benyon (86)	6000	0.0528	0.108	105	0.140	164	0.0897	70	0.134	153
	11000	0.0494	0.0989	100	0.128	159	0.0821	66	0.122	149
	30000	0.0442	0.0854	93	0.110	149	0.0709	60	0.106	139
	78000	0.0398	0.0743	87	0.0959	141	0.0617	55	0.0919	131
Proctor (101) Mass transfer y = 2.0	11000	0.0530	0.163	207	0.171	223	0.142	169	0.163	207
	30000	0.0515	0.141	173	0.148	187	0.123	139	0.141	173
	78000	0.0502	0.122	144	0.129	157	0.107	113	0.122	144
Proctor (101) Mass transfer y = 1.5	11000	0.0789	0.310	293	0.329	317	0.289	266	0.307	289
	22000	0.0780	0.280	257	0.298	280	0.261	233	0.278	254
	78000	0.0774	0.233	201	0.247	220	0.217	181	0.231	198
Proctor (101) Heat transfer y = 1.5	6000	0.138	0.339	145	0.360	161	0.316	129	0.336	143
	11000	0.136	0.310	127	0.329	142	0.289	112	0.307	125
	20000	0.135	0.284	111	0.302	124	0.265	97	0.282	109
	78000	0.131	0.233	78	0.247	89	0.217	66	0.231	77

Continued.....

Table No.7.5 Continued

Reference	Reynolds Number	ϕ_R	ϕ_{P1}	$\%_1$	ϕ_{P2}	$\%_2$	ϕ_{P3}	$\%_3$	ϕ_{P4}	$\%_4$
Smith (117)	300	0.471	0.476	1	0.505	7	0.441	-6	0.468	-1
	11000	0.306	0.281	-8	0.298	-3	0.260	-15	0.277	-10
	78000	0.242	0.211	-13	0.244	-7	0.196	-19	0.208	-14
	100000	0.235	0.204	-13	0.216	-8	0.189	-20	0.200	-15
Chakrabarti (21)	1.6	34.8	1.24	-96	1.40	-96	1.16	-97	1.29	-96
	160	0.744	0.636	-15	—	—	—	—	—	—
	120	0.858	—	—	0.745	-13	—	—	—	—
	200	0.675	—	—	—	—	0.575	-15	—	—
	150	0.767	—	—	—	—	—	—	0.665	-13
	2800	0.420	0.418	0	0.470	12	0.391	-7	0.434	3
	11000	0.405	0.343	-15	0.385	-5	0.320	-21	0.355	-12
	78000	0.401	0.257	-36	0.289	-28	0.241	-40	0.267	-33

Table No.7.6 The effectiveness of inserts of alternate twist direction for heat transfer enhancement based on the constant power criterion

Configuration	$Re_{oP} \times 10^{-4}$ for Reynolds numbers of		$(Nu/Nu_o)_P$ at Reynolds numbers of		$(Nu/Nu_o)_P^*$ at Reynolds numbers of	
	15500	104000	15500	104000	15500	104000
1K	2.77	18.6	0.848	0.841	0.953	0.963
3K	3.79	26.1	0.809	0.750	0.912	0.862
4K	3.66	25.0	0.808	0.770	0.910	0.884
5K	4.94	33.5	0.820	0.842	0.927	0.970
6K	7.12	50.1	0.817	0.799	0.926	0.924
7K	5.08	33.1	1.02	0.986	1.15	1.14
8K	5.58	39.1	0.611	0.600	0.692	0.692
9K	5.63	39.1	0.646	0.620	0.731	0.715
1KS	2.92	20.1	0.902	0.868	1.01	0.994
3KS	3.87	26.4	0.815	0.805	0.919	0.925

The configurations of the inserts are shown in Figure 1.6

The symbols used in this table are the same as those given in Table 7.1, except that the empty tube friction and heat transfer factors are evaluated using denotation B - P of Table 5.5 and denotation A - P of Table 5.6, respectively.

FIGURES

Figure No.1.1 Schematic diagram of a slat blockage and a segmental blockage

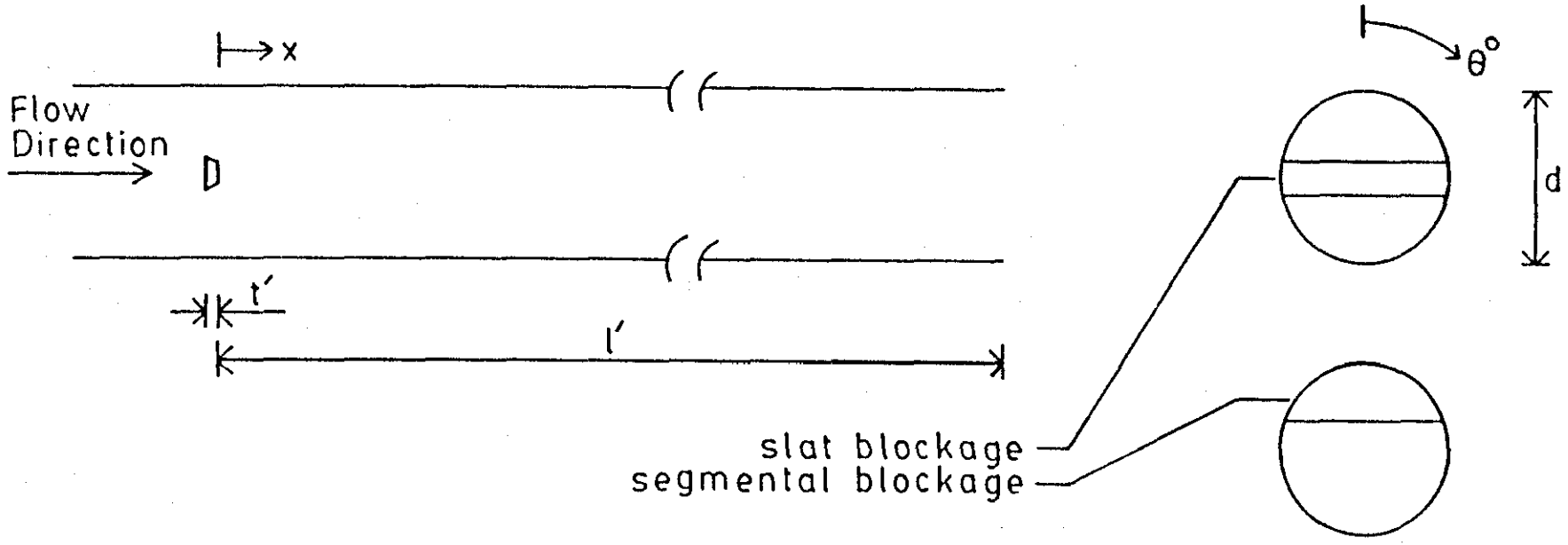

d = tube diameter
l' = tube length downstream of the blockage
t' = thickness of the blockage
x = distance downstream of the blockage
θ° = angular coordinate

Figure No.1.2 The arrangement of helices to form a twisted tape and a Kenics static mixer

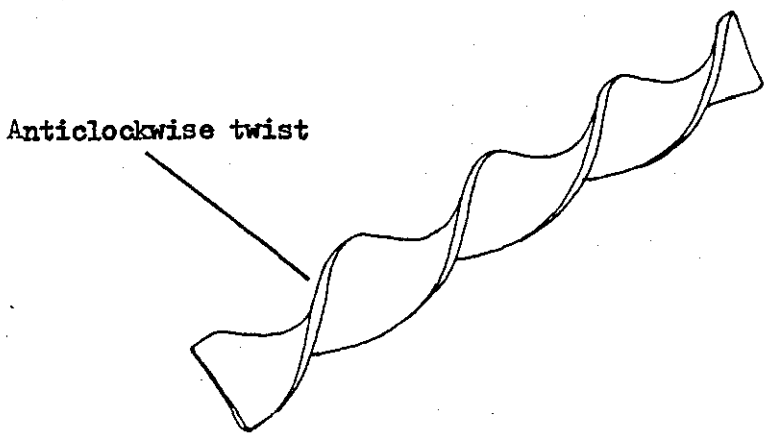

(a) Twisted tape

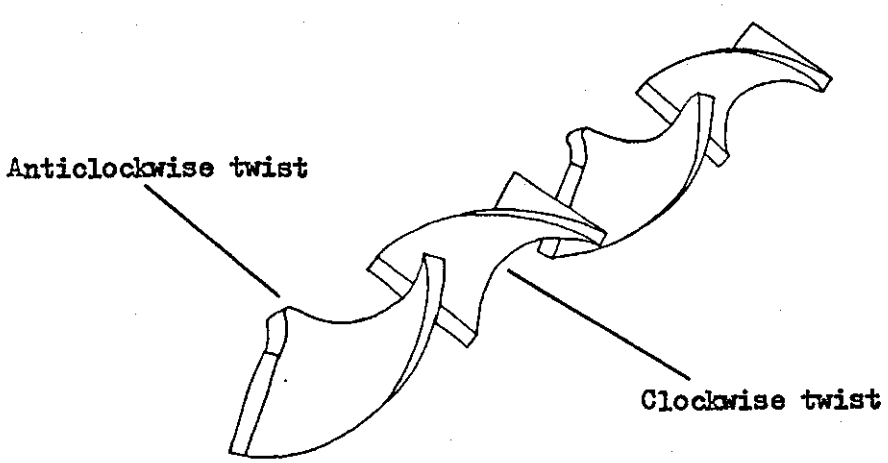

(b) Kenics static mixer

Note

Anticlockwise and clockwise helices may also be referred to as 'lefthand rotation' and 'righthand rotation' elements or helices.

Figure No.1.3 Diagrams of some commercially available motionless in-line mixers*

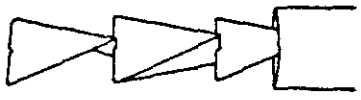

Etoflo LV process line mixer

Standard elements of a Komax motionless mixer

Lightnin in-line blender turbulent flow module

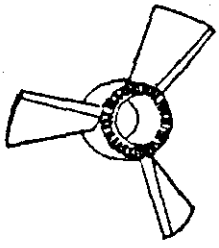

Single element, Lightnin in-line blender

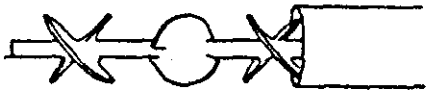

Standard Ross LPD motionless mixer

Ross LLPD motionless mixer

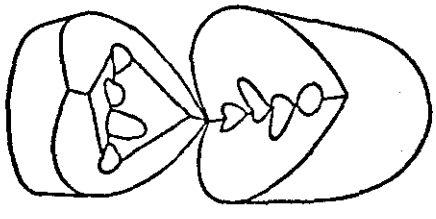

Two elements of a Ross ISG mixer

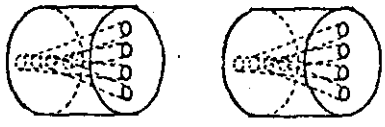

Schematic diagram showing the flow channels within two consecutive elements of a Ross ISG mixer

*Reproduced by permission from photographs and drawings supplied by the manufacturer's of the respective mixers.

Figure No.1.4 Photograph of the various arrangements of the swirl flow inducing inserts

[A] Stainless steel inserts manufactured by the Kenics Corporation

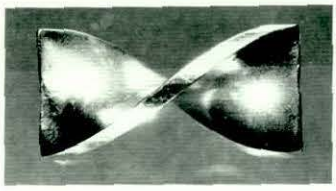

Anticlockwise, or lefthand rotation

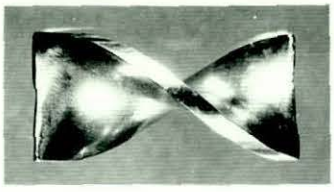

Clockwise, or righthand rotation

[B] Inserts formed from solder alloy (Grade J)

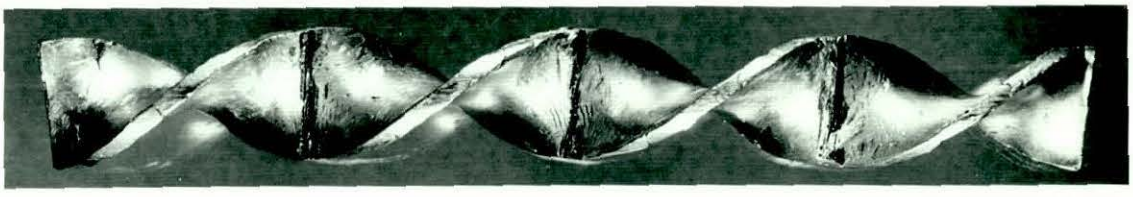

a. Four inserts of anticlockwise twist with aligned edges (Twisted tape)

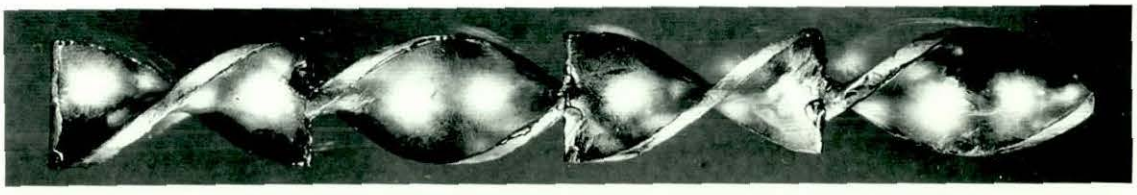

b. Four inserts of anticlockwise twist with perpendicular edges

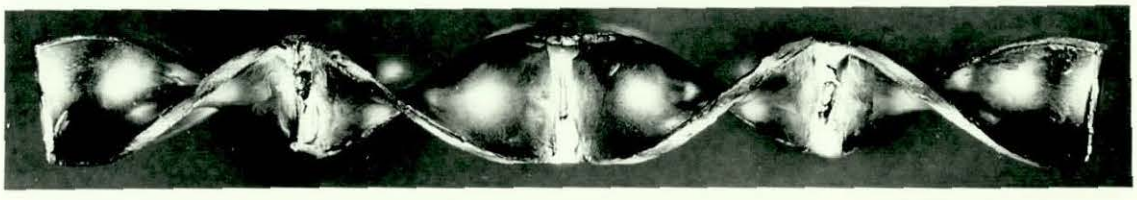

c. Four inserts of alternate twist with aligned edges

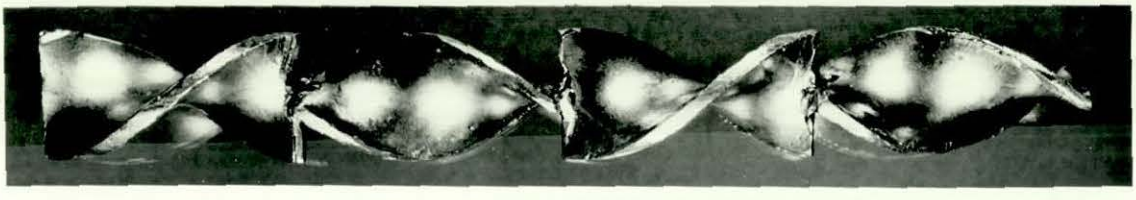

d. Four inserts of alternate twist with perpendicular edges (Kenics mixer)

Figure No.1.5 Details of configurations using inserts of identical twist direction

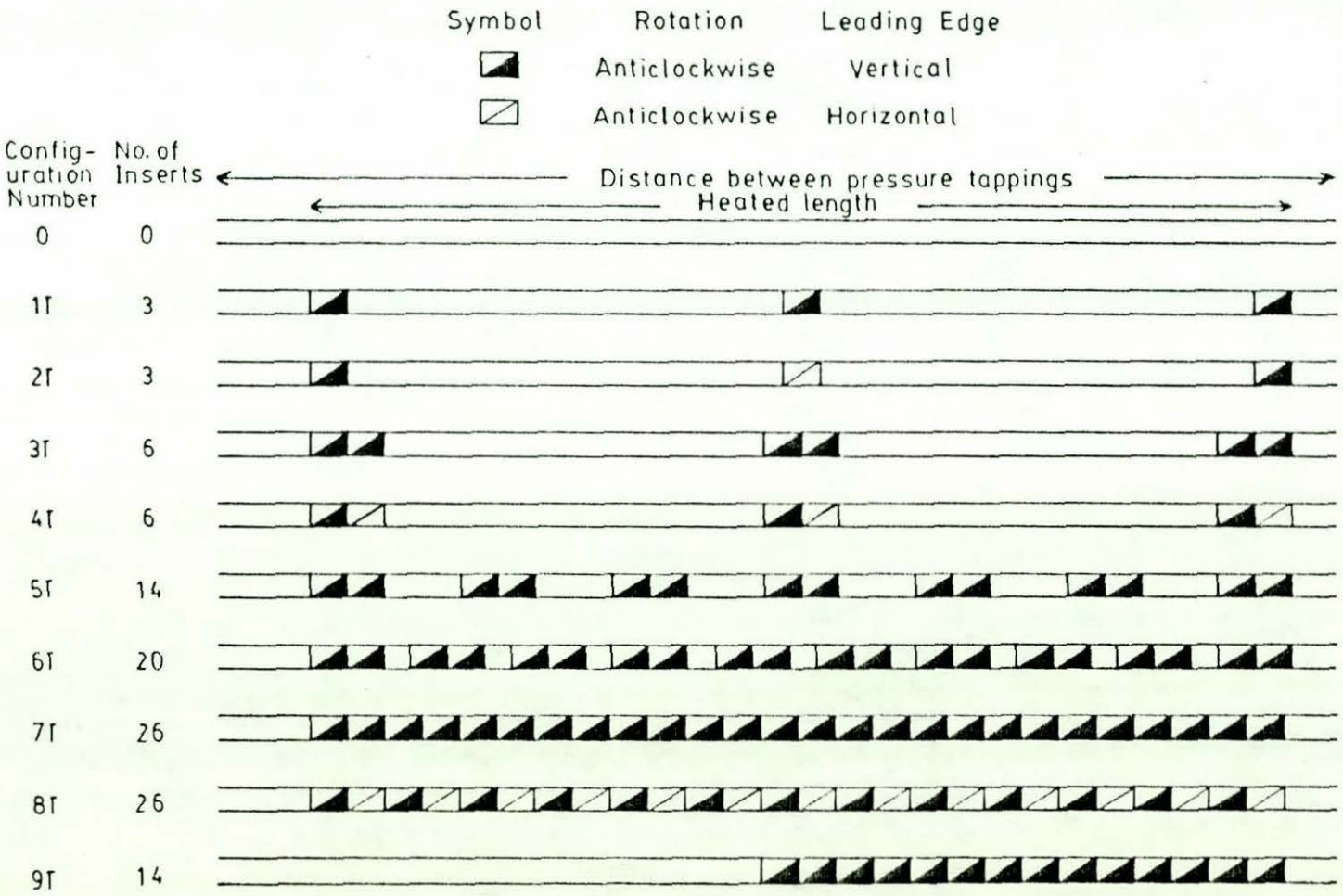

Figure No. 1.6 Details of configurations using inserts of alternate twist direction

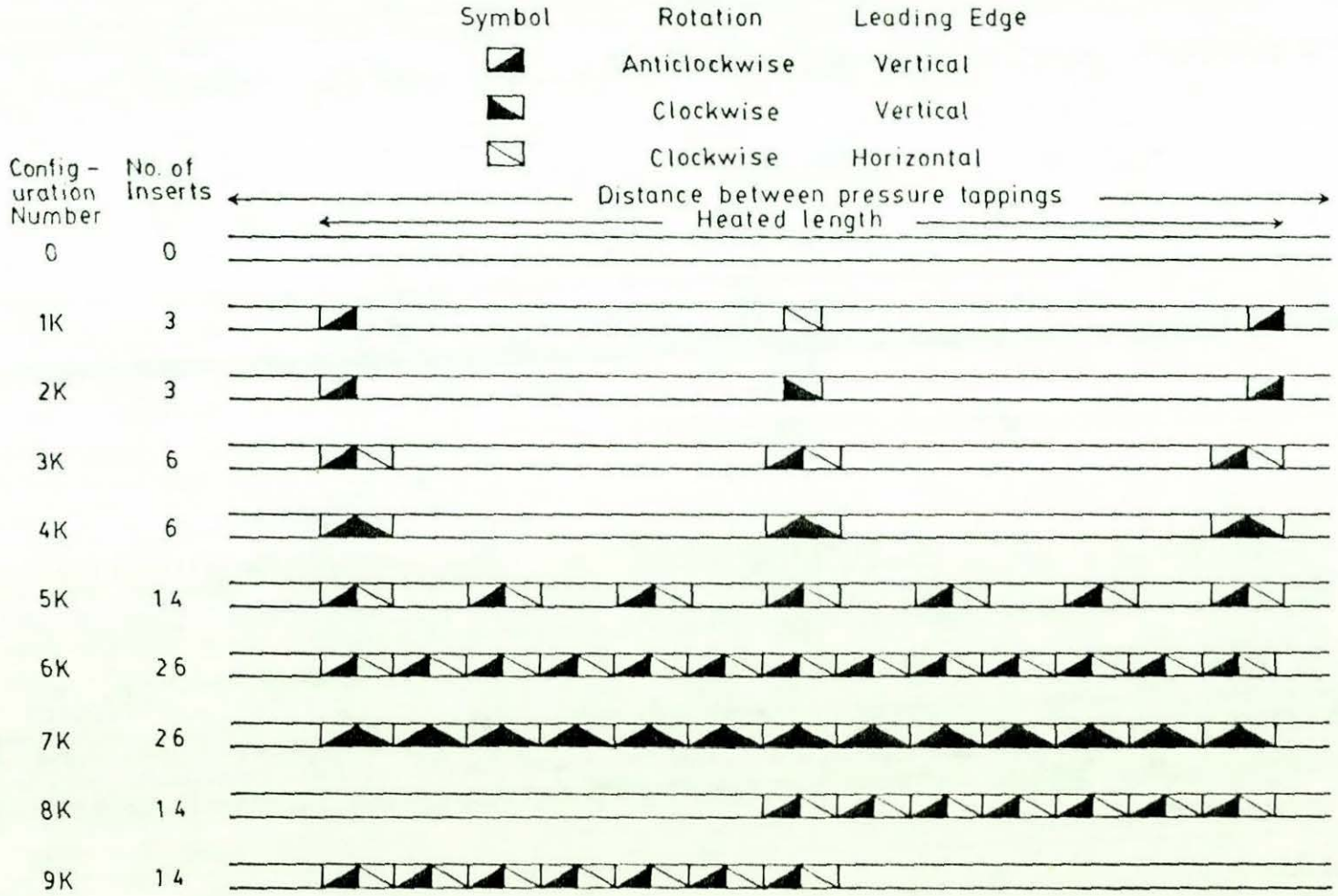

Figure No.1.7 Photograph of an original stainless steel Pall ring and those adapted for insertion into a tube (20 mm i.d.)

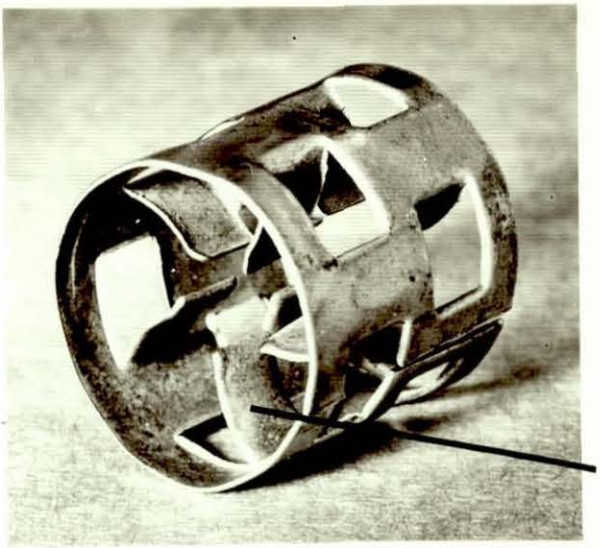

Original one inch (25·4 mm) Pall ring

An inset of the Pall ring

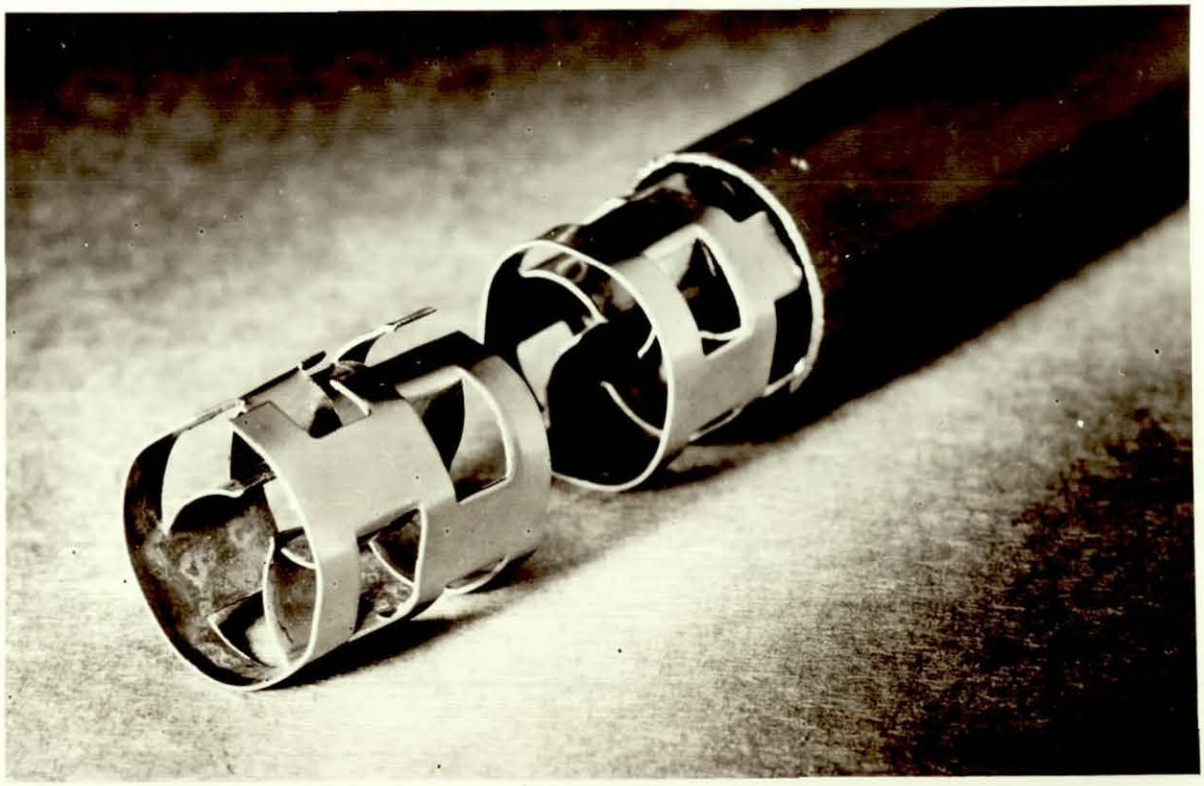

Adapted Pall rings

(The insets of all of the Pall rings have the same curve direction)

Figure No. 1.8 Details of configurations using pall rings

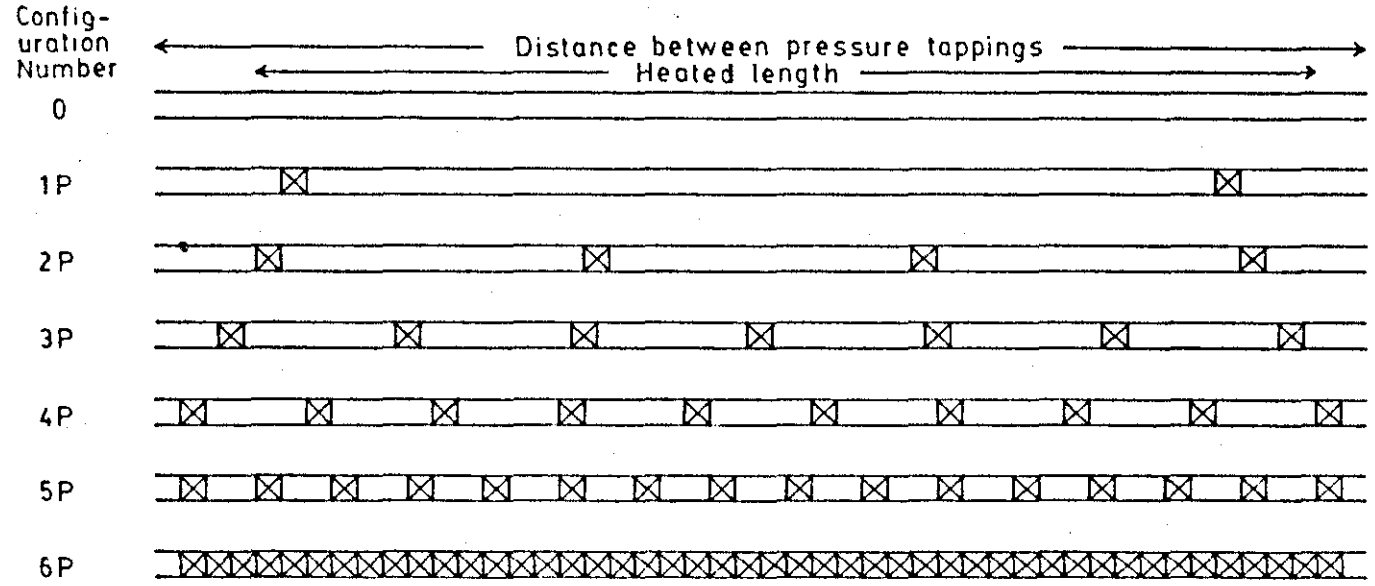

Configuration	No. of inserts	Spacing, inches (mm)	A′, Heat transfer	A′, Pressure drop
1P	2	36 (914)	0·960	0·955
2P	4	12 (305)	0·919	0·915
3P	7	6 (152)	0·879	0·862
4P	10	4 (102)	0·838	0·816
5P	16	2 (51)	0·717	0·705
6P	46	———	0·152	0·152

A′ = fraction of the tube wall area that is not covered by the material of the pall rings.

Figure No. 2.1 Flow Diagram of the Experimental Facility

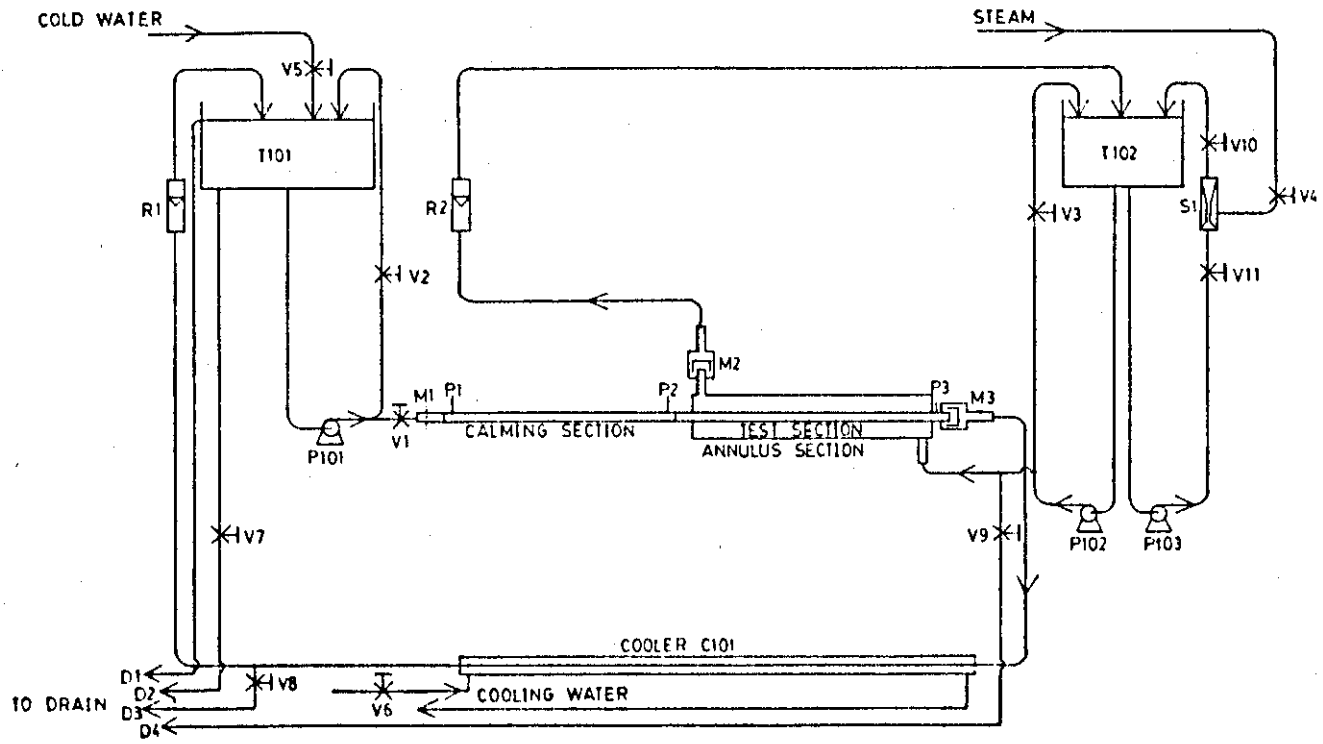

Figure No. 2.2 Manometer Layout and Associated Tubing Network

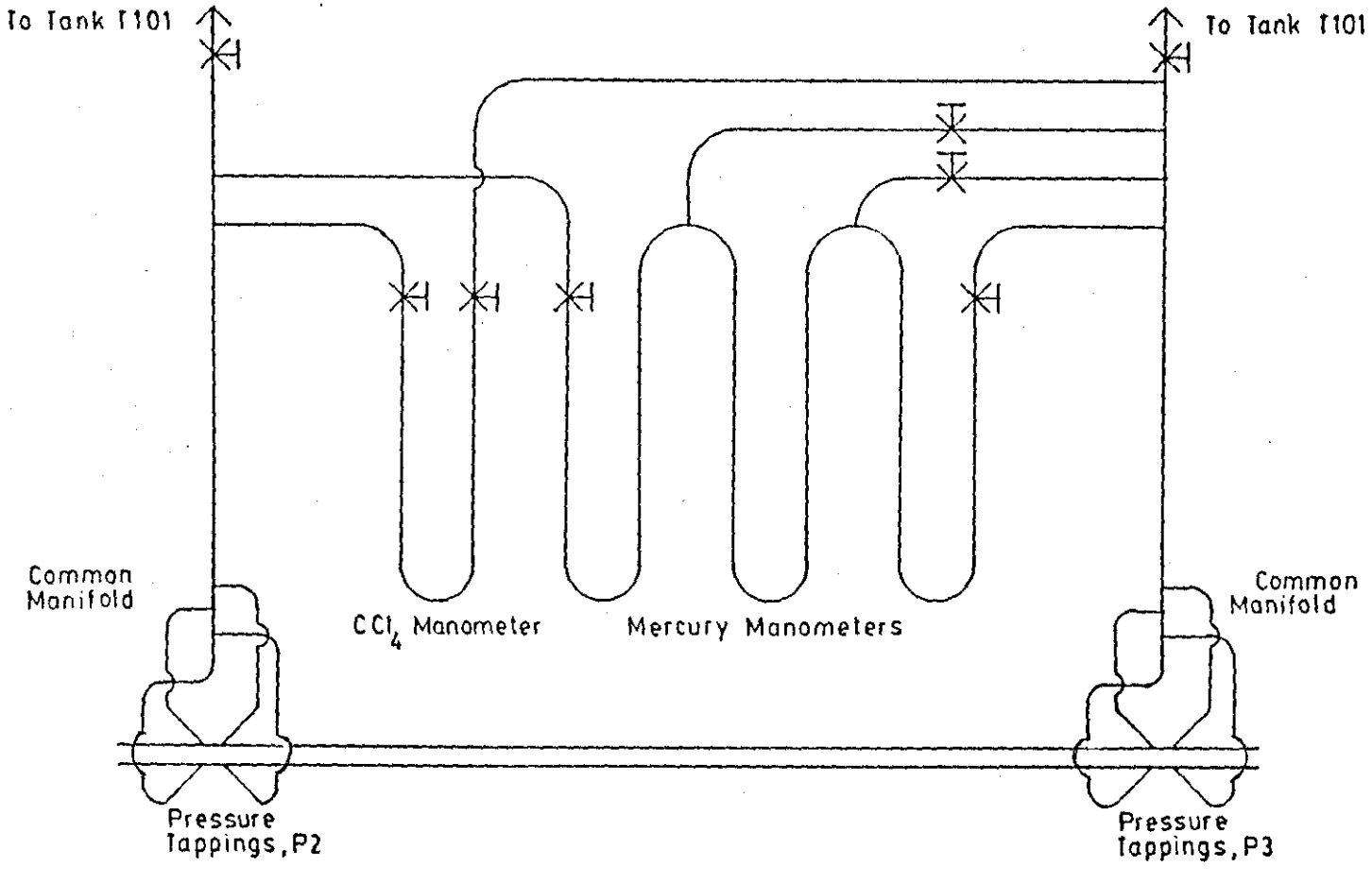

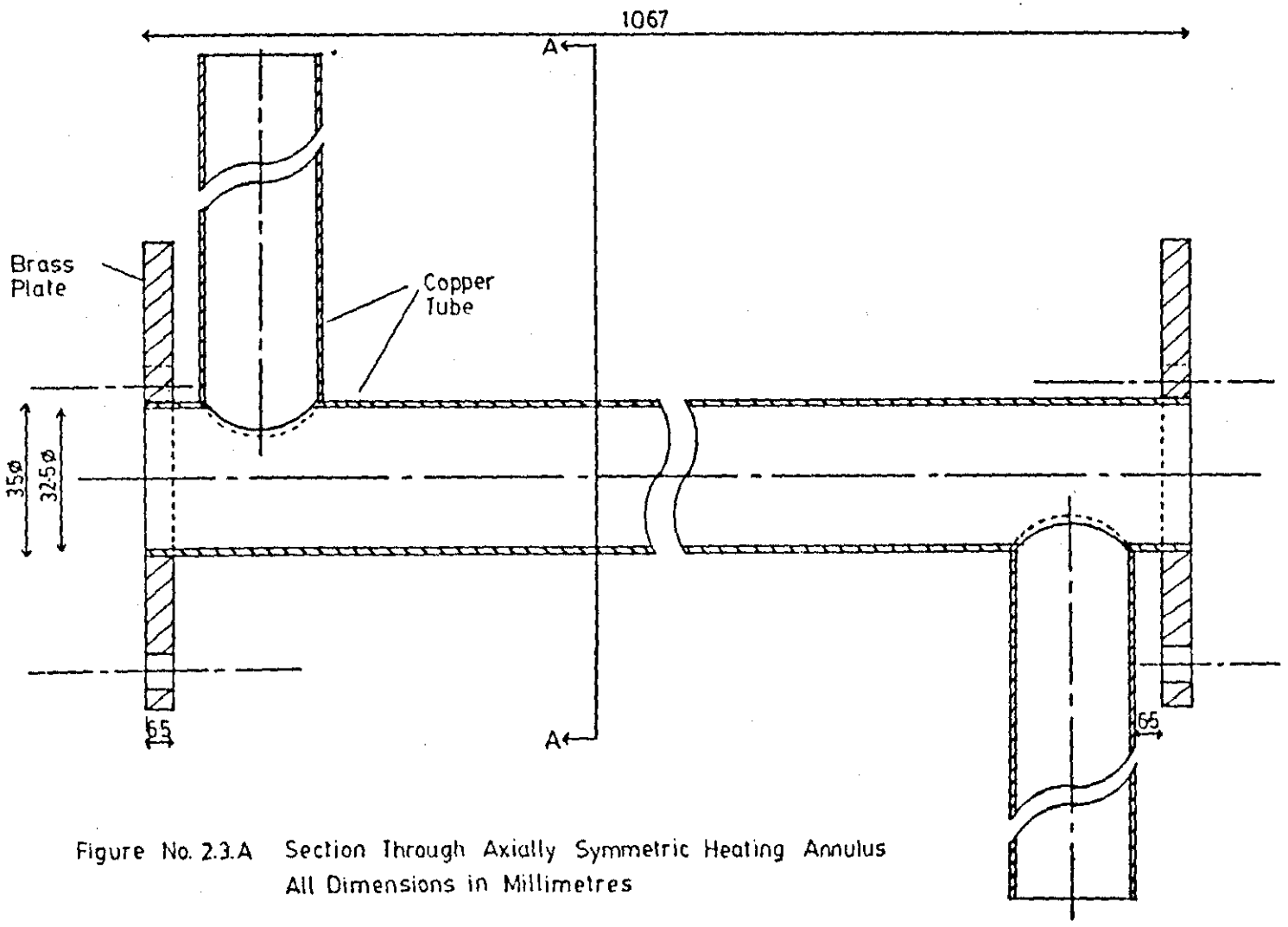

Figure No. 2.3.A Section Through Axially Symmetric Heating Annulus
All Dimensions in Millimetres

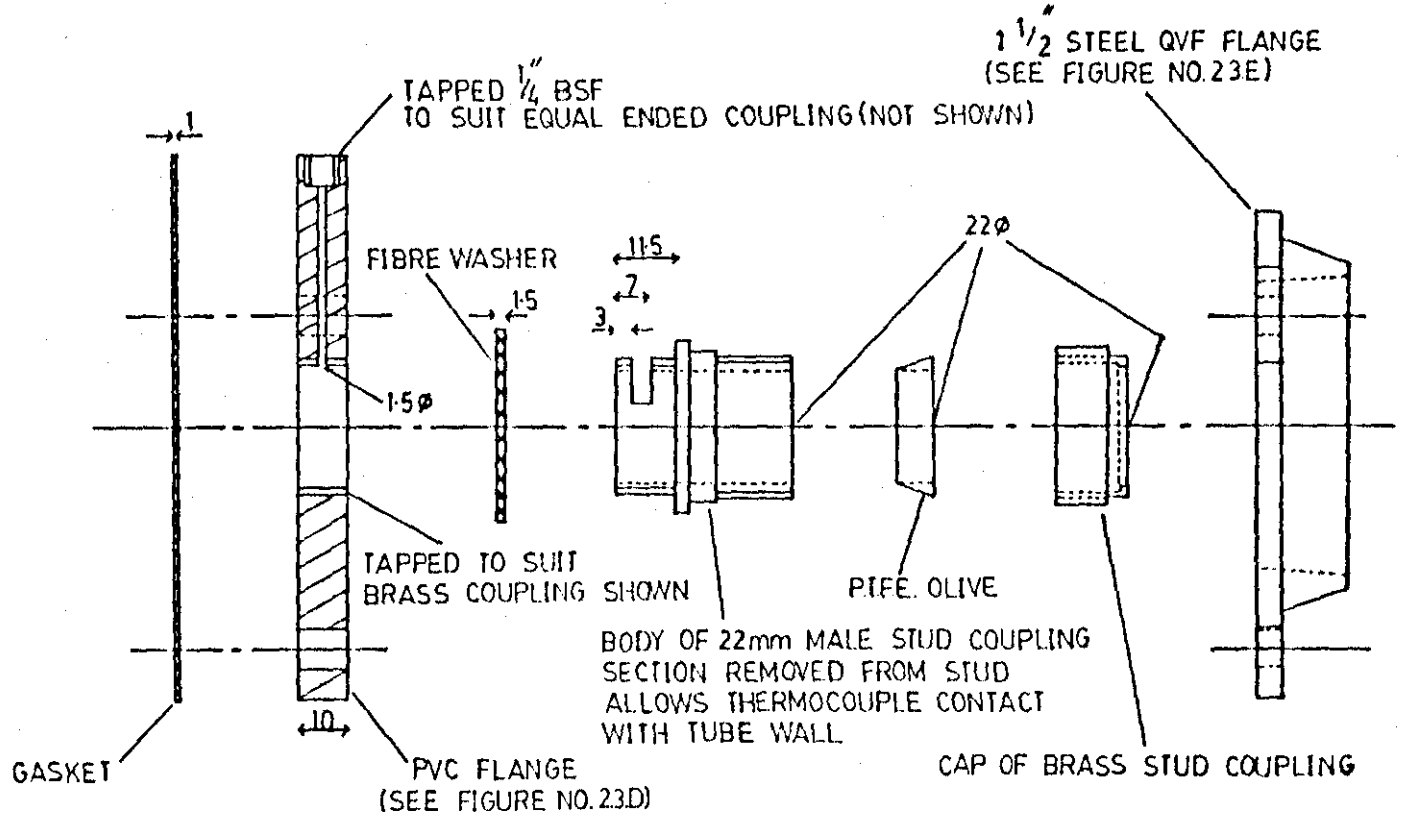

Figure No. 2.3.B Side Elevation of the Dismantled Flanges and Fittings of each of the End Flanges of the Annulus Length

All Dimensions in Millimetres

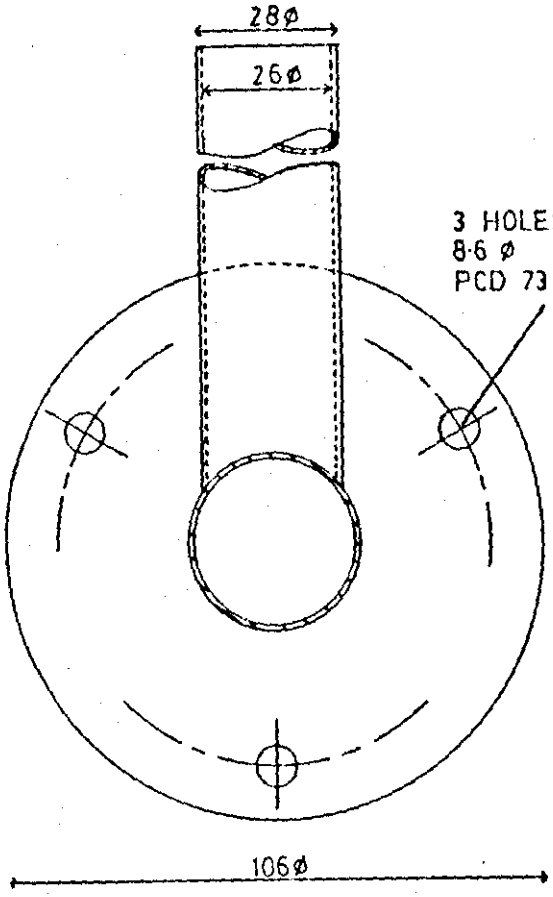

Figure No. 2.3.C View from A-A (Figure No. 2.3A)
All Dimensions in Millimetres

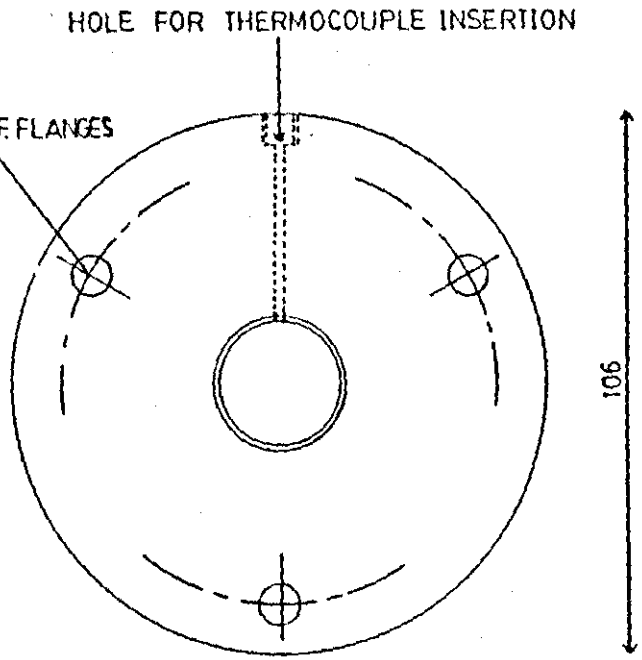

Figure No. 2.3.D Front Elevation of P.V.C. Flange
All Dimensions in Millimetres

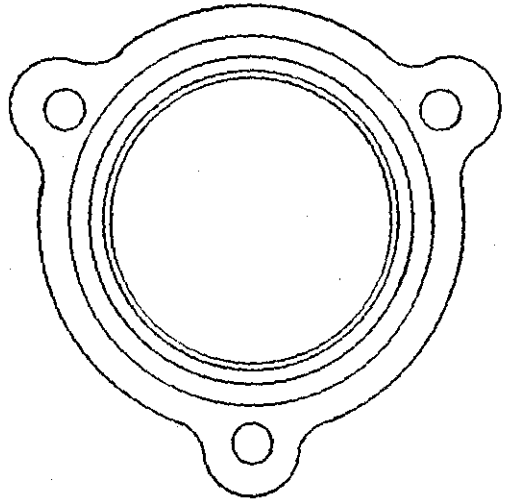

Figure No. 2.3.E
Front Elevation of
Steel Q.V.F. Flange ($1\frac{1}{2}''$)

Figure No. 24 Relative Locations of the Pressure and Temperature Sensors

(See Figure No. 2.1 for locations relative to other equipment)

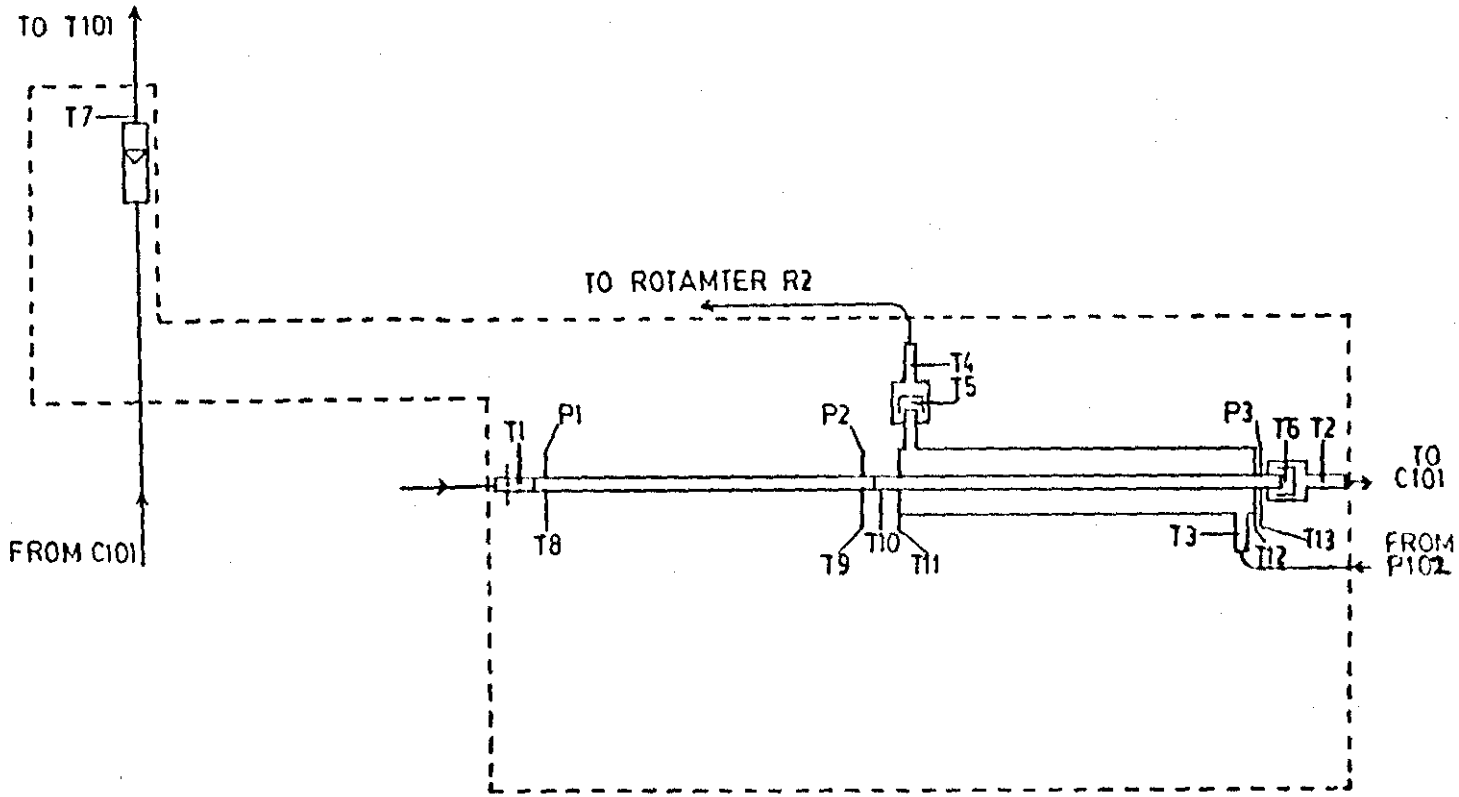

Figure No.25 Constructional details of the adiabatic mixing chambers

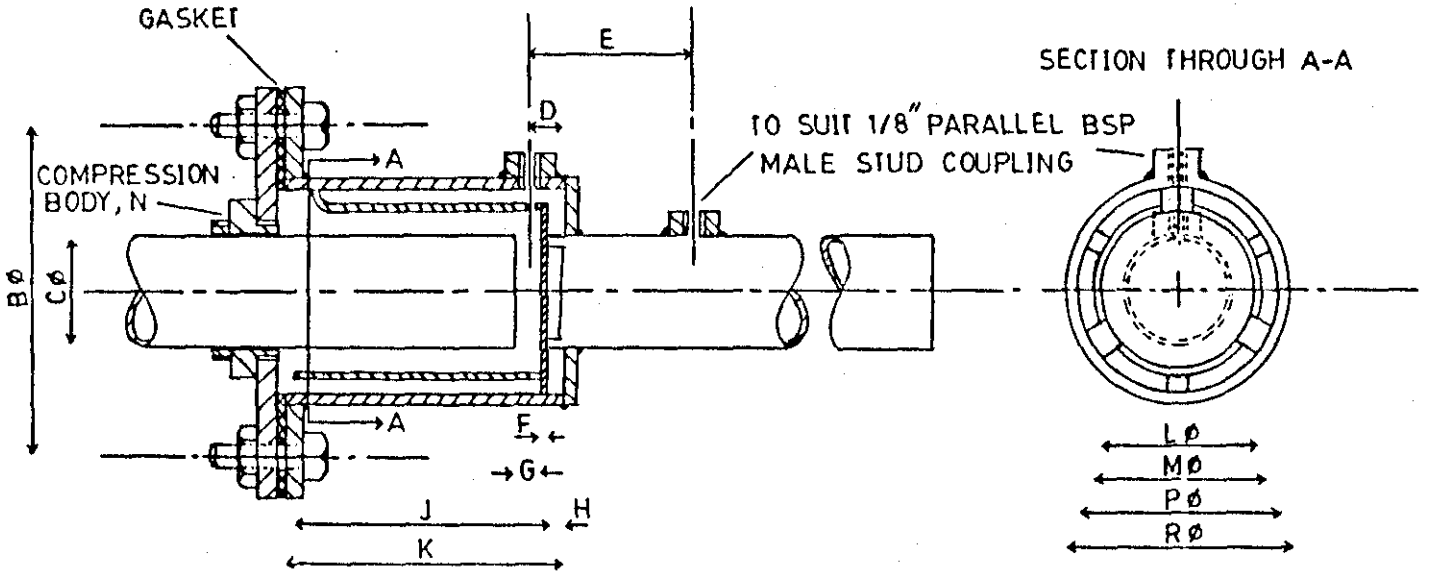

	TUBE SIDE		ANNULUS SIDE	
	DIMENSION	MATERIAL	DIMENSION	MATERIAL
Bø	75		86	
Cø	22	COPPER	28	COPPER
D	7		8	
E	20		20	
F	1	COPPER	1	COPPER
G	5		6	
J	50	COPPER	50	COPPER
H	3		4	
K	57	STEEL	59	STEEL
Lø	32	COPPER	38	COPPER
Mø	34	COPPER	40	COPPER
Pø	40	STEEL	48	STEEL
Rø	43	STEEL	52	STEEL

All dimensions in millimetres

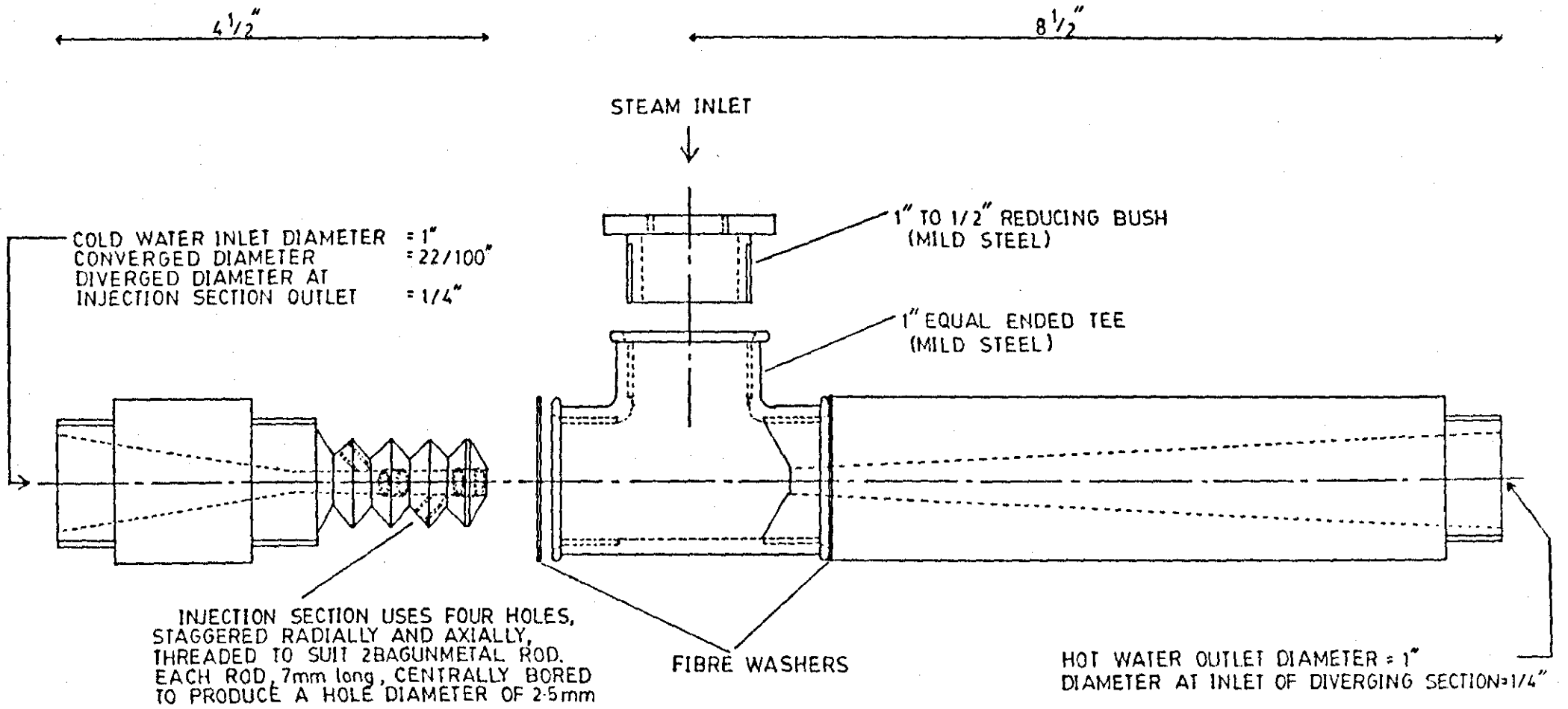

ALL PARTS CONSTRUCTED FROM BRASS UNLESS OTHERWISE STATED

Figure No. 2.6 STEAM INJECTOR

Figure No.27 Equipment for the sensing of Tube Wall Temperatures

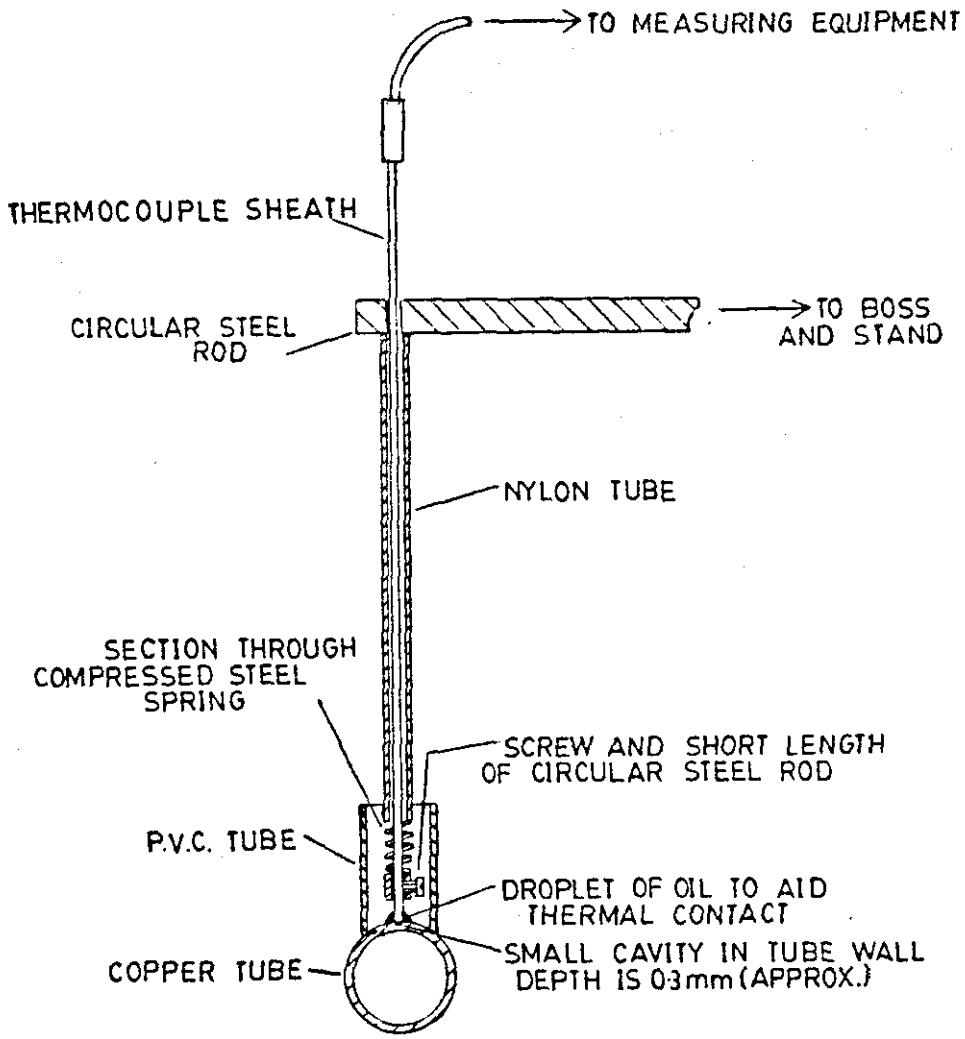

Figure No.4.1 The Effect of Temperature on the Specific Gravity of Carbon Tetrachloride

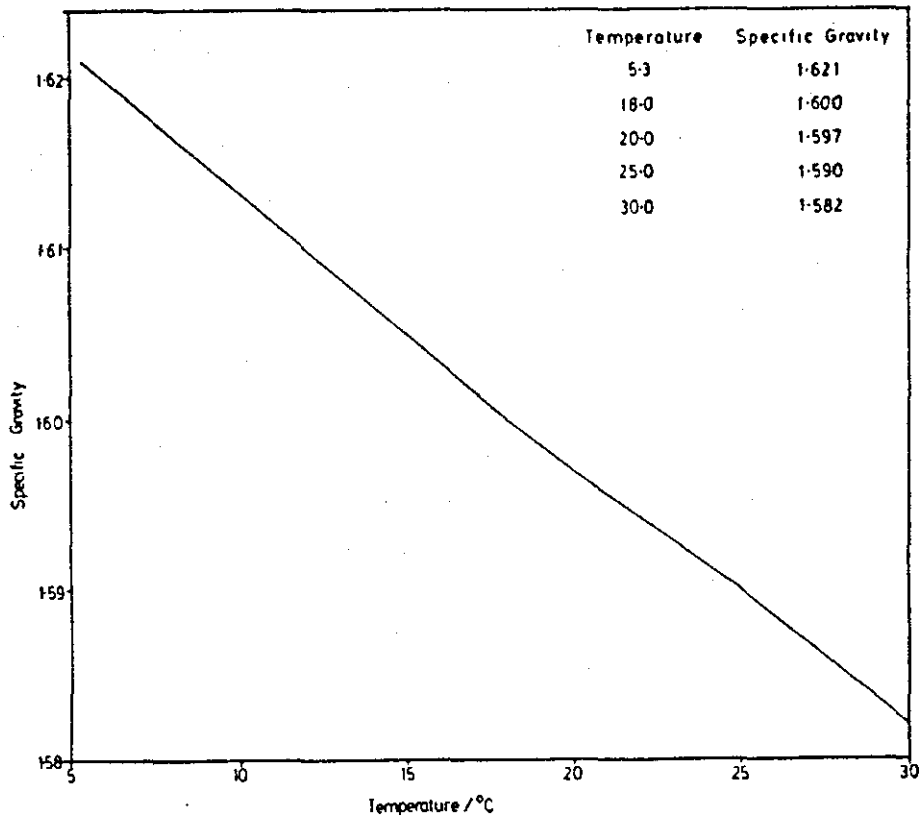

Figure No.4.2 The Effect of Temperature on the Specific Gravity of Mercury

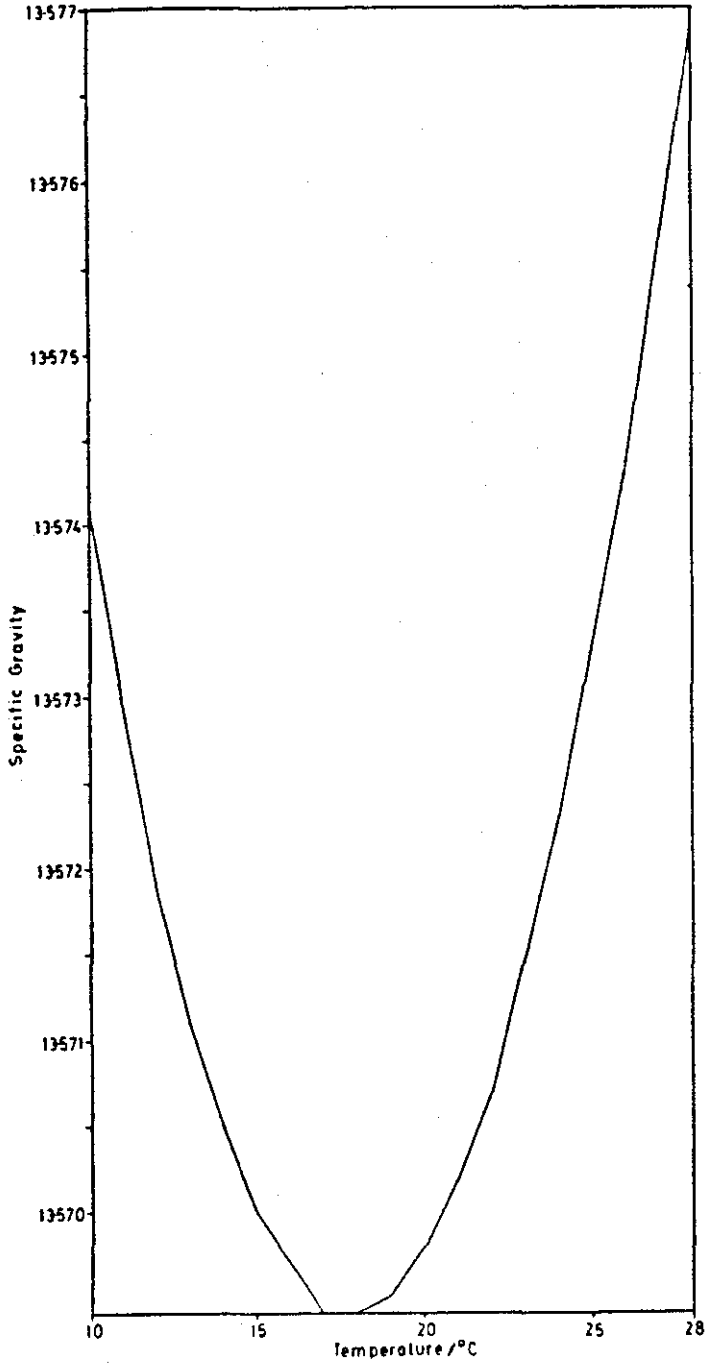

Figure No.4.3 Explanatory Diagram for the Conversion of Differential Fluid Heads to Differential Pressures (See Section 4.4)

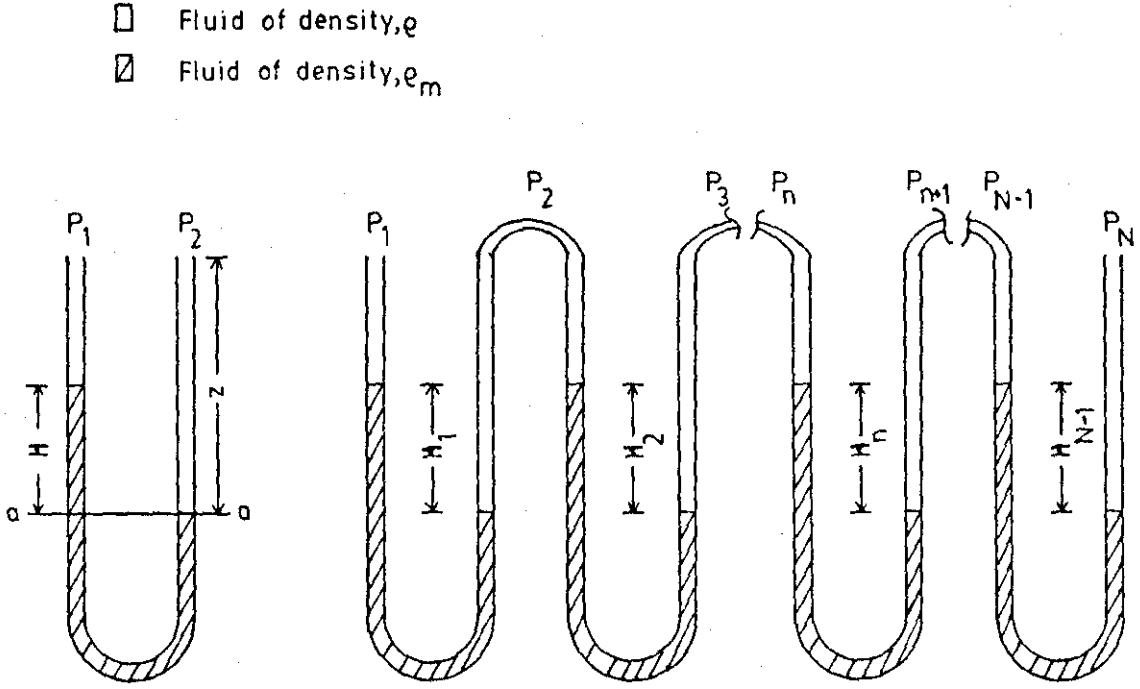

Figure No. 4.4 The Effect of Temperature on Rotameter Metering

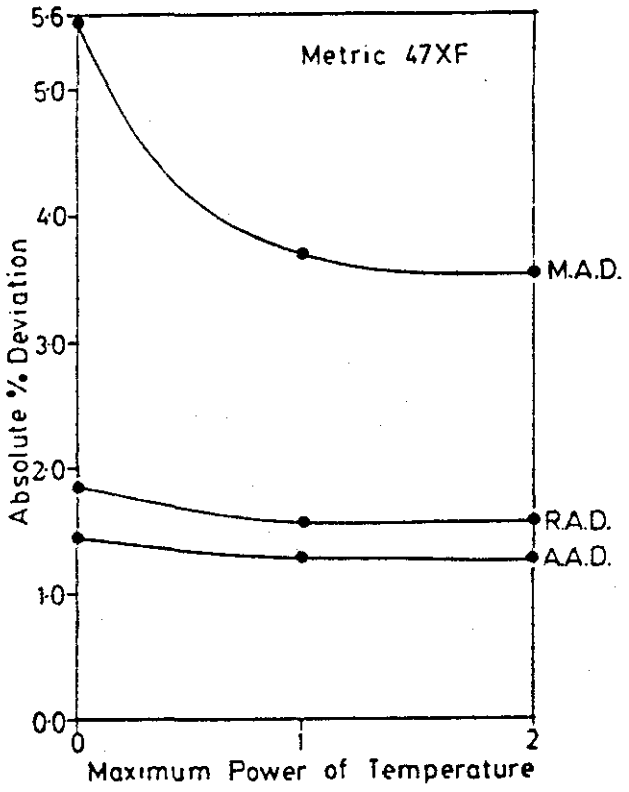

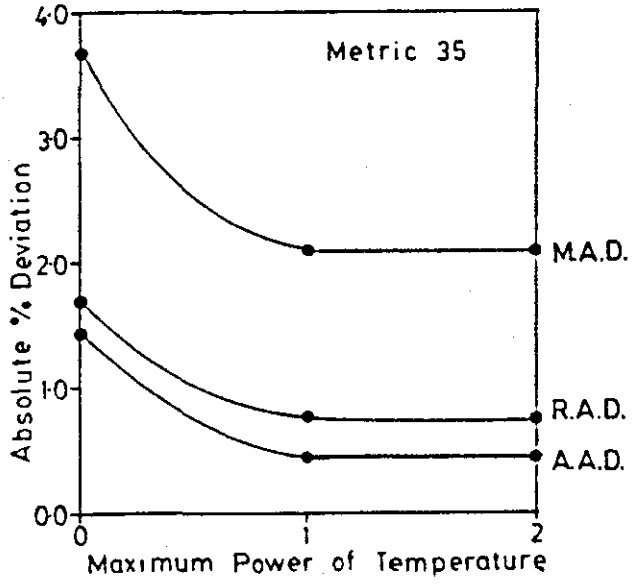

Figure No. 5.1 (See Table 5.1)
Friction Factor Comparisons
Type: Pall Rings (Isothermal)

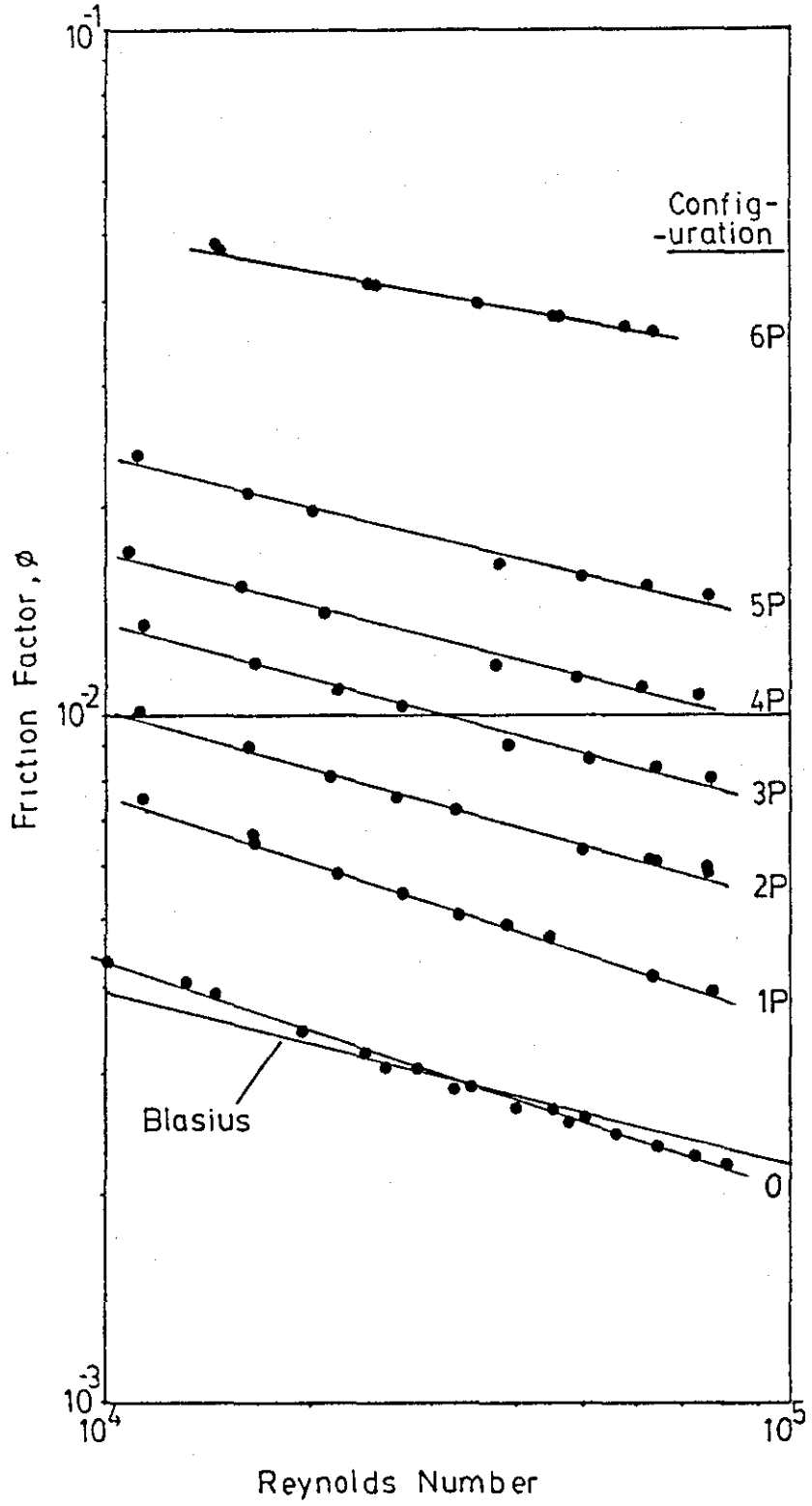

Figure No.5.2 (See Table 5.2)
Friction Factor Comparisons
Type: Pall Rings (Heating data)

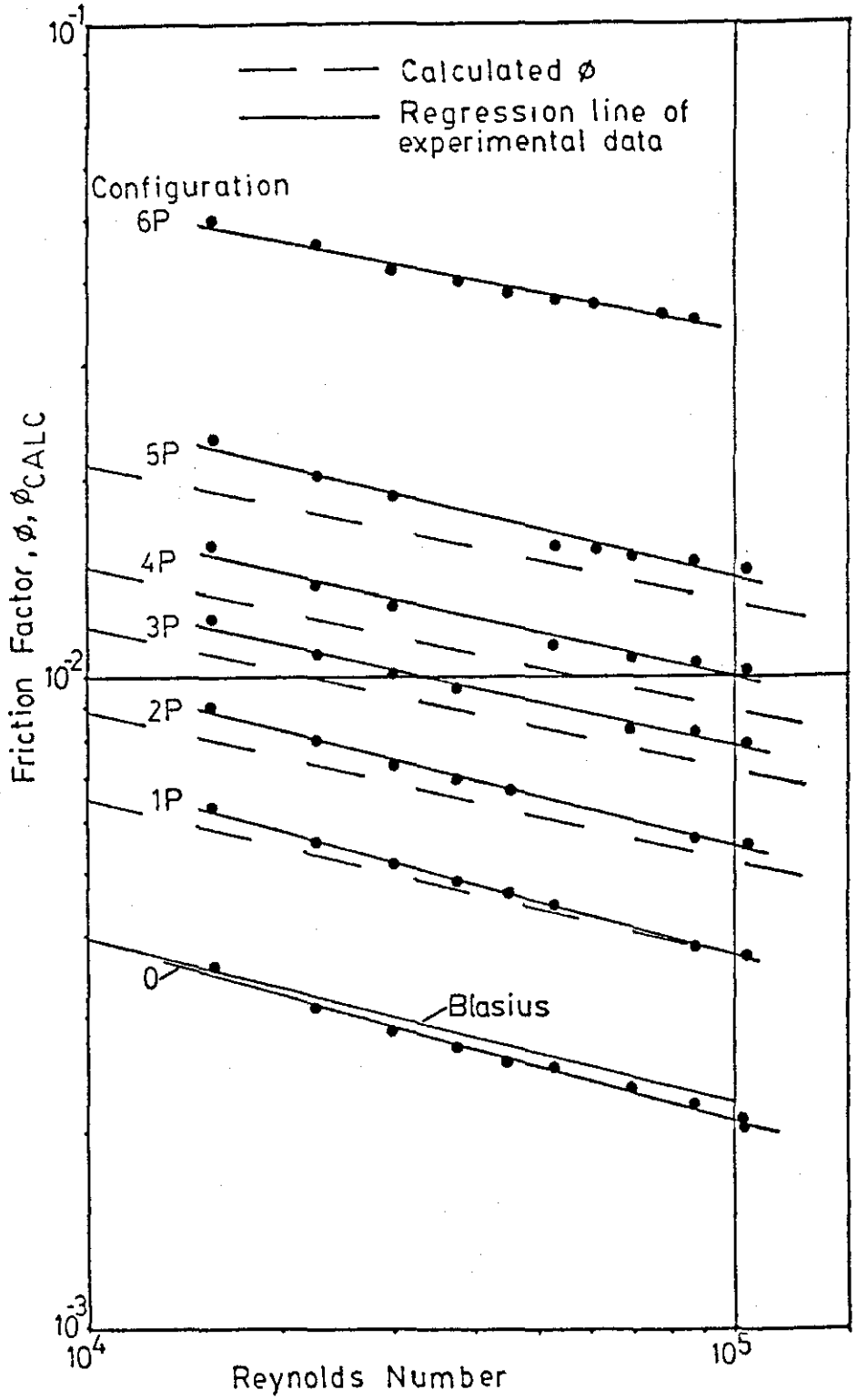

Figure No. 5.3
Heat Transfer Comparisons
Type: Configuration 1P (Denotation D of Table 5.3)

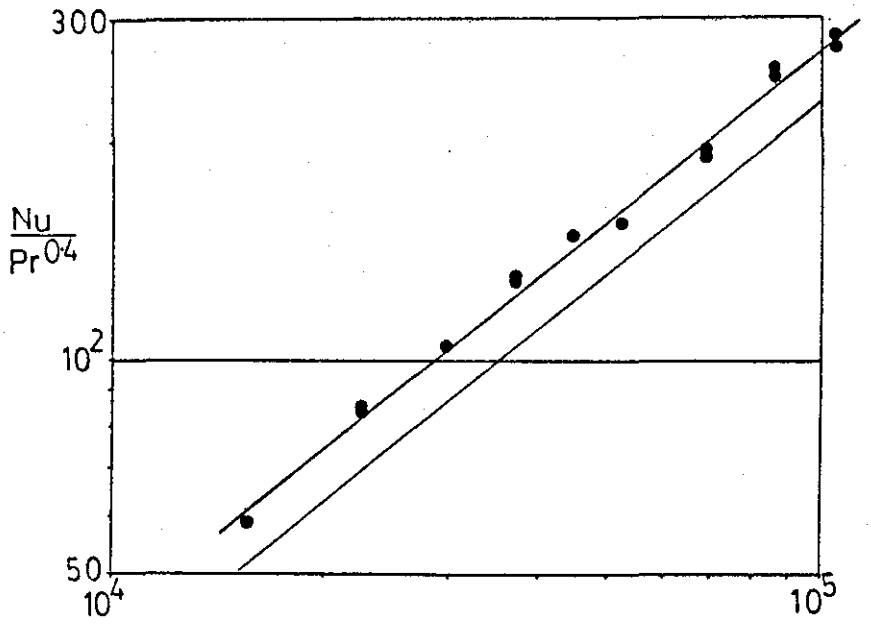

Figure No. 5.4
Heat Transfer Comparisons
Type: Configuration 2P (Denotation E of Table 5.3)

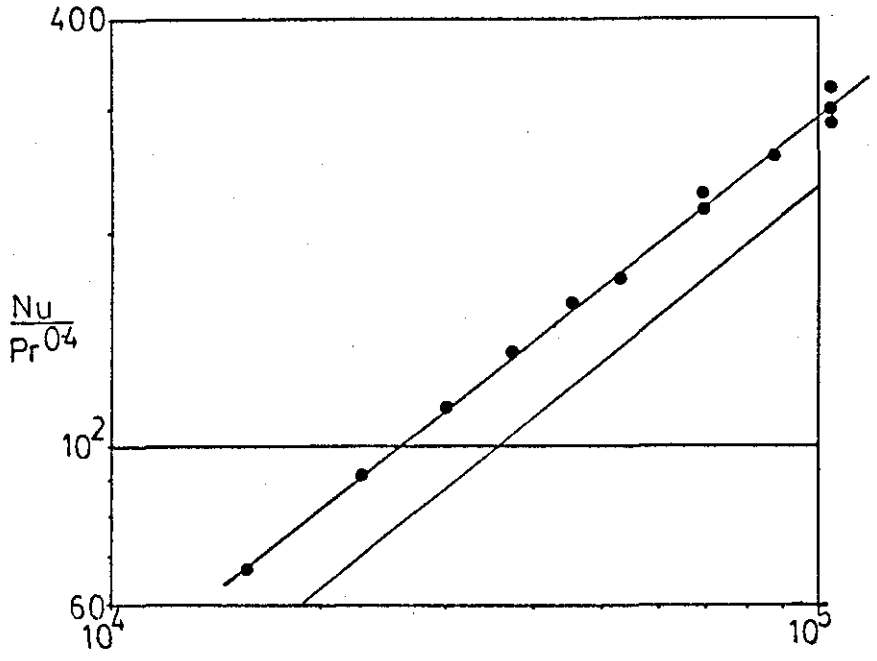

Figure No. 5.5
Heat Transfer Comparisons
Type: Configuration 3P (Denotation F of Table 5.3)

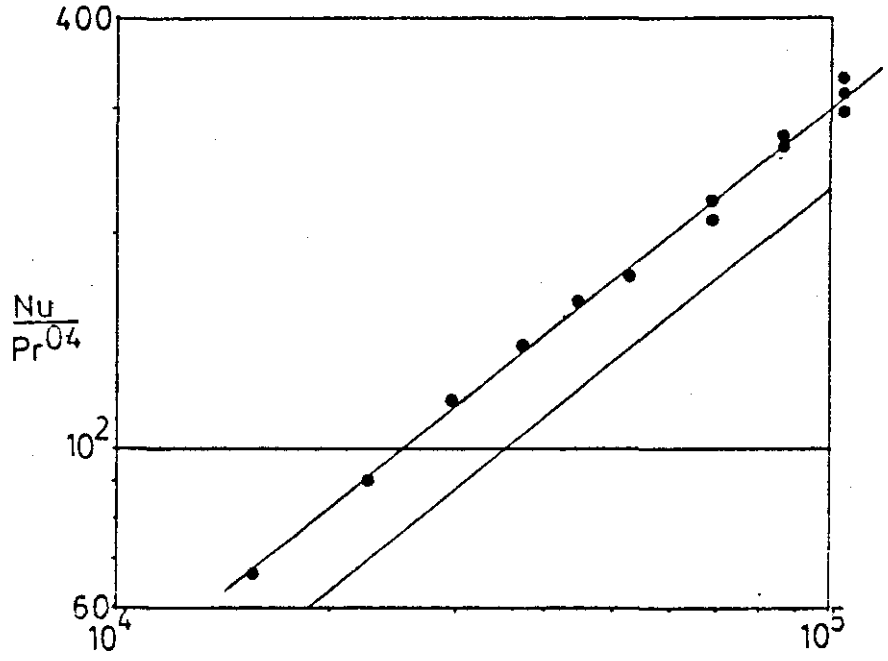

Figure No. 5.6
Heat Transfer Comparisons
Type: Configuration 4P (Denotation G of Figure 5.3)

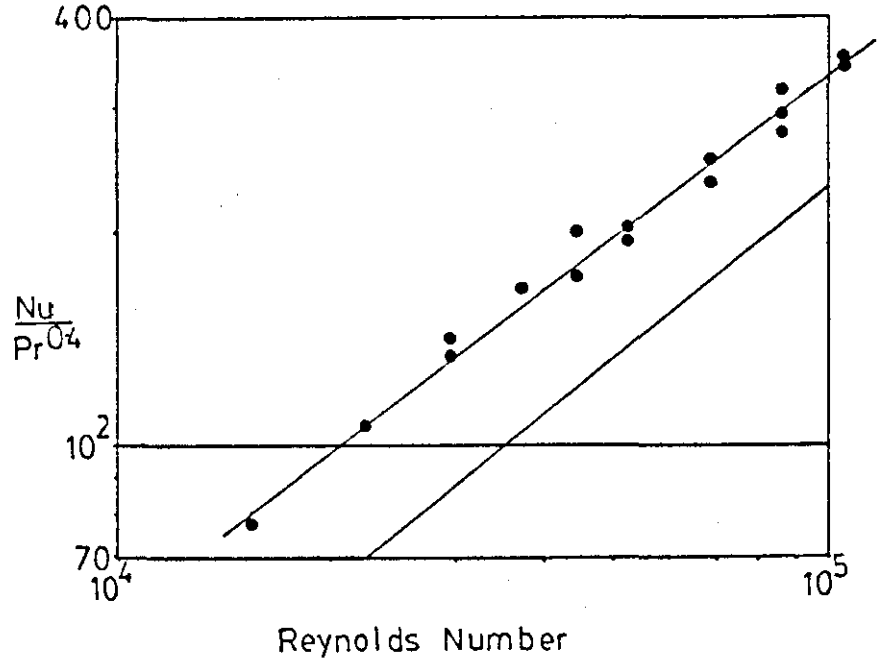

Figure No. 5.7
Heat Transfer Comparisons
Type: Configuration 5P (Denotation H of Table 5.3)

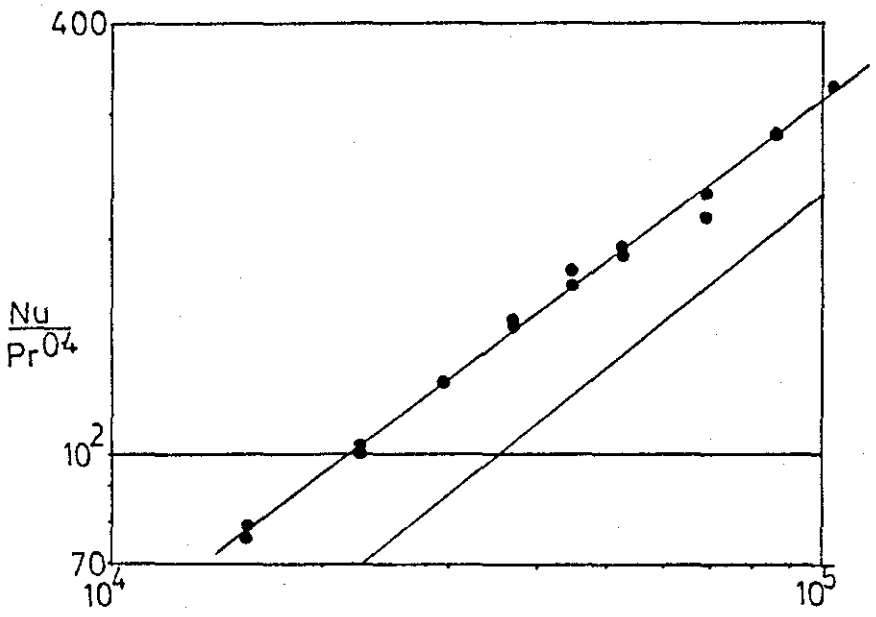

Figure No. 5.8
Heat Transfer Comparisons
Type: Configuration 6P (Denotation I of Table 5.3)

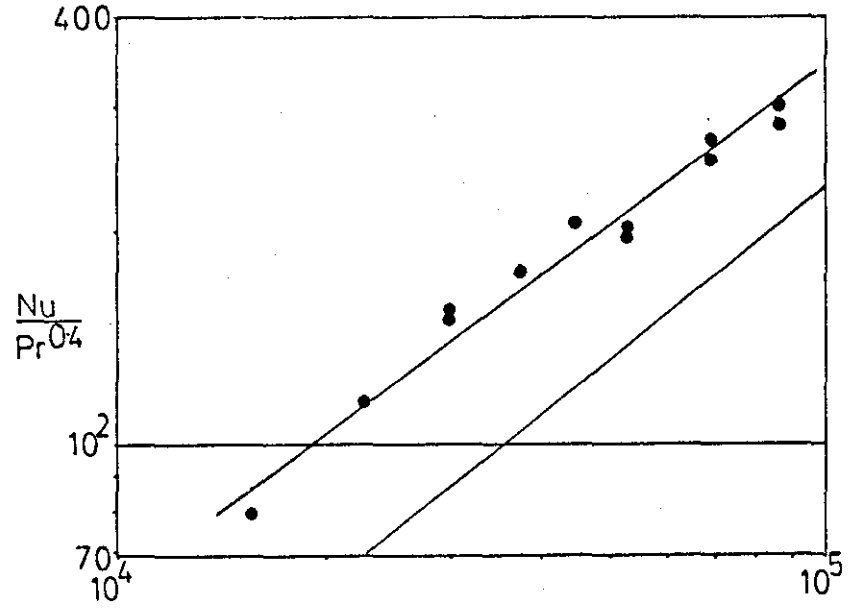

Figure No.5.9 (See Table 5.3)
Heat Transfer Comparisons
Type: Pall Rings

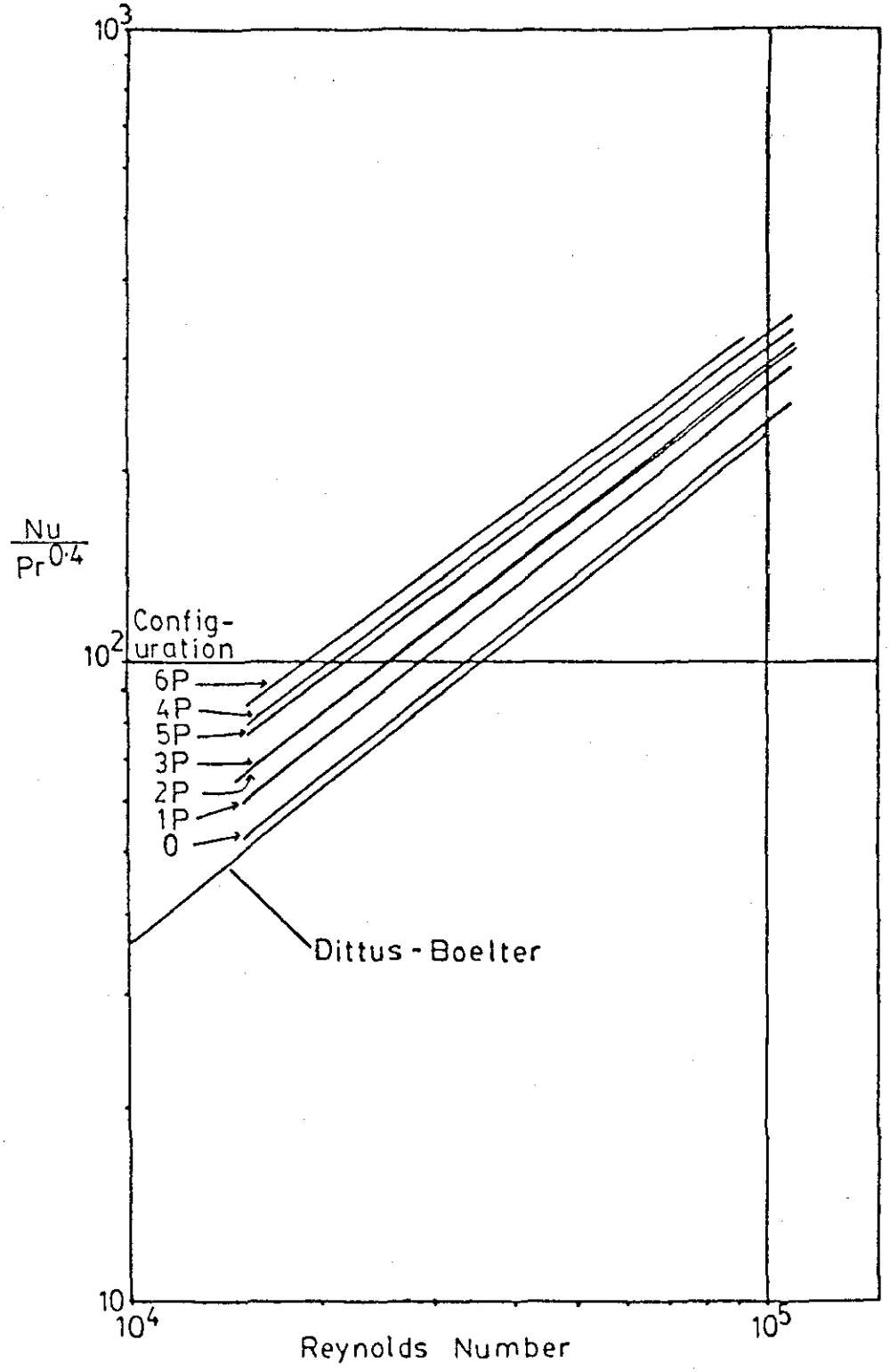

Figure No. 5.10 The effect of surface coverage on the Re exponent, E, and multiplier, F. (Pall Rings)

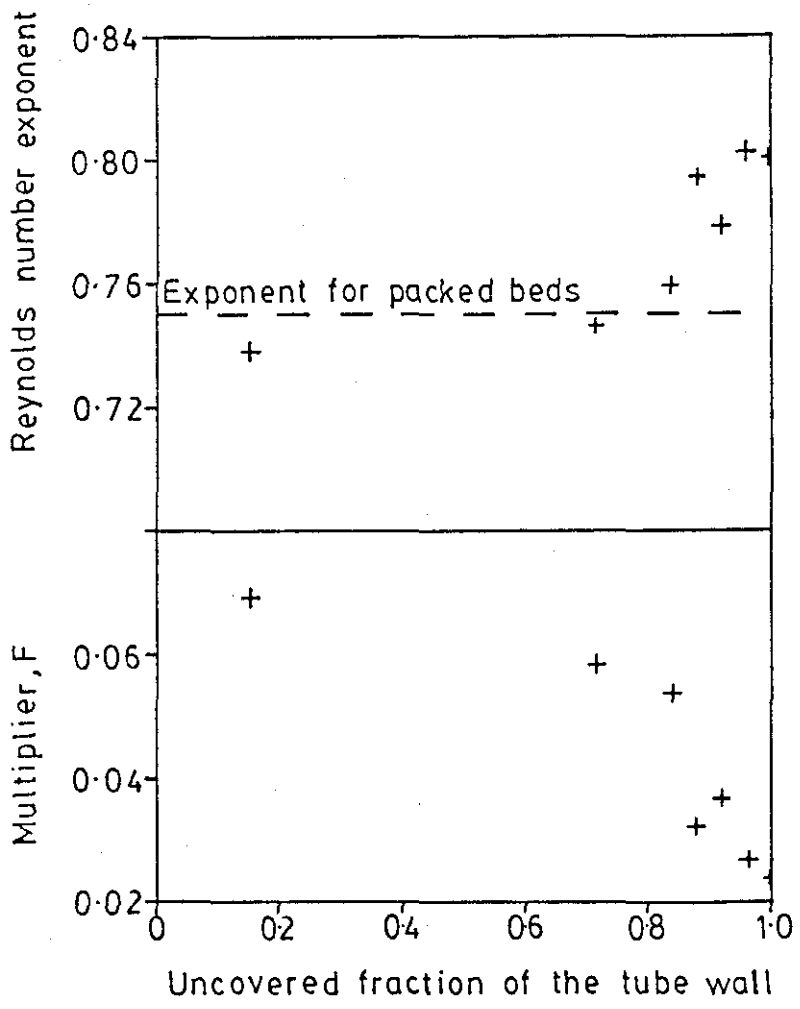

Figure No.5.11 The effect of surface coverage on the Re exponent, B, and multiplier, A. (Isothermal data, Pall Rings)

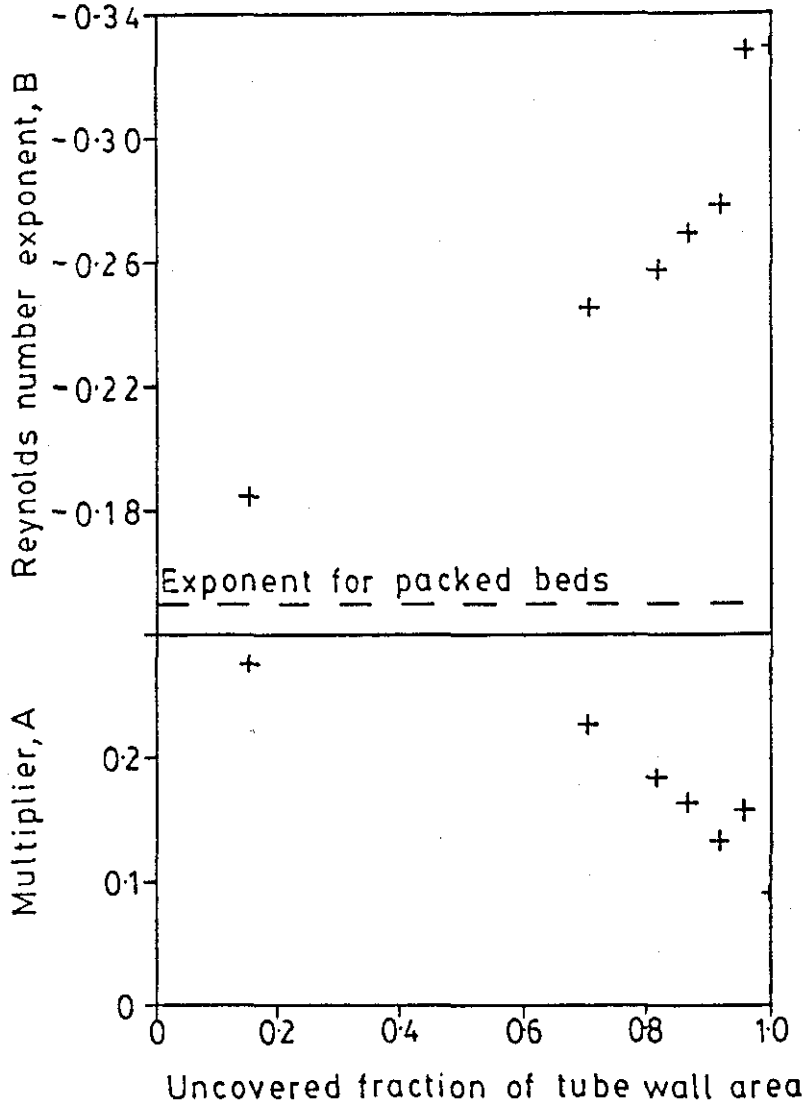

Figure No. 5.12 The variation of the friction and heat transfer factors with the number of pall rings in a tube.

The data shown is obtained by using the regression equations of Tables 5.2 and 5.3.

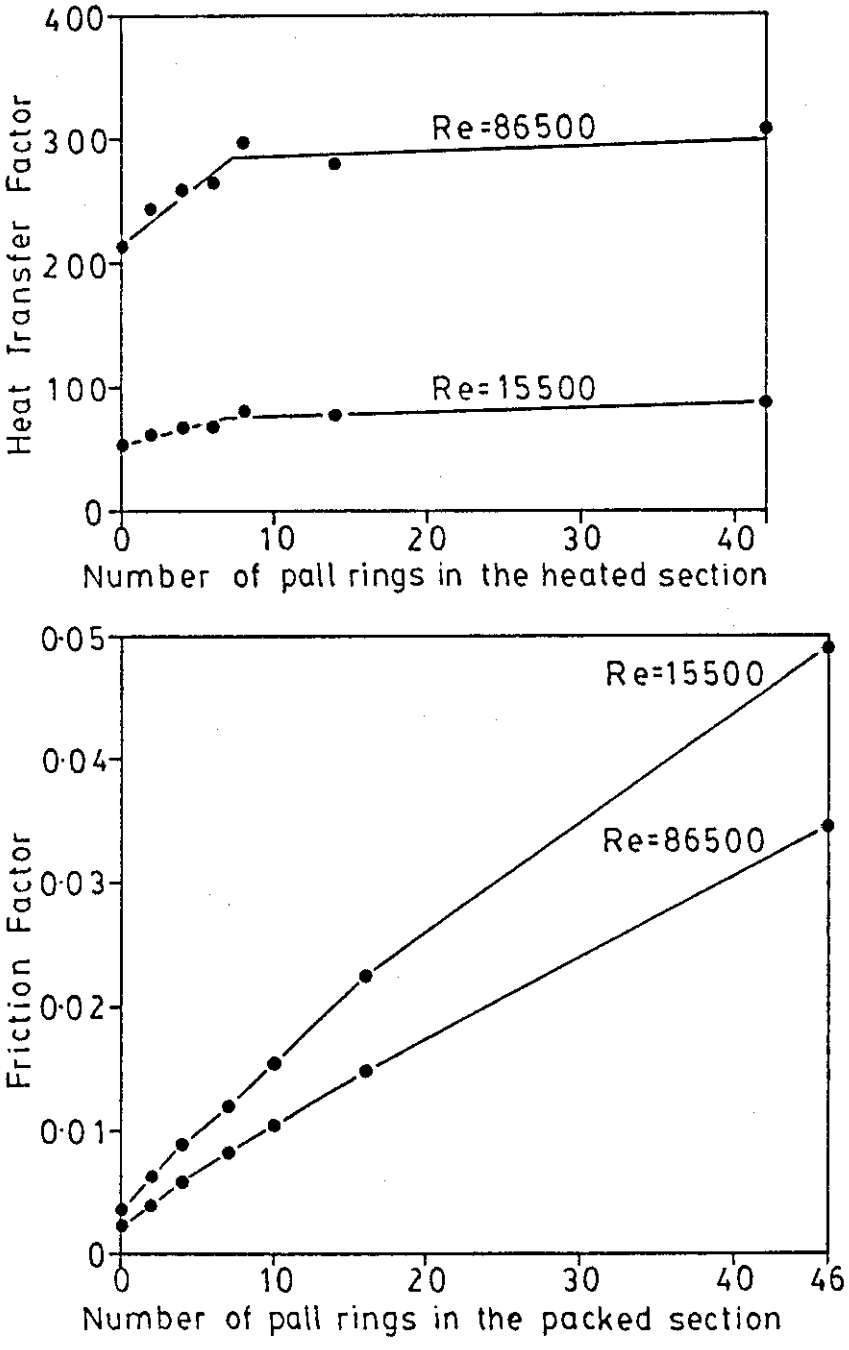

Figure No. 5.13 (See Table 5.4, Denotation H)
Friction Factor Comparisons
Type: Empty Tube (Isothermal, Room temp.)

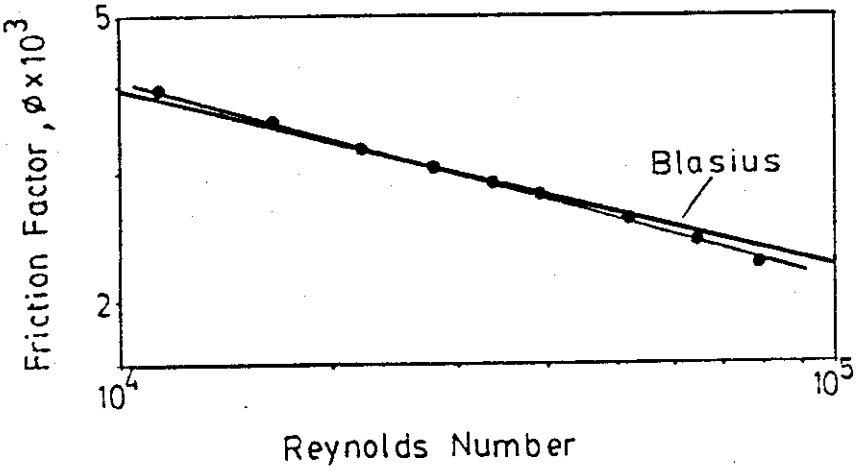

Figure No. 5.14 (See Table 5.5, Denotation K)
Friction Factor Comparisons
Type: Empty Tube (Heating)

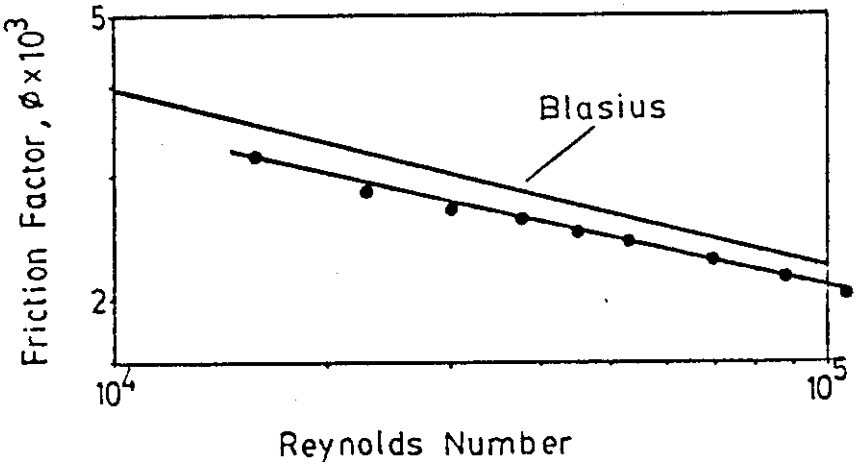

Figure No.5.15 (See Table 5.6, Denotation I)
Heat Transfer Comparisons
Type: Empty Tube

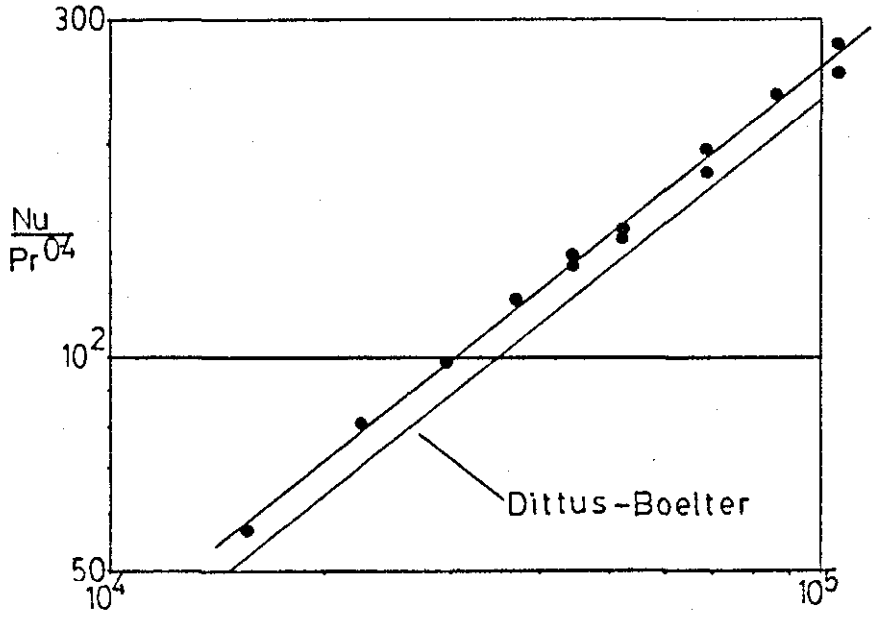

Figure No.5.16 (See Table 5.6, Denotation K)
Heat Transfer Comparisons
Type: Empty Tube

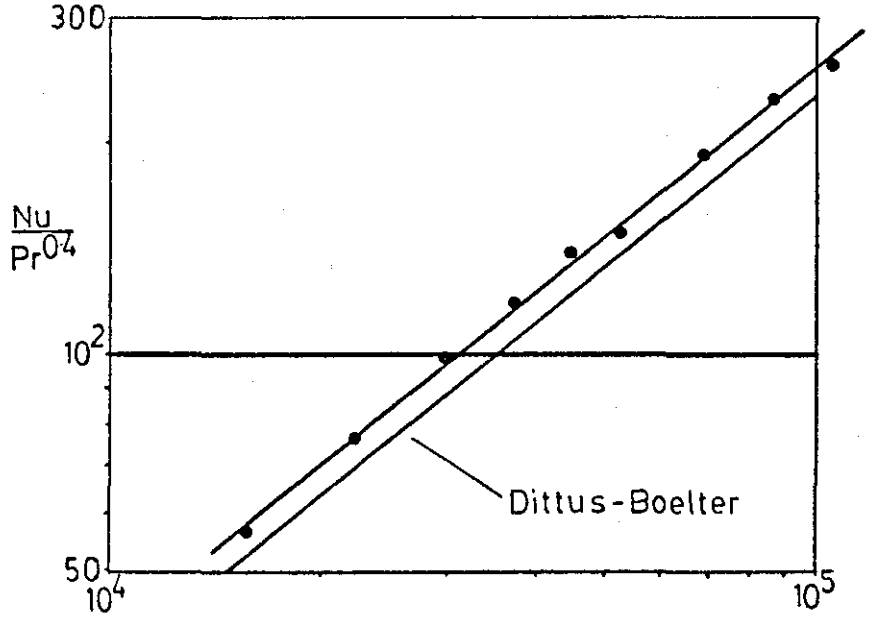

Figure No. 5.17 (See Table 5.6, Denotation N)
Heat Transfer Comparisons
Type: Empty Tube

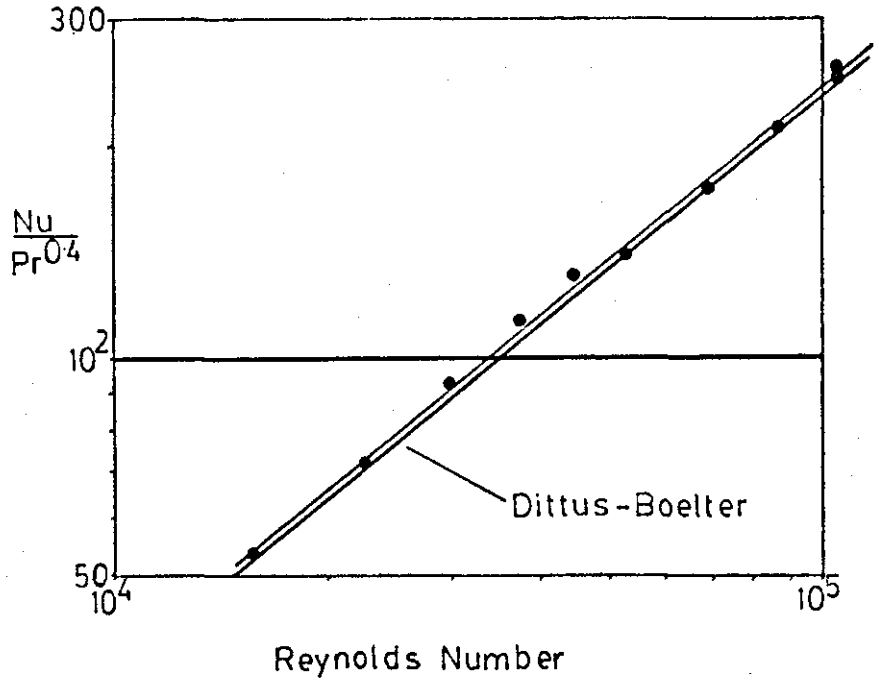

Figure No. 5.18
Friction Factor Results (Isothermal)
Type: Swirl Inducers (Identical twist)
Denotations refer to Table 5.7

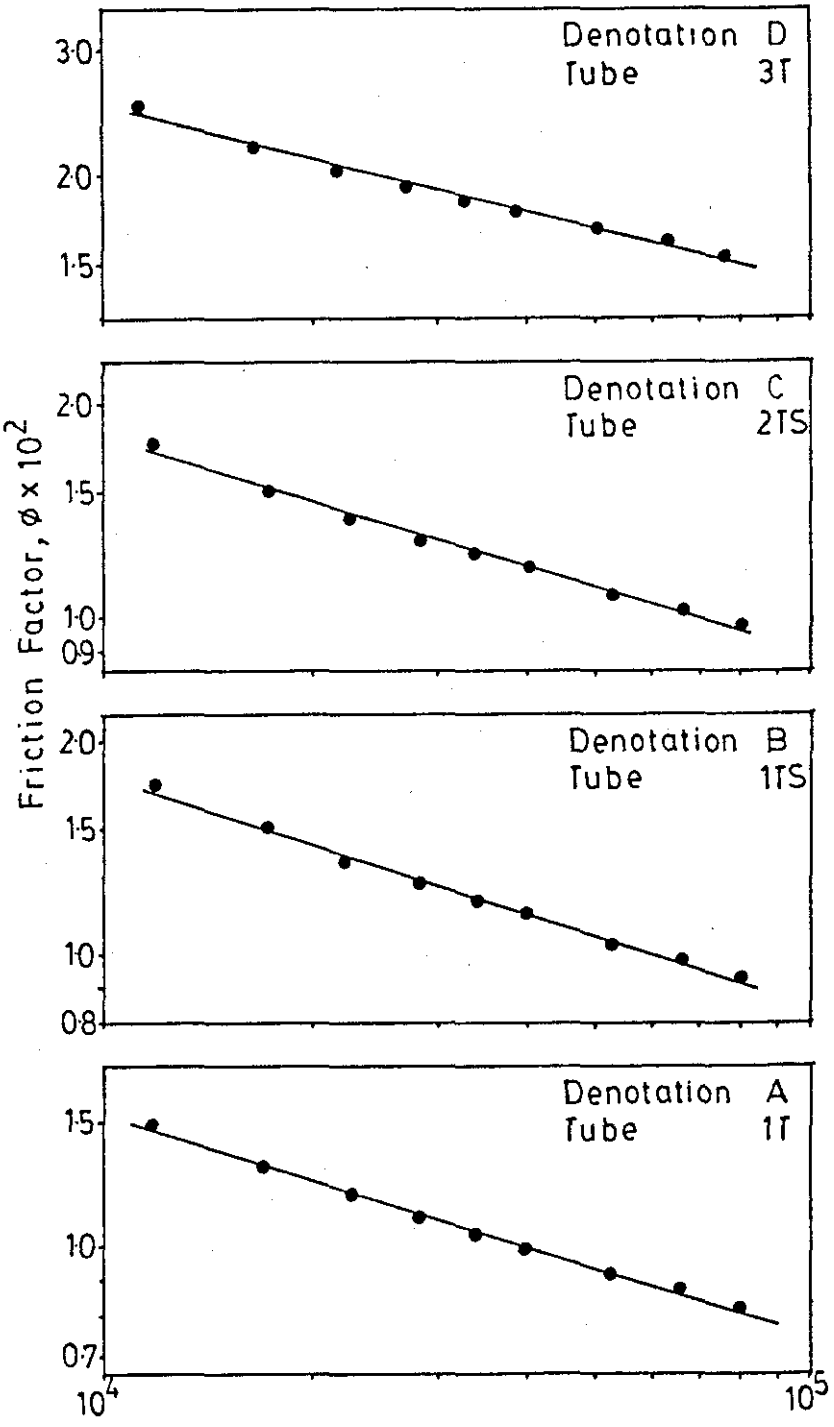

Figure No. 5.19
Friction Factor Results (Isothermal)
Type: Swirl Inducers (Identical twist)
Denotations refer to Table 5.7

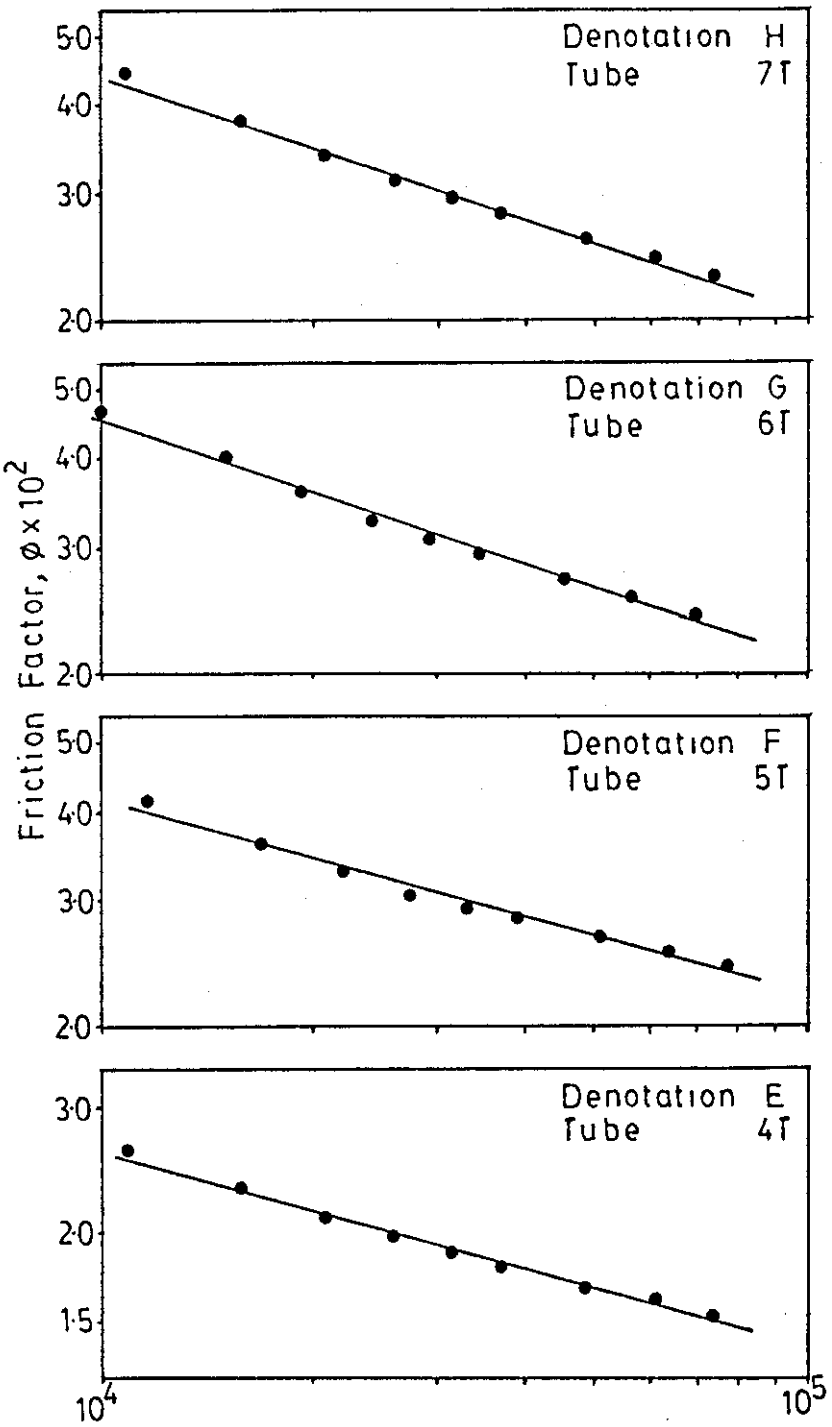

Figure No.5.20
Friction Factor Results (Isothermal)
Type: Swirl Inducers (Identical twist)
Denotations refer to Table 5.7

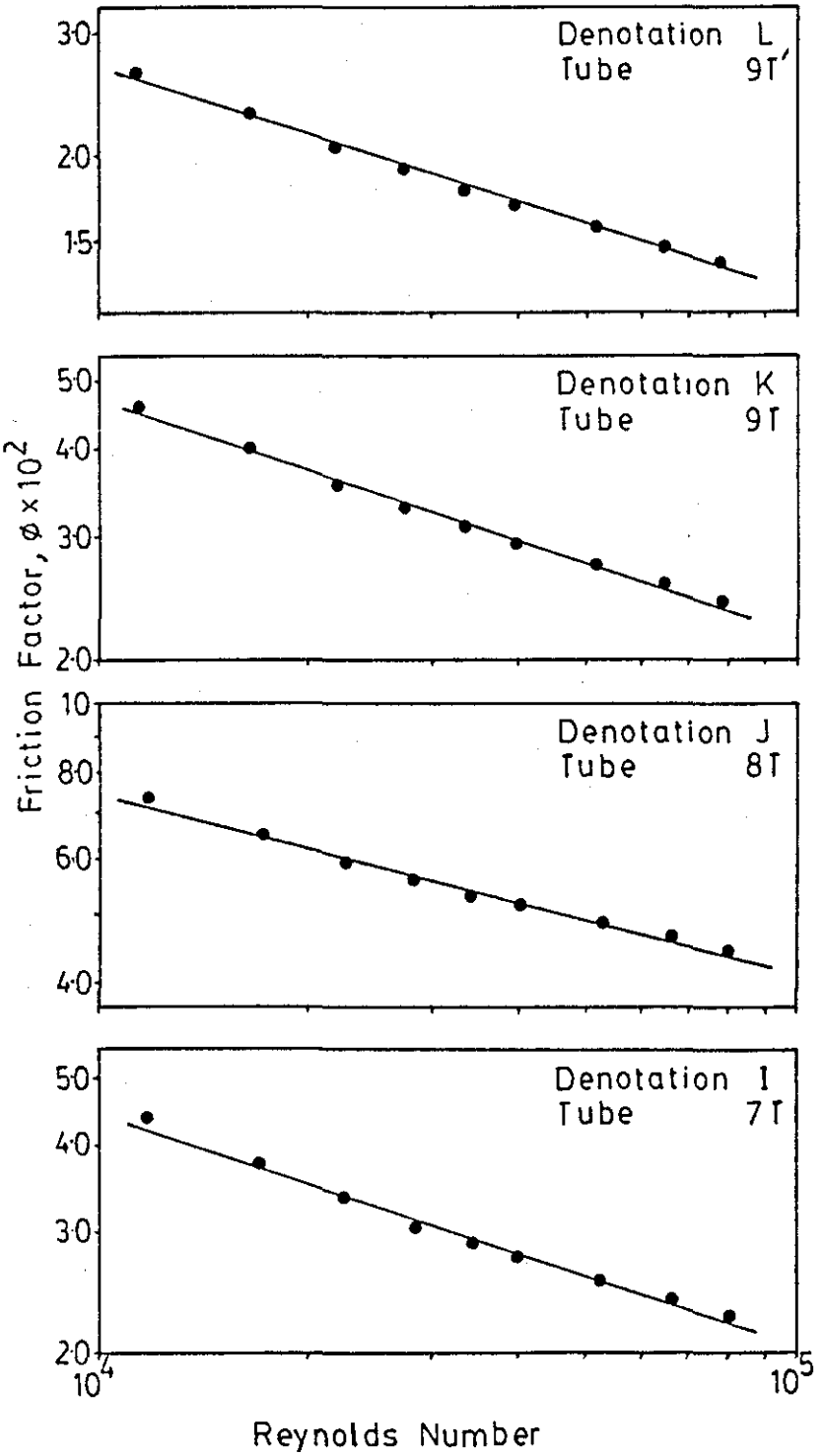

Figure No.5.21
Friction Factor Results (Isothermal)
Type: Swirl Inducers (Identical twist)

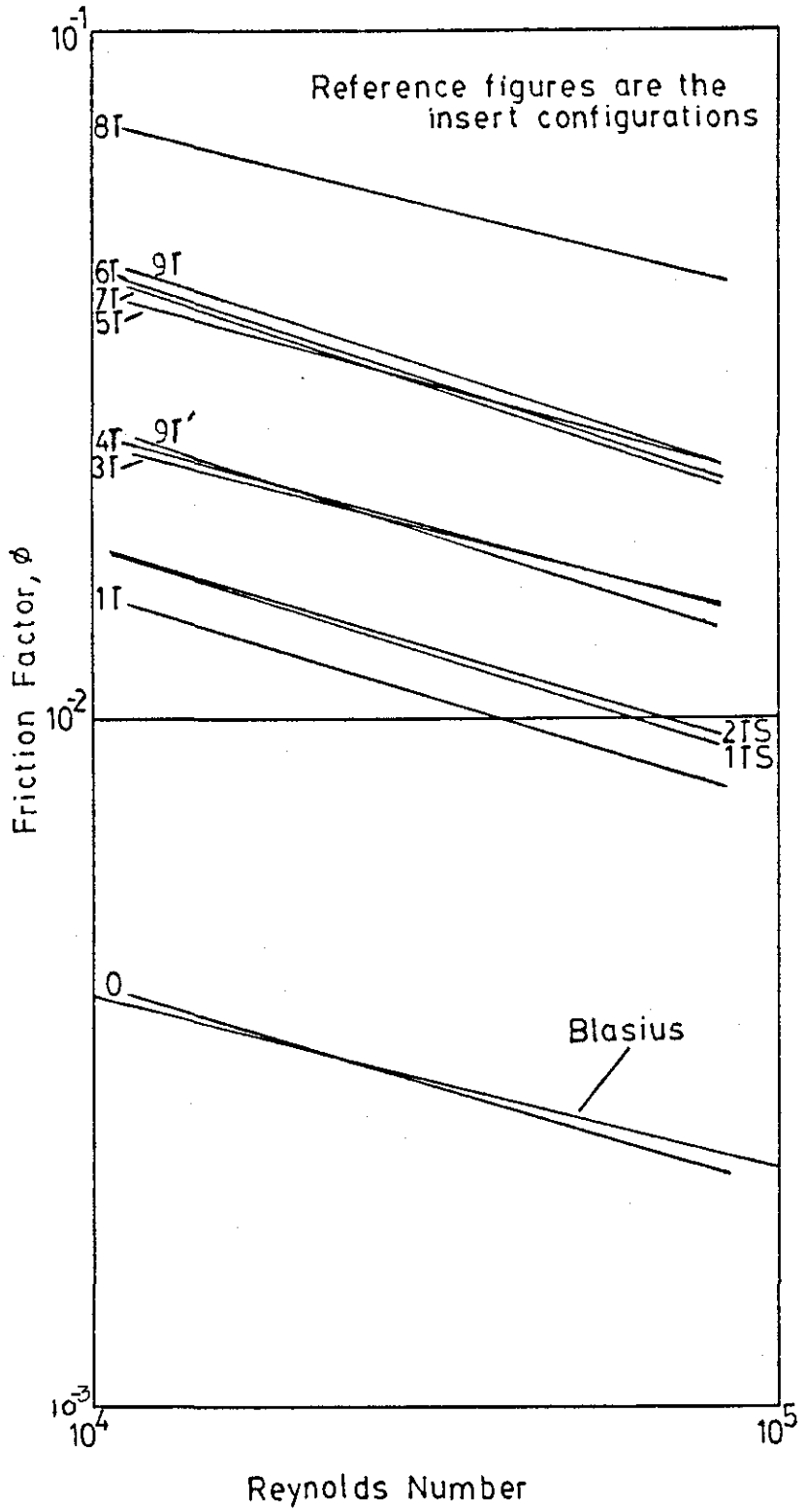

Figure No. 5.22
Friction Factor Results (Isothermal)
Type: Swirl Inducers (Identical twist)

Denotations for tube 0 refer to Table 5.4
other denotations refer to Table 5.7.

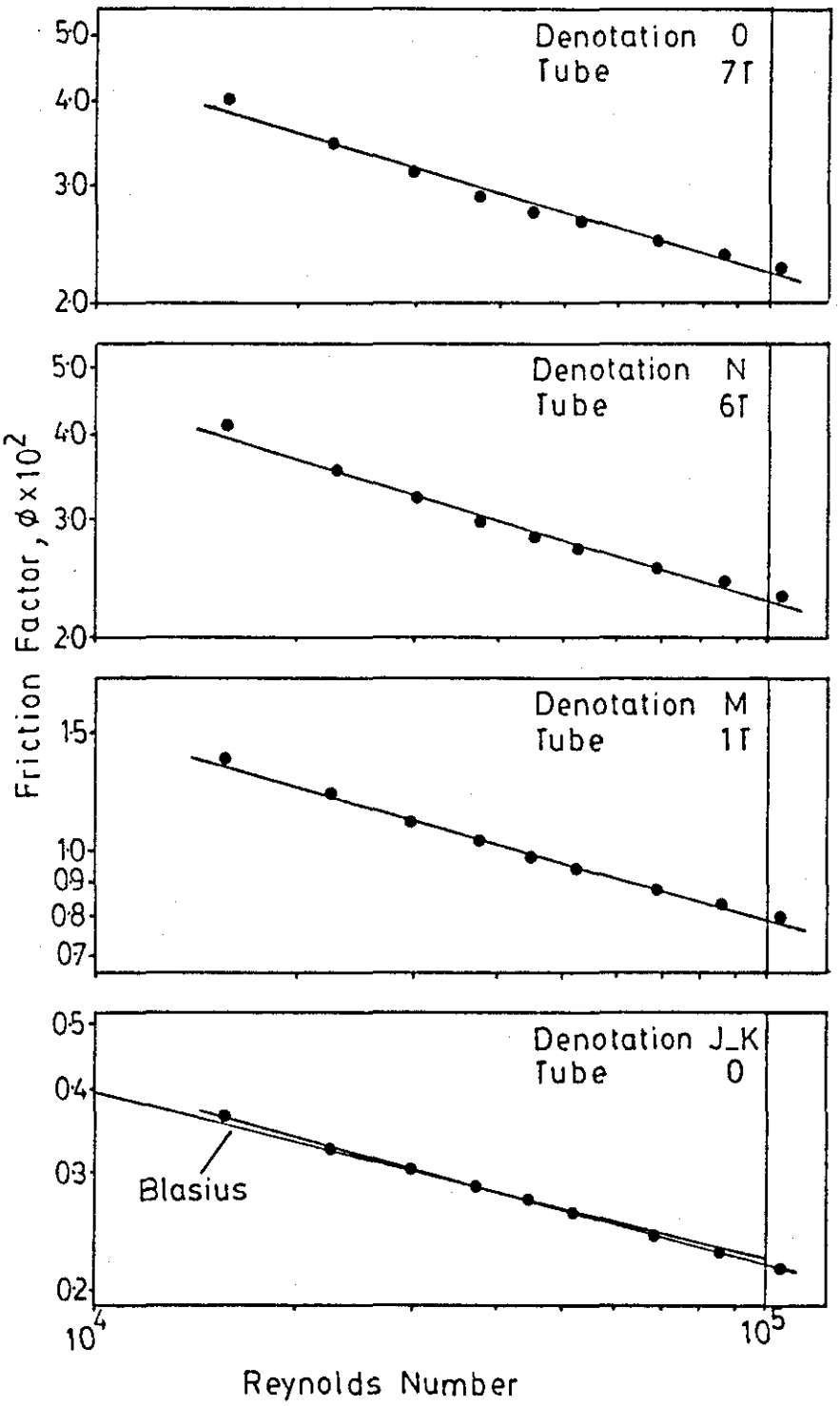

Figure No. 5.23
Friction Factor Results (Isothermal)
Type: Swirl Inducers (Identical twist)
Denotations refer to Table 5.7

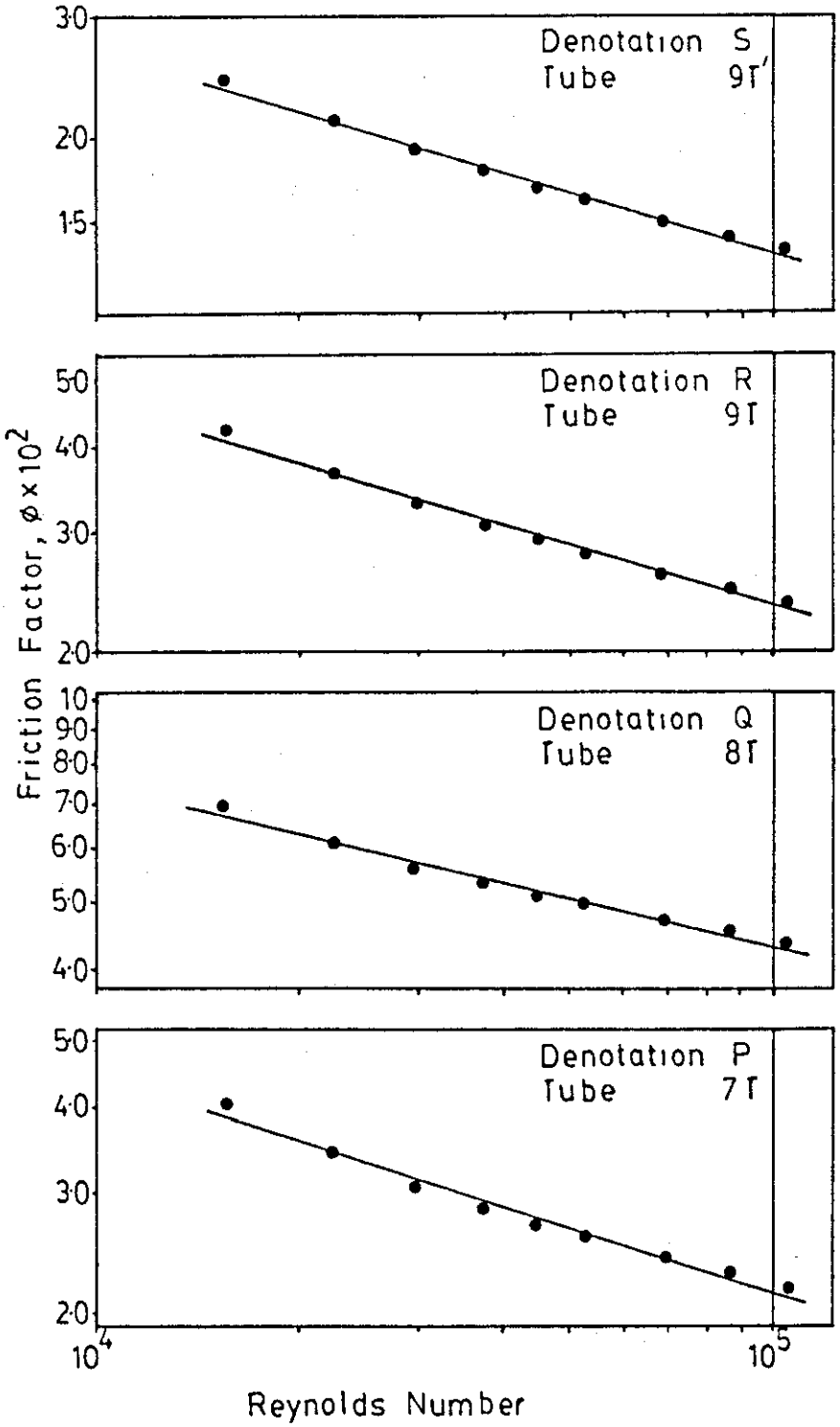

Figure No. 5.24
Friction Factor Results (Isothermal)
Type: Swirl Inducers (Identical twist)

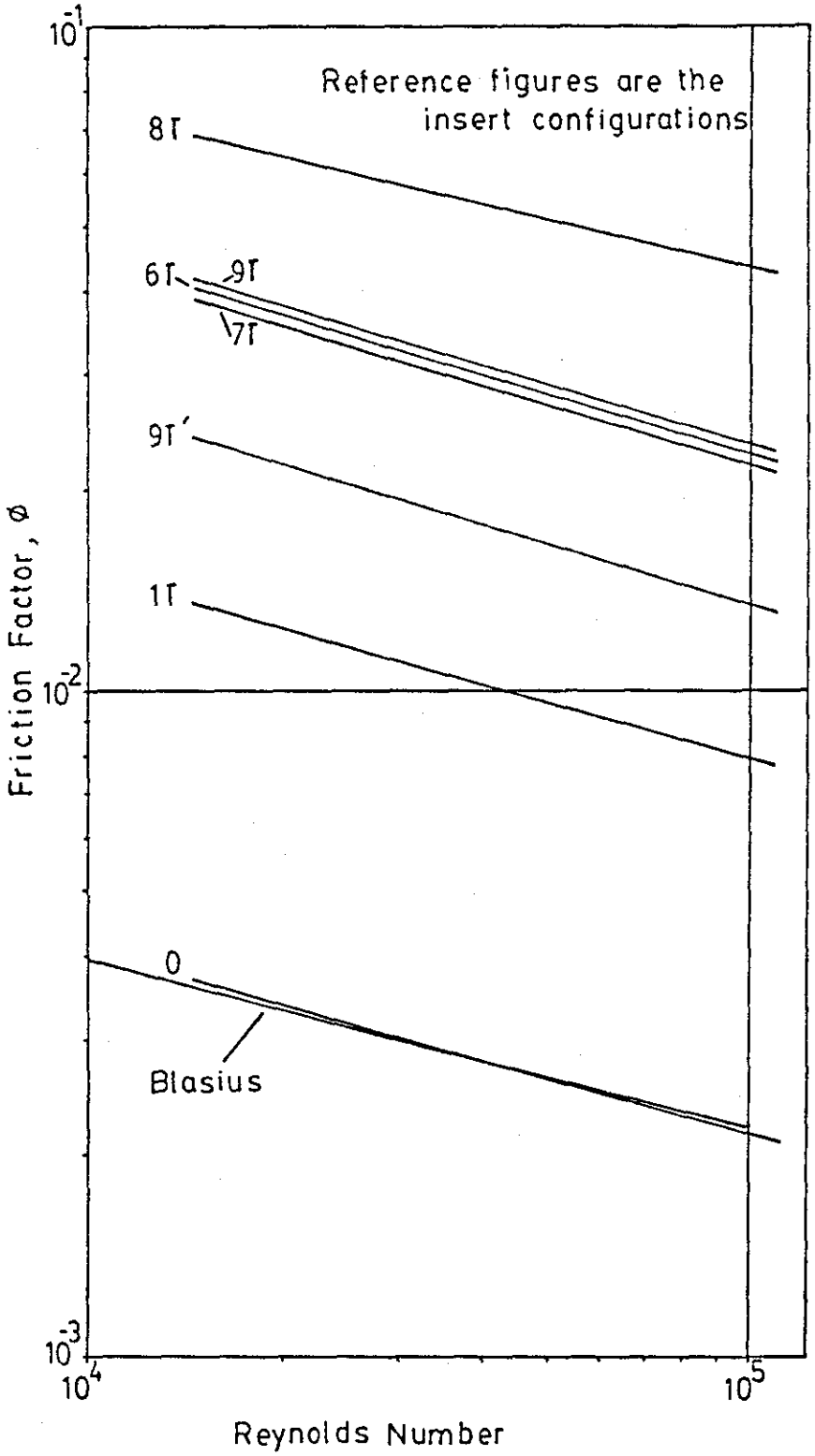

Figure No.5.25 (See Table 5.8)
Friction Factor Results (Isothermal)
Type: Swirl Inducers (Alternate twist)

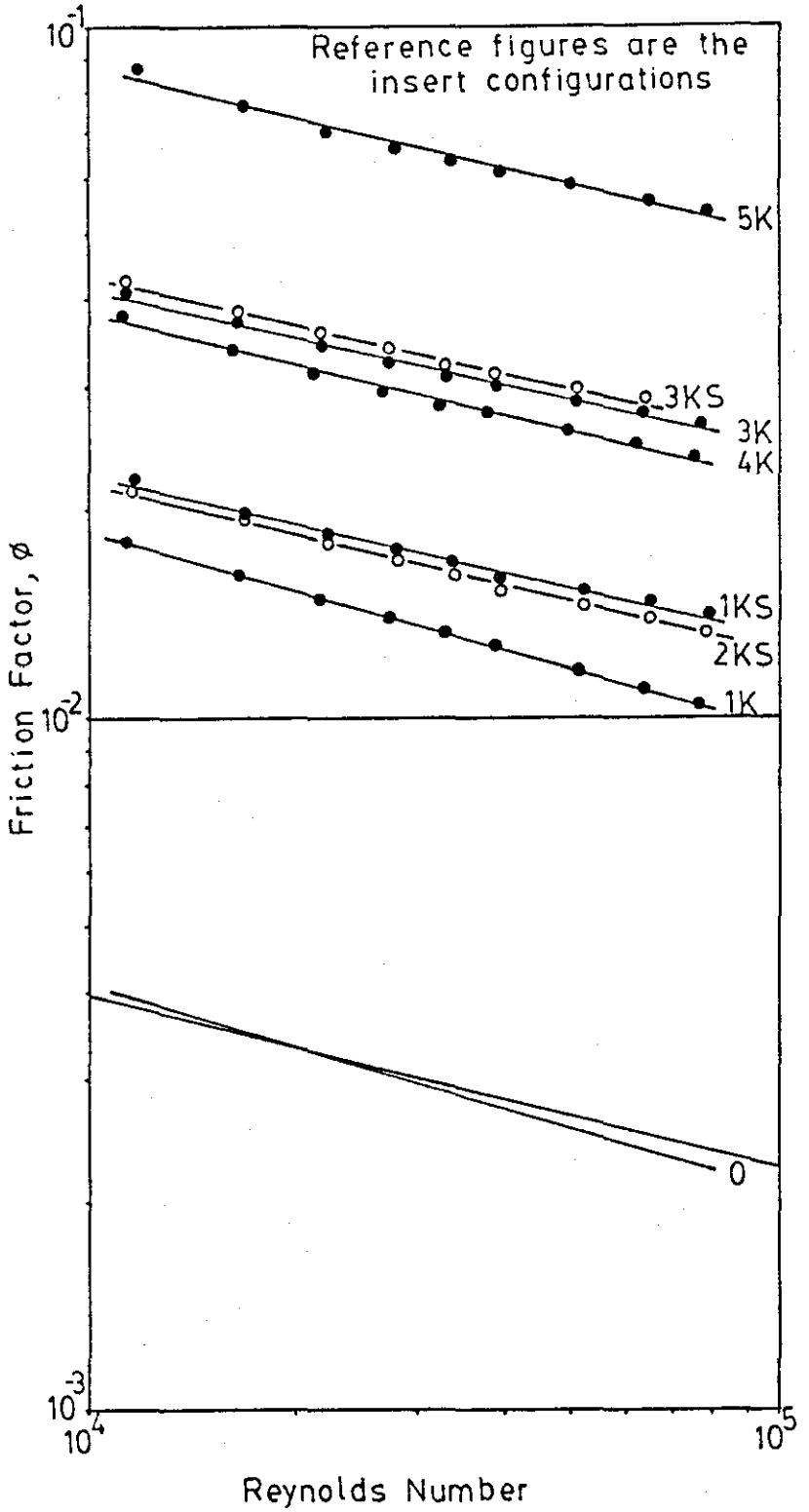

Figure No. 5.26
Friction Factor Results (Isothermal)
Type: Swirl Inducers (Alternate twist)
Denotations refer to Table 5.8

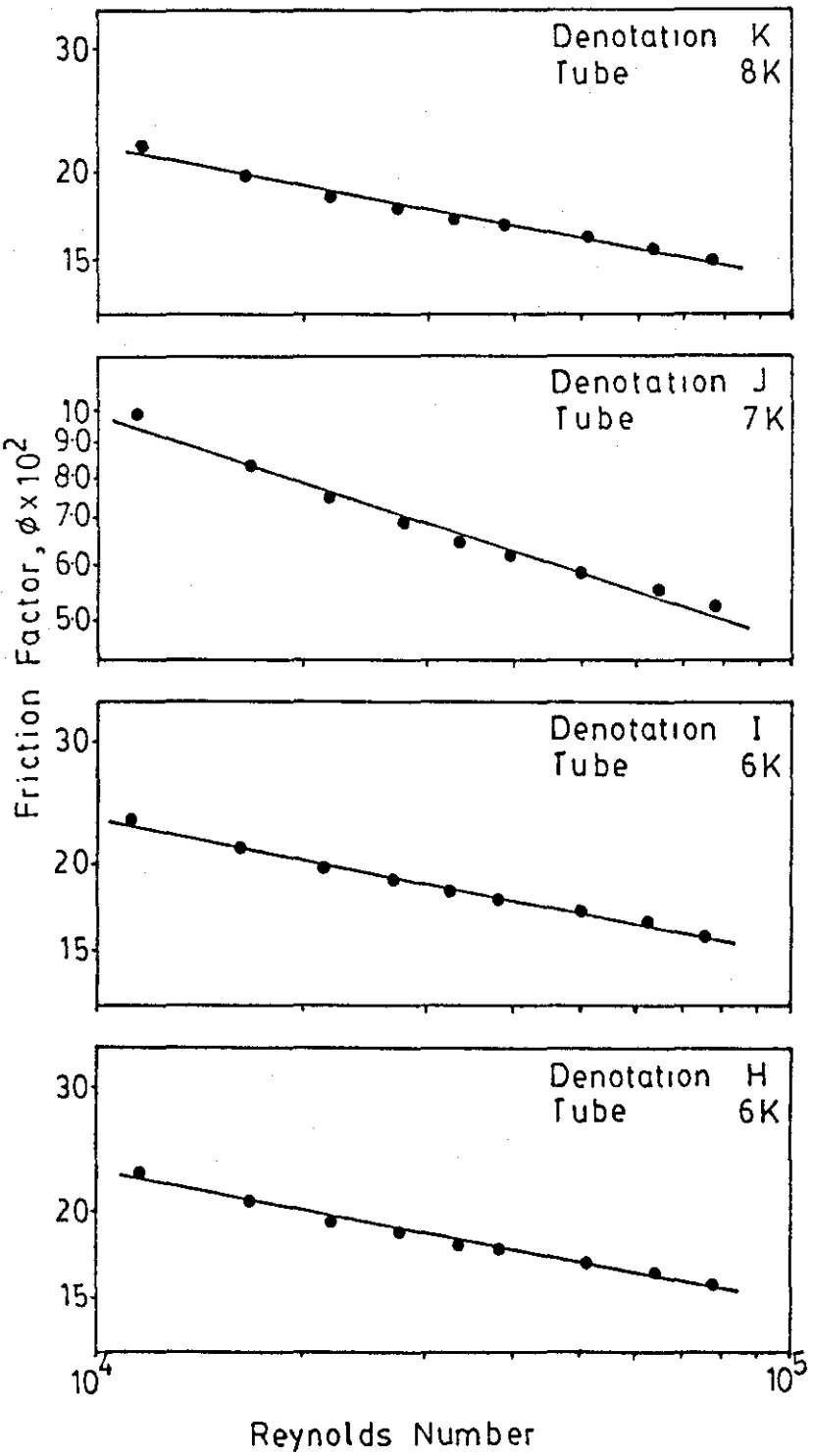

Figure No.5.27
Friction Factor Results (Isothermal)
Type: Swirl Inducers (Alternate twist)
Denotations refer to Table 5.8

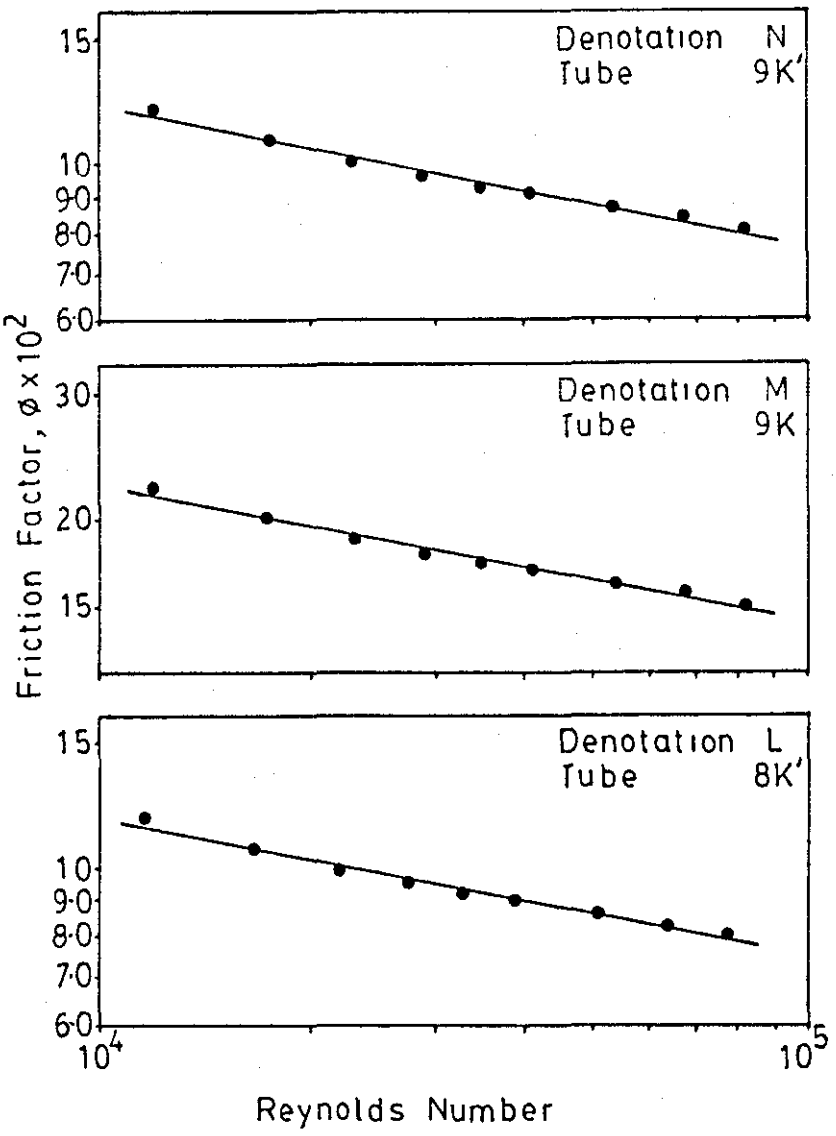

Figure No.5.28
Friction Factor Results (Isothermal)
Type:Swirl Inducers (Alternate twist)

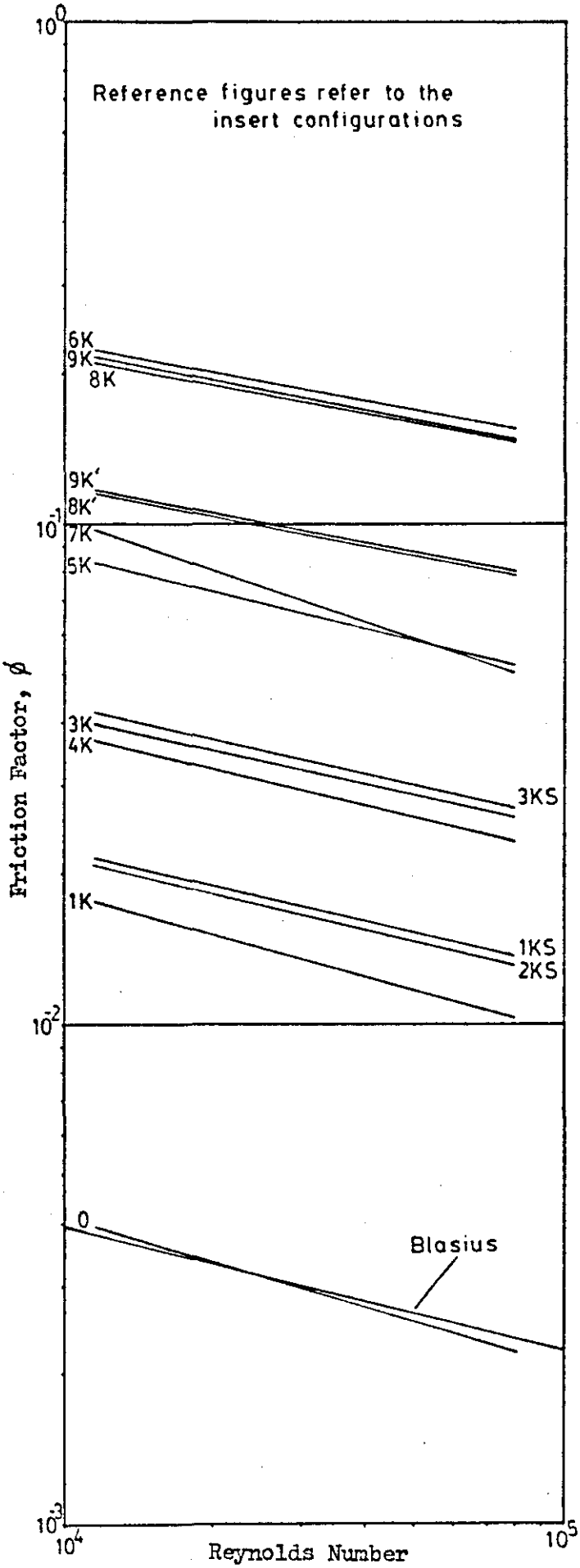

Figure No.5.29
Friction Factor Results (Isothermal)
Type: Swirl Inducers (Alternate twist)

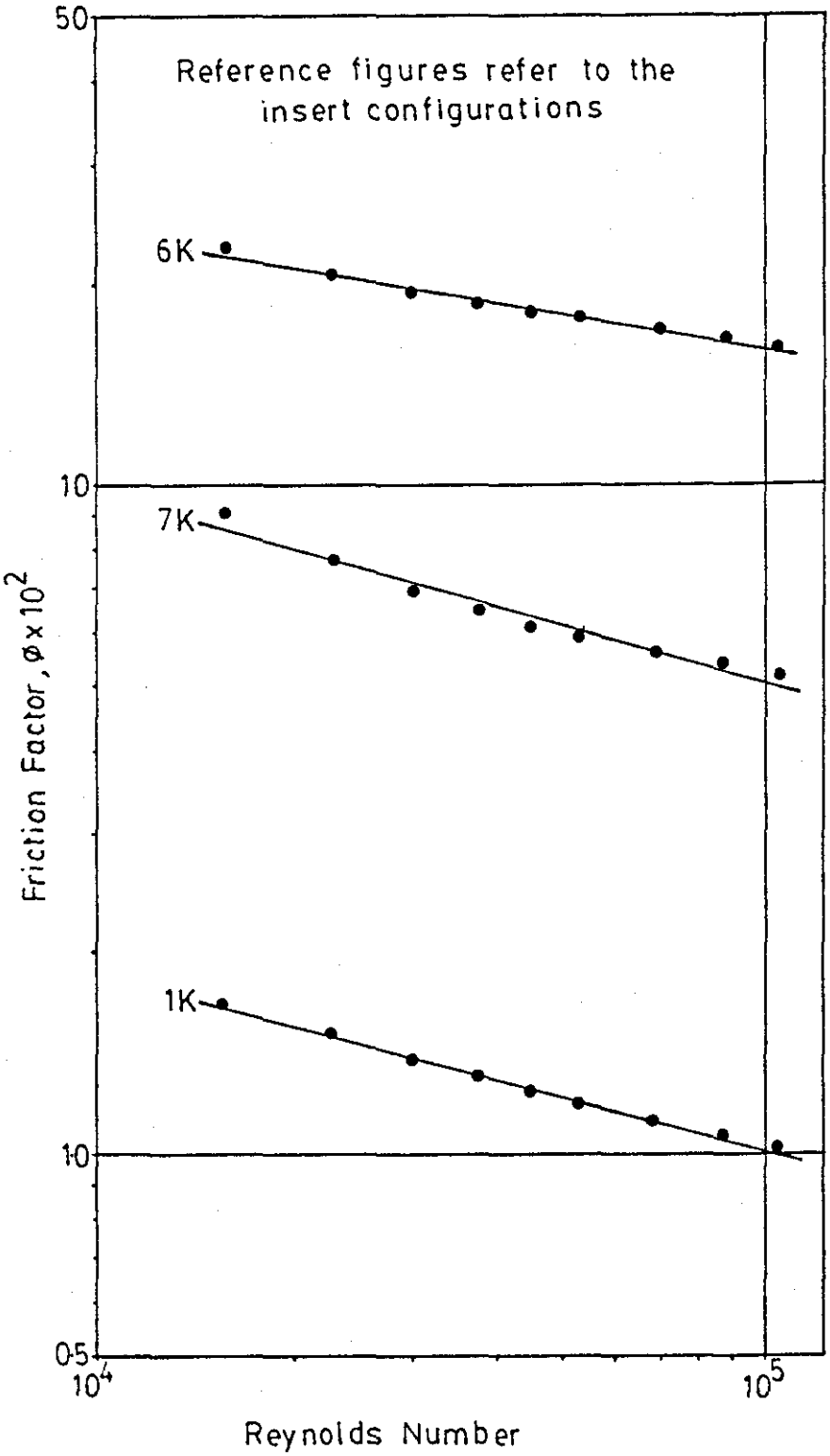

Figure No. 5.30
Friction Factor Results (Heating)
Type: Swirl Inducers (Identical twist)
Denotations refer to Table 5.9

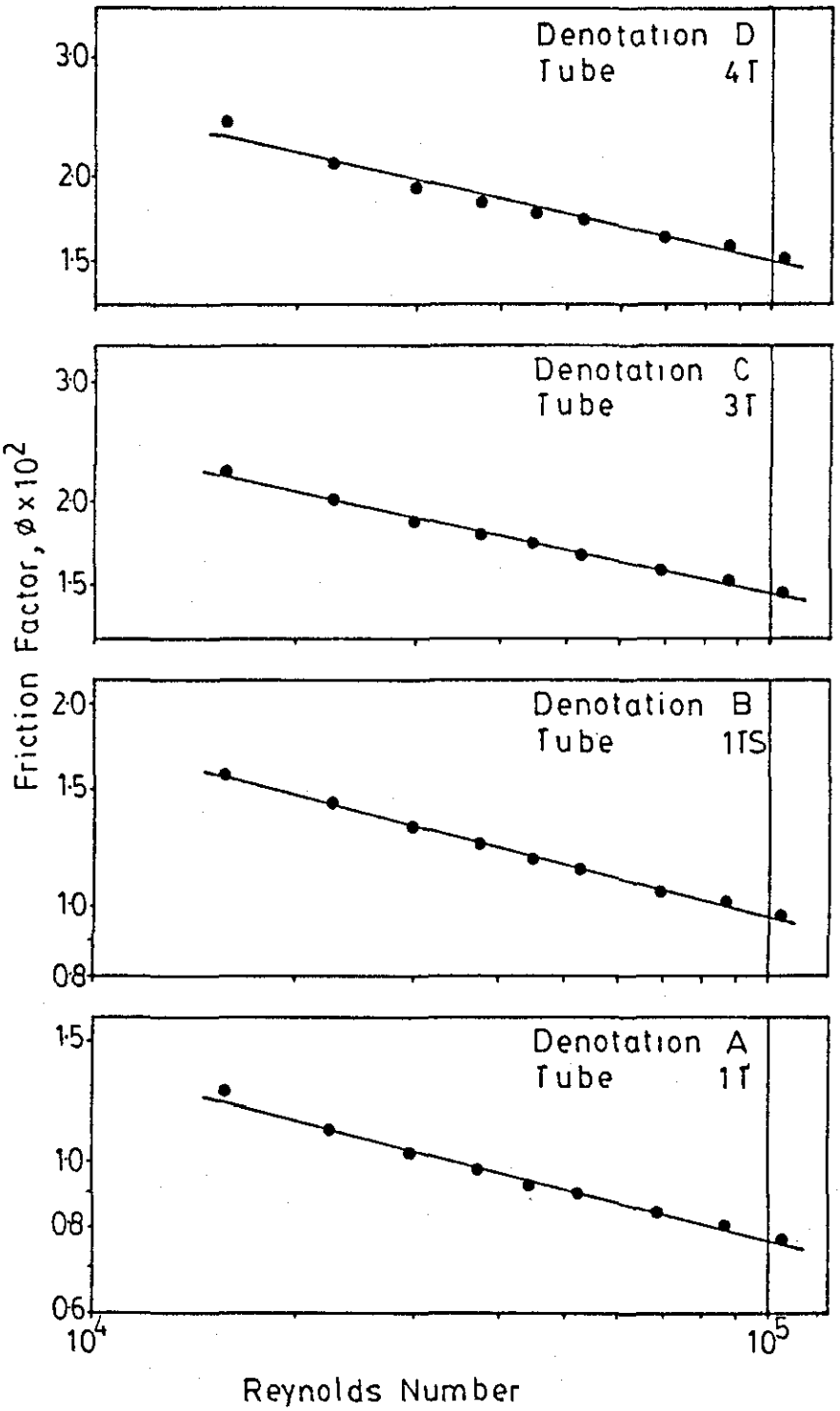

Figure No.5.31
Friction Factor Results (Heating)
Type: Swirl Inducers (Identical twist)
Denotations refer to Table 5.9

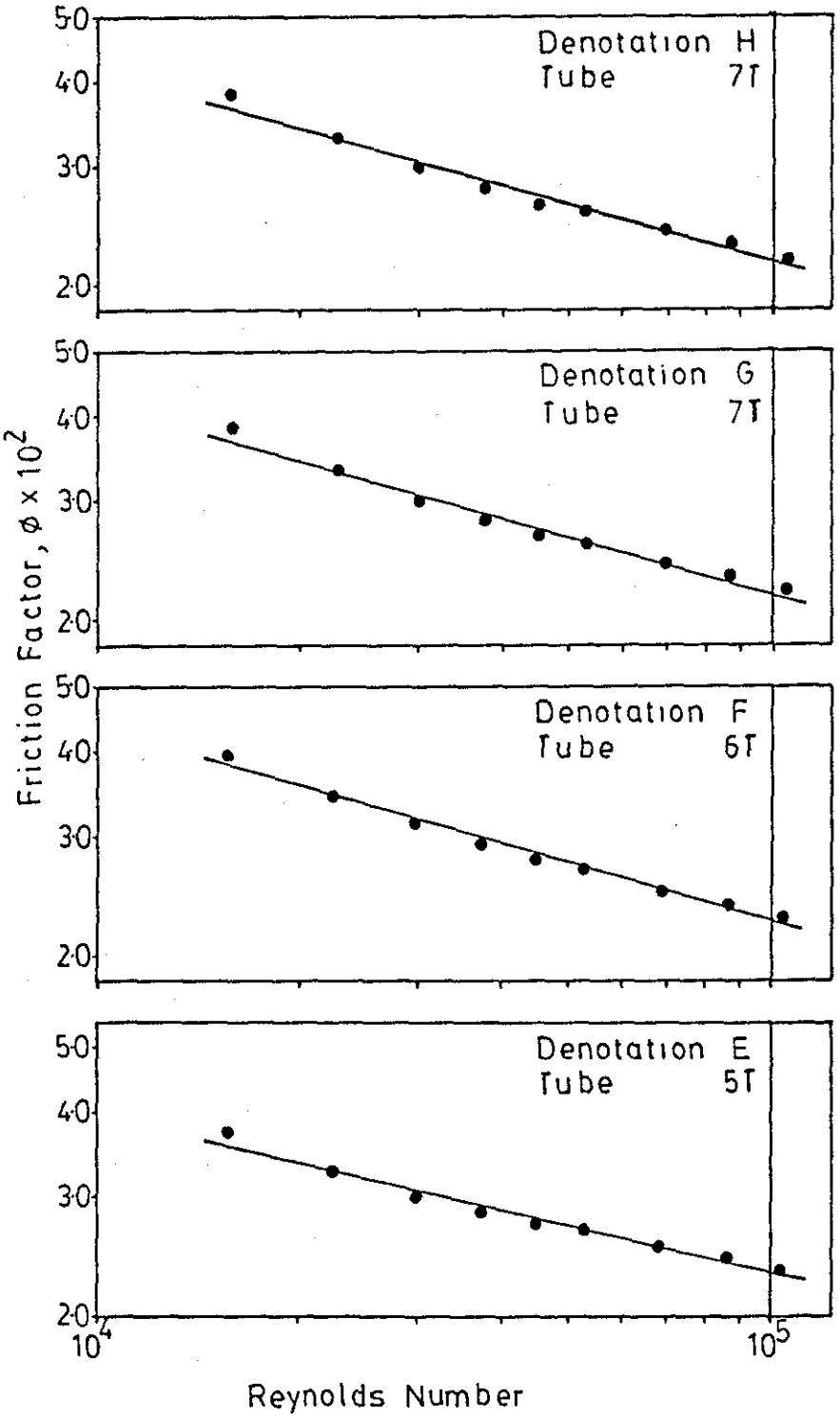

Figure No. 5.32
Friction Factor Results (Heating)
Type: Swirl Inducers (Identical twist)
Denotations refer to Table 5.9

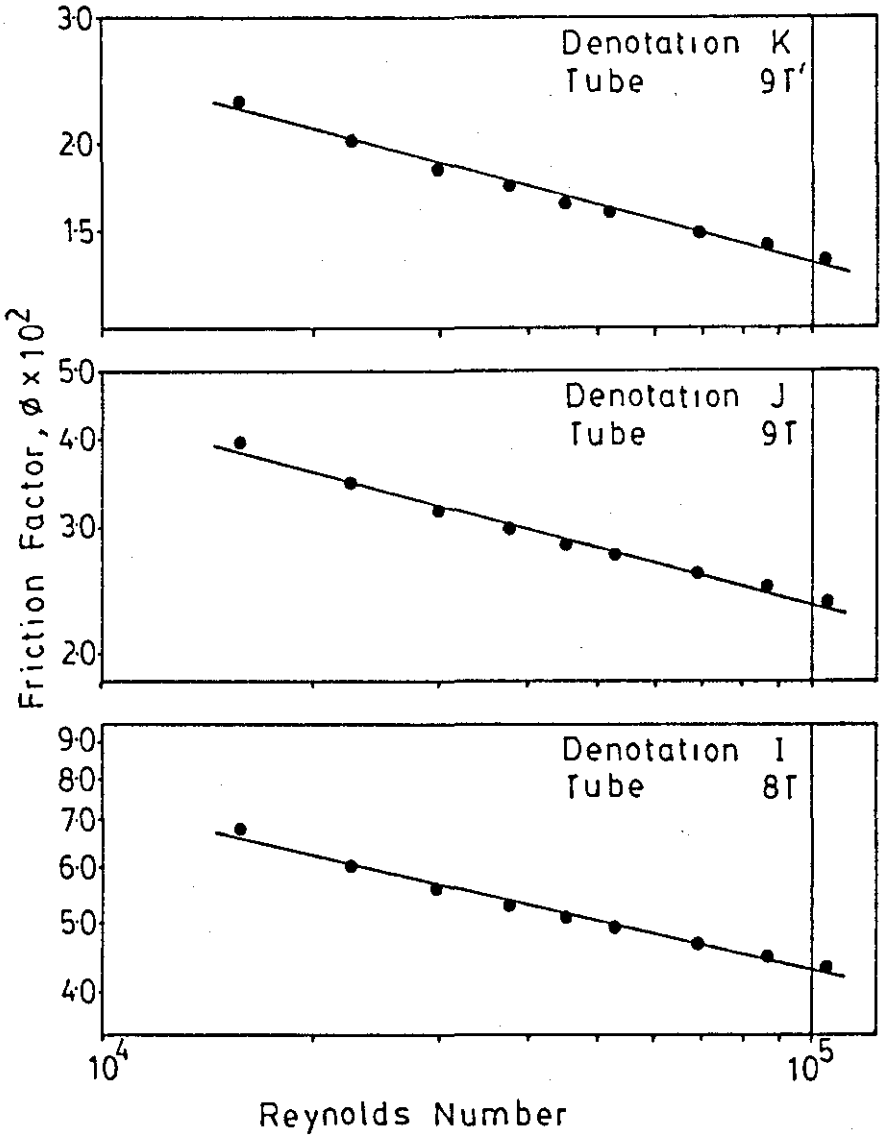

Figure No. 5.33
Friction Factor Results (Heating)
Type: Swirl Inducers (Identical twist)

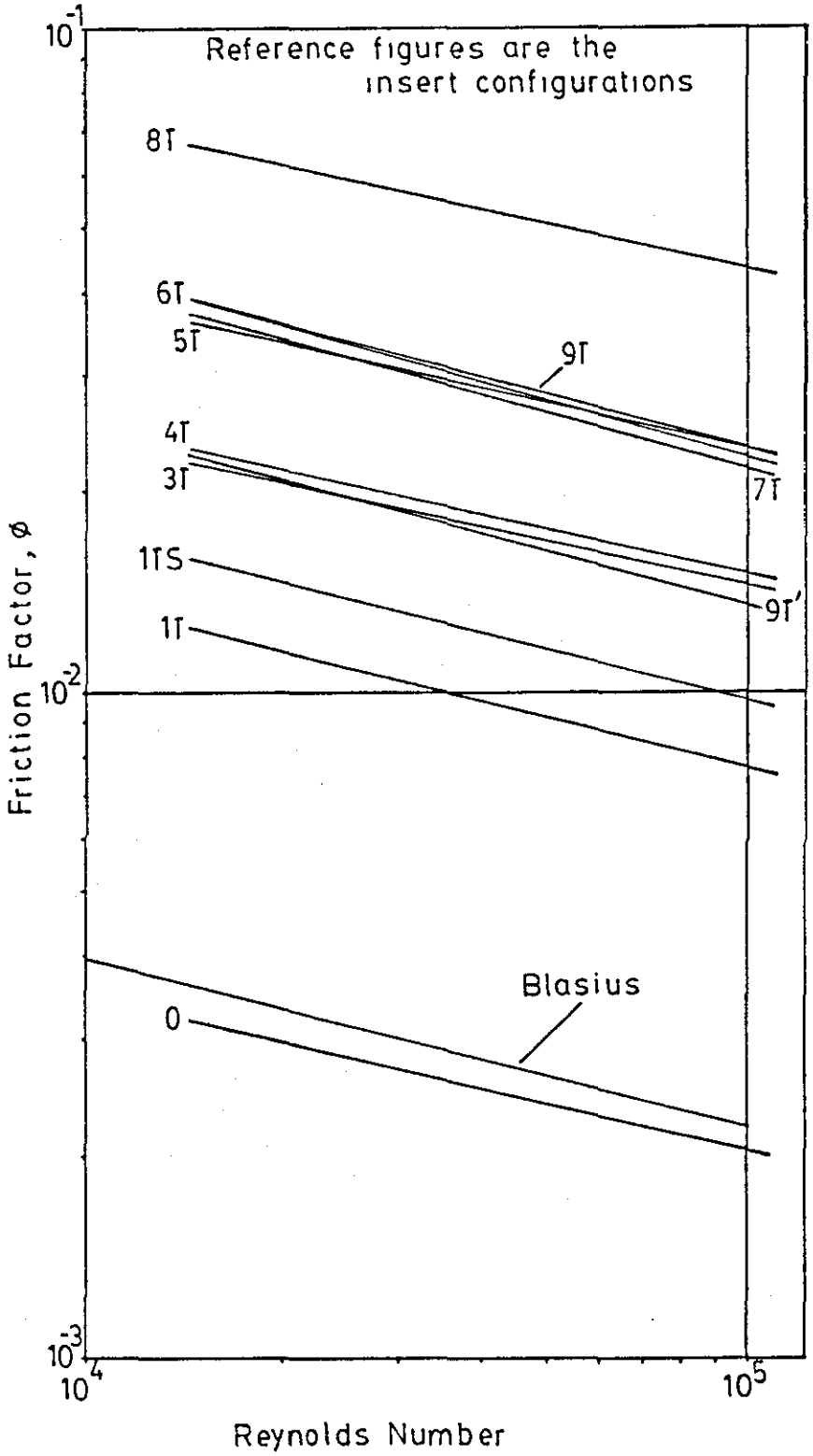

Figure No.5.34
Friction Factor Results (Heating)
Type: Swirl Inducers (Alternate twist)

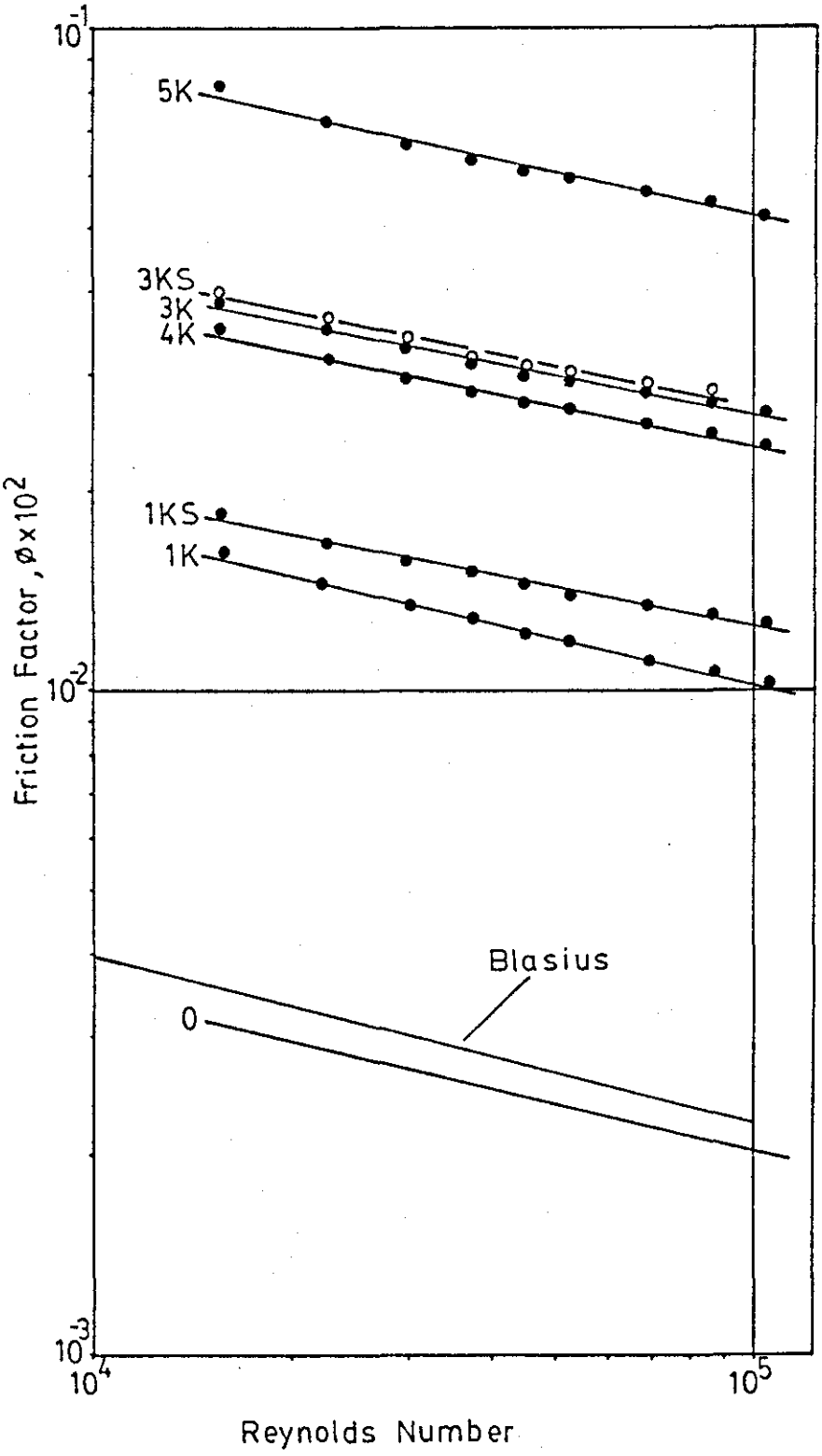

Figure No. 5.35
Friction Factor Results (Heating)
Type: Swirl Inducers (Alternate twist)
Denotations refer to Table 5.10

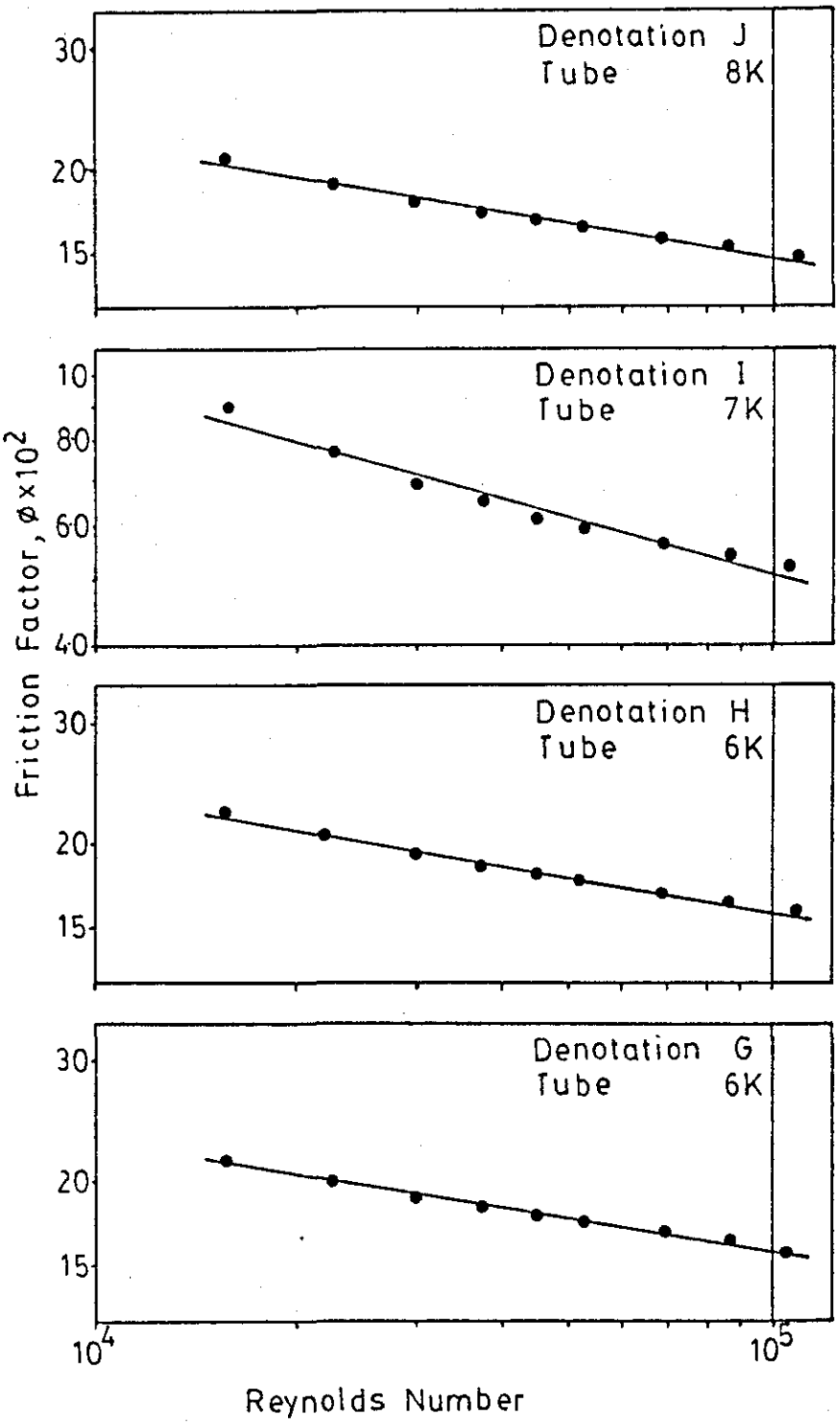

Figure No. 5.36
Friction Factor Results (Heating)
Type: Swirl Inducers (Alternate twist)
Denotations refer to Table 5.10

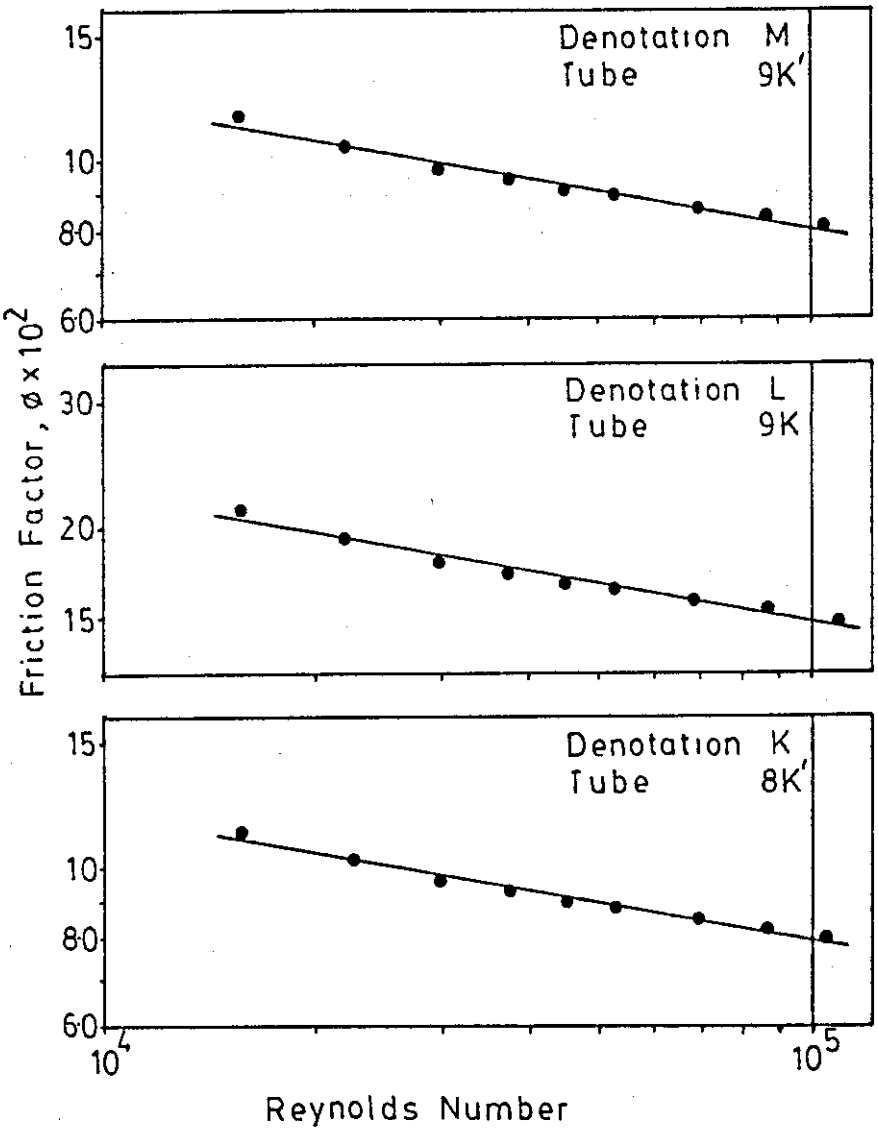

Figure No.5.37
Friction Factor Results (Heating)
Type:Swirl Inducers (Alternate twist)

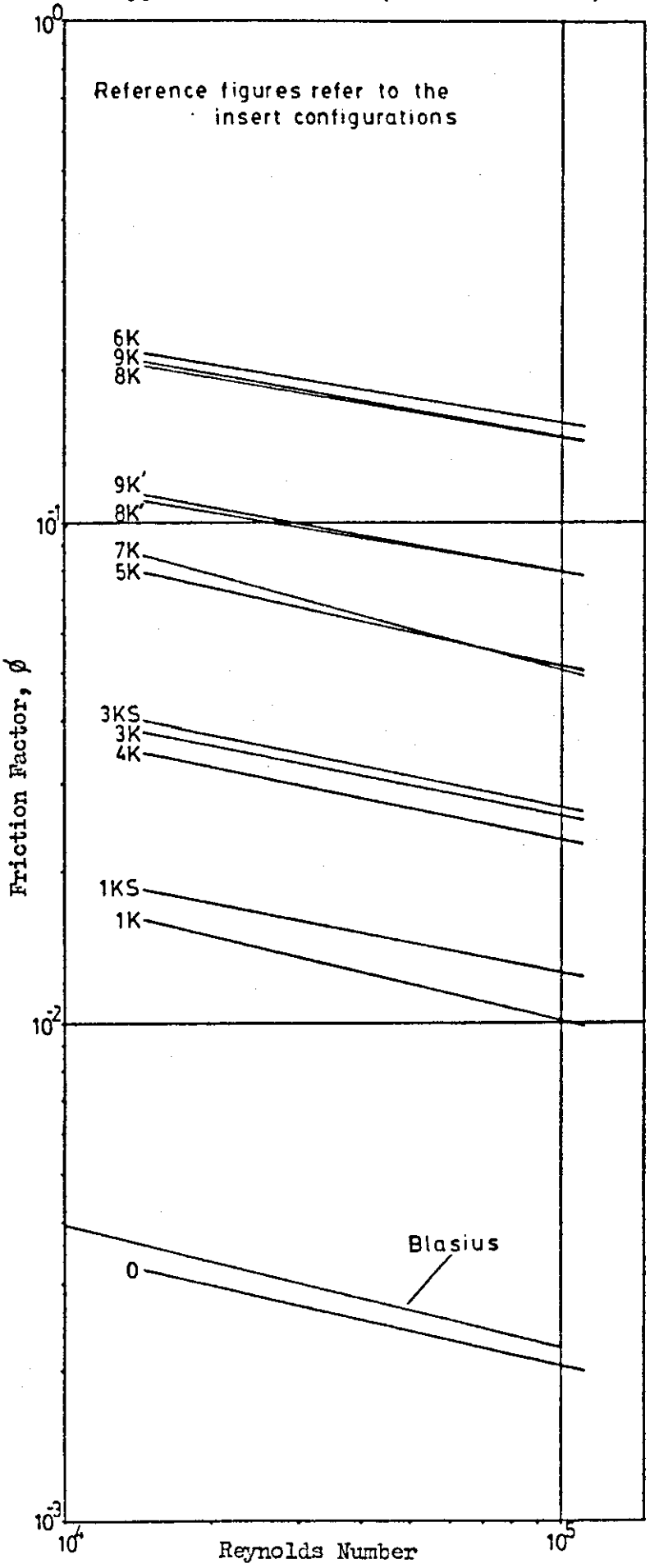

Figure No.5.38
Heat Transfer Results
Type: Swirl Inducers (Identical twist)
Reference figures are the insert configurations

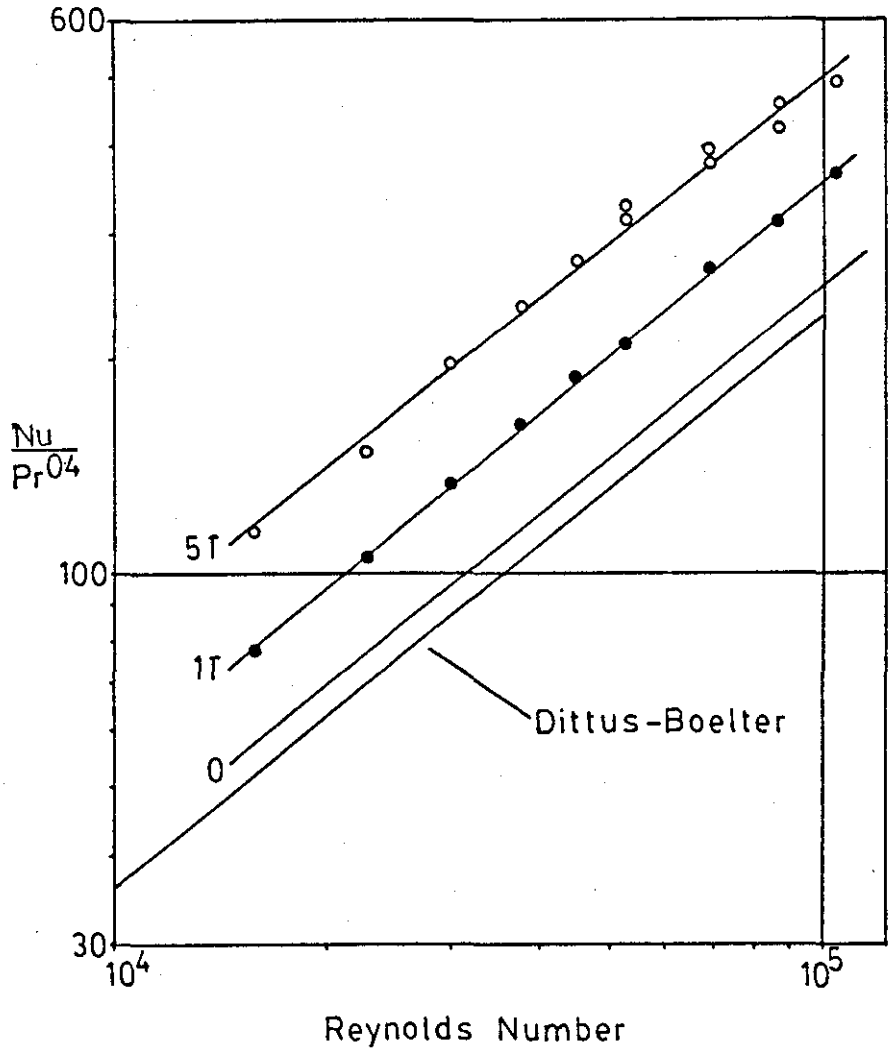

Figure No.5.39
Heat Transfer Results
Type: Swirl Inducers (Identical twist)
Reference figures are the insert configurations

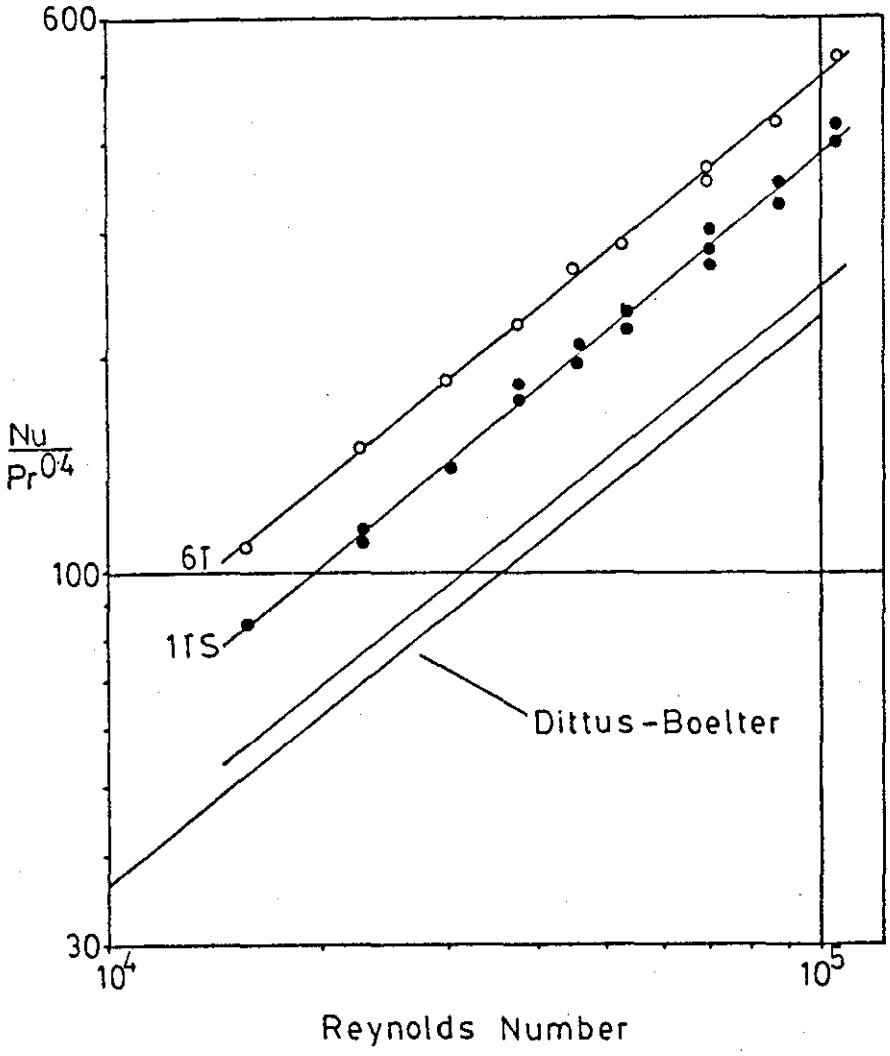

Figure No.5.40
Heat Transfer Results
Type: Swirl Inducers (Identical twist)
Reference figures are the insert configurations

The results for configuration 7T refer to denotation G of Table 5.11

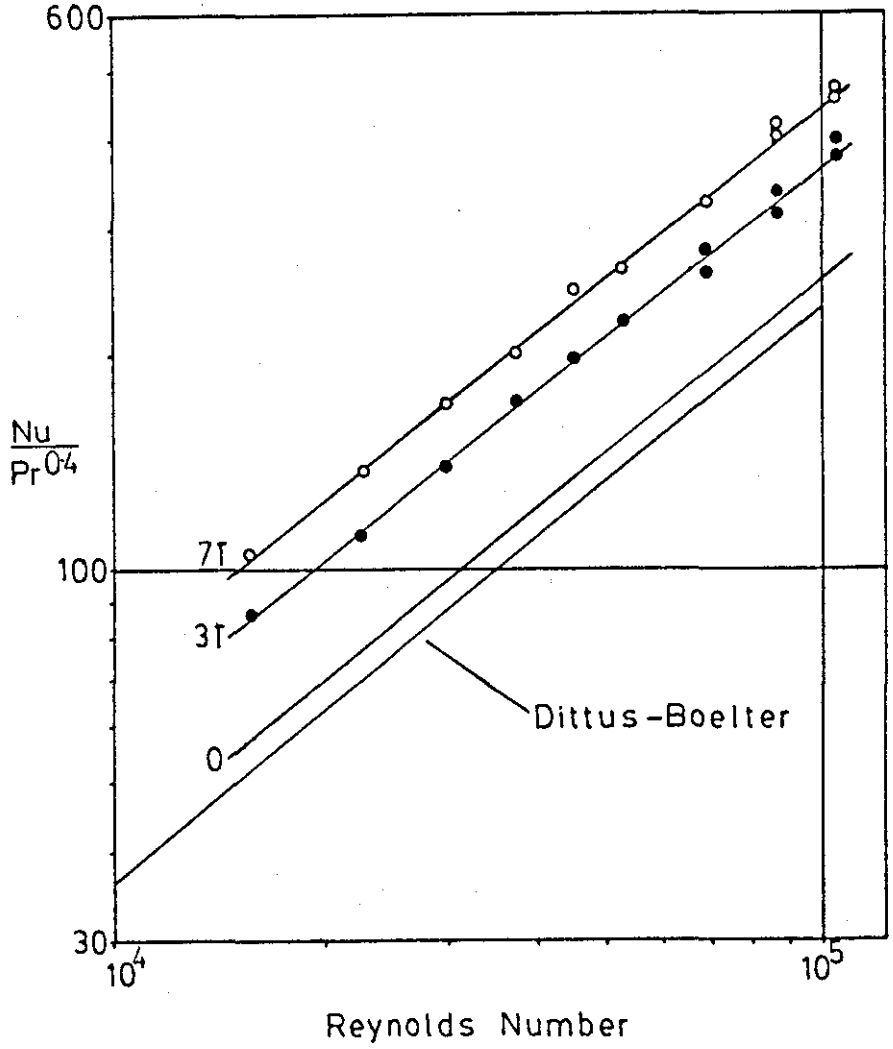

Figure No.5.41
Heat Transfer Results
Type: Swirl Inducers (Identical twist)
Reference figures are the insert configurations

The results for configuration 7T refer to denotation H of Table 5.11

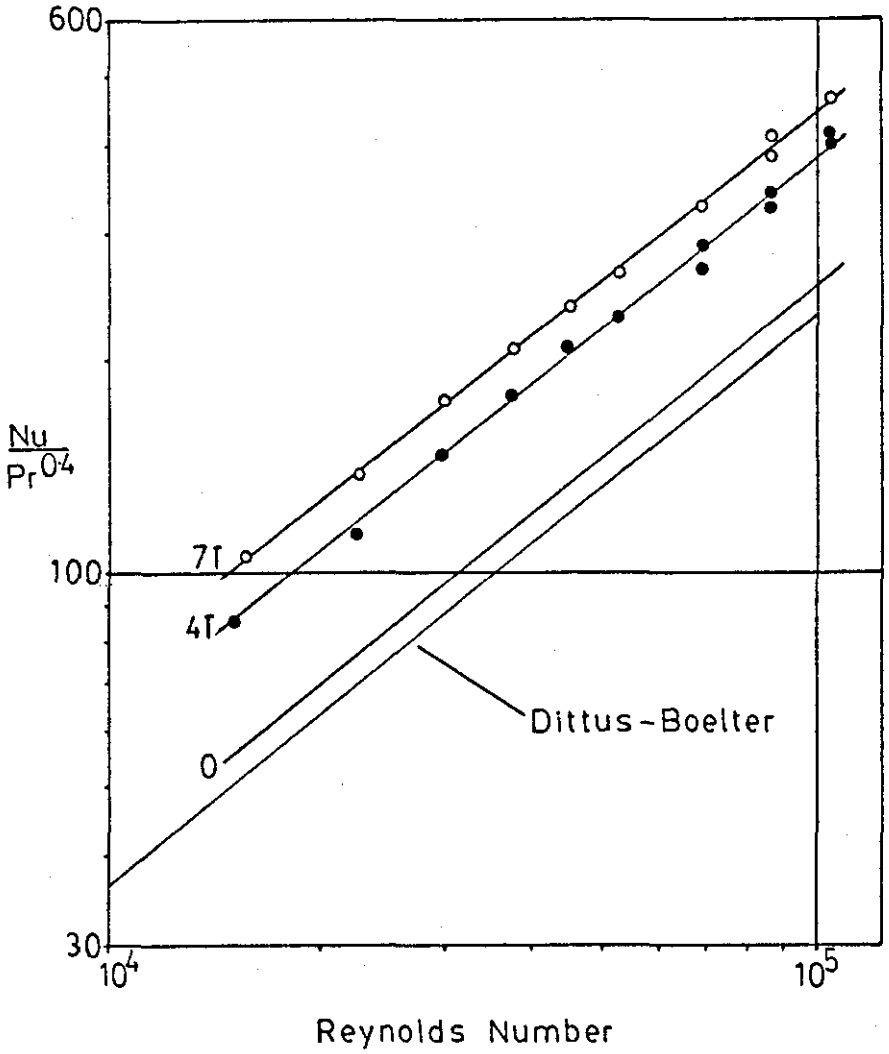

Figure No.5.42
Heat Transfer Results
Type: Swirl Inducers (Identical twist)
Reference figures are the insert configurations

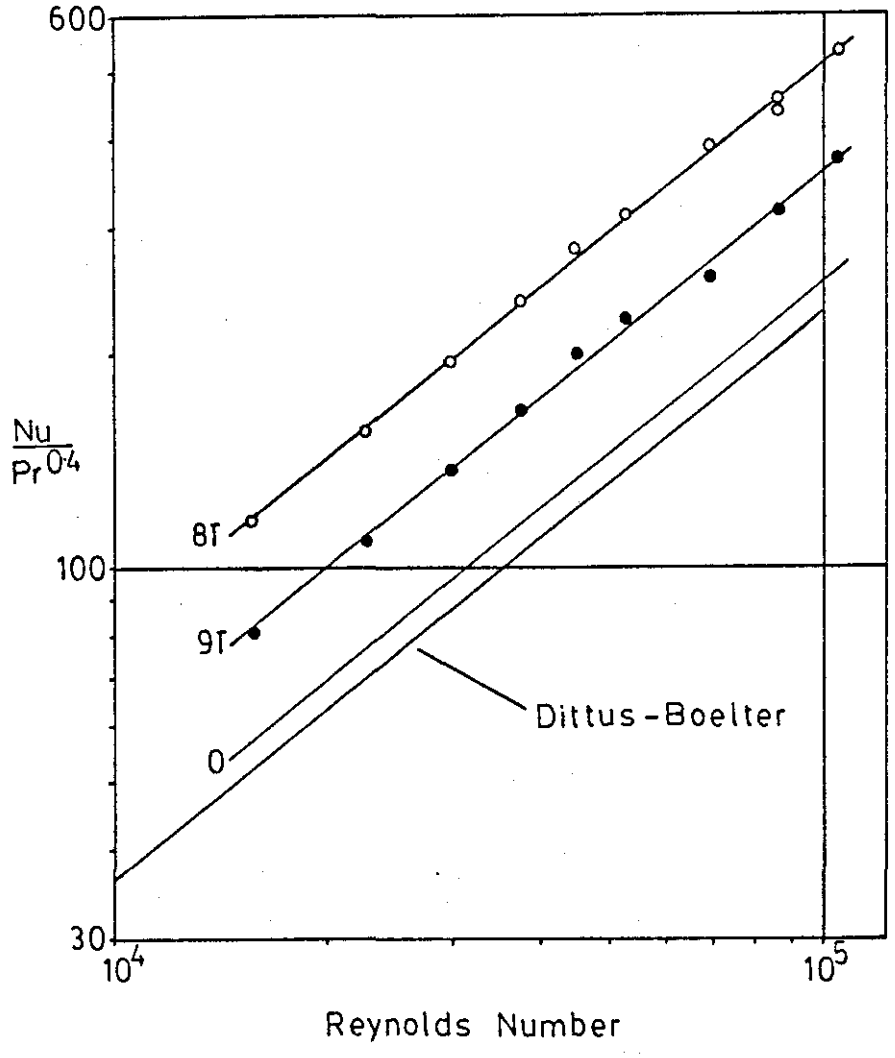

Figure No.5.43
Heat Transfer Factors calculated using the regression equations of Table 5.11
Type : Swirl Inducers (Identical twist)

For configuration 7T the equation is based on the results for rotameter, R2, scale readings of 7·5 and 10

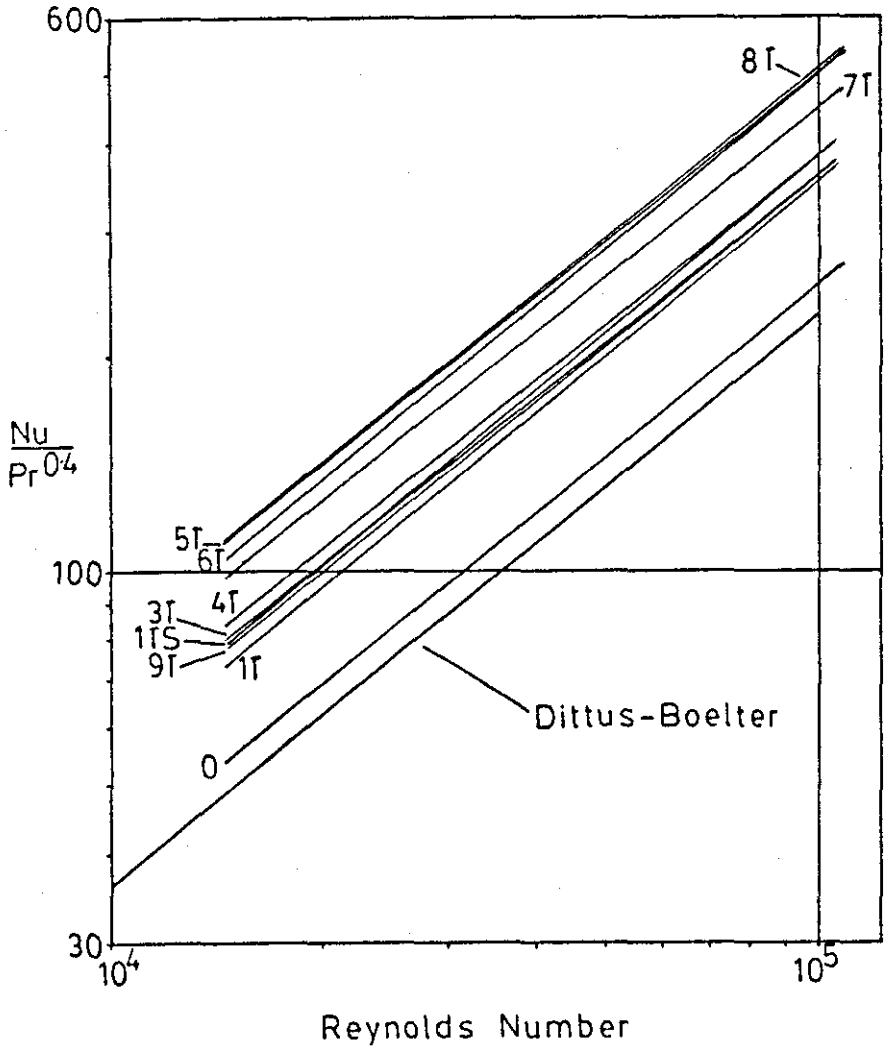

Figure No.5.44
Heat Transfer Results
Type: Swirl Inducers (Alternate twist)
Reference figures are the insert configurations

The results for configuration 6K refer to denotation H of Table 5.12

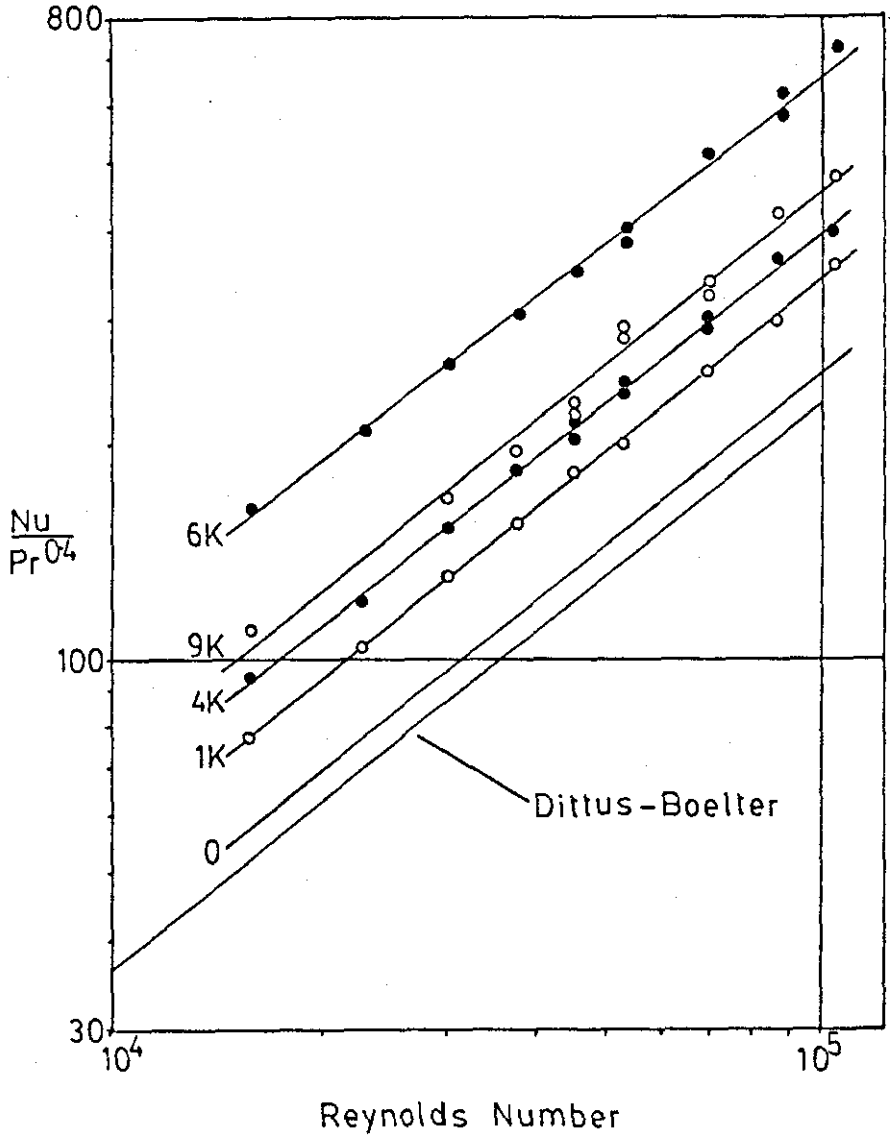

Figure No. 5.45
Heat Transfer Results
Type: Swirl Inducers (Alternate twist)
Reference figures are the insert configurations

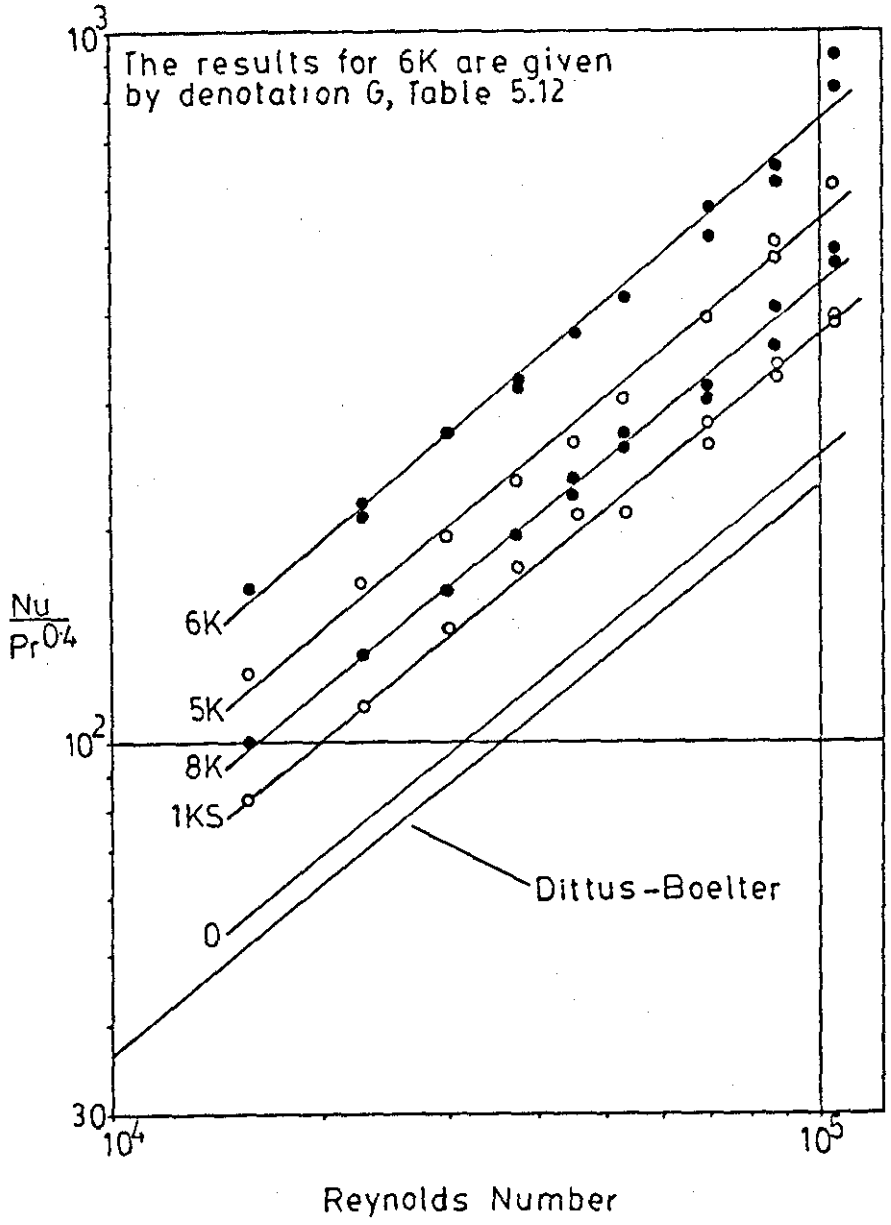

Figure No. 5.46
Heat Transfer Results
Type: Swirl Inducers (Alternate twist)
Reference figures are the insert configurations

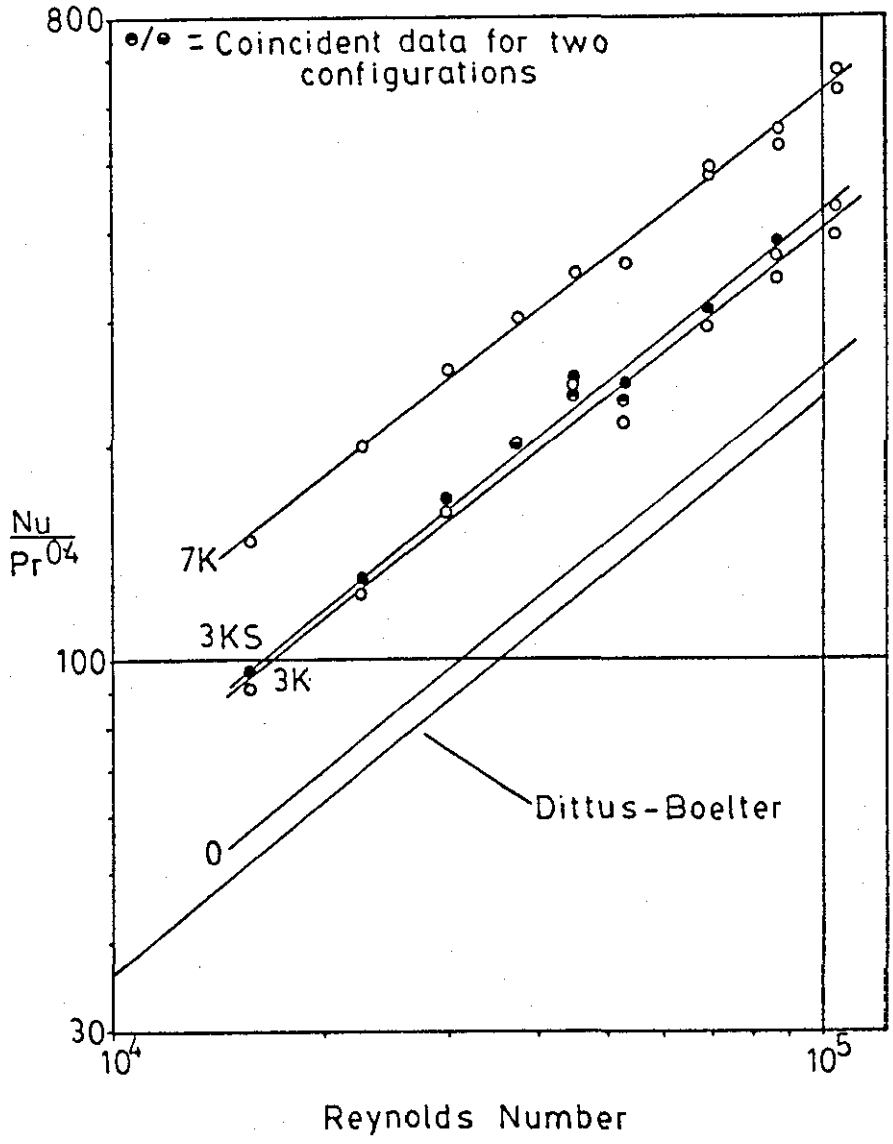

Figure No.5.47
Heat Transfer Factors calculated using the regression equations of Table 5.12
Type : Swirl Inducers (Alternate twist)

For configuration 6K the equation shown is based on the results for rotameter, R2, scale readings of 7·5 and 10

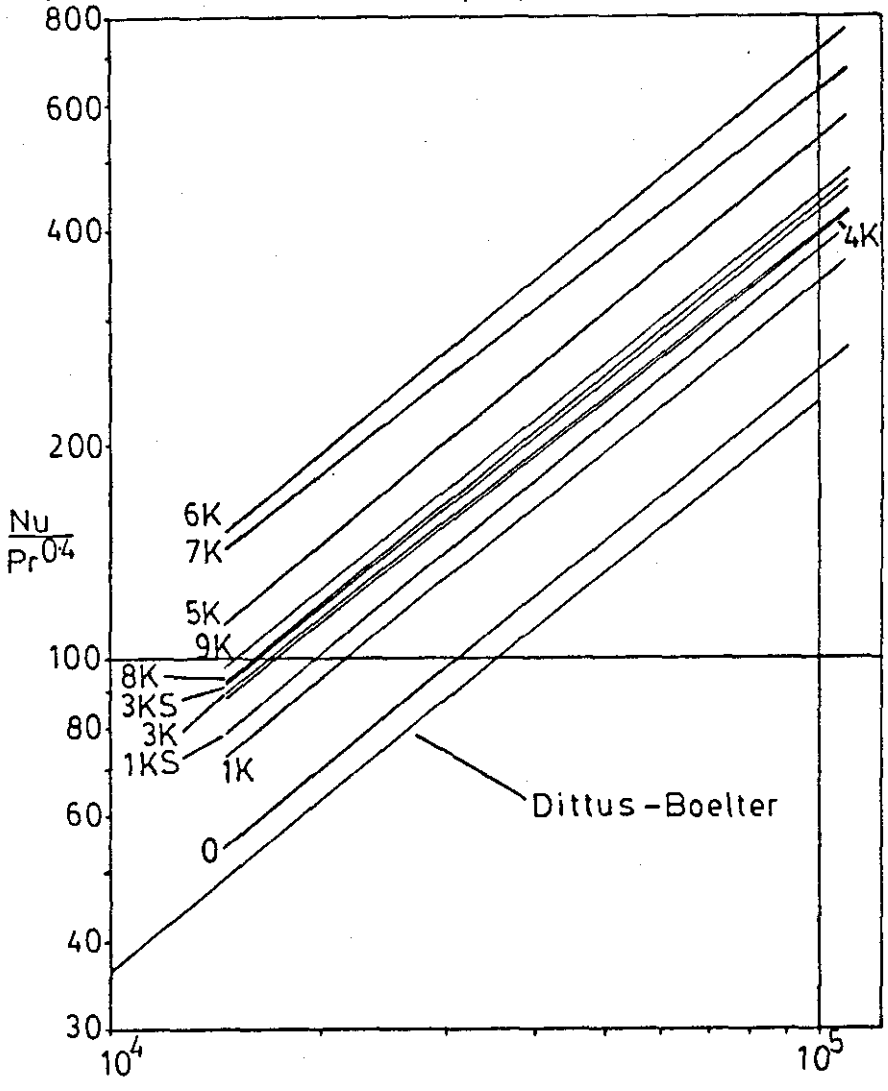

Figure No.5.48 The effect of unoccupied fraction of tube length on the regression parameters A,B (Inserts of identical twist direction)

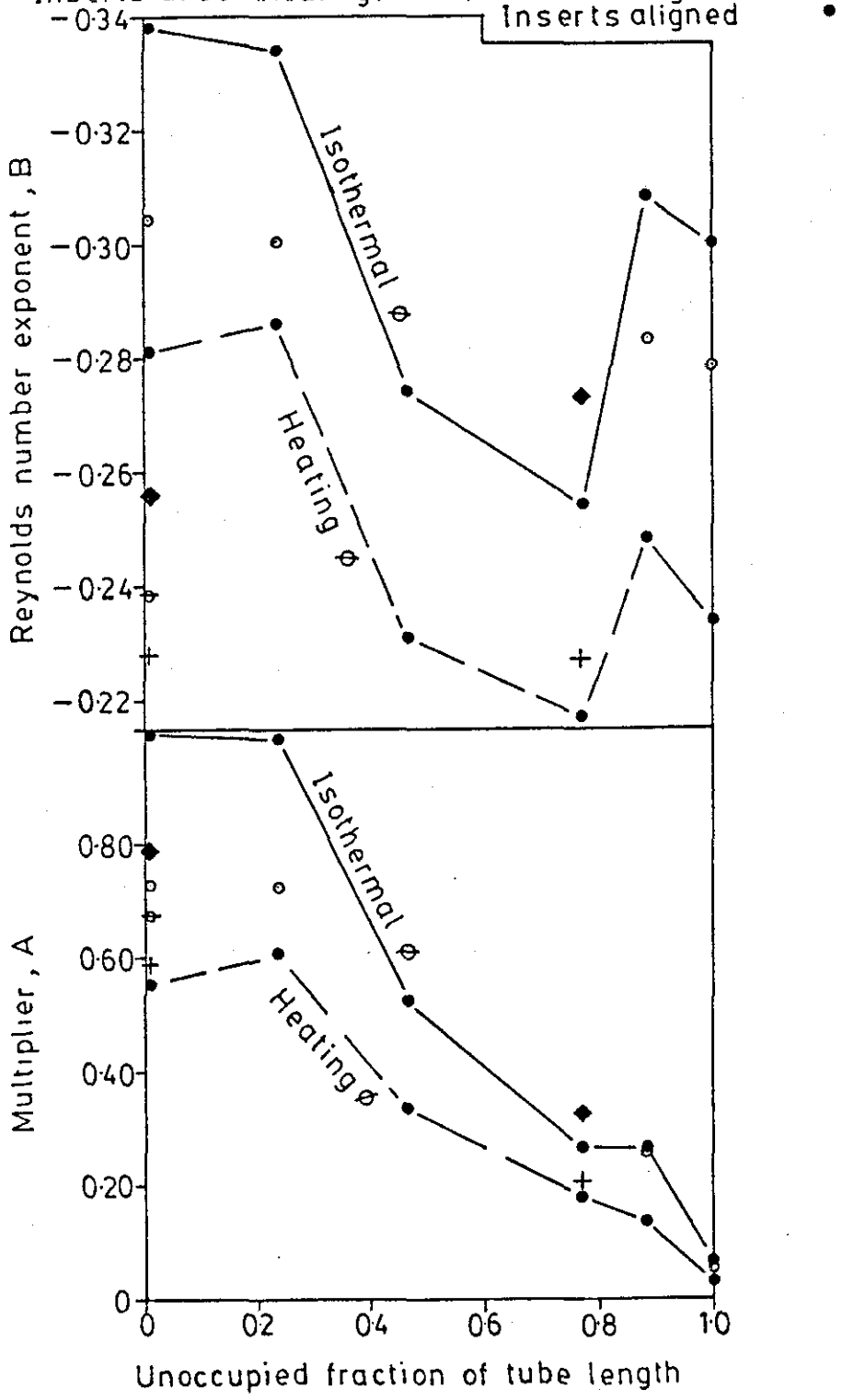

Figure No.5.49 The effect of unoccupied fraction of tube length on the multiplier, A

(Inserts of alternate twist direction)

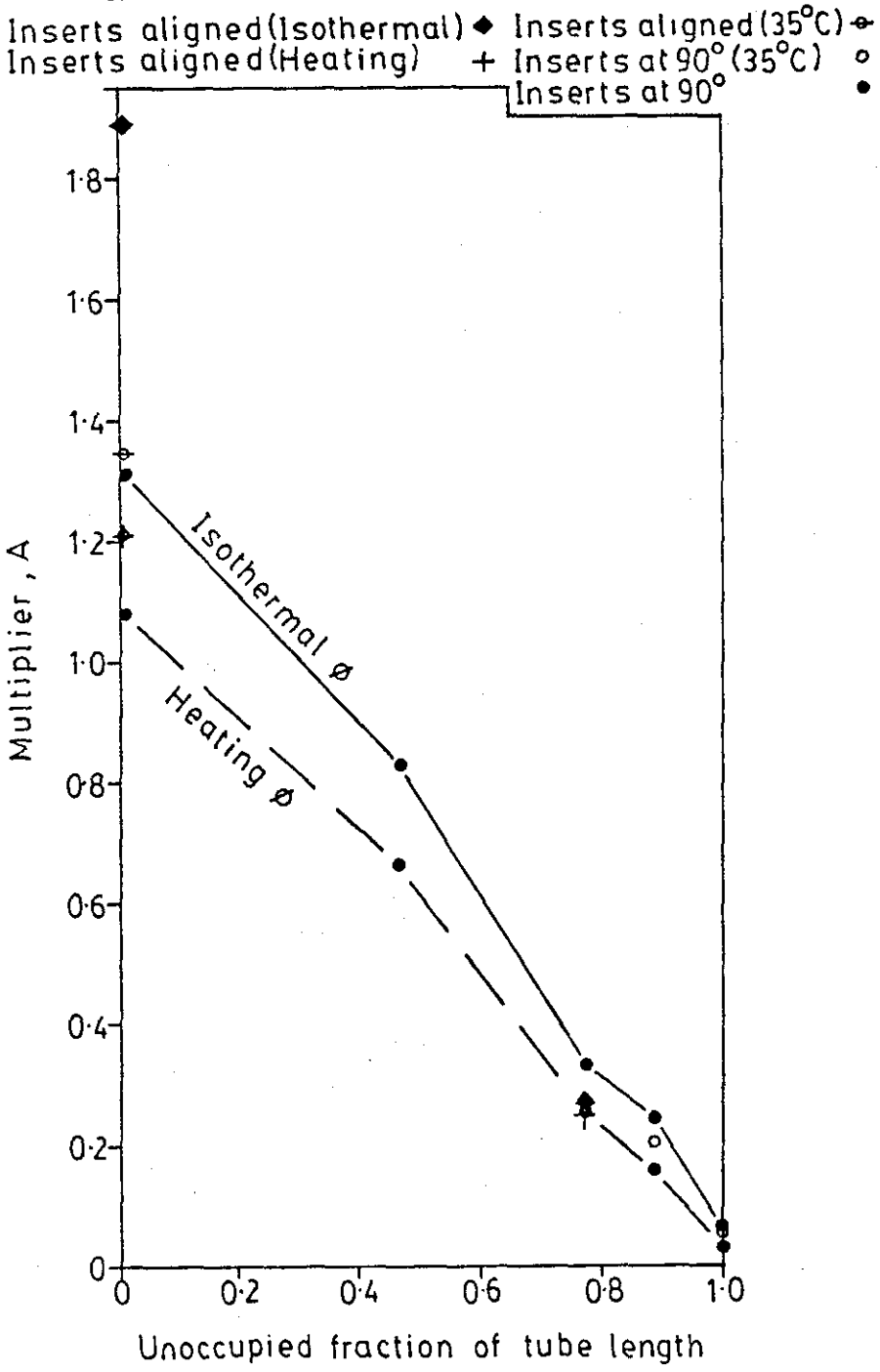

Figure No.5.50 The effect of unoccupied fraction of tube length on the Re exponent, B (Inserts of alternate twist direction)

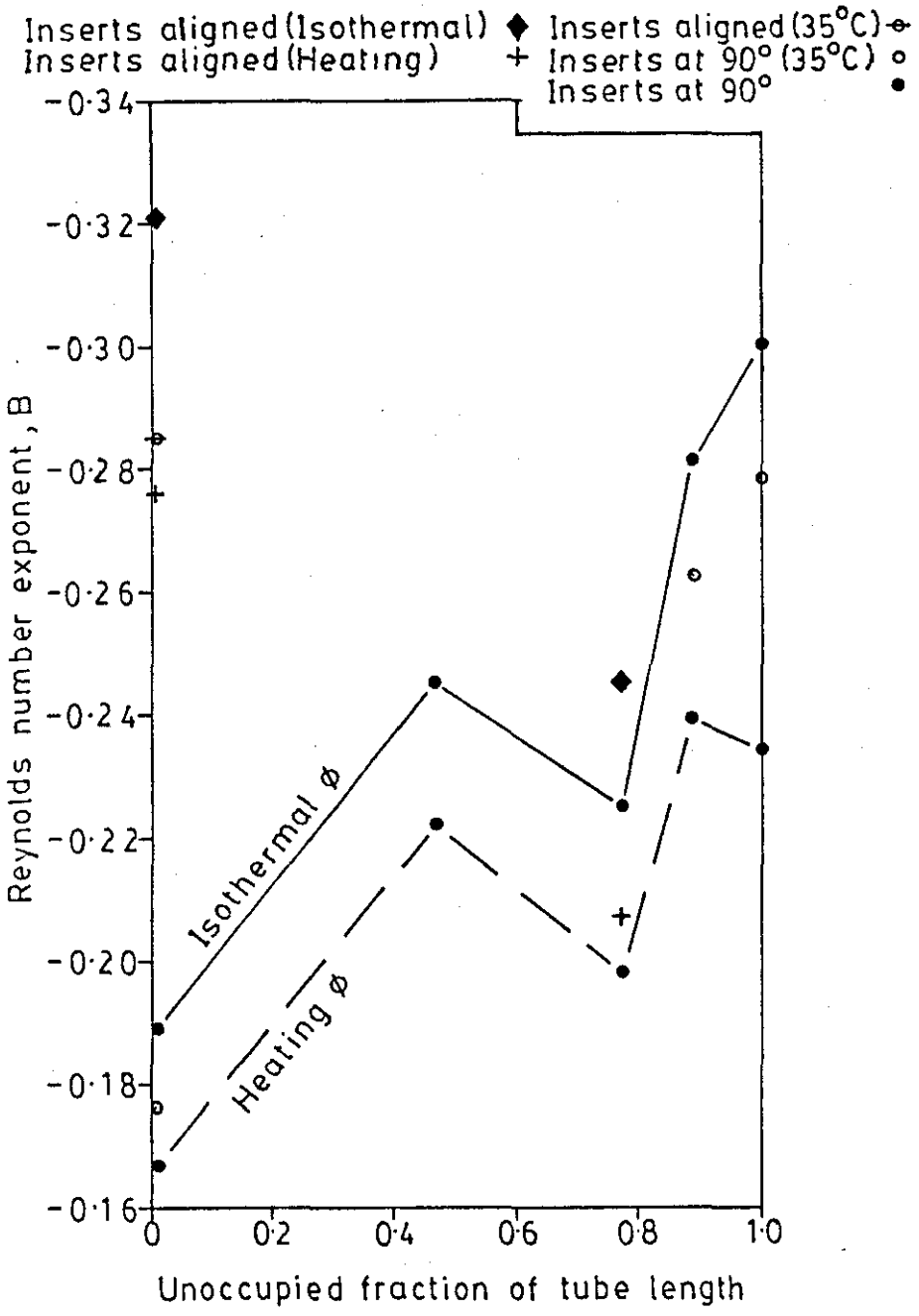

Figure No.5.51 The effect of the unoccupied fraction of the tube length on the regression parameters F,E

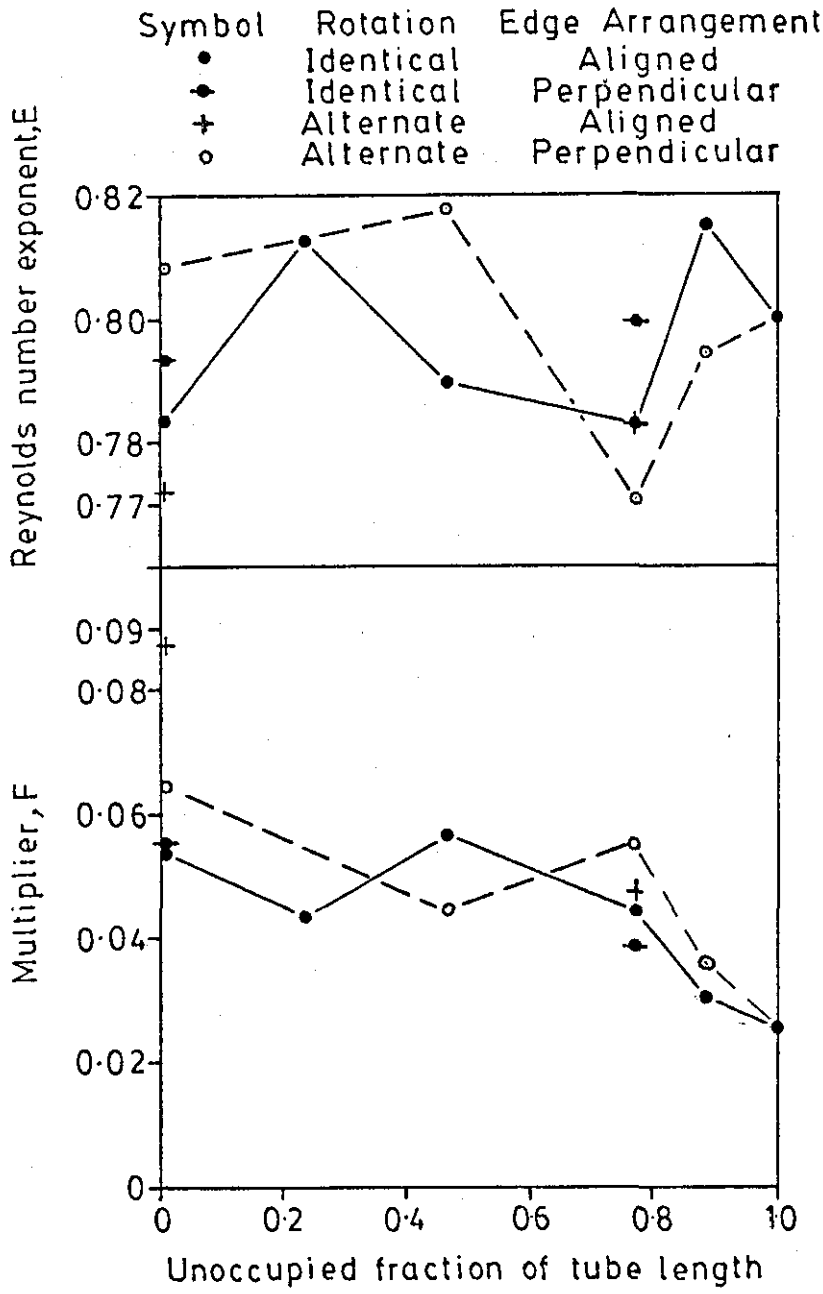

Figure No.5.52 Friction factor ratio versus the number of inserts

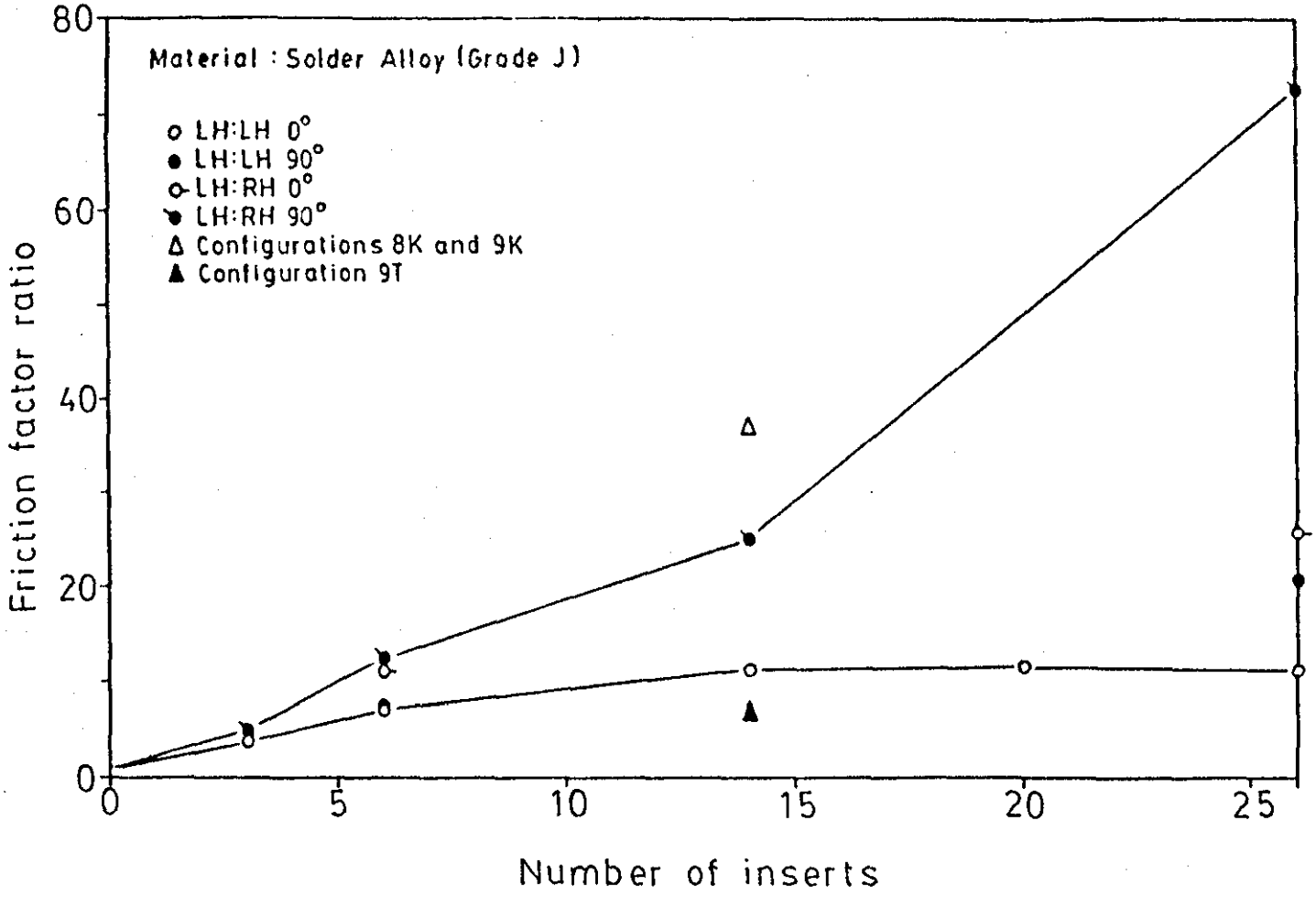

Figure No.5.53 Friction factor ratio versus the number of inserts

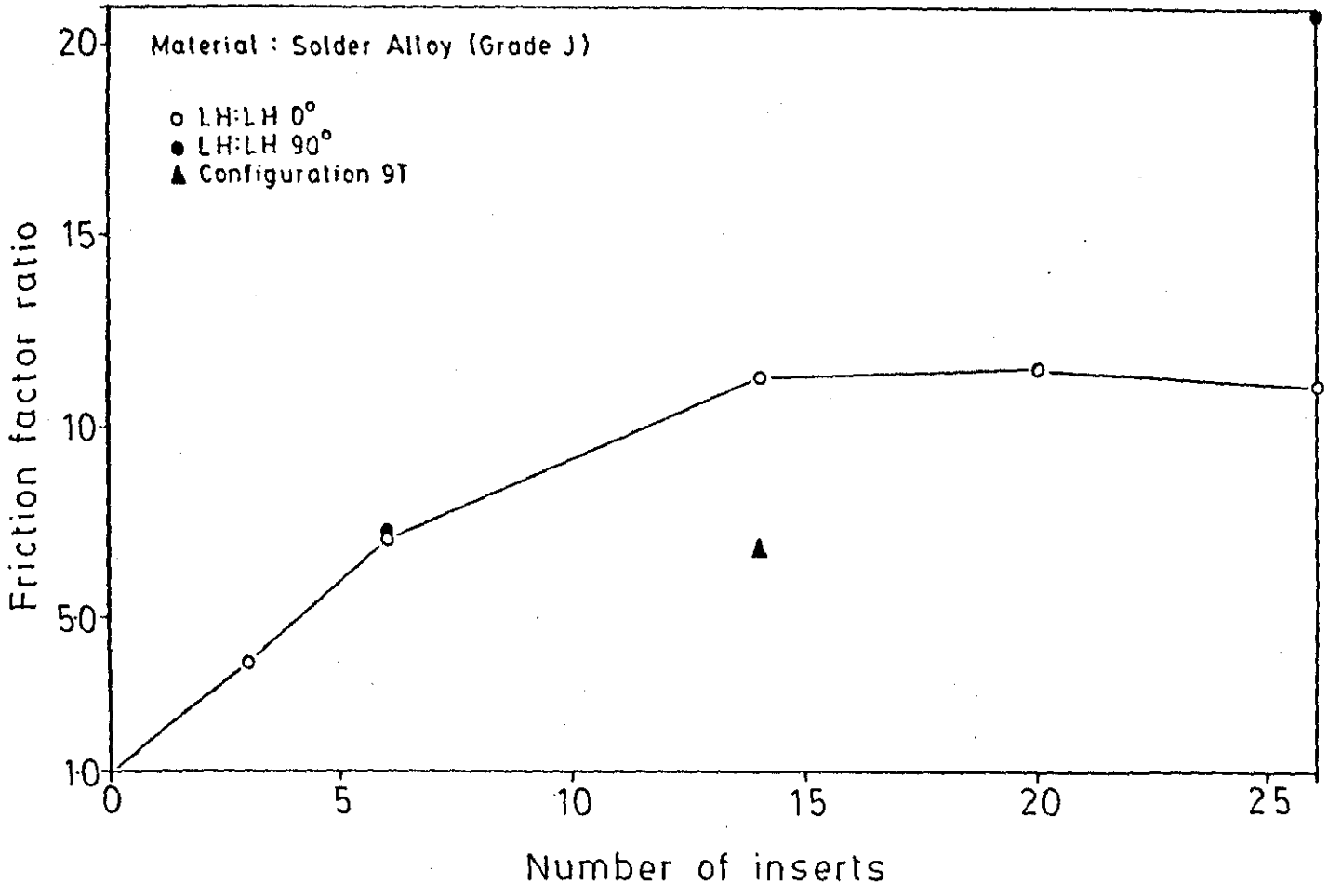

Figure No.5.54 Heat transfer factor ratio versus the number of inserts

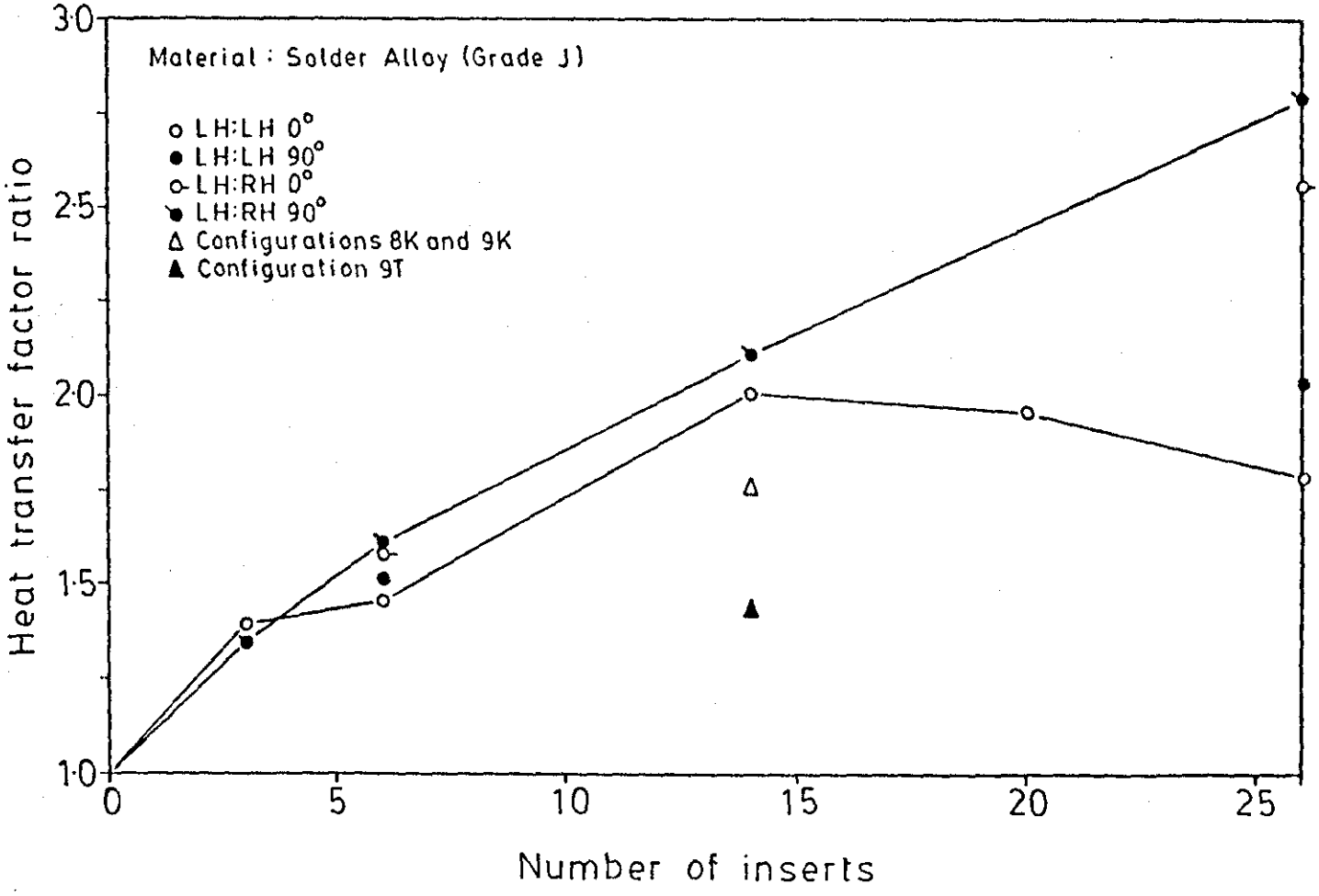

Figure No.7.1 Comparison of the heat transfer and flow resistance obtained using stainless steel pall rings (present work) and roughened tubes (Norris (6,pp.16-26)).

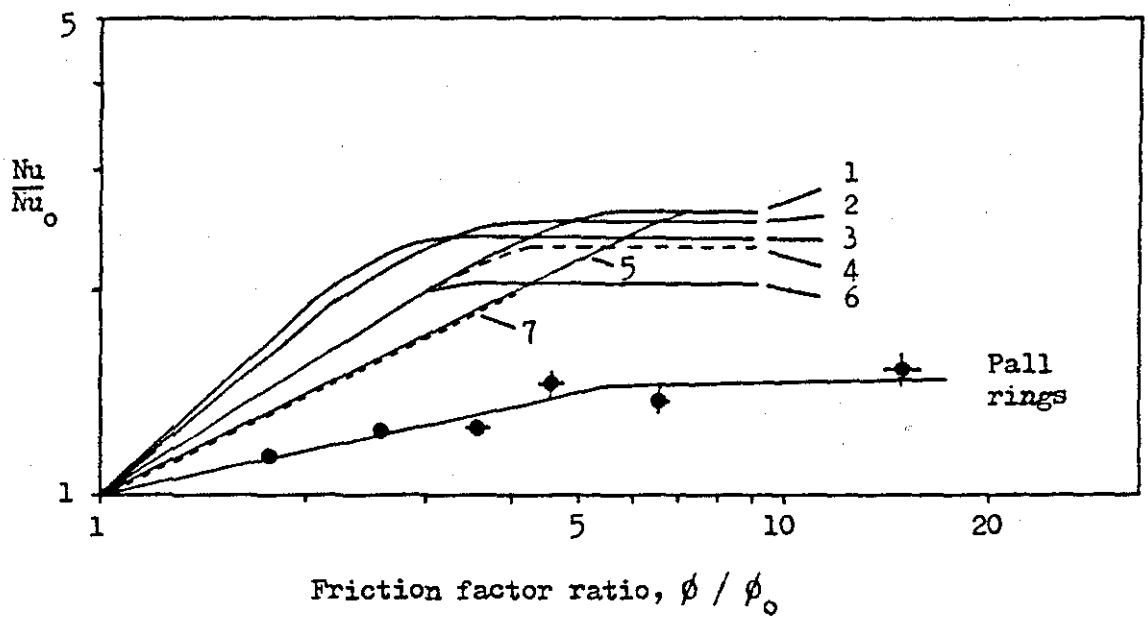

Symbols

● Average of the ratios obtained using pall rings at Reynolds numbers of 15500 and 86500. The short lines through the points indicate the effect of Reynolds number.	Pr = 4.94
1 Square ribs (large spacing)	Pr = 0.7
2 Sand grain roughness	Pr = 4
3 Sand grain roughness	Pr = 6
4 Wire type ribs	Pr = 0.7
5 Rectangular ribs (large spacing)	Pr = 0.7
6 Sand grain roughness	Pr = 0.7
7 Square ribs and V-shaped grooves (small spacing)	Pr = 0.7

Figure No.7.2 Comparison of the heat transfer and friction factor increases, relative to an empty tube operating at the same Reynolds numbers, produced by swirl inducing inserts

The points represent the mean of the ratios evaluated at Reynolds numbers of 15500 and 104000.

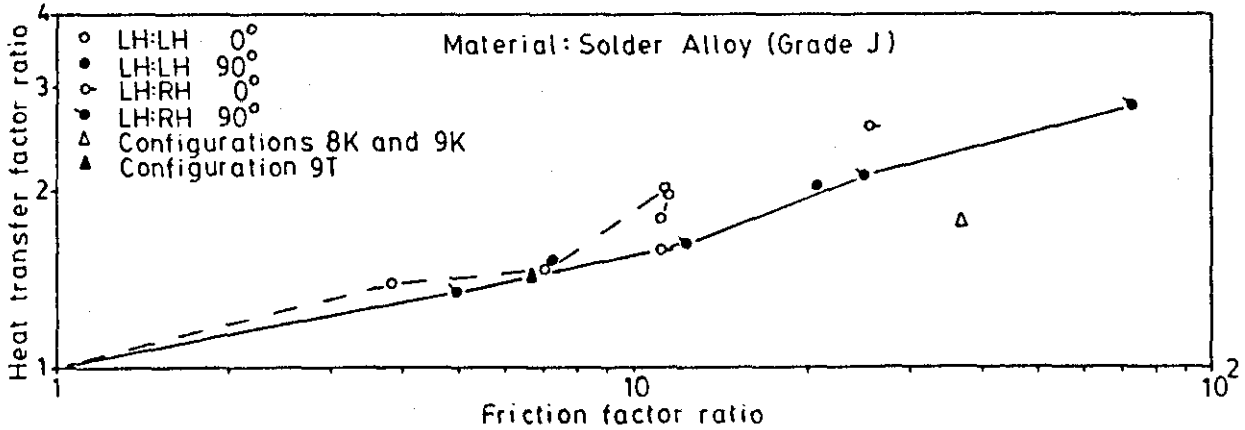

Figure No.7.3 Comparison of the friction factors evaluated using modified forms of equations (1.80) to (1.83) and the correlation proposed by Chakrabarti [21]

Denotation	Modified Equation
1	(1.80)
2	(1.81)
3	(1.82)
4	(1.83)

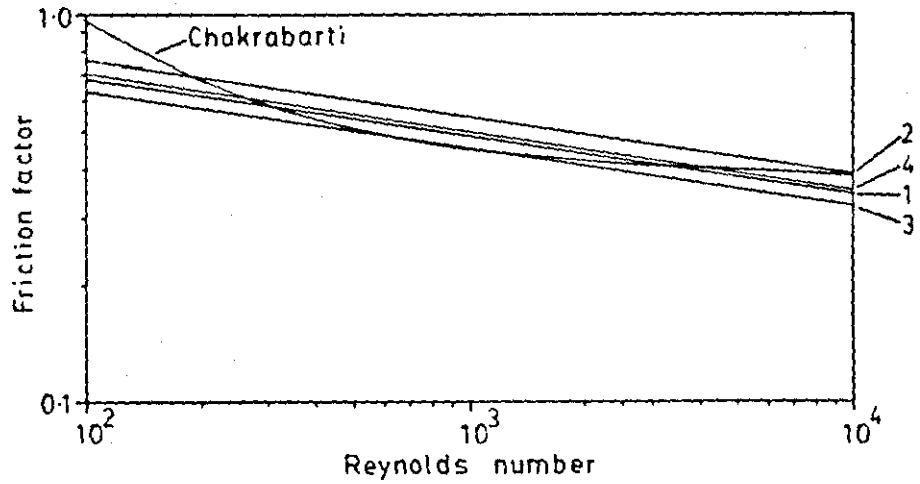

Figure No.7.4 Comparison of the friction factor characteristics of the Kenics static mixer system in the laminar and turbulent flow regimes.

Denotation	Source and conditions
A	Present work, empty tube, heat transfer.
B	Present work, configuration 9K, heat transfer.
C	Present work, configuration 6K, heat transfer.
D	Average $\emptyset$, determined using references (24) and (60), for a Kenics mixer with d = 15.7mm, average y = 1.61. Turbulent flow correlation.
E	As for D except correlation for laminar flow is used.
F	Proctor (101), Kenics mixer, d = 12.7mm, y = 1.5, heat transfer.
G	Lin et.al. (78), empty tube, heat transfer.
H	Lin et.al. (78), similar to configuration 9K, tube length = 1016mm, tube length occupied by Kenics mixers = 540mm, d = 12.7mm, y = 1.6, heat transfer.
J	Lin et.al. (78), Kenics mixer, d = 12.7mm, y = 1.6, heat transfer.

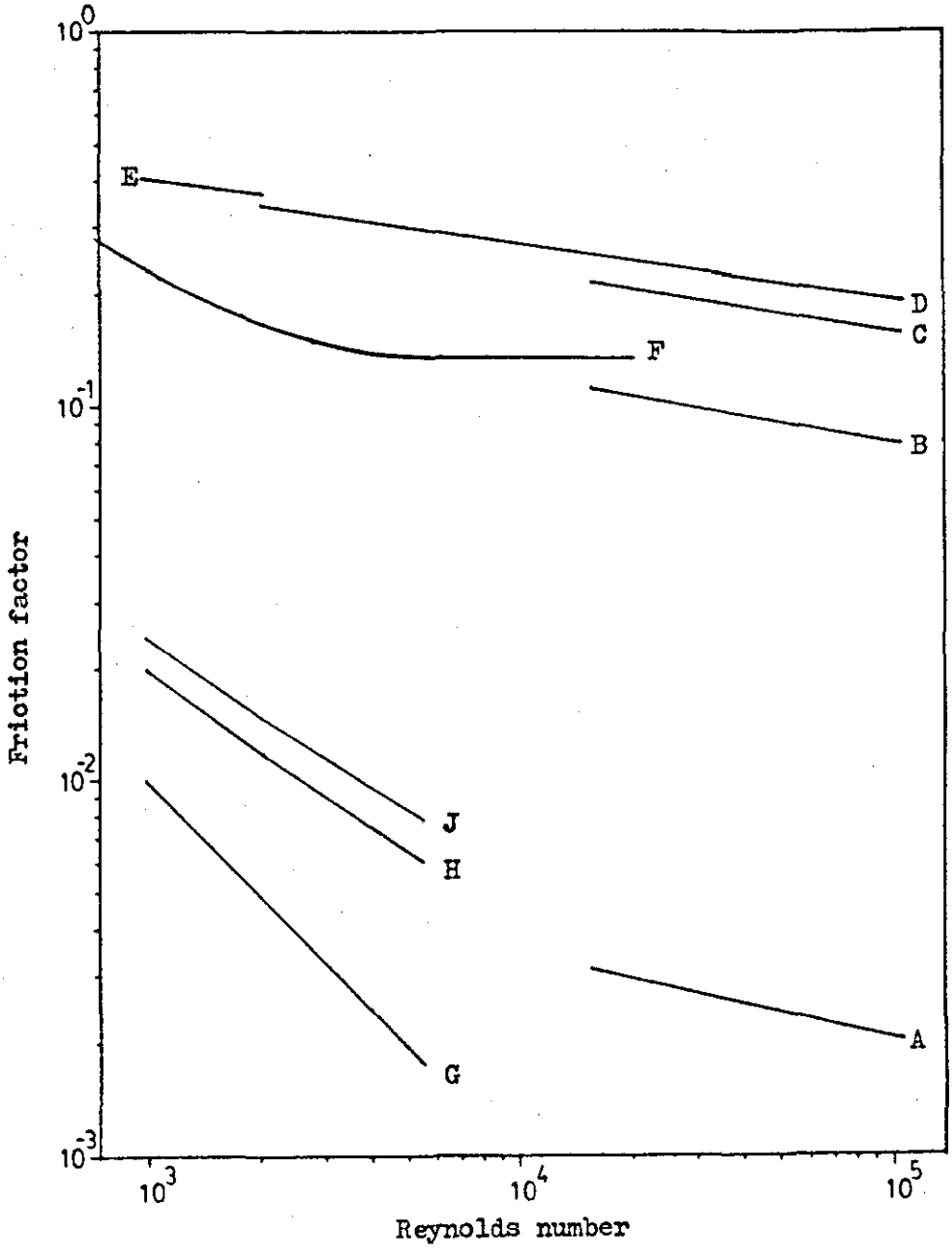

Figure No.7.5 Comparison of the heat transfer characteristics of the Kenics static mixer system in the laminar and turbulent flow regimes.

Denotation	Source and conditions
A	Present work, empty tube.
B	Present work, configuration 9K.
C	Present work, Kenics mixer, configuration 6K.
D	Chen (25), Kenics mixer, turbulent flow, $Nu = 0.078\ Re^{0.8}\ Pr^{0.33}$
E	Chen (25), Kenics mixer, laminar flow, $Nu = 2.25\ (Re\ Pr)^{0.33}$
F	Lin et.al. (78), empty tube.
G	Lin et.al. (78), similar to configuration 9K, tube length = 1016mm, tube length occupied by Kenics mixers = 540mm, d = 12.7mm, y = 1.6.
H	Lin et.al. (78), Kenics mixer, d = 12.7mm, y = 1.6.

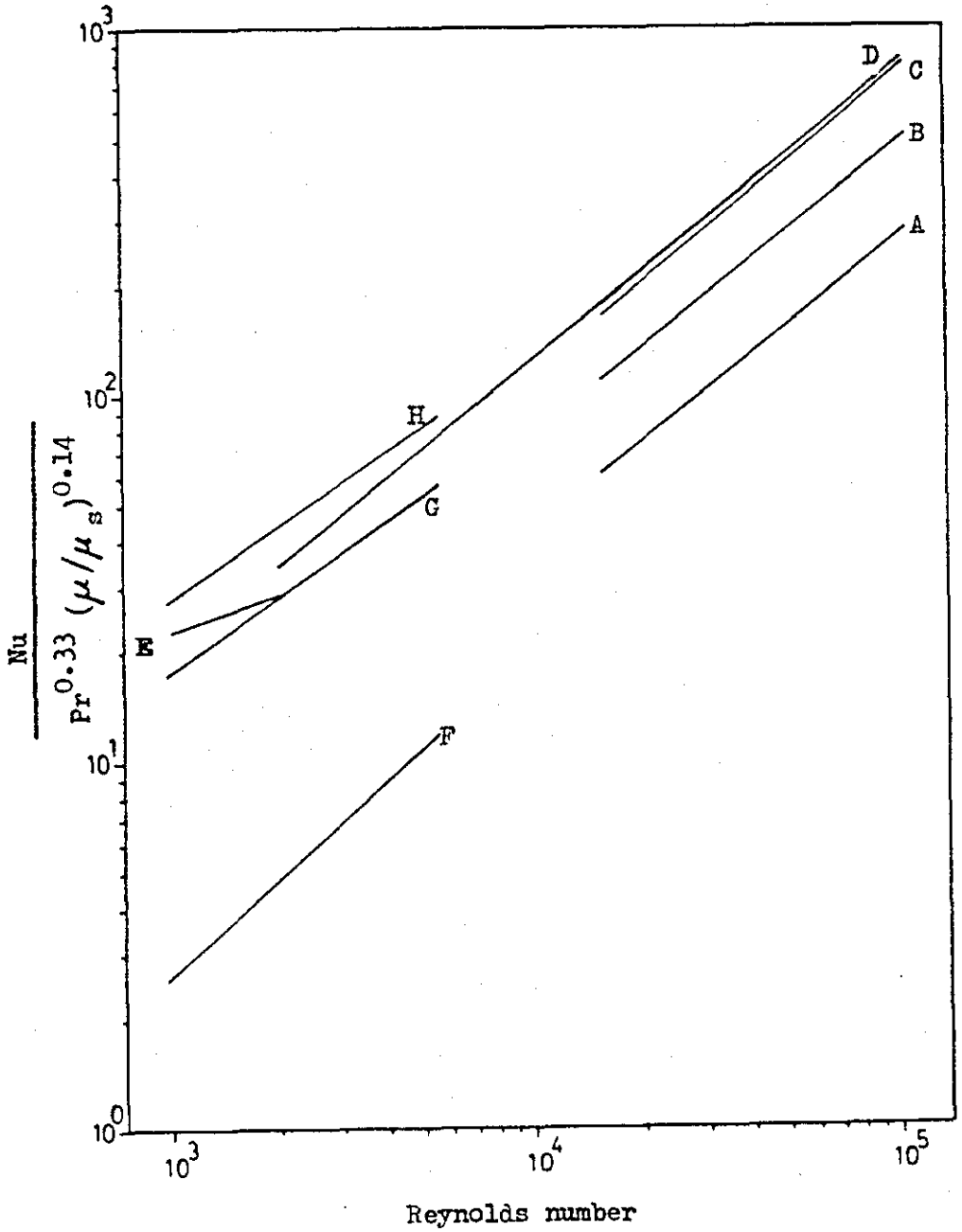

APPENDICES

Appendix A.1

The hydraulic, or equivalent, flow concept

The equivalent diameter of a tube containing inserts is found using the equation

$$D_e = \frac{4\ (\text{Cross sectional free area})}{(\text{Wetted perimeter})} \qquad (A.1.1)$$

For the twisted tape arrangement, for which Gambill, Bundy and Wansbrough (49, 50) call D_e the "nominal" equivalent diameter, it is found that

$$D_e = \frac{\pi d^2 - 4 \delta d}{(\pi + 2) d - 2\delta} \qquad (A.1.2)$$

The fluid velocity to be used with this "nominal" equivalent diameter is given by

$$u_e = \frac{uA_f}{A_c} = \frac{u}{1 - \left[\frac{4\delta}{\pi d}\right]} \qquad (A.1.3)$$

The length to be used in the friction factor calculation is the axial tube length, as used without the equivalent diameter correction.

Gambill et. al. (49, 50) do not use the area correction given by equation (A.1.3); they prefer to use a resultant fluid velocity and path length, at the tube wall, based on the rotating forced vortex slug flow model. This model has been used by a number of authors, for instance, Smithberg and Landis (118) and Migay (83). The model is described here for completeness, and further to show that other definitions of an "equivalent" diameter may be proposed. The work below is taken almost wholly from the report by Gambill et. al. (49).

For a continuous twisted tape

l = axial distance travelled by a slug of fluid while it is rotating through 360^o

$$= 2yd \qquad (A.1.4)$$

$$l_{si}^2 = \text{(actual distance travelled by a point on the outside surface of the fluid slug while rotating through } 360^o)^2$$

$$= (\pi d)^2 + (2yd)^2 \qquad (A.1.5)$$

$$\Rightarrow l_{si} = \frac{l}{2y}(4y^2 + \pi^2)^{0.5} \qquad (A.1.6)$$

Gambill et. al. neglect the tape thickness, hence in their work, the axial fluid velocity, u, is the velocity based on the tube bore, and it is not a function of distance from the tube centreline (by definition of the slug flow concept). However, there appears to be no reason why the velocity, u, *should not be substituted for the* corrected velocity, u_e, in the following equations.

For the forced vortex model

$$u_t = \text{tangential fluid velocity}$$

$$= u\frac{\pi}{2y}\frac{R}{r} \qquad (A.1.7)$$

So that at the wall of the tube

$$u_t = u_{ti} = \frac{\pi}{2y}u \qquad (A.1.8)$$

Hence the resultant fluid velocity at the tube wall is given by

$$u_{ri}^2 = u^2 + \left[\frac{\pi}{2y}u\right]^2 \qquad (A.1.9)$$

$$u_{ri} = \frac{u}{2y}(4y^2 + \pi^2)^{0.5}$$

The "true" equivalent diameter, here denoted by D_H, is considered by Gambill et. al. (49) to be obtained from a "true" flow area and corresponding wetted perimeter; hence

$$\text{"True" flow area} = \frac{\text{Volume}}{\text{Path length}} \qquad (A.1.10)$$

Neglecting the thickness of the tape, the volume of the slug of fluid over an increment (dR) is $2\pi R(4yr)(dR)$, and the path length is obtained from

$$(\text{Path length})^2 = (2\pi R)^2 + (4yr)^2 \qquad (A.1.11)$$

Hence

$$A_f' = \text{"true" flow area}$$

$$= \int_0^r \frac{8\pi Rry \quad (dR)}{\left[(2\pi R)^2 + (4yr)^2\right]^{0.5}} \qquad (A.1.12)$$

From Gradshteyn and Rhzhik (52, p. 86, equation 2.271) it is found that

$$\int \frac{R\,(dR)}{(a + cR^2)^{0.5}} = \frac{(a + cR^2)^{0.5}}{c} \qquad (A.1.13)$$

Hence

$$A_f' = \frac{8\,r^2y^2}{\pi}\left[\left[1 + \left[\frac{\pi}{2y}\right]^2\right]^{0.5} - 1\right] \qquad (A.1.14)$$

If the thickness of the tape is also considered then

$$A_f'' = \text{corrected true flow area}$$

$$= \frac{8\,r^2y^2}{\pi}\left[\left[1 + \left[\frac{\pi}{2y}\right]^2\right]^{0.5} - 1\right] - 2\,r\,\delta \qquad (A.1.15)$$

Gambill et. al. (49) define the wetted perimeter by

$$\text{Wetted perimeter} = \frac{\text{Area exposed}}{\text{Path length along the area}} \qquad (A.1.16)$$

where

$$\text{Tube area exposed} = 2\pi r^2\,(4y) \qquad (A.1.17)$$

$$\text{Path length at the tube wall} = r\left[(4y)^2 + 4\pi^2\right]^{0.5} \qquad (A.1.18)$$

and Wetted perimeter of the tape = 4r

Hence it can be shown that

$$\text{Wetted perimeter} = \frac{2\pi r^2\,(4y)}{r\left[4\pi^2 + (4y)^2\right]^{0.5}} + 4r$$

$$= 4r\left[\frac{\pi\,y}{(\pi^2 + 4y^2)^{0.5}} + 1\right] \qquad (A.1.19)$$

and Hydraulic diameter

$$= D_H = \frac{8ry^2}{\pi}\left[\frac{X - 2yX^{0.5}}{2y\,(\pi y + X^{0.5})}\right] \qquad \text{(A.1.20)}$$

where

$$X = (4y^2 + \pi^2) \qquad \text{(A.1.21)}$$

If allowance is made for the covering of part of the tube wall by the tape edges, then

$$\text{Wetted perimeter} = \frac{2\pi r^2 (4y) - 2\delta}{r\left[4\pi^2 + (4y)^2\right]^{0.5}} + 4r$$

$$= 4r\left[\frac{\pi y - (\delta/4r^2)}{\left[\pi^2 + 4y^2\right]^{0.5}} + 1\right] \qquad \text{(A.1.22)}$$

Using the corrected true flow area and wetted perimeter it is found that

$$D'_H = \text{corrected hydraulic diameter}$$

$$= \frac{\frac{4ry}{\pi}\left[X - 2yX^{0.5}\right] - 2\delta X^{0.5}}{\left[\pi y - (\delta/4r^2) + X^{0.5}\right]} \qquad \text{(A.1.23)}$$

where X is given by equation (A.1.21).

Appendix A.2

Representation of the data in BS 1042 (13)

(a) Expansion corrections

The following equation was applied to allow for the effect of temperature on the diameter of the tube and orifices :

$$\text{Diameter at } t, {}^{o}C = (\text{Diameter at } 20^{o}C)\left[1 + c\,(t - 20)\right] \qquad (A.2.1)$$

For the steel orifice plate and pipe, both of which were produced from 302 stainless steel :

$$c = \text{expansion coefficient} = 17.28 \times 10^{-6}\ m\ m^{-1}\ {}^{o}C^{-1}$$

For the brass plate :

$$c = 18.9\ m\ m^{-1}\ {}^{o}C^{-1}$$

(b) Discharge coefficient

$$m_o = \left[\frac{D_o}{d}\right]^2 = \left[\frac{\text{Orifice diameter}}{\text{Tube diameter}}\right]^2 \qquad (A.2.2)$$

For $m_o < 0.15$, with a corner tapped orifice plate, Figure 18a in BS 1042: 1943 and Figure 35 in BS 1042: Part 1: 1964 can be approximated by :

$$\text{Discharge coefficient} = 0.03938 m_o + 0.5956 \qquad (A.2.3)$$

(c) Fluid density and viscosity correlations

See section 4.3.2

(d) Reynolds number correction

For $m_o < 0.15$ the data of BS 1042 is correlated by :

$$\text{Multiplier} = (547.5\ Re_+^{-0.8951})m_o + \left[\frac{40.63 - 3.369\ \ln(Re_+)}{1000}\right] + 1$$

where Re_+ = Reynolds number of the flow through the orifice (A.2.4)

(e) Extra tolerance due to the Reynolds number

Correlating the data in BS 1042 it is found that

Extra tolerance = (Multiplier from (d) above).(25%) (A.2.5)

(f) Correction for diameter = $0.02723m_o + 1.000859$ (A.2.6)

(g) Extra tolerance for diameter = $2.9342m_o + 0.4842$ % (A.2.7)

(h) Basic tolerance = 0.8167%, for $m_o < 0.5$ (A.2.8)

Appendix A.3

The computer program (EX-6010) used for the analysis of the raw experimental data and for the pressure drop calculations

```
10 REM PROGRAM FOR TUBESIDE PROPERTIES,FLOW PARAMETERS AND PRESSURE DROPS
20 REM AXIAL CONDUCTION LOSSES ARE CALCULATED
30 REM DATA OBTAINED FROM FILES #1 AND #4 (CREATED BY INPUT)
40 REM LINES 40-680
50 REM DIM STATEMENTS,PROCESS INFORMATION,PRINT FOMAT,DATA READ
60 DIM N(100),H(100,6),M(100),S(100),T(100,25),D(100,5),V(100),Z(100)
70 DIM U(100),H(100,6),P(100),F(100),Q(100,5),Y(9,1),O(100,6)
80 DIM K(100,15),A(100,15),C(15,5)
90 DIM W(100,15),R(100)
100 PRINT'X=1 . . . . ISOTHERMAL'
110 PRINT'X=2 . . . . DIABATIC (TEST SECTION)'
120 PRINT'CHOSEN VALUE OF X IS':
130 INPUT X
140 REM DEFAULT VALUE OF A=0 ALLOWS TUBE WALL AREA TO BE FOUND
150 PRINT'CROSS SECTIONAL AREA OF TUBE/SQ.INS. IS':
160 INPUT A
170 PRINT'TUBE MATERIAL IS':
180 INPUT A$(5)
190 PRINT'TOTAL INSERTED LENGTH/INS. IS':
200 INPUT L1
210 F$='<##########'
220 G$='RUN NUMBER'
230 H$='  TEMP./C  '
240 I$=' HEAD/CM.  '
250 J$=' ROTAM/CM. '
260 K$='D/G./CU.CM. '
270 L$=' VISC./CP. '
280 M$='SPEC. GRAV.'
290 N$='Q/CU.FT./S.'
300 D$='#.#####^^^^'
310 P$='VEL./FT./S.'
320 Q$='  P/PSI.   '
330 R$='RE/NO UNITS'
340 S$=' FRICTION  '
350 T$='  COLBURN  '
360 U$='  BLASIUS  '
370 V$='  D.K.M.   '
380 W$=' COLEBROOK '
390 O$=' NIKURADSE '
400 B$='   ROUSE   '
410 PRINT'FIRST RUN NUMBER ON DATA FILE IS':
420 INPUT O1
430 PRINT'LAST RUN NUMBER ON DATA FILE IS':
440 INPUT Y1
450 PRINT'FIRST RUN NUMBER':
460 INPUT O
470 PRINT'LAST RUN NUMBER':
480 INPUT Y
490 PRINT'HOW MANY F EQUATIONS':
500 INPUT M
510 PRINT'LENGTH/INS. IS':
520 INPUT L
530 L3=L
540 E=0.000005*12
550 PRINT'I.D./INS. IS':
560 INPUT D
570 PRINT'O.D./INS. IS':
580 INPUT D1
590 DEFINE FILE#4='DAY5DH-6010'
600 DEFINE FILE#1='TH5-6010'
610 FOR I=O1 TO Y
620 READ #1,N(I),H(I,0),M(I),S(I),T(I,1),T(I,2),T(I,3),T(I,4),T(I,6),T(I,25)
630 IF X=1 GO TO 650
640 READ #4,T(I,9),T(I,10),T(I,8),T(I,7),T(I,22),T(I,23),Z(I)
650 NEXT I
660 CLOSE #4
670 CLOSE #1
680 P=0
690 REM LINES 690-1060
700 REM CALCULATE RE,PRESSURE DROP,FRICTION,HEAT LOSSES
710 FOR I=O TO Y
720 GOSUB 2690
730  D(I,3)=1-((((T(I,6)-3.9863)^2)*(T(I,6)+288.9414))/(508929.2*(T(I,6)+68.12963)))
740 IF X=2 GO TO 770
```

Appendix A.3 Continued

```
750 T=(T(I,1)+T(I,2))/2
760 GO TO 890
770 T(I,11)=(T(I,7)+T(I,8))/2
780 T(I,18)=(T(I,8)+T(I,10))/2
790 T(I,19)=(T(I,10)+T(I,9))/2
800 T(I,12)=(T(I,22)+T(I,23))/2
810 GOSUB 2900
820 T=T(I,1)
830 GOSUB 2840
840 T(I,21)=(H(I,5)/(C*Q(I,2)*3600*D(I,2)*62.427961*1.8))+T(I,1)
850 T=T(I,2)
860 GOSUB 2840
870 T(I,14)=T(I,2)-(H(I,6)/(C*Q(I,2)*3600*D(I,2)*62.427961*1.8))
880 T=(T(I,21)+T(I,2))/2
890 GOSUB 2840
900 D(I,1)=R
910 V(I)=V
920 T(I,20)=T
930 Q(I,1)=Q(I,2)*D(I,2)/D(I,1)
940 U(I)=Q(I,1)*183.34649/(D^2)
950 R(I)=7741.92*D*U(I)*D(I,1)/V(I)
960 IF L1=0 GO TO 990
970 P=0.0396*(R(I)^(-0.25))*(L3-L1)*D(I,1)*(U(I)^2)/(D*18.553609)
980 GO TO 1000
990 P=0
1000 P(I)=(H(I,0)*(S(I)-1)*D(I,3)*0.014223343)-P
1010 IF L1=0 GO TO 1030
1020 L=L1
1030 F(I)=18.553609*P(I)*D/(L*D(I,1)*(U(I)^2))
1040 P=0
1050 L=L3
1060 NEXT I
1070 REM LINES 1070-1380
1080 REM PRINT STATEMENTS OF SOME CALCULATED DATA
1090 PRINT LIN(4)
1100 PRINT'DATE:':
1110 INPUT A$
1120 PRINT
1130 PRINT'TABLE NO.':
1140 INPUT A$(2)
1150 PRINT
1160 PRINT'GEOMETRY:':
1170 INPUT A$(3)
1180 PRINT LIN(3)
1190 PRINT TAB(15):G$:TAB(29):H$:TAB(44):I$:TAB(57):J$
1200 FOR I=0 TO Y
1210 PRINT TAB(19):N(I):TAB(29):
1220 PRINT USING D$,T(I,20):
1230 PRINT TAB(46):H(I,0):TAB(61):M(I)
1240 NEXT I
1250 PRINT'LENGTH/INS.=':L
1260 PRINT'DIA./INS.=':D
1270 PRINT'ROUGH/INS.=':E
1280 PRINT
1290 PRINT TAB(15):K$:TAB(29):L$:TAB(43):M$:TAB(57):N$
1300 FOR I=0 TO Y
1310 PRINT TAB(15):
1320 PRINT USING D$,D(I,1):
1330 PRINT TAB(29):
1340 PRINT USING D$,V(I):
1350 PRINT TAB(44):S(I):
1360 PRINT TAB(57):
1370 PRINT USING D$,Q(I,1)
1380 NEXT I
1390 REM LINES 1390-1620
1400 REM DATA OF OTHER WORKERS AT SAME RE
1410 FOR I=0 TO Y
1420 F=0.0396*(R(I)^(-0.25))
1430 K(I,1)=0.023*(R(I)^(-0.2))
1440 K(I,2)=F
1450 K(I,3)=(0.00140+(0.125*(R(I)^(-0.32))))/2
1460 W=(E/(3.7*D))
1470 W(I,4)=1.255/(R(I)*((2*F)^0.5))
1480 K(I,4)=((-4*((LOG(W+W(I,4)))/LOG(10)))^(-2))/2
1490 IF ABS(K(I,4)-F)<0.0000000001 GO TO 1520
1500 F=K(I,4)
1510 GO TO 1470
1520 W(I,5)=(LOG(R(I)*((2*F)^0.5)))/LOG(10)
1530 K(I,5)=(((4*W(I,5))-0.40)^(-2))/2
1540 IF ABS(K(I,5)-F)<0.0000000001 GO TO 1570
1550 F=K(I,5)
```

Appendix A.3 Continued

```
1560 GO TO 1520
1570 W(I,6)=(LOG(R(I)*((2*F)^0.5)))/LOG(10)
1580 K(I,6)=(((4.06*W(I,6))-0.6)^(-2))/2
1590 IF ABS(K(I,6)-F)<0.0000000001 GO TO 1620
1600 F=K(I,6)
1610 GO TO 1570
1620 NEXT I
1630 REM LINES 1630-1830
1640 REM CALCULATE MEAN,MAXM.,AND MINM. RATIO OF EXPTL. TO REFERENCE FRICTION
1650 FOR J=1 TO M
1660 F1=0
1670 F2=0
1680 F3=1000000
1690 FOR I=0 TO Y
1700 A(I,J)=F(I)/K(I,J)
1710 F1=F1+A(I,J)
1720 IF A(I,J)<F3 GO TO 1770
1730 IF A(I,J)>F2 GO TO 1750
1740 GO TO 1790
1750 F2=A(I,J)
1760 GO TO 1790
1770 F3=A(I,J)
1780 IF I=0 GO TO 1730
1790 NEXT I
1800 C(J,2)=F1/(Y+1-0)
1810 C(J,0)=F2
1820 C(J,1)=F3
1830 NEXT J
1840 REM LINES 1840-2460
1850 REM PRINT STATEMENTS WITH OPTION ON REFERENCE PRINT OUTS
1860 PRINT
1870 PRINT TAB(15):P$:TAB(29):Q$:TAB(43):R$:TAB(57):S$
1880 FOR I=0 TO Y
1890 PRINT TAB(15):
1900 PRINT USING D$,U(I):
1910 PRINT TAB(29):
1920 PRINT USING D$,P(I):
1930 PRINT TAB(43):
1940 PRINT USING D$,R(I):
1950 PRINT TAB(57):
1960 PRINT USING D$,F(I)
1970 NEXT I
1980 PRINT
1990 PRINT'DO YOU WANT A PRINT OUT OF REFERENCE DATA':
2000 INPUT A$(4)
2010 PRINT
2020 FOR J=1 TO M STEP 4
2030 IF J=1 THEN GO TO 2050
2040 IF J=5 THEN GO TO 2080
2050 PRINT TAB(15):T$:TAB(29):U$:TAB(43):V$:TAB(57):W$
2060 IF A$(4)='NO' GO TO 2230
2070 GO TO 2100
2080 PRINT TAB(15):O$:TAB(29):B$
2090 IF A$(4)='NO' GO TO 2230
2100 FOR I=0 TO Y
2110 PRINT TAB(15):
2120 PRINT USING D$,K(I,J):
2130 PRINT TAB(29):
2140 IF J=5 GO TO 2210
2150 PRINT USING D$,K(I,J+1):
2160 PRINT TAB(43):
2170 PRINT USING D$,K(I,J+2):
2180 PRINT TAB(57):
2190 PRINT USING D$,K(I,J+3)
2200 GO TO 2220
2210 PRINT USING D$,K(I,J+1)
2220 NEXT I
2230 PRINT
2240 PRINT'MEAN RATIOS ARE'
2250 Q=2
2260 PRINT TAB(15):
2270 PRINT USING D$,C(J,Q):
2280 PRINT TAB(29):
2290 IF J=5 GO TO 2360
2300 PRINT USING D$,C(J+1,Q):
2310 PRINT TAB(43):
2320 PRINT USING D$,C(J+2,Q):
2330 PRINT TAB(57):
2340 PRINT USING D$,C(J+3,Q)
2350 GO TO 2370
2360 PRINT USING D$,C(J+1,Q)
```

Appendix A.3 Continued

```
2370 IF Q=1 GO TO 2450
2380 IF Q=0 GO TO 2420
2390 PRINT'MAXIMUM RATIOS ARE'
2400 Q=0
2410 GO TO 2260
2420 PRINT'MINIMUM RATIOS ARE'
2430 Q=1
2440 GO TO 2260
2450 PRINT
2460 NEXT J
2470 REM LINES 2470-2660
2480 REM FILE CALCULATED DATA
2490 DEFINE FILE#2='DAY5AH-6010', ASC SEP,50
2500 DEFINE FILE#5='DAY5EH-6010', ASC SEP,500
2510 DEFINE FILE#3='DAY5BH-6010', ASC SEP,500
2520 IF O=01 GO TO 2580
2530 FOR I=01 TO (O-1)
2540 READ #2,R(I),F(I)
2550 READ#3,Q(I,2),U(I),R(I),D(I,2),V(I)
2560 READ #5,H(I,3),H(I,4),H(I,5),H(I,6),T(I,11),T(I,12),T(I,18),T(I,19),T(I,14),T(I,20)
2570 NEXT I
2580 FOR I=O TO Y
2590 WRITE #2,R(I),F(I)
2600 WRITE #3,Q(I,2),U(I),R(I),D(I,2),V(I)
2610 IF X=1 GO TO 2630
2620 WRITE #5,H(I,3),H(I,4),H(I,5),H(I,6),T(I,11),T(I,12),T(I,18),T(I,19),T(I,14),T(I,20)
2630 NEXT I
2640 CLOSE #3
2650 CLOSE #2
2660 CLOSE #5
2670 PRINT
2680 STOP
2690 REM SUBROUTINE LINES 2690-2830
2700 REM TUBESIDE VOLUME FLOW AND DENSITY AT ROTAMETER
2710 Y(1,1)=0.00340162026987
2720 Y(2,1)=2.597274544769E-6
2730 Y(3,1)=0.001274380370887
2740 Y(4,1)=3.2853189679B3E-6
2750 Y(5,1)=1.3010310944146-5
2760 Y(6,1)=-1.130686733131E-7
2770 Y(7,1)=6.012183950688E-8
2780 Y(8,1)=-3.622024147276E-8
2790 Y(9,1)=1.465898163272E-9
2800 Q(I,3)=Y(1,1)+(Y(2,1)*T(I,25))+(Y(3,1)*M(I))+(Y(4,1)*T(I,25)*M(I))+(Y(5,1)*(M(I)^2))+(Y(6,1)*T(I,25)*(M(I)^2))
2810 Q(I,2)=Q(I,3)+(Y(7,1)*(T(I,25)^2))+(Y(8,1)*(T(I,25)^2)*M(I))+(Y(9,1)*(T(I,25)^2)*(M(I)^2))
2820 D(I,2)=1-((((T(I,25)-3.9863)^2)*(T(I,25)+288.9414))/(508929.2*(T(I,25)+68.12963)))
2830 RETURN
2840 REM SUBROUTINE LINES 2840-2890
2850 REM DENSITY,SPECIFIC HEAT,AND VISCOSITY AT DUMMY TEMPERATURE,T
2860 R=1-((((T-3.9863)^2)*(T+288.9414))/(508929.2*(T+68.12963)))
2870 C=1
2880 V=100/((2.1482*((T-8.435)+((8078.4+((T-8.435)^2))^0.5)))-120)
2890 RETURN
2900 REM SUBROUTINE LINES 2900-3120
2910 REM AXIAL CONDUCTION LOSSES
2920 IF A$(5)='STEEL' GO TO 2980
2930 O(I,5)=221.2-((11/720)*((T(I,11)*1.8)+32))
2940 O(I,6)=221.2-((11/720)*((T(I,12)*1.8)+32))
2950 O(I,3)=221.2-((11/720)*((T(I,19)*1.8)+32))
2960 O(I,4)=221.2-((11/720)*((T(I,18)*1.8)+32))
2970 GO TO 3020
2980 REM THERMAL COND. OF STEEL
2990 REM THERMAL COND. OF STEEL
3000 REM THERMAL COND. OF STEEL
3010 REM THERMAL COND. OF STEEL
3020 IF A>0 GO TO 3040
3030 A=3.1415927*((D1^2)-(D^2))/576
3040 X1=2/12
3050 X2=2/12
3060 X3=38/12
3070 X4=2/12
3080 H(I,5)=O(I,5)*A*(T(I,8)-T(I,7))*1.8/X3
3090 H(I,6)=O(I,6)*A*(T(I,22)-T(I,23))*1.8/X4
3100 H(I,3)=O(I,3)*A*(T(I,9)-T(I,10))*1.8/X1
3110 H(I,4)=O(I,4)*A*(T(I,10)-T(I,8))*1.8/X2
3120 RETURN
3130 END
```

Appendix A.4

The computer program (FRICTION-6010) used for the regression analysis of the friction factors and Reynolds numbers

```
 10 REM PROGRAM FOR LN-LN LINEAR REGRESSION OF RE AND FRICTION FACTORS
 20 REM DATA OBTAINED FROM FILE #2 , CREATED BY EX-6010 , OR BY ON-LINE INPUT
 30 REM LINES 30-330
 40 REM DIM STATEMENTS.PRINT FORMAT,
 50 REM AND RUN NUMBER STATEMENTS AND DATA INPUT OR READ
 60 DIM A$(10),R(500),F(500,5),S(500,5)
 70 DIM G$(10),A(40)
 80 A$(3)='+#.#####^^^^'
 90 PRINT'IS DATA ON FILE':
100 INPUT A$(1)
110 IF A$(1)='NO' GO TO 160
120 PRINT'FIRST RUN ON DATA FILE':
130 INPUT O1
140 PRINT'LAST RUN ON DATA FILE':
150 INPUT Y1
160 PRINT'FIRST RUN':
170 INPUT O
180 PRINT'LAST RUN':
190 INPUT Y
200 IF A$(1)='YES' GO TO 270
210 PRINT'DATA INPUTS'
220 PRINT'INPUT RE,F'
230 FOR I=O TO Y
240 INPUT R(I),F(I,1)
250 NEXT I
260 GO TO 360
270 PRINT'NAME #2':
280 INPUT A$(2)
290 DEFINE FILE#2=A$(2), ASC SEP,50
300 FOR I=O1 TO Y1
310 READ #2,R(I),F(I,1)
320 NEXT I
330 CLOSE #2
340 REM LINES 340-560
350 REM LN-LN LINEAR REGRESSION
360 C1=0
370 Z=0
380 E=0
390 F=0
400 W=0
410 G=0
420 S=0
430 Q4=0
440 FOR I=0 TO Y
450 Z=Z+(LOG(F(I,1)))
460 Q4=Q4+((LOG(F(I,1)))^2)
470 F=F+(LOG(R(I)))
480 W=W+((LOG(F(I,1)))*(LOG(R(I))))
490 G=G+((LOG(R(I)))^2)
500 NEXT I
510 X=(Y+1-O)
520 E=((X*W)-(F*Z))/((X*G)-(F^2))
530 C1=((G*Z)-(W*F))/((X*G)-(F^2))
540 GOSUB 580
550 PRINT LIN(2)
560 GOSUB 900
570 STOP
580 REM SUBROUTINE LINES 580-890
590 REM COMPARISON OF CALCULATED AND EXPERIMENTAL RESULTS
600 REM CALCULATE DATA FOR USE IN REGRESSION ANALYSIS
610 PRINT LIN(4)
620 PRINT TAB(20):'COMPARISON WITH REGRESSION ANALYSIS'
630 PRINT
640 PRINT TAB(20):'% ERROR IS EXP-CALC/EXP'
650 PRINT
660 PRINT TAB(15):'REYNOLDS NO':TAB(30):'  EXPTL F  ':TAB(45):' CALCED F ':TAB(60):'  % ERROR  '
670 F2=0
680 F3=0
```

Appendix A.4 Continued

```
690 FOR I=0 TO Y
700 F(I,3)=(C1+(E*LOG(R(I))))
710 F(I,2)=EXP(F(I,3))
720 S(I,1)=((LOG(F(I,1)))-F(I,3))
730 S=S+(S(I,1)^2)
740 S(I,2)=(F(I,1)-F(I,2))*100/F(I,1)
750 PRINT TAB(15):
760 PRINT USING A$(3),R(I):
770 PRINT TAB(30):
780 PRINT USING A$(3),F(I,1):
790 PRINT TAB(45):
800 PRINT USING A$(3),F(I,2):
810 PRINT TAB(60):
820 PRINT USING A$(3),S(I,2)
830 F2=F2+(S(I,2)^2)
840 F3=F3+ABS(S(I,2))
850 NEXT I
860 PRINT
870 PRINT'LOG-LOG REGRESSION LINE IS':
880 PRINT'F=':EXP(C1):'*(RE^':E:')'
890 RETURN
900 REM SUBROUTINE LINES 900-1630
910 REM REGRESSION ANALYSIS USING STUDENTS T-DISTRIBUTION
920 REM VALUES OF T READ FROM FILE
930 REM OPTION TO FILE EXPERIMENTAL DATA IS GIVEN
940 DEFINE FILE#7='T-DIST-6010'
950 FOR K=1 TO 33
960 READ #7,A(K)
970 NEXT K
980 CLOSE #7
990 IF (X-2)>120 GO TO 1050
1000 IF (X-2)>60 GO TO 1070
1010 IF (X-2)>40 GO TO 1090
1020 IF (X-2)>30 GO TO 1110
1030 X7=A(X-2)
1040 GO TO 1120
1050 X7=A(33)
1060 GO TO 1120
1070 X7=A(32)
1080 GO TO 1120
1090 X7=A(31)
1100 GO TO 1120
1110 X7=A(30)
1120 F4=(F3/X)
1130 F5=((F2/X)^0.5)
1140 X6=((1/X)+(((F/X)^2)/(G-((F/X)*F))))^0.5
1150 X5=X7*((S/(X-2))^0.5)*X6
1160 X4=((G-(F*F/X))^(-0.5))
1170 X3=X7*((S/(X-2))^0.5)*X4
1180 Q3=(W-(F*Z/X))/((((G-(F*F/X))^0.5)*((Q4-(Z*Z/X))^0.5))
1190 Q2=Q3^2
1200 F6=C1-X5
1210 Q6=EXP(F6)
1220 F7=C1+X5
1230 Q7=EXP(F7)
1240 F8=E-X3
1250 F9=E+X3
1260 Q5=EXP(C1)
1270 PRINT TAB(15):'RESULTS OF REGRESSION ANALYSIS'
1280 PRINT
1290 PRINT TAB(15):'Z...SUM OF LOG(F)':TAB(50):Z
1300 PRINT TAB(15):'F...SUM OF LOG(RE)':TAB(50):F
1310 PRINT TAB(15):'W...SUM OF LOG(F)*LOG(RE)':TAB(50):W
1320 PRINT TAB(15):'G...SUM OF (LOG(RE)^2)':TAB(50):G
1330 PRINT TAB(15):'X...TOTAL NUMBER OF RUNS USED':TAB(50):X
1340 PRINT TAB(15):'S...SUM OF (DEVIATIONS^2)':TAB(50):S
1350 PRINT TAB(15):'E...SLOPE OF REGRESSION LINE':TAB(50):E
1360 PRINT TAB(15):'C1...LOG(CONST) IN F EQUATION':TAB(50):C1
1370 PRINT TAB(15):'X7...T(5) IN CONFIDENCE ANALYSIS':TAB(50):X7
1380 PRINT TAB(15):'X6...MULT. IN LOG(CONST) ANALYSIS':TAB(50):X6
1390 PRINT TAB(15):'X4...MULT. IN SLOPE ANALYSIS':TAB(50):X4
1400 PRINT TAB(15):'X5...INTERVAL ON LOG(CONST)':TAB(50):X5
1410 PRINT TAB(15):'X3...INTERVAL ON SLOPE':TAB(50):X3
1420 PRINT TAB(15):'F6...MIN. LOG(CONST)':TAB(50):F6
1430 PRINT TAB(15):'F7...MAX. LOG(CONST)':TAB(50):F7
```

Appendix A.4 Continued

```
1440 PRINT TAB(15):'Q6...MIN. CONST':TAB(50):Q6
1450 PRINT TAB(15):'Q7...MAX. CONST':TAB(50):Q7
1460 PRINT TAB(15):'Q5...REGRESSION CONST':TAB(50):Q5
1470 PRINT TAB(15):'F8...MIN. SLOPE':TAB(50):F8
1480 PRINT TAB(15):'F9...MAX. SLOPE':TAB(50):F9
1490 PRINT TAB(15):'Q4...SUM OF (LOG(F)^2)':TAB(50):Q4
1500 PRINT TAB(15):'Q3...CORRELATION COEFFICIENT/R':TAB(50):Q3
1510 PRINT TAB(15):'Q2...R^2':TAB(50):Q2
1520 PRINT TAB(15):'F4...AV. ABS. DEV. ':TAB(50):F4
1530 PRINT TAB(15):'F5...R.M.S. ABS. DEV.':TAB(50):F5
1540 PRINT LIN(2)
1550 PRINT'STATE FILENAME OR NO':
1560 INPUT G$(5)
1570 IF G$(5)='NO' GO TO 1630
1580 DEFINE FILE#6=G$(5), ASC SEP,500
1590 FOR I=0 TO Y
1600 WRITE #6,R(I),F(I,1)
1610 NEXT I
1620 CLOSE #6
1630 RETURN
1640 END
```

Appendix A.5

The computer program (HEAT2-6010) used for the conversion of the experimental heat transfer data into dimensionless form

```
10 REM PROGRAM FOR RAW HEATING DATA TO NU FORM
20 REM DATA OBTAINED FROM #1,#4,#5,#3, OF EX-6010
30 REM LINES 30-640
40 REM DIM STATEMENTS,PROCESS INFORMATION.PRINT FORMAT,DATA READ
50 DIM O(100,5),G(100,5),A(60),M(100),C(100,9),H(100,10)
60 DIM Q(100,7),U(100,2),R(100),N(100),D(100,7),V(100),Y(9,2),T(100,25)
70 DIM P(100,5),K(100),B(100,5),S(100,5),Z(100),D$(25)
80 PRINT'ERROR CRITERION FOR RE EXPONENT IS':
90 INPUT X8
100 PRINT'ERROR CRITERION FOR RESISTANCE IS':
110 INPUT X9
120 B$='#.#####^^^^'
130 D$(1)=' RUN NUMBER '
140 D$(2)='(HO/HI)MEAS'
150 D$(3)='(HO/HI)CORR'
160 D$(4)='CORR/HIMEAS'
170 D$(5)='   CORR1   '
180 D$(6)='   CORR2   '
190 D$(7)='   CORR3   '
200 D$(8)='   CORR4   '
210 D$(9)=' LMTD MEAS '
220 D$(10)=' OUT T AV  '
230 D$(11)='INSI. T AV. '
240 D$(12)=' LMTD CORR '
250 D$(13)='HO CORR/BEU'
260 D$(14)='EXP NUSSELT'
270 D$(15)='CAL NUSSELT'
280 D$(16)=' % CA-EX/EX'
290 D$(17)='VEL. /FT..S.'
300 D$(18)='  SLOPE E   '
310 D$(19)=' RE NUMBER '
320 Z$(2)='+#.#####^^^^'
330 PRINT'TUBE MATERIAL IS':
340 INPUT AS
350 PRINT'CROSS SECTIONAL AREA OF TUBE AND INSERTS/SQ.FT. IS':
360 INPUT A
370 PRINT'FIRST RUN NUMBER ON DATA FILE IS':
380 INPUT O1
390 PRINT'LAST RUN NUMBER ON DATA FILE IS':
400 INPUT Y1
410 DEFINE FILE#5='DAY5EA-6010', ASC SEP,500
420 DEFINE FILE#3='DAY5BA-6010', ASC SEP,500
430 DEFINE FILE#2='DAY5DA-6010'
440 DEFINE FILE#1='TA5-6010'
450 FOR I=O1 TO Y1
460 READ #1,N(I),S(I,4),M(I),S(I,5),T(I,1),T(I,2),T(I,3),T(I,4),T(I,6),T(I,25)
470 READ #3,Q(I,2),U(I,1),R(I),D(I,2),V(I)
480 READ #5,H(I,3),H(I,4),H(I,5),H(I,6),T(I,11),T(I,12),T(I,18),T(I,19),T(I,14),T(I,20)
490 READ #2,T(I,9),T(I,10),T(I,8),T(I,7),T(I,22),T(I,23),Z(I)
500 NEXT I
510 CLOSE #1
520 CLOSE #2
530 CLOSE #3
540 CLOSE #5
550 PRINT 'FIRST RUN NUMBER IS':
560 INPUT O
570 PRINT'LAST RUN NUMBER IS':
580 INPUT Y
590 PRINT'TUBE I.D./INS.=':
600 INPUT D
610 PRINT'TUBE O.D./INS.=':
620 INPUT D1
630 L=42/12
640 PRINT LIN(2)
650 REM LINES 650-1010
660 REM HEAT FLOWS,CORRECTED HEAT FLOWS AND TEMPERATURES,LMTD AND OVERALL HTC
670 FOR I=O TO Y
680 GOSUB 2530
690 T=T(I,4)
700 GOSUB 2670
710 D(I,3)=R
720 T(I,15)=(T(I,3)+T(I,4))/2
730 T=T(I,15)
740 GOSUB 2670
```

Appendix A.5 Continued

```
750 D(I,4)=R
760 C(I,4)=C3
770 T=T(I,20)
780 GOSUB 2670
790 C(I,1)=C3
800 T(I,13)=((H(I,3)+H(I,4)+H(I,5))/(C(I,1)*Q(I,2)*3600*D(I,2)*62.427961*1.8))+T(I,1)
810 T(I,16)=(T(I,13)+T(I,14))/2
820 T=T(I,16)
830 GOSUB 2670
840 D(I,5)=R
850 C(I,5)=C3
860 Q(I,5)=Q(I,2)*D(I,2)/D(I,5)
870 H(I,7)=Q(I,2)*3600*D(I,2)*62.427961*C(I,5)*(T(I,14)-T(I,13))*1.8
880 U(I,2)=(Q(I,5)*576)/(3.1415927*(D^2))
890 H(I,2)=Q(I,3)*D(I,3)*3600*62.427961*C(I,4)*(T(I,3)-T(I,4))*1.8
900 H(I,8)=H(I,2)-(H(I,3)+H(I,4)+H(I,5)+H(I,6))
910 T=(T(I,1)+T(I,2))/2
920 GOSUB 2670
930 C(I,2)=C3
940 H(I,1)=Q(I,2)*3600*D(I,2)*62.427961*C(I,2)*(T(I,2)-T(I,1))*1.8
950 P(I,1)=H(I,7)/H(I,8)
960 P(I,2)=H(I,1)/H(I,2)
970 P(I,3)=(H(I,3)+H(I,4)+H(I,5)+H(I,6))/H(I,2)
980 T(I,5)=((T(I,4)-T(I,13))-(T(I,3)-T(I,14)))/LOG((T(I,4)-T(I,13))/(T(I,3)-T(I,14)))
990 K(I)=H(I,7)/(3.1415927*(D1/12)*L*T(I,5)*1.8)
1000 T(I,17)=((T(I,4)-T(I,1))-(T(I,3)-T(I,2)))/LOG((T(I,4)-T(I,1))/(T(I,3)-T(I,2)))
1010 NEXT I
1020 REM LINES 1020-1390
1030 REM PRINT STATEMENTS OF CALCULATED DATA
1040 PRINT LIN(2)
1050 PRINT TAB(15):D$(1):TAB(29):D$(2):TAB(43):D$(3):TAB(57):D$(4)
1060 FOR I=0 TO Y
1070 PRINT TAB(19):N(I):
1080 PRINT TAB(29):
1090 PRINT USING B$,P(I,2):
1100 PRINT TAB(43):
1110 PRINT USING B$,P(I,1):
1120 PRINT TAB(57):
1130 PRINT USING B$,P(I,3)
1140 NEXT I
1150 PRINT
1160 PRINT TAB(15):D$(5):TAB(29):D$(6):TAB(43):D$(7):TAB(57):D$(8)
1170 FOR I=0 TO Y
1180 PRINT TAB(15):
1190 PRINT USING B$,H(I,3):
1200 PRINT TAB(29):
1210 PRINT USING B$,H(I,4):
1220 PRINT TAB(43):
1230 PRINT USING B$,H(I,5):
1240 PRINT TAB(57):
1250 PRINT USING B$,H(I,6)
1260 NEXT I
1270 PRINT
1280 PRINT TAB(15):D$(9):TAB(29):D$(12):TAB(43):D$(10):TAB(57):D$(11)
1290 FOR I=0 TO Y
1300 PRINT TAB(15):
1310 PRINT USING B$,T(I,17):
1320 PRINT TAB(29):
1330 PRINT USING B$,T(I,5):
1340 PRINT TAB(43):
1350 PRINT USING B$,T(I,15):
1360 PRINT TAB(57):
1370 PRINT USING B$,T(I,16)
1380 NEXT I
1390 PRINT
1400 REM LINES 1400-1680
1410 REM INPUT OF CALCULATION REQUIREMENTS
1420 REM CALCULATION OF RE AND PR
1430 PRINT'ONE TEMPERATURE,FIRST RUN NUMBER IS':
1440 INPUT O2
1450 PRINT'ONE TEMPERATURE,LAST RUN NUMBER IS':
1460 INPUT Y2
1470 G1=0
1480 FOR I=O2 TO Y2
1490 D(I,0)=100/((2.1482*((T(I,16)-8.435)+((8078.4+((T(I,16)-8.435)^2))^0.5)))-120)
1500 O(I,3)=7741.92*D*U(I,2)*D(I,5)/D(I,0)
1510 O(I,1)=0.00587*(1+(0.00281*(T(I,16)-20)))/0.017307
1520 G(I,1)=C(I,5)*D(I,0)*2.4190883/O(I,1)
1530 G1=G1+G(I,1)
1540 NEXT I
1550 FOR I=O2 TO Y2
```

Appendix A.5 Continued

```
1560 G(I,2)=G1/(Y2+1-02)
1570 NEXT I
1580 PRINT'DO YOU WANT TO INCLUDE MORE RESULTS':
1590 INPUT G$(1)
1600 IF G$(1)='YES' GO TO 1430
1610 PRINT'CHOSEN PRANDTL NUMBER EXPONENT IS':
1620 INPUT Z9
1630 PRINT'DO YOU WANT TO USE MEAN PRANDTL NUMBERS':
1640 INPUT G$(2)
1650 PRINT'RE EXPONENT IS':
1660 INPUT F1
1670 PRINT'GEOMETRY:':
1680 INPUT E$
1690 REM LINES 1690-2000
1700 REM LN-LN LINEAR REGRESSION
1710 C=0
1720 C2=0.0001
1730 B4=1000000
1740 G$(4)='NO'
1750 PRINT
1760 PRINT TAB(15):'RESISTANCE ':TAB(29):' INCREMENT ':TAB(43):'  EXPONENT ':TAB(57):'SUM ERS SQ'
1770 Z=0
1780 F=0
1790 W=0
1800 S=0
1810 E=0
1820 C1=0
1830 G=0
1840 Q4=0
1850 FOR I=0 TO Y
1860 IF G$(2)='YES' GO TO 1890
1870 G(I,3)=G(I,1)
1880 GO TO 1900
1890 G(I,3)=G(I,2)
1900 B(I,3)=(1/((1/K(I))-C))
1910 B(I,4)=(LOG(B(I,3)*D1/(12*O(I,1)*(G(I,3)^Z9))))
1920 Z=Z+B(I,4)
1930 Q4=Q4+(B(I,4)^2)
1940 F=F+(LOG(O(I,3)))
1950 W=W+((LOG(B(I,3)*D1/(12*O(I,1)*(G(I,3)^Z9))))*(LOG(O(I,3))))
1960 G=G+((LOG(O(I,3)))^2)
1970 NEXT I
1980 X=(Y+1-0)
1990 E=((X*W)-(F*Z))/((X*G)-(F^2))
2000 C1=((G*Z)-(W*F))/((X*G)-(F^2))
2010 REM LINES 2010-2290
2020 REM COMPARISON OF EXPTL. AND CALCULATED RESULTS
2030 FOR I=0TO Y
2040 S(I,1)=(B(I,4)-(C1+(E*LOG(O(I,3)))))
2050 S=S+(S(I,1)^2)
2060 NEXT I
2070 PRINT TAB(15):
2080 PRINT USING B$,C:
2090 PRINT TAB(29):
2100 PRINT USING B$,C2:
2110 PRINT TAB(43):
2120 PRINT USING B$,E:
2130 PRINT TAB(57):
2140 PRINT USING B$,S
2150 IF G$(4)='YES' GO TO 2270
2160 IF ABS(E-F1)<X8 GO TO 2270
2170 IF E<F1 GO TO 2250
2180 GO TO 2210
2190 IF C2<X9 GO TO 2270
2200 IF S<B4 GO TO 2240
2210 C=C-C2
2220 C2=C2/10
2230 GO TO 1770
2240 B4=S
2250 C=C+C2
2260 GO TO 1770
2270 GOSUB 2720
2280 PRINT LIN(4)
2290 GOSUB 3030
2300 REM LINES 2300-2400
2310 REM DECISIONS ON NEW CALCULATION METHOD
2320 PRINT'TRY ANOTHER RE AND/OR PR EXPONENT':
2330 INPUT G$(3)
2340 IF G$(3)='YES' GO TO 1610
2350 PRINT'DO YOU WANT TO STATE THE RESISTANCE':
2360 INPUT G$(4)
```

Appendix A.5 Continued

```
2370 IF G$(4)='NO' GO TO 2410
2380 PRINT'RESISTANCE ,C, IS':
2390 INPUT C
2400 GO TO 1750
2410 REM LINES 2410-2510
2420 REM FILE CALCULATED DATA
2430 DEFINE FILE#4='DAY5CA-6010', ASC SEP,500
2440 IF O=01 GO TO 2480
2450 FOR I=01 TO (O-1)
2460 READ #4,T(I,5),T(I,13),T(I,16),K(I),U(I,2)
2470 NEXT I
2480 FOR I=O TO Y
2490 WRITE #4,T(I,5),T(I,13),T(I,16),K(I),U(I,2)
2500 NEXT I
2510 CLOSE #4
2520 STOP
2530 REM SUBROUTINE LINES 2530-2660
2540 REM ANNULUS FLUID FLOWRATE
2550 Y(1,1)=0.002911610712545
2560 Y(2,1)=1.089821240896E-5
2570 Y(3,1)=0.0007601237919062
2580 Y(4,1)=-6.3082666912362-7
2590 Y(5,1)=9.7547162312142-6
2600 Y(6,1)=-2.2316818171222-8
2610 Y(7,1)=-7.1418425395822-8
2620 Y(8,1)=1.1914734199262-8
2630 Y(9,1)=-2.138529076046E-10
2640 Q(I,7)=Y(1,1)+(Y(2,1)*T(I,4))+(Y(3,1)*Z(I))+(Y(4,1)*T(I,4)*Z(I))+(Y(5,1)*(Z(I)^2))+(Y(6,1)*T(I,4)*(Z(I)^2))
2650 Q(I,3)=Q(I,7)+(Y(7,1)*(T(I,4)^2))+(Y(8,1)*(T(I,4)^2)*Z(I))+(Y(9,1)*(T(I,4)^2)*(Z(I)^2))
2660 RETURN
2670 REM SUBROUTINE LINES 2670-2710
2680 REM DENSITY AND SPECIFIC HEAT AT DUMMY TEMPERATURE,T
2690 R=1-((((T-3.9863)^2)*(T+288.9414))/(508929.2*(T+68.12963)))
2700 C3=1
2710 RETURN
2720 REM SUBROUTINE LINES 2720-3020
2730 REM PRINT OUT OF RESULTS AND COMPARISON
2740 PRINT LIN(4)
2750 PRINT'DATA INPUTS:'
2760 PRINT'RESISTANCE STATED:':G$(4)
2770 PRINT'GEOMETRY:':E$
2780 PRINT LIN(2)
2790 PRINT TAB(5):D$(13):TAB(19):D$(19):TAB(33):D$(14):TAB(47):D$(15):TAB(61):D$(16)
2800 F2=0
2810 F3=0
2820 FOR I=O TO Y
2830 B(I,5)=EXP(B(I,4))
2840 S(I,2)=EXP(C1+(E*LOG(O(I,3))))
2850 B(I,0)=(S(I,2)-B(I,5))*100/B(I,5)
2860 PRINT TAB(5);
2870 PRINT USING B$,H(I,7);
2880 PRINT TAB(19);
2890 PRINT USING B$,O(I,3);
2900 PRINT TAB(33);
2910 PRINT USING B$,B(I,5);
2920 PRINT TAB(47);
2930 PRINT USING B$,S(I,2);
2940 PRINT TAB(61);
2950 PRINT USING Z$(2),B(I,0)
2960 F2=F2+(B(I,0)^2)
2970 F3=F3+ABS(B(I,0))
2980 NEXT I
2990 PRINT
3000 PRINT'LOG-LOG REGRESSION LINE IS':
3010 PRINT'(NU/PR"':Z9:')=':EXP(C1):'*(RE"':E:')'
3020 RETURN
3030 REM SUBROUTINE LINES 3030-3810
3040 REM REGRESSION ANALYSIS USING STUDENTS T-DISTRIBUTION
3050 REM VALUES OF T READ FROM FILE
3060 REM OPTION TO FILE EXPERIMENTAL DATA IS GIVEN
3070 DEFINE FILE#7='T-DIST-6010'
3080 FOR K=1 TO 33
3090 READ #7,A(K)
3100 NEXT K
3110 CLOSE #7
3120 IF (X-2)>120 GO TO 3180
3130 IF (X-2)>60 GO TO 3200
3140 IF (X-2)>40 GO TO 3220
3150 IF (X-2)>30 GO TO 3240
3160 X7=A(X-2)
3170 GO TO 3250
```

Appendix A.5 Continued

```
3180 X7=A(33)
3190 GO TO 3250
3200 X7=A(32)
3210 GO TO 3250
3220 X7=A(31)
3230 GO TO 3250
3240 X7=A(30)
3250 F4=(F3/X)
3260 F5=((E2/X)^0.5)
3270 X6=((1/X)+(((F/X)^2)/(G-((F/X)*F))))^0.5
3280 X5=X7*((S/(X-2))^0.5)*X6
3290 X4=((G-(F*F/X))^(-0.5))
3300 X3=X7*((S/(X-2))^0.5)*X4
3310 Q3=(W-(F*Z/X))/(((G-(F*F/X))^0.5)*((Q4-(Z*Z/X))^0.5))
3320 Q2=Q3^2
3330 F6=C1-X5
3340 Q6=EXP(F6)
3350 F7=C1+X5
3360 Q7=EXP(F7)
3370 F8=E-X3
3380 F9=E+X3
3390 Q5=EXP(C1)
3400 PRINT TAB(15):'RESULTS OF REGRESSION ANALYSIS'
3410 PRINT LIN(2)
3420 PRINT TAB(15):'Z...SUM OF LOG(NU)':TAB(50):Z
3430 PRINT TAB(15):'F...SUM OF LOG(RE)':TAB(50):F
3440 PRINT TAB(15):'W...SUM OF LOG(NU)*LOG(RE)':TAB(50):W
3450 PRINT TAB(15):'G...SUM OF (LOG(RE)^2)':TAB(50):G
3460 PRINT TAB(15):'X...TOTAL NUMBER OF RUNS USED':TAB(50):X
3470 PRINT TAB(15):'S...SUM OF (DEVIATIONS^2)':TAB(50):S
3480 PRINT TAB(15):'C...OUTER RESISTANCE TO TRANSFER':TAB(50):C
3490 PRINT TAB(15):'E...SLOPE OF REGRESSION LINE':TAB(50):E
3500 PRINT TAB(15):'C1...LOG(CONST) IN NU EQUATION':TAB(50):C1
3510 PRINT TAB(15):'X7...T(5) IN CONFIDENCE ANALYSIS':TAB(50):X7
3520 PRINT TAB(15):'X6...MULT. IN LOG(CONST) ANALYSIS':TAB(50):X6
3530 PRINT TAB(15):'X4...MULT. IN SLOPE ANALYSIS':TAB(50):X4
3540 PRINT TAB(15):'X5...INTERVAL ON LOG(CONST':TAB(50):X5
3550 PRINT TAB(15):'X3...INTERVAL ON SLOPE':TAB(50):X3
3560 PRINT TAB(15):'F6...MIN. LOG(CONST)':TAB(50):F6
3570 PRINT TAB(15):'F7...MAX. LOG(CONST)':TAB(50):F7
3580 PRINT TAB(15):'Q6...MIN. CONST':TAB(50):Q6
3590 PRINT TAB(15):'Q7...MAX. CONST':TAB(50):Q7
3600 PRINT TAB(15):'Q5...REGRESSION CONST':TAB(50):Q5
3610 PRINT TAB(15):'F8...MIN.SLOPE':TAB(50):F8
3620 PRINT TAB(15):'F9...MAX.SLOPE':TAB(50):F9
3630 PRINT TAB(15):'Q4...SUM OF (LOG(NU)^2)':TAB(50):Q4
3640 PRINT TAB(15):'Q3...CORRELATION COEFFICIENT/R':TAB(50):Q3
3650 PRINT TAB(15):'Q2...R^2':TAB(50):Q2
3660 PRINT TAB(15):'F4...AV. ABS. DEV.':TAB(50):F4
3670 PRINT TAB(15):'F5...R.M.S. ABS. DEV.':TAB(50):F5
3680 PRINT LIN(2)
3690 PRINT'FILE RESULTS':
3700 INPUT G$(5)
3710 IF G$(5)='NO' GO TO 3810
3720 DEFINE FILE#6='DAY5FA-6010', ASC SEP,50
3730 IF O=01 GO TO 3770
3740 FOR I=01 TO (O-1)
3750 READ #6,O(I,3),B(I,5)
3760 NEXT I
3770 FOR I=O TO Y
3780 WRITE #6,O(I,3),B(I,5)
3790 NEXT I
3800 CLOSE #6
3810 RETURN
3820 END
```

Appendix A.6

The data file (T-DIST-6010) which contains the values of "t_1" that are obtained from Student's t-distribution, see Perry and Chilton (97, p. 1-40)

This data file is used by the computer programs FRICTION-6010 and HEAT2-6010 to calculate the 95% confidence intervals on the regression constants and slopes. The data is shown as it is arranged in the computer file.

```
12.706
4.303
3.182
2.776
2.571
2.447
2.365
2.306
2.262
2.228
2.201
2.179
2.160
2.145
2.131
2.120
2.110
2.101
2.093
2.086
2.08
2.074
2.069
2.064
2.06
2.056
2.052
2.048
2.045
2.042
2.021
2.000
1.980
1.960
```

Appendix A.7

Definitions of the symbols in the computer programs used for the analysis of the experimental data

Definitions of print formats are not considered.

E, F, and H refer to the computer programs 'EX-6010', 'FRICTION-6010', and 'HEAT2-6010', respectively.

Symbol	Program	Definition
A	E	Cross sectional area of tube wall, ins^2
A	H	Cross sectional area of tube wall, ft^2
A$	H	Tube material
A$(1)	F	Answer to 'IS DATA ON FILE ?'
A$(2)	F	Name of file #2
A$(4)	E	Answer to 'DO YOU WANT A PRINT OUT OF REFERENCE DATA ?'
A$(5)	E	Tube material
A(K)	F,H	Appropriate value of t_1 from Student's t-distribution
A(I,K)	E	Ratio of experimental and reference friction factor
B4	H	Sum of the squares of the deviations of the calculated and experimental values of $\ln(Nu/Pr^{0.4})$
B(I,0)	H	Percentage difference of the experimental and calculated values of $(Nu/Pr^{0.4})$
B(I,3)	H	(dh/d_o), Btu ft^{-2} hr^{-1} $^oF^{-1}$
B(I,4)	H	$\ln(Nu/Pr^{Z9})$
B(I,5)	H	(Nu/Pr^{Z9})
C	E	Specific heat capacity, Btu lb^{-1} $^oF^{-1}$
C	H	Tube wall, scale, and annulus, fluid resistances to heat transfer, ft^2 hr ^oF Btu^{-1}
C1	F	Logarithm of the constant in the friction factor equation
C1	H	Logarithm of the constant in the heat transfer factor equation

Symbol	Program	Definition
C2	H	Incremental change in C, ft^2 hr ^oF Btu^{-1}
C3	H	Specific heat capacity, Btu lb^{-1} $^oF^{-1}$
C(I,1)	H	Specific heat at T(I,20), Btu lb^{-1} $^oF^{-1}$
C(I,2)	H	Specific heat at the mean of the inlet and outlet temperatures, Btu lb^{-1} $^oF^{-1}$
C(I,4)	H	Specific heat at T(I,15), Btu lb^{-1} $^oF^{-1}$
C(I,5)	H	Specific heat at T(I,16), Btu lb^{-1} $^oF^{-1}$
C(J,0)	E	Maximum ratio of experimental to reference friction factor
C(J,1)	E	Minimum ratio of experimental to reference friction factor
C(J,2)	E	Mean ratio of experimental to reference friction factors
D	E,H	Tube inside diameter, ins
D1	E,H	Tube outside diameter, ins
D(I,0)	H	Fluid viscosity at T(I,16), cP
D(I,1)	E	Fluid density at mean temperature of fluid, g cm^{-3}
D(I,2)	E,H	Fluid density at temperature of the rotameter (R1), g cm^{-3}
D(I,3)	E	Fluid density at the temperature of the manometer, g cm^{-3}
D(I,4)	H	Fluid density at T(I,15), g cm^{-3}
D(I,5)	H	Fluid density at T(I,16), g cm^{-3}
E	E	Tube roughness, ins
E	F,H	Reynolds number exponent
E$\not$	H	Insert configuration
F	E	Dummy friction factor
F	F,H	Temporary sum of ln(Re)
F1	E	Sum of the ratios of the experimental and reference friction factors
F1	H	Stated Reynolds number exponent
F2	E	Temporary maximum value of the ratio of the experimental and reference friction factor

Symbol	Program	Definition
F2	F,H	Sum of the squares of the % differences between the experimental and calculated values
F3	E	Temporary minimum value of the ratio of the experimental and reference friction factor
F3	F,H	Sum of the % differences between the experimental and calculated values
F4	F,H	Average absolute % deviation
F5	F,H	Root mean square absolute % deviation
F6	F,H	Minimum value of the ln(constant in the regression equation)
F7	F,H	Maximum value of the ln(constant in the regression equation)
F8	F,H	Minimum slope of the regression line
F9	F,H	Maximum slope of the regression line
F(I)	E	Experimental friction factor
F(I,1)	F	Experimental friction factor
F(I,2)	F	Calculated friction factor
F(I,3)	F	ln(calculated friction factor)
G	F,H	Temporary sum of $(\ln(Re))^2$
G1	H	Temporary sum of Prandtl numbers
G$(1)	H	Answer to 'DO YOU WANT TO INCLUDE MORE RESULTS ?'
G$(2)	H	Answer to 'DO YOU WANT TO USE MEAN PRANDTL NUMBERS ?'
G$(3)	H	Answer to 'TRY ANOTHER RE AND/OR PR EXPONENT ?'
G$(4)	H	Answer to 'DO YOU WANT TO STATE THE RESISTANCE ?'
G$(5)	F,H	Name of file #6
G(I,1)	H	Prandtl number
G(I,2)	H	Mean Prandtl number
G(I,3)	H	Chosen Prandtl number
H(I,0)	E	Differential head of manometer fluid, cm
H(I,1)	H	Uncorrected heat gain by tube fluid, Btu hr^{-1}

Symbol	Program	Definition
H(I,2)	H	Uncorrected heat loss by annulus side fluid, Btu hr^{-1}
H(I,3)	E,H	Axial conduction loss between T11 and T10, Btu hr^{-1}
H(I,4)	E,H	Axial conduction loss between T10 and T9, Btu hr^{-1}
H(I,5)	E,H	Axial conduction loss between T9 and T8, Btu hr^{-1}
H(I,6)	E,H	Axial conduction loss between T12 and T13, Btu hr^{-1}
H(I,7)	H	Corrected heat gain by tube side fluid, Btu hr^{-1}
H(I,8)	H	Corrected heat loss by annulus fluid, Btu hr^{-1}
I	E,F,H	Run number on data file
J	E	Reference number for the friction factor equation
J = 1	E	Colburn, equation (1.4)
J = 2	E	Blasius, equation (1.1) with a constant of 0.0396
J = 3	E	Drew et. al., equation (1.5)
J = 4	E	Colebrook, equation (1.11)
J = 5	E	Nikuradse, equation (1.7)
J = 6	E	Rouse, equation (1.10)
K	F,H	Reference number for t_1 in t-distribution
K(I)	H	Overall heat transfer coefficient, Btu ft^{-2} hr^{-1} $^oF^{-1}$
K(I,J)	E	Reference friction factor
L	E	Dummy length, either L1 or L3, ins
L	H	Heated length of tube
L1	E	Packed length of tube, ins
L3	E	Length of tube between pressure tappings, ins
M	E	Number of reference friction factor equations
M(I)	E,H	Scale reading on rotameter (R1)

Symbol	Program	Definition
N(I)	E,H	Run number
O	E,F,H	First run number, relative to position in data file
O1	E,F,H	First run number on data file
O2	H	First run number to be considered in one set of data
O(I,1)	H	Fluid thermal conductivity, Btu ft^{-1} hr^{-1} $^{o}F^{-1}$
O(I,3)	E	Tube wall thermal conductivity at T(I,19), Btu ft^{-1} hr^{-1} $^{o}F^{-1}$
O(I,4)	E	Tube wall thermal conductivity at T(I,18), Btu ft^{-1} hr^{-1} $^{o}F^{-1}$
O(I,5)	E	Tube wall thermal conductivity at T(1,11), Btu ft^{-1} hr^{-1} $^{o}F^{-1}$
O(I,6)	E	Tube wall thermal conductivity at T(I,12), Btu ft^{-1} hr^{-1} $^{o}F^{-1}$
P	E	Empty tube length correction for pressure drop, psi
P(I)	E	Pressure drop corrected for end effects, psi
P(I,1)	H	Ratio of corrected heat output and heat input
P(I,2)	H	Ratio of uncorrected heat output and heat input
P(I,3)	H	Ratio of axial conduction losses and heat input
Q2	F,H	Square of the correlation coefficient i.e. R^2
Q3	F,H	Correlation coefficient $(R^2)^{0.5}$
Q4	F,H	Sum of the squares of ln(friction factor or heat transfer factor)
Q5	F,H	Regression constant in least squares equation
Q6	F,H	Minimum constant (95% confidence) in regression equation

Symbol	Program	Definition
Q7	F,H	Maximum constant (95% confidence) in regression equation
Q(I,1)	E	Volumetric flowrate of tube side fluid at T(I,20), $ft^3\ s^{-1}$
Q(I,2)	E,H	Volumetric flowrate of tube side fluid at T(1,25), $ft^3\ s^{-1}$
Q(I,3)	E	Sum of first six terms in rotameter calibration equation, $ft^3\ s^{-1}$
Q(I,3)	H	Volumetric flowrate of annulus fluid at T(I,4), $ft^3\ s^{-1}$
Q(I,5)	H	Volumetric flowrate of tube side fluid at T(I,16), $ft^3\ s^{-1}$
Q(I,7)	H	Sum of the first six terms in the rotameter (R2) calibration equation, $ft^3\ s^{-1}$
R	E,H	Dummy fluid density, g cm^{-3}
R(I)	E,F,H	Mean Reynolds number between the pressure tappings
S	F,H	Sum of the squares of S(I,1)
S(I)	E	Specific gravity of the manometer fluid at T(I,6)
S(I,1)	F,H	Deviations of the logarithms of the calculated and experimental friction, or heat transfer, factors
S(I,2)	F	Percentage deviation of the calculated and experimental friction factor
S(I,2)	H	Calculated heat transfer factor
S(I,4)	H	Differential head of manometer fluid, cm
S(I,5)	H	Specific gravity of manometer fluid at T(I,6)
T	E,H	Dummy temperature, ^oC
T(I,1)	E,H	T1, ^oC
T(I,2)	E,H	T2, ^oC
T(I,3)	E,H	T3, ^oC
T(I,4)	E,H	T4, ^oC
T(I,5)	H	Corrected log mean temperature difference, ^oC

Symbol	Program	Definition
T(I,6)	E,H	Ambient air temperature, ^{o}C
T(I,7)	E,H	T8, ^{o}C
T(I,8)	E,H	T9, ^{o}C
T(I,9)	E,H	T11, ^{o}C
T(I,10)	E,H	T10, ^{o}C
T(1,11)	E,H	(T8 + T9)/2, ^{o}C
T(I,12)	E,H	(T12 + T13)/2, ^{o}C
T(I,13)	H	Corrected value of T1, ^{o}C
T(I,14)	E,H	Corrected value of T2, ^{o}C
T(I,15)	H	Average annulus fluid temperature, ^{o}C
T(I,16)	H	Corrected average tube fluid temperature, ^{o}C
T(I,17)	H	Uncorrected log mean temperature difference, ^{o}C
T(I,18)	E,H	(T9 + T10)/2, ^{o}C
T(I,19)	E,H	(T11 + T12)/2, ^{o}C
T(I,20)	E,H	Average fluid temperature between pressure tappings
T(I,21)	E	Corrected value of T1, ^{o}C
T(I,22)	E,H	T12, ^{o}C
T(I,23)	E,H	T13, ^{o}C
T(I,25)	E,H	T7, ^{o}C
U(I)	E	Mean fluid velocity between the pressure tappings, ft s^{-1}
U(I,1)	H	Mean fluid velocity between the pressure tappings, ft s^{-1}
U(I,2)	H	Mean fluid velocity along the heated length, ft s^{-1}
V	E	Dummy fluid viscosity, cP
V(I)	E,H	Mean fluid viscosity between the pressure tappings, cP
W	E	(e/(3.7 d))
W	F,H	Sum of the products of ln(Re) and ln(Ø or Nu/Pr^{Z9})
W(I,4)	E	$1.255/(Re\ (2Ø)^{0.5})$
W(I,5)	E	$\log_{10}(Re\ (2Ø)^{0.5})$
W(I,6)	E	$\log_{10}(Re\ (2Ø)^{0.5})$

Symbol	Program	Definition
X	E	Reference number for the mode of operation
X	F,H	Number of experimental tests considered
X1	E	Distance between T11 and T10, ft
X2	E	Distance between T10 and T9, ft
X3	E	Distance between T9 and T8, ft
X3	F,H	95% confidence interval on the regression slope
X4	E	Distance between T12 and T13, ft
X4	F,H	A multiplier in the slope analysis
X5	F,H	Interval on ln(regression constant)
X6	F,H	A multiplier in the regression constant analysis
X7	F,H	Appropriate value of t_1 from t-distribution
X8	H	Error criterion on the Re exponent
X9	H	Error criterion on the heat transfer resistance, ft^2 hr ^oF Btu^{-1}
Y	E,F,H	Last run number, relative to position in data file
Y1	E,F,H	Last run number on data file
Y(1 to 9,1)	E	Constants in the calibration equation for rotameter (R1)
Y(1 to 9,1)	H	Constants in the calibration equation for rotameter (R2)
Z	F,H	Sum of ln(ϕ or Nu/Pr^{Z9})
Z9	H	Prandtl number exponent
Z(I)	E,H	Scale reading on rotameter (R2)

Appendix A.8

Samples of the raw experimental data

This appendix presents samples of the raw experimental data which has been processed using the computer programs. Experimental data obtained under isothermal conditions is referenced by line number 620 of the prcgram EX-6010, see Appendix A.3. Data obtained under heating conditions is referenced by line numbers 620 and 640 in EX-6010, and by line numbers 460 and 490 in HEAT2-6010, see Appendix A.5. (See Appendix A.7 for the definitions of the symbols used in these programs). To produce a clear presentation the data "read" by line numbers 620 and 640, in EX-6010, will be referred to as "File A" and "File B", respectively. The title of each table in this appendix states the configuration number of the tube, the conditions, and the denotation/table number of the regression equation produced by using the data.

The data in Table A.8.n, where n = a natural number, were used to produce the processed results that are presented in Table A.9.n. The data in Table A.8.2 were used to produce friction factor and heat transfer factor results. These processed results are presented in Table A.9.2 (friction factor) and Table A.9.4 (heat transfer factor). For the reason of uniformity in presentation the raw data of these tests have been specified by two table numbers i.e. A.8.2 and A.8.4. The data in Table A.8.9 were similarly used to produce friction factor (Table A.9.9) and heat transfer factor (Table A.9.12) results. Here again the raw data is specified by two table numbers i.e. A.8.9 and A.8.12.

****
TABLE NO.A.8.1 CONFIGURATION O (ISOTHERMAL DATA)
(DENOTATION H OF TABLE 5.4)
****

****
* FILE A *
****

1,5.15,2,1.594,21.07,20.88,0,0,21.95,19.63
2,9.65,4,1.594,21.15,20.78,0,0,22,19.5
3,15.6,6,1.594,21.49,20.93,0,0,22.05,19.85
4,22.95,8,1.594,21.78,21.34,0,0,22.15,20.25
5,31.65,10,1.594,21.73,21.34,0,0,22.25,20.4
6,42,12,1.594,21.46,21.27,0,0,22.25,20.3
7,66.75,16,1.594,21.54,21.34,0,0,22.4,20.63
8,97.95,20,1.594,21.83,21.63,0,0,22.45,21.1
9,134,24,1.593,21.88,21.66,0,0,22.6,21.29
10,134.3,24,1.593,21.88,21.59,0,0,22.6,21.22
11,97.85,20,1.593,21.83,21.68,0,0,22.55,21.17
12,66.75,16,1.593,21.51,21.32,0,0,22.5,20.65
13,42.05,12,1.594,21.44,21.24,0,0,22.3,20.45
14,31.65,10,1.594,21.61,21.34,0,0,22.35,20.35
15,22.95,8,1.594,21.63,21.29,0,0,22.15,20.3
16,15.6,6,1.594,21.37,21,0,0,22.1,19.88
17,9.6,4,1.594,21.12,20.75,0,0,22,19.68
18,5.15,2,1.594,21.32,20.85,0,0,22,19.48
19,5.15,2,1.594,21.29,20.88,0,0,22,19.4
20,9.65,4,1.594,21.12,20.78,0,0,22.05,19.5
21,15.6,6,1.594,21.39,21.02,0,0,22.1,19.8
22,22.95,8,1.594,21.61,21.29,0,0,22.25,20.13
23,31.65,10,1.594,21.54,21.37,0,0,22.3,20.35
24,42.1,12,1.594,21.44,21.27,0,0,22.3,20.45
25,66.8,16,1.593,21.51,21.37,0,0,22.5,20.5
26,97.9,20,1.593,21.88,21.68,0,0,22.55,21.02
27,134.25,24,1.593,21.85,21.56,0,0,22.65,21.17

****
TABLE NO.A.8.2 CONFIGURATION O (HEATING DATA)
(DENOTATION K OF TABLE 5.5)
****

****
* FILE A *
****

1,4.1,2,1.594,30.54,39.39,82.32,77.55,21.8,32.18
2,4.1,2,1.594,30.66,39.44,82.41,77.62,21.8,32.4
3,4.15,2,1.595,30.68,39.59,82.39,77.55,21.55,32.6
4,7.95,4,1.594,31.32,38.78,82.9,77.14,22.4,33.29
5,7.95,4,1.593,31.27,38.76,82.85,77.07,22.55,33.37
6,8,4,1.593,31.29,38.8,82.83,77.1,22.6,33.46
7,13.1,6,1.593,31.76,38.27,83.29,76.66,23.05,33.95
8,13.15,6,1.593,31.78,38.32,83.24,76.66,23.05,33.93
9,13.2,6,1.593,31.76,38.27,83.29,76.68,23.05,33.93
10,19.75,8,1.593,32.2,37.9,83.6,76.34,23,34.24
11,19.8,8,1.593,32.13,37.85,83.62,76.41,23,34.32
12,19.85,8,1.593,32.1,37.83,83.62,76.37,23,34.32
13,27.9,10,1.592,32.5,37.63,83.95,76.24,23.75,34.46
14,27.7,10,1.592,32.5,37.6,83.81,76.02,23.85,34.44
15,27.9,10,1.592,32.48,37.58,83.9,76.22,23.85,34.49
16,37.1,12,1.593,32.75,37.2,84.02,75.86,23.1,34.07
17,37.05,12,1.593,32.75,37.23,84.02,75.88,23.2,34.1
18,37.05,12,1.593,32.83,37.33,84.02,75.81,23.2,34.32
19,59.7,16,1.591,33.15,36.93,84.49,75.6,24.05,34.51
20,59.75,16,1.591,33.17,36.95,84.39,75.55,24.2,34.66
21,59.75,16,1.591,33.12,36.9,84.51,75.55,24.2,34.59
22,88.55,20,1.591,33.41,36.61,84.76,75.19,24.5,34.71
23,88.6,20,1.591,33.44,36.68,84.78,75.29,24.5,34.73
24,88.65,20,1.591,33.32,36.54,84.78,75.29,24.5,34.66
25,122.25,24,1.591,33.56,36.32,84.9,74.93,24.45,34.9
26,122.25,24,1.591,33.59,36.34,84.9,75.02,24.55,34.85
27,122.25,24,1.591,33.54,36.32,85,75.14,24.55,34.73

****
* FILE B *
****

41.22,31.22,30.07,29.78,67.32,43.6,10
41.34,31.34,30.1,29.98,67.59,43.71,10
41.44,31.51,30.22,30.1,67.9,43.86,10
40.46,32,30.73,30.78,67.15,42.37,10
40.29,31.95,30.76,30.78,67.15,42.32,10
40.37,32,30.73,30.76,67.07,42.34,10
39.8,32.48,31.15,31.22,66.88,41.39,10
40.05,32.5,31.2,31.27,66.86,41.46,10
39.98,32.5,31.2,31.27,66.83,41.46,10
39.61,32.9,31.56,31.73,66.5,40.76,10
39.56,32.93,31.59,31.71,66.6,40.76,10
39.49,32.88,31.56,31.71,66.6,40.73,10
39.15,33.17,31.93,32.05,66.29,40.22,10
39.17,33.2,31.88,32,66.24,40.15,10
39.24,33.24,31.98,32.08,66.14,40.27,10
39.02,32.98,32.08,32.08,65.39,39.32,10
39.07,33.02,32.13,32.2,65.49,39.32,10
39.17,33.17,32.18,32.35,65.73,39.54,10
38.73,33.59,32.73,32.73,65.61,39,10
38.9,33.71,32.83,32.85,65.61,39.02,10
38.76,33.51,32.73,32.73,65.49,38.95,10
38.88,33.9,33.02,33.02,65.44,38.68,10
38.8,33.93,33.1,33.1,65.51,38.63,10
38.8,33.83,33,32.98,65.54,38.51,10
38.66,34.07,33.2,33.27,65.56,38.29,10
38.61,34.05,33.05,33.2,65.54,38.24,10
38.63,34.02,33.05,33.17,65.54,38.24,10

****
TABLE NO.A.8.3 CONFIGURATION O (HEATING DATA)
(DENOTATION I OF TABLE 5.6)
****

****
* FILE A *
****

1,4.2,2,1.592,30.83,39.2,82.9,77.17,23.3,32.98
2,4.25,2,1.592,30.88,39.24,82.9,77.19,23.3,33.12
3,4.25,2,1.592,30.85,39.2,82.83,77.14,23.25,33.1
4,8.15,4,1.592,31.51,38.61,83.38,76.66,23.9,33.63
5,8.15,4,1.592,31.49,38.59,83.36,76.59,23.9,33.59
6,8.2,4,1.592,31.39,38.44,83.33,76.61,23.85,33.61
7,13.2,6,1.591,32.03,37.95,83.74,76.37,24.45,34.02
8,13.25,6,1.591,31.98,37.93,83.67,76.17,24.55,34.02
9,13.3,6,1.591,32,37.9,83.74,76.32,24.5,34.2
10,19.75,8,1.59,32.45,37.63,84.1,76,24.75,34.34
11,19.75,8,1.59,32.5,37.73,84.07,75.95,24.75,34.46
12,19.8,8,1.59,32.45,37.6,84,76,24.7,34.44
13,27.55,10,1.59,32.65,37.25,84.32,75.62,24.95,34.37
14,27.6,10,1.59,32.68,37.28,84.32,75.67,24.9,34.29
15,27.55,10,1.59,32.73,37.25,84.32,75.79,25,34.41
16,36.7,12,1.593,33.05,37.03,84.46,75.57,23.15,34.07
17,36.75,12,1.592,32.98,37,84.44,75.52,23.3,34.02
18,36.75,12,1.592,32.98,37.03,84.46,75.48,23.4,34.12
19,58.9,16,1.592,33.44,36.73,84.9,75.26,23.6,34.24
20,58.95,16,1.592,33.27,36.56,84.78,75.21,23.8,34.1
21,59.05,16,1.592,33.39,36.76,84.83,75.07,23.85,34.24
22,87.3,20,1.592,33.56,36.39,85.1,74.81,23.75,34.39
23,87.4,20,1.592,33.51,36.37,85.26,74.98,23.8,34.37
24,87.35,20,1.592,33.54,36.41,85.19,74.86,23.85,34.37
25,120.7,24,1.592,33.8,36.27,85.36,74.76,23.75,34.49
26,120.8,24,1.592,33.78,36.24,85.21,74.6,23.75,34.39
27,120.7,24,1.591,33.76,36.17,85.26,74.81,23.95,34.39

****
* FILE B *
****

40.54,31.83,30.71,30.78,66.4,42.85,7.5
40.59,31.85,30.76,30.78,66.57,42.93,7.5
40.63,31.88,30.73,30.76,66.67,42.85,7.5
39.98,32.63,31.34,31.46,66.02,41.56,7.5
39.78,32.5,31.2,31.41,65.95,41.37,7.5
39.76,32.45,31.15,31.25,66.05,41.17,7.5
39.46,33.02,31.76,31.98,65.39,40.29,7.5
39.44,33,31.73,31.83,65.49,40.22,7.5
39.46,33.02,31.83,31.91,65.49,40.49,7.5
39.24,33.44,32.25,32.45,65.05,39.63,7.5
39.32,33.51,32.33,32.53,65.17,39.68,7.5
39.2,33.46,32.28,32.58,65.17,39.66,7.5
39.12,33.83,32.48,32.68,64.9,39.32,7.5
39.12,33.85,32.53,32.68,64.88,39.29,7.5
39.22,33.85,32.53,32.75,64.88,39.32,7.5
39.02,33.76,32.78,32.2,63.78,38.95,7.5
39,33.71,32.7,32.1,63.78,38.85,7.5
38.93,33.68,32.68,32.18,63.76,38.83,7.5
38.95,34.15,33.17,32.63,63.66,38.54,7.5
38.78,33.98,33,32.5,63.73,38.39,7.5
38.9,34.17,33.1,32.53,63.76,38.41,7.5
38.8,34.41,33.32,32.85,63.71,38.17,7.5
38.83,34.41,33.27,32.8,63.73,38.15,7.5
38.83,34.41,33.29,32.83,63.73,38.15,7.5
38.76,34.63,33.56,33.07,63.61,37.7,7.5
38.78,34.71,33.56,33.07,63.49,37.73,7.5
38.78,34.68,33.56,33.07,63.59,37.73,7.5

****
TABLE NO.A.8.4 CONFIGURATION O (HEATING DATA)
(DENOTATION K OF TABLE 5.6)
****

****
* FILE A *
****

SEE TABLE NO.A.8.2

****
* FILE B *
****

SEE TABLE A.8.2

****
TABLE NO.A.8.5 CONFIGURATION 0 (HEATING DATA)
(DENOTATION N OF TABLE 5.6)
****

****
* FILE A *
****

1,4.1,2,1.592,30.93,39.12,82.78,77.29,23.45,32.38
2,4.15,2,1.592,30.93,39.1,82.71,77.19,23.55,32.38
3,4.15,2,1.592,30.98,39.15,82.71,77.19,23.6,32.48
4,8.1,4,1.592,31.56,38.37,83.26,76.71,23.8,32.83
5,8.15,4,1.592,31.56,38.39,83.29,76.73,23.85,32.83
6,8.15,4,1.592,31.66,38.46,83.26,76.68,23.9,33.07
7,13.45,6,1.591,32.18,38.05,83.67,76.37,23.95,33.32
8,13.45,6,1.591,32.1,37.98,83.57,76.26,24,33.41
9,13.5,6,1.591,32.1,38.02,83.67,76.27,24.05,33.39
10,20.1,8,1.591,32.38,37.58,84,75.9,24.2,33.76
11,20.15,8,1.591,32.45,37.68,84.1,76.02,24.3,33.78
12,20.2,8,1.591,32.48,37.7,84,75.9,24.35,33.76
13,28.05,10,1.591,32.7,37.3,84.39,75.79,24.4,33.9
14,28.05,10,1.591,32.8,37.43,84.22,75.6,24.55,34
15,28.05,10,1.591,32.68,37.3,84.29,75.62,24.55,33.9
16,37.55,12,1.591,32.93,37,84.51,75.35,24.35,33.76
17,37.6,12,1.591,32.98,37,84.51,75.33,24.45,33.66
18,37.6,12,1.591,32.98,37.05,84.49,75.29,24.5,33.76
19,60.4,16,1.59,33.34,36.68,84.95,75.05,24.7,34.02
20,60.4,16,1.59,33.39,36.76,84.85,74.95,24.85,34.07
21,60.4,16,1.59,33.39,36.76,85.02,75.05,24.85,34.05
22,89.45,20,1.59,33.51,36.37,85.21,74.74,25,34.07
23,89.5,20,1.59,33.51,36.39,85.21,74.71,25,34.12
24,89.5,20,1.59,33.56,36.44,85.24,74.76,25.05,34.29
25,123.5,24,1.59,33.8,36.29,85.5,74.64,25.25,34.49
26,123.55,24,1.59,33.73,36.24,85.45,74.64,25.3,34.39
27,123.5,24,1.59,33.85,36.37,85.5,74.69,25.3,34.44

****
* FILE B *
****

40.61,32.35,30.93,30.56,67.93,42.61,7.5
40.29,32.3,30.85,30.59,68.24,42.61,7.5
40.34,32.33,30.76,30.66,68.19,42.71,7.5
39.37,32.78,31.41,31.2,67.76,41.39,7.5
39.24,32.75,31.37,31.2,67.8,41.34,7.5
39.29,32.88,31.41,31.32,67.78,41.41,7.5
39.22,33.27,31.98,31.8,67.29,40.46,7.5
39.27,33.2,31.95,31.76,67.37,40.59,7.5
39.05,33.22,31.9,31.83,67.27,40.59,7.5
38.95,33.51,32.38,32.15,67.17,39.9,7.5
39.02,33.59,32.45,32.23,67.12,40,7.5
38.78,33.54,32.15,32.18,67.1,39.98,7.5
38.51,33.66,32.53,32.38,66.9,39.34,7.5
38.71,33.78,32.63,32.48,66.86,39.46,7.5
38.46,33.68,32.55,32.45,66.81,39.37,7.5
38.27,33.68,32.68,32.25,66.02,38.68,7.5
38.27,33.68,32.63,32.2,66.12,38.66,7.5
38.29,33.73,32.65,32.15,66.19,38.71,7.5
38.05,34,33.1,32.63,65.83,38.24,7.5
38.12,34.12,33.15,32.68,65.95,38.32,7.5
38.05,34.07,33.12,32.7,65.9,38.24,7.5
38.07,34.27,33.32,32.88,65.85,37.9,7.5
38.02,34.24,33.32,32.93,65.76,37.95,7.5
38.2,34.37,33.41,33.07,65.98,37.98,7.5
38.15,34.63,33.73,33.24,65.93,37.78,7.5
37.98,34.54,33.54,33.22,65.88,37.63,7.5
38.17,34.61,33.61,33.34,65.9,37.73,7.5

****
TABLE NO.A.8.6 CONFIGURATION 1T (ISOTHERMAL DATA)
(DENOTATION A OF TABLE 5.7)
****

****
* FILE A *
****

1,17.45,2,1.594,22.63,22.58,0,0,22,20.23
2,32.15,4,1.594,22.45,22.4,0,0,22,20.3
3,51.1,6,1.594,22.9,22.88,0,0,21.95,21.05
4,74.55,8,1.594,22.63,22.63,0,0,21.95,20.83
5,102.35,10,1.594,22.38,22.35,0,0,22.05,20.9
6,135.65,12,1.594,22.38,22.38,0,0,22,20.95
7,10.15,16,13.5707,22.5,22.53,0,0,21.95,21.24
8,15.1,20,13.5707,22.63,22.63,0,0,22,21.56
9,20.9,24,13.5707,22.58,22.58,0,0,22,21.63
10,20.95,24,13.5707,22.6,22.6,0,0,22,21.66
11,15.1,20,13.5707,22.63,22.63,0,0,22,21.56
12,10.175,16,13.5707,22.55,22.55,0,0,21.95,21.2
13,135.7,12,1.594,22.38,22.38,0,0,22.05,21.07
14,102.35,10,1.594,22.38,22.3,0,0,22.05,20.88
15,74.6,8,1.594,22.6,22.6,0,0,22,20.8
16,51.1,6,1.594,22.9,22.83,0,0,21.95,20.93
17,32.15,4,1.594,22.43,22.38,0,0,22,20.25
18,17.45,2,1.594,22.55,22.5,0,0,22.05,20
19,17.45,2,1.594,22.55,22.45,0,0,22.05,19.9
20,32.15,4,1.594,22.48,22.4,0,0,22,20.4
21,51.1,6,1.594,22.88,22.8,0,0,22,20.7
22,74.6,8,1.594,22.65,22.6,0,0,22.05,20.7
23,102.35,10,1.594,22.4,22.33,0,0,22.1,20.8
24,135.7,12,1.594,22.4,22.35,0,0,22.1,21
25,10.175,16,13.5707,22.58,22.55,0,0,22,21.29
26,15.1,20,13.5707,22.65,22.63,0,0,22.05,21.59
27,20.9,24,13.5707,22.58,22.6,0,0,22,21.66

****
TABLE NO.A.8.7 CONFIGURATION 6K (ISOTHERMAL DATA)
(DENOTATION I OF TABLE 5.8)
****

****
* FILE A *
****
1,12.35,2,13.5699,20.78,20.55,0,0,20.25,19.03
2,23.6,4,13.5699,20.68,20.45,0,0,20.25,19
3,38.55,6,13.5699,20.63,20.4,0,0,20.25,19.2
4,58,8,13.5699,20.65,20.43,0,0,20.25,19.18
5,81.65,10,13.5699,20.63,20.4,0,0,20.3,19.25
6,110.4,12,13.5699,20.63,20.33,0,0,20.3,19.3
7,182.1,16,13.5699,20.53,20.3,0,0,20.3,19.35
8,275.95,20,13.57,20.43,20.28,0,0,20.4,19.45
9,388.35,24,13.57,20.38,20.25,0,0,20.45,19.3
10,387.75,24,13.57,20.35,20.25,0,0,20.45,19.85
11,275.8,20,13.57,20.4,20.25,0,0,20.45,19.48
12,182.3,16,13.5699,20.55,20.33,0,0,20.35,19.35
13,110.4,12,13.5699,20.5,20.23,0,0,20.35,19.33
14,81.5,10,13.5699,20.5,20.3,0,0,20.3,19.23
15,57.95,8,13.57,20.45,20.3,0,0,20.5,19.08
16,38.5,6,13.57,20.53,20.25,0,0,20.4,19.05
17,23.65,4,13.5699,20.48,20.2,0,0,20.35,18.98
18,12.35,2,13.57,20.53,20.28,0,0,20.5,18.88
19,12.35,2,13.57,20.53,20.2,0,0,20.45,18.93
20,23.65,4,13.57,20.53,20.23,0,0,20.45,19
21,38.6,6,13.57,20.53,20.23,0,0,20.4,19.08
22,57.9,8,13.57,20.45,20.18,0,0,20.5,19.18
23,81.55,10,13.57,20.43,20.18,0,0,20.45,19.2
24,110.4,12,13.57,20.4,20.18,0,0,20.4,19.2
25,182.25,16,13.57,20.4,20.18,0,0,20.45,19.33
26,275.95,20,13.57,20.43,20.28,0,0,20.45,19.38
27,388.15,24,13.57,20.35,20.15,0,0,20.5,19.48

****
TABLE NO.A.8.8 CONFIGURATION 1T (HEATING DATA)
(DENOTATION A OF TABLE 5.9)
****

****
* FILE A *
****
1,15.3,2,1.595,29.83,40.15,83.52,76.44,21.55,32.05
2,15.35,2,1.595,29.8,40.15,83.48,76.39,21.65,32.15
3,15.35,2,1.594,29.88,40.22,83.6,76.49,21.8,32.23
4,28.5,4,1.594,30.8,39.15,84.1,75.98,21.9,32.43
5,28.55,4,1.594,30.8,39.2,84.12,76.07,22,32.55
6,28.55,4,1.594,30.8,39.15,84,75.9,22.05,32.53
7,45.95,6,1.594,31.46,38.49,84.39,75.52,21.95,32.83
8,45.95,6,1.594,31.51,38.59,84.54,75.6,22.1,32.83
9,45.95,6,1.594,31.51,38.54,84.46,75.6,22.2,32.93
10,67.95,8,1.595,31.98,38.07,84.68,75.26,21.5,33.12
11,68,8,1.595,31.93,38.02,84.73,75.31,21.6,33.07
12,67.95,8,1.595,31.9,38.02,84.71,75.31,21.7,33.12
13,93.7,10,1.595,32.28,37.65,84.98,75.1,21.05,33.37
14,93.6,10,1.595,32.28,37.63,85.02,75.12,21.15,33.29
15,93.6,10,1.595,32.3,37.65,84.95,75.02,21.2,33.24
16,126.05,12,1.595,32.63,37.35,85.12,74.9,21.15,33.32
17,126,12,1.595,32.68,37.38,85.1,74.9,21.35,33.32
18,126.05,12,1.594,32.6,37.3,85.12,74.9,21.8,33.32
19,9.6,16,13.5707,33.2,37.03,85.38,74.5,21.9,33.83
20,9.575,16,13.5707,33.07,36.93,85.38,74.55,22,33.68
21,9.575,16,13.5707,33.12,36.98,85.36,74.5,22.05,33.8
22,14.35,20,13.5709,33.39,36.61,85.57,74.26,22.2,33.9
23,14.35,20,13.571,33.39,36.59,85.64,74.26,22.35,33.88
24,14.35,20,13.5711,33.44,36.66,85.74,74.31,22.55,33.9
25,20.05,24,13.5712,33.59,36.34,85.81,74.02,22.6,33.95
26,20.1,24,13.5712,33.54,36.29,85.81,73.98,22.65,33.98
27,20.1,24,13.5714,33.54,36.29,85.93,74.14,22.85,33.98

****
* FILE B *
****
41.27,30.63,29.78,29.8,66.19,40.49,7.5
41.37,30.71,29.56,29.59,66.21,40.51,7.5
41.59,30.78,29.54,29.63,66.24,40.59,7.5
40.51,31.46,30.46,40.49,65.98,39.59,7.5
40.68,31.56,30.61,30.54,66,39.63,7.5
40.41,31.56,30.68,30.61,65.95,39.61,7.5
40.24,32.1,31.29,31.15,65.73,38.98,7.5
40.59,32.23,31.39,31.22,65.68,39.02,7.5
40.66,32.3,31.39,31.02,65.71,39.07,7.5
40.41,32.65,31.98,31.59,65.63,38.63,7.5
40.32,32.6,31.93,31.54,65.59,38.56,7.5
40.32,32.65,31.9,31.51,65.59,38.56,7.5
40.27,32.95,32.28,31.83,65.41,38.24,7.5
40.12,32.93,32.23,31.78,65.56,38.24,7.5
40.15,32.93,32.23,31.78,65.44,38.2,7.5
39.1,32.9,32.63,31.95,62.61,37.88,7.5
39.24,33.02,32.73,32.23,63.83,37.9,7.5
39.15,32.95,32.6,32.18,64.21,37.83,7.5
39.41,33.66,33.22,32.85,64.67,37.48,7.5
39.34,33.59,33.15,32.8,64.57,37.43,7.5
39.17,33.66,33.17,32.85,64.57,37.45,7.5
39.05,33.9,33.46,33.15,64.6,37.15,7.5
38.9,33.88,33.29,33.05,64.48,37.13,7.5
39.1,33.98,33.46,33.12,64.23,37.18,7.5
39.1,34.12,33.66,33.24,64.24,36.78,7.5
39.07,34.15,33.66,33.29,63.95,36.83,7.5
39.15,34,33.59,33.15,64.02,36.68,7.5

****
TABLE NO.A.8.9 CONFIGURATION 6K (HEATING DATA)
(DENOTATION H OF TABLE 5.10)
****

****
* FILE A *
****

1,12.35,2,13.5697,27.17,42.85,84.32,75.81,19.55,35.12
2,12.35,2,13.5697,27.17,42.88,84.34,75.79,19.7,35.05
3,12.35,2,13.5698,27.17,42.9,84.29,75.83,19.75,35.05
4,23.65,4,13.5698,29.07,41.02,84.59,75.4,20,34.98
5,23.65,4,13.5698,29.02,40.93,84.54,75.38,20.1,34.95
6,23.65,4,13.5698,29.05,40.98,84.56,75.36,20.05,35.02
7,38.75,6,13.5699,30.2,39.95,84.85,75.07,20.25,34.9
8,38.75,6,13.57,30.2,39.93,84.93,75.19,20.4,34.78
9,38.75,6,13.57,30.07,39.76,84.85,75.17,20.5,34.76
10,58.1,8,13.5701,30.93,39.1,85.14,74.76,20.8,34.83
11,58.15,8,13.5701,30.88,39.05,85.26,74.98,20.8,34.78
12,58,8,13.5701,30.93,39.05,85.14,74.83,20.8,34.8
13,81.75,10,13.57,31.49,38.51,85.33,74.67,20.35,34.71
14,81.85,10,13.57,31.44,38.49,85.38,74.76,20.55,34.73
15,81.95,10,13.5701,31.49,38.49,85.29,74.71,20.65,34.78
16,110.95,12,13.5697,31.95,38.05,85.43,74.55,19.6,34.39
17,110.9,12,13.5698,31.93,38.02,85.43,74.57,19.85,34.41
18,111,12,13.5698,31.9,38.07,85.47,74.48,19.85,34.59
19,183.1,16,13.5698,32.63,37.53,85.62,74.31,20.1,34.71
20,183.05,16,13.5699,32.6,37.5,85.64,74.38,20.2,34.73
21,183.1,16,13.5699,32.6,37.53,85.67,74.26,20.2,34.78
22,278,20,13.57,32.95,36.98,85.86,74.19,20.6,34.88
23,277.95,20,13.5701,32.88,36.95,85.74,74.1,20.65,34.73
24,277.8,20,13.5701,33,37.02,85.88,74.26,20.65,34.85
25,393.3,24,13.5699,33.32,36.73,85.98,74.12,20.2,34.56
26,393.2,24,13.5699,33.27,36.68,85.98,74.07,20.2,34.51
27,393.3,24,13.5699,33.22,36.66,86,73.98,20.15,34.49

****
* FILE B *
****

38.51,28.38,27.07,27.05,65.63,42.39,10
38.22,28.23,26.95,26.98,65.46,42.44,10
38.44,28.3,26.98,27.05,65.44,42.34,10
38.61,30.15,28.75,28.85,65.07,40.88,10
38.51,30.15,28.68,28.78,65.34,40.76,10
38.54,30.15,28.68,28.78,65.29,40.85,10
38.59,31.17,29.68,29.85,64.93,39.88,10
38.56,31.22,29.71,29.93,64.93,39.88,10
38.44,31.12,29.66,29.85,64.74,39.76,10
38.63,31.9,30.49,30.66,64.76,39.2,10
38.54,31.83,30.41,30.61,64.52,39.17,10
38.61,31.85,30.46,30.66,64.64,39.22,10
38.68,32.43,31.02,31.17,64.43,38.73,10
38.51,32.38,30.95,31.12,64.14,38.68,10
38.68,32.48,31.05,31.22,64.31,38.78,10
38.39,32.55,31.54,31.46,62.98,38.1,10
38.44,32.55,31.51,31.51,63.34,37.98,10
38.41,32.63,31.59,31.54,63.44,38.02,10
38.46,33.27,32.13,32.13,63.34,37.6,10
38.44,33.29,32.23,32.23,63.41,37.6,10
38.51,33.34,32.15,32.25,63.46,37.6,10
38.24,33.76,32.58,32.65,63.51,37.28,10
38.17,33.71,32.55,32.63,63.54,37.2,10
38.24,33.73,32.5,32.63,63.51,37.2,10
38.32,34.07,32.85,33.05,63.49,37.08,10
38.15,33.98,32.83,32.85,63.34,36.95,10
38.22,34,32.9,32.9,63.51,37.08,10

****
TABLE NO.A.8.10 CONFIGURATION 7T (HEATING DATA)
(DENOTATION H OF TABLE 5.11)
****

****
* FILE A *
****

1,45.5,2,1.59,29.05,41.05,84.07,75.86,25.05,33.85
2,45.5,2,1.59,29,41.07,84,75.86,25.15,33.9
3,45.5,2,1.59,29.07,41.1,84.02,75.9,25.15,33.8
4,82.5,4,1.589,30.34,39.71,84.49,75.6,25.5,34.05
5,82.55,4,1.589,30.29,39.76,84.59,75.6,25.5,34.05
6,82.6,4,1.589,30.41,39.8,84.59,75.62,25.5,34.12
7,130.35,6,1.589,31.2,38.98,84.85,75.07,25.45,34.15
8,130.25,6,1.589,31.2,39.02,84.85,75.05,25.5,34.12
9,130.1,6,1.589,31.1,38.93,84.78,74.98,25.5,34.05
10,8.85,8,13.5738,31.71,38.41,85.05,74.79,25.55,34.24
11,8.9,8,13.5738,31.61,38.29,85.05,74.83,25.55,34.17
12,8.9,8,13.5739,31.59,38.27,85.14,74.93,25.6,34.17
13,12.2,10,13.5724,32.13,37.85,85.36,74.6,24.1,34.32
14,12.2,10,13.5724,32.15,37.9,85.38,74.64,24.1,34.32
15,12.2,10,13.5724,32.03,37.83,85.45,74.69,24.1,34.34
16,16.35,12,13.5722,32.48,37.53,85.48,74.57,23.85,34.17
17,16.35,12,13.5723,32.45,37.48,85.45,74.48,23.95,34.22
18,16.35,12,13.5723,32.53,37.55,85.48,74.5,24,34.29
19,26.4,16,13.5724,32.98,37.03,85.79,74.14,24.15,34.41
20,26.4,16,13.5725,32.98,37.03,85.74,74.1,24.25,34.51
21,26.4,16,13.5726,32.98,37.05,85.81,74.19,24.3,34.63
22,39.4,20,13.5729,33.39,36.78,85.98,73.98,24.6,34.66
23,39.35,20,13.5729,33.32,36.68,85.95,74,24.6,34.63
24,39.35,20,13.5729,33.37,36.78,85.95,74,24.65,34.78
25,54.75,24,13.5731,33.51,36.39,86.1,73.8,24.85,34.83
26,54.7,24,13.5732,33.56,36.44,86.15,73.85,24.95,34.8
27,54.85,24,13.5732,33.61,36.49,86.1,73.78,24.95,34.9

****
* FILE B *
****

39.05,30.27,29.07,29.02,67.2,41.46,7.5
39.37,30.29,29.07,29.02,67.41,41.46,7.5
39.1,30.34,29,29.12,67.39,41.46,7.5
38.85,31.49,30.24,30.56,66.76,40.29,7.5
38.78,31.44,30.32,30.27,66.9,40.15,7.5
38.93,31.56,30.49,30.37,66.79,40.29,7.5
38.61,32.25,31.1,31.15,66.43,39.49,7.5
38.56,32.25,31,31.07,66.36,39.46,7.5
38.61,32.2,30.93,31.07,66.29,39.44,7.5
38.61,32.7,31.63,31.59,66.07,38.88,7.5
38.46,32.68,31.54,31.49,66.07,38.9,7.5
38.51,32.63,31.56,31.46,66.02,38.78,7.5
38.27,33.02,31.95,31.85,65.9,38.44,7.5
38.24,33.07,31.93,31.85,65.83,38.54,7.5
38.2,32.95,31.68,31.56,65.98,38.44,7.5
38.66,33.05,32.4,32.43,65.17,38.1,7.5
38.63,33.05,32.43,32.35,65.15,38.1,7.5
38.66,33.12,32.4,32.43,65.12,38.2,7.5
38.51,33.59,32.83,32.9,64.93,37.73,7.5
38.54,33.54,32.83,32.83,65.12,37.7,7.5
38.63,33.66,32.93,32.9,65.2,37.78,7.5
38.54,33.95,33.29,33.27,65,37.45,7.5
38.56,34.44,33.34,33.32,65.02,36.9,7.5
38.66,34.24,33.32,33.27,65.05,37.23,7.5
38.51,34.22,33.32,33.39,64.98,37.2,7.5
38.61,34.24,33.41,33.56,65.05,37.15,7.5
38.54,34.27,33.27,33.37,65.12,37.18,7.5

****
TABLE NO.A.8.11 CONFIGURATION 6K (HEATING DATA)
(DENOTATION G OF TABLE 5.12)
****

****
* FILE A *
****

1,11.85,2,13.5706,27.9,42.1,84.88,75.31,21.85,34.56
2,11.85,2,13.5707,27.9,42.02,84.76,75.24,22,34.59
3,11.85,2,13.5708,27.9,42.1,84.78,75.19,22.1,34.63
4,23.1,4,13.571,29.71,40.34,85.07,74.88,22.4,34.37
5,23.15,4,13.5712,29.56,40.34,85.14,74.83,22.6,34.49
6,23.15,4,13.5711,29.61,40.2,85.12,74.95,22.5,34.54
7,37.8,6,13.5713,30.76,39.41,85.36,74.57,22.75,34.56
8,37.8,6,13.5712,30.73,39.32,85.36,74.5,22.6,34.51
9,37.75,6,13.5714,30.71,39.32,85.4,74.62,22.85,34.56
10,56.95,8,13.571,31.46,38.63,85.52,74.38,22.3,34.56
11,56.95,8,13.571,31.44,38.59,85.64,74.45,22.3,34.61
12,56.95,8,13.571,31.39,38.61,85.64,74.43,22.3,34.51
13,80.1,10,13.5715,32,38.15,85.79,74.24,23,34.54
14,80.25,10,13.5714,31.98,38.15,85.71,74.12,22.9,34.59
15,80.1,10,13.5715,31.85,38.05,85.79,74.24,22.95,34.51
16,108.95,12,13.5706,32.43,37.78,85.81,74.07,21.85,34.07
17,109,12,13.5706,32.33,37.68,85.76,74.02,21.8,33.95
18,108.95,12,13.5706,32.43,37.78,85.86,74,21.85,34.07
19,180.05,16,13.5708,32.93,37.15,86.07,73.85,22.1,34.02
20,180.2,16,13.5708,32.8,37.1,86.17,73.93,22.15,34.02
21,180.2,16,13.5709,32.9,37.18,86.12,73.95,22.25,34.07
22,272.6,20,13.571,33.27,36.73,86.22,73.66,22.3,33.98
23,272.55,20,13.571,33.27,36.76,86.24,73.78,22.35,34.02
24,272.45,20,13.5712,33.2,36.7,86.27,73.83,22.6,33.93
25,382.55,24,13.5713,33.44,36.41,86.39,73.59,22.7,33.73
26,382.65,24,13.5713,33.49,36.46,86.39,73.56,22.75,33.83
27,382.6,24,13.5713,33.44,36.44,86.37,73.56,22.7,33.83

****
* FILE B *
****

37.35,29.07,27.71,27.83,66.21,42.12,7.5
37.2,29.07,27.78,27.78,66.1,42.05,7.5
37.18,29.1,27.8,27.8,65.98,42.07,7.5
37.23,30.59,29.46,29.59,65.17,40.66,7.5
37.25,30.59,29.44,29.39,65.27,40.68,7.5
37.23,30.66,29.49,29.46,65.41,40.71,7.5
37.5,31.71,30.44,30.51,65.07,40.02,7.5
37.45,31.73,30.46,30.59,65.07,39.93,7.5
37.45,31.66,30.46,30.46,64.9,39.9,7.5
37.48,32.4,31.17,31.17,64.62,39.24,7.5
37.58,32.38,31.15,31.17,64.6,39.29,7.5
37.48,32.35,31.1,31.05,64.57,39.24,7.5
37.6,32.85,31.66,31.63,64.36,38.83,7.5
37.6,32.9,31.8,31.76,64.21,38.88,7.5
37.5,32.83,31.63,31.61,64.4,38.78,7.5
37.9,33.02,31.93,31.63,63.66,38.02,7.5
37.78,32.95,31.8,31.54,63.61,37.88,7.5
37.93,33.02,31.95,31.76,63.66,37.95,7.5
37.83,33.49,32.4,32.13,63.63,37.48,7.5
37.85,33.54,32.3,32.1,63.76,37.43,7.5
37.88,33.59,32.4,32.13,63.76,37.53,7.5
38.07,34.15,32.9,32.65,63.61,37.38,7.5
38.02,34.05,32.88,32.63,63.63,37.33,7.5
37.98,34,32.8,32.58,63.61,37.25,7.5
38,34.34,33.12,32.88,63.46,37.1,7.5
38,34.37,33.12,32.78,63.49,37.08,7.5
37.93,34.29,33.1,32.75,63.54,37.1,7.5

****
TABLE NO.A.8.12 CONFIGURATION 6K (HEATING DATA)
(DENOTATION H OF TABLE 5.12)
****

****
* FILE A *
****

SEE TABLE A.8.9

****
* FILE B *
****

SEE TABLE A.8.9

Appendix A.9

Sample computer outputs of the processed results

This appendix shows the format of the outputs that were obtained using the computer programs EX-6010, FRICTION-6010, and HEAT2-6010. The sample results which are presented were used in the reliability estimations in Chapter 6.

The computer program HEAT2-6010 "READ "s data from files which have been created by the program EX-6010. The outputs obtained using the latter program have not been included in this thesis unless pressure loss data is required.

****

TABLE NO.A.9.1 ISOTHERMAL FRICTION FACTORS CALCULATED USING THE DATA IN
TABLE A.8.1
(RESULTING CORRELATION IS DENOTATION H OF TABLE 5.4)

****

OUTPUT USING EX-6010

X=1 . . . . ISOTHERMAL
X=2 . . . . DIABATIC (TEST SECTION)
CHOSEN VALUE OF X IS !1
CROSS SECTIONAL AREA OF TUBE/SQ.INS. IS !0
TUBE MATERIAL IS !COPPER
TOTAL INSERTED LENGTH/INS. IS !0
FIRST RUN NUMBER ON DATA FILE IS !1
LAST RUN NUMBER ON DATA FILE IS !81
FIRST RUN NUMBER !1
LAST RUN NUMBER !27
HOW MANY F EQUATIONS !6
LENGTH/INS. IS !48
I.D./INS. IS !0.7874016
O.D./INS. IS !0.8661417

DATE: !****

TABLE NO. !A.9.1

GEOMETRY: !CONFIGURATION 0

RUN NUMBER	TEMP./C	HEAD/CM.	ROTAM/CM.
1	2.09750E+01	5.15	2
2	2.09650E+01	9.65	4
3	2.12100E+01	15.6	6
4	2.15600E+01	22.95	8
5	2.15350E+01	31.65	10
6	2.13650E+01	42	12
7	2.14400E+01	66.75	16
8	2.17300E+01	97.95	20
9	2.17700E+01	134	24
10	2.17350E+01	134.3	24
11	2.17550E+01	97.85	20
12	2.14150E+01	66.75	16
13	2.13400E+01	42.05	12
14	2.14750E+01	31.65	10
15	2.14600E+01	22.95	8
16	2.11850E+01	15.6	6
17	2.09350E+01	9.6	4
18	2.10850E+01	5.15	2
19	2.10850E+01	5.15	2
20	2.09500E+01	9.65	4
21	2.12050E+01	15.6	6
22	2.14500E+01	22.95	8
23	2.14550E+01	31.65	10
24	2.13550E+01	42.1	12
25	2.14400E+01	66.8	16
26	2.17800E+01	97.9	20
27	2.17050E+01	134.25	24

LENGTH/INS.= 48
DIA./INS.= .7874016
ROUGH/INS.= 6.E-05

Continued

D/G./CU.CM.	VISC./CP.	SPEC. GRAV.	Q/CU.FT./S.
9.98027E-01	9.81463E-01	1.594	6.17276E-03
9.98029E-01	9.81699E-01	1.594	8.95836E-03
9.97976E-01	9.75953E-01	1.594	1.18405E-02
9.97899E-01	9.67839E-01	1.594	1.48161E-02
9.97904E-01	9.68415E-01	1.594	1.78786E-02
9.97942E-01	9.72346E-01	1.594	2.10276E-02
9.97925E-01	9.70609E-01	1.594	2.76067E-02
9.97861E-01	9.63936E-01	1.594	3.45503E-02
9.97852E-01	9.63022E-01	1.593	4.18485E-02
9.97860E-01	9.63822E-01	1.593	4.18475E-02
9.97855E-01	9.63365E-01	1.593	3.45514E-02
9.97931E-01	9.71187E-01	1.593	2.76068E-02
9.97947E-01	9.72927E-01	1.594	2.10297E-02
9.97918E-01	9.69799E-01	1.594	1.78777E-02
9.97921E-01	9.70146E-01	1.594	1.48164E-02
9.97981E-01	9.76537E-01	1.594	1.18408E-02
9.98036E-01	9.82406E-01	1.594	8.96005E-03
9.98003E-01	9.78878E-01	1.594	6.17182E-03
9.98003E-01	9.78878E-01	1.594	6.17125E-03
9.98033E-01	9.82052E-01	1.594	8.95833E-03
9.97977E-01	9.76070E-01	1.594	1.18399E-02
9.97923E-01	9.70377E-01	1.594	1.48141E-02
9.97922E-01	9.70262E-01	1.594	1.78776E-02
9.97944E-01	9.72578E-01	1.594	2.10298E-02
9.97925E-01	9.70609E-01	1.593	2.76048E-02
9.97850E-01	9.62793E-01	1.593	3.45497E-02
9.97866E-01	9.64509E-01	1.593	4.18468E-02

VEL./FT./S.	P/PSI.	RE/NO UNITS	FRICTION
1.82540E+00	4.34154E-02	1.13154E+04	3.97342E-03
2.64916E+00	8.13502E-02	1.64179E+04	3.53493E-03
3.50149E+00	1.31507E-01	2.18267E+04	3.27121E-03
4.38141E+00	1.93463E-01	2.75386E+04	3.07375E-03
5.28707E+00	2.66796E-01	3.32114E+04	2.91101E-03
6.21828E+00	3.54043E-01	3.89045E+04	2.79249E-03
8.16384E+00	5.62656E-01	5.11674E+04	2.57477E-03
1.02172E+01	8.25641E-01	6.44762E+04	2.41234E-03
1.23754E+01	1.12757E+00	7.81690E+04	2.24565E-03
1.23751E+01	1.13009E+00	7.81030E+04	2.25076E-03
1.02175E+01	8.23390E-01	6.45160E+04	2.40563E-03
8.16388E+00	5.61696E-01	5.11374E+04	2.57033E-03
6.21890E+00	3.54460E-01	3.88853E+04	2.79522E-03
5.28679E+00	2.66790E-01	3.31627E+04	2.91121E-03
4.38150E+00	1.93463E-01	2.74743E+04	3.07354E-03
3.50157E+00	1.31506E-01	2.18143E+04	3.27099E-03
2.64966E+00	8.09287E-02	1.64093E+04	3.51527E-03
1.82513E+00	4.34149E-02	1.13433E+04	3.97468E-03
1.82495E+00	4.34149E-02	1.13423E+04	3.97542E-03
2.64915E+00	8.13493E-02	1.64120E+04	3.53490E-03
3.50131E+00	1.31506E-01	2.18230E+04	3.27149E-03
4.38083E+00	1.93459E-01	2.74636E+04	3.07440E-03
5.28677E+00	2.66793E-01	3.31469E+04	2.91126E-03
6.21892E+00	3.54882E-01	3.88993E+04	2.79853E-03
8.16329E+00	5.62116E-01	5.11639E+04	2.57265E-03
1.02170E+01	8.23811E-01	6.45509E+04	2.40710E-03
1.23749E+01	1.12966E+00	7.80466E+04	2.24995E-03

DO YOU WANT A PRINT OUT OF REFERENCE DATA ?NO

	COLBURN	BLASIUS	D.K.M.	COLEBROOK
MEAN RATIOS ARE				
	1.01748E+00	9.91858E-01	9.88681E-01	1.00126E+00
MAXIMUM RATIOS ARE				
	1.11839E+00	1.03601E+00	1.03245E+00	1.06004E+00
MINIMUM RATIOS ARE				
	9.29439E-01	9.48212E-01	9.36206E-01	9.30835E-01

	NIKURADSE	ROUSE
MEAN RATIOS ARE		
	1.01067E+00	1.01095E+00
MAXIMUM RATIOS ARE		
	1.06361E+00	1.06034E+00
MINIMUM RATIOS ARE		
	9.47400E-01	9.50178E-01

STOP AT LINE 2680

Continued

OUTPUT USING FRICTION-6010

IS DATA ON FILE !YES
FIRST RUN ON DATA FILE !1
LAST RUN ON DATA FILE !27
FIRST RUN !1
LAST RUN !27
NAME #2 !DAY5AE-6010

COMPARISON WITH REGRESSION ANALYSIS

% ERROR IS EXP-CALC/EXP

REYNOLDS NO	EXPTL F	CALCED F	% ERROR
+1.13154E+04	+3.97342E-03	+3.96277E-03	+2.68169E-01
+1.64179E+04	+3.53493E-03	+3.55955E-03	-6.96370E-01
+2.18267E+04	+3.27121E-03	+3.27899E-03	-2.37890E-01
+2.75386E+04	+3.07375E-03	+3.06644E-03	+2.37745E-01
+3.32114E+04	+2.91101E-03	+2.90524E-03	+1.98319E-01
+3.89045E+04	+2.79249E-03	+2.77569E-03	+6.01631E-01
+5.11674E+04	+2.57477E-03	+2.56486E-03	+3.84610E-01
+6.44762E+04	+2.41234E-03	+2.39948E-03	+5.33086E-01
+7.81690E+04	+2.24565E-03	+2.26988E-03	-1.07941E+00
+7.81030E+04	+2.25076E-03	+2.27044E-03	-8.74489E-01
+6.45160E+04	+2.40563E-03	+2.39905E-03	+2.73477E-01
+5.11374E+04	+2.57033E-03	+2.56530E-03	+1.95935E-01
+3.88853E+04	+2.79522E-03	+2.77609E-03	+6.84378E-01
+3.31627E+04	+2.91121E-03	+2.90647E-03	+1.62942E-01
+2.74743E+04	+3.07354E-03	+3.06850E-03	+1.63935E-01
+2.18143E+04	+3.27099E-03	+3.27953E-03	-2.60840E-01
+1.64093E+04	+3.51527E-03	+3.56009E-03	-1.27503E+00
+1.13433E+04	+3.97468E-03	+3.95996E-03	+3.70390E-01
+1.13423E+04	+3.97542E-03	+3.96006E-03	+3.86369E-01
+1.64120E+04	+3.53490E-03	+3.55992E-03	-7.07642E-01
+2.18230E+04	+3.27149E-03	+3.27915E-03	-2.33919E-01
+2.74636E+04	+3.07440E-03	+3.06885E-03	+1.80616E-01
+3.31469E+04	+2.91126E-03	+2.90687E-03	+1.50819E-01
+3.88993E+04	+2.79853E-03	+2.77580E-03	+8.12240E-01
+5.11639E+04	+2.57265E-03	+2.56491E-03	+3.00592E-01
+6.45509E+04	+2.40710E-03	+2.39868E-03	+3.49969E-01
+7.80466E+04	+2.24995E-03	+2.27091E-03	-9.31498E-01

LOG-LOG REGRESSION LINE IS F= .05843918127178 *(RE^ -.2883076533968)

RESULTS OF REGRESSION ANALYSIS

Z...SUM OF LOG(F)	-157.4704932419
F...SUM OF LOG(RE)	280.2448611224
W...SUM OF LOG(F)*LOG(RE)	-1637.257592084
G...SUM OF (LOG(RE)^2)	2918.503885161
X...TOTAL NUMBER OF RUNS USED	27
S...SUM OF (DEVIATIONS^2)	.0008360183474446
E...SLOPE OF REGRESSION LINE	-.2883076533968
C1...LOG(CONST) IN F EQUATION	-2.839768701921
X7...T(5) IN CONFIDENCE ANALYSIS	2.06
X6...MULT. IN LOG(CONST) ANALYSIS	3.334873976075
X4...MULT. IN SLOPE ANALYSIS	.3207607135248
X5...INTERVAL ON LOG(CONST)	.03972688809818
X3...INTERVAL ON SLOPE	.003821081415343
F6...MIN. LOG(CONST)	-2.879495590019
F7...MAX. LOG(CONST)	-2.800041813823
Q6...MIN. CONST	.05616308491116
Q7...MAX. CONST	.0608075199772
Q5...REGRESSION CONST	.05843918127178
F8...MIN. SLOPE	-.2921287348121
F9...MAX. SLOPE	-.2844865719814
Q4...SUM OF (LOG(F)^2)	919.2145086018
Q3...CORRELATION COEFFICIENT/R	-.9994829901673
Q2...R^2	.9989662476338
F4...AV. ABS. DEV.	.4649010358941
F5...R.M.S. ABS. DEV.	.5577575274292

STATE FILENAME OR NO !NO
STOP AT LINE 570

****

TABLE NO.A.9.2 NON-ISOTHERMAL FRICTION FACTORS CALCULATED USING THE DATA IN TABLE A.8.2
(RESULTING CORRELATION IS DENOTATION K OF TABLE 5.5)

****

OUTPUT USING EX-6010

X=1 . . . . ISOTHERMAL
X=2 . . . . DIABATIC (TEST SECTION)
CHOSEN VALUE OF X IS !2
CROSS SECTIONAL AREA OF TUBE/SQ.INS. IS !0
TUBE MATERIAL IS !COPPER
TOTAL INSERTED LENGTH/INS. IS !0
FIRST RUN NUMBER ON DATA FILE IS !1
LAST RUN NUMBER ON DATA FILE IS !81
FIRST RUN NUMBER !55
LAST RUN NUMBER !81
HOW MANY F EQUATIONS !6
LENGTH/INS. IS !48
I.D./INS. IS !0.7874016
O.D./INS. IS !0.8661417

DATE: !****

TABLE NO. !A.9.2

GEOMETRY: !CONFIGURATION 0

RUN NUMBER	TEMP./C	HEAD/CM.	ROTAM/CM.
1	3.49650E+01	4.1	2
2	3.50500E+01	4.1	2
3	3.51350E+01	4.15	2
4	3.50500E+01	7.95	4
5	3.50150E+01	7.95	4
6	3.50450E+01	8	4
7	3.50150E+01	13.1	6
8	3.50500E+01	13.15	6
9	3.50150E+01	13.2	6
10	3.50500E+01	19.75	8
11	3.49900E+01	19.8	8
12	3.49650E+01	19.85	8
13	3.50650E+01	27.9	10
14	3.50500E+01	27.7	10
15	3.50300E+01	27.9	10
16	3.49750E+01	37.1	12
17	3.49900E+01	37.05	12
18	3.50800E+01	37.05	12
19	3.50400E+01	59.7	16
20	3.50600E+01	59.75	16
21	3.50100E+01	59.75	16
22	3.50100E+01	88.55	20
23	3.50600E+01	88.6	20
24	3.49300E+01	88.65	20
25	3.49400E+01	122.25	24
26	3.49650E+01	122.25	24
27	3.49300E+01	122.25	24

LENGTH/INS.= 48
DIA./INS.= .7874016
ROUGH/INS.= 6.E-05

Continued

D/G./CU.CM.	VISC./CP.	SPEC. GRAV.	Q/CU.FT./S.
9.94075E-01	7.23027E-01	1.594	6.28204E-03
9.94046E-01	7.21804E-01	1.594	6.28360E-03
9.94017E-01	7.20584E-01	1.595	6.28504E-03
9.94046E-01	7.21804E-01	1.594	9.10850E-03
9.94058E-01	7.22307E-01	1.593	9.10894E-03
9.94048E-01	7.21876E-01	1.593	9.10965E-03
9.94058E-01	7.22307E-01	1.593	1.20194E-02
9.94046E-01	7.21804E-01	1.593	1.20194E-02
9.94058E-01	7.22307E-01	1.593	1.20193E-02
9.94046E-01	7.21804E-01	1.593	1.50153E-02
9.94066E-01	7.22667E-01	1.593	1.50155E-02
9.94075E-01	7.23027E-01	1.593	1.50154E-02
9.94041E-01	7.21588E-01	1.592	1.80975E-02
9.94046E-01	7.21804E-01	1.592	1.80973E-02
9.94053E-01	7.22091E-01	1.592	1.80975E-02
9.94072E-01	7.22883E-01	1.593	2.12614E-02
9.94066E-01	7.22667E-01	1.593	2.12618E-02
9.94036E-01	7.21373E-01	1.593	2.12640E-02
9.94049E-01	7.21948E-01	1.591	2.78605E-02
9.94042E-01	7.21660E-01	1.591	2.78617E-02
9.94060E-01	7.22379E-01	1.591	2.78607E-02
9.94060E-01	7.22379E-01	1.591	3.48040E-02
9.94042E-01	7.21660E-01	1.591	3.48047E-02
9.94087E-01	7.23532E-01	1.591	3.48027E-02
9.94084E-01	7.23387E-01	1.591	4.20936E-02
9.94075E-01	7.23027E-01	1.591	4.20937E-02
9.94087E-01	7.23532E-01	1.591	4.20927E-02

VEL./FT./S.	P/PSI.	RE/NO UNITS	FRICTION
1.85772E+00	3.45649E-02	1.55700E+04	3.06646E-03
1.85818E+00	3.45649E-02	1.55998E+04	3.06502E-03
1.85861E+00	3.50472E-02	1.56294E+04	3.10646E-03
2.69356E+00	6.70130E-02	2.26130E+04	2.82801E-03
2.69369E+00	6.68978E-02	2.25986E+04	2.82284E-03
2.69390E+00	6.73178E-02	2.26136E+04	2.84015E-03
3.55439E+00	1.10221E-01	2.98195E+04	2.67119E-03
3.55439E+00	1.10641E-01	2.98399E+04	2.68141E-03
3.55435E+00	1.11062E-01	2.98191E+04	2.69164E-03
4.44032E+00	1.66175E-01	3.72775E+04	2.58055E-03
4.44040E+00	1.66595E-01	3.72344E+04	2.58694E-03
4.44036E+00	1.67016E-01	3.72158E+04	2.59349E-03
5.35180E+00	2.34310E-01	4.49427E+04	2.50478E-03
5.35173E+00	2.32625E-01	4.49289E+04	2.48682E-03
5.35180E+00	2.34304E-01	4.49119E+04	2.50469E-03
6.28743E+00	3.12149E-01	5.27069E+04	2.41758E-03
6.28753E+00	3.11721E-01	5.27232E+04	2.41420E-03
6.28820E+00	3.11721E-01	5.28218E+04	2.41376E-03
8.23889E+00	5.00490E-01	6.91538E+04	2.25752E-03
8.23925E+00	5.00890E-01	6.91838E+04	2.25915E-03
8.23897E+00	5.00890E-01	6.91138E+04	2.25926E-03
1.02922E+01	7.42268E-01	8.63379E+04	2.14542E-03
1.02924E+01	7.42687E-01	8.64242E+04	2.14658E-03
1.02918E+01	7.43106E-01	8.61997E+04	2.14793E-03
1.24479E+01	1.02477E+00	1.04278E+05	2.02485E-03
1.24479E+01	1.02474E+00	1.04329E+05	2.02481E-03
1.24476E+01	1.02474E+00	1.04255E+05	2.02488E-03

DO YOU WANT A PRINT OUT OF REFERENCE DATA !NO

	COLBURN	BLASIUS	D.K.M.	COLEBROOK
MEAN RATIOS ARE	9.14644E-01	9.06529E-01	9.01043E-01	9.06852E-01
MAXIMUM RATIOS ARE	9.31810E-01	9.29417E-01	9.20282E-01	9.25376E-01
MINIMUM RATIOS ARE	8.87753E-01	8.64997E-01	8.64587E-01	8.85884E-01

	NIKURADSE	ROUSE
MEAN RATIOS ARE	9.17995E-01	9.19159E-01
MAXIMUM RATIOS ARE	9.36045E-01	9.37802E-01
MINIMUM RATIOS ARE	8.89897E-01	8.88182E-01

STOP AT LINE 2680

Continued

OUTPUT USING FRICTION-6010

IS DATA ON FILE !YES
FIRST RUN ON DATA FILE !1
LAST RUN ON DATA FILE !81
FIRST RUN !55
LAST RUN !81
NAME #2 !DAY5AA-6010

COMPARISON WITH REGRESSION ANALYSIS

% ERROR IS EXP-CALC/EXP

REYNOLDS NO	EXPTL F	CALCED F	% ERROR
+1.55700E+04	+3.06646E-03	+3.09396E-03	-8.96757E-01
+1.55998E+04	+3.06502E-03	+3.09269E-03	-9.02879E-01
+1.56294E+04	+3.10646E-03	+3.09144E-03	+4.83497E-01
+2.26130E+04	+2.82801E-03	+2.85706E-03	-1.02720E+00
+2.25986E+04	+2.82284E-03	+2.85745E-03	-1.22576E+00
+2.26136E+04	+2.84015E-03	+2.85704E-03	-5.94585E-01
+2.98195E+04	+2.67119E-03	+2.69323E-03	-8.25280E-01
+2.98399E+04	+2.68141E-03	+2.69284E-03	-4.26067E-01
+2.98191E+04	+2.69164E-03	+2.69324E-03	-5.93386E-02
+3.72775E+04	+2.58055E-03	+2.56791E-03	+4.89913E-01
+3.72344E+04	+2.58694E-03	+2.56854E-03	+7.11104E-01
+3.72158E+04	+2.59349E-03	+2.56882E-03	+9.51525E-01
+4.49427E+04	+2.50478E-03	+2.46743E-03	+1.49135E+00
+4.49289E+04	+2.48682E-03	+2.46759E-03	+7.73281E-01
+4.49119E+04	+2.50469E-03	+2.46779E-03	+1.47336E+00
+5.27069E+04	+2.41758E-03	+2.38490E-03	+1.35152E+00
+5.27232E+04	+2.41420E-03	+2.38475E-03	+1.21998E+00
+5.28218E+04	+2.41376E-03	+2.38380E-03	+1.24127E+00
+6.91538E+04	+2.25752E-03	+2.25058E-03	+3.07583E-01
+6.91838E+04	+2.25915E-03	+2.25037E-03	+3.88637E-01
+6.91138E+04	+2.25926E-03	+2.25086E-03	+3.72182E-01
+8.63379E+04	+2.14542E-03	+2.14644E-03	-4.79380E-02
+8.64242E+04	+2.14658E-03	+2.14599E-03	+2.74543E-02
+8.61997E+04	+2.14793E-03	+2.14718E-03	+3.51384E-02
+1.04278E+05	+2.02485E-03	+2.06166E-03	-1.81790E+00
+1.04329E+05	+2.02481E-03	+2.06145E-03	-1.80960E+00
+1.04255E+05	+2.02488E-03	+2.06176E-03	-1.82130E+00

LOG-LOG REGRESSION LINE IS F= .02428815511698 *(RE^ -.2134584589251)

RESULTS OF REGRESSION ANALYSIS

Z...SUM OF LOG(F)	-161.9584223293
F...SUM OF LOG(RE)	288.4810813837
W...SUM OF LOG(F)*LOG(RE)	-1732.448950068
G...SUM OF (LOG(RE)^2)	3091.672523157
X...TOTAL NUMBER OF RUNS USED	27
S...SUM OF (DEVIATIONS^2)	.002733603710147
E...SLOPE OF REGRESSION LINE	-.2134584589251
C1...LOG(CONST) IN F EQUATION	-3.717766491221
X7...T(5) IN CONFIDENCE ANALYSIS	2.06
X6...MULT. IN LOG(CONST) ANALYSIS	3.490041286815
X4...MULT. IN SLOPE ANALYSIS	.3261487389009
X5...INTERVAL ON LOG(CONST)	.07517882926313
X3...INTERVAL ON SLOPE	.00702555595799
F6...MIN. LOG(CONST)	-3.792945320484
F7...MAX. LOG(CONST)	-3.642587661958
Q6...MIN. CONST	.02252914847343
Q7...MAX. CONST	.02618449959092
Q5...REGRESSION CONST	.02428815511698
F8...MIN. SLOPE	-.2204840148831
F9...MAX. SLOPE	-.2064329029672
Q4...SUM OF (LOG(F)^2)	971.9322121885
Q3...CORRELATION COEFFICIENT/R	-.9968243137816
Q2...R^2	.993658712546
F4...AV. ABS. DEV.	.8434241895094
F5...R.M.S. ABS. DEV.	1.007660491307

STATE FILENAME OR NO !NO
STOP AT LINE 570

****

TABLE NO.A.9.3 HEAT TRANSFER FACTORS CALCULATED USING THE DATA IN TABLE A.8.3
(RESULTING CORRELATION IS DENOTATION I OF TABLE 5.6)

****

OUTPUT USING HEAT2-6010

ERROR CRITERION FOR RE EXPONENT IS !0.0000001
ERROR CRITERION FOR RESISTANCE IS !0.00000001
TUBE MATERIAL IS !COPPER
CROSS SECTIONAL AREA OF TUBE AND INSERTS/SQ.FT. IS !0
FIRST RUN NUMBER ON DATA FILE IS !1
LAST RUN NUMBER ON DATA FILE IS !81
FIRST RUN NUMBER IS !28
LAST RUN NUMBER IS !54
TUBE I.D./INS.= !0.7874016
TUBE O.D./INS.= !0.8661417

RUN NUMBER	(HO/HI)MEAS	(HO/HI)CORR	CORR/HIMEAS
1	9.79371E-01	9.79318E-01	2.59875E-03
2	9.81764E-01	9.81716E-01	2.61506E-03
3	9.84016E-01	9.83973E-01	2.64380E-03
4	1.02650E+00	1.02655E+00	2.19710E-03
5	1.01888E+00	1.01892E+00	2.18454E-03
6	1.01925E+00	1.01929E+00	2.22310E-03
7	1.02961E+00	1.02967E+00	1.98490E-03
8	1.01688E+00	1.01692E+00	1.96157E-03
9	1.01932E+00	1.01936E+00	1.96171E-03
10	1.02401E+00	1.02406E+00	1.78459E-03
11	1.03141E+00	1.03147E+00	1.78402E-03
12	1.03086E+00	1.03091E+00	1.80770E-03
13	1.02034E+00	1.02037E+00	1.65176E-03
14	1.02620E+00	1.02624E+00	1.65938E-03
15	1.02259E+00	1.02263E+00	1.68620E-03
16	1.01505E+00	1.01507E+00	1.56090E-03
17	1.02179E+00	1.02182E+00	1.56372E-03
18	1.02257E+00	1.02260E+00	1.55053E-03
19	1.01387E+00	1.01389E+00	1.43149E-03
20	1.02125E+00	1.02128E+00	1.45212E-03
21	1.02575E+00	1.02579E+00	1.42539E-03
22	1.02066E+00	1.02069E+00	1.34609E-03
23	1.03248E+00	1.03253E+00	1.35262E-03
24	1.03108E+00	1.03112E+00	1.34518E-03
25	1.04593E+00	1.04599E+00	1.31057E-03
26	1.04070E+00	1.04076E+00	1.30388E-03
27	1.03516E+00	1.03521E+00	1.32810E-03

CORR1	CORR2	CORR3	CORR4
1.46771E+01	1.88846E+00	6.21247E-03	3.95924E+01
1.47276E+01	1.83787E+00	1.77498E-03	3.97430E+01
1.47444E+01	1.93904E+00	2.66248E-03	4.00456E+01
1.23852E+01	2.17491E+00	1.06490E-02	4.11266E+01
1.22675E+01	2.19181E+00	1.86361E-02	4.13290E+01
1.23181E+01	2.19182E+00	8.87445E-03	4.18337E+01
1.08519E+01	2.12422E+00	1.95221E-02	4.22077E+01
1.08519E+01	2.14109E+00	8.87381E-03	4.24935E+01
1.08519E+01	2.00620E+00	7.09896E-03	4.20387E+01
9.77336E+00	2.00610E+00	1.77463E-02	4.27485E+01
9.79012E+00	1.98922E+00	1.77461E-02	4.28657E+01
9.67227E+00	1.98923E+00	2.66192E-02	4.28994E+01
8.91383E+00	2.27574E+00	1.77458E-02	4.30188E+01
8.88011E+00	2.22515E+00	1.33093E-02	4.30357E+01
9.04856E+00	2.22515E+00	1.95202E-02	4.29852E+01
8.86337E+00	1.65199E+00	5.14635E-02	4.17614E+01
8.91396E+00	1.70258E+00	5.32387E-02	4.19298E+01
8.84661E+00	1.68572E+00	4.43654E-02	4.19299E+01
8.08808E+00	1.65191E+00	4.79118E-02	4.22505E+01
8.08825E+00	1.65195E+00	4.43636E-02	4.26208E+01
7.97015E+00	1.80362E+00	5.05741E-02	4.26375E+01
7.39717E+00	1.83728E+00	4.17001E-02	4.29578E+01
7.44771E+00	1.92157E+00	4.17003E-02	4.30251E+01
7.44771E+00	1.88785E+00	4.08130E-02	4.30251E+01
6.95899E+00	1.80352E+00	4.34733E-02	4.35817E+01
6.85785E+00	1.93835E+00	4.34733E-02	4.33296E+01
6.90841E+00	1.88779E+00	4.34733E-02	4.34976E+01

Continued

LMTD MEAS	LMTD CORR	OUT T AV	INSI. T AV.
4.50071E+01	4.50118E+01	8.00350E+01	3.50104E+01
4.49719E+01	4.49767E+01	8.00450E+01	3.50554E+01
4.49468E+01	4.49517E+01	7.99850E+01	3.50203E+01
4.49597E+01	4.49633E+01	8.00200E+01	3.50563E+01
4.49348E+01	4.49384E+01	7.99750E+01	3.50363E+01
4.50548E+01	4.50585E+01	7.99700E+01	3.49112E+01
4.50611E+01	4.50640E+01	8.00550E+01	3.49869E+01
4.49605E+01	4.49635E+01	7.99200E+01	3.49519E+01
4.50757E+01	4.50786E+01	8.00300E+01	3.49469E+01
4.49942E+01	4.49966E+01	8.00500E+01	3.50374E+01
4.48794E+01	4.48819E+01	8.00100E+01	3.51124E+01
4.49599E+01	4.49624E+01	8.00000E+01	3.50224E+01
4.49888E+01	4.49909E+01	7.99700E+01	3.49478E+01
4.49846E+01	4.49867E+01	7.99950E+01	3.49778E+01
4.50352E+01	4.50373E+01	8.00550E+01	3.49878E+01
4.49303E+01	4.49320E+01	8.00150E+01	3.50381E+01
4.49454E+01	4.49472E+01	7.99800E+01	3.49881E+01
4.49199E+01	4.49216E+01	7.99700E+01	3.50031E+01
4.49202E+01	4.49215E+01	8.00800E+01	3.50835E+01
4.50070E+01	4.50083E+01	7.99950E+01	3.49135E+01
4.47990E+01	4.48004E+01	7.99500E+01	3.50735E+01
4.48767E+01	4.48778E+01	7.99550E+01	3.49738E+01
4.50782E+01	4.50793E+01	8.01200E+01	3.49388E+01
4.49468E+01	4.49479E+01	8.00250E+01	3.49738E+01
4.49024E+01	4.49033E+01	8.00600E+01	3.50339E+01
4.47714E+01	4.47723E+01	7.99050E+01	3.50089E+01
4.49502E+01	4.49511E+01	8.00350E+01	3.49639E+01

ONE TEMPERATURE,FIRST RUN NUMBER IS 128
ONE TEMPERATURE,LAST RUN NUMBER IS 154
DO YOU WANT TO INCLUDE MORE RESULTS !NO
CHOSEN PRANDTL NUMBER EXPONENT IS !0.4
DO YOU WANT TO USE MEAN PRANDTL NUMBERS !NO
RE EXPONENT IS !0.8
GEOMETRY: !CONFIGURATION 0

RESISTANCE	INCREMENT	EXPONENT	SUM ERS SQ
.00000E+00	1.00000E-04	3.42832E-01	2.61557E-02
1.00000E-04	1.00000E-04	3.60148E-01	2.70407E-02
2.00000E-04	1.00000E-04	3.79371E-01	2.78618E-02
3.00000E-04	1.00000E-04	4.00845E-01	2.85766E-02
4.00000E-04	1.00000E-04	4.25008E-01	2.91279E-02
5.00000E-04	1.00000E-04	4.52423E-01	2.94407E-02
6.00000E-04	1.00000E-04	4.83828E-01	2.94225E-02
7.00000E-04	1.00000E-04	5.20219E-01	2.89712E-02
8.00000E-04	1.00000E-04	5.62971E-01	2.80111E-02
9.00000E-04	1.00000E-04	6.14055E-01	2.66077E-02
1.00000E-03	1.00000E-04	6.76428E-01	2.53229E-02
1.10000E-03	1.00000E-04	7.54786E-01	2.63485E-02
1.20000E-03	1.00000E-04	8.57242E-01	3.75051E-02
1.10000E-03	1.00000E-05	7.54786E-01	2.63485E-02
1.11000E-03	1.00000E-05	7.63768E-01	2.67841E-02
1.12000E-03	1.00000E-05	7.72997E-01	2.73201E-02
1.13000E-03	1.00000E-05	7.82483E-01	2.79711E-02
1.14000E-03	1.00000E-05	7.92239E-01	2.87539E-02
1.15000E-03	1.00000E-05	8.02277E-01	2.96875E-02
1.14000E-03	1.00000E-06	7.92239E-01	2.87539E-02
1.14100E-03	1.00000E-06	7.93230E-01	2.88402E-02
1.14200E-03	1.00000E-06	7.94223E-01	2.89279E-02
1.14300E-03	1.00000E-06	7.95220E-01	2.90172E-02
1.14400E-03	1.00000E-06	7.96219E-01	2.91081E-02
1.14500E-03	1.00000E-06	7.97222E-01	2.92006E-02
1.14600E-03	1.00000E-06	7.98227E-01	2.92947E-02
1.14700E-03	1.00000E-06	7.99235E-01	2.93904E-02
1.14800E-03	1.00000E-06	8.00246E-01	2.94877E-02
1.14700E-03	1.00000E-07	7.99235E-01	2.93904E-02
1.14710E-03	1.00000E-07	7.99336E-01	2.94000E-02
1.14720E-03	1.00000E-07	7.99437E-01	2.94097E-02
1.14730E-03	1.00000E-07	7.99538E-01	2.94194E-02
1.14740E-03	1.00000E-07	7.99639E-01	2.94291E-02
1.14750E-03	1.00000E-07	7.99740E-01	2.94389E-02
1.14760E-03	1.00000E-07	7.99841E-01	2.94486E-02
1.14770E-03	1.00000E-07	7.99943E-01	2.94584E-02
1.14780E-03	1.00000E-07	8.00044E-01	2.94681E-02
1.14770E-03	1.00000E-08	7.99943E-01	2.94584E-02
1.14771E-03	1.00000E-08	7.99953E-01	2.94593E-02
1.14772E-03	1.00000E-08	7.99963E-01	2.94603E-02
1.14773E-03	1.00000E-08	7.99973E-01	2.94613E-02
1.14774E-03	1.00000E-08	7.99983E-01	2.94623E-02
1.14775E-03	1.00000E-08	7.99993E-01	2.94632E-02
1.14776E-03	1.00000E-08	8.00003E-01	2.94642E-02
1.14775E-03	1.00000E-09	7.99993E-01	2.94632E-02
1.14775E-03	1.00000E-09	7.99994E-01	2.94633E-02
1.14775E-03	1.00000E-09	7.99995E-01	2.94634E-02
1.14775E-03	1.00000E-09	7.99996E-01	2.94635E-02
1.14775E-03	1.00000E-09	7.99997E-01	2.94636E-02
1.14775E-03	1.00000E-09	7.99998E-01	2.94637E-02
1.14775E-03	1.00000E-09	7.99999E-01	2.94638E-02
1.14775E-03	1.00000E-09	8.00000E-01	2.94639E-02
1.14775E-03	1.00000E-10	7.99999E-01	2.94638E-02
1.14775E-03	1.00000E-10	7.99999E-01	2.94638E-02
1.14775E-03	1.00000E-10	7.99999E-01	2.94639E-02

Continued

DATA INPUTS:
RESISTANCE STATED: NO
GEOMETRY: CONFIGURATION 0

HO CORR/BEU	RE NUMBER	EXP NUSSELT	CAL NUSSELT	% CA-EX/EX
2.11053E+04	1.55965E+04	5.67426E+01	5.81168E+01	+2.42191E+00
2.10828E+04	1.56127E+04	5.67326E+01	5.81649E+01	+2.52468E+00
2.10566E+04	1.56015E+04	5.66579E+01	5.81315E+01	+2.60087E+00
2.59564E+04	2.26216E+04	8.12311E+01	7.82524E+01	-3.66690E+00
2.59556E+04	2.26119E+04	8.12997E+01	7.82256E+01	-3.78114E+00
2.57722E+04	2.25560E+04	7.97756E+01	7.80707E+01	-2.13706E+00
2.85596E+04	2.98041E+04	9.73796E+01	9.75661E+01	+1.91524E-01
2.87043E+04	2.97833E+04	9.88198E+01	9.75116E+01	-1.32377E+00
2.84663E+04	2.97835E+04	9.66449E+01	9.75122E+01	+8.97405E-01
3.12240E+04	3.72699E+04	1.18308E+02	1.16671E+02	-1.38371E+00
3.15276E+04	3.73277E+04	1.21708E+02	1.16816E+02	-4.01933E+00
3.10443E+04	3.72606E+04	1.16969E+02	1.16648E+02	-2.74842E-01
3.34208E+04	4.48363E+04	1.38915E+02	1.35264E+02	-2.62821E+00
3.34198E+04	4.48616E+04	1.38963E+02	1.35325E+02	-2.61812E+00
3.28391E+04	4.48728E+04	1.32771E+02	1.35352E+02	+1.94351E+00
3.39766E+04	5.27733E+04	1.45356E+02	1.54102E+02	+6.01671E+00
3.43177E+04	5.27198E+04	1.48956E+02	1.53977E+02	+3.37098E+00
3.45755E+04	5.27374E+04	1.52127E+02	1.54018E+02	+1.24357E+00
3.68048E+04	6.92092E+04	1.80922E+02	1.91429E+02	+5.80763E+00
3.68031E+04	6.89728E+04	1.79687E+02	1.90906E+02	+6.24353E+00
3.77006E+04	6.91954E+04	1.96052E+02	1.91399E+02	-2.37359E+00
3.95536E+04	8.62711E+04	2.27707E+02	2.28334E+02	+2.75115E-01
3.99731E+04	8.62106E+04	2.32476E+02	2.28206E+02	-1.83682E+00
4.01131E+04	8.62708E+04	2.37816E+02	2.28333E+02	-3.98735E+00
4.17568E+04	1.04469E+05	2.77433E+02	2.66114E+02	-4.07975E+00
4.15873E+04	1.04416E+05	2.76136E+02	2.66006E+02	-3.66863E+00
4.07408E+04	1.04322E+05	2.51428E+02	2.65815E+02	+5.72229E+00

LOG-LOG REGRESSION LINE IS (NU/PR^ .4)= .02569677710738 *(RE^ .7999999491549)

RESULTS OF REGRESSION ANALYSIS

Z...SUM OF LOG(NU)	131.9222904492
F...SUM OF LOG(RE)	288.4747837498
W...SUM OF LOG(NU)*LOG(RE)	1417.014208161
G...SUM OF (LOG(RE)^2)	3091.541208877
X...TOTAL NUMBER OF RUNS USED	27
S...SUM OF (DEVIATIONS^2)	.02946390113782
C...OUTER RESISTANCE TO TRANSFER	.0011477562
E...SLOPE OF REGRESSION LINE	.7999999491549
C1...LOG(CONST) IN NU EQUATION	-3.661389699327
X7...T(5) IN CONFIDENCE ANALYSIS	2.06
X6...MULT. IN LOG(CONST) ANALYSIS	3.489362542729
X4...MULT. IN SLOPE ANALYSIS	.3260922346366
X5...INTERVAL ON LOG(CONST	.2467677692193
X3...INTERVAL ON SLOPE	.02306124752462
F6...MIN. LOG(CONST)	-3.908157468546
F7...MAX. LOG(CONST)	-3.414621930108
Q6...MIN. CONST	.02007746035411
Q7...MAX. CONST	.03288883863098
Q5...REGRESSION CONST	.02569677710738
F8...MIN.SLOPE	.7769387016303
F9...MAX.SLOPE	.8230611966795
Q4...SUM OF (LOG(NU)^2)	650.6218430127
Q3...CORRELATION COEFFICIENT/R	.997561233224
Q2...R^2	.9951284140314
F4...AV. ABS. DEV.	2.853298060231
F5...R.M.S. ABS. DEV.	3.329137271869

FILE RESULTS !YES
TRY ANOTHER RE AND/OR PR EXPONENT !NO
DO YOU WANT TO STATE THE RESISTANCE !NO
STOP AT LINE 2520

****

TABLE NO.A.9.4 HEAT TRANSFER FACTORS CALCULATED USING THE DATA IN TABLE A.8.4
(RESULTING CORRELATION IS DENOTATION K OF TABLE 5.6)

****

OUTPUT USING HEAT2-6010

ERROR CRITERION FOR RE EXPONENT IS !0.0000001
ERROR CRITERION FOR RESISTANCE IS !0.00000001
TUBE MATERIAL IS !COPPER
CROSS SECTIONAL AREA OF TUBE AND INSERTS/SQ.FT. IS !0
FIRST RUN NUMBER ON DATA FILE IS !1
LAST RUN NUMBER ON DATA FILE IS !81
FIRST RUN NUMBER IS 155
LAST RUN NUMBER IS !81
TUBE I.D./INS.= !0.7874016
TUBE O.D./INS.= !0.8661417

RUN NUMBER	(HO/HI)MEAS	(HO/HI)CORR	CORR/HIMEAS
1	1.00635E+00	1.00636E+00	2.64177E-03
2	9.94447E-01	9.94433E-01	2.64888E-03
3	9.98939E-01	9.98936E-01	2.63187E-03
4	1.01849E+00	1.01853E+00	2.16387E-03
5	1.01910E+00	1.01914E+00	2.14708E-03
6	1.03081E+00	1.03088E+00	2.16644E-03
7	1.01891E+00	1.01894E+00	1.85962E-03
8	1.03137E+00	1.03143E+00	1.87979E-03
9	1.02198E+00	1.02202E+00	1.86580E-03
10	1.01774E+00	1.01777E+00	1.68054E-03
11	1.02844E+00	1.02849E+00	1.69332E-03
12	1.02455E+00	1.02459E+00	1.68340E-03
13	1.03954E+00	1.03960E+00	1.55912E-03
14	1.02282E+00	1.02285E+00	1.54727E-03
15	1.03751E+00	1.03756E+00	1.55775E-03
16	1.00097E+00	1.00097E+00	1.46109E-03
17	1.01020E+00	1.01022E+00	1.46895E-03
18	1.00613E+00	1.00614E+00	1.45923E-03
19	1.02262E+00	1.02265E+00	1.32476E-03
20	1.02844E+00	1.02848E+00	1.33425E-03
21	1.01465E+00	1.01467E+00	1.31281E-03
22	1.00460E+00	1.00461E+00	1.23098E-03
23	1.02575E+00	1.02578E+00	1.23983E-03
24	1.01940E+00	1.01943E+00	1.24940E-03
25	1.00591E+00	1.00591E+00	1.18540E-03
26	1.01139E+00	1.01141E+00	1.20082E-03
27	1.02450E+00	1.02453E+00	1.20406E-03

CORR1	CORR2	CORR3	CORR4
1.68508E+01	1.93920E+00	2.57400E-02	3.98740E+01
1.68506E+01	2.09094E+00	1.06508E-02	4.01420E+01
1.67323E+01	2.17522E+00	1.06507E-02	4.04098E+01
1.42558E+01	2.14136E+00	4.43747E-03	4.16595E+01
1.40538E+01	2.00647E+00	1.77498E-03	4.17437E+01
1.41042E+01	2.14136E+00	2.66248E-03	4.15758E+01
1.23349E+01	2.24240E+00	6.21213E-03	4.28565E+01
1.27223E+01	2.19181E+00	6.21209E-03	4.27051E+01
1.26044E+01	2.19181E+00	6.21209E-03	4.26547E+01
1.13068E+01	2.25914E+00	1.50857E-02	4.32796E+01
1.11721E+01	2.25913E+00	1.06487E-02	4.34475E+01
1.11384E+01	2.22542E+00	1.33109E-02	4.34980E+01
1.00769E+01	2.09046E+00	1.06482E-02	4.38365E+01
1.00600E+01	2.22534E+00	1.06483E-02	4.38705E+01
1.01105E+01	2.12417E+00	8.87353E-03	4.35005E+01
1.01782E+01	1.51727E+00	.00000E+00	4.38415E+01
1.01950E+01	1.50041E+00	6.21136E-03	4.40094E+01
1.01105E+01	1.66897E+00	1.50845E-02	4.40417E+01
8.66141E+00	1.44973E+00	.00000E+00	4.47499E+01
8.74551E+00	1.48342E+00	1.77452E-03	4.47162E+01
8.84680E+00	1.31487E+00	.00000E+00	4.46326E+01
8.39155E+00	1.48338E+00	.00000E+00	4.50035E+01
8.20622E+00	1.39909E+00	.00000E+00	4.52053E+01
8.37478E+00	1.39911E+00	1.77449E-03	4.54578E+01
7.73441E+00	1.46650E+00	6.21053E-03	4.58620E+01
7.68389E+00	1.68565E+00	1.33084E-02	4.59126E+01
7.76815E+00	1.63508E+00	1.06468E-02	4.59126E+01

Continued

LMTD MEAS	LMTD CORR	OUT T AV	INSI. T AV.
4.49391E+01	4.49436E+01	7.99350E+01	3.49608E+01
4.49354E+01	4.49400E+01	8.00150E+01	3.50458E+01
4.48041E+01	4.48088E+01	7.99700E+01	3.51307E+01
4.49646E+01	4.49681E+01	8.00200E+01	3.50465E+01
4.49395E+01	4.49431E+01	7.99600E+01	3.50114E+01
4.49141E+01	4.49176E+01	7.99650E+01	3.50415E+01
4.49599E+01	4.49628E+01	7.99750E+01	3.50120E+01
4.49000E+01	4.49028E+01	7.99500E+01	3.50471E+01
4.49699E+01	4.49728E+01	7.99850E+01	3.50121E+01
4.49154E+01	4.49178E+01	7.99700E+01	3.50475E+01
4.50208E+01	4.50233E+01	8.00150E+01	3.49875E+01
4.50257E+01	4.50281E+01	7.99950E+01	3.49625E+01
4.50176E+01	4.50197E+01	8.00950E+01	3.50628E+01
4.48515E+01	4.48536E+01	7.99150E+01	3.50478E+01
4.50176E+01	4.50197E+01	8.00600E+01	3.50278E+01
4.49394E+01	4.49412E+01	7.99400E+01	3.49731E+01
4.49351E+01	4.49369E+01	7.99500E+01	3.49881E+01
4.48094E+01	4.48112E+01	7.99150E+01	3.50781E+01
4.49566E+01	4.49580E+01	8.00450E+01	3.50384E+01
4.48624E+01	4.48639E+01	7.99700E+01	3.50584E+01
4.49702E+01	4.49717E+01	8.00300E+01	3.50084E+01
4.48897E+01	4.48908E+01	7.99750E+01	3.50087E+01
4.49025E+01	4.49037E+01	8.00350E+01	3.50587E+01
4.50322E+01	4.50334E+01	8.00350E+01	3.49287E+01
4.48785E+01	4.48795E+01	7.99150E+01	3.49389E+01
4.49006E+01	4.49016E+01	7.99600E+01	3.49639E+01
4.50473E+01	4.50483E+01	8.00700E+01	3.49289E+01

ONE TEMPERATURE,FIRST RUN NUMBER IS !55
ONE TEMPERATURE,LAST RUN NUMBER IS !81
DO YOU WANT TO INCLUDE MORE RESULTS !NO
CHOSEN PRANDTL NUMBER EXPONENT IS !0.4
DO YOU WANT TO USE MEAN PRANDTL NUMBERS !NO
RE EXPONENT IS !0.8
GEOMETRY: !CONFIGURATION 0

RESISTANCE	INCREMENT	EXPONENT	SUM ERS SQ
.00000E+00	1.00000E-04	3.81781E-01	3.38491E-02
1.00000E-04	1.00000E-04	4.03120E-01	3.48545E-02
2.00000E-04	1.00000E-04	4.27092E-01	3.56644E-02
3.00000E-04	1.00000E-04	4.54241E-01	3.61656E-02
4.00000E-04	1.00000E-04	4.85275E-01	3.61972E-02
5.00000E-04	1.00000E-04	5.21145E-01	3.55345E-02
6.00000E-04	1.00000E-04	5.63154E-01	3.38719E-02
7.00000E-04	1.00000E-04	6.13158E-01	3.08243E-02
8.00000E-04	1.00000E-04	6.73906E-01	2.60083E-02
9.00000E-04	1.00000E-04	7.49708E-01	1.94391E-02
1.00000E-03	1.00000E-04	8.47840E-01	1.32035E-02
9.00000E-04	1.00000E-05	7.49708E-01	1.94391E-02
9.10000E-04	1.00000E-05	7.58358E-01	1.87278E-02
9.20000E-04	1.00000E-05	7.67236E-01	1.80182E-02
9.30000E-04	1.00000E-05	7.76352E-01	1.73150E-02
9.40000E-04	1.00000E-05	7.85717E-01	1.66240E-02
9.50000E-04	1.00000E-05	7.95343E-01	1.59518E-02
9.60000E-04	1.00000E-05	8.05241E-01	1.53063E-02
9.50000E-04	1.00000E-06	7.95343E-01	1.59518E-02
9.51000E-04	1.00000E-06	7.96320E-01	1.58859E-02
9.52000E-04	1.00000E-06	7.97300E-01	1.58203E-02
9.53000E-04	1.00000E-06	7.98283E-01	1.57549E-02
9.54000E-04	1.00000E-06	7.99268E-01	1.56899E-02
9.55000E-04	1.00000E-06	8.00257E-01	1.56252E-02
9.54000E-04	1.00000E-07	7.99268E-01	1.56899E-02
9.54100E-04	1.00000E-07	7.99367E-01	1.56834E-02
9.54200E-04	1.00000E-07	7.99466E-01	1.56769E-02
9.54300E-04	1.00000E-07	7.99565E-01	1.56705E-02
9.54400E-04	1.00000E-07	7.99663E-01	1.56640E-02
9.54500E-04	1.00000E-07	7.99762E-01	1.56575E-02
9.54600E-04	1.00000E-07	7.99861E-01	1.56510E-02
9.54700E-04	1.00000E-07	7.99960E-01	1.56446E-02
9.54800E-04	1.00000E-07	8.00059E-01	1.56381E-02
9.54700E-04	1.00000E-08	7.99960E-01	1.56446E-02
9.54710E-04	1.00000E-08	7.99970E-01	1.56439E-02
9.54720E-04	1.00000E-08	7.99980E-01	1.56433E-02
9.54730E-04	1.00000E-08	7.99990E-01	1.56426E-02
9.54740E-04	1.00000E-08	8.00000E-01	1.56420E-02

Continued

DATA INPUTS:
RESISTANCE STATED: NO
GEOMETRY: CONFIGURATION 0

HO CORR/BEU	RE NUMBER	EXP NUSSELT	CAL NUSSELT	% CA-EX/EX
2.22985E+04	1.55687E+04	5.59697E+01	5.76765E+01	+3.04947E+00
2.21261E+04	1.55985E+04	5.53615E+01	5.77648E+01	+4.34118E+00
2.24589E+04	1.56280E+04	5.68915E+01	5.78522E+01	+1.68876E+00
2.72661E+04	2.26115E+04	7.69129E+01	7.77426E+01	+1.07882E+00
2.73778E+04	2.25970E+04	7.74999E+01	7.77030E+01	+2.61961E-01
2.74529E+04	2.26121E+04	7.79487E+01	7.77443E+01	-2.62222E-01
3.14079E+04	2.98177E+04	9.88245E+01	9.70009E+01	-1.84526E+00
3.15523E+04	2.98382E+04	9.99538E+01	9.70542E+01	-2.90100E+00
3.14075E+04	2.98174E+04	9.87812E+01	9.70001E+01	-1.80306E+00
3.43599E+04	3.72756E+04	1.18076E+02	1.15967E+02	-1.78627E+00
3.44820E+04	3.72325E+04	1.18322E+02	1.15860E+02	-2.08087E+00
3.45424E+04	3.72140E+04	1.18702E+02	1.15814E+02	-2.43350E+00
3.72772E+04	4.49408E+04	1.39888E+02	1.34681E+02	-3.72193E+00
3.70585E+04	4.49270E+04	1.39191E+02	1.34648E+02	-3.26402E+00
3.70596E+04	4.49100E+04	1.38042E+02	1.34608E+02	-2.48798E+00
3.79919E+04	5.27049E+04	1.46541E+02	1.52995E+02	+4.40357E+00
3.82486E+04	5.27212E+04	1.48885E+02	1.53032E+02	+2.78541E+00
3.84224E+04	5.28198E+04	1.51540E+02	1.53261E+02	+1.13609E+00
4.22941E+04	6.91516E+04	1.91153E+02	1.90124E+02	-5.38028E-01
4.22955E+04	6.91817E+04	1.92279E+02	1.90190E+02	-1.08645E+00
4.22950E+04	6.91117E+04	1.90971E+02	1.90036E+02	-4.89239E-01
4.47315E+04	8.63358E+04	2.24994E+02	2.27064E+02	+9.19982E-01
4.52916E+04	8.64220E+04	2.33511E+02	2.27245E+02	-2.68348E+00
4.50107E+04	8.61975E+04	2.26949E+02	2.26773E+02	-7.75844E-02
4.66649E+04	1.04275E+05	2.56949E+02	2.64084E+02	+2.77682E+00
4.64951E+04	1.04327E+05	2.53544E+02	2.64188E+02	+4.19812E+00
4.70024E+04	1.04253E+05	2.59868E+02	2.64038E+02	+1.60472E+00

LOG-LOG REGRESSION LINE IS (NU/PR^ .4)= .02553852344398 *(RE^ .8000000250654)

RESULTS OF REGRESSION ANALYSIS

Z...SUM OF LOG(NU)	131.7595537008
F...SUM OF LOG(RE)	288.4798275568
W...SUM OF LOG(NU)*LOG(RE)	1415.297991185
G...SUM OF (LOG(RE)^2)	3091.646349576
X...TOTAL NUMBER OF RUNS USED	27
S...SUM OF (DEVIATIONS^2)	.01564201812853
C...OUTER RESISTANCE TO TRANSFER	.0009547399999999
E...SLOPE OF REGRESSION LINE	.8000000250654
C1...LOG(CONST) IN NU EQUATION	-3.667567243519
X7...T(5) IN CONFIDENCE ANALYSIS	2.06
X6...MULT. IN LOG(CONST) ANALYSIS	3.489911554643
X4...MULT. IN SLOPE ANALYSIS	.3261379957883
X5...INTERVAL ON LOG(CONST	.1798282960535
X3...INTERVAL ON SLOPE	.01680525111958
F6...MIN. LOG(CONST)	-3.847395539573
F7...MAX. LOG(CONST)	-3.487738947466
Q6...MIN. CONST	.02133523090504
Q7...MAX. CONST	.03056991427003
Q5...REGRESSION CONST	.02553852344398
F8...MIN.SLOPE	.7831947739458
F9...MAX.SLOPE	.816805276185
Q4...SUM OF (LOG(NU)^2)	649.0170472644
Q3...CORRELATION COEFFICIENT/R	.9987027017554
Q2...R^2	.9974070864936
F4...AV. ABS. DEV.	2.063180809844
F5...R.M.S. ABS. DEV.	2.416174212201

FILE RESULTS !YES
TRY ANOTHER RE AND/OR PR EXPONENT !NO
DO YOU WANT TO STATE THE RESISTANCE !NO
STOP AT LINE 2520

****

TABLE NO.A.9.5 HEAT TRANSFER FACTORS CALCULATED USING THE DATA IN TABLE A.8.5
(RESULTING CORRELATION IS DENOTATION N OF TABLE 5.6)

****

OUTPUT USING HEAT2-6010

ERROR CRITERION FOR RE EXPONENT IS !0.0000001
ERROR CRITERION FOR RESISTANCE IS !0.00000001
TUBE MATERIAL IS !COPPER
CROSS SECTIONAL AREA OF TUBE AND INSERTS/SQ.FT. IS !0
FIRST RUN NUMBER ON DATA FILE IS !1
LAST RUN NUMBER ON DATA FILE IS !81
FIRST RUN NUMBER IS !1
LAST RUN NUMBER IS !27
TUBE I.D./INS.= !0.7874016
TUBE O.D./INS.= !0.8661417

RUN NUMBER	(HO/HI)MEAS	(HO/HI)CORR	CORR/HIMEAS
1	9.99609E-01	9.99608E-01	2.84560E-03
2	9.91746E-01	9.91723E-01	2.83525E-03
3	9.91845E-01	9.91822E-01	2.83378E-03
4	1.00952E+00	1.00954E+00	2.33878E-03
5	1.01094E+00	1.01096E+00	2.33507E-03
6	1.00362E+00	1.00363E+00	2.32225E-03
7	1.03027E+00	1.03033E+00	2.08253E-03
8	1.03067E+00	1.03073E+00	2.08153E-03
9	1.02504E+00	1.02510E+00	2.03956E-03
10	1.02767E+00	1.02773E+00	1.86430E-03
11	1.03617E+00	1.03624E+00	1.86060E-03
12	1.03163E+00	1.03169E+00	1.85860E-03
13	1.03200E+00	1.03206E+00	1.74014E-03
14	1.03636E+00	1.03643E+00	1.73299E-03
15	1.02812E+00	1.02817E+00	1.71618E-03
16	1.00729E+00	1.00731E+00	1.60486E-03
17	9.92721E-01	9.92709E-01	1.60962E-03
18	1.00291E+00	1.00292E+00	1.60726E-03
19	1.00219E+00	1.00219E+00	1.46741E-03
20	1.01120E+00	1.01122E+00	1.47009E-03
21	1.00410E+00	1.00410E+00	1.45921E-03
22	1.01369E+00	1.01371E+00	1.39426E-03
23	1.01787E+00	1.01790E+00	1.38210E-03
24	1.01984E+00	1.01987E+00	1.39652E-03
25	1.02916E+00	1.02919E+00	1.33893E-03
26	1.04221E+00	1.04227E+00	1.34973E-03
27	1.04637E+00	1.04643E+00	1.35127E-03

CORR1	CORR2	CORR3	CORR4
1.39183E+01	2.39419E+00	3.28373E-02	4.25646E+01
1.34637E+01	2.44479E+00	2.30749E-02	4.30849E+01
1.34973E+01	2.64713E+00	8.87499E-03	4.28326E+01
1.11049E+01	2.30976E+00	1.86361E-02	4.43336E+01
1.09365E+01	2.32663E+00	1.50864E-02	4.44850E+01
1.08015E+01	2.47834E+00	7.98684E-03	4.43335E+01
1.00262E+01	2.17474E+00	1.59726E-02	4.51110E+01
1.02284E+01	2.10732E+00	1.68600E-02	4.50263E+01
9.82416E+00	2.22533E+00	6.21160E-03	4.48584E+01
9.16686E+00	1.90493E+00	2.04085E-02	4.58527E+01
9.14992E+00	1.92176E+00	1.95210E-02	4.56004E+01
8.82992E+00	2.34326E+00	2.66201E-03	4.56005E+01
8.17281E+00	1.90489E+00	1.33095E-02	4.63427E+01
8.30745E+00	1.93858E+00	1.33094E-02	4.60735E+01
8.05487E+00	1.90488E+00	8.87301E-03	4.61411E+01
7.73479E+00	1.68572E+00	3.81541E-02	4.59772E+01
7.73479E+00	1.77002E+00	3.81543E-02	4.61788E+01
7.68420E+00	1.82058E+00	4.43656E-02	4.62121E+01
6.82477E+00	1.51708E+00	4.17012E-02	4.63995E+01
6.74043E+00	1.63506E+00	4.17009E-02	4.64662E+01
6.70678E+00	1.60135E+00	3.72647E-02	4.65170E+01
6.40337E+00	1.60131E+00	3.90383E-02	4.70059E+01
6.36970E+00	1.55075E+00	3.46020E-02	4.67705E+01
6.45383E+00	1.61815E+00	3.01654E-02	4.70893E+01
5.93138E+00	1.51696E+00	4.34724E-02	4.73423E+01
5.79667E+00	1.68554E+00	2.83905E-02	4.75111E+01
5.99878E+00	1.68553E+00	2.39542E-02	4.73762E+01

Continued

LMTD MEAS	LMTD CORR	OUT T AV	INSI. T AV.
4.49965E+01	4.50019E+01	8.00350E+01	3.50198E+01
4.49219E+01	4.49275E+01	7.99500E+01	3.50096E+01
4.48719E+01	4.48774E+01	7.99500E+01	3.50597E+01
4.50198E+01	4.50241E+01	7.99850E+01	3.49607E+01
4.50348E+01	4.50391E+01	8.00100E+01	3.49707E+01
4.49099E+01	4.49141E+01	7.99700E+01	3.50557E+01
4.49012E+01	4.49045E+01	8.00200E+01	3.51116E+01
4.48712E+01	4.48745E+01	7.99150E+01	3.50366E+01
4.49059E+01	4.49092E+01	7.99700E+01	3.50566E+01
4.49544E+01	4.49571E+01	7.99500E+01	3.49771E+01
4.49799E+01	4.49827E+01	8.00600E+01	3.50621E+01
4.48445E+01	4.48473E+01	7.99500E+01	3.50871E+01
4.50604E+01	4.50627E+01	8.00900E+01	3.49975E+01
4.47653E+01	4.47677E+01	7.99100E+01	3.51125E+01
4.49345E+01	4.49369E+01	7.99550E+01	3.49875E+01
4.49169E+01	4.49189E+01	7.99300E+01	3.49628E+01
4.48805E+01	4.48825E+01	7.99200E+01	3.49878E+01
4.48260E+01	4.48281E+01	7.98900E+01	3.50128E+01
4.49101E+01	4.49117E+01	8.00000E+01	3.50083E+01
4.47456E+01	4.47472E+01	7.99000E+01	3.50733E+01
4.48791E+01	4.48807E+01	8.00350E+01	3.50733E+01
4.49276E+01	4.49289E+01	7.99750E+01	3.49386E+01
4.49022E+01	4.49035E+01	7.99600E+01	3.49486E+01
4.48928E+01	4.48941E+01	8.00000E+01	3.49986E+01
4.48950E+01	4.48961E+01	8.00700E+01	3.50438E+01
4.49323E+01	4.49333E+01	8.00450E+01	3.49838E+01
4.48574E+01	4.48584E+01	8.00950E+01	3.51088E+01

ONE TEMPERATURE,FIRST RUN NUMBER IS !1
ONE TEMPERATURE,LAST RUN NUMBER IS !27
DO YOU WANT TO INCLUDE MORE RESULTS !NO
CHOSEN PRANDTL NUMBER EXPONENT IS !0.4
DO YOU WANT TO USE MEAN PRANDTL NUMBERS !NO
RE EXPONENT IS !0.8
GEOMETRY: !CONFIGURATION 0

RESISTANCE	INCREMENT	EXPONENT	SUM ERS SQ
.00000E+00	1.00000E-04	3.69566E-01	2.88975E-02
1.00000E-04	1.00000E-04	3.88211E-01	2.96671E-02
2.00000E-04	1.00000E-04	4.08915E-01	3.03026E-02
3.00000E-04	1.00000E-04	4.32055E-01	3.07358E-02
4.00000E-04	1.00000E-04	4.58107E-01	3.08749E-02
5.00000E-04	1.00000E-04	4.87689E-01	3.05973E-02
6.00000E-04	1.00000E-04	5.21614E-01	2.97448E-02
7.00000E-04	1.00000E-04	5.60983E-01	2.81276E-02
8.00000E-04	1.00000E-04	6.07327E-01	2.55585E-02
9.00000E-04	1.00000E-04	6.62867E-01	2.19867E-02
1.00000E-03	1.00000E-04	7.30970E-01	1.79503E-02
1.10000E-03	1.00000E-04	8.17097E-01	1.61380E-02
1.00000E-03	1.00000E-05	7.30970E-01	1.79503E-02
1.01000E-03	1.00000E-05	7.38655E-01	1.75884E-02
1.02000E-03	1.00000E-05	7.46525E-01	1.72482E-02
1.03000E-03	1.00000E-05	7.54585E-01	1.69349E-02
1.04000E-03	1.00000E-05	7.62845E-01	1.66548E-02
1.05000E-03	1.00000E-05	7.71313E-01	1.64146E-02
1.06000E-03	1.00000E-05	7.79997E-01	1.62225E-02
1.07000E-03	1.00000E-05	7.88907E-01	1.60875E-02
1.08000E-03	1.00000E-05	7.98054E-01	1.60201E-02
1.09000E-03	1.00000E-05	8.07446E-01	1.60323E-02
1.08000E-03	1.00000E-06	7.98054E-01	1.60201E-02
1.08100E-03	1.00000E-06	7.98981E-01	1.60175E-02
1.08200E-03	1.00000E-06	7.99912E-01	1.60158E-02
1.08300E-03	1.00000E-06	8.00845E-01	1.60148E-02
1.08200E-03	1.00000E-07	7.99912E-01	1.60158E-02
1.08210E-03	1.00000E-07	8.00005E-01	1.60156E-02
1.08200E-03	1.00000E-08	7.99912E-01	1.60158E-02
1.08201E-03	1.00000E-08	7.99921E-01	1.60158E-02
1.08202E-03	1.00000E-08	7.99931E-01	1.60157E-02
1.08203E-03	1.00000E-08	7.99940E-01	1.60157E-02
1.08204E-03	1.00000E-08	7.99949E-01	1.60157E-02
1.08205E-03	1.00000E-08	7.99959E-01	1.60157E-02
1.08206E-03	1.00000E-08	7.99968E-01	1.60157E-02
1.08207E-03	1.00000E-08	7.99977E-01	1.60157E-02
1.08208E-03	1.00000E-08	7.99986E-01	1.60157E-02
1.08209E-03	1.00000E-08	7.99996E-01	1.60157E-02
1.08210E-03	1.00000E-08	8.00005E-01	1.60156E-02
1.08209E-03	1.00000E-09	7.99996E-01	1.60157E-02
1.08209E-03	1.00000E-09	7.99997E-01	1.60157E-02
1.08209E-03	1.00000E-09	7.99998E-01	1.60157E-02
1.08209E-03	1.00000E-09	7.99999E-01	1.60157E-02
1.08209E-03	1.00000E-09	8.00000E-01	1.60157E-02

Continued

DATA INPUTS:
RESISTANCE STATED: NO
GEOMETRY: CONFIGURATION 0

HO CORR/BEU	RE NUMBER	EXP NUSSELT	CAL NUSSELT	% CA-EX/EX
2.06351E+04	1.55901E+04	5.29953E+01	5.39243E+01	+1.75300E+00
2.05844E+04	1.55870E+04	5.29266E+01	5.39155E+01	+1.86841E+00
2.05865E+04	1.56041E+04	5.30423E+01	5.39629E+01	+1.73553E+00
2.48769E+04	2.25650E+04	7.16490E+01	7.24857E+01	+1.16776E+00
2.49501E+04	2.25695E+04	7.19757E+01	7.24972E+01	+7.24624E-01
2.48450E+04	2.26119E+04	7.18355E+01	7.26061E+01	+1.07268E+00
2.83039E+04	2.98656E+04	9.10401E+01	9.07069E+01	-3.65957E-01
2.83537E+04	2.98227E+04	9.14210E+01	9.06027E+01	-8.95079E-01
2.85471E+04	2.98342E+04	9.24980E+01	9.06307E+01	-2.01876E+00
3.13334E+04	3.72146E+04	1.11337E+02	1.08162E+02	-2.85160E+00
3.15151E+04	3.72781E+04	1.12637E+02	1.08309E+02	-3.84262E+00
3.14543E+04	3.72963E+04	1.12916E+02	1.08351E+02	-4.04243E+00
3.34121E+04	4.48721E+04	1.27568E+02	1.25627E+02	-1.52119E+00
3.36319E+04	4.49768E+04	1.31575E+02	1.25862E+02	-4.34207E+00
3.35579E+04	4.48631E+04	1.29667E+02	1.25607E+02	-3.13137E+00
3.47392E+04	5.26884E+04	1.40795E+02	1.42848E+02	+1.45824E+00
3.43102E+04	5.27128E+04	1.36954E+02	1.42901E+02	+4.34206E+00
3.47388E+04	5.27409E+04	1.41528E+02	1.42962E+02	+1.01350E+00
3.73601E+04	6.91018E+04	1.69628E+02	1.77457E+02	+4.61573E+00
3.76966E+04	6.91921E+04	1.75661E+02	1.77643E+02	+1.12844E+00
3.76964E+04	6.91918E+04	1.74222E+02	1.77642E+02	+1.96323E+00
3.99685E+04	8.62059E+04	2.05634E+02	2.11803E+02	+2.99997E+00
4.02490E+04	8.62238E+04	2.10508E+02	2.11838E+02	+6.32124E-01
4.02497E+04	8.63123E+04	2.10724E+02	2.12012E+02	+6.11203E-01
4.20929E+04	1.04489E+05	2.44056E+02	2.47037E+02	+1.22130E+00
4.24308E+04	1.04363E+05	2.50125E+02	2.46798E+02	-1.32997E+00
4.26002E+04	1.04624E+05	2.55380E+02	2.47291E+02	-3.16745E+00

LOG-LOG REGRESSION LINE IS (NU/PR^ .4)= .02385083222045 *(RE^ .7999999962321)

RESULTS OF REGRESSION ANALYSIS

Z...SUM OF LOG(NU)	129.9134952665
F...SUM OF LOG(RE)	288.4797161219
W...SUM OF LOG(NU)*LOG(RE)	1395.582218311
G...SUM OF (LOG(RE)^2)	3091.655044051
X...TOTAL NUMBER OF RUNS USED	27
S...SUM OF (DEVIATIONS^2)	.01601569572334
C...OUTER RESISTANCE TO TRANSFER	.001082094
E...SLOPE OF REGRESSION LINE	.7999999962321
C1...LOG(CONST) IN NU EQUATION	-3.735936168317
X7...T(5) IN CONFIDENCE ANALYSIS	2.06
X6...MULT. IN LOG(CONST) ANALYSIS	3.487862577316
X4...MULT. IN SLOPE ANALYSIS	.3259460571525
X5...INTERVAL ON LOG(CONST	.181856775319
X3...INTERVAL ON SLOPE	.0169947919586
F6...MIN. LOG(CONST)	-3.917792943636
F7...MAX. LOG(CONST)	-3.554079392999
Q6...MIN. CONST	.01988493351831
Q7...MAX. CONST	.02860769924546
Q5...REGRESSION CONST	.02385083222045
F8...MIN.SLOPE	.7830052042735
F9...MAX.SLOPE	.8169947881907
Q4...SUM OF (LOG(NU)^2)	631.1332593698
Q3...CORRELATION COEFFICIENT/R	.998673331579
Q2...R^2	.997348423207
F4...AV. ABS. DEV.	2.067273862603
F5...R.M.S. ABS. DEV.	2.429325865437

FILE RESULTS !YES
TRY ANOTHER RE AND/OR PR EXPONENT !NO
DO YOU WANT TO STATE THE RESISTANCE !NO
STOP AT LINE 2520

****
TABLE NO.A.9.6 ISOTHERMAL FRICTION FACTORS CALCULATED USING THE DATA IN
TABLE A.8.6
(RESULTING CORRELATION IS DENOTATION A OF TABLE 5.7)
****

OUTPUT USING EX-6010

X=1 . . . . ISOTHERMAL
X=2 . . . . DIABATIC (TEST SECTION)
CHOSEN VALUE OF X IS !1
CROSS SECTIONAL AREA OF TUBE/SQ.INS. IS !0
TUBE MATERIAL IS !COPPER
TOTAL INSERTED LENGTH/INS. IS !42
FIRST RUN NUMBER ON DATA FILE IS !1
LAST RUN NUMBER ON DATA FILE IS !81
FIRST RUN NUMBER !55
LAST RUN NUMBER !81
HOW MANY F EQUATIONS 16
LENGTH/INS. IS !48
I.D./INS. IS !0.7874016
O.D./INS. IS !0.8661417

DATE: !****

TABLE NO. !A.9.6

GEOMETRY: !CONFIGURATION 1T

RUN NUMBER	TEMP./C	HEAD/CM.	ROTAM/CM.
1	2.26050E+01	17.45	2
2	2.24250E+01	32.15	4
3	2.28900E+01	51.1	6
4	2.26300E+01	74.55	8
5	2.23650E+01	102.35	10
6	2.23800E+01	135.65	12
7	2.25150E+01	10.15	16
8	2.26300E+01	15.1	20
9	2.25800E+01	20.9	24
10	2.26000E+01	20.95	24
11	2.26300E+01	15.1	20
12	2.25500E+01	10.175	16
13	2.23800E+01	135.7	12
14	2.23400E+01	102.35	10
15	2.26000E+01	74.6	8
16	2.28650E+01	51.1	6
17	2.24050E+01	32.15	4
18	2.25250E+01	17.45	2
19	2.25000E+01	17.45	2
20	2.24400E+01	32.15	4
21	2.28400E+01	51.1	6
22	2.26250E+01	74.6	8
23	2.23650E+01	102.35	10
24	2.23750E+01	135.7	12
25	2.25650E+01	10.175	16
26	2.26400E+01	15.1	20
27	2.25900E+01	20.9	24

LENGTH/INS.= 48
DIA./INS.= .7874016
ROUGH/INS.= 6.E-05

Continued

D/G./CU.CM.	VISC./CP.	SPEC. GRAV.	Q/CU.FT./S.
9.97661E-01	9.44244E-01	1.594	6.17934E-03
9.97703E-01	9.48242E-01	1.594	8.96901E-03
9.97594E-01	9.37969E-01	1.594	1.18588E-02
9.97655E-01	9.43691E-01	1.594	1.48272E-02
9.97716E-01	9.49580E-01	1.594	1.78890E-02
9.97713E-01	9.49245E-01	1.594	2.10419E-02
9.97682E-01	9.46239E-01	13.5707	2.76221E-02
9.97655E-01	9.43691E-01	13.5707	3.45631E-02
9.97667E-01	9.44797E-01	13.5707	4.18991E-02
9.97662E-01	9.44354E-01	13.5707	4.18596E-02
9.97655E-01	9.43691E-01	13.5707	3.45631E-02
9.97674E-01	9.45462E-01	13.5707	2.76217E-02
9.97713E-01	9.49245E-01	1.594	2.10436E-02
9.97722E-01	9.50139E-01	1.594	1.78886E-02
9.97662E-01	9.44354E-01	1.594	1.48267E-02
9.97600E-01	9.38516E-01	1.594	1.18574E-02
9.97707E-01	9.48688E-01	1.594	8.96849E-03
9.97679E-01	9.46017E-01	1.594	6.17758E-03
9.97685E-01	9.46573E-01	1.594	6.17682E-03
9.97699E-01	9.47907E-01	1.594	8.97000E-03
9.97606E-01	9.39065E-01	1.594	1.18547E-02
9.97656E-01	9.43801E-01	1.594	1.48255E-02
9.97716E-01	9.49580E-01	1.594	1.78876E-02
9.97714E-01	9.49357E-01	1.594	2.10426E-02
9.97670E-01	9.45130E-01	13.5707	2.76231E-02
9.97653E-01	9.43469E-01	13.5707	3.45635E-02
9.97664E-01	9.44576E-01	13.5707	4.18595E-02

VEL./FT./S.	P/PSI.	RE/NO UNITS	FRICTION
1.82735E+00	1.41902E-01	1.17697E+04	1.48162E-02
2.65231E+00	2.61031E-01	1.70118E+04	1.29364E-02
3.50690E+00	4.14529E-01	2.27370E+04	1.17524E-02
4.38469E+00	6.04405E-01	2.82576E+04	1.09608E-02
5.29012E+00	8.29335E-01	3.38833E+04	1.03315E-02
6.22250E+00	1.09907E+00	3.98691E+04	9.89614E-03
8.16840E+00	1.73929E+00	5.25016E+04	9.08826E-03
1.02209E+01	2.58807E+00	6.58701E+04	8.63748E-03
1.23785E+01	3.58064E+00	7.96824E+04	8.14721E-03
1.23787E+01	3.58957E+00	7.97202E+04	8.16741E-03
1.02209E+01	2.58807E+00	6.58701E+04	8.63748E-03
8.16830E+00	1.74376E+00	5.25437E+04	9.11194E-03
6.22301E+00	1.09947E+00	3.98724E+04	9.89815E-03
5.29001E+00	8.29332E-01	3.38629E+04	1.03319E-02
4.38455E+00	6.04817E-01	2.82370E+04	1.09689E-02
3.50648E+00	4.14530E-01	2.27211E+04	1.17552E-02
2.65216E+00	2.61030E-01	1.70029E+04	1.29379E-02
1.82683E+00	1.41900E-01	1.17445E+04	1.48242E-02
1.82660E+00	1.41901E-01	1.17362E+04	1.48278E-02
2.65260E+00	2.61030E-01	1.70196E+04	1.29336E-02
3.50568E+00	4.14529E-01	2.27029E+04	1.17604E-02
4.38420E+00	6.04817E-01	2.82511E+04	1.09708E-02
5.28971E+00	8.29331E-01	3.38807E+04	1.03331E-02
6.22270E+00	1.09946E+00	3.98658E+04	9.89901E-03
8.16870E+00	1.74374E+00	5.25646E+04	9.11097E-03
1.02211E+01	2.58805E+00	6.58862E+04	8.63719E-03
1.23786E+01	3.58065E+00	7.97015E+04	8.14711E-03

DO YOU WANT A PRINT OUT OF REFERENCE DATA !NO

	COLBURN	BLASIUS	D.K.M.	COLEBROOK
MEAN RATIOS ARE				
	3.68558E+00	3.59656E+00	3.58463E+00	3.62898E+00
MAXIMUM RATIOS ARE				
	4.20005E+00	3.89730E+00	3.88545E+00	3.98872E+00
MINIMUM RATIOS ARE				
	3.38496E+00	3.45664E+00	3.41133E+00	3.38999E+00

	NIKURADSE	ROUSE
MEAN RATIOS ARE		
	3.66367E+00	3.66494E+00
MAXIMUM RATIOS ARE		
	4.00261E+00	3.99081E+00
MINIMUM RATIOS ARE		
	3.45126E+00	3.46155E+00

STOP AT LINE 2680

Continued

OUTPUT USING FRICTION-6010

IS DATA ON FILE !YES
FIRST RUN ON DATA FILE !1
LAST RUN ON DATA FILE !81
FIRST RUN !55
LAST RUN !81
NAME #2 !DAY5AK-6010

COMPARISON WITH REGRESSION ANALYSIS

% ERROR IS EXP-CALC/EXP

REYNOLDS NO	EXPTL F	CALCED F	% ERROR
+1.17697E+04	+1.48162E-02	+1.45132E-02	+2.04444E+00
+1.70118E+04	+1.29364E-02	+1.29553E-02	-1.45810E-01
+2.27370E+04	+1.17524E-02	+1.18471E-02	-8.05766E-01
+2.82576E+04	+1.09608E-02	+1.10793E-02	-1.08119E+00
+3.38833E+04	+1.03315E-02	+1.04763E-02	-1.40084E+00
+3.98691E+04	+9.89614E-03	+9.96390E-03	-6.84732E-01
+5.25016E+04	+9.08826E-03	+9.15338E-03	-7.16589E-01
+6.58701E+04	+8.63748E-03	+8.53520E-03	+1.18411E+00
+7.96824E+04	+8.14721E-03	+8.04876E-03	+1.20849E+00
+7.97202E+04	+8.16741E-03	+8.04758E-03	+1.46716E+00
+6.58701E+04	+8.63748E-03	+8.53520E-03	+1.18411E+00
+5.25437E+04	+9.11194E-03	+9.15112E-03	-4.29982E-01
+3.98724E+04	+9.89815E-03	+9.96365E-03	-6.61753E-01
+3.38629E+04	+1.03319E-02	+1.04782E-02	-1.41644E+00
+2.82370E+04	+1.09689E-02	+1.10818E-02	-1.02912E+00
+2.27211E+04	+1.17552E-02	+1.18497E-02	-8.03573E-01
+1.70029E+04	+1.29379E-02	+1.29574E-02	-1.50878E-01
+1.17445E+04	+1.48242E-02	+1.45228E-02	+2.03289E+00
+1.17362E+04	+1.48278E-02	+1.45260E-02	+2.03527E+00
+1.70196E+04	+1.29336E-02	+1.29535E-02	-1.53724E-01
+2.27029E+04	+1.17604E-02	+1.18526E-02	-7.83745E-01
+2.82511E+04	+1.09708E-02	+1.10801E-02	-9.96679E-01
+3.38807E+04	+1.03331E-02	+1.04765E-02	-1.38820E+00
+3.98658E+04	+9.89901E-03	+9.96416E-03	-6.58109E-01
+5.25646E+04	+9.11097E-03	+9.15000E-03	-4.28343E-01
+6.58862E+04	+8.63719E-03	+8.53455E-03	+1.18829E+00
+7.97015E+04	+8.14711E-03	+8.04816E-03	+1.21456E+00

*LOG-LOG REGRESSION LINE IS F= .2609799143938 *(RE^ -.3082567570791)*

RESULTS OF REGRESSION ANALYSIS

Z...SUM OF LOG(F)	-122.8905467233
F...SUM OF LOG(RE)	281.0031744471
W...SUM OF LOG(F)*LOG(RE)	-1281.924284659
G...SUM OF (LOG(RE)^2)	2934.078086143
X...TOTAL NUMBER OF RUNS USED	27
S...SUM OF (DEVIATIONS^2)	.003530821944723
E...SLOPE OF REGRESSION LINE	-.3082567570791
C1...LOG(CONST) IN F EQUATION	-1.343311830966
X7...T(5) IN CONFIDENCE ANALYSIS	2.06
X6...MULT. IN LOG(CONST) ANALYSIS	3.37672313756
X4...MULT. IN SLOPE ANALYSIS	.3239227880822
X5...INTERVAL ON LOG(CONST)	.08266669562957
X3...INTERVAL ON SLOPE	.007930062797276
F6...MIN. LOG(CONST)	-1.425978526596
F7...MAX. LOG(CONST)	-1.260645135337
Q6...MIN. CONST	.2402732343882
Q7...MAX. CONST	.2834710902795
Q5...REGRESSION CONST	.2609799143938
F8...MIN. SLOPE	-.3161868198764
F9...MAX. SLOPE	-.3003266942818
Q4...SUM OF (LOG(F)^2)	560.2456789734
Q3...CORRELATION COEFFICIENT/R	-.9980562700362
Q2...R^2	.9961163181585
F4...AV. ABS. DEV.	1.010921525038
F5...R.M.S. ABS. DEV.	1.139772548202

STATE FILENAME OR NO !NO
STOP AT LINE 570

****

TABLE NO.A.9.7 ISOTHERMAL FRICTION FACTORS CALCULATED USING THE DATA IN
TABLE A.8.7
(RESULTING CORRELATION IS DENOTATION I OF TABLE 5.8)

****

OUTPUT USING EX-6010

X=1 . . . . ISOTHERMAL
X=2 . . . . DIABATIC (TEST SECTION)
CHOSEN VALUE OF X IS !1
CROSS SECTIONAL AREA OF TUBE/SQ.INS. IS !0
TUBE MATERIAL IS !COPPER
TOTAL INSERTED LENGTH/INS. IS !41.6
FIRST RUN NUMBER ON DATA FILE IS !1
LAST RUN NUMBER ON DATA FILE IS !81
FIRST RUN NUMBER !1
LAST RUN NUMBER !27
HOW MANY F EQUATIONS !6
LENGTH/INS. IS !48
I.D./INS. IS !0.7874016
O.D./INS. IS !0.8661417

DATE: !****

TABLE NO. !A.9.7

GEOMETRY: !CONFIGURATION 6K

RUN NUMBER	TEMP./C	HEAD/CM.	ROTAM/CM.
1	2.06650E+01	12.35	2
2	2.05650E+01	23.6	4
3	2.05150E+01	38.55	6
4	2.05400E+01	58	8
5	2.05150E+01	81.65	10
6	2.04800E+01	110.4	12
7	2.04150E+01	182.1	16
8	2.03550E+01	275.95	20
9	2.03150E+01	388.35	24
10	2.03000E+01	387.75	24
11	2.03250E+01	275.8	20
12	2.04400E+01	182.3	16
13	2.03650E+01	110.4	12
14	2.04000E+01	81.5	10
15	2.03750E+01	57.95	8
16	2.03900E+01	38.5	6
17	2.03400E+01	23.65	4
18	2.04050E+01	12.35	2
19	2.03650E+01	12.35	2
20	2.03800E+01	23.65	4
21	2.03800E+01	38.6	6
22	2.03150E+01	57.9	8
23	2.03050E+01	81.55	10
24	2.02900E+01	110.4	12
25	2.02900E+01	182.25	16
26	2.03550E+01	275.95	20
27	2.02500E+01	388.15	24

LENGTH/INS.= 48
DIA./INS.= .7874016
ROUGH/INS.= 6.E-05

Continued

D/G./CU.CM.	VISC./CP.	SPEC. GRAV.	Q/CU.FT./S.
9.98094E-01	9.88808E-01	13.5699	6.16801E-03
9.98115E-01	9.91197E-01	13.5699	8.95269E-03
9.98126E-01	9.92394E-01	13.5699	1.18311E-02
9.98120E-01	9.91795E-01	13.5699	1.47986E-02
9.98126E-01	9.92394E-01	13.5699	1.78582E-02
9.98133E-01	9.93234E-01	13.5699	2.10086E-02
9.98147E-01	9.94796E-01	13.5699	2.75817E-02
9.98159E-01	9.96242E-01	13.57	3.45191E-02
9.98168E-01	9.97208E-01	13.57	4.18174E-02
9.98171E-01	9.97570E-01	13.57	4.18223E-02
9.98166E-01	9.96966E-01	13.57	3.45193E-02
9.98141E-01	9.94195E-01	13.5699	2.75818E-02
9.98157E-01	9.96001E-01	13.5699	2.10086E-02
9.98150E-01	9.95157E-01	13.5699	1.78575E-02
9.98155E-01	9.95760E-01	13.57	1.47967E-02
9.98152E-01	9.95398E-01	13.57	1.18290E-02
9.98162E-01	9.96604E-01	13.5699	8.95207E-03
9.98149E-01	9.95037E-01	13.57	6.16658E-03
9.98157E-01	9.96001E-01	13.57	6.16689E-03
9.98154E-01	9.95639E-01	13.57	8.95234E-03
9.98154E-01	9.95639E-01	13.57	1.18293E-02
9.98168E-01	9.97208E-01	13.57	1.47979E-02
9.98170E-01	9.97449E-01	13.57	1.78567E-02
9.98173E-01	9.97812E-01	13.57	2.10062E-02
9.98173E-01	9.97812E-01	13.57	2.75806E-02
9.98159E-01	9.96242E-01	13.57	3.45182E-02
9.98181E-01	9.98780E-01	13.57	4.18185E-02

VEL./FT./S.	P/PSI.	RE/NO UNITS	FRICTION
1.82400E+00	2.19839E+00	1.12235E+04	2.32495E-01
2.64748E+00	4.20092E+00	1.62517E+04	2.10876E-01
3.49870E+00	6.86215E+00	2.14512E+04	1.97238E-01
4.37623E+00	1.03248E+01	2.68476E+04	1.89683E-01
5.28103E+00	1.45351E+01	3.23790E+04	1.83370E-01
6.21266E+00	1.96540E+01	3.80592E+04	1.79158E-01
8.15645E+00	3.24203E+01	4.98891E+04	1.71455E-01
1.02079E+01	4.91309E+01	6.23476E+04	1.65884E-01
1.23662E+01	6.91431E+01	7.54570E+04	1.59075E-01
1.23676E+01	6.90360E+01	7.54388E+04	1.58790E-01
1.02080E+01	4.91036E+01	6.23030E+04	1.65789E-01
8.15649E+00	3.24556E+01	4.99193E+04	1.71641E-01
6.21265E+00	1.96537E+01	3.79543E+04	1.79153E-01
5.28081E+00	1.45083E+01	3.22886E+04	1.83042E-01
4.37568E+00	1.03154E+01	2.67383E+04	1.89551E-01
3.49808E+00	6.85306E+00	2.13833E+04	1.97042E-01
2.64730E+00	4.20974E+00	1.61632E+04	2.11338E-01
1.82357E+00	2.19829E+00	1.11513E+04	2.32579E-01
1.82367E+00	2.19831E+00	1.11411E+04	2.32556E-01
2.64738E+00	4.20969E+00	1.61792E+04	2.11324E-01
3.49818E+00	6.87090E+00	2.13787E+04	1.97543E-01
4.37602E+00	1.03064E+01	2.67019E+04	1.89355E-01
5.28058E+00	1.45169E+01	3.22136E+04	1.83163E-01
6.21196E+00	1.96537E+01	3.78818E+04	1.79189E-01
8.15614E+00	3.24462E+01	4.97378E+04	1.71601E-01
1.02077E+01	4.91304E+01	6.23459E+04	1.65892E-01
1.23665E+01	6.91066E+01	7.53413E+04	1.58980E-01

DO YOU WANT A PRINT OUT OF REFERENCE DATA !NO

	COLBURN	BLASIUS	D.K.M.	COLEBROOK
MEAN RATIOS ARE	6.43200E+01	6.27341E+01	6.25340E+01	6.33203E+01
MAXIMUM RATIOS ARE	6.56234E+01	6.65782E+01	6.57887E+01	6.56777E+01
MINIMUM RATIOS ARE	6.29283E+01	6.01253E+01	6.01135E+01	6.14888E+01

	NIKURADSE	ROUSE
MEAN RATIOS ARE	6.39188E+01	6.39390E+01
MAXIMUM RATIOS ARE	6.66499E+01	6.68056E+01
MINIMUM RATIOS ARE	6.18585E+01	6.17350E+01

STOP AT LINE 2680

Continued

OUTPUT USING FRICTION-6010

IS DATA ON FILE !YES
FIRST RUN ON DATA FILE !1
LAST RUN ON DATA FILE !27
FIRST RUN !1
LAST RUN !27
NAME #2 !DAY5AC-6010

COMPARISON WITH REGRESSION ANALYSIS

% ERROR IS EXP-CALC/EXP

REYNOLDS NO	EXPTL F	CALCED F	% ERROR
+1.12235E+04	+2.32495E-01	+2.26735E-01	+2.47769E+00
+1.62517E+04	+2.10876E-01	+2.11338E-01	-2.19160E-01
+2.14512E+04	+1.97238E-01	+2.00483E-01	-1.64489E+00
+2.68476E+04	+1.89683E-01	+1.92116E-01	-1.28284E+00
+3.23790E+04	+1.83370E-01	+1.85400E-01	-1.10695E+00
+3.80592E+04	+1.79158E-01	+1.79794E-01	-3.54665E-01
+4.98891E+04	+1.71455E-01	+1.70783E-01	+3.91999E-01
+6.23476E+04	+1.65884E-01	+1.63702E-01	+1.31570E+00
+7.54570E+04	+1.59075E-01	+1.57874E-01	+7.55190E-01
+7.54388E+04	+1.58790E-01	+1.57881E-01	+5.72766E-01
+6.23030E+04	+1.65789E-01	+1.63724E-01	+1.24578E+00
+4.99193E+04	+1.71641E-01	+1.70763E-01	+5.11431E-01
+3.79543E+04	+1.79153E-01	+1.79888E-01	-4.10454E-01
+3.22886E+04	+1.83042E-01	+1.85498E-01	-1.34170E+00
+2.67383E+04	+1.89551E-01	+1.92265E-01	-1.43170E+00
+2.13833E+04	+1.97042E-01	+2.00604E-01	-1.80767E+00
+1.61632E+04	+2.11338E-01	+2.11558E-01	-1.03816E-01
+1.11513E+04	+2.32579E-01	+2.27013E-01	+2.39327E+00
+1.11411E+04	+2.32556E-01	+2.27052E-01	+2.36667E+00
+1.61792E+04	+2.11324E-01	+2.11518E-01	-9.14942E-02
+2.13787E+04	+1.97543E-01	+2.00612E-01	-1.55329E+00
+2.67019E+04	+1.89355E-01	+1.92315E-01	-1.56319E+00
+3.22136E+04	+1.83163E-01	+1.85580E-01	-1.31967E+00
+3.78818E+04	+1.79189E-01	+1.79953E-01	-4.26674E-01
+4.97378E+04	+1.71601E-01	+1.70882E-01	+4.19014E-01
+6.23459E+04	+1.65892E-01	+1.63703E-01	+1.31943E+00
+7.53413E+04	+1.58980E-01	+1.57920E-01	+6.67202E-01

LOG-LOG REGRESSION LINE IS F= 1.333211694619 *(RE^ -.1899642463292)

RESULTS OF REGRESSION ANALYSIS

Z...SUM OF LOG(F)	-45.3460160229
F...SUM OF LOG(RE)	279.5840254583
W...SUM OF LOG(F)*LOG(RE)	-471.3610591593
G...SUM OF (LOG(RE)^2)	2904.58270088
X...TOTAL NUMBER OF RUNS USED	27
S...SUM OF (DEVIATIONS^2)	.004448244788742
E...SLOPE OF REGRESSION LINE	-.1899642463292
C1...LOG(CONST) IN F EQUATION	.2875908392545
X7...T(5) IN CONFIDENCE ANALYSIS	2.06
X6...MULT. IN LOG(CONST) ANALYSIS	3.365064712045
X4...MULT. IN SLOPE ANALYSIS	.3244392802055
X5...INTERVAL ON LOG(CONST)	.09246661848358
X3...INTERVAL ON SLOPE	.00891507466007
F6...MIN. LOG(CONST)	.1951242207709
F7...MAX. LOG(CONST)	.380057457738
Q6...MIN. CONST	1.215461962734
Q7...MAX. CONST	1.462368611413
Q5...REGRESSION CONST	1.333211694619
F8...MIN. SLOPE	-.1988793209893
F9...MAX. SLOPE	-.1810491716692
Q4...SUM OF (LOG(F)^2)	76.50509779353
Q3...CORRELATION COEFFICIENT/R	-.9935748916057
Q2...R^2	.9871910652293
F4...AV. ABS. DEV.	1.077569068767
F5...R.M.S. ABS. DEV.	1.280361771172

STATE FILENAME OR NO !NO
STOP AT LINE 570

****

TABLE NO.A.9.8 NON-ISOTHERMAL FRICTION FACTORS CALCULATED USING THE DATA IN TABLE A.8.8
(RESULTING CORRELATION IS DENOTATION A OF TABLE 5.9)

****

OUTPUT USING EX-6010

X=1 . . . . ISOTHERMAL
X=2 . . . . DIABATIC (TEST SECTION)
CHOSEN VALUE OF X IS !2
CROSS SECTIONAL AREA OF TUBE/SQ.INS. IS !0
TUBE MATERIAL IS !COPPER
TOTAL INSERTED LENGTH/INS. IS !42
FIRST RUN NUMBER ON DATA FILE IS !1
LAST RUN NUMBER ON DATA FILE IS !54
FIRST RUN NUMBER !28
LAST RUN NUMBER !54
HOW MANY F EQUATIONS !6
LENGTH/INS. IS !48
I.D./INS. IS !0.7874016
O.D./INS. IS !0.8661417

DATE: !****

TABLE NO. !A.9.8

GEOMETRY: !CONFIGURATION !T

RUN NUMBER	TEMP./C	HEAD/CM.	ROTAM/CM.
1	3.49900E+01	15.3	2
2	3.49750E+01	15.35	2
3	3.50500E+01	15.35	2
4	3.49748E+01	28.5	4
5	3.50000E+01	28.55	4
6	3.49750E+01	28.55	4
7	3.49750E+01	45.95	6
8	3.50500E+01	45.95	6
9	3.50250E+01	45.95	6
10	3.50250E+01	67.95	8
11	3.49750E+01	68	8
12	3.49600E+01	67.95	8
13	3.49650E+01	93.7	10
14	3.49550E+01	93.6	10
15	3.49750E+01	93.6	10
16	3.49900E+01	126.05	12
17	3.50300E+01	126	12
18	3.49500E+01	126.05	12
19	3.51150E+01	9.6	16
20	3.50000E+01	9.575	16
21	3.50500E+01	9.575	16
22	3.50000E+01	14.35	20
23	3.49900E+01	14.35	20
24	3.50500E+01	14.35	20
25	3.49650E+01	20.05	24
26	3.49150E+01	20.1	24
27	3.49150E+01	20.1	24

LENGTH/INS.= 48
DIA./INS.= .7874016
ROUGH/INS.= 6.E-05

Continued

D/C./CU.CM.	VISC./CP.	SPEC. GRAV.	Q/CU.FT./S.
9.94066E-01	7.22667E-01	1.595	6.28128E-03
9.94072E-01	7.22883E-01	1.595	6.28187E-03
9.94046E-01	7.21804E-01	1.594	6.28254E-03
9.94072E-01	7.22885E-01	1.594	9.10231E-03
9.94063E-01	7.22523E-01	1.594	9.10323E-03
9.94072E-01	7.22883E-01	1.594	9.10301E-03
9.94072E-01	7.22883E-01	1.594	1.20111E-02
9.94046E-01	7.21804E-01	1.594	1.20114E-02
9.94054E-01	7.22163E-01	1.594	1.20121E-02
9.94054E-01	7.22163E-01	1.595	1.50068E-02
9.94072E-01	7.22883E-01	1.595	1.50061E-02
9.94077E-01	7.23099E-01	1.595	1.50064E-02
9.94075E-01	7.23027E-01	1.595	1.80887E-02
9.94078E-01	7.23171E-01	1.595	1.80880E-02
9.94072E-01	7.22883E-01	1.595	1.80878E-02
9.94066E-01	7.22667E-01	1.595	2.12558E-02
9.94053E-01	7.22091E-01	1.595	2.12561E-02
9.94080E-01	7.23243E-01	1.594	2.12555E-02
9.94023E-01	7.20871E-01	13.5707	2.78565E-02
9.94063E-01	7.22523E-01	13.5707	2.78543E-02
9.94046E-01	7.21804E-01	13.5707	2.78556E-02
9.94063E-01	7.22523E-01	13.5709	3.47991E-02
9.94066E-01	7.22667E-01	13.571	3.47989E-02
9.94046E-01	7.21804E-01	13.5711	3.47997E-02
9.94075E-01	7.23027E-01	13.5712	4.20898E-02
9.94092E-01	7.23748E-01	13.5712	4.20892E-02
9.94092E-01	7.23748E-01	13.5714	4.20892E-02

VEL./FT./S.	P/PSI.	RE/NO UNITS	FRICTION
1.85749E+00	1.24198E-01	1.55758E+04	1.25955E-02
1.85767E+00	1.24616E-01	1.55727E+04	1.26355E-02
1.85787E+00	1.24395E-01	1.55972E+04	1.26107E-02
2.69173E+00	2.30669E-01	2.25644E+04	1.11399E-02
2.69200E+00	2.31084E-01	2.25778E+04	1.11578E-02
2.69194E+00	2.31081E-01	2.25662E+04	1.11581E-02
3.55193E+00	3.71780E-01	2.97755E+04	1.03113E-02
3.55202E+00	3.71772E-01	2.98200E+04	1.03108E-02
3.55221E+00	3.71761E-01	2.98070E+04	1.03093E-02
4.43781E+00	5.50843E-01	3.72381E+04	9.78713E-03
4.43762E+00	5.51249E-01	3.72001E+04	9.79502E-03
4.43771E+00	5.50812E-01	3.71899E+04	9.78680E-03
5.34919E+00	7.59477E-01	4.48330E+04	9.28739E-03
5.34899E+00	7.58617E-01	4.48225E+04	9.27754E-03
5.34891E+00	7.58612E-01	4.48394E+04	9.27782E-03
6.28577E+00	1.02227E+00	5.27085E+04	9.05338E-03
6.28586E+00	1.02181E+00	5.27505E+04	9.04918E-03
6.28569E+00	1.02033E+00	5.26665E+04	9.03629E-03
8.23771E+00	1.64483E+00	6.92454E+04	8.48175E-03
8.23707E+00	1.64030E+00	6.90844E+04	8.45940E-03
8.23746E+00	1.64029E+00	6.91553E+04	8.45869E-03
1.02907E+01	2.45976E+00	8.63089E+04	8.12750E-03
1.02907E+01	2.45969E+00	8.62914E+04	8.12736E-03
1.02909E+01	2.45962E+00	8.63949E+04	8.12691E-03
1.24467E+01	3.43677E+00	1.04319E+05	7.76236E-03
1.24466E+01	3.44562E+00	1.04216E+05	7.78243E-03
1.24466E+01	3.44552E+00	1.04216E+05	7.78219E-03

DO YOU WANT A PRINT OUT OF REFERENCE DATA ?NO

	COLBURN	BLASIUS	D.K.M.	COLEBROOK
MEAN RATIOS ARE				
	3.50557E+00	3.47223E+00	3.45145E+00	3.47447E+00
MAXIMUM RATIOS ARE				
	3.78737E+00	3.56442E+00	3.56273E+00	3.65049E+00
MINIMUM RATIOS ARE				
	3.40360E+00	3.40888E+00	3.39892E+00	3.40373E+00

	NIKURADSE	ROUSE
MEAN RATIOS ARE		
	3.51684E+00	3.52116E+00
MAXIMUM RATIOS ARE		
	3.66703E+00	3.65996E+00
MINIMUM RATIOS ARE		
	3.46417E+00	3.46910E+00

STOP AT LINE 2680

Continued

OUTPUT USING FRICTION-6010

IS DATA ON FILE !YES
FIRST RUN ON DATA FILE !1
LAST RUN ON DATA FILE !54
FIRST RUN !28
LAST RUN !54
NAME #2 !DAY5AL-6010

COMPARISON WITH REGRESSION ANALYSIS

% ERROR IS EXP-CALC/EXP

REYNOLDS NO	EXPTL F	CALCED F	% ERROR
+1.55758E+04	+1.25955E-02	+1.22781E-02	+2.51994E+00
+1.55727E+04	+1.26355E-02	+1.22787E-02	+2.82339E+00
+1.55972E+04	+1.26107E-02	+1.22739E-02	+2.67048E+00
+2.25644E+04	+1.11399E-02	+1.12009E-02	-5.47714E-01
+2.25778E+04	+1.11578E-02	+1.11993E-02	-3.71467E-01
+2.25662E+04	+1.11581E-02	+1.12007E-02	-3.81762E-01
+2.97755E+04	+1.03113E-02	+1.04573E-02	-1.41588E+00
+2.98200E+04	+1.03108E-02	+1.04534E-02	-1.38308E+00
+2.98070E+04	+1.03093E-02	+1.04545E-02	-1.40895E+00
+3.72381E+04	+9.78713E-03	+9.89368E-03	-1.08865E+00
+3.72001E+04	+9.79502E-03	+9.89619E-03	-1.03282E+00
+3.71899E+04	+9.78680E-03	+9.89686E-03	-1.12451E+00
+4.48330E+04	+9.28739E-03	+9.44906E-03	-1.74068E+00
+4.48225E+04	+9.27754E-03	+9.44960E-03	-1.85463E+00
+4.48394E+04	+9.27782E-03	+9.44872E-03	-1.84201E+00
+5.27085E+04	+9.05338E-03	+9.07773E-03	-2.68980E-01
+5.27505E+04	+9.04918E-03	+9.07594E-03	-2.95702E-01
+5.26665E+04	+9.03629E-03	+9.07952E-03	-4.78448E-01
+6.92454E+04	+8.48175E-03	+8.48435E-03	-3.05943E-02
+6.90844E+04	+8.45940E-03	+8.48924E-03	-3.52755E-01
+6.91553E+04	+8.45869E-03	+8.48709E-03	-3.35638E-01
+8.63089E+04	+8.12750E-03	+8.03377E-03	+1.15327E+00
+8.62914E+04	+8.12736E-03	+8.03417E-03	+1.14659E+00
+8.63949E+04	+8.12691E-03	+8.03179E-03	+1.17044E+00
+1.04319E+05	+7.76236E-03	+7.66529E-03	+1.25049E+00
+1.04216E+05	+7.78243E-03	+7.66718E-03	+1.48090E+00
+1.04216E+05	+7.78219E-03	+7.66718E-03	+1.47790E+00

LOG-LOG REGRESSION LINE IS F= .1341941159953 *(RE^ -.2477309575456)

RESULTS OF REGRESSION ANALYSIS

Z...SUM OF LOG(F)	-125.6886679893
F...SUM OF LOG(RE)	288.4582346297
W...SUM OF LOG(F)*LOG(RE)	-1345.144758668
G...SUM OF (LOG(RE)^2)	3091.198860959
X...TOTAL NUMBER OF RUNS USED	27
S...SUM OF (DEVIATIONS^2)	.005232291650687
E...SLOPE OF REGRESSION LINE	-.2477309575456
C1...LOG(CONST) IN F EQUATION	-2.008467900448
X7...T(5) IN CONFIDENCE ANALYSIS	2.06
X6...MULT. IN LOG(CONST) ANALYSIS	3.487080145885
X4...MULT. IN SLOPE ANALYSIS	.3258969821803
X5...INTERVAL ON LOG(CONST)	.103921430701
X3...INTERVAL ON SLOPE	.009712332161132
F6...MIN. LOG(CONST)	-2.112389331149
F7...MAX. LOG(CONST)	-1.904546469747
Q6...MIN. CONST	.1209486345762
Q7...MAX. CONST	.1488901535008
Q5...REGRESSION CONST	.1341941159953
F8...MIN. SLOPE	-.2574432897067
F9...MAX. SLOPE	-.2380186253845
Q4...SUM OF (LOG(F)^2)	585.6808865027
Q3...CORRELATION COEFFICIENT/R	-.995502980257
Q2...R^2	.9910261837005
F4...AV. ABS. DEV.	1.172139000599
F5...R.M.S. ABS. DEV.	1.386457744505

STATE FILENAME OR NO !NO
STOP AT LINE 570

****
TABLE NO.A.9.9 NON-ISOTHERMAL FRICTION FACTORS CALCULATED USING THE DATA IN
TABLE A.8.9
(RESULTING CORRELATION IS DENOTATION H OF TABLE 5.10)
****

OUTPUT USING EX-6010

X=1 . . . . ISOTHERMAL
X=2 . . . . DIABATIC (TEST SECTION)
CHOSEN VALUE OF X IS 2
CROSS SECTIONAL AREA OF TUBE/SQ.INS. IS 0
TUBE MATERIAL IS 1COPPER
TOTAL INSERTED LENGTH/INS. IS 141.6
FIRST RUN NUMBER ON DATA FILE IS 1
LAST RUN NUMBER ON DATA FILE IS 181
FIRST RUN NUMBER 28
LAST RUN NUMBER 54
HOW MANY F EQUATIONS 6
LENGTH/INS. IS 48
I.D./INS. IS 0.7874016
O.D./INS. IS 0.8661417

DATE: 1****

TABLE NO. 1A.9.9

GEOMETRY: 1CONFIGURATION 6K

RUN NUMBER	TEMP./C	HEAD/CM.	ROTAM/CM.
1	3.50100E+01	12.35	2
2	3.50250E+01	12.35	2
3	3.50350E+01	12.35	2
4	3.50450E+01	23.65	4
5	3.49750E+01	23.65	4
6	3.50150E+01	23.65	4
7	3.50750E+01	38.75	6
8	3.50650E+01	38.75	6
9	3.49150E+01	38.75	6
10	3.50150E+01	58.1	8
11	3.49650E+01	58.15	8
12	3.49900E+01	58	8
13	3.50000E+01	81.75	10
14	3.49650E+01	81.85	10
15	3.49900E+01	81.95	10
16	3.50000E+01	110.95	12
17	3.49750E+01	110.9	12
18	3.49850E+01	111	12
19	3.50800E+01	183.1	16
20	3.50500E+01	183.05	16
21	3.50650E+01	183.1	16
22	3.49650E+01	278	20
23	3.49150E+01	277.95	20
24	3.50100E+01	277.8	20
25	3.50250E+01	393.3	24
26	3.49750E+01	393.2	24
27	3.49400E+01	393.3	24

LENGTH/INS.= 48
DIA./INS.= .7874016
ROUGH/INS.= 6.E-05

Continued

D/G./CU.CM.	VISC./CP.	SPEC. GRAV.	Q/CU.FT./S.
9.94060E-01	7.22379E-01	13.5697	6.30031E-03
9.94054E-01	7.22163E-01	13.5697	6.29992E-03
9.94051E-01	7.22020E-01	13.5697	6.29994E-03
9.94048E-01	7.21876E-01	13.5698	9.11975E-03
9.94072E-01	7.22883E-01	13.5698	9.11933E-03
9.94058E-01	7.22307E-01	13.5698	9.11991E-03
9.94037E-01	7.21445E-01	13.5699	1.20263E-02
9.94041E-01	7.21588E-01	13.57	1.20254E-02
9.94092E-01	7.23748E-01	13.57	1.20247E-02
9.94058E-01	7.22307E-01	13.5701	1.50193E-02
9.94075E-01	7.23027E-01	13.5701	1.50187E-02
9.94066E-01	7.22667E-01	13.5701	1.50190E-02
9.94063E-01	7.22523E-01	13.57	1.80989E-02
9.94075E-01	7.23027E-01	13.57	1.80988E-02
9.94066E-01	7.22667E-01	13.5701	1.80993E-02
9.94063E-01	7.22523E-01	13.5697	2.12640E-02
9.94072E-01	7.22883E-01	13.5698	2.12639E-02
9.94068E-01	7.22739E-01	13.5698	2.12653E-02
9.94036E-01	7.21373E-01	13.5698	2.78622E-02
9.94046E-01	7.21804E-01	13.5699	2.78620E-02
9.94041E-01	7.21588E-01	13.5699	2.78625E-02
9.94075E-01	7.23027E-01	13.57	3.48044E-02
9.94092E-01	7.23748E-01	13.5701	3.48030E-02
9.94060E-01	7.22379E-01	13.5701	3.48048E-02
9.94054E-01	7.22163E-01	13.5699	4.20933E-02
9.94072E-01	7.22883E-01	13.5699	4.20924E-02
9.94084E-01	7.23387E-01	13.5699	4.20918E-02

VEL./FT./S.	P/PSI.	RE/NO UNITS	FRICTION
1.86312E+00	2.19889E+00	1.56291E+04	2.23789E-01
1.86301E+00	2.19883E+00	1.56327E+04	2.23811E-01
1.86301E+00	2.19881E+00	1.56358E+04	2.23808E-01
2.69688E+00	4.21051E+00	2.26387E+04	2.04518E-01
2.69676E+00	4.21042E+00	2.26067E+04	2.04528E-01
2.69693E+00	4.21047E+00	2.26258E+04	2.04507E-01
3.55642E+00	6.89870E+00	2.98715E+04	1.92694E-01
3.55616E+00	6.89854E+00	2.98635E+04	1.92716E-01
3.55594E+00	6.89838E+00	2.97741E+04	1.92726E-01
4.44151E+00	1.03429E+01	3.72619E+04	1.85225E-01
4.44133E+00	1.03518E+01	3.72240E+04	1.85397E-01
4.44141E+00	1.03251E+01	3.72429E+04	1.84913E-01
5.35221E+00	1.45549E+01	4.48890E+04	1.79498E-01
5.35219E+00	1.45721E+01	4.48581E+04	1.79709E-01
5.35234E+00	1.45897E+01	4.48813E+04	1.79918E-01
6.28818E+00	1.97573E+01	5.27390E+04	1.76521E-01
6.28817E+00	1.97476E+01	5.27131E+04	1.76432E-01
6.28857E+00	1.97654E+01	5.27268E+04	1.76570E-01
8.23940E+00	3.26044E+01	6.92122E+04	1.69673E-01
8.23936E+00	3.25951E+01	6.91712E+04	1.69625E-01
8.23950E+00	3.26040E+01	6.91927E+04	1.69666E-01
1.02923E+01	4.95018E+01	8.62629E+04	1.65083E-01
1.02919E+01	4.94927E+01	8.61749E+04	1.65064E-01
1.02924E+01	4.94660E+01	8.63399E+04	1.64963E-01
1.24478E+01	7.00401E+01	1.04451E+05	1.59691E-01
1.24475E+01	7.00222E+01	1.04346E+05	1.59654E-01
1.24473E+01	7.00408E+01	1.04273E+05	1.59699E-01

DO YOU WANT A PRINT OUT OF REFERENCE DATA ?NO

	COLBURN	BLASIUS	D.K.M.	COLEBROOK
MEAN RATIOS ARE	6.74839E+01	6.69367E+01	6.65164E+01	6.69219E+01
MAXIMUM RATIOS ARE	7.00382E+01	7.24959E+01	7.10305E+01	7.00401E+01
MINIMUM RATIOS ARE	6.57630E+01	6.31870E+01	6.31586E+01	6.46738E+01

	NIKURADSE	ROUSE
MEAN RATIOS ARE	6.77554E+01	6.78442E+01
MAXIMUM RATIOS ARE	7.16146E+01	7.18768E+01
MINIMUM RATIOS ARE	6.50064E+01	6.48820E+01

STOP AT LINE 2680

Continued

OUTPUT USING FRICTION-6010

IS DATA ON FILE !YES
FIRST RUN ON DATA FILE !1
LAST RUN ON DATA FILE !54
FIRST RUN !28
LAST RUN !54
NAME #2 !DAY5AD-6010

COMPARISON WITH REGRESSION ANALYSIS

% ERROR IS EXP-CALC/EXP

REYNOLDS NO	EXPTL F	CALCED F	% ERROR
+1.56291E+04	+2.23789E-01	+2.18153E-01	+2.51858E+00
+1.56327E+04	+2.23811E-01	+2.18144E-01	+2.53216E+00
+1.56358E+04	+2.23808E-01	+2.18137E-01	+2.53414E+00
+2.26387E+04	+2.04518E-01	+2.04815E-01	-1.44999E-01
+2.26067E+04	+2.04528E-01	+2.04864E-01	-1.64576E-01
+2.26258E+04	+2.04507E-01	+2.04835E-01	-1.60440E-01
+2.98715E+04	+1.92694E-01	+1.95372E-01	-1.38958E+00
+2.98635E+04	+1.92716E-01	+1.95380E-01	-1.38240E+00
+2.97741E+04	+1.92726E-01	+1.95480E-01	-1.42893E+00
+3.72619E+04	+1.85225E-01	+1.88155E-01	-1.58139E+00
+3.72240E+04	+1.85397E-01	+1.88187E-01	-1.50500E+00
+3.72429E+04	+1.84913E-01	+1.88171E-01	-1.76211E+00
+4.48890E+04	+1.79498E-01	+1.82282E-01	-1.55139E+00
+4.48581E+04	+1.79709E-01	+1.82304E-01	-1.44364E+00
+4.48813E+04	+1.79918E-01	+1.82288E-01	-1.31682E+00
+5.27390E+04	+1.76521E-01	+1.77349E-01	-4.69032E-01
+5.27131E+04	+1.76432E-01	+1.77363E-01	-5.27690E-01
+5.27268E+04	+1.76570E-01	+1.77356E-01	-4.45076E-01
+6.92122E+04	+1.69673E-01	+1.69328E-01	+2.03663E-01
+6.91712E+04	+1.69625E-01	+1.69345E-01	+1.65046E-01
+6.91927E+04	+1.69666E-01	+1.69336E-01	+1.94763E-01
+8.62629E+04	+1.65083E-01	+1.63096E-01	+1.20349E+00
+8.61749E+04	+1.65064E-01	+1.63125E-01	+1.17474E+00
+8.63399E+04	+1.64963E-01	+1.63071E-01	+1.14642E+00
+1.04451E+05	+1.59691E-01	+1.57869E-01	+1.14071E+00
+1.04346E+05	+1.59654E-01	+1.57896E-01	+1.10134E+00
+1.04273E+05	+1.59699E-01	+1.57915E-01	+1.11737E+00

LOG-LOG REGRESSION LINE IS F= 1.129360048657 *(RE^ -.1702628475737)

RESULTS OF REGRESSION ANALYSIS

Z...SUM OF LOG(F)	-45.83408781996
F...SUM OF LOG(RE)	288.4872971325
W...SUM OF LOG(F)*LOG(RE)	-491.3222346023
G...SUM OF (LOG(RE)^2)	3091.790438899
X...TOTAL NUMBER OF RUNS USED	27
S...SUM OF (DEVIATIONS^2)	.004822717869633
E...SLOPE OF REGRESSION LINE	-.1702628475737
C1...LOG(CONST) IN F EQUATION	.1216511436777
X7...T(5) IN CONFIDENCE ANALYSIS	2.06
X6...MULT. IN LOG(CONST) ANALYSIS	3.492878799161
X4...MULT. IN SLOPE ANALYSIS	.3264076834912
X5...INTERVAL ON LOG(CONST)	.09993708101647
X3...INTERVAL ON SLOPE	.009339067567217
F6...MIN. LOG(CONST)	.02171406266123
F7...MAX. LOG(CONST)	.2215882246942
Q6...MIN. CONST	1.021951528589
Q7...MAX. CONST	1.248057352842
Q5...REGRESSION CONST	1.129360048657
F8...MIN. SLOPE	-.1796019151409
F9...MAX. SLOPE	-.1609237800065
Q4...SUM OF (LOG(F)^2)	78.08297625586
Q3...CORRELATION COEFFICIENT/R	-.9912538690631
Q2...R^2	.9825842329325
F4...AV. ABS. DEV.	1.122428712339
F5...R.M.S. ABS. DEV.	1.332488213839

STATE FILENAME OR NO !NO
STOP AT LINE 570

****

TABLE NO.A.9.10 HEAT TRANSFER FACTORS CALCULATED USING THE DATA IN TABLE A.8.10
(RESULTING CORRELATION IS DENOTATION H OF TABLE 5.11)

****

OUTPUT USING HEAT2-6010

ERROR CRITERION FOR RE EXPONENT IS !0.0000001
ERROR CRITERION FOR RESISTANCE IS !0.00000001
TUBE MATERIAL IS !COPPER
CROSS SECTIONAL AREA OF TUBE AND INSERTS/SQ.FT. IS !0
FIRST RUN NUMBER ON DATA FILE IS !1
LAST RUN NUMBER ON DATA FILE IS !81
FIRST RUN NUMBER IS !1
LAST RUN NUMBER IS !27
TUBE I.D./INS.= !0.7874016
TUBE O.D./INS.= !0.8661417

RUN NUMBER	(HO/HI)MEAS	(HO/HI)CORR	CORR/HIMEAS
1	9.80789E-01	9.80752E-01	1.94129E-03
2	9.95043E-01	9.95033E-01	1.98703E-03
3	9.94091E-01	9.94079E-01	1.97933E-03
4	1.02431E+00	1.02435E+00	1.75965E-03
5	1.02373E+00	1.02377E+00	1.74747E-03
6	1.01740E+00	1.01743E+00	1.73812E-03
7	1.01972E+00	1.01975E+00	1.57139E-03
8	1.02286E+00	1.02289E+00	1.56860E-03
9	1.02412E+00	1.02416E+00	1.57164E-03
10	1.04559E+00	1.04565E+00	1.48591E-03
11	1.04651E+00	1.04658E+00	1.48826E-03
12	1.04754E+00	1.04761E+00	1.49421E-03
13	1.02583E+00	1.02586E+00	1.40081E-03
14	1.03313E+00	1.03317E+00	1.39590E-03
15	1.04018E+00	1.04024E+00	1.41248E-03
16	1.04950E+00	1.04957E+00	1.36293E-03
17	1.03964E+00	1.03970E+00	1.35246E-03
18	1.03666E+00	1.03671E+00	1.34815E-03
19	1.03277E+00	1.03281E+00	1.25904E-03
20	1.03368E+00	1.03373E+00	1.26983E-03
21	1.04061E+00	1.04066E+00	1.27168E-03
22	1.04844E+00	1.04850E+00	1.21950E-03
23	1.04351E+00	1.04356E+00	1.24478E-03
24	1.05906E+00	1.05914E+00	1.23811E-03
25	1.05102E+00	1.05108E+00	1.19576E-03
26	1.05102E+00	1.05108E+00	1.20031E-03
27	1.04932E+00	1.04938E+00	1.20244E-03

CORR1	CORR2	CORR3	CORR4
1.47979E+01	2.02376E+00	4.43842E-03	4.32758E+01
1.53032E+01	2.05749E+00	4.43842E-03	4.36283E+01
1.47641E+01	2.25986E+00	1.06522E-02	4.35947E+01
1.24038E+01	2.10777E+00	2.84011E-02	4.45076E+01
1.23702E+01	1.88856E+00	4.43773E-03	4.49784E+01
1.24206E+01	1.80421E+00	1.06503E-02	4.45580E+01
1.07182E+01	1.93895E+00	4.43726E-03	4.53011E+01
1.06339E+01	2.10757E+00	6.21224E-03	4.52341E+01
1.08025E+01	2.14130E+00	1.24245E-02	4.51503E+01
9.95957E+00	1.80395E+00	3.54960E-03	4.57243E+01
9.74059E+00	1.92198E+00	4.43705E-03	4.56906E+01
9.90912E+00	1.80397E+00	8.87411E-03	4.58088E+01
8.84734E+00	1.80388E+00	8.87367E-03	4.61801E+01
8.71252E+00	1.92189E+00	7.09895E-03	4.58941E+01
8.84742E+00	2.14110E+00	1.06487E-02	4.63144E+01
9.45377E+00	1.09578E+00	2.66193E-03	4.55273E+01
9.40323E+00	1.04520E+00	7.09850E-03	4.54937E+01
9.33577E+00	1.21378E+00	2.66193E-03	4.52749E+01
8.29080E+00	1.28114E+00	6.21082E-03	4.57477E+01
8.42562E+00	1.19686E+00	.00000E+00	4.61172E+01
8.37496E+00	1.23056E+00	2.66176E-03	4.61168E+01
7.73452E+00	1.11252E+00	1.77442E-03	4.63369E+01
6.94231E+00	1.85413E+00	1.77441E-03	4.72972E+01
7.44787E+00	1.55075E+00	4.43606E-03	4.67916E+01
7.22889E+00	1.51704E+00	6.21044E-03	4.67246E+01
7.36364E+00	1.39904E+00	1.33078E-02	4.69263E+01
7.19515E+00	1.68560E+00	8.87210E-03	4.69933E+01

Continued

LMTD MEAS	LMTD CORR	OUT T AV	INSI. T AV.
4.48883E+01	4.48939E+01	7.99650E+01	3.50447E+01
4.48663E+01	4.48718E+01	7.99300E+01	3.50298E+01
4.48466E+01	4.48522E+01	7.99600E+01	3.50797E+01
4.50195E+01	4.50237E+01	8.00450E+01	3.50209E+01
4.50695E+01	4.50737E+01	8.00950E+01	3.50208E+01
4.49996E+01	4.50038E+01	8.01050E+01	3.51008E+01
4.48625E+01	4.48658E+01	7.99600E+01	3.50866E+01
4.48327E+01	4.48359E+01	7.99500E+01	3.51066E+01
4.48577E+01	4.48610E+01	7.98800E+01	3.50116E+01
4.48364E+01	4.48391E+01	7.99200E+01	3.50571E+01
4.49667E+01	4.49694E+01	7.99400E+01	3.49471E+01
4.50819E+01	4.50846E+01	8.00350E+01	3.49271E+01
4.49429E+01	4.49452E+01	7.99800E+01	3.49875E+01
4.49388E+01	4.49411E+01	8.00100E+01	3.50225E+01
4.50945E+01	4.50968E+01	8.00700E+01	3.49275E+01
4.49563E+01	4.49582E+01	8.00250E+01	3.50029E+01
4.49345E+01	4.49364E+01	7.99650E+01	3.49629E+01
4.48840E+01	4.48859E+01	7.99900E+01	3.50379E+01
4.48527E+01	4.48542E+01	7.99650E+01	3.50033E+01
4.48079E+01	4.48094E+01	7.99200E+01	3.50033E+01
4.48792E+01	4.48807E+01	8.00000E+01	3.50133E+01
4.47570E+01	4.47582E+01	7.99800E+01	3.50836E+01
4.48379E+01	4.48392E+01	7.99750E+01	3.49986E+01
4.47643E+01	4.47655E+01	7.99750E+01	3.50736E+01
4.48351E+01	4.48362E+01	7.99500E+01	3.49488E+01
4.48351E+01	4.48362E+01	8.00000E+01	3.49988E+01
4.47240E+01	4.47250E+01	7.99400E+01	3.50488E+01

ONE TEMPERATURE,FIRST RUN NUMBER IS !1
ONE TEMPERATURE,LAST RUN NUMBER IS !27
DO YOU WANT TO INCLUDE MORE RESULTS !NO
CHOSEN PRANDTL NUMBER EXPONENT IS !0.4
DO YOU WANT TO USE MEAN PRANDTL NUMBERS !NO
RE EXPONENT IS !0.8
GEOMETRY: !CONFIGURATION 7T

RESISTANCE	INCREMENT	EXPONENT	SUM ERS SQ
.00000E+00	1.00000E-04	2.44750E-01	1.32098E-02
1.00000E-04	1.00000E-04	2.60830E-01	1.41270E-02
2.00000E-04	1.00000E-04	2.79212E-01	1.50833E-02
3.00000E-04	1.00000E-04	3.00440E-01	1.60506E-02
4.00000E-04	1.00000E-04	3.25247E-01	1.69767E-02
5.00000E-04	1.00000E-04	3.54649E-01	1.77685E-02
6.00000E-04	1.00000E-04	3.90099E-01	1.82644E-02
7.00000E-04	1.00000E-04	4.33764E-01	1.81933E-02
8.00000E-04	1.00000E-04	4.89040E-01	1.71321E-02
9.00000E-04	1.00000E-04	5.61624E-01	1.45803E-02
1.00000E-03	1.00000E-04	6.62045E-01	1.09401E-02
1.10000E-03	1.00000E-04	8.12877E-01	1.52809E-02
1.00000E-03	1.00000E-05	6.62045E-01	1.09401E-02
1.01000E-03	1.00000E-05	6.74304E-01	1.06680E-02
1.02000E-03	1.00000E-05	6.87075E-01	1.04592E-02
1.03000E-03	1.00000E-05	7.00394E-01	1.03355E-02
1.04000E-03	1.00000E-05	7.14299E-01	1.03242E-02
1.05000E-03	1.00000E-05	7.28834E-01	1.04596E-02
1.06000E-03	1.00000E-05	7.44049E-01	1.07843E-02
1.07000E-03	1.00000E-05	7.59996E-01	1.13521E-02
1.08000E-03	1.00000E-05	7.76736E-01	1.22302E-02
1.09000E-03	1.00000E-05	7.94338E-01	1.35039E-02
1.10000E-03	1.00000E-05	8.12877E-01	1.52809E-02
1.09000E-03	1.00000E-06	7.94338E-01	1.35039E-02
1.09100E-03	1.00000E-06	7.96148E-01	1.36570E-02
1.09200E-03	1.00000E-06	7.97968E-01	1.38151E-02
1.09300E-03	1.00000E-06	7.99797E-01	1.39786E-02
1.09400E-03	1.00000E-06	8.01636E-01	1.41474E-02
1.09300E-03	1.00000E-07	7.99797E-01	1.39786E-02
1.09310E-03	1.00000E-07	7.99981E-01	1.39952E-02
1.09320E-03	1.00000E-07	8.00164E-01	1.40119E-02
1.09310E-03	1.00000E-08	7.99981E-01	1.39952E-02
1.09311E-03	1.00000E-08	7.99999E-01	1.39969E-02
1.09312E-03	1.00000E-08	8.00017E-01	1.39985E-02
1.09311E-03	1.00000E-09	7.99999E-01	1.39969E-02
1.09311E-03	1.00000E-09	8.00001E-01	1.39970E-02
1.09311E-03	1.00000E-10	7.99999E-01	1.39969E-02
1.09311E-03	1.00000E-10	7.99999E-01	1.39969E-02
1.09311E-03	1.00000E-10	7.99999E-01	1.39969E-02
1.09311E-03	1.00000E-10	8.00000E-01	1.39969E-02

Continued

DATA INPUTS:
RESISTANCE STATED: NO
GEOMETRY: CONFIGURATION 7T

HO CORR/BEU	RE NUMBER	EXP NUSSELT	CAL NUSSELT	% CA-EX/EX
3.03049E+04	1.56206E+04	1.05335E+02	1.04958E+02	-3.58328E-01
3.04826E+04	1.56167E+04	1.06720E+02	1.04937E+02	-1.67083E+00
3.03788E+04	1.56307E+04	1.06096E+02	1.05012E+02	-1.02147E+00
3.42803E+04	2.26127E+04	1.37597E+02	1.41104E+02	+2.54880E+00
3.46466E+04	2.26126E+04	1.40791E+02	1.41104E+02	+2.22176E-01
3.43556E+04	2.26498E+04	1.38540E+02	1.41289E+02	+1.98473E+00
3.75502E+04	2.98655E+04	1.75645E+02	1.76276E+02	+3.59570E-01
3.77429E+04	2.98769E+04	1.78530E+02	1.76330E+02	-1.23257E+00
3.77895E+04	2.98192E+04	1.78763E+02	1.76058E+02	-1.51336E+00
4.03973E+04	3.72828E+04	2.18841E+02	2.10506E+02	-3.80872E+00
4.02753E+04	3.71999E+04	2.14582E+02	2.10132E+02	-2.07378E+00
4.02751E+04	3.71851E+04	2.12819E+02	2.10065E+02	-1.29424E+00
4.15677E+04	4.48709E+04	2.38608E+02	2.44135E+02	+2.31624E+00
4.17863E+04	4.49022E+04	2.43087E+02	2.44271E+02	+4.87074E-01
4.21497E+04	4.48177E+04	2.47388E+02	2.43903E+02	-1.40863E+00
4.31228E+04	5.27381E+04	2.71916E+02	2.77816E+02	+2.16986E+00
4.29527E+04	5.26970E+04	2.68342E+02	2.77643E+02	+3.46594E+00
4.28683E+04	5.27771E+04	2.67633E+02	2.77980E+02	+3.86645E+00
4.53175E+04	6.91017E+04	3.35825E+02	3.44865E+02	+2.69180E+00
4.53181E+04	6.91034E+04	3.37332E+02	3.44871E+02	+2.23488E+00
4.55435E+04	6.91191E+04	3.42451E+02	3.44934E+02	+7.25063E-01
4.73900E+04	8.64639E+04	4.20915E+02	4.12597E+02	-1.97612E+00
4.69690E+04	8.63172E+04	3.98065E+02	4.12037E+02	+3.50984E+00
4.76702E+04	8.64484E+04	4.33959E+02	4.12538E+02	-4.93620E+00
4.86954E+04	1.04295E+05	4.84677E+02	4.79371E+02	-1.09477E+00
4.86951E+04	1.04399E+05	4.84809E+02	4.79752E+02	-1.04319E+00
4.86954E+04	1.04504E+05	4.92201E+02	4.80138E+02	-2.45077E+00

LOG-LOG REGRESSION LINE IS (NU/PR^ .4)= .04635092319319 *(RE^ .7999999882138)

RESULTS OF REGRESSION ANALYSIS

Z...SUM OF LOG(NU)	147.8597659962
F...SUM OF LOG(RE)	288.4883115845
W...SUM OF LOG(NU)*LOG(RE)	1587.360917234
G...SUM OF (LOG(RE)^2)	3091.82107692
X...TOTAL NUMBER OF RUNS USED	27
S...SUM OF (DEVIATIONS^2)	.01399695064936
C...OUTER RESISTANCE TO TRANSFER	.0010931103
E...SLOPE OF REGRESSION LINE	.7999999882138
C1...LOG(CONST) IN NU EQUATION	-3.0715140693
X7...T(5) IN CONFIDENCE ANALYSIS	2.06
X6...MULT. IN LOG(CONST) ANALYSIS	3.491230162414
X4...MULT. IN SLOPE ANALYSIS	.3262520027667
X5...INTERVAL ON LOG(CONST	.1701736886814
X3...INTERVAL ON SLOPE	.01590256275516
F6...MIN. LOG(CONST)	-3.241687757982
F7...MAX. LOG(CONST)	-2.901340380619
Q6...MIN. CONST	.03909785167078
Q7...MAX. CONST	.05494951740448
Q5...REGRESSION CONST	.04635092319319
F8...MIN.SLOPE	.7840974254586
F9...MAX.SLOPE	.8159025509689
Q4...SUM OF (LOG(NU)^2)	815.749360487
Q3...CORRELATION COEFFICIENT/R	.9988380901982
Q2...R^2	.9976775304307
F4...AV. ABS. DEV.	1.94316691917
F5...R.M.S. ABS. DEV.	2.275276664451

The results in this table were obtained three days after the acquisition of the data in Tables A.8.5 and A.9.5.The value of the heat transfer resistance,C,used overleaf is that obtained from Table A.9.5.

Continued

```
FILE RESULTS !NO
TRY ANOTHER RE AND/OR PR EXPONENT !NO
DO YOU WANT TO STATE THE RESISTANCE !YES
RESISTANCE ,C, IS !0.001082094
```

RESISTANCE	INCREMENT	EXPONENT	SUM ERS SQ
1.08209E-03	1.00000E-10	7.80348E-01	1.24610E-02

DATA INPUTS:
RESISTANCE STATED: YES
GEOMETRY: CONFIGURATION 7T

HO CORR/BEU	RE NUMBER	EXP NUSSELT	CAL NUSSELT	% CA-EX/EX
3.03049E+04	1.56206E+04	1.04213E+02	1.04273E+02	+5.71629E-02
3.04826E+04	1.56167E+04	1.05569E+02	1.04253E+02	-1.24640E+00
3.03788E+04	1.56307E+04	1.04958E+02	1.04326E+02	-6.02600E-01
3.42803E+04	2.26127E+04	1.35688E+02	1.39168E+02	+2.56429E+00
3.46466E+04	2.26126E+04	1.38793E+02	1.39167E+02	+2.69596E-01
3.43556E+04	2.26498E+04	1.36606E+02	1.39346E+02	+2.00582E+00
3.75502E+04	2.98655E+04	1.72548E+02	1.72909E+02	+2.09660E-01
3.77429E+04	2.98769E+04	1.75332E+02	1.72961E+02	-1.35249E+00
3.77895E+04	2.98192E+04	1.75555E+02	1.72700E+02	-1.62585E+00
4.03973E+04	3.72828E+04	2.14053E+02	2.05587E+02	-3.95511E+00
4.02753E+04	3.71999E+04	2.09973E+02	2.05231E+02	-2.25871E+00
4.02751E+04	3.71851E+04	2.08285E+02	2.05167E+02	-1.49698E+00
4.15677E+04	4.48709E+04	2.32925E+02	2.37564E+02	+1.99151E+00
4.17863E+04	4.49022E+04	2.37193E+02	2.37693E+02	+2.11014E-01
4.21497E+04	4.48177E+04	2.41282E+02	2.37344E+02	-1.63219E+00
4.31228E+04	5.27381E+04	2.64561E+02	2.69482E+02	+1.86004E+00
4.29527E+04	5.26970E+04	2.61175E+02	2.69318E+02	+3.11780E+00
4.28683E+04	5.27771E+04	2.60506E+02	2.69637E+02	+3.50525E+00
4.53175E+04	6.91017E+04	3.24677E+02	3.32747E+02	+2.48556E+00
4.53181E+04	6.91034E+04	3.26086E+02	3.32753E+02	+2.04471E+00
4.55435E+04	6.91191E+04	3.30868E+02	3.32813E+02	+5.87901E-01
4.73900E+04	8.64639E+04	4.03556E+02	3.96350E+02	-1.78581E+00
4.69690E+04	8.63172E+04	3.82498E+02	3.95825E+02	+3.48426E+00
4.76702E+04	8.64484E+04	4.15530E+02	3.96294E+02	-4.62932E+00
4.86954E+04	1.04295E+05	4.61785E+02	4.58800E+02	-6.46422E-01
4.86951E+04	1.04399E+05	4.61912E+02	4.59156E+02	-5.96752E-01
4.86954E+04	1.04504E+05	4.68625E+02	4.59517E+02	-1.94355E+00

LOG-LOG REGRESSION LINE IS (NU/PR^ .4)= .05567065607497 *(RE^ .7803486534724)

RESULTS OF REGRESSION ANALYSIS

Z...SUM OF LOG(NU)	147.137309012
F...SUM OF LOG(RE)	288.4883115845
W...SUM OF LOG(NU)*LOG(RE)	1579.457020376
G...SUM OF (LOG(RE)^2)	3091.82107692
X...TOTAL NUMBER OF RUNS USED	27
S...SUM OF (DEVIATIONS^2)	.01246102899163
C...OUTER RESISTANCE TO TRANSFER	.001082094
E...SLOPE OF REGRESSION LINE	.7803486534724
C1...LOG(CONST) IN NU EQUATION	-2.888302091784
X7...T(5) IN CONFIDENCE ANALYSIS	2.06
X6...MULT. IN LOG(CONST) ANALYSIS	3.491230162414
X4...MULT. IN SLOPE ANALYSIS	.3262520027667
X5...INTERVAL ON LOG(CONST	.160565653147
X3...INTERVAL ON SLOPE	.01500470134531
F6...MIN. LOG(CONST)	-3.048867744931
F7...MAX. LOG(CONST)	-2.727736438637
Q6...MIN. CONST	.04741257714192
Q7...MAX. CONST	.06536708474085
Q5...REGRESSION CONST	.05567065607497
F8...MIN.SLOPE	.7653439521271
F9...MAX.SLOPE	.7953533548177
Q4...SUM OF (LOG(NU)^2)	807.5626227125
Q3...CORRELATION COEFFICIENT/R	.9989127130863
Q2...R^2	.9978266083654
F4...AV. ABS. DEV.	1.783957303205
F5...R.M.S. ABS. DEV.	2.145206493441

```
FILE RESULTS !YES
TRY ANOTHER RE AND/OR PR EXPONENT !NO
DO YOU WANT TO STATE THE RESISTANCE !NO
STOP AT LINE 2520
```

****

TABLE NO.A.9.11 HEAT TRANSFER FACTORS CALCULATED USING THE DATA IN TABLE A.8.11
(RESULTING CORRELATION IS DENOTATION G OF TABLE 5.12)

****

OUTPUT USING HEAT2-6010

ERROR CRITERION FOR RE EXPONENT IS 10.0000001
ERROR CRITERION FOR RESISTANCE IS 10.00000001
TUBE MATERIAL IS 1COPPER
CROSS SECTIONAL AREA OF TUBE AND INSERTS/SQ.FT. IS 10
FIRST RUN NUMBER ON DATA FILE IS 11
LAST RUN NUMBER ON DATA FILE IS 181
FIRST RUN NUMBER IS 155
LAST RUN NUMBER IS 181
TUBE I.D./INS.= 10.7874016
TUBE O.D./INS.= 10.8661417

RUN NUMBER	(HO/HI)MEAS	(HO/HI)CORR	CORR/HIMEAS
1	9.96348E-01	9.96343E-01	1.57234E-03
2	9.95967E-01	9.95960E-01	1.56870E-03
3	9.94337E-01	9.94328E-01	1.54888E-03
4	1.01403E+00	1.01405E+00	1.41311E-03
5	1.01646E+00	1.01648E+00	1.40226E-03
6	1.01233E+00	1.01234E+00	1.42325E-03
7	1.02787E+00	1.02790E+00	1.32758E-03
8	1.01413E+00	1.01415E+00	1.31972E-03
9	1.02406E+00	1.02410E+00	1.32402E-03
10	1.03070E+00	1.03074E+00	1.26920E-03
11	1.02325E+00	1.02328E+00	1.26549E-03
12	1.03138E+00	1.03142E+00	1.26219E-03
13	1.02759E+00	1.02762E+00	1.21572E-03
14	1.02739E+00	1.02743E+00	1.19845E-03
15	1.03593E+00	1.03598E+00	1.21646E-03
16	1.03320E+00	1.03324E+00	1.20198E-03
17	1.03316E+00	1.03320E+00	1.20572E-03
18	1.02275E+00	1.02277E+00	1.19262E-03
19	1.02583E+00	1.02586E+00	1.15361E-03
20	1.04356E+00	1.04362E+00	1.16252E-03
21	1.04470E+00	1.04475E+00	1.16310E-03
22	1.02226E+00	1.02229E+00	1.11593E-03
23	1.03941E+00	1.03945E+00	1.12632E-03
24	1.04405E+00	1.04410E+00	1.13167E-03
25	1.04140E+00	1.04145E+00	1.08941E-03
26	1.03898E+00	1.03902E+00	1.08879E-03
27	1.05111E+00	1.05117E+00	1.08980E-03

CORR1	CORR2	CORR3	CORR4
1.39577E+01	2.29396E+00	1.06539E-02	4.05025E+01
1.37050E+01	2.17588E+00	.00000E+00	4.04357E+01
1.36207E+01	2.19274E+00	.00000E+00	4.02006E+01
1.11922E+01	1.90562E+00	1.15392E-02	4.12152E+01
1.12259E+01	1.93935E+00	4.43821E-03	4.13494E+01
1.10741E+01	1.97306E+00	2.66291E-03	4.15339E+01
9.75863E+00	2.14144E+00	6.21268E-03	4.21252E+01
9.64066E+00	2.14143E+00	1.15377E-02	4.22767E+01
9.75869E+00	2.02341E+00	.00000E+00	4.20418E+01
8.56161E+00	2.07380E+00	.00000E+00	4.26834E+01
8.76381E+00	2.07381E+00	1.77490E-03	4.25656E+01
8.64591E+00	2.10754E+00	4.43729E-03	4.25994E+01
8.00516E+00	2.00625E+00	2.66218E-03	4.29375E+01
7.92087E+00	1.85449E+00	3.54952E-03	4.26014E+01
7.87039E+00	2.02311E+00	1.77479E-03	4.30889E+01
8.22401E+00	1.83760E+00	2.66214E-02	4.31265E+01
8.13984E+00	1.93878E+00	2.30722E-02	4.32784E+01
8.27455E+00	1.80388E+00	1.68600E-02	4.32445E+01
7.31379E+00	1.83749E+00	2.39578E-02	4.39859E+01
7.26320E+00	2.09037E+00	1.77466E-02	4.42885E+01
7.22946E+00	2.00606E+00	2.39578E-02	4.41200E+01
6.60563E+00	2.10707E+00	2.21817E-02	4.41208E+01
6.68995E+00	1.97223E+00	2.21818E-02	4.42387E+01
6.70684E+00	2.02281E+00	1.95201E-02	4.43399E+01
6.16746E+00	2.05644E+00	2.12939E-02	4.43407E+01
6.11689E+00	2.10701E+00	3.01665E-02	4.44248E+01
6.13380E+00	2.00588E+00	3.10538E-02	4.44750E+01

Continued

LMTD MEAS	LMTD CORR	OUT T AV	INSI. T AV.
4.50553E+01	4.50605E+01	8.00950E+01	3.49952E+01
4.50008E+01	4.50060E+01	8.00000E+01	3.49551E+01
4.49456E+01	4.49508E+01	7.99850E+01	3.49951E+01
4.49496E+01	4.49535E+01	7.99750E+01	3.50211E+01
4.50345E+01	4.50384E+01	7.99850E+01	3.49461E+01
4.51296E+01	4.51335E+01	8.00350E+01	3.49011E+01
4.48715E+01	4.48745E+01	7.99650E+01	3.50818E+01
4.48954E+01	4.48985E+01	7.99300E+01	3.50218E+01
4.49862E+01	4.49893E+01	8.00100E+01	3.50118E+01
4.48757E+01	4.48782E+01	7.99500E+01	3.50423E+01
4.49997E+01	4.50022E+01	8.00450E+01	3.50123E+01
4.50055E+01	4.50080E+01	8.00350E+01	3.49973E+01
4.48858E+01	4.48879E+01	8.00150E+01	3.50727E+01
4.47953E+01	4.47974E+01	7.99150E+01	3.50627E+01
4.50120E+01	4.50141E+01	8.00150E+01	3.49477E+01
4.47590E+01	4.47607E+01	7.99400E+01	3.51030E+01
4.48090E+01	4.48108E+01	7.98900E+01	3.50030E+01
4.47461E+01	4.47478E+01	7.99300E+01	3.51030E+01
4.48010E+01	4.48024E+01	7.99600E+01	3.50384E+01
4.49832E+01	4.49846E+01	8.00500E+01	3.49484E+01
4.48794E+01	4.48808E+01	8.00350E+01	3.50384E+01
4.47860E+01	4.47871E+01	7.99400E+01	3.49987E+01
4.48455E+01	4.48467E+01	8.00100E+01	3.50137E+01
4.49519E+01	4.49530E+01	8.00500E+01	3.49487E+01
4.48857E+01	4.48867E+01	7.99900E+01	3.49239E+01
4.48193E+01	4.48203E+01	7.99750E+01	3.49739E+01
4.48463E+01	4.48472E+01	7.99650E+01	3.49389E+01

ONE TEMPERATURE,FIRST RUN NUMBER IS !55
ONE TEMPERATURE,LAST RUN NUMBER IS !81
DO YOU WANT TO INCLUDE MORE RESULTS !NO
CHOSEN PRANDTL NUMBER EXPONENT IS !0.4
DO YOU WANT TO USE MEAN PRANDTL NUMBERS !NO
RE EXPONENT IS !0.8
GEOMETRY: !*CONFIGURATION 6K*

RESISTANCE	INCREMENT	EXPONENT	SUM ERS SQ
.00000E+00	1.00000E-04	1.76525E-01	6.01764E-03
1.00000E-04	1.00000E-04	1.89228E-01	6.58265E-03
2.00000E-04	1.00000E-04	2.03919E-01	7.21561E-03
3.00000E-04	1.00000E-04	2.21113E-01	7.92033E-03
4.00000E-04	1.00000E-04	2.41517E-01	8.69509E-03
5.00000E-04	1.00000E-04	2.66139E-01	9.52648E-03
6.00000E-04	1.00000E-04	2.96465E-01	1.03779E-02
7.00000E-04	1.00000E-04	3.34796E-01	1.11718E-02
8.00000E-04	1.00000E-04	3.84902E-01	1.17757E-02
9.00000E-04	1.00000E-04	4.53487E-01	1.21093E-02
1.00000E-03	1.00000E-04	5.53934E-01	1.32891E-02
1.10000E-03	1.00000E-04	7.18513E-01	2.89962E-02
1.20000E-03	1.00000E-04	1.06272E+00	2.92383E-01
1.10000E-03	1.00000E-05	7.18513E-01	2.89962E-02
1.11000E-03	1.00000E-05	7.41234E-01	3.39772E-02
1.12000E-03	1.00000E-05	7.65645E-01	4.04718E-02
1.13000E-03	1.00000E-05	7.91967E-01	4.89877E-02
1.14000E-03	1.00000E-05	8.20466E-01	6.02322E-02
1.13000E-03	1.00000E-06	7.91967E-01	4.89877E-02
1.13100E-03	1.00000E-06	7.94714E-01	4.99756E-02
1.13200E-03	1.00000E-06	7.97483E-01	5.09913E-02
1.13300E-03	1.00000E-06	8.00275E-01	5.20358E-02
1.13200E-03	1.00000E-07	7.97483E-01	5.09913E-02
1.13210E-03	1.00000E-07	7.97762E-01	5.10944E-02
1.13220E-03	1.00000E-07	7.98040E-01	5.11978E-02
1.13230E-03	1.00000E-07	7.98319E-01	5.13016E-02
1.13240E-03	1.00000E-07	7.98597E-01	5.14056E-02
1.13250E-03	1.00000E-07	7.98876E-01	5.15099E-02
1.13260E-03	1.00000E-07	7.99156E-01	5.16145E-02
1.13270E-03	1.00000E-07	7.99435E-01	5.17193E-02
1.13280E-03	1.00000E-07	7.99715E-01	5.18245E-02
1.13290E-03	1.00000E-07	7.99995E-01	5.19300E-02
1.13300E-03	1.00000E-07	8.00275E-01	5.20358E-02
1.13290E-03	1.00000E-08	7.99995E-01	5.19300E-02
1.13291E-03	1.00000E-08	8.00023E-01	5.19405E-02
1.13290E-03	1.00000E-09	7.99995E-01	5.19300E-02
1.13290E-03	1.00000E-09	7.99998E-01	5.19310E-02
1.13290E-03	1.00000E-09	8.00000E-01	5.19321E-02
1.13290E-03	1.00000E-10	7.99998E-01	5.19310E-02
1.13290E-03	1.00000E-10	7.99998E-01	5.19311E-02
1.13290E-03	1.00000E-10	7.99998E-01	5.19313E-02
1.13290E-03	1.00000E-10	7.99998E-01	5.19314E-02
1.13290E-03	1.00000E-10	7.99999E-01	5.19315E-02
1.13290E-03	1.00000E-10	7.99999E-01	5.19316E-02
1.13290E-03	1.00000E-10	7.99999E-01	5.19317E-02
1.13290E-03	1.00000E-10	7.99999E-01	5.19318E-02

Continued

DATA INPUTS:
RESISTANCE STATED: NO
GEOMETRY: CONFIGURATION 6K

HO CORR/BEU	RE NUMBER	EXP NUSSELT	CAL NUSSELT	% CA-EX/EX
3.59001E+04	1.56160E+04	1.63202E+02	1.56918E+02	-3.85021E+00
3.56990E+04	1.56040E+04	1.61226E+02	1.56822E+02	-2.73169E+00
3.59033E+04	1.56170E+04	1.64328E+02	1.56927E+02	-4.50404E+00
3.89118E+04	2.26181E+04	2.08246E+02	2.11049E+02	+1.34583E+00
3.94649E+04	2.25862E+04	2.16538E+02	2.10811E+02	-2.64486E+00
3.87697E+04	2.25668E+04	2.03108E+02	2.10666E+02	+3.72111E+00
4.17696E+04	2.98698E+04	2.68265E+02	2.63636E+02	-1.72551E+00
4.14783E+04	2.98333E+04	2.60636E+02	2.63378E+02	+1.05208E+00
4.15764E+04	2.98282E+04	2.60953E+02	2.63342E+02	+9.15509E-01
4.32460E+04	3.72775E+04	3.08300E+02	3.14757E+02	+2.09450E+00
4.31261E+04	3.72561E+04	3.01153E+02	3.14613E+02	+4.46933E+00
4.35468E+04	3.72432E+04	3.13581E+02	3.14526E+02	+3.01254E-01
4.47047E+04	4.49511E+04	3.57513E+02	3.65603E+02	+2.26301E+00
4.48517E+04	4.49430E+04	3.66715E+02	3.65551E+02	-3.17480E-01
4.50680E+04	4.48387E+04	3.66422E+02	3.64872E+02	-4.22843E-01
4.56892E+04	5.28415E+04	4.04367E+02	4.16101E+02	+2.90179E+00
4.56871E+04	5.27342E+04	4.01654E+02	4.15424E+02	+3.42836E+00
4.56890E+04	5.28415E+04	4.04973E+02	4.16101E+02	+2.74761E+00
4.72196E+04	6.91433E+04	4.84304E+02	5.15963E+02	+6.53694E+00
4.81152E+04	6.90194E+04	5.31354E+02	5.15223E+02	-3.03576E+00
4.78921E+04	6.91441E+04	5.23580E+02	5.15968E+02	-1.45394E+00
4.83664E+04	8.63079E+04	5.67262E+02	6.16111E+02	+8.61135E+00
4.87865E+04	8.63343E+04	5.97670E+02	6.16261E+02	+3.11068E+00
4.89255E+04	8.62212E+04	5.99504E+02	6.15615E+02	+2.68747E+00
5.02159E+04	1.04231E+05	7.47618E+02	7.16504E+02	-4.16177E+00
5.02164E+04	1.04336E+05	7.57848E+02	7.17082E+02	-5.37926E+00
5.07242E+04	1.04264E+05	8.27577E+02	7.16682E+02	-1.34000E+01

LOG-LOG REGRESSION LINE IS (NU/PR^ .4)= .06931364897477 *(RE^ .79999994031)

RESULTS OF REGRESSION ANALYSIS

Z...SUM OF LOG(NU)	158.7200607881
F...SUM OF LOG(RE)	288.4826760183
W...SUM OF LOG(NU)*LOG(RE)	1703.366939507
G...SUM OF (LOG(RE)^2)	3091.700138797
X...TOTAL NUMBER OF RUNS USED	27
S...SUM OF (DEVIATIONS^2)	.05193182397299
C...OUTER RESISTANCE TO TRANSFER	.0011329017
E...SLOPE OF REGRESSION LINE	.79999994031
C1...LOG(CONST) IN NU EQUATION	-2.669113437276
X7...T(5) IN CONFIDENCE ANALYSIS	2.06
X6...MULT. IN LOG(CONST) ANALYSIS	3.491256650678
X4...MULT. IN SLOPE ANALYSIS	.3262608590583
X5...INTERVAL ON LOG(CONST	.3277900603508
X3...INTERVAL ON SLOPE	.03063225576958
F6...MIN. LOG(CONST)	-2.996903497627
F7...MAX. LOG(CONST)	-2.341323376926
Q6...MIN. CONST	.0499414730771
Q7...MAX. CONST	.09620024477013
Q5...REGRESSION CONST	.06931364897477
F8...MIN.SLOPE	.7693676845404
F9...MAX.SLOPE	.8306321960796
Q4...SUM OF (LOG(NU)^2)	939.1035347375
Q3...CORRELATION COEFFICIENT/R	.9957090711494
Q2...R^2	.9914365543691
F4...AV. ABS. DEV.	3.326456520066
F5...R.M.S. ABS. DEV.	4.297539219538

The results in this table were obtained three days after the acqusition of the data in Tables A.8.3 and A.9.3.The value of the heat *transfer resistance*,C,used overleaf is that obtained from Table A.9.3.

Continued

```
FILE RESULTS !NO
TRY ANOTHER RE AND/OR PR EXPONENT !NO
DO YOU WANT TO STATE THE RESISTANCE !YES
RESISTANCE ,C, IS !0.0011477562
```

RESISTANCE	INCREMENT	EXPONENT	SUM ERS SQ
1.14775E-03	1.00000E-10	8.44274E-01	7.14565E-02

DATA INPUTS:
RESISTANCE STATED: YES
GEOMETRY: CONFIGURATION 6K

HO CORR/BEU	RE NUMBER	EXP NUSSELT	CAL NUSSELT	% CA-EX/EX
3.59001E+04	1.56160E+04	1.66959E+02	1.58716E+02	-4.93674E+00
3.56990E+04	1.56040E+04	1.64892E+02	1.58613E+02	-3.80789E+00
3.59033E+04	1.56170E+04	1.68138E+02	1.58726E+02	-5.59790E+00
3.89118E+04	2.26181E+04	2.14401E+02	2.16997E+02	+1.21096E+00
3.94649E+04	2.25862E+04	2.23204E+02	2.16739E+02	-2.89632E+00
3.87697E+04	2.25668E+04	2.08963E+02	2.16582E+02	+3.64592E+00
4.17696E+04	2.98698E+04	2.78562E+02	2.74424E+02	-1.48529E+00
4.14783E+04	2.98333E+04	2.70349E+02	2.74141E+02	+1.40273E+00
4.15764E+04	2.98282E+04	2.70691E+02	2.74102E+02	+1.26009E+00
4.32460E+04	3.72775E+04	3.21982E+02	3.30867E+02	+2.75967E+00
4.31261E+04	3.72561E+04	3.14197E+02	3.30707E+02	+5.25461E+00
4.35468E+04	3.72432E+04	3.27751E+02	3.30611E+02	+8.72584E-01
4.47047E+04	4.49511E+04	3.76039E+02	3.87514E+02	+3.05166E+00
4.48517E+04	4.49430E+04	3.86235E+02	3.87456E+02	+3.16147E-01
4.50680E+04	4.48387E+04	3.85924E+02	3.86697E+02	+2.00184E-01
4.56892E+04	5.28415E+04	4.28224E+02	4.44207E+02	+3.73241E+00
4.56871E+04	5.27342E+04	4.25199E+02	4.43445E+02	+4.29123E+00
4.56890E+04	5.28415E+04	4.28905E+02	4.44207E+02	+3.56781E+00
4.72196E+04	6.91433E+04	5.18945E+02	5.57411E+02	+7.41233E+00
4.81152E+04	6.90194E+04	5.73370E+02	5.56568E+02	-2.93045E+00
4.78921E+04	6.91441E+04	5.64304E+02	5.57417E+02	-1.22050E+00
4.83664E+04	8.63079E+04	6.15390E+02	6.72171E+02	+9.22690E+00
4.87865E+04	8.63343E+04	6.51334E+02	6.72345E+02	+3.22573E+00
4.89255E+04	8.62212E+04	6.53538E+02	6.71601E+02	+2.76393E+00
5.02159E+04	1.04231E+05	8.33578E+02	7.88257E+02	-5.43689E+00
5.02164E+04	1.04336E+05	8.46285E+02	7.88928E+02	-6.77746E+00
5.07242E+04	1.04264E+05	9.34207E+02	7.88464E+02	-1.56008E+01

LOG-LOG REGRESSION LINE IS (NU/PR^ .4)= .04571908369612 *(RE^ .8442746752726)

RESULTS OF REGRESSION ANALYSIS

Z...SUM OF LOG(NU)	160.2571516085
F...SUM OF LOG(RE)	288.4826760183
W...SUM OF LOG(NU)*LOG(RE)	1720.205988856
G...SUM OF (LOG(RE)^2)	3091.700138797
X...TOTAL NUMBER OF RUNS USED	27
S...SUM OF (DEVIATIONS^2)	.07145658682372
C...OUTER RESISTANCE TO TRANSFER	.0011477562
E...SLOPE OF REGRESSION LINE	.8442746752726
C1...LOG(CONST) IN NU EQUATION	-3.085239481898
X7...T(5) IN CONFIDENCE ANALYSIS	2.06
X6...MULT. IN LOG(CONST) ANALYSIS	3.491256650678
X4...MULT. IN SLOPE ANALYSIS	.3262608590583
X5...INTERVAL ON LOG(CONST	.3845033482964
X3...INTERVAL ON SLOPE	.03593216004376
F6...MIN. LOG(CONST)	-3.469742830195
F7...MAX. LOG(CONST)	-2.700736133602
Q6...MIN. CONST	.03112503405084
Q7...MAX. CONST	.0671560587082
Q5...REGRESSION CONST	.04571908369612
F8...MIN.SLOPE	.8083425152289
F9...MAX.SLOPE	.8802068353164
Q4...SUM OF (LOG(NU)^2)	957.9661178467
Q3...CORRELATION COEFFICIENT/R	.9947068302724
Q2...R^2	.9894416781906
F4...AV. ABS. DEV.	3.884638755978
F5...R.M.S. ABS. DEV.	5.00633828187

```
FILE RESULTS !YES
TRY ANOTHER RE AND/OR PR EXPONENT !NO
DO YOU WANT TO STATE THE RESISTANCE !NO
STOP AT LINE 2520
```

****

TABLE NO.A.9.12 HEAT TRANSFER FACTORS CALCULATED USING THE DATA IN TABLE A.8.12
(RESULTING CORRELATION IS DENOTATION H OF TABLE 5.12)

****

OUTPUT USING HEAT2-6010

ERROR CRITERION FOR RE EXPONENT IS !0.0000001
ERROR CRITERION FOR RESISTANCE IS !0.00000001
TUBE MATERIAL IS !COPPER
CROSS SECTIONAL AREA OF TUBE AND INSERTS/SQ.FT. IS !0
FIRST RUN NUMBER ON DATA FILE IS !1
LAST RUN NUMBER ON DATA FILE IS !54
FIRST RUN NUMBER IS !28
LAST RUN NUMBER IS !54
TUBE I.D./INS.= !0.7874016
TUBE O.D./INS.= !0.8661417

RUN NUMBER	(HO/HI)MEAS	(HO/HI)CORR	CORR/HIMEAS
1	1.00214E+00	1.00214E+00	1.47225E-03
2	9.99294E-01	9.99293E-01	1.44878E-03
3	1.01121E+00	1.01123E+00	1.47565E-03
4	1.02368E+00	1.02371E+00	1.33819E-03
5	1.02357E+00	1.02360E+00	1.35675E-03
6	1.02088E+00	1.02091E+00	1.34653E-03
7	1.03493E+00	1.03497E+00	1.25393E-03
8	1.03699E+00	1.03704E+00	1.25676E-03
9	1.03911E+00	1.03916E+00	1.25940E-03
10	1.02044E+00	1.02046E+00	1.17234E-03
11	1.03036E+00	1.03039E+00	1.17601E-03
12	1.02107E+00	1.02109E+00	1.17571E-03
13	1.02883E+00	1.02886E+00	1.13006E-03
14	1.03713E+00	1.03717E+00	1.12275E-03
15	1.03368E+00	1.03372E+00	1.13175E-03
16	1.02908E+00	1.02911E+00	1.05357E-03
17	1.02930E+00	1.02933E+00	1.07398E-03
18	1.03054E+00	1.03057E+00	1.05970E-03
19	1.04192E+00	1.04196E+00	1.02418E-03
20	1.04656E+00	1.04660E+00	1.02711E-03
21	1.03912E+00	1.03916E+00	1.01977E-03
22	1.03745E+00	1.03748E+00	9.86858E-04
23	1.05041E+00	1.05046E+00	9.91550E-04
24	1.03933E+00	1.03937E+00	9.95993E-04
25	1.04465E+00	1.04469E+00	9.70526E-04
26	1.04025E+00	1.04029E+00	9.61589E-04
27	1.03979E+00	1.03983E+00	9.53999E-04

CORR1	CORR2	CORR3	CORR4
1.70758E+01	2.20981E+00	1.77581E-03	3.90742E+01
1.68403E+01	2.15924E+00	2.66374E-03	3.87046E+01
1.70928E+01	2.22670E+00	6.21537E-03	3.88394E+01
1.42591E+01	2.36112E+00	8.87711E-03	4.06767E+01
1.40906E+01	2.47918E+00	8.87719E-03	4.13322E+01
1.41412E+01	2.47918E+00	8.87719E-03	4.10966E+01
1.25054E+01	2.51260E+00	1.50892E-02	4.21259E+01
1.23706E+01	2.54631E+00	1.95271E-02	4.21259E+01
1.23370E+01	2.46202E+00	1.68645E-02	4.20090E+01
1.13420E+01	2.37746E+00	1.50877E-02	4.29858E+01
1.13084E+01	2.39435E+00	1.77504E-02	4.26334E+01
1.13926E+01	2.34375E+00	1.77503E-02	4.27507E+01
1.05326E+01	2.37731E+00	1.33118E-02	4.32235E+01
1.03305E+01	2.41104E+00	1.50868E-02	4.28207E+01
1.04483E+01	2.41101E+00	1.50867E-02	4.29377E+01
9.84183E+00	1.70282E+00	7.09929E-03	4.18498E+01
9.92606E+00	1.75341E+00	.00000E+00	4.26565E+01
9.74066E+00	1.75339E+00	4.43702E-03	4.27571E+01
8.74599E+00	1.92184E+00	.00000E+00	4.32968E+01
8.67858E+00	1.78696E+00	.00000E+00	4.34143E+01
8.71222E+00	2.00612E+00	8.87334E-03	4.34983E+01
7.54940E+00	1.98916E+00	6.21101E-03	4.41214E+01
7.51575E+00	1.95545E+00	7.09833E-03	4.43066E+01
7.59996E+00	2.07346E+00	1.15348E-02	4.42562E+01
7.16164E+00	2.05651E+00	1.77450E-02	4.44248E+01
7.02695E+00	1.93853E+00	1.77452E-03	4.43919E+01
7.11116E+00	1.85423E+00	.00000E+00	4.44584E+01

Continued

LMTD MEAS	LMTD CORR	OUT T AV	INSI. T AV.
4.49597E+01	4.49642E+01	8.00650E+01	3.50061E+01
4.49449E+01	4.49494E+01	8.00650E+01	3.50211E+01
4.49270E+01	4.49314E+01	8.00600E+01	3.50311E+01
4.49358E+01	4.49393E+01	7.99950E+01	3.50417E+01
4.49709E+01	4.49745E+01	7.99600E+01	3.49716E+01
4.49311E+01	4.49346E+01	7.99600E+01	3.50116E+01
4.48850E+01	4.48878E+01	7.99600E+01	3.50722E+01
4.49950E+01	4.49978E+01	8.00600E+01	3.50621E+01
4.50950E+01	4.50978E+01	8.00100E+01	3.49121E+01
4.49259E+01	4.49282E+01	7.99500E+01	3.50125E+01
4.51467E+01	4.51491E+01	8.01200E+01	3.49626E+01
4.49861E+01	4.49884E+01	7.99850E+01	3.49876E+01
4.49754E+01	4.49774E+01	8.00000E+01	3.49979E+01
4.50814E+01	4.50834E+01	8.00700E+01	3.49629E+01
4.49862E+01	4.49882E+01	8.00000E+01	3.49879E+01
4.49476E+01	4.49493E+01	7.99900E+01	3.49982E+01
4.49828E+01	4.49845E+01	8.00000E+01	3.49731E+01
4.49469E+01	4.49486E+01	7.99750E+01	3.49831E+01
4.48086E+01	4.48099E+01	7.99650E+01	3.50785E+01
4.48849E+01	4.48862E+01	8.00100E+01	3.50485E+01
4.48219E+01	4.48233E+01	7.99650E+01	3.50635E+01
4.49518E+01	4.49529E+01	8.00250E+01	3.49637E+01
4.48986E+01	4.48998E+01	7.99200E+01	3.49137E+01
4.49529E+01	4.49541E+01	8.00700E+01	3.50087E+01
4.48925E+01	4.48934E+01	8.00500E+01	3.50239E+01
4.49160E+01	4.49169E+01	8.00250E+01	3.49739E+01
4.49134E+01	4.49144E+01	7.99900E+01	3.49389E+01

ONE TEMPERATURE,FIRST RUN NUMBER IS !28
ONE TEMPERATURE,LAST RUN NUMBER IS !54
DO YOU WANT TO INCLUDE MORE RESULTS !NO
CHOSEN PRANDTL NUMBER EXPONENT IS !0.4
DO YOU WANT TO USE MEAN PRANDTL NUMBERS !NO
RE EXPONENT IS !0.8
GEOMETRY: !CONFIGURATION 6K

RESISTANCE	INCREMENT	EXPONENT	SUM ERS SQ
.00000E+00	1.00000E-04	1.96880E-01	6.77898E-03
1.00000E-04	1.00000E-04	2.13114E-01	7.44509E-03
2.00000E-04	1.00000E-04	2.32301E-01	8.17761E-03
3.00000E-04	1.00000E-04	2.55340E-01	8.96287E-03
4.00000E-04	1.00000E-04	2.83545E-01	9.76210E-03
5.00000E-04	1.00000E-04	3.18915E-01	1.04853E-02
6.00000E-04	1.00000E-04	3.64668E-01	1.09433E-02
7.00000E-04	1.00000E-04	4.26372E-01	1.07821E-02
8.00000E-04	1.00000E-04	5.14698E-01	9.61441E-03
9.00000E-04	1.00000E-04	6.53599E-01	9.81566E-03
1.00000E-03	1.00000E-04	9.14951E-01	6.07524E-02
9.00000E-04	1.00000E-05	6.53599E-01	9.81566E-03
9.10000E-04	1.00000E-05	6.72150E-01	1.05192E-02
9.20000E-04	1.00000E-05	6.91898E-01	1.15597E-02
9.30000E-04	1.00000E-05	7.12975E-01	1.30533E-02
9.40000E-04	1.00000E-05	7.35534E-01	1.51574E-02
9.50000E-04	1.00000E-05	7.59754E-01	1.80858E-02
9.60000E-04	1.00000E-05	7.85848E-01	2.21328E-02
9.70000E-04	1.00000E-05	8.14070E-01	2.77076E-02
9.60000E-04	1.00000E-06	7.85848E-01	2.21328E-02
9.61000E-04	1.00000E-06	7.88570E-01	2.26135E-02
9.62000E-04	1.00000E-06	7.91314E-01	2.31099E-02
9.63000E-04	1.00000E-06	7.94079E-01	2.36224E-02
9.64000E-04	1.00000E-06	7.96866E-01	2.41515E-02
9.65000E-04	1.00000E-06	7.99676E-01	2.46979E-02
9.66000E-04	1.00000E-06	8.02508E-01	2.52620E-02
9.65000E-04	1.00000E-07	7.99676E-01	2.46979E-02
9.65100E-04	1.00000E-07	7.99958E-01	2.47535E-02
9.65200E-04	1.00000E-07	8.00240E-01	2.48093E-02
9.65100E-04	1.00000E-08	7.99958E-01	2.47535E-02
9.65110E-04	1.00000E-08	7.99986E-01	2.47590E-02
9.65120E-04	1.00000E-08	8.00014E-01	2.47646E-02
9.65110E-04	1.00000E-09	7.99986E-01	2.47590E-02
9.65111E-04	1.00000E-09	7.99989E-01	2.47596E-02
9.65112E-04	1.00000E-09	7.99992E-01	2.47602E-02
9.65113E-04	1.00000E-09	7.99994E-01	2.47607E-02
9.65114E-04	1.00000E-09	7.99997E-01	2.47613E-02
9.65115E-04	1.00000E-09	8.00000E-01	2.47618E-02
9.65114E-04	1.00000E-10	7.99997E-01	2.47613E-02
9.65114E-04	1.00000E-10	7.99998E-01	2.47613E-02
9.65114E-04	1.00000E-10	7.99998E-01	2.47614E-02
9.65114E-04	1.00000E-10	7.99998E-01	2.47614E-02
9.65114E-04	1.00000E-10	7.99998E-01	2.47615E-02
9.65114E-04	1.00000E-10	7.99999E-01	2.47615E-02
9.65114E-04	1.00000E-10	7.99999E-01	2.47616E-02
9.65114E-04	1.00000E-10	7.99999E-01	2.47617E-02
9.65114E-04	1.00000E-10	8.00000E-01	2.47617E-02

Continued

DATA INPUTS:
RESISTANCE STATED: NO
GEOMETRY: CONFIGURATION 6K

HO CORR/BEU	RE NUMBER	EXP NUSSELT	CAL NUSSELT	% CA-EX/EX
3.96676E+04	1.56279E+04	1.64706E+02	1.60011E+02	-2.85022E+00
3.97416E+04	1.56315E+04	1.65619E+02	1.60041E+02	-3.36811E+00
3.97918E+04	1.56346E+04	1.66316E+02	1.60066E+02	-3.75767E+00
4.37667E+04	2.26372E+04	2.14810E+02	2.15223E+02	+1.92605E-01
4.36185E+04	2.26052E+04	2.12119E+02	2.14979E+02	+1.34849E+00
4.36942E+04	2.26243E+04	2.13796E+02	2.15125E+02	+6.21797E-01
4.70943E+04	2.98698E+04	2.71857E+02	2.68669E+02	-1.17284E+00
4.69945E+04	2.98619E+04	2.67631E+02	2.68611E+02	+3.66437E-01
4.68007E+04	2.97724E+04	2.61713E+02	2.67967E+02	+2.38988E+00
4.92878E+04	3.72601E+04	3.19662E+02	3.20646E+02	+3.07777E-01
4.92870E+04	3.72222E+04	3.13588E+02	3.20385E+02	+2.16760E+00
4.89854E+04	3.72411E+04	3.10587E+02	3.20515E+02	+3.19650E+00
5.10365E+04	4.48872E+04	3.66671E+02	3.72159E+02	+1.49672E+00
5.12559E+04	4.48562E+04	3.69651E+02	3.71954E+02	+6.23108E-01
5.08927E+04	4.48795E+04	3.61893E+02	3.72108E+02	+2.82271E+00
5.21072E+04	5.27371E+04	4.03228E+02	4.23374E+02	+4.99603E+00
5.20211E+04	5.27112E+04	3.98677E+02	4.23207E+02	+6.15281E+00
5.27085E+04	5.27249E+04	4.25610E+02	4.23295E+02	-5.43966E-01
5.48455E+04	6.92102E+04	5.33531E+02	5.26219E+02	-1.37046E+00
5.48458E+04	6.91692E+04	5.28251E+02	5.25970E+02	-4.31807E-01
5.51823E+04	6.91907E+04	5.51998E+02	5.26101E+02	-4.69154E+00
5.63508E+04	8.62608E+04	6.17325E+02	6.27598E+02	+1.66409E+00
5.69091E+04	8.61728E+04	6.64809E+02	6.27086E+02	-5.67432E+00
5.62103E+04	8.63378E+04	6.07485E+02	6.28046E+02	+3.38463E+00
5.76672E+04	1.04449E+05	7.33038E+02	7.31399E+02	-2.23561E-01
5.76672E+04	1.04344E+05	7.29911E+02	7.30813E+02	+1.23601E-01
5.81748E+04	1.04271E+05	7.81489E+02	7.30404E+02	-6.53681E+00

LOG-LOG REGRESSION LINE IS (NU/PR^ .4)= .07063680006552 *(RE^ .7999999859741)

RESULTS OF REGRESSION ANALYSIS

Z...SUM OF LOG(NU)	159.2333666428
P...SUM OF LOG(RE)	288.4860991298
W...SUM OF LOG(NU)*LOG(RE)	1708.865267162
G...SUM OF (LOG(RE)^2)	3091.765413692
X...TOTAL NUMBER OF RUNS USED	27
S...SUM OF (DEVIATIONS^2)	.02476176123341
C...OUTER RESISTANCE TO TRANSFER	.0009651147999999
E...SLOPE OF REGRESSION LINE	.7999999859741
C1...LOG(CONST) IN NU EQUATION	-2.650204022898
X7...T(5) IN CONFIDENCE ANALYSIS	2.06
X6...MULT. IN LOG(CONST) ANALYSIS	3.492757609555
X4...MULT. IN SLOPE ANALYSIS	.3263976793339
X5...INTERVAL ON LOG(CONST	.2264417118143
X3...INTERVAL ON SLOPE	.02116094430327
F6...MIN. LOG(CONST)	-2.876645734712
F7...MAX. LOG(CONST)	-2.423762311084
Q6...MIN. CONST	.0563233698627
Q7...MAX. CONST	.08858769522597
Q5...REGRESSION CONST	.07063680006552
F8...MIN.SLOPE	.7788390416709
F9...MAX.SLOPE	.8211609302774
Q4...SUM OF (LOG(NU)^2)	945.1160426868
Q3...CORRELATION COEFFICIENT/R	.9979454077331
Q2...R^2	.9958950368156
F4...AV. ABS. DEV.	2.313932620648
F5...R.M.S. ABS. DEV.	3.01272276741

The results in tables A.8.4 and A.9.4 were obtained 7 days after the acquisition of the results that are presented in this table. The value of the heat transfer resistance used overleaf is that obtained from Table A.9.4.

Continued

```
FILE RESULTS !NO
TRY ANOTHER RE AND/OR PR EXPONENT !NO
DO YOU WANT TO STATE THE RESISTANCE !YES
RESISTANCE ,C, IS !0.0009547400
```

RESISTANCE	INCREMENT	EXPONENT	SUM ERS SQ
9.54740E-04	1.00000E-10	7.71875E-01	1.98428E-02

DATA INPUTS:
RESISTANCE STATED: YES
GEOMETRY: CONFIGURATION 6K

HO CORR/BEU	RE NUMBER	EXP NUSSELT	CAL NUSSELT	% CA-EX/EX
3.96676E+04	1.56279E+04	1.62134E+02	1.58534E+02	-2.22054E+00
3.97416E+04	1.56315E+04	1.63020E+02	1.58562E+02	-2.73415E+00
3.97918E+04	1.56346E+04	1.63695E+02	1.58587E+02	-3.12050E+00
4.37667E+04	2.26372E+04	2.10458E+02	2.11026E+02	+2.70033E-01
4.36185E+04	2.26052E+04	2.07872E+02	2.10795E+02	+1.40602E+00
4.36942E+04	2.26243E+04	2.09484E+02	2.10933E+02	+6.91930E-01
4.70943E+04	2.98698E+04	2.64925E+02	2.61383E+02	-1.33716E+00
4.69945E+04	2.98619E+04	2.60910E+02	2.61329E+02	+1.60747E-01
4.68007E+04	2.97724E+04	2.55276E+02	2.60725E+02	+2.13431E+00
4.92878E+04	3.72601E+04	3.10118E+02	3.10017E+02	-3.23622E-02
4.92870E+04	3.72222E+04	3.04394E+02	3.09774E+02	+1.76725E+00
4.89854E+04	3.72411E+04	3.01568E+02	3.09895E+02	+2.76133E+00
5.10365E+04	4.48872E+04	3.54166E+02	3.57943E+02	+1.06630E+00
5.12559E+04	4.48562E+04	3.56943E+02	3.57752E+02	+2.26861E-01
5.08927E+04	4.48795E+04	3.49706E+02	3.57895E+02	+2.34187E+00
5.21072E+04	5.27371E+04	3.88157E+02	4.05360E+02	+4.43179E+00
5.20211E+04	5.27112E+04	3.83936E+02	4.05206E+02	+5.53991E+00
5.27085E+04	5.27249E+04	4.08853E+02	4.05287E+02	-8.72180E-01
5.48455E+04	6.92102E+04	5.07473E+02	4.99992E+02	-1.47423E+00
5.48458E+04	6.91692E+04	5.02689E+02	4.99763E+02	-5.82063E-01
5.51823E+04	6.91907E+04	5.24150E+02	4.99883E+02	-4.62965E+00
5.63508E+04	8.62608E+04	5.82681E+02	5.92636E+02	+1.70841E+00
5.69091E+04	8.61728E+04	6.24791E+02	5.92169E+02	-5.22132E+00
5.62103E+04	8.63378E+04	5.73916E+02	5.93044E+02	+3.33295E+00
5.76672E+04	1.04449E+05	6.84715E+02	6.86948E+02	+3.26103E-01
5.76672E+04	1.04344E+05	6.81972E+02	6.86417E+02	+6.51805E-01
5.81748E+04	1.04271E+05	7.26778E+02	6.86046E+02	-5.60437E+00

LOG-LOG REGRESSION LINE IS (NU/PR^ .4)= .09182385048846 *(RE^ .7718753144495)

RESULTS OF REGRESSION ANALYSIS

Z...SUM OF LOG(NU)	158.202451924
F...SUM OF LOG(RE)	288.4860991298
W...SUM OF LOG(NU)*LOG(RE)	1697.586289684
G...SUM OF (LOG(RE)^2)	3091.765413692
X...TOTAL NUMBER OF RUNS USED	27
S...SUM OF (DEVIATIONS^2)	.01984279781869
C...OUTER RESISTANCE TO TRANSFER	.00095474
E...SLOPE OF REGRESSION LINE	.7718753144495
C1...LOG(CONST) IN NU EQUATION	-2.387883205858
X7...T(5) IN CONFIDENCE ANALYSIS	2.06
X6...MULT. IN LOG(CONST) ANALYSIS	3.492757609555
X4...MULT. IN SLOPE ANALYSIS	.3263976793339
X5...INTERVAL ON LOG(CONST	.2027062396314
X3...INTERVAL ON SLOPE	.0189428679566
F6...MIN. LOG(CONST)	-2.590589445489
F7...MAX. LOG(CONST)	-2.185176966226
Q6...MIN. CONST	.07497583289126
Q7...MAX. CONST	.1124578306554
Q5...REGRESSION CONST	.09182385048846
F8...MIN.SLOPE	.7529324464929
F9...MAX.SLOPE	.7908181824061
Q4...SUM OF (LOG(NU)^2)	932.5758158896
Q3...CORRELATION COEFFICIENT/R	.9982306290075
Q2...R^2	.9964643886887
F4...AV. ABS. DEV.	2.098007775191
F5...R.M.S. ABS. DEV.	2.699323561068

```
FILE RESULTS !YES
TRY ANOTHER RE AND/OR PR EXPONENT !NO
DO YOU WANT TO STATE THE RESISTANCE !NO
STOP AT LINE 2520
```

Appendix A.10

Estimation of the entrance and exit losses for a twisted tape

Using the forced vortex model, outlined in Appendix A.1, Gambill et. al. (49) show that the pressure loss due to swirl formation is given by

$$\Delta p_s = \frac{\pi^2 \rho u^2}{16 y^2} \qquad \text{(A.10.1)}$$

This term represents an actual useful energy loss if the swirl totally decays in the pipe section connecting the twisted tape exit and the downstream pressure tapping.

To estimate the pressure losses associated with changes in the cross section of ducts, Kays (58) uses the following nomenclature :-

$$\frac{\Delta p_e}{\rho g} = \frac{K_c u^2}{2g} \qquad \text{(A.10.2)}$$

and

$$\frac{\Delta p_c}{\rho g} = \frac{K_e u^2}{2g} \qquad \text{(A.10.3)}$$

where

$$K_e = 1 - 2K_{d3}\sigma + \sigma^2 (2K_{d1} - 1) \qquad \text{(A.10.4)}$$

and

$$K_c = \frac{1 - K_{eb1}\sigma^2 c_c^2 - 2c_c + 2c_c^2 K_{d3}}{c_c^2} - (1 - \sigma^2) \qquad \text{(A.10.5)}$$

The suffixes, 1 and 3, refer to the ducts upstream and downstream of the contraction. K_{eb} and K_d are respectively kinetic energy and momentum correction factors; the reader should consult reference (58) if a more detailed description is required.

For a uniform velocity distribution upstream of the contraction, equation (A.10.5) reduces to

$$K_c \approx \frac{1 - 2c_c + c_c^2 (2K_{d3} - 1)}{c_c^2} \qquad \text{(A.10.6)}$$

In equations (A.10.4) to (A.10.6), c_c is the ratio of the flow areas of the vena contracta and contracted duct: it is dependent on the

ratio of the flow areas, σ, downstream and upstream of the contraction. For the present work using solder alloy inserts, $\sigma = 0.822$ and tentatively using the data of Kays, which applies for circular ducts, it is found that $c_c = 0.78$. Further requirements for the use of the above equations, again using the circular duct correlations, are

$$K_d = 1.09068\,(8\phi) + 0.05584\,(8\phi)^{0.5} + 1 \qquad \text{(A.10.7)}$$

$$K_{eb} = -1.735\,(8\phi)^{1.5} + 3.272\,(8\phi) + 0.0883\,(8\phi)^{0.5} + 1 \qquad \text{(A.10.8)}$$

The total pressure drop across the twisted tape is given by

$$\Delta p = 4\,\phi\,\frac{l}{d}\,\rho\,u^2 \qquad \text{(A.10.9)}$$

Combining equations (A.10.1), (A.10.2), (A.10.3), and (A.10.9), gives

$$\frac{\Delta p'}{\Delta p} = \frac{\frac{\bar{u}^2}{8y^2} + K_e + K_c}{8\,\phi\,\frac{l}{d}} \qquad \text{(A.10.10)}$$

where $\Delta p'$ is the sum of the pressure losses due to the swirl formation and flow area changes.

Appendix A.11

Determination of the heat transfer coefficients in selected regions of a double pipe heat exchanger

Figure A.11 is a schematic diagram of the apparatus. The tube side and annulus side fluid flowrates and densities are Q(I,2), Q(I,3), D(I,2), and D(I,3).* A heat balance over the unpacked section of the tube shows that

$$q_o = Q(I,2)\, D(I,2)\, c_p\, (Y - T(I,13)) \qquad (A.11.1)$$

$$= Q(I,3)\, D(I,3)\, c_p\, (Y1 - T(I,4)) \qquad (A.11.2)$$

$$= U_o\, A_o \left[\frac{(Y1 - Y) - (T(I,4) - T(I,13))}{\ln \left[\frac{Y1 - Y}{T(I,4) - T(I,13)} \right]} \right] \qquad (A.11.3)$$

where U_o and A_o are the overall heat transfer coefficient and the outer tube wall area over the unpacked section of the tube.

Similarly, a heat balance over the packed section shows that

$$q_p = Q(I,2)\, D(I,2)\, c_p\, (T(I,14) - Y) \qquad (A.11.4)$$

$$= Q(I,3)\, D(I,3)\, c_p\, (T(I,3) - Y1) \qquad (A.11.5)$$

$$= U_p\, A_p \left[\frac{(T(I,3) - T(I,14)) - (Y1 - Y)}{\ln \left[\frac{T(I,3) - T(I,14)}{Y1 - Y} \right]} \right] \qquad (A.11.6)$$

The total heat flowrate, through the entire tube wall, is given by

$$q = Q(I,2)\, D(I,2)\, c_p\, (T(I,14) - T(I,13)) \qquad (A.11.7)$$

$$= Q(I,3)\, D(I,3)\, c_p\, (T(I,3) - (T(I,4)) \qquad (A.11.8)$$

$$= q_o + q_p \qquad (A.11.9)$$

---

* These symbols, and those used later to represent the fluid temperatures, have been used in the computer program that is presented later in this appendix. This avoids confusion in relating the present discussion to the computer program.

Figure No. A.11 Schematic diagram of a double pipe heat exchanger with the tube containing a continuous length of inserts which does not extend along the total tube length

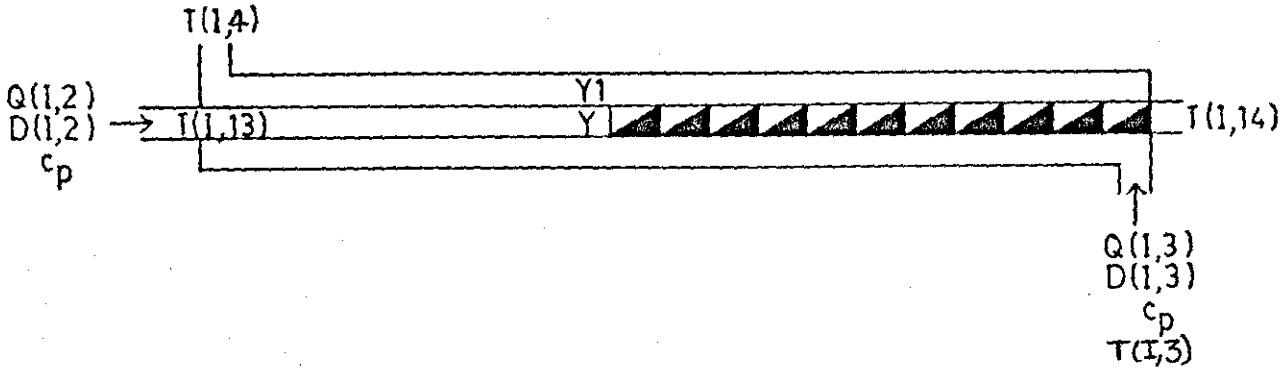

Substituting equations (A.11.1) and (A.11.5) into equations (A.11.9) and (A.11.7), and rearranging, we obtain

$$Y1 = T(I,3) - \frac{Q(I,2)\ D(I,2)\ (T(I,14) - Y)}{Q(I,3)\ D(I,3)} \qquad (A.11.10)$$

Alternatively, using equations (A.11.2), (A.11.4), (A.11.9), and (A.11.7), and rearranging, we obtain

$$Y1 = T(I,4) + \frac{Q(I,2)\ D(I,2)\ (Y - T(I,13))}{Q(I,3)\ D(I,3)} \qquad (A.11.11)$$

The total heat flow may also be written in the form

$$q = U\ A_T \left[\frac{(T(I,3) - T(I,14)) - (T(I,4) - T(I,13))}{\ln \left[\frac{T(I,3) - T(I,14)}{T(I,4) - T(I,13)} \right]} \right] \qquad (A.11.12)$$

where

$$\frac{1}{U} = C + \frac{d_o}{d\ h} \qquad (A.11.13)$$

Similarly,

$$\frac{1}{U_o} = C_o + \frac{d_o}{d\ h_o} \quad \text{for the empty tube section} \qquad (A.11.14)$$

and

$$\frac{1}{U_p} = C_p + \frac{d_o}{d\ h_p} \quad \text{for the packed section} \qquad (A.11.15)$$

The above equations were used to analyse the experimental results of the present work. The two methods considered for the analysis are outlined below.

Case 1. For $C = C_s = C_p$

(i) Assume a value for the tube side fluid temperature, Y.

(ii) Calculate the average Reynolds number and Prandtl number in the empty tube section.

(iii) Using an entrance length modification of the Dittus-Boelter equation, which is considered later, determine the tube side heat transfer coefficient in the empty tube section and the film resistance d_o/dh_o.

(iv) Calculate the overall heat transfer resistance,

$1/U_o$, using the result of (iii) and the assumption that C_o equals the heat transfer resistance, C, determined from previous empty tube tests.

(v) Calculate an estimated annulus fluid temperature, Y1, using equation (A.11.10) or (A.11.11). Hence find the estimated logarithmic mean temperature difference for the empty tube section.

(vi) Estimate the heat flowrate through the wall of the empty tube section using equations (A.11.1) and (A.11.3). If the difference between the two heat flows is not below a prespecified limit then adjust the value of Y and go to (ii).

(vii) Calculate q_p using equation (A.11.4). Calculate the LMTD over the packed section and hence obtain the value of $1/U_p$ using equation (A.11.6).

(viii) Assuming that C_p equals the heat transfer resistance, C, find h_p using equation (A.11.15).

Case 2. For $C \neq C_o \neq C_p$

Equation (5.8) is a modification of the Dittus-Boelter equation which allows its use for annuli. Using this information with the adaptation of the Dittus-Boelter equation that was suggested by McAdams, see equation (1.22), it is expected that for a given annulus and fluid velocity :

$$h_a = (\text{Constant})\ (1 + 0.011\ T_{av}) \qquad \text{(A.11.16)}$$

$$= A + B\ T_{av} \qquad \text{(A.11.17)}$$

where T_{av} is the average annulus fluid temperature measured in ^oF. Substituting equation (A.11.17) into equation (5.7) and rearranging, we obtain

$$\frac{1}{C - \left[\frac{x_w\ d_o}{k_w\ d_m}\right] - (R_i + R_o)} = A + BT_{av} \qquad \text{(A.11.18)}$$

The tube wall resistance to heat transfer can be calculated. The value of C can be determined from the previous empty tube tests which used an average annulus fluid temperature of 80^oC. This average annulus fluid temperature varied only slightly (maximum deviations of

$\pm$ 0.13°C) and therefore a regression analysis of equation (A.11.18) is not suitable. An alternative procedure is to substitute equation (A.11.16) into equation (5.7) and neglect the scale resistances, hence

$$h_a = \frac{1}{C - \frac{x_w d_o}{k_w d_m}} = (\text{Constant})\ (1 + 0.011\ T_{av}) \qquad (A.11.19)$$

For each of the experimental values of T_{av} a value of the "constant" can be calculated. The mean value of the "constant" so obtained may then be used in equation (A.11.19) in order to estimate the value of h_a at any given fluid temperature. Using this procedure with the estimated mean annulus fluid temperature along the empty and packed tube sections, the values of C_o and C_p may be estimated for each experimental test. These values can be used in (iv) and (viii) of the previous case considered above.

Estimation of the heat transfer coefficient in the empty tube section

This section considers the derivation of the equation that was used to estimate the heat transfer coefficient in the relatively short (l/d = 24.9) empty section of the tube.

The empty tube tests of the present work showed that

$$\frac{Nu}{Pr^{0.4}} = 0.0253\ Re^{0.8} \qquad (A.11.20)$$

These results were obtained using a tube length to diameter ratio, (l/d), of 53.34.

A heat transfer coefficient determined using the Dittus-Boelter equation, (1.19), is the assymptotic value of the coefficient in an empty tube. Substituting this value into equation (1.27) and equating to equation (A.11.20) shows that X = 5.37, in the present work. The heat transfer coefficient in the empty section of a tube containing inserts may therefore be estimated using

$$\frac{Nu}{Pr^{0.4}} = 0.023\ Re^{0.8} \left[1 + 5.37\left[\frac{d}{l}\right]\right] \qquad (A.11.21)$$

where l = length of the empty tube section

The experimental data was analysed using the techniques that have been described above. The analysis was performed using the computer program that is presented in the following pages of this appendix.

```
10 REM PROGRAM FOR ESTIMATION OF FILM COEFFICIENTS IN SELECTED REGIONS
20 REM DATA OBTAINED FROM FILES #1,#3,#4,#5, OF HEAT2-6010
30 REM IF THE EMPTY TUBE SECTION IS DOWNSTREAM OF THE PACKED SECTION
40 REM THEN INSERT APPROPRIATE NU EQUATION AS LINE 1530
50 REM LINES 50-570
60 REM DIM STATEMENTS,PROCESS INFORMATION,DATA READ
70 DIM A$(4),Q(100,7),U(100,2),R(100),N(100),D(100,7),V(100),Y(9,1),M(100)
80 DIM T(100,25),H(100,10),K(100,8),E(100)
90 DIM B(100,5),S(100,5),Z(100,6),G(100,2),O(100,4)
100 DEFINE FILE#1='TH5-6010'
110 DEFINE FILE#3='DAY5BH-6010', ASC SEP,500
120 DEFINE FILE#5='DAY5EH-6010', ASC SEP,500
130 DEFINE FILE#4='DAY5CH-6010', ASC SEP,500
140 PRINT'FIRST RUN ON DATA FILE':
150 INPUT O8
160 PRINT'LAST RUN ON DATA FILE':
170 INPUT Y8
180 FOR I=O8 TO Y8
190 READ#1,N(I),S(I,4),M(I),S(I,5),T(I,1),T(I,2),T(I,3),T(I,4),T(I,6),T(I,25)
200 READ#3,Q(I,2),U(I,1),R(I),D(I,2),V(I)
210 READ#5,H(I,3),H(I,4),H(I,5),H(I,6),T(I,11),T(I,12),T(I,18),T(I,19),T(I,14),T(I,20)
220 READ#4,T(I,5),T(I,13),T(I,16),K(I,1),E(I),U(I,2)
230 NEXT I
240 CLOSE #1
250 CLOSE #3
260 CLOSE #5
270 CLOSE #4
280 PRINT'FIRST RUN NUMBER IS':
290 INPUT O9
300 PRINT'LAST RUN NUMBER IS':
310 INPUT Y9
320 PRINT'ALLOWABLE ERROR ON HEAT FLUX':
330 INPUT E
340 PRINT'INITIAL TEMPERATURE INCREMENT':
350 INPUT X1
360 PRINT'INITIAL EST. TEMP. AT EMPTY/PACKED JUNCTION':
370 INPUT Y6
380 PRINT'USE EQUATION 1 OR 2':
390 INPUT A
400 PRINT'TUBE I.D./INS.':
410 INPUT D
420 PRINT'TUBE O.D./INS.':
430 INPUT D1
440 PRINT'TOTAL HEATED LENGTH/INS.':
450 INPUT L1
460 PRINT'EMPTY TUBE LENGTH/INS.':
470 INPUT L
480 PRINT'ROTAMETER SCALE READING ON R2':
490 INPUT Z9
500 A1=3.1415927*D1*L/144
510 A2=3.1415927*D1*(L1-L)/144
520 GOSUB 1800
530 PRINT'AVERAGE RESISTANCE,C/BEU':
540 INPUT C
550 PRINT'USE AVERAGE C THROUGHOUT':
560 INPUT A$(4)
570 IF A$(4)='YES' GO TO 640
580 REM LINE 600
590 REM CALCULATE ANNULUS SIDE COEFFICIENT IF CASE 2 IS USED
600 GOSUB 1620
610 REM LINES 610-1120
620 REM CALCULATION OF TEMPERATURES AT EMPTY/PACKED INTERFACE AND
630 REM CALCULATION OF HEAT FLUXES OVER SECTIONS OF THE TUBE
640 FOR I=O9 TO Y9
650 Y=Y6
660 X=X1
670 M=1
680 PRINT LIN(1)
690 PRINT 'RUN NUMBER':N(I):TAB(16):
700 N=0
710 GOSUB 1390
720 IF A<2 GO TO 750
730 Y1=(Q(I,2)*D(I,2)*(Y-T(I,13))/(Q(I,3)*D(I,3)))+T(I,4)
740 GO TO 760
750 Y1=T(I,3)-((Q(I,2)*D(I,2)*(T(I,14)-Y))/(Q(I,3)*D(I,3)))
760 Z1=Q(I,2)*D(I,2)*62.427961*3600*1.8*(Y-T(I,13))
770 Y2=((Y1-Y)-(T(I,4)-T(I,13)))/LOG((Y1-Y)/(T(I,4)-T(I,13)))
780 Z2=B1*A1*Y2*1.8
790 Z3=Z1-Z2
800 IF ABS(Z3)<E GO TO 870
810 IF Z3<0 GO TO 840
```

```
820 Y=Y-X
830 X=X/10
840 Y=Y+X
850 N=N+1
860 GO TO 710
870 B(I,1)=B
880 N=N+1
890 PRINT'NO. OF ITERATIONS':N
900 K(I,6)=K5
910 B(I,2)=B1
920 Z(I,1)=Y
930 Z(I,2)=Y1
940 Z(I,3)=((T(I,3)-T(I,14))-(Y1-Y))/LOG((T(I,3)-T(I,14))/(Y1-Y))
950 Z(I,4)=Q(I,2)*D(I,2)*62.427961*1.8*3600*(T(I,14)-Y)
960 Z(I,5)=Z(I,3)*A2*1.8/Z(I,4)
970 IF A$(4)='YES' GO TO 1020
980 K7=1/(K2*(1+(0.011*(((Y1+T(I,3))*0.9)+32))))
990 K8=221.2-((11/720)*((((Y1+T(I,3)+Y+T(I,14))/4)*1.8)+32))
1000  K(I,7)=K7+(((D1-D)*D1)/(K8*K4*12))
1010 GO TO 1030
1020 K(I,7)=C
1030 B(I,3)=D1/(D*(Z(I,5)-K(I,7)))
1040 G(I,1)=G1
1050 O(I,3)=O3
1060 M=0
1070 GOSUB 1390
1080 B(I,4)=D*B(I,3)/(O1*12*(G1^0.4))
1090 O(I,4)=O3
1100 G(I,2)=G1
1110 NEXT I
1120 PRINT LIN(1)
1130 REM LINES 1130-1290
1140 REM OPTION TO FILE RESULTS
1150 PRINT'FILE RESULTS':
1160 INPUT A$(1)
1170 IF A$(1)='NO' GO TO 1320
1180 DEFINE FILE#2='SIGMA-6010', ASC SEP,500
1190 DEFINE FILE#7='SIGMAS-6010', ASC SEP,50
1200 PRINT LIN(1)
1210 PRINT'REYNOLDS NUMBER,NU/(PR^0.4)'
1220 PRINT LIN(1)
1230 FOR I=09 TO Y9
1240 WRITE#2,B(I,1),B(I,2),B(I,3),Z(I,1),Z(I,2),O(I,3),G(I,1),G(I,2),K(I,6),K(I,7)
1250 WRITE#7,O(I,4),B(I,4)
1260 PRINT O(I,4),B(I,4)
1270 NEXT I
1280 CLOSE #2
1290 CLOSE #7
1300 REM LINES 1300-1370
1310 REM OPTIONS TO USE DIFFERENT CALCULATION METHODS
1320 PRINT'TRY ANOTHER RESISTANCE':
1330 INPUT A$(2)
1340 IF A$(2)='YES' GO TO 530
1350 PRINT'TRY ANOTHER HEAT BALANCE ETC.':
1360 INPUT A$(3)
1370 IF A$(3)='YES' GO TO 320
1380 STOP
1390 REM SUBROUTINE LINES 1390-1610
1400 REM CALCULATION OF RE,PR,AND NU IN EMPTY TUBE SECTION
1410 IF M=1 GO TO 1440
1420 T=(Y+T(I,14))/2
1430 GO TO 1450
1440 T=(Y+T(I,13))/2
1450 D7=1-((((T-3.9863)^2)*(T+288.9414))/(508929.2*(T+68.12963)))
1460 Q1=Q(I,2)*D(I,2)/D7
1470 U2=(Q1*576)/(3.1415927*(D^2))
1480 D0=100/((2.1482*((T-8.435)+((8078.4+((T-8.435)^2))^0.5)))-120)
1490 O1=0.00587*(1+(0.00281*(T-20)))/0.017307
1500 O3=7741.92*D*U2*D7/D0
1510 O2=1
1520 G1=O2*D0*2.14190883/O1
1530 B=0.023*(O3^0.8)*(G1^0.4)*(1+(5.37*(D/L)))
1540 IF A$(4)='YES' GO TO 1590
1550 K3=1/(K2*(1+(0.011*(((Y1+T(I,4))*0.9)+32))))
1560 K6=221.2-((11/720)*((((Y1+T(I,4)+Y+T(I,13))/4)*1.8)+32))
1570 K5=K3+(((D1-D)*D1)/(K6*K4*12))
1580 GO TO 1600
1590 K5=C
1600 B1=1/(K5+(D1/(12*B*O1)))
1610 RETURN
1620 REM SUBROUTINE LINES 1620-1770
```

```
1630 REM ESTIMATION OF ANNULUS SIDE FILM COEFFICIENT USING CASE 2
1640 K1=0
1650 K4=(D1-D)/LOG(D1/D)
1660 FOR I=09 TO Y9
1670 T(I,23)=(T(I,3)+T(I,4)+T(I,13)+T(I,14))/4
1680 T(I,24)=((T(I,3)+T(I,4))*0.9)+32
1690 K(I,2)=221.2-((11/720)*((T(I,23)*1.8)+32))
1700 K(I,4)=1/(C-((((D1-D)*D1)/(K(I,2)*K4*12)))
1710 K(I,5)=K(I,4)/(1+(0.011*T(I,24)))
1720 K1=K1+K(I,5)
1730 NEXT I
1740 K2=K1/(Y9+1-09)
1750 PRINT LIN(2)
1760 PRINT'OUTSIDE H=':K2:'*(1+(0.011*T/F))'
1770 RETURN
1780 REM SUBROUTINE LINES 1780-1940
1790 REM ANNULUS SIDE VOLUME FLOW AND DENSITY AT ROTAMETER
1800 Y(1,1)=0.002911610712545
1810 Y(2,1)=1.089821240896E-5
1820 Y(3,1)=0.0007601237919062
1830 Y(4,1)=-6.308266691236E-7
1840 Y(5,1)=9.7547162312l4E-6
1850 Y(6,1)=-2.231681817122E-8
1860 Y(7,1)=-7.141842539582E-8
1870 Y(8,1)=1.1914734199l6E-8
1880 Y(9,1)=-2.138529076046E-10
1890 FOR I=09 TO Y9
1900 Q(I,7)=Y(1,1)+(Y(2,1)*T(I,4))+(Y(3,1)*Z9)+(Y(4,1)*T(I,4)*Z9)+(Y(5,1)*(Z9^2))+(Y(6,1)*T(I,4)*(Z9^2))
1910 Q(I,3)=Q(I,7)+(Y(7,1)*(T(I,4)^2))+(Y(8,1)*(T(I,4)^2)*Z9)+(Y(9,1)*(T(I,4)^2)*(Z9^2))
1920 D(I,3)=1-((((T(I,4)-3.9863)^2)*(T(I,4)+288.9414))/(508929.2*(T(I,4)+68.126963)))
1930 NEXT I
1940 RETURN
1950 END
```

Appendix A.12

Prediction of the friction factor characteristics of the Kenics static mixer arrangement

The empty tube friction factor characteristics may be presented in the form :

$$\phi_o = A\, Re^{-B} \qquad (A.12.1)$$

Equations (1.80) to (1.83) have the general form :

$$K = \frac{\phi}{\phi_o} = G\, D^H\, J^Q\, Re^{0.104} \qquad (A.12.2)$$

where J = y in equations (1.80) and (1.82),

J = y/(y-1) in equations (1.81) and (1.83),

and G, H, and Q are constants.

Combining equations (A.12.1) and (A.12.2) it is found that for the commercial Kenics mixer

$$\phi = A\, G\, D^H\, J^Q\, Re^{(0.104-B)} \qquad (A.12.3)$$

Converting this equation to the equivalent flow basis, gives

$$\phi_e = A\, G \left[\frac{\phi_e}{\phi}\right] \left[\frac{D}{D_e}\right]^H D_e^H\, J^Q \left[\frac{Re}{Re_e}\right]^{(0.104-B)} Re_e^{(0.104-B)} \qquad (A.12.4)$$

where $\frac{\phi_e}{\phi}$ = (friction factor defined using the equivalent flow basis) / (friction factor defined using the tube diameter and the superficial fluid velocity)

$$= \left[\frac{D_e}{D}\right] \left[\frac{A_c}{A_f}\right]^2 \qquad (A.12.5)$$

and $$\frac{Re_e}{Re} = \left[\frac{D_e}{D}\right] \left[\frac{A_f}{A_c}\right] \qquad (A.12.6)$$

The geometrical details of the mixer to be considered can be substituted into equation (A.12.4), so that

$$\phi = \frac{A\ G \left[\frac{\phi_e}{\phi}\right]_K \left[\frac{D}{D_e}\right]_K^H D^H\ J^Q \left[\frac{Re}{Re_e}\right]_K^{(0.104-B)} Re^{(0.104-B)}}{\left[\frac{\phi_e}{\phi}\right] \left[\frac{D}{D_e}\right]^H \left[\frac{Re}{Re_e}\right]^{(0.104-B)}} \qquad (A.12.7)$$

where the subscript "K" refers to the commercial Kenics mixers. Since (D/D_e) and (A_c/A_f) are only dependent on the relative thickness of the inserts, (δ/d), it is found that for the commercial Kenics mixers ($\delta/d = 0.1$ for $d < 38$ mm):

$$(\phi_e / \phi)_K = 0.4225$$

$$(D/D_e)_K = 1.802$$

$$(Re_e/Re)_K = 0.6357$$

The above values can be substituted into equation (A.12.7) to yield an expression which should allow the prediction of the pressure drop across a configuration of alternately twisting helices with perpendicular leading edges.

In Table 7.5 the predicted values of the friction factor, at Reynolds numbers of 11000 and 78000, were determined using the actual empty tube correlation, i.e. denotation A-I of Table 5.4. Similarly, the predicted results for the heat transfer conditions were determined using denotation B-P of Table 5.5. The empty tube friction factor correlation used when predicting the results of other workers was

$$\phi_o = 0.0396\ Re^{-0.25}$$

This is not a good representation of the empty tube results of Chakrabarti (21) and it is only for consistency that this correlation has been used in the prediction of those results.